https://ntrs.nasa.gov/search.jsp?R=19780005096 2020-03-22T06:46:32+00:00Z

NASA CR 152051

(NASA-CR-152051) SIMULATION STUDY OF GUST ALLEVIATION IN A TILT ROTOR AIRCRAFT, VOLUME 2 (Boeing Vertol Co., Philadelphia, Pa.) 349 p HC A15/MF A01 CSCL 01C

N78-13039

Unclas
G3/05 55040

SIMULATION STUDY OF GUST ALLEVIATION IN A TILT ROTOR AIRCRAFT VOLUME II

A. K. AMOS

H. R. ALEXANDER

JUNE 1977

PREPARED UNDER CONTRACT NAS2-8048-4R

FOR

NATIONAL AERONAUTICS AND SPACE ADMINISTRATION
AMES RESEARCH CENTER

BY

BOEING VERTOL COMPANY
A DIVISION OF THE BOEING COMPANY
P. O. BOX 16858
PHILADELPHIA, PENNSYLVANIA 191

DEC 1977
RECEIVED
NASA STI FACILITY

D210-11231-2

NASA CR 152051

SIMULATION STUDY OF GUST ALLEVIATION IN A TILT ROTOR AIRCRAFT VOLUME II

A. K. AMOS

H. R. ALEXANDER

JUNE 1977

PREPARED UNDER CONTRACT NAS2-8048-4R

FOR

NATIONAL AERONAUTICS AND SPACE ADMINISTRATION
AMES RESEARCH CENTER

BY

BOEING VERTOL COMPANY
A DIVISION OF THE BOEING COMPANY
P. O. BOX 16858
PHILADELPHIA, PENNSYLVANIA 19142

D210-11231-2

REV LTR

THE BOEING COMPANY

VERTOL DIVISION · PHILADELPHIA, PENNSYLVANIA

CODE IDENT. NO. 77272

NUMBER D210-11231-2

TITLE SIMULATION STUDY OF GUST ALLEVIATION IN A TILT ROTOR AIRCRAFT - VOLUME II

ORIGINAL RELEASE DATE _____. FOR THE RELEASE DATE OF SUBSEQUENT REVISIONS, SEE THE REVISION SHEET. FOR LIMITATIONS IMPOSED ON THE DISTRIBUTION AND USE OF INFORMATION CONTAINED IN THIS DOCUMENT, SEE THE LIMITATIONS SHEET.

MODEL _____ CONTRACT NAS2-8048-4R

ISSUE NO. _____ ISSUED TO: _____

PREPARED BY	A. K. Amos A. K. Amos	DATE	6/8/77
APPROVED BY	H. K. Alexander	DATE	6/8/77
APPROVED BY	J. P. Magee	DATE	6/8/77
APPROVED BY		DATE	

FORM 46260 (6/66)

LIMITATIONS

This document is controlled by Organization 7420

All revisions to this document shall be approved by the above noted organization prior to release.

ACTIVE SHEET RECORD

SHEET NUMBER	REV LTR	ADDED SHEETS				SHEET NUMBER	REV LTR	ADDED SHEETS			
		SHEET NUMBER	REV LTR	SHEET NUMBER	REV LTR			SHEET NUMBER	REV LTR	SHEET NUMBER	REV LTR
a											
b						AII.21					
c						AII.22					
d						AIII.1					
e						AIII.2					
f						AIII.3					
g						AIII.4					
h						AIII.5					
i						AIII.6					
ii						AIII.7					
iii						AIV.0					
iv						AIV.1					
v						AIV.2					
vi						AIV.3					
AI.1						AIV.4					
AI.2						AIV.5					
AI.3						AIV.6					
AI.4						AIV.7					
AI.5						AIV.8					
AI.6						AIV.9					
AI.7						AIV.10					
AI.8						AIV.11					
AI.9						AIV.12					
AI.10						AIV.13					
AI.11						AIV.14					
AII.1						AIV.15					
AII.2						AIV.16					
AII.3						AIV.17					
AII.4						AIV.18					
AII.5						AIV.19					
AII.6						AIV.20					
AII.7						AIV.21					
AII.8						AIV.22					
AII.9						AIV.23					
AII.10						AIV.24					
AII.11						AIV.25					
AII.12						AIV.26					
AII.13						AIV.27					
AII.14						AIV.28					
AII.15						AIV.29					
AII.16						AIV.30					
AII.17						AIV.31					
AII.18						AIV.32					
AII.19						AIV.33					
AII.20						AIV.34					

FORM 46283 (12/69)

ACTIVE SHEET RECORD

SHEET NUMBER	REV LTR	ADDED SHEETS				SHEET NUMBER	REV LTR	ADDED SHEETS			
		SHEET NUMBER	REV LTR	SHEET NUMBER	REV LTR			SHEET NUMBER	REV LTR	SHEET NUMBER	REV LTR
AIV.35						AIV.80					
AIV.36						AIV.81					
AIV.37						AIV.82					
AIV.38						AIV.83					
AIV.39						AIV.84					
AIV.40						AIV.85					
AIV.41						AIV.86					
AIV.42						AIV.87					
AIV.43						AIV.88					
AIV.44						AIV.89					
AIV.45						AIV.90					
AIV.46						AIV.91					
AIV.47						AIV.92					
AIV.48						AIV.93					
AIV.49						AIV.94					
AIV.50						AIV.95					
AIV.51						AIV.96					
AIV.52						AIV.97					
AIV.53						AIV.98					
AIV.54						AIV.99					
AIV.55						AIV.100					
AIV.56						AIV.101					
AIV.57						AIV.102					
AIV.58						AIV.103					
AIV.59						AIV.104					
AIV.60						AIV.105					
AIV.61						AIV.106					
AIV.62						AIV.107					
AIV.63						AIV.108					
AIV.64						AIV.109					
AIV.65						AIV.110					
AIV.66						AIV.111					
AIV.67						AIV.112					
AIV.68						AIV.113					
AIV.69						AIV.114					
AIV.70						AIV.115					
AIV.71						AIV.116					
AIV.72						AIV.117					
AIV.73						AIV.118					
AIV.74						AIV.119					
AIV.75						AIV.120					
AIV.76						AIV.121					
AIV.77						AIV.122					
AIV.78						AIV.123					
AIV.79						AIV.124					

FORM 46283 (12/66)

ACTIVE SHEET RECORD

SHEET NUMBER	REV LTR	ADDED SHEETS				SHEET NUMBER	REV LTR	ADDED SHEETS			
		SHEET NUMBER	REV LTR	SHEET NUMBER	REV LTR			SHEET NUMBER	REV LTR	SHEET NUMBER	REV LTR
AIV.125						AIV.170					
AIV.126						AIV.171					
AIV.127						AIV.172					
AIV.128						AIV.173					
AIV.129						AIV.174					
AIV.130						AIV.175					
AIV.131						AIV.176					
AIV.132						AIV.177					
AIV.133						AIV.178					
AIV.134						AIV.179					
AIV.135						AIV.180					
AIV.136						AIV.181					
AIV.137						AIV.182					
AIV.138						AIV.183					
AIV.139						AIV.184					
AIV.140						AIV.185					
AIV.141						AIV.186					
AIV.142						AIV.187					
AIV.143						AIV.188					
AIV.144						AIV.189					
AIV.145						AIV.190					
AIV.146						AIV.191					
AIV.147						AIV.192					
AIV.148						AIV.193					
AIV.149						AIV.194					
AIV.150						AIV.195					
AIV.151						AIV.196					
AIV.152						AIV.197					
AIV.153						AIV.198					
AIV.154						AIV.199					
AIV.155						AIV.200					
AIV.156						AIV.201					
AIV.157						AIV.202					
AIV.158						AIV.203					
AIV.159						AIV.204					
AIV.160						AIV.205					
AIV.161						AIV.206					
AIV.162						AIV.207					
AIV.163						AIV.208					
AIV.164						AIV.209					
AIV.165						AIV.210					
AIV.166						AIV.211					
AIV.167						AIV.212					
AIV.168						AIV.213					
AIV.169						AIV.214					

FORM 46283 (7/67)

ACTIVE SHEET RECORD

SHEET NUMBER	REV LTR	ADDED SHEETS				SHEET NUMBER	REV LTR	ADDED SHEETS			
		SHEET NUMBER	REV LTR	SHEET NUMBER	REV LTR			SHEET NUMBER	REV LTR	SHEET NUMBER	REV LTR
AIV.215						AIV.261					
AIV.216						AIV.262					
AIV.217						AIV.263					
AIV.218						AIV.264					
AIV.219						AIV.265					
AIV.220						AIV.266					
AIV.221						AIV.267					
AIV.222						AIV.268					
AIV.223						AIV.269					
AIV.224						AIV.270					
AIV.225						AIV.271					
AIV.226						AIV.272					
AIV.227						AIV.273					
AIV.228						AIV.274					
AIV.230						AIV.275					
AIV.231						AIV.276					
AIV.232						AIV.277					
AIV.233						AIV.278					
AIV.234						AIV.279					
AIV.235						AIV.280					
AIV.236						AIV.281					
AIV.237						AIV.282					
AIV.238						AIV.283					
AIV.239						AIV.284					
AIV.240						AIV.285					
AIV.241						AIV.286					
AIV.242						AIV.287					
AIV.243						AIV.288					
AIV.244						AIV.290					
AIV.245						AIV.291					
AIV.246						AIV.292					
AIV.247						AIV.293					
AIV.248						AIV.294					
AIV.249						AIV.295					
AIV.250						AIV.296					
AIV.251						AIV.297					
AIV.252						AIV.298					
AIV.253						AIV.299					
AIV.254						AIV.300					
AIV.255						AIV.301					
AIV.256						AIV.302					
AIV.257						AIV.303					
AIV.258						AIV.304					
AIV.259						AIV.305					
AIV.260						AIV.306					

ACTIVE SHEET RECORD

SHEET NUMBER	REV LTR	ADDED SHEETS				SHEET NUMBER	REV LTR	ADDED SHEETS			
		SHEET NUMBER	REV LTR	SHEET NUMBER	REV LTR			SHEET NUMBER	REV LTR	SHEET NUMBER	REV LTR
AIV.307											
AIV.308											
AIV.309											
AIV.310											
AIV.311											
AIV.312											
AIV.313											
AIV.314											
AIV.315											
AIV.316											
AIV.317											
AIV.318											
AIV.319											
AIV.320											
AIV.321											
AIV.322											
AIV.323											
AIV.324											
AIV.325											
AIV.326											
AIV.327											
AIV.328											
AIV.329											
AIV.330											
AIV.331											
AIV.332											
AIV.332											
AIV.333											
AIV.334											
AIV.335											
AIV.336											
AIV.337											

FORM 46283 (12/69)

REVISIONS			
LTR	DESCRIPTION	DATE	APPROVAL

ABSTRACT

The response to vertical turbulence in cruise of the HTR XV-15 design is studied. This design is a modified version of the XV-15 with a hingeless fiberglass soft-in-plane rotor system. The parameters of a gust alleviation system are determined and the performance of the system is evaluated over a range of cruise velocities and altitudes. The study is performed using simulation techniques and the mathematical model includes detailed dynamic representation of the wing and rotor. Volume I is a summary report of the study, while Volume II contains details of analytical and other data used in the study.

FOREWORD

The studies summarized in this report were performed by the Boeing Vertol Company for the National Aeronautics and Space Administration, Ames Research Center under NASA Contract NAS2 8048-4. Mr. T. Galloway was the NASA Technical Monitor over the greater part of the program; Mr. G. Callas was the Technical Monitor for a short time at the beginning of the program.

Mr. H. R. Alexander was the Boeing Vertol Project Manager. Dr. Anthony K. Amos was Project Engineer for methodology and dynamic simulation development. Mr. J. P. Magee, Tilt Rotor Program Manager, and M. A. McVeigh, who developed the basic vehicle simulation, also made significant contributions. Very substantial contributions were also made by George Knott and Austin Mollenkoff of the Simulation Staff of Boeing Computer Services.

SUMMARY

This volume presents background material to the study of gust response and alleviation of the HTR XV-15. The study is summarized in Volume I of this report, where a full discussion of the technical issue is given, along with comparisons of the HTR XV-15 and other transport aircraft. It is shown that gust alleviation is probably a requirement for passenger acceptance, and the derivation and evaluation of a gust alleviation system is described. The system selected provides approximately 70% alleviation of cabin normal acceleration over the cruise speed range and altitude range. The material given in this volume is arranged in appendices and consists of:

Appendix (I) - Dynamic Treatment of Wing in the Simulation Mathematical Model.

Appendix (II) - Incorporation of Rotor Structural Dynamic Effects in the Simulation Mathematical Model.

Appendix (III) - Study of Influence of Pitch Response on Blade and Rotor Response.

Appendix (IV) - Complete Response Data for Matrix of Speeds, Altitudes and Center of Gravity Locations.

1.0 INTRODUCTION

1.1 WING AND ROTOR DYNAMIC REPRESENTATION

The gust response investigation was performed using a simulation mathematical model initially developed for real time simulation. This used a quasistatic approach to wing structural dynamics and rotor forces and moments, and full force effects were developed on a fully non-linear basis. This was considered essential for handling quality evaluations and exploration of rotor loads under maneuvering conditions. For investigation of transient gust response behavior it was decided -

(i) That a dynamic representation of the wing and rotor would be required.

(ii) That the most practical way of accomplishing an adequate dynamic representative was to use a linear perturbation approach.

Accordingly the section of the mathematical model dealing with the wing and rotor were provided with additional linear perturbation equations. The basic model was used to set up trim conditions. For gust response work the linear models of wing and rotor evaluated the perturbation response due to turbulence and control motion while the basic model was used in computing other effects. Rotor generalized forces and equations are calculated by drawing on a data bank of matrices of partial derivatives computed off line and stored on tape for a range of flight and

altitude conditions. This methodology and the interface with the basic full force model is discussed in detail in Appendices I and II.

1.2 STUDY OF PITCH FREEDOME ON BLADE AND ROTOR RESPONSE

A matter of concern at the outset of the study was the possible adverse effect of direct lift control, using flaps or spoilers, on rotor response. It was felt initially that the flap operation would reduce the alleviation in angle of attack produced by aircraft vertical motion; this was expected to lead to increased blade response. When this was not observed to happen in the gust alleviation simulation a study was undertaken to understand the reason. It was found that the pitching response of the aircraft to the gust and the flap application was such that the net angle of attack, the dominant input in blade and rotor response, did not vary much. The impact of this variable was examined by suppression of the freedom of the aircraft to respond in pitch; this caused the anticipated increase in blade response. This study is presented in Appendix III.

1.3 RESPONSE DATA FOR AIRCRAFT AND ROTOR SYSTEM OVER MATRIX OF ALTITUDES AND SPEEDS

Appendix IV compiles the response data, alleviation system characteristics and random turbulence response with and without alleviation for speeds of 200 Knots, 240 Knots and 280 Knots at altitudes of 1524m, (5,000 Feet), 3049m

(10,000 Feet), and 4573m (15,000 Feet). The gross weight is 5,596 Kg (13,000 Lb) and data for forward and aft center of gravity location are given.

APPENDIX I

DYNAMIC TREATMENT OF WING IN MATHEMATICAL MODEL FOR SIMULATION

I.1 INTRODUCTION

A quasi-static treatment of wing vertical bending is included in the full force mathematical model which was modified for study of the Hingeless Rotor XV-15 aircraft (HTR XV-15). This treatment is adequate for piloted studies. In gust alleviation control studies, however, it is considered that transient and time delay effects associated with wing vertical bending may impact the system design and behavior. Consequently the quasi-static treatment was replaced by a full dynamic treatment in the model used for gust alleviation control work.

The mathematical equations representing each of the two treatments are summarized in Paragraphs I.2 and I.3, and the derivation of the dynamic representation is given in Paragraph I.4. Paragraph I.2 presents a detailed derivation of the equations for the full dynamic treatment.

In the quasi-static treatment, the wing vertical bending deflections of the wing tips and aerodynamic centers are obtained directly in each time frame from Equations (1) through (4) using current values of the four aerodynamic terms and the aircraft roll acceleration. Deflection rates are computed by time-frame differentiation.

The dynamic simulation consists of determining the wing bending modal acceleration at each time frame according to Equation (5) using current values of the indicated aerodynamic loads, the aircraft vertical and roll accelerations, and the wing bending modal deflections and velocities. The latter two are obtained by numerical integration of the previous acceleration. The deflection at the wing aerodynamic center is assumed to be related to that at the wing tip by a constant ratio as indicated in Equation (6).

For programming purposes, the constants K'_{w1} through K'_{w6} in Equations (5) and (6) are to be regarded as input data replacing the constants Kw_1 through Kw_{10} defined for real time piloted simulation activity.

I.2 QUASI-STATIC TREATMENT

Wing vertical bending deflections are obtained by equating the wing static resistance to bending deformation to the dynamic loads which produce wing bending. These include:

- o aircraft inertia loads
- o wing aerodynamic loads
- o nacelle-rotor aerodynamic loads, and
- o nacelle-rotor aerodynamic rolling moment.

Thus the wing tip deflection is given by:

$$k_{1t} = Kw_1 \, Z^N_{aero} + Kw_2 Z^W_{aero} - Kw_3 L^N_{aero} - Kw_4 \, \bar{a}_t - Kw_5 \, \bar{a}_{wac}$$

Equation (1)

where

Z^N_{aero} = Nacelle vertical load

L^N_{aero} = Nacelle rolling moment

Z^w_{aero} = Total wing aerodynamic load

$\bar{a}_t$ = Wing tip acceleration

$$= \frac{Z_{aero}}{m} + Y_N \dot{p} \qquad \text{Equation (2)}$$

$\bar{a}_{wac}$ = Wing Aerodynamic center acceleration

$$= \frac{Z_{aero}}{m} \pm Y_{wac} \dot{p} \qquad \text{Equation (3)}$$

$\dot{p}$ = Aircraft roll acceleration

Kw_1 thru Kw_5 are constants reflecting wing flexibility and loading distributions. The corresponding deflection at the wing aerodynamic center is given by:

$$h_{wac} = Kw_6 \, Z^N_{aero} + Kw_7 \, Z^w_{aero} - Kw_8 \, L^N_{aero} - Kw_9 \, \bar{a}_t - Kw_{10} \, \bar{a}_{wac}$$

Equation (4)

where Kw_6 thru Kw_{10} are constants corresponding to Kw_1 thru Kw_5 for the tip deflection.

I.3 DYNAMIC TREATMENT

The internal resistance of the wing to vertical bending is taken as the sum of static and dynamic components. The dynamic component is comprised of both inertial and damping terms.

The applicable equations are obtained as in the quasi-static treatment except that the dynamic loads considered

now include the internal dynamic loads. The resulting equations are:

$$\ddot{h}_{1t} = \omega_{w1}^2 \left[-K'_{w1} Z^N_{aero} - K'_{w2} Z^w_{aero} - K'_{w3} L^N_{aero} + K'_{w4} \dot{w} + Sw K'_{w5} \dot{p} \right]$$

$$- \omega_{w1}^2 + h_{1t} - 2\xi_{w1}\, \omega_{w1} \dot{h}_{1t} \qquad \text{Equation (5)}$$

$$h_{1wac} = K'_{w6}\, h_{1t} \qquad \text{Equation (6)}$$

where - Z^N_{aero}, Z^w_{aero}, L^N_{aero}, $\dot{p}$ are as defined above,

w = Aircraft vertical acceleration

ω_{w1} = Wing vertical bending frequency (1st symmetric mode)

Sw = +1 for right wing

= -1 for left wing

ξ_{w1} = Percent critical damping of the wing vertical bending mode,

K'_{w1} thru K'_{w6} are constants related to, but not identical with the constants in the quasi-static equations.

I.4 DERIVATION OF DIFFERENTIAL EQUATION FOR WING VERTICAL BENDING STRUCTURAL EFFECTS

The derivation is based on the differential equation for a slender beam subjected to external dynamic loading.

$$\text{i.e. } \frac{d^2}{dy^2} \left(EI - \frac{d^2 Z}{dy^2} \right) + m(y) \frac{d^2 Z}{dt^2} = p(t,y) \qquad \text{Equation (7)}$$

where $p(t,y)$ is the external loading per unit length,

$m(y)$ is the beam mass per unit length,

$Z(t,y)$ is the beam deflection (vertically upward for the wing).

Double integration leads to the alternate form:

$$EI \frac{d^2 Z}{dy^2} = (M_b(t,y) \qquad \text{Equation (8)}$$

where $M_b(t,y)$ is the bending moment due to the combined external loading and beam inertia loading.

The external loading consists of

(a) Wing aerodynamic loading distributed along the wing span.

(b) Nacelle-rotor aerodynamic load, concentrated at the wing tip.

(c) Nacelle-rotor aerodynamic rolling moment (rotor torque) acting at the wing tip.

(d) Nacelle-rotor inertia loads also concentrated at the wing tip.

The wing aerodynamic loading is assumed to be elliptically distributed along the span,

i.e. $\ell\ (y,t) = \ell o(t) \left[1 - (\frac{2y}{b})^2\right]^{1/2}$

The bending moment at spanwise location y, due to this loading is:

$$M_b^{wA}(y\ ,\ t) = \int_{y_1}^{b/2} \ell(y,t)\ (y-y_1)\ dy$$

$$= \frac{\ell o b^2}{4}\left[1/2\ (\text{Sin}\ \theta - \theta\ \cos\ \theta) - 1/6\ \sin^3\theta\right]$$

Equation (9)

where $\theta = \cos^{-1}\ \frac{2y_1}{b}$

The nacelle-rotor vertical load and rolling moment due to aerodynamics, denoted by F^N and T^N respectively produce the bending moment

$$M_b^{NA}\ (y_1,\ t) = T^N + \frac{F^N b}{2}\ (1-\cos\ \theta)$$

Equation (10)

Nacelle-rotor inertia load, excluding gravitational component, is expressed by:

$$G_N = -\ M_N\ \ddot{Z}_T$$

where $\ddot{Z}_T$ is the wing tip vertical acceleration, and is composed of aircraft vertical and roll contributions and wing bending components.

i.e. $\ddot{Z}_T = -\dot{w} - S_w\ Y_N\ \dot{p} + \ddot{h}_T$

$S_w = +1$ for right wing

$= -1$ for left wing

The corresponding wing bending moment is

$$M_b^{NG} = \frac{M_N b}{2}\ (-\dot{w} - S_w\ Y_N\ \dot{p} + \ddot{h}_T)\ (1-\cos\ \theta)$$

Equation (11)

The wing inertia loading is

$$G_w\ (y,t) = -M_w\ \ddot{Z}$$

where $\ddot{Z} = -\dot{w} - S_w\ y\ \dot{p} + \ddot{h}$

The bending moment due to this, assuming uniform mass distribution is

$$M_b^{wG}\ (y_1,\ t) = \int_{y_1}^{b/2} G_w(y,\ t)\ (y-y_1)\ dy$$

$$= \frac{M_w b^2}{4} \Big[(1-\cos\ \theta - 1/2\ \sin^2\ \theta)\ \dot{w}$$

$$+ S_w\ \frac{b}{12}\ (2-3\ \cos\ \theta + \cos^3\ \theta)\ p\Big]$$

$$- M_w \int_{y_1}^{b/2} \ddot{h}\ (y - y_1)\ dy$$

Introducing wing bending mode shape

$$h = \phi\ (y)\ h_1\ (t)$$

$$h_T \quad \phi\ (b/2)\ h_1\ (t)$$

yields

$$M_b^{wG}\ (y\ ,\ t) = \frac{M_w b^2}{4} \Big[(1 - \cos\ \theta - 1/2\ \sin^2\ \theta)\ \dot{w}$$

$$+ S_w\ \frac{b}{12}\ (2-3\ \cos\ \theta + \cos^3\ \theta)\ \dot{p}\Big]$$

$$- m_w \Big[\int_{y_1}^{b/2} \phi\ (y)\ (y-y_1)\ dy]\ \ddot{h}_1\Big]$$

Equation (12)

Substitution of Equations 9 thru 12 in Equation 8 and assuming a linear variation of EI

i.e. $EI = EI_o\ (1 - a \cos\theta)$

$$\frac{d^2Z}{dy^2} = \frac{M_b(t, y)}{EI}$$

$$= \frac{\ell o b^2}{8EI}\left[\frac{(\sin\theta - \theta\cos\theta) - 1/3\sin^3\theta}{1 - a\cos\theta}\right]$$

$$+ \frac{T^N}{EI_o}\left[\frac{1}{1 - a\cos\theta}\right] + \frac{F^N b}{2EI_o}\left[\frac{1 - \cos\theta}{1 - a\cos\theta}\right]$$

$$+ \frac{\dot{w}b}{2EI_o}\left[\frac{m_N\ (1 - \cos\theta) + m_w b/2\ (1 - \cos\theta - 1/2\sin^2\theta)}{1 - a\cos\theta}\right]$$

$$+ \frac{S_w \dot{p} b}{2EI_o}\left[\frac{m_N Y_N\ (1 - \cos\theta) + \frac{m_w b^2}{24}\ (2 - 3\cos\theta + \cos^3\theta)}{1 - a\cos\theta}\right]$$

$$- \frac{m_N \phi(b/2) b \ddot{h}_1}{2EI_o}\left[\frac{1 - \cos\theta}{1 - a\cos\theta}\right] - \frac{m_w b^2 h_1}{4EI_o}\left[\frac{\frac{4}{b^2}\int_{y_1}^{b/2} \ddot{h}\ (y - y_1)\,dy}{1 - a\cos\theta}\right]$$

Equation (13)

Integrating twice and setting of y to b/2, the wing tip deflection is obtained as

$$Z\ (b/2) = \phi\ (b/2)\ h_1$$

$$= - K_{w1}\ Z^N_{aero} - K_{w2}\ Z^W_{aero} - K_{w3}\ L^N_{aero}$$

$$+ K_{w4}\ \dot{W} + S_w\ K_{w5}\ \dot{p} - K_{w6}\ \ddot{h}_1$$

where $Z^W_{aero} = -\frac{\bar{\Lambda}\ell ob}{8}$

$$Z^N_{aero} = -F^N$$

$$L^N_{aero} = -T^N$$

$$K_{w1} = \frac{b}{2EI_o} \int_o^{b/2} \int_o^{b/2} \frac{1 - \cos\theta}{1 - a\cos\theta}\, dy_1\, dy_1$$

$$K_{w2} = \frac{b}{2\bar{\Lambda}EI_o} \int_o^{b/2} \int_o^{b/2} \frac{(\sin\theta - \theta\cos\theta) - 1/3\sin^3\theta}{1 - a\cos\theta}\, dy_1\, dy_1$$

$$K_{w3} = \frac{1}{EI_o} \int_o^{b/2} \int_o^{b/2} \frac{1}{1 - a\cos\theta}\, dy_1\, dy_1$$

$$K_{w4} = \frac{b}{2EI_o} \int_o^{b/2} \int_o^{b/2} \frac{m_N(1-\cos\theta) + \frac{m_w b}{2}(1-\cos\theta - 1/2\sin^2\theta)}{1 - a\cos\theta}\, dy_1\, dy_1$$

$$K_{w5} = \frac{b}{2EI_o} \int_o^{b/2} \int_o^{b/2} \frac{m_N y_N(1-\cos\theta) + \frac{m_w b^2}{24}(2 - 3\cos\theta + \cos^3\theta)}{1 - a\cos\theta}\, dy_1\, dy_1$$

$$K_{w6} = \frac{b}{2EI} \int_o^{b/2} \int_o^{b/2} \frac{m_N\phi(b/2)(1-\cos\theta) + \frac{2m_{vy}}{b}\int_o^{b/2}\phi(y)\, y\, dy}{1 - a\cos\theta}\, dy_1\, dy_1$$

Assuming the bending mode shape is normalized to a unit tip deflection, i.e., $\phi(b/2) = 1$, the above equation becomes

$$\ddot{h}_1 + \frac{1}{K_{w6}} h_1 = \frac{1}{K_{w6}}\Big[-K_{w1}\, Z^N_{aero} - K_{w2} Z^W_{aero} - K_{w3} L^N_{aero} + K_{w4}\, \dot{w} + S_w\, K_{w5}\, \dot{p}\Big]$$

It can be demonstrated that $K_{w6} = \frac{1}{\omega^2_{w1}}$ where ω_{w1} is the natural frequency of the wing first vertical bending mode.

Hence

$$\ddot{h}_1 = -\omega^2_{w1}\, h_1 - 2\xi_{w1}\, \omega_{w1}\, \dot{h}_1 + \omega^2_{w1}\Big[-K_{w1}\, Z^N_{aero} - K_{w2}\, Z^W_{aero} - K_{w3}\, L^N_{aero} + K_{w4}\, \dot{w} + S_w\, K_{w5}\, \dot{p}\Big] \qquad \text{(Equation 1.)}$$

The term $2\xi_{w1}\, \omega_{w1}\, \dot{h}_1$ has been added to account for structural damping in the mode.

APPENDIX II

INCORPORATION OF ROTOR STRUCTURAL DYNAMIC EFFECTS IN TILT-ROTOR AIRCRAFT MATHEMATICAL MODELLING FOR SIMULATOR STUDIES OF GUST ALLEVIATION

II.1 INTRODUCTION

A full force mathematical simulation model for real time piloted evaluations of the proposed 1985 tilt-rotor transport is to be modified for a study of gust alleviation systems using rotor feedback control. One aspect of the modification involves the introduction of rotor dynamic derivatives to permit consideration of blade transient structural response effects in the simulations.

The mathematical equations representing the full force model are documented in Reference II.1 and II.2. This document outlines procedures for incorporating the derivatives in the full force model and presents the applicable equations.

II.2 BASIC APPROACH

To introduce rotor derivatives in the model, it is necessary to separate the rotor forces and moments into two parts: a steady part resulting from aircraft trim conditions, and perturbations away from steady trim conditions under the combined effects of gust velocities and control feedback inputs. This is shown schematically in Figure AII.1.

Computation of the steady components is to be based on the existing rotor equations of the full force model but restricted to trim conditions only. The perturbation components are to be computed from a set of predetermined derivative coefficients and appropriate rotor perturbation degrees of freedom. The force and moment components will be obtained as summations of products of the coefficients and the perturbation degrees of freedom, as defined on Pages AII.7 and AII.8.

II.3 ROTOR DYNAMIC DERIVATIVE COEFFICIENTS

A set of derivative coefficients for each rotor and each flight condition to be simulated will be computed prior to the simulation and stored on a peripheral device. At the start of the simulation, the coefficients for the particular flight condition under investigation will be loaded into core and used to evaluate all perturbations and maneuvers about the specified flight condition.

Each set of coefficients will consist of three 15 by 15 matrices identified as inertial matrix (DM), damping matrix (DC), and stiffness matrix (DK). The matrix size reflects the perturbation degrees of freedom pertinent to the analysis (excluding gust velocity components), as discussed below. The non-zero elements of each of these matrices are identified by dots in the charted matrices shown on Tables AII.1,AII.2 and AII.3.

II.4 ROTOR PERTURBATION DEGREES OF FREEDOM

The perturbation degrees of freedom considered in the analysis comprise three components of gust velocity and the following variables and their first two time derivatives:

(a) hub translations and rotations (6 components);

(b) blade flexible mode D.O.F. in quasi-normal coordinates (6 components: 2 modes with three quasi-normal coordinates each); and

(c) blade collective and cyclic pitch (3 components).

Perturbations in the hub translations and rotations and in the blade pitch angles are obtained as the difference between their current (instantaneous) values and their values under trim conditions, as indicated on Pages AII.8 and AII.10. The trim values of the variables involved (see list on Page AII.10) are computed once and saved for reuse throughout the simulation of a given flight condition. The rotor hub accelerations involved in the relations cited above which are not currently computed in the full force model, need to be included in the computations either by a time frame differentiation of the associated velocities or by use of the equations shown on Page AII.11.

Perturbations in the blade flexible mode degrees of freedom are obtained by numerical integration of their

equations given on Pages AII.12 thru AII.17. These degrees of freedom represent, mathematically, signals with significant high frequency components. For example, typical blade frequencies in cruise are 0.73 and 1.4 per rev. These give rise to rotor modes of frequency 0.27, 1.73, 0.4 and 2.4 per rev which in absolute terms are .81, 5.19, 1.2 and 7.2 Hz. The turbulence spectrum does not have a high rate of attenuation with frequency and the inputs at these frequencies may be significant. To ensure adequate representation of the rotor transient response in the gust environment, it is necessary that the numerical integration of the blade equations be performed more often than that of the total system equations and for this reason fast and slow loops are defined in the calculation as indicated in Figure AII.1.

The gust velocity components are to be considered as perturbations about the trim airspeed components and used as such in the force and moment calculations.

II.5 EQUATIONS & RELATIONS

II.5.1 Right Rotor Hub Perturbation Forces and Moments

$$\Delta T_R = \Delta F_x^R$$

$$\Delta SF_R = -\Delta F_y^R \cos \xi_{HR} + \Delta F_z^R \sin \xi_{HR}$$

$$\Delta NF_R = -\Delta F_y^R \sin \xi_{HR} - \Delta F_z^R \cos \xi_{HR}$$

$$\Delta Q_R = \Delta M_x^R$$

$$\Delta PM_R = \Delta M_y^R \cos \xi_{HR} - \Delta M_z^R \sin \xi_{HR}$$

$$\Delta YM_R = \Delta M_y^R \sin \xi_{HR} + \Delta M_z^R \cos \xi_{HR}$$

II.5.2 <u>Left Rotor Hub Perturbation Forces and Moments</u>

$$\Delta T_L = \Delta F_x^L$$

$$\Delta SF_L = \Delta F_y^L \cos \xi_{HL} - \Delta F_z^L \sin \xi_{HL}$$

$$\Delta NF_L = -\Delta F_y^L \sin \xi_{HL} - \Delta F_z^L \cos \xi_{HL}$$

$$\Delta Q_L = \Delta M_x^L$$

$$\Delta PM_L = \Delta M_y^L \cos \xi_{HL} - \Delta M_z^L \sin \xi_{HL}$$

$$\Delta YM_L = -\Delta M_y^L \sin \xi_{HL} - \Delta M_z^L \cos \xi_{HL}$$

where ΔF_x, ΔF_y, ΔF_z, ΔM_x, ΔM_y, ΔM_z are defined on the following page, and ΔF_x, ΔF_y, ΔF_z, ΔM_x, ΔM_y, ΔM_z are obtained from the same definitions by replacing the right rotor coefficients and perturbations by the left rotor equivalents.

$$\Delta F_x^R = -DK_{1,5}^R\ \Delta\theta_{RR} - DK_{1,13}^R\ \Delta\theta_{75R} - DC_{1,1}^R\ \Delta U_{RR} - DC_{1,3}^R\ \Delta W_{RR}$$

$$-DC_{1,4}^R\ \Delta p_{RR} - DC_{1,7}^R\ \Delta\dot{\beta}_{10R} - DC_{1,10}^R\Delta\dot{\beta}_{20R} - DM_{1,1}^R\ \Delta\dot{U}_{RR}$$

$$-DM_{1,7}^R\ \Delta\ddot{\beta}_{10R} - DM_{1,10}^R\Delta\ddot{\beta}_{20R} + DC_{1,1}^R U_g + DC_{1,3}^R\ W_g.$$

$$\Delta F_y = -DK_{2,6}^R\ \Delta\psi_{RR} - DK_{2,9}^R\ \Delta\beta_{1SR} - DK_{2,12}^R\Delta\beta_{2SR} - DK_{2,14}^R\Delta A_{1R}$$

$$-DC_{2,2}^R\ \Delta V_{RR} - DC_{2,5}^R\ \Delta g_{RR} - DC_{2,8}^R\ \Delta\dot{\beta}_{1CR} - DC_{2,11}^R\Delta\dot{\beta}_{2CR}$$

$$-DM_{2,2}^R\ \Delta\dot{V}_{RR} - DM_{2,8}^R\ \Delta\ddot{\beta}_{1CR} - DM_{2,11}^R\Delta\ddot{\beta}_{2CR} + DC_{2,2}^R\ V_g.$$

$$\Delta F_z^R = -DK_{3,5}^R\ \Delta\theta_{RR} - DK_{3,8}^R\ \Delta\beta_{1CR} - DK_{3,11}^R\Delta\beta_{2CR} - DK_{3,15}^R\Delta B_{1R}$$

$$-DC_{3,3}^R\ \Delta W_{RR} - DC_{3,6}^R\ \Delta r_{RR} - DC_{3,9}^R\ \Delta\dot{\beta}_{1SR} - DC_{3,12}^R\Delta\dot{\beta}_{2SR}$$

$$-DM_{3,3}^R\ \Delta\dot{W}_{RR} - DM_{3,9}^R\ \Delta\ddot{\beta}_{1SR} - DM_{3,12}^R\Delta\ddot{\beta}_{2SR} + DC_{3,3}^R\ W_g.$$

$$\Delta M_x^R = -DK_{4,13}^R\Delta\theta_{75R} - DC_{4,1}^R\ \Delta U_{RR} - DC_{4,4}^R\Delta p_{RR} - DC_{4,7}^R\Delta\dot{\beta}_{10R}$$

$$-DC_{4,10}^R\Delta\dot{\beta}_{20R} - DM_{4,4}^R\Delta\dot{p}_{RR} - DM_{4,7}^R\Delta\ddot{\beta}_{10R} - DM_{4,10}^R\Delta\ddot{\beta}_{20R} + DC_{4,1}^R\ U_g.$$

$$\Delta M_y^R = -DK_{5,6}^R\ \Delta\psi_{RR} - DK_{5,9}^R\ \Delta\beta_{1SR} - DK_{5,12}^R\Delta\beta_{2SR} - DK_{5,14}^R\Delta A_{1R}$$

$$-DC_{5,2}^R\Delta V_{RR} - DC_{5,3}^R\Delta W_{RR} - DC_{5,5}^R\Delta q_{RR} - DC_{5,6}^R\Delta r_{RR} - DC_{5,8}\Delta\dot{\beta}_{1CR}$$

$$-DC_{5,9}\Delta\dot{\beta}_{1\ R} - DC_{5,11}\ \Delta\dot{\beta}_{2CR} - DC_{5,12}\ \Delta\dot{\beta}_{2SR} - DM_{5,5}\ \Delta\dot{q}_{RR}$$

$$-DM_{5,8}\Delta\ddot{\beta}_{1CR} - DM_{5,11}\ \Delta\ddot{\beta}_{2CR} + DC_{5,2}\ V_g$$

$$\Delta M_z^R = -DK_{6,5}^R \Delta\theta_{RR} - DK_{6,8}^R \Delta\beta_{1CR} - DK_{6,11}^R \Delta\beta_{2CR} - DK_{6,15}^R \Delta B_{1R}$$

$$-DC_{6,3}^R \Delta W_{RR} - DC_{6,5}^R \Delta q_{RR} - DC_{6,6}^R \Delta r_{RR} - DC_{6,8}^R \Delta\dot{\beta}_{1CR}$$

$$-DC_{6,9}^R \Delta\dot{\beta}_{1SR} - DC_{6,11}^R \Delta\dot{\beta}_{2CR} - DC_{6,12}^R \Delta\dot{\beta}_{2SR} - DM_{6,6}^R \Delta\dot{r}_{RR}$$

$$-DM_{6,9}^R \Delta\ddot{\beta}_{1SR} - DM_{6,12}^R \Delta\ddot{\beta}_{2SR} + DC_{6,3}^R W_g.$$

II.5.3 <u>Right Rotor Hub Perturbations</u>

$$\Delta\theta_{RR} = \theta - \theta^\circ + \theta_{TR} - \theta_{TR}^\circ$$

$$\Delta\psi_{RR} = \psi - \psi^\circ$$

$$\Delta U_{RR} = U_{RR} - U_{RR}^\circ$$

$$\Delta V_{RR} = V_{RR} - V_{RR}^\circ$$

$$\Delta W_{RR} = W_{RR} - W_{RR}^\circ$$

$$\Delta W_{RR} = W_{RR} - W_{RR}^\circ$$

$$\Delta p_{RR} = - P_{NR}^N - P_{NR}^{NO}$$

$$\Delta q_{RR} = Q_{NR}^N - Q_{NR}^{NO}$$

$$\Delta r_{RR} = - R_{NR}^N - R_{NR}^{NO}$$

$$\Delta\dot{U}_{RR} = \dot{U}_{RR} - \dot{U}_{RR}^\circ$$

$$\Delta\dot{V}_{RR} = \dot{V}_{RR} - \dot{V}_{RR}^\circ$$

$$\Delta\dot{W}_{RR} = \dot{W}_{RR} \quad \dot{W}_{RR}^\circ$$

$$\Delta\dot{p}_{RR} = - \dot{P}_{NR}^N - \dot{P}_{NR}^{NO}$$

$$\Delta\dot{q}_{RR} = \dot{Q}^{N}_{NR} - \dot{Q}^{NO}_{NR}$$

$$\Delta\dot{r}_{RR} = - \dot{R}^{N}_{NR} - \dot{R}^{NO}_{NR}$$

II.5.4 <u>Right Rotor Blade Pitch Perturbations</u>

$$\Delta\theta_{75R} = \theta_{75R} - \theta^{\circ}_{75R}$$

$$\Delta A_{1R} = A_{1R} - A^{\circ}_{1R}$$

$$\Delta B_{1R} = B_{1R} - B^{\circ}_{1R}$$

II.5.6 <u>Left Rotor Blade Pitch Perturbations</u>

$$\Delta\theta_{RL} = \theta - \theta^{\circ} + \theta_{TL} - \theta^{\circ}_{TL}$$

$$\Delta\psi_{RL} = \psi - \psi^{\circ}$$

$$\Delta U_{RL} = U_{RL} - U^{\circ}_{RL}$$

$$\Delta V_{RL} = V_{RL} - V^{\circ}_{RL}$$

$$\Delta W_{RL} = W_{RL} - W^{\circ}_{RL}$$

$$\Delta p_{RL} = P^{N}_{NL} - P^{NO}_{NL}$$

$$\Delta q_{RL} = Q^{N}_{NL} - Q^{NO}_{NL}$$

$$\Delta r_{RL} = R^{N}_{NL} - R^{NO}_{NL}$$

$$\Delta\dot{U}_{RL} = \dot{U}_{RL} - \dot{U}^{\circ}_{RL}$$

$$\Delta\dot{V}_{RL} = \dot{V}_{RL} - \dot{V}^{\circ}_{RL}$$

$$\Delta\dot{W}_{RL} = \dot{W}_{RL} - \dot{W}^{\circ}_{RL}$$

$$\Delta\dot{p}_{RL} = \dot{P}^{N}_{NL} - \dot{P}^{NO}_{NL}$$

$$\Delta\dot{q}_{RL} = \dot{Q}^{N}_{NL} - \dot{Q}^{NO}_{NL}$$

$$\Delta\dot{r}_{RL} = \dot{R}^{N}_{NL} - \dot{R}^{NO}_{NL}$$

II.5.6 Left Rotor Blade Pitch Perturbations

$$\Delta\theta_{75L} = \theta_{75L} - \theta^{\circ}_{75L}$$

$$\Delta A_{1L} = A_{1L} - A^{\circ}_{1L}$$

$$\Delta B_{1L} = B_{1L} - B^{\circ}_{1L}$$

II.5.7 Trim Parameters to Save (For Perturbation Components)

Aircraft: Pitch Angle:

Yaw Angle:

Right Wing Twist Angle:

Left Wing Twist Angle:

Right Rotor:

Hub Velocities: U°_{RR}, V°_{RR}, W°_{RR}

P^{NO}_{NR}, P^{NO}_{NR}, P^{NO}_{NR}

Hub Accelerations: $\dot{U}^{\circ}_{RR}$, $\dot{V}^{\circ}_{RR}$, $\dot{W}^{\circ}_{RR}$

$\dot{P}^{NO}_{NR}$, $\dot{Q}^{NO}_{NR}$, $\dot{R}^{NO}_{NR}$

Blade Pitch: O°_{75R}, A°_{1R}, B°_{1R}

Left Rotor:

Hub Velocities: U°_{RL}, V°_{RL}, W°_{RL}

P^{NO}_{NL}, Q^{NO}_{NL}, R^{NO}_{NL}

Hub Accelerations: $\dot{U}^{\circ}_{LR}$, $\dot{V}^{\circ}_{RL}$, $\dot{W}^{\circ}_{RL}$

$\dot{P}^{NO}_{NL}$, $\dot{Q}^{NO}_{NL}$, $\dot{R}^{NO}_{NL}$

Blade Pitch: O°_{75L}, A°_{1L}, B°_{1L}

II.5.8 Right Rotor Hub Accelerations in Shaft Axes

$$\dot{U}_{RR} = \dot{U} - \ddot{X}_{CG} - (Z_{CG} - h_{1R})\,\dot{q} - Y_N\dot{r} - (\dot{Z}_{CG} - \dot{h}_{1R})q$$

$$\dot{V}_{RR} = \dot{V} + (Z_{CG} - h_{1R})\dot{p} - (X_{CG} - L_S)\,\dot{r} + (\dot{Z}_{CG} - \dot{h}_{1R})\,p - \dot{X}_{CG}r$$

$$\dot{W}_{RR} = \dot{W} - \ddot{Z}_{CG} + \ddot{h}_{1R} + Y_N\dot{p} + (X_{CG} - L_S)\,\dot{q} + \dot{X}_{CG}\,g$$

$$\dot{P}^N_{NR} = -\dot{p}$$

$$\dot{Q}^N_{NR} = \dot{q}$$

$$\dot{R}^N_{NR} = -\dot{r}$$

II.5.9 Left Rotor Hub Accelerations in Shaft Axes

$$\dot{U}_{RL} = \dot{U} - \ddot{X}_{CG} -)Z_{CG} - h_{1L})\,\dot{q} + Y_N\dot{r} - (\dot{Z}_{CG} - \dot{h}_{1L})\,q$$

$$\dot{V}_{RL} = \dot{V} + (Z_{CG} - h_{1L})\dot{p} - (X_{CG} - L_S)\,\dot{r} + (\dot{Z}_{CG} - \dot{h}_{1L})p - \dot{X}_{CG}r$$

$$\dot{W}_{RL} = \dot{W} - \ddot{Z}_{CG} + \ddot{h}_{1L} - Y_N\dot{p} = (X_{CG} - L_S)\,\dot{q} + \dot{X}_{CG}q$$

$$\dot{P}^N_{NL} = \dot{p}$$

$$\dot{Q}^N_{NL} = \dot{q}$$

$$\dot{R}^N_{NL} = \dot{r}$$

NOTE: Time frame differentiation of the corresponding velocities may be used for computing the above accelerations in place of the equations specified.

II.5.10 Blade Transient Response Equations

$$\Delta\ddot{\beta}_{10R} = \frac{1}{(DM^R_{7,7}\cdot DM^R_{10,10} - DM^R_{7,10}\cdot DM^R_{10,7})}$$

$$\Big[(DM^R_{7,10}\cdot DC^R_{10,7} - DM^R_{10,10}\cdot DC^R_{7.7})\quad \Delta\dot{\beta}_{10R}$$

$$+ (DM^R_{7,10}\cdot DC^R_{10,10} - DM^R_{10,10}\cdot DC^R_{7,10})\quad \Delta\dot{\beta}_{20R}$$

$$+ (DM^R_{7,10}\cdot DK^R_{10,7} - DM^R_{10,10}\cdot DK^R_{7,7})\quad \Delta\beta_{10R}$$

$$+ (DM^R_{7,10}\cdot DK^R_{10,10} - DM^R_{10,10}\cdot DK^R_{7,10})\quad \Delta\beta_{20R}$$

$$+ (DM^R_{7,10}\cdot DM^R_{10,1} - DM^R_{10,10}\cdot DM^R_{7,1})\quad \Delta\dot{U}_{RR}$$

$$+ (DM^R_{7,10}\cdot DM^R_{10,4} - DM^R_{10,10}\cdot DM^R_{7.4})\quad \Delta\dot{p}_{RR}$$

$$+ (DM^R_{7,10}\cdot DC^R_{10,1} - DM^R_{10,10}\cdot DC^R_{7,1})\quad \Delta U_{RR}$$

$$+ (DM^R_{7,10}\cdot DC^R_{10,4} - DM^R_{10,10}\cdot DC^R_{7,4})\quad \Delta p_{RR}$$

$$+ (DM^R_{7,10}\cdot DK^R_{10,13} - DM^R_{10,10}\cdot DK^R_{7,13})\quad \Delta\theta_{75R}$$

$$- (DM^R_{7,10}\cdot DC^R_{10,1} - DM^R_{10,10}\cdot DC^R_{7,1})\quad U_g\Big]$$

$$\Delta\ddot{\beta}_{20R} = \frac{1}{(DM^R_{7,7}\cdot DM^R_{10,10} - DM^R_{7,10}\cdot DM^R_{10,7})}$$

$$\Big[(DM^R_{10,7}\cdot DC^R_{7,7} - DM^R_{7,7}\cdot DC^R_{10,7})\ \Delta\dot{\beta}_{10R}$$

$$+ (DM^R_{10,7}\cdot DC^R_{7,10} - DM^R_{7,7}\cdot DC^R_{10,10})\ \Delta\dot{\beta}_{20R}$$

$$+ (DM^R_{10,7}\cdot DK^R_{7,7} - DM^R_{7,7}\cdot DK^R_{10,7})\ \Delta\beta_{10R}$$

$$+ (DM^R_{10,7}\cdot DK^R_{7,10} - DM^R_{7,7}\cdot DK^R_{10,10})\ \Delta\beta_{20R}$$

$$+ (DM^R_{10,7}\cdot DM^R_{7,1} - DM^R_{7,7}\cdot DM^R_{10,1})\ \Delta\dot{U}_{RR}$$

$$+ (DM^R_{10,7}\cdot DM^R_{7,4} - DM^R_{7,7}\cdot DM^R_{10,4})\ \Delta\dot{p}_{RR}$$

$$+ (DM^R_{10,7}\cdot DC^R_{7,1} - DM^R_{7,7}\cdot DC^R_{10,1})\ \Delta U_{RR}$$

$$+ (DM^R_{10,7}\cdot DC^R_{7,4} - DM^R_{7,7}\cdot DC^R_{10,4})\ \Delta p_{RR}$$

$$+ (DM^R_{10,7}\cdot DK^R_{7,13} - DM^R_{7,7}\cdot DK^R_{10,13})\ \Delta\theta_{75R}$$

$$- (DM^R_{10,7}\cdot DC^R_{7,1} - DM^R_{7,7}\cdot DC^R_{10,1})\ U_g\Big]$$

$$
\begin{aligned}
\Delta\ddot{\beta}_{1CR} = \frac{1}{(DM^R_{8,8}\cdot DM^R_{11,11} - DM^R_{8,11}\cdot DM^R_{11,8})}
&\Big[(DM^R_{8,11}\cdot DC^R_{11,8} - DM^R_{11,11}\cdot DC^R_{8,8}) && \Delta\dot{\beta}_{1CR} \\
&+ (DM^R_{8,11}\cdot DC^R_{11,9} - DM^R_{11,11}\cdot DC^R_{8,9}) && \Delta\dot{\beta}_{1SR} \\
&+ (DM^R_{8,11}\cdot DC^R_{11,11} - DM^R_{11,11}\cdot DC^R_{8,11}) && \Delta\dot{\beta}_{2CR} \\
&+ (DM^R_{8,11}\cdot DC^R_{11,12} - DM^R_{11,11}\cdot DC^R_{8,12}) && \Delta\dot{\beta}_{2SR} \\
&+ (DM^R_{8,11}\cdot DK^R_{11,8} - DM^R_{11,11}\cdot DK^R_{8,8}) && \Delta\beta_{1CR} \\
&+ (DM^R_{8,11}\cdot DK^R_{11,9} - DM^R_{11,11}\cdot DK^R_{8,9}) && \Delta\beta_{1SR} \\
&+ (DM^R_{8,11}\cdot DK^R_{11,11} - DM^R_{11,11}\cdot DK^R_{8,11}) && \Delta\beta_{2CR} \\
&+ (DM^R_{8,11}\cdot DK^R_{11,12} - DM^R_{11,11}\cdot DK^R_{8,12}) && \Delta\beta_{2SR} \\
&+ (DM^R_{8,11}\cdot DM^R_{11,2} - DM^R_{11,11}\cdot DM^R_{8,2}) && \Delta\dot{V}_{RR} \\
&+ (DM^R_{8,11}\cdot DM^R_{11,5} - DM^R_{11,11}\cdot DM^R_{8,5}) && \Delta\dot{q}_{RR} \\
&+ (DM^R_{8,11}\cdot DC^R_{11,2} - DM^R_{11,11}\cdot DC^R_{8,2}) && \Delta V_{RR} \\
&+ (DM^R_{8,11}\cdot DC^R_{11,5} - DM^R_{11,11}\cdot DC^R_{8,5}) && \Delta q_{RR} \\
&+ (DM^R_{8,11}\cdot DC^R_{11,6} - DM^R_{11,11}\cdot DC^R_{8,6}) && \Delta r_{RR} \\
&+ (DM^R_{8,11}\cdot DK^R_{11,6} - DM^R_{11,11}\cdot DK^R_{8,6}) && \Delta\psi_{RR} \\
&+ (DM^R_{8,11}\cdot DK^R_{11,14} - DM^R_{11,11}\cdot DK^R_{8,14}) && \Delta A_{1R} \\
&- (DM^R_{8,11}\cdot DC^R_{11,2} - DM^R_{11,11}\cdot DC^R_{8,2}) && V_g\Big]
\end{aligned}
$$

$$\Delta\ddot{\beta}_{2CR} = \frac{1}{(DM^R_{8,8} \cdot DM^R_{11,11} - DM^R_{8,11} \cdot DM^R_{11,8})}$$

$$\Big[(DM^R_{11,8} \cdot DC^R_{8,8} - DM^R_{8,8} \cdot DC^R_{11,8}) \quad \Delta\dot{\beta}_{1CR}$$

$$+ (DM^R_{11,8} \cdot DC^R_{8,9} - DM^R_{8,8} \cdot DC^R_{11,9}) \quad \Delta\dot{\beta}_{1SR}$$

$$+ (DM^R_{11,8} \cdot DC^R_{8,11} - DM^R_{8,8} \cdot DC^R_{11,11}) \quad \Delta\dot{\beta}_{2CR}$$

$$+ (DM^R_{11,8} \cdot DC^R_{8,12} - DM^R_{8,8} \cdot DC^R_{11,12}) \quad \Delta\dot{\beta}_{2SR}$$

$$+ (DM^R_{11,8} \cdot DK^R_{8,8} - DM^R_{8,8} \cdot DK^R_{11,8}) \quad \Delta\beta_{1CR}$$

$$+ (DM^R_{11,8} \cdot DK^R_{8,9} - DM^R_{8,8} \cdot DK^R_{11,9}) \quad \Delta\beta_{1SR}$$

$$+ (DM^R_{11,8} \cdot DK^R_{8,11} - DM^R_{8,8} \cdot DK^R_{11,11}) \quad \Delta\beta_{2CR}$$

$$+ (DM^R_{11,8} \cdot DK^R_{8,12} - DM^R_{8,8} \cdot DK^R_{11,12}) \quad \Delta\beta_{2SR}$$

$$+ (DM^R_{11,8} \cdot DM^R_{8,2} - DM^R_{8,8} \cdot DM^R_{11,2}) \quad \Delta\dot{V}_{RR}$$

$$+ (DM^R_{11,8} \cdot DM^R_{8,5} - DM^R_{8,8} \cdot DM^R_{11,5}) \quad \Delta\dot{q}_{RR}$$

$$+ (DM^R_{11,8} \cdot DC^R_{8,2} - DM^R_{8,8} \cdot DC^R_{11,2}) \quad \Delta V_{RR}$$

$$+ (DM^R_{11,8} \cdot DC^R_{8,5} - DM^R_{8,8} \cdot DC^R_{11,5}) \quad \Delta q_{RR}$$

$$+ (DM^R_{11,8} \cdot DC^R_{8,6} - DM^R_{8,8} \cdot DC^R_{11,6}) \quad \Delta r_{RR}$$

$$+ (DM^R_{11,8} \cdot DK^R_{8,6} - DM^R_{8,8} \cdot DK^R_{11,6}) \quad \Delta\psi_{RR}$$

$$+ (DM^R_{11,8} \cdot DK^R_{8,14} - DM^R_{8,8} \cdot DK^R_{11,14}) \quad \Delta A_{1R}$$

$$- (DM^R_{11,8} \cdot DC^R_{8,2} - DM^R_{8,8} \cdot DC^R_{11,2}) \quad V_g \Big]$$

$$\Delta\ddot{\beta}_{1SR} = \frac{1}{(DM^R_{9,9} \cdot DM^R_{12,12} - DM^R_{9,12} \cdot DM^R_{12,9})}$$

$$\Big[(DM^R_{9,12} \cdot DC^R_{12,8} - DM^R_{12,12} \cdot DC_{9,9}) \quad \Delta\dot{\beta}_{1CR}$$

$$+ (DM_{9,12} \cdot DC_{12,9} - DM_{12,12} \cdot DC_{9,9}) \quad \Delta\dot{\beta}_{1SR}$$

$$+ (DM^R_{9,12} \cdot DC^R_{12,11} - DM^R_{12,12} \cdot DC^R_{9,11}) \quad \Delta\dot{\beta}_{2CR}$$

$$+ (DM^R_{9,12} \cdot DC^R_{12,12} - DM^R_{12,12} \cdot DC^R_{9,12}) \quad \Delta\dot{\beta}_{2SR}$$

$$+ (DM^R_{9,12} \cdot DK^R_{12,8} - DM^R_{12,12} \cdot DK^R_{9,8}) \quad \Delta\beta_{1CR}$$

$$+ (DM^R_{9,12} \cdot DK^R_{12,9} - DM^R_{12,12} \cdot DK^R_{9,9}) \quad \Delta\beta_{1SR}$$

$$+ (DM^R_{9,12} \cdot DK^R_{12,11} - DM^R_{12,12} \cdot DK^R_{9,11}) \quad \Delta\beta_{2CR}$$

$$+ (DM^R_{9,12} \cdot DK^R_{12,12} - DM^R_{12,12} \cdot DK^R_{9,12}) \quad \Delta\beta_{2SR}$$

$$+ (DM^R_{9,12} \cdot DM^R_{12,3} - DM^R_{12,12} \cdot DM^R_{9,3}) \quad \Delta\dot{W}_{RR}$$

$$+ (DM^R_{9,12} \cdot DM^R_{12,6} - DM^R_{12,12} \cdot DM^R_{9,6}) \quad \Delta\dot{r}_{RR}$$

$$+ (DM^R_{9,12} \cdot DC^R_{12,3} - DM^R_{12,12} \cdot DC^R_{9,3}) \quad \Delta W_{RR}$$

$$+ (DM^R_{9,12} \cdot DC^R_{12,5} - DM^R_{12,12} \cdot DC^R_{9,5}) \quad \Delta q_{RR}$$

$$+ (DM_{9,12} \cdot DC_{12,6} - DM_{12,12} \cdot DC_{9,6}) \quad \Delta r_{RR}$$

$$+ (DM_{9,12} \cdot DK_{12,5} - DM_{12,12} \cdot DK_{9,5}) \quad \Delta\theta_{RR}$$

$$+ (DM_{9,12} \cdot DK_{12,15} - DM_{12,12} \cdot DK_{9,15}) \quad \Delta B_{1R}$$

$$- (DM_{9,12} \cdot DC_{12,3} - DM_{12,12} - DC_{9,3}) \quad W_g \Big]$$

$$
\begin{aligned}
\Delta\ddot{\beta}_{2SR} = \frac{1}{(DM^R_{9,9} \cdot DM^R_{12,12} - DM^R_{12,9} \cdot DM^R_{9,12})} \Big[& (DM^R_{12,9} \cdot DC^R_{9,8} - DM^R_{9,9} \cdot DC^R_{12,8}) \quad \Delta\dot{\beta}_{1CR} \\
+ & (DM^R_{12,9} \cdot DC^R_{9,9} - DM^R_{9,9} \cdot DC^R_{12,9}) \quad \Delta\dot{\beta}_{1SR} \\
+ & (DM^R_{12,9} \cdot DC^R_{9,11} - DM^R_{9,9} \cdot DC^R_{12,11}) \quad \Delta\dot{\beta}_{2CR} \\
+ & (DM^R_{12,9} \cdot DC^R_{9,12} - DM^R_{9,9} \cdot DC^R_{12,12}) \quad \Delta\dot{\beta}_{2SR} \\
+ & (DM^R_{12,9} \cdot DK^R_{9,8} - DM^R_{9,9} \cdot DK^R_{12,8}) \quad \Delta\beta_{1CR} \\
+ & (DM^R_{12,9} \cdot DK^R_{9,9} - DM^R_{9,9} \cdot DK^R_{12,9}) \quad \Delta\beta_{1SR} \\
+ & (DM^R_{12,9} \cdot DK^R_{9,11} - DM^R_{9,9} \cdot DK^R_{12,11}) \quad \Delta\beta_{2CR} \\
+ & (DM^R_{12,9} \cdot DK^R_{9,12} - DM^R_{9,9} \cdot DK^R_{12,12}) \quad \Delta\beta_{2SR} \\
+ & (DM^R_{12,9} \cdot DM^R_{9,3} - DM^R_{9,9} \cdot DM^R_{12,3}) \quad \Delta\dot{W}_{RR} \\
+ & (DM^R_{12,9} \cdot DM^R_{9,6} - DM^R_{9,9} \cdot DM^R_{12,6}) \quad \Delta\dot{r}_{RR} \\
+ & (DM^R_{12,9} \cdot DC^R_{9,3} - DM^R_{9,9} \cdot DC^R_{12,3}) \quad \Delta W_{RR} \\
+ & (DM^R_{12,9} \cdot DC^R_{9,5} - DM^R_{9,9} \cdot DC^R_{12,5}) \quad \Delta q_{RR} \\
+ & (DM^R_{12,9} \cdot DC^R_{9,6} - DM^R_{9,9} \cdot DC^R_{12,6}) \quad \Delta r_{RR} \\
+ & (DM^R_{12,9} \cdot DK^R_{9,5} - DM^R_{9,9} \cdot DK^R_{12,5}) \quad \Delta\theta_{RR} \\
+ & (DM^R_{12,9} \cdot DK^R_{9,15} - DM^R_{9,9} \cdot DK^R_{12,15}) \quad \Delta\beta_{1R} \\
- & (DM^R_{12,9} \cdot DC^R_{9,3} - DM^R_{9,9} \cdot DC^R_{12,3}) \quad W_g \Big]
\end{aligned}
$$

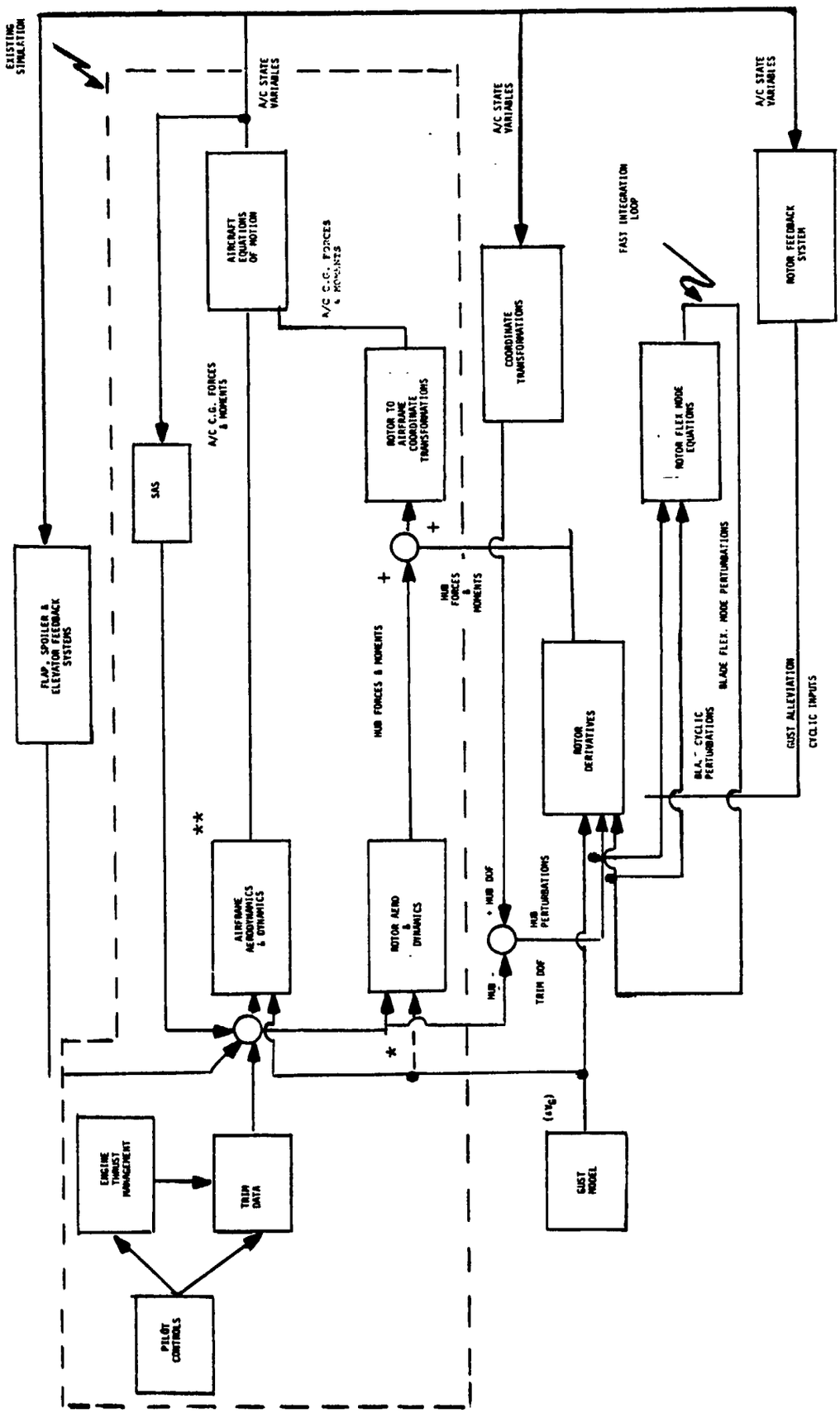

* GUST INPUTS TO EXISTING ROTOR TREATMENT TO BE ELIMINATED.
**WING FLEXIBILITY TREATMENT TO BE REVIEWED.

FIGURE AII.1.SCHEMATIC OF GUST ALLEVIATION SYSTEM INTERFACE WITH PILOTED SIMULATION MODEL

ROW \ COL	1	2	3	4	5	6	7	8	9	10	11	12	13	14	15
1	●						●			●					
2		●						●			●				
3			●						●			●			
4				●			●			●					
5					●			●			●				
6						●			●			●			
7	●			●			●			●					
8		●			●			●			●				
9			●			●			●			●			
10	●			●			●			●					
11		●			●			●			●				
12			●			●			●			●			
13													●		
14														●	
15															●

TABLE AII.1. NON-ZERO ELEMENTS OF INERTIA MATRIX (DM)

ROW \ COL	1	2	3	4	5	6	7	8	9	10	11	12	13	14	15
1	●		●	●			●			●					
2		●			●			●			●				
3			●			●			●			●			
4	●			●			●			●					
5		●	●		●	●		●	●		●	●			
6			●		●	●		●	●		●	●			
7	●			●			●			●					
8		●			●	●		●	●		●	●			
9			●		●	●		●	●		●	●			
10	●			●			●			●					
11		●			●	●		●	●		●	●			
12			●		●	●		●	●		●	●			
13													●		
14														●	●
15														●	●

TABLE AII.2. NON-ZERO ELEMENTS OF DAMPING MATRIX (DC)

ROW \ COL	1	2	3	4	5	6	7	8	9	10	11	12	13	14	15
1					●								●		
2						●			●			●		●	
3					●			●			●				●
4													●		
5						●			●			●		●	
6					●			●			●				●
7							●			●			●		
8						●		●	●		●	●		●	
9					●			●	●		●	●			●
10							●			●			●		
11						●		●	●		●	●		●	
12					●			●	●		●	●			●
13													●		
14														●	●
15														●	●

TABLE AII.3. NON-ZERO ELEMENTS OF STIFFNESS MATRIX (DK)

REFERENCES

II.1. McVeigh, M. A. and Widdison, C. W., "Equations, Control Diagrams and Data for A Mathematical Model of a 1985-ERA Tilt Rotor Aircraft". Boeing Vertol Document

II.2. McVeigh, M. A. and Rosenstein, H. R., "Mathematical Modelling of A Commercial V/STOL Tilt Rotor Transport". Boeing Vertol Document No. D210-10928-1, March 1975.

APPENDIX III

A STUDY OF AIRCRAFT PITCH RESPONSE EFFECT ON BLADE AND ROTOR RESPONSE

AIII.1 INTRODUCTION

Blade and rotor load response did not fall into pattern anticipated. It had been expected that blade loads would increase significantly when direct lift control was used to alleviate normal acceleration response to turbulence. When this was not found to be so, a brief study was made using discrete gust excitation to explore the cause. The results of this study are shown in Figures AIII.1 through AIII.4.

AIII.2 RESPONSE TO 500 FEET, 10 FT/SEC (1-COSINE) GUST

Figures AIII.1 and AIII.2 show the response of a number of variables to a discrete gust, in a series of cases. The first two records are taken with the peaks in perturbation angle of attack do not change much, although there are differences in pitch acceleration, aircraft attitude, and normal acceleration. Angle of attack seems to dominate the rotor response.

The third record is the system response, with alleviation and the pitch degree of freedom frozen. The perturbated angle of attack is about 50% higher than the basic case shown in record 1. Record 4 is the response without alleviation with the pitch freedom frozen. This shows a similar level of peak blade response to 1 and 2, and a reduction with respect

to 3. This shows that under the artificial condition of no pitch freedom, the blade response increases with alleviation. It also shows that with the pitch freedom present, the perturbation response of the rotor has an initial peak associated with the initial peaking angle of attack, and a second peak associated with over-swing angle of attack. With the alleviation system considered here the second peak is more severe than the first.

AIII.3 RESPONSE TO 1,000 FEET, 10 FEET PER SECOND (1-COSINE) GUST

Figures AIII.3 and AIII.4 show response to a 1,000 foot (1-cosine) gust. The results and conclusions are substantially the same as those from the 500 foot gust length case.

ORIGINAL PAGE IS
OF POOR QUALITY

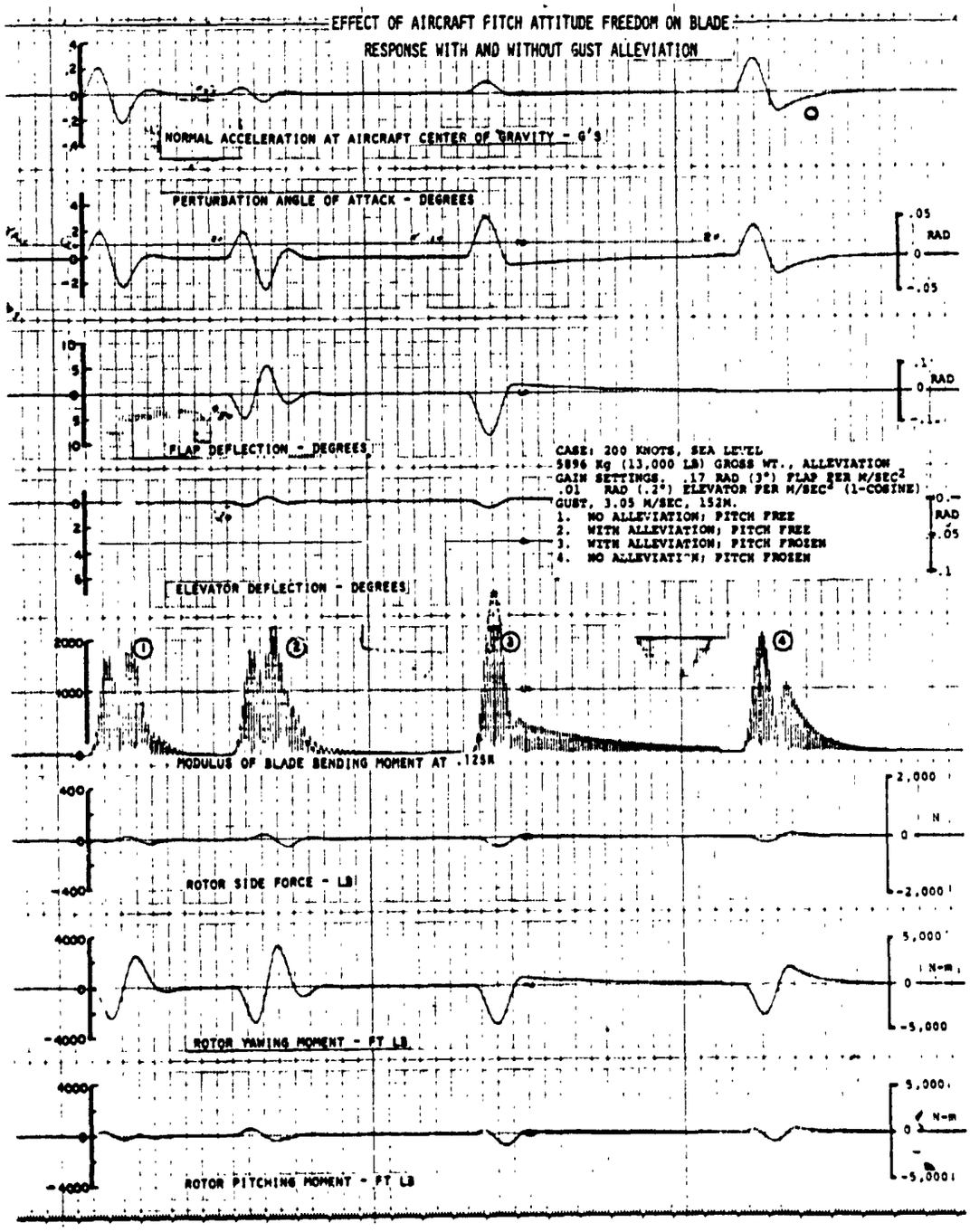

FIGURE AIII.1. EFFECT OF AIRCRAFT PITCH ATTITUDE FREEDOM ON BLADE RESPONSE WITH AND WITHOUT GUST ALLEVIATION.

ORIGINAL PAGE IS
OF POOR QUALITY

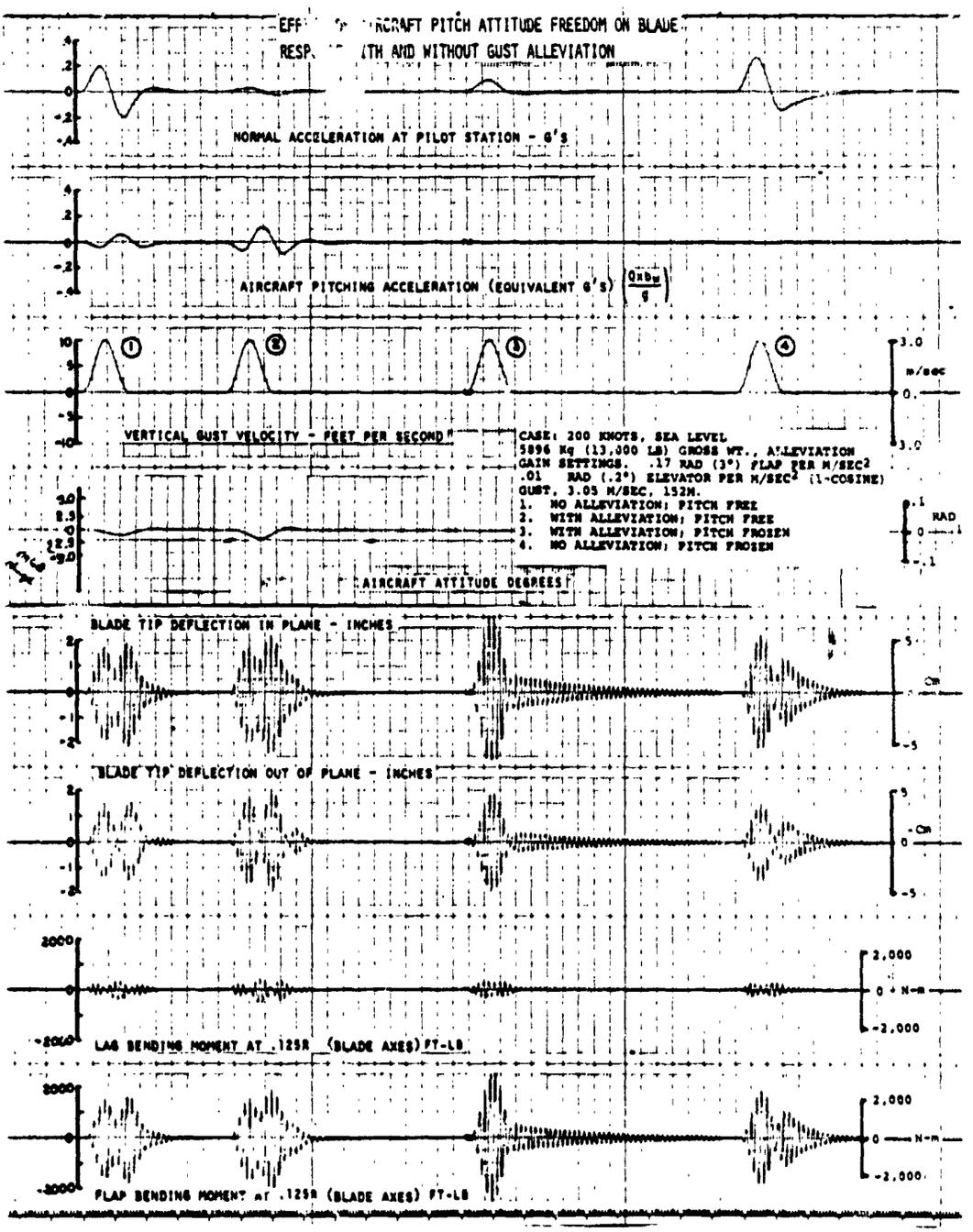

FIGURE AIII.2. EFFECT OF AIRCRAFT PITCH ATTITUDE FREEDOM ON BLADE RESPONSE WITH AND WITHOUT GUST ALLEVIATION.

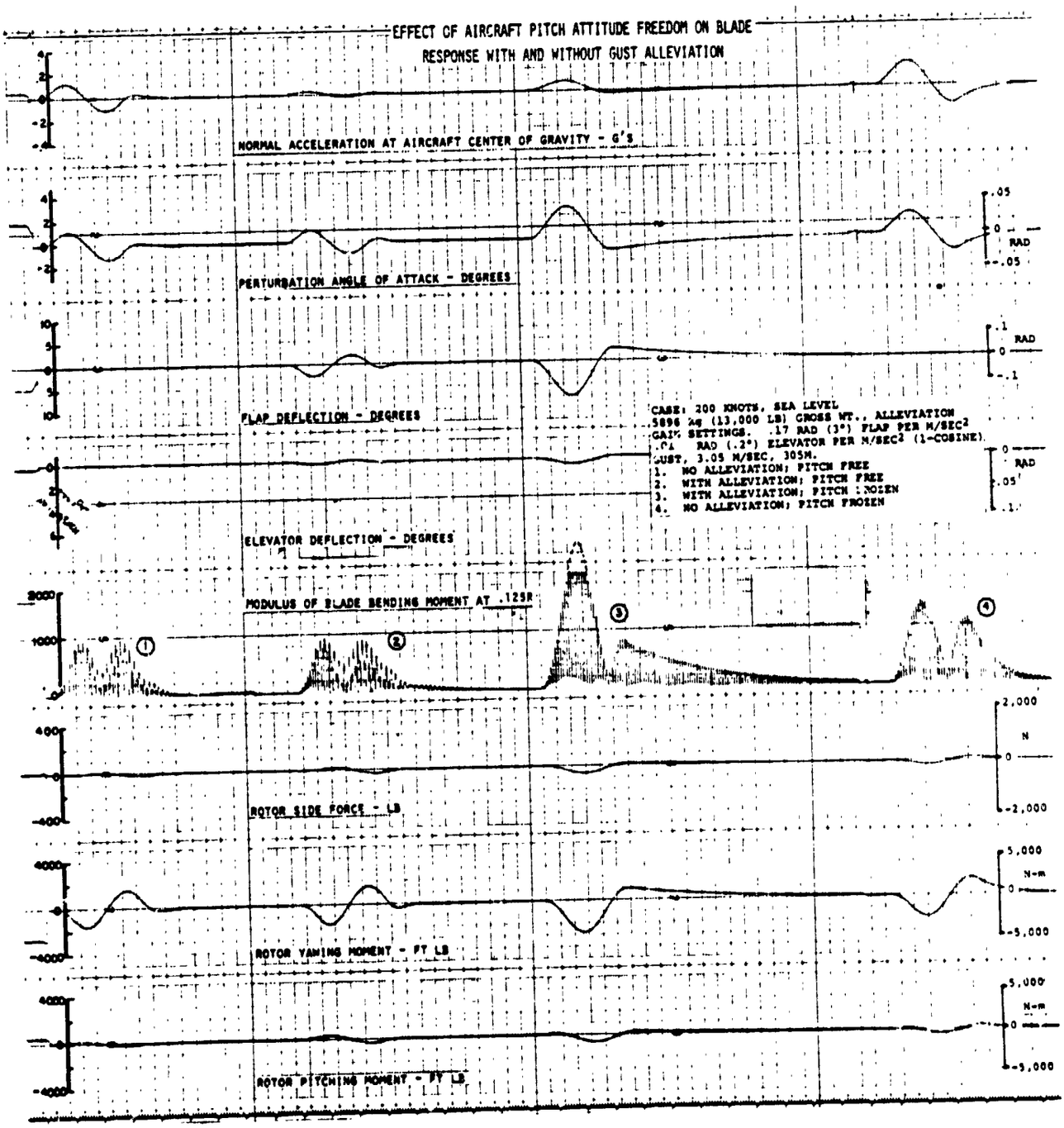

FIGURE AIII.3. EFFECT OF AIRCRAFT PITCH ATTITUDE FREEDOM ON BLADE RESPONSE WITH AND WITHOUT GUST ALLEVIATION.

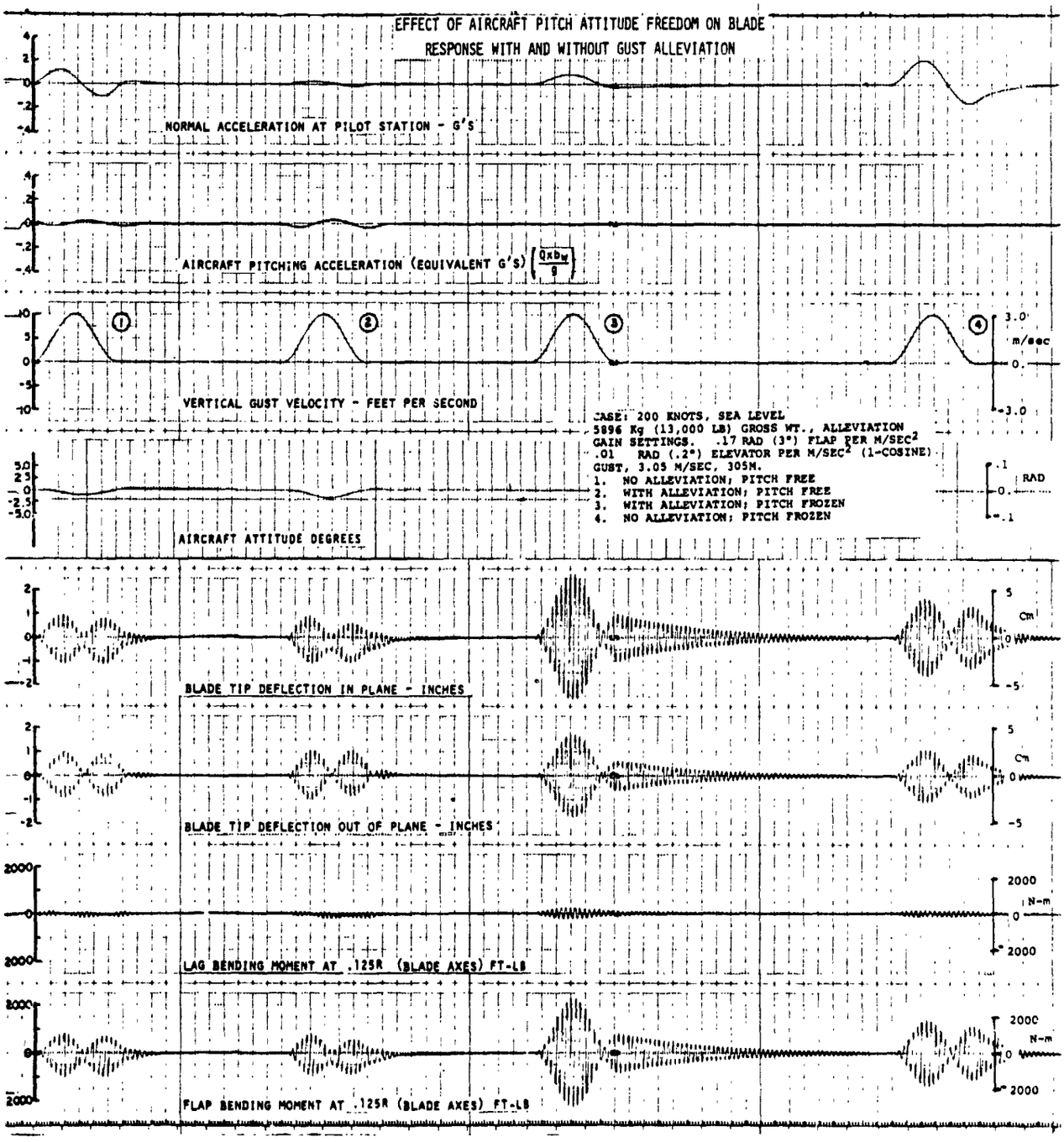

FIGURE AIII.4. EFFECT OF AIRCRAFT PITCH ATTITUDE FREEDOM ON BLADE RESPONSE WITH AND WITHOUT GUST ALLEVIATION.

ORIGINAL PAGE IS
OF POOR QUALITY

APPENDIX IV

RESPONSE DATA FOR MATRIX OF SPEEDS, ALTITUDES AND CENTER OF GRAVITY LOCATIONS

AIV.1 INTRODUCTION

Appendix IV is a compilation of frequency response, system requirement, and random response data for alleviated and unalleviated conditions. Because of the number and length of titles which could be required to adequately dispute each plot, a coded system has been adopted. In this system the exact description of the plot is given by the values of six indices. Thus in a figure designated

Figure A, B, C, X, Y, Z

A indicates the type of plot

B indicates altitude and speed

C indicates location of center of gravity

X indicates variable plotted

Y indicates forcing function

Z indicates type of alleviation

The meanings of values assigned to ABC XYZ are listed in Table AIV.1. For example, Figure 4.6.1.0.0.2 would mean that it showed random response data for the second growth of aircraft variables at a speed of 240 knots at 4,573 meters (15,000 feet) with the center of gravity at the forward limit, alleviation system gains F=4.0, E=0.6 with acceleration sensing. The use of this type of data is discussed fully in Volume I.

TABLE AIV.1. KEY TO FIGURE TITLES (A,B,C,X,Y,Z) OF APPENDIX IV.

A - TYPE OF DATA

1. Frequency Response
2. System Requirements
3. Random Response Sheet 1
4. Randon Response Sheet 2
5. RMS Response

B - FLIGHT CONDITIONS

1. 200 Kt, 1524m, 5,000 Ft
2. 200 Kt, 3049m, 10,000 Ft
3. 200 Kt, 4576m, 15,000 Ft
4. 240 Kt, 1524m, 5,000 Ft
5. 240 Kt, 3049m, 10,000 Ft
6. 240 Kt, 4576m, 15,000 Ft
7. 280 Kt, 1524m, 5,000 Ft
8. 280 Kt, 3049m, 10,000 Ft
9. 280 Kt, 4576m, 15,000 Ft

C - LOCATION OF CENTER OF GRAVITY

1. Forward
2. Aft

X - VARIABLE WHOSE FREQUENCY RESPONSE IS PLOTTED

0. Not Applicable
1. Cabin Acceleration
2. Pitch Acceleration
3. C.G. Acceleration
4. α
5. Hub Yawing Moment
6. Hub Pitching Moment

Y - FORCING FUNCTION

0. Not Applicable
1. Gust
2. Flap
3. Elevator
4. A_1
5. B_1

Z - ALLEVIATION SYSTEM DESCRIPTION

0. Not applicable
1. No Alleviation
2. $\ddot{Z}$ Sensing F=4.0, E=0.6
3. $\ddot{Z}$ Sensing F=4.0, E=0.7
4. $\ddot{Z}$ Sensing F=4.0, E=0.8
5. α Sensing F=4.0, E=0.6
6. $\ddot{Z}$ Sensing F=4.8, E=.72
7. $\ddot{Z}$ Sensing F=4.4, E-.77
8. $\ddot{Z}$ Sensing F=3.34, E=.51

K+E LOGARITHMIC • 2 X 3 CYCLES
KEUFFEL & ESSER CO. MADE IN U.S.A.
46 7323

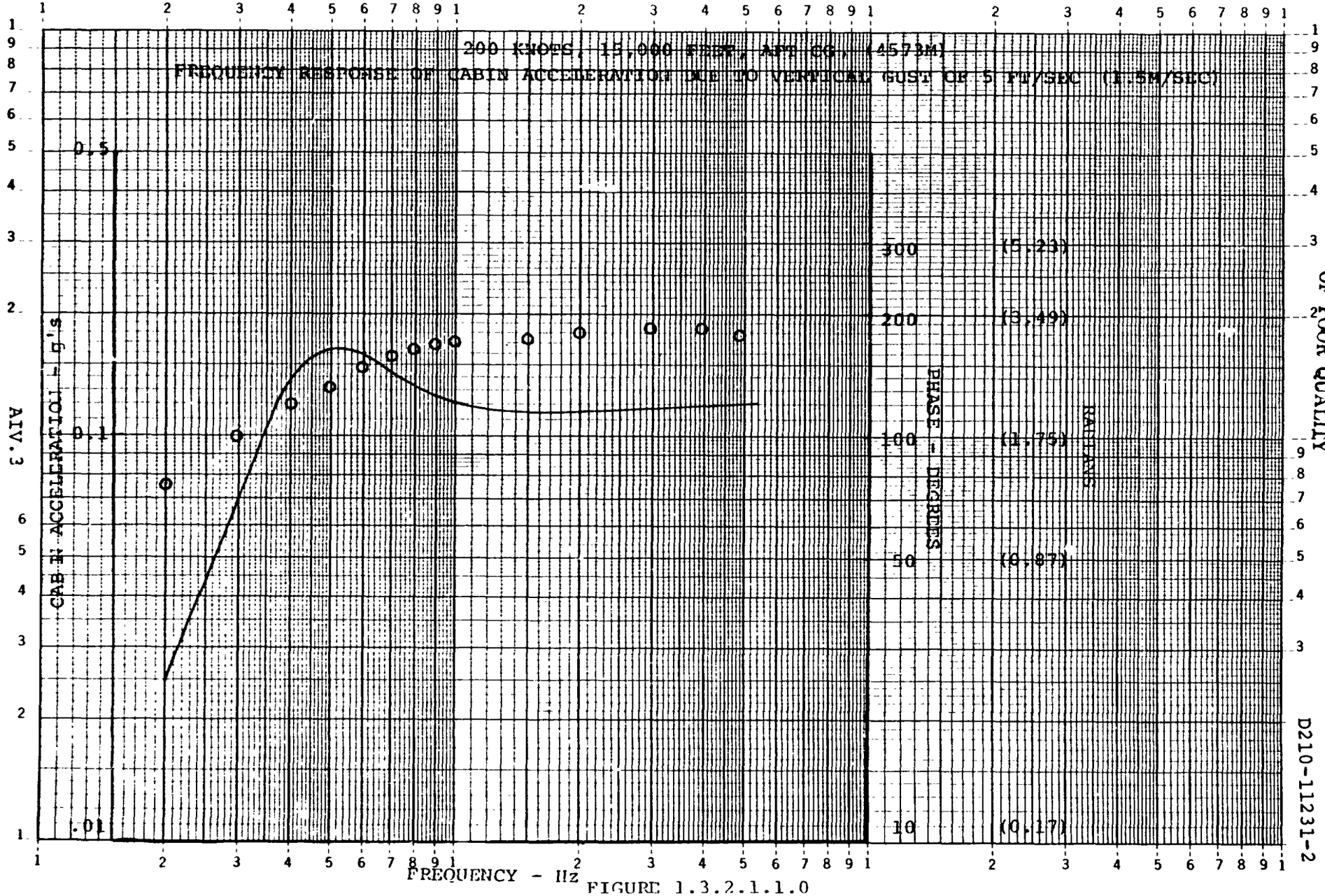

FIGURE 1.3.2.1.1.0

ORIGINAL PAGE IS
OF POOR QUALITY

K·E LOGARITHMIC • 2 X 3 CYCLES
KEUFFEL & ESSER CO MADE IN U.S.A.

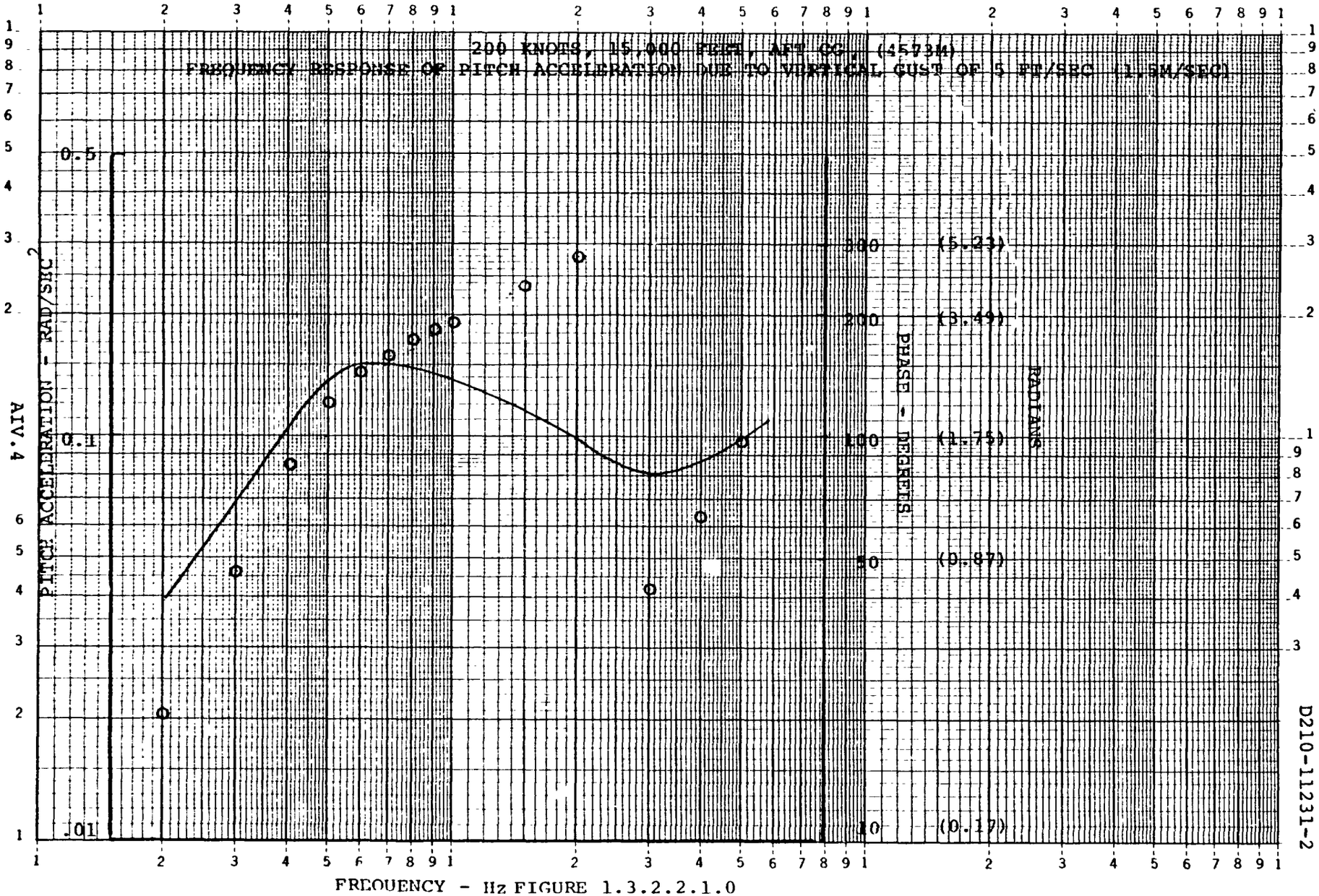

FIGURE 1.3.2.2.1.0

K•E LOGARITHMIC • 2 X 3 CYCLES
KEUFFEL & ESSER CO MADE IN U.S.A.
46 7323

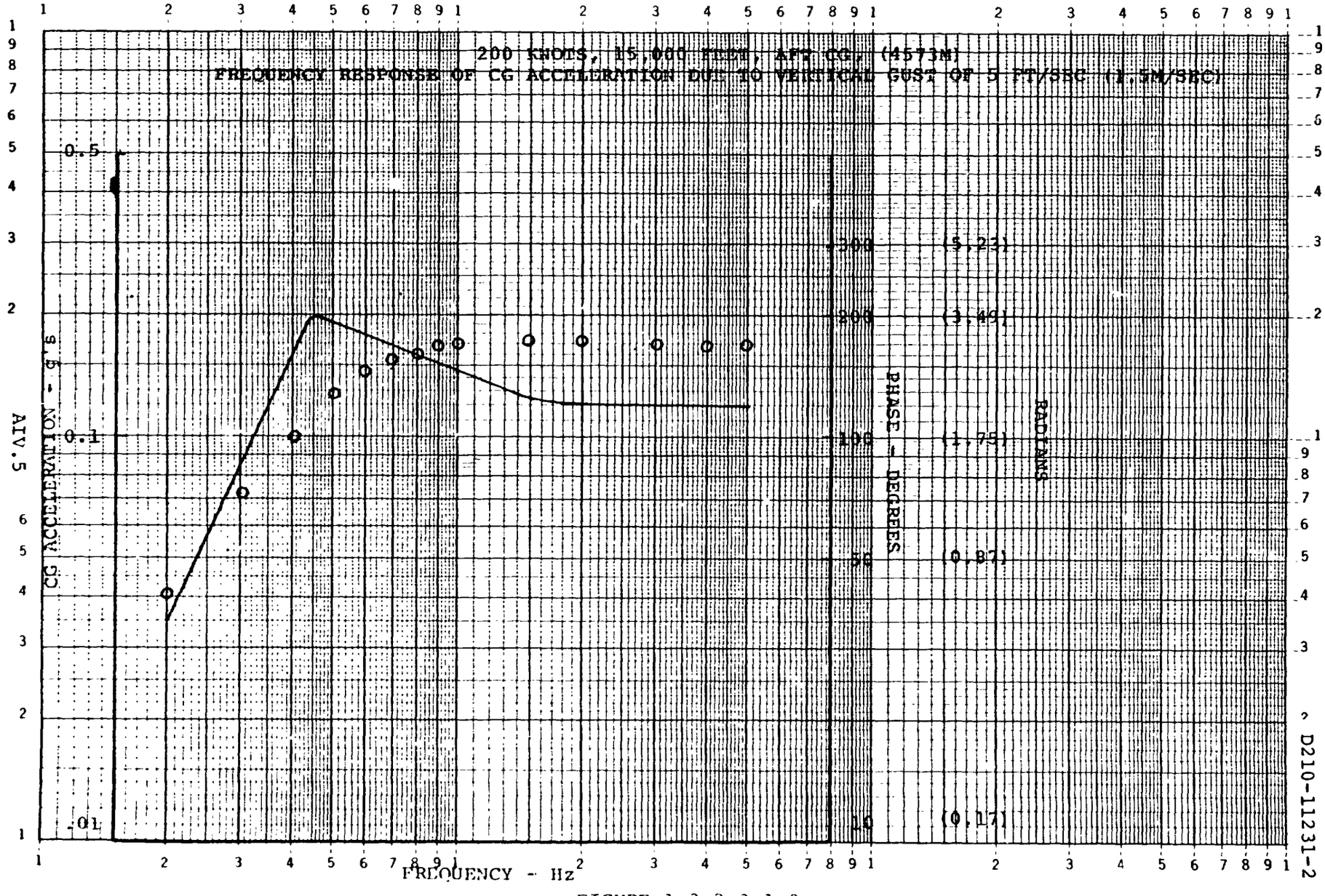

FIGURE 1.3.2.3.1.0

K+E LOGARITHMIC • 2 X 3 CYCLES
KEUFFEL & ESSER CO. MADE IN U.S.A.

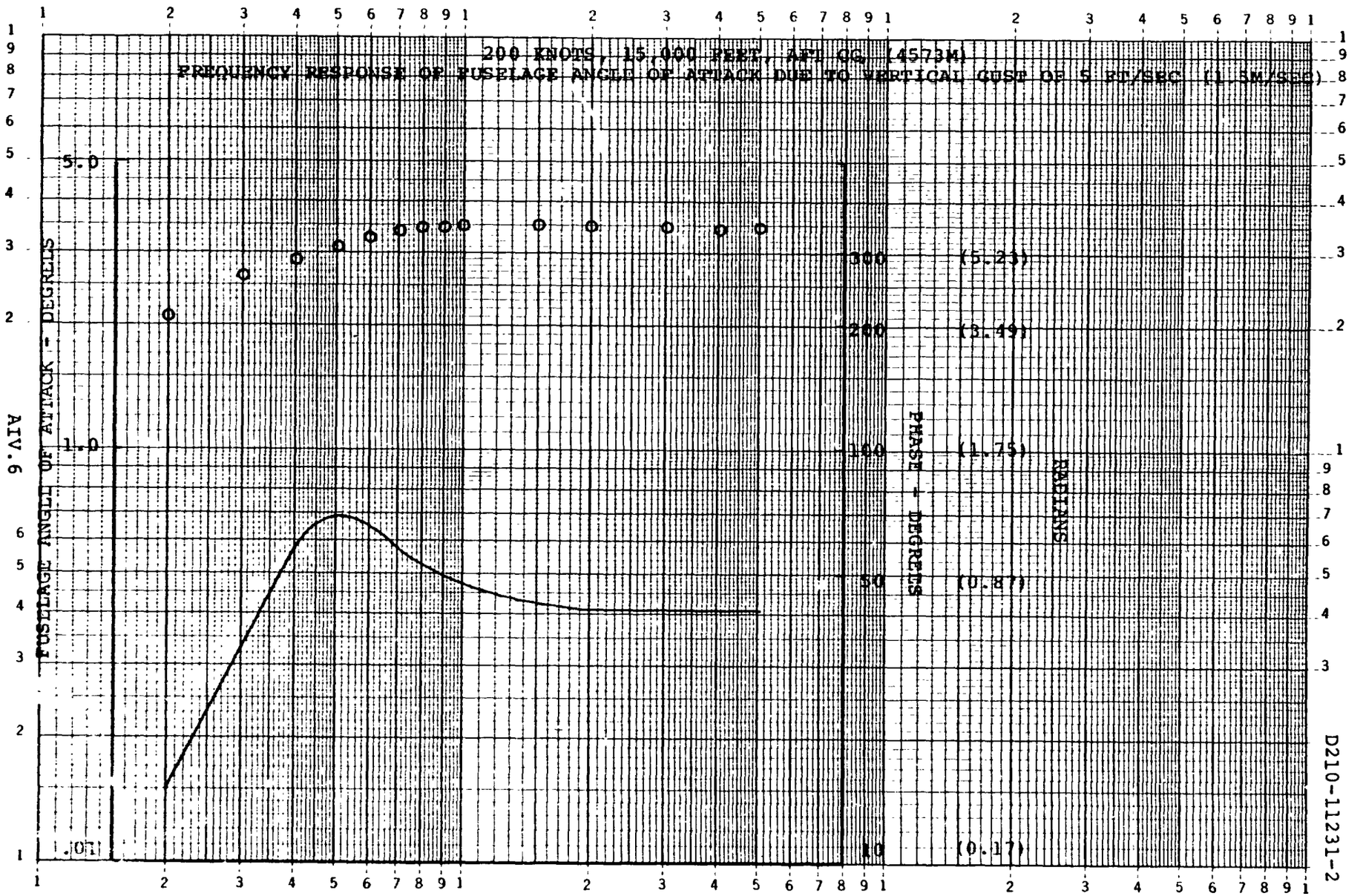

FIGURE 1.3.2.4.1.0

K•Σ LOGARITHMIC • 2 X 3 CYCLES
KEUFFEL & ESSER CO MADE IN U.S.A.
46 7323

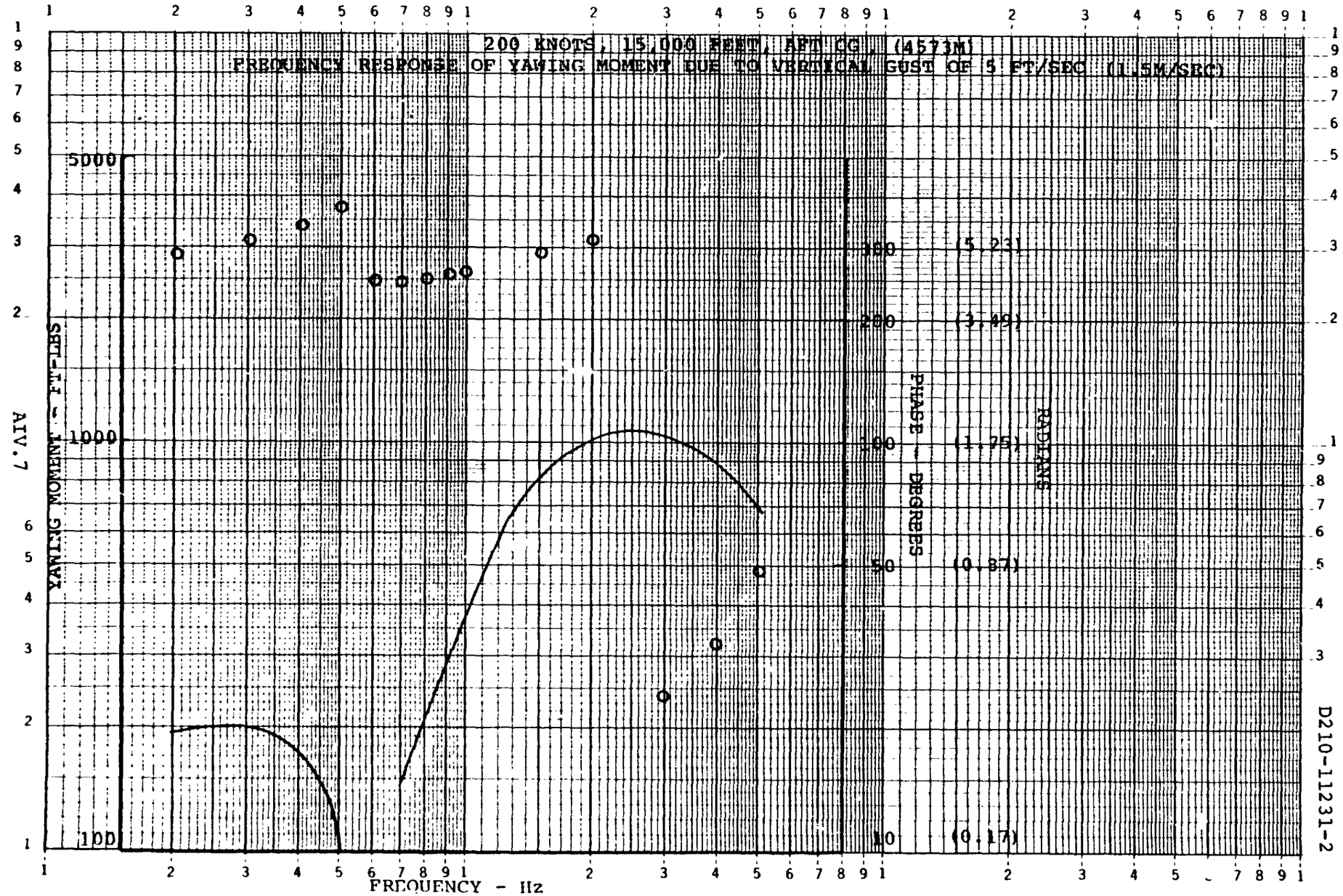

FIGURE 1.3.2.5.1.0

K•E LOGARITHMIC • 2 X 3 CYCLES
KEUFFEL & ESSER CO. MADE IN U.S.A.

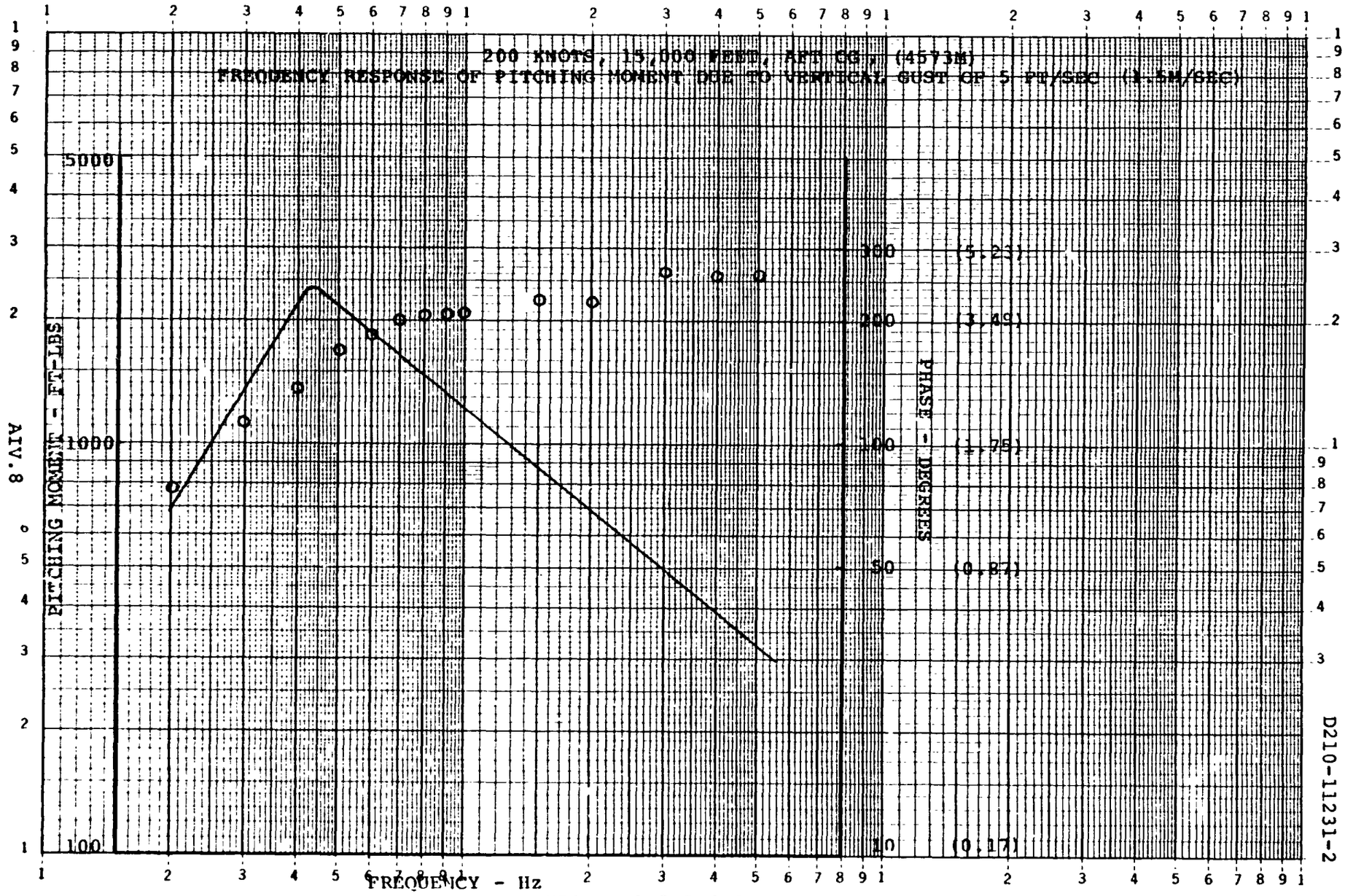

FIGURE 1.3.2.6.1.0

K•E LOGARITHMIC • 2 X 3 CYCLES
KEUFFEL & ESSER CO. MADE IN U.S.A.

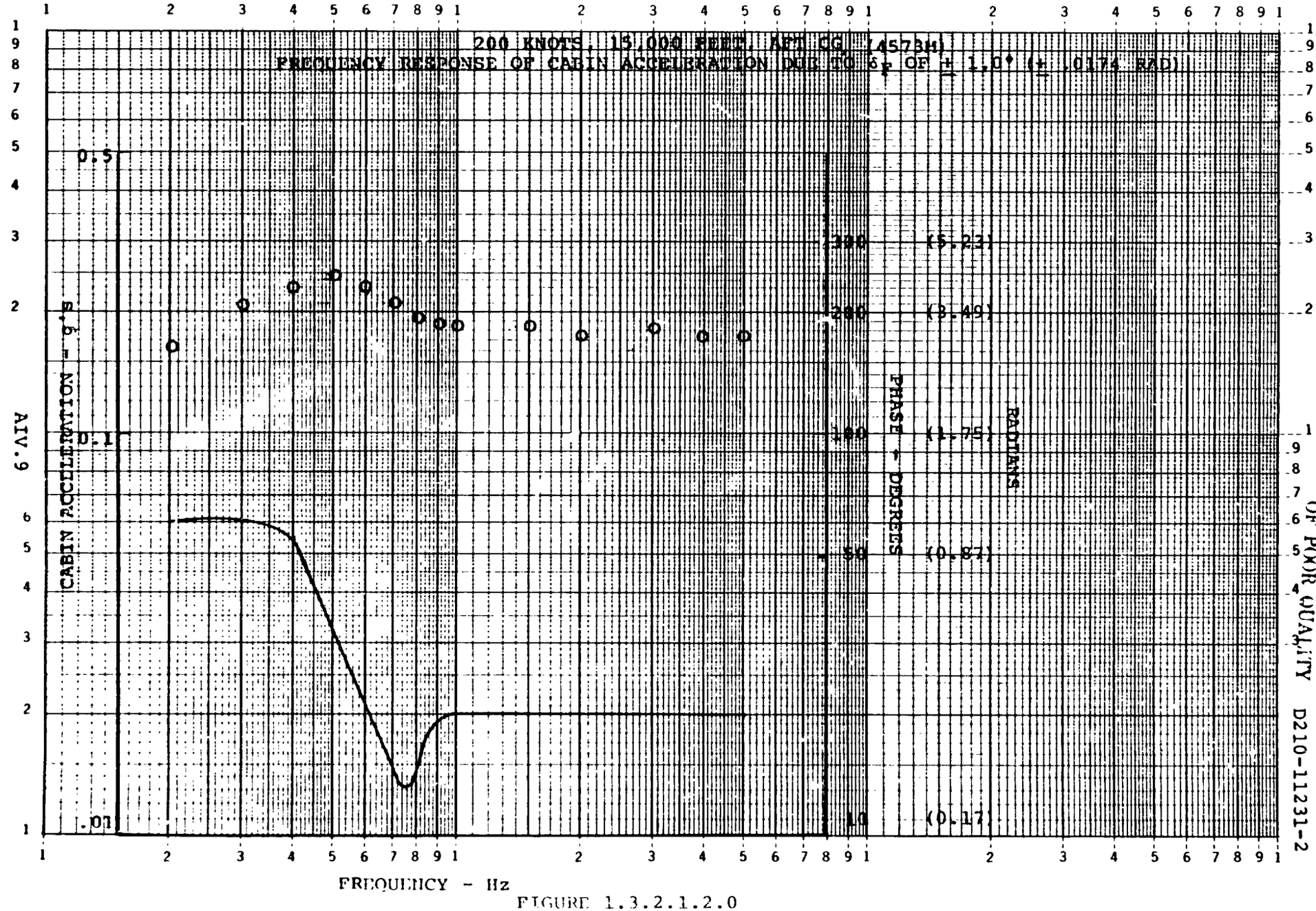

FIGURE 1.3.2.1.2.0

ORIGINAL PAGE IS
OF POOR QUALITY

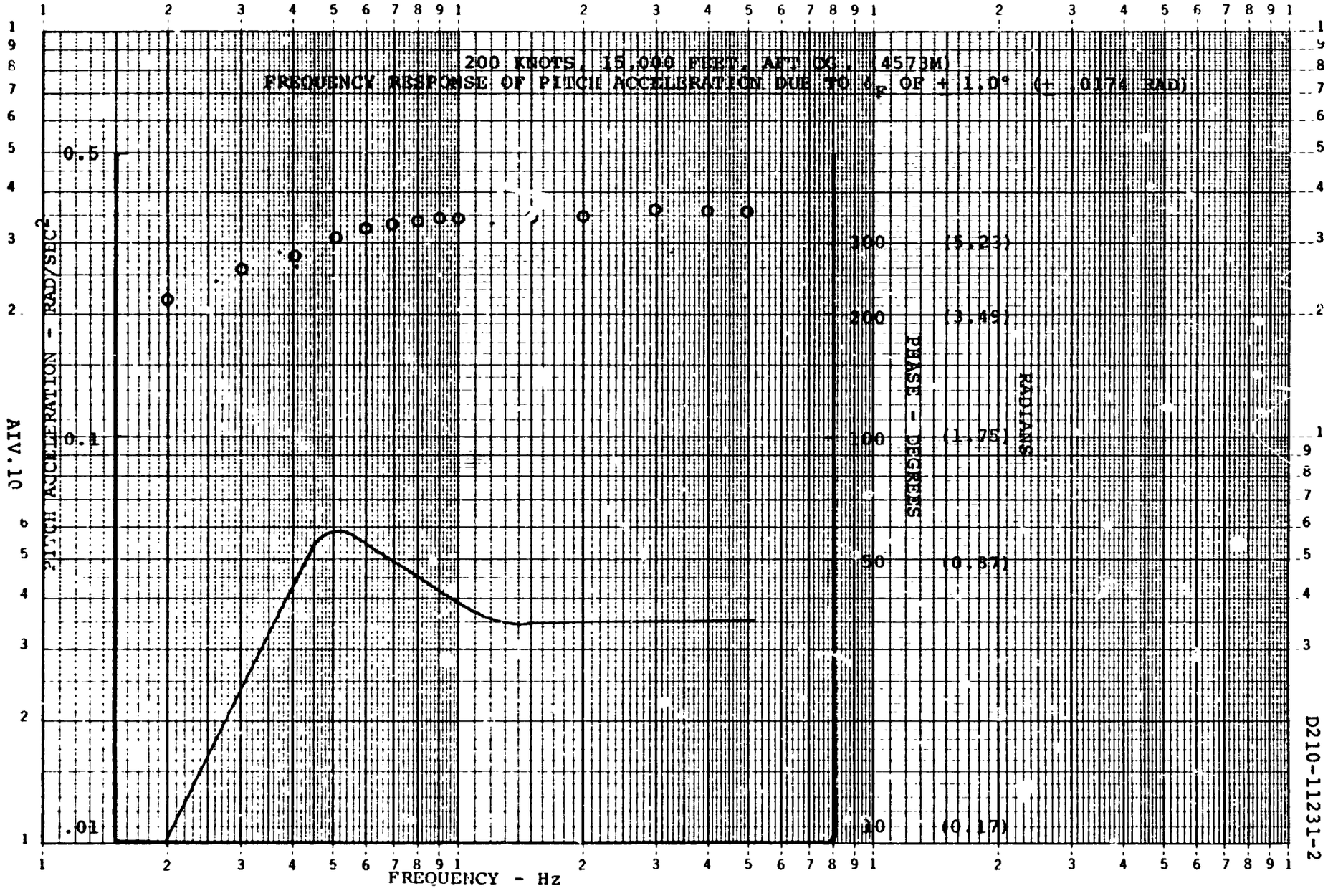

FIGURE 1.3.2.2.2.0

K•E LOGARITHMIC • 2 X 3 CYCLES
KEUFFEL & ESSER CO. MADE IN U.S.A.

46 7323

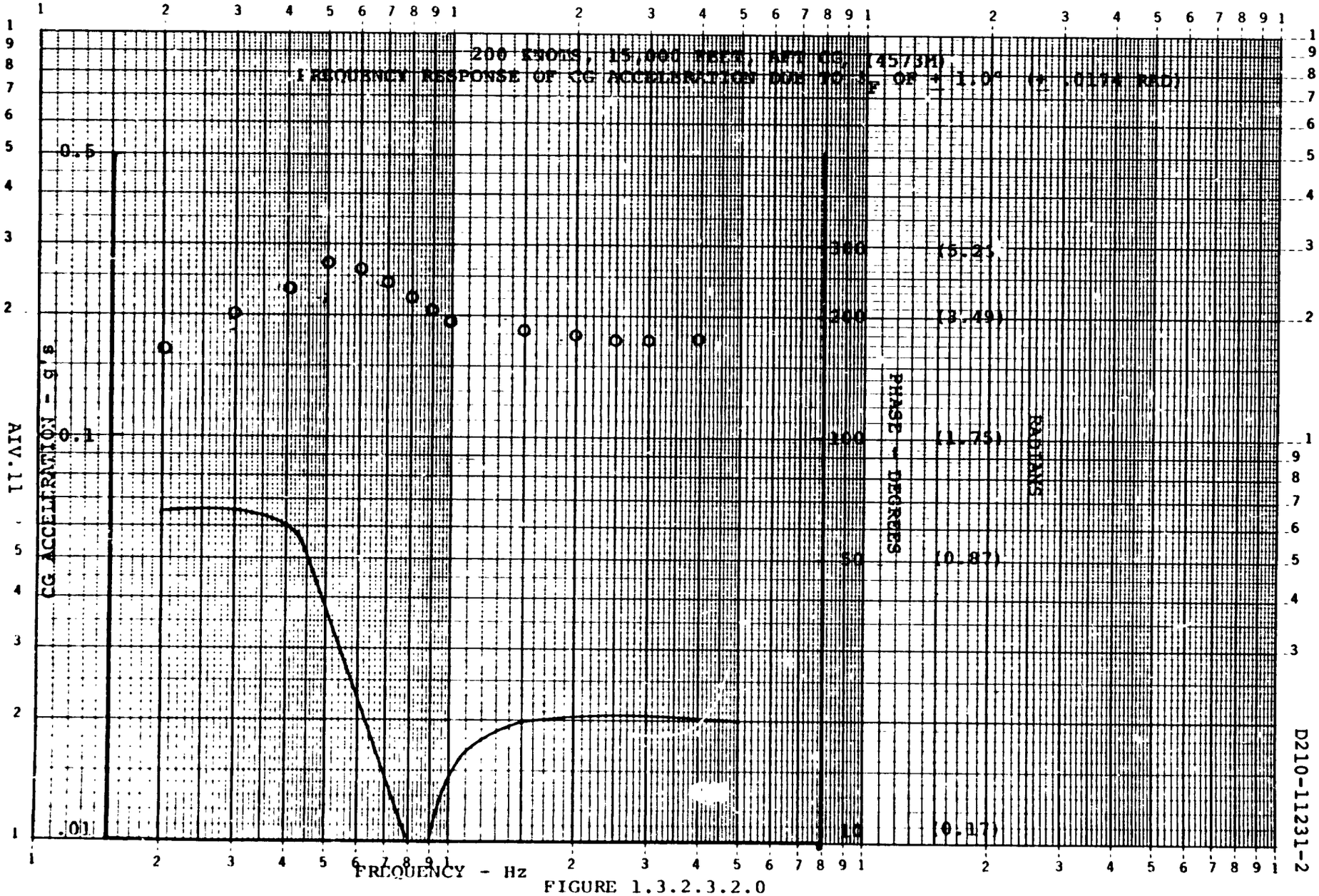

FIGURE 1.3.2.3.2.0

K·E LOGARITHMIC • 2 X 3 CYCLES KEUFFEL & ESSER CO. MADE IN U.S.A.

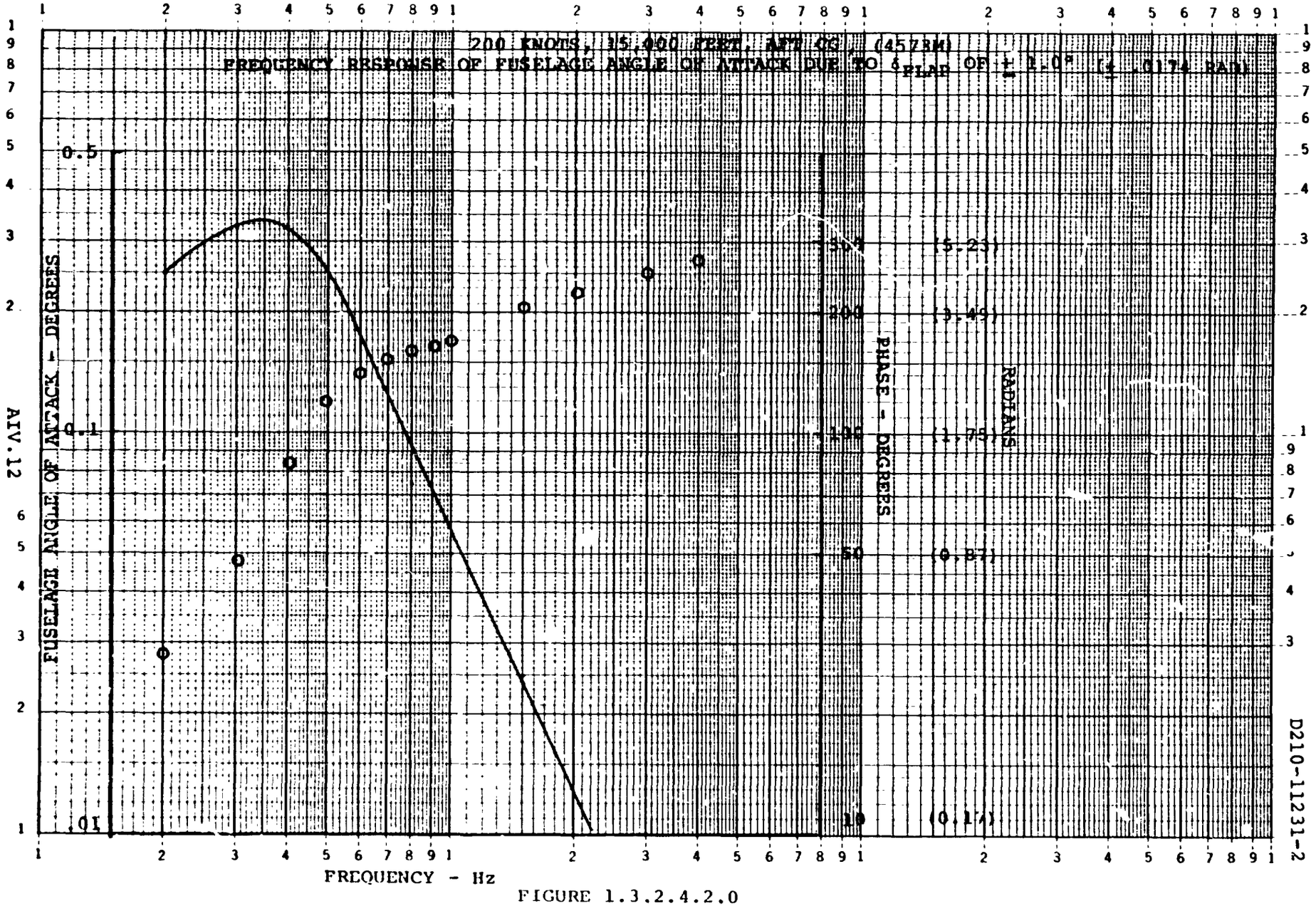

FIGURE 1.3.2.4.2.0

K+E LOGARITHMIC • 2 X 3 CYCLES
KEUFFEL & ESSER CO. MADE IN U.S.A.
46 7323

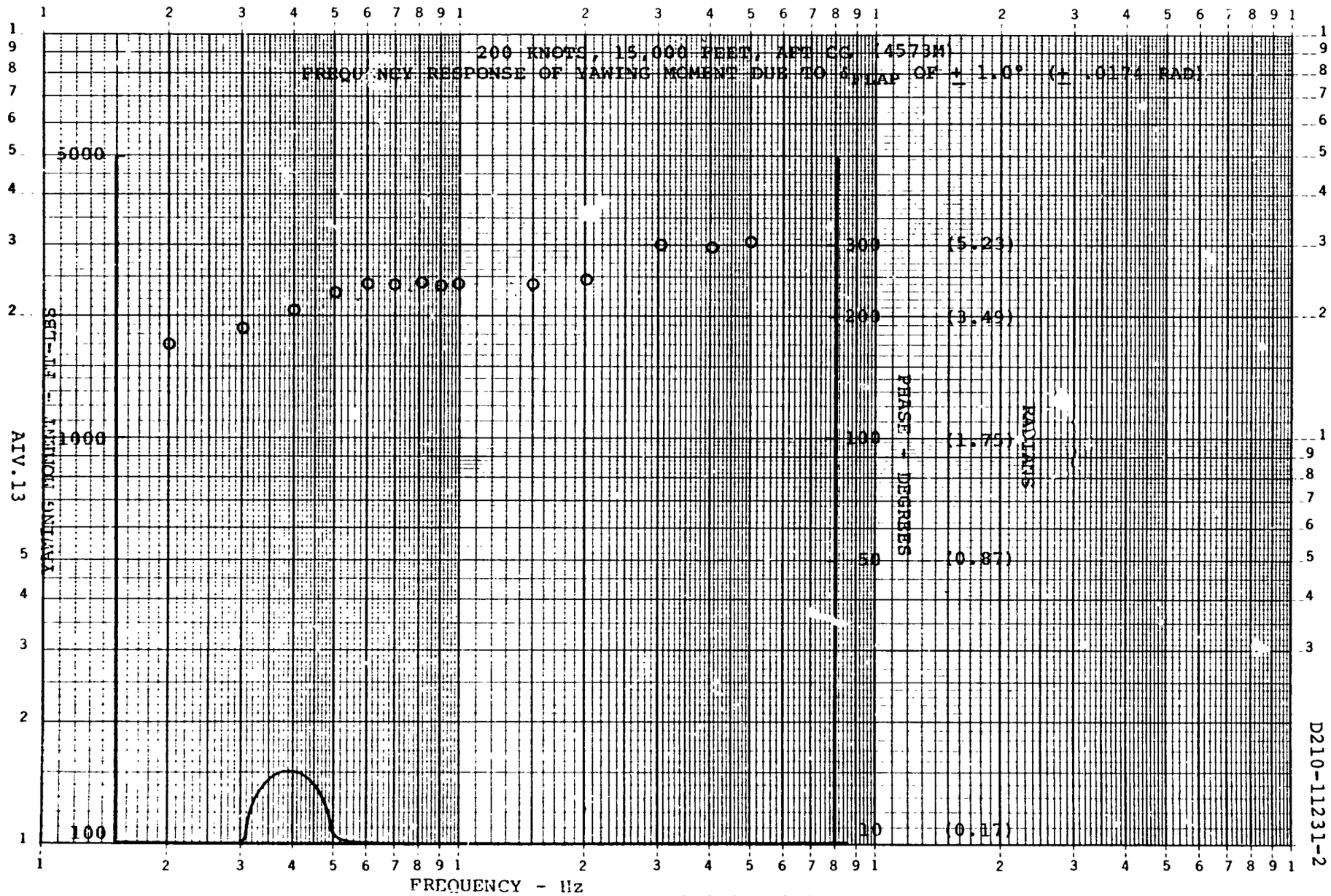

FIGURE 1.3.2.5.2.0

K•E LOGARITHMIC • 2 X 3 CYCLES
KEUFFEL & ESSER CO MADE IN U.S.A.
46 7323

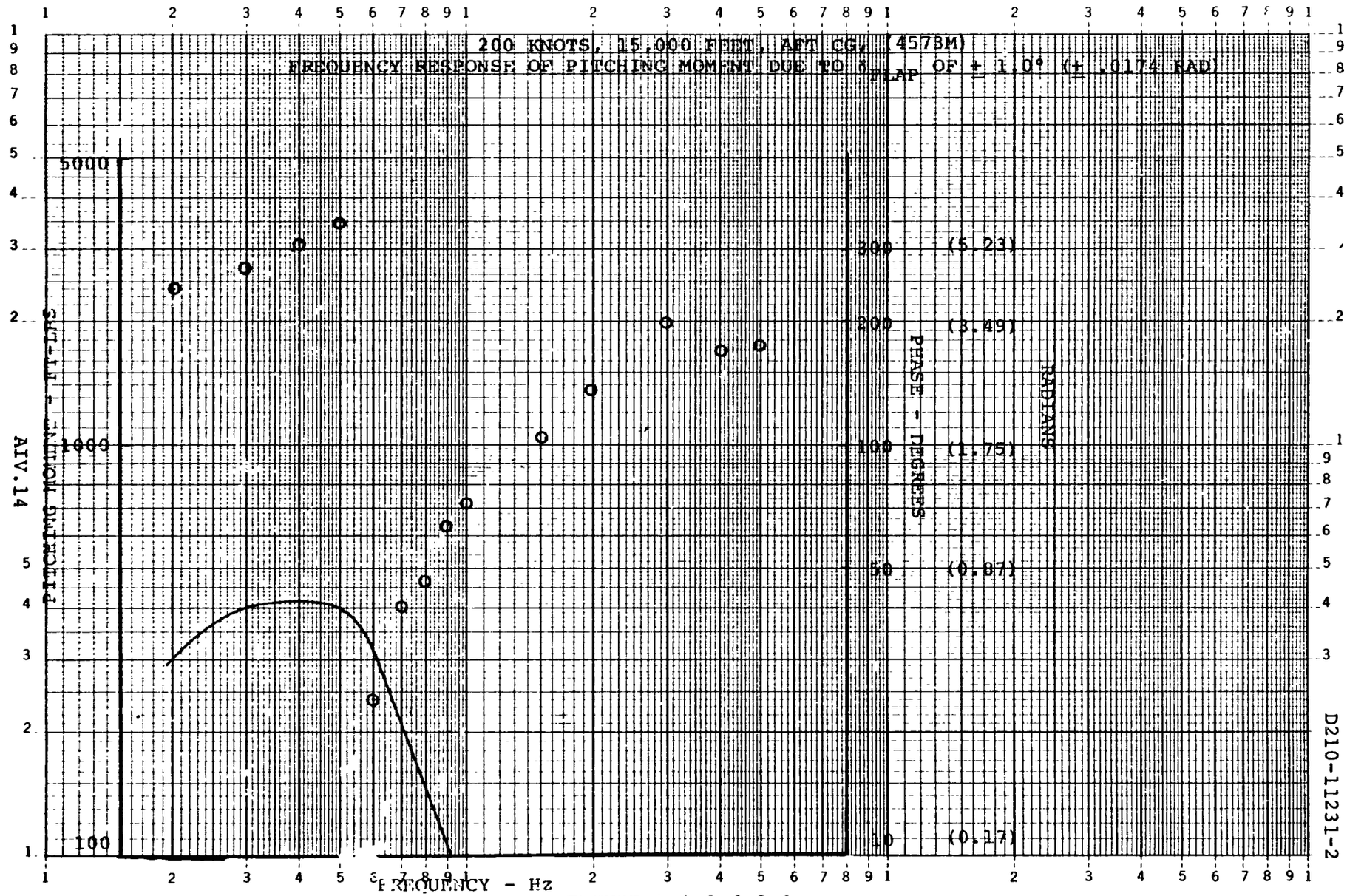

FIGURE 1.3.2.6.2.0

K+E LOGARITHMIC • 2 X 3 CYCLES
KEUFFEL & ESSER CO MADE IN U.S.A.

46 7323

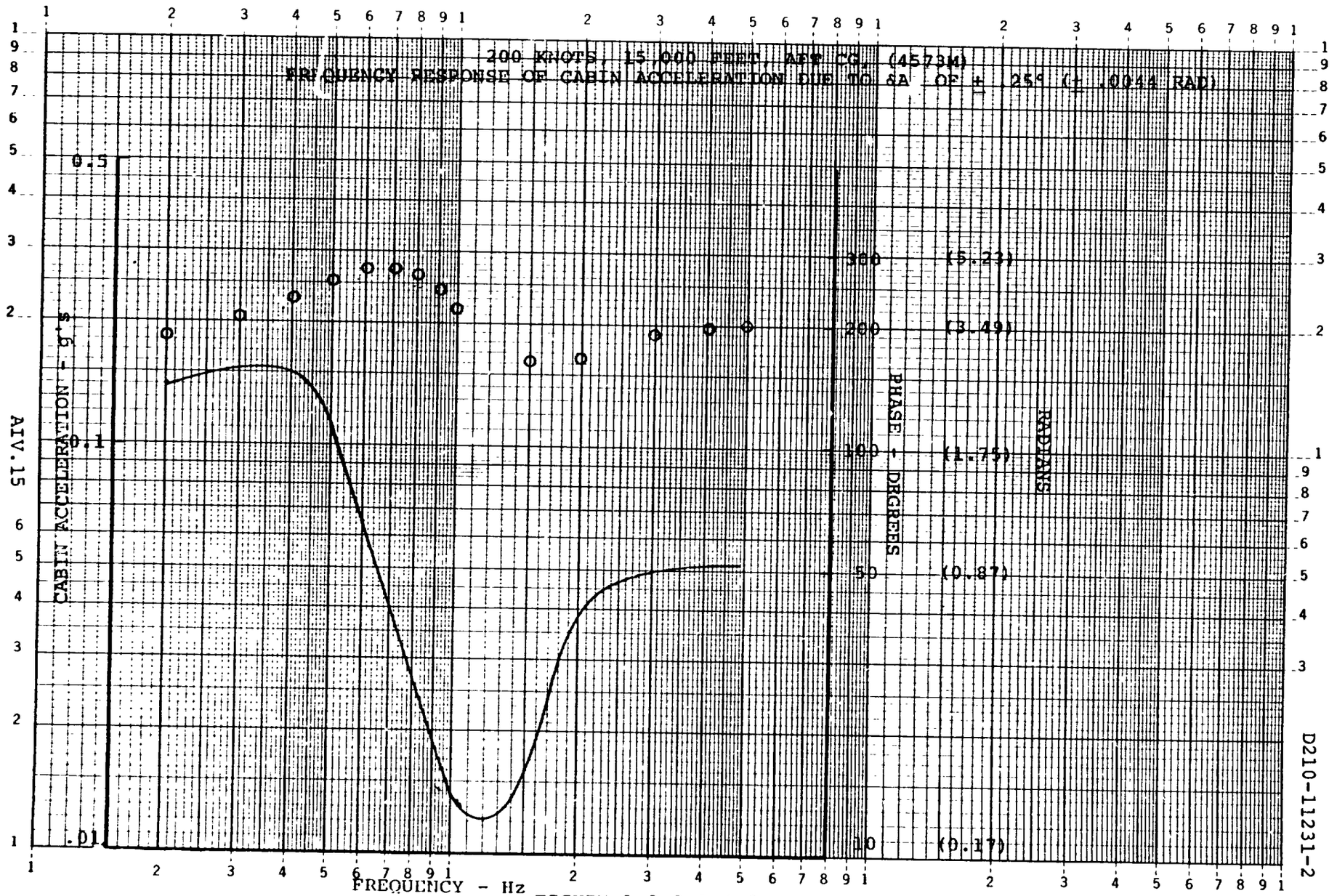

FIGURE 1.3.2.1.4.0

AIV.15

D210-11231-2

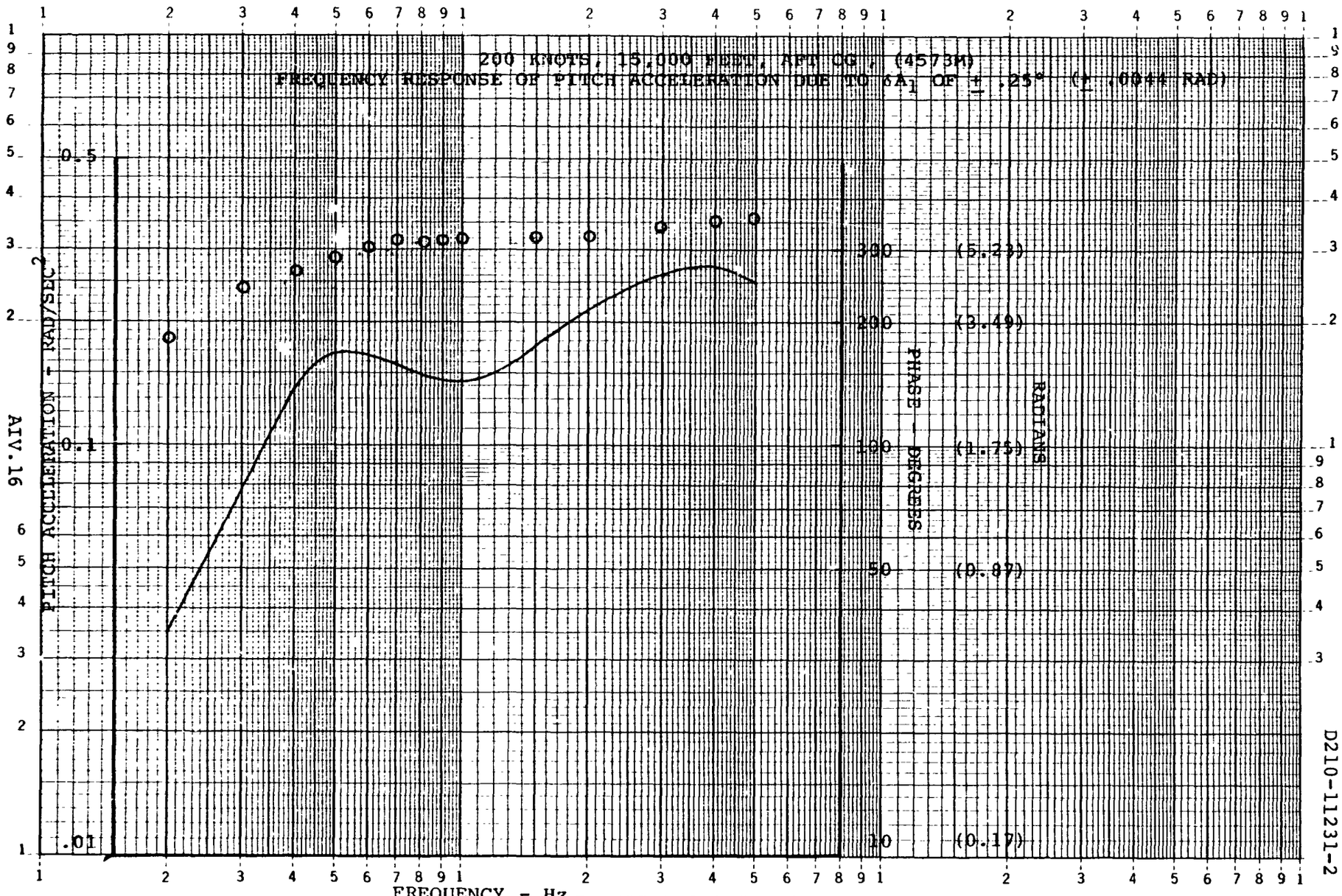

FIGURE 1.3.2.2.4.0

K•E LOGARITHMIC •2 X 3 CYCLES
KEUFFEL & ESSER CO MADE IN U.S.A.
46 7323

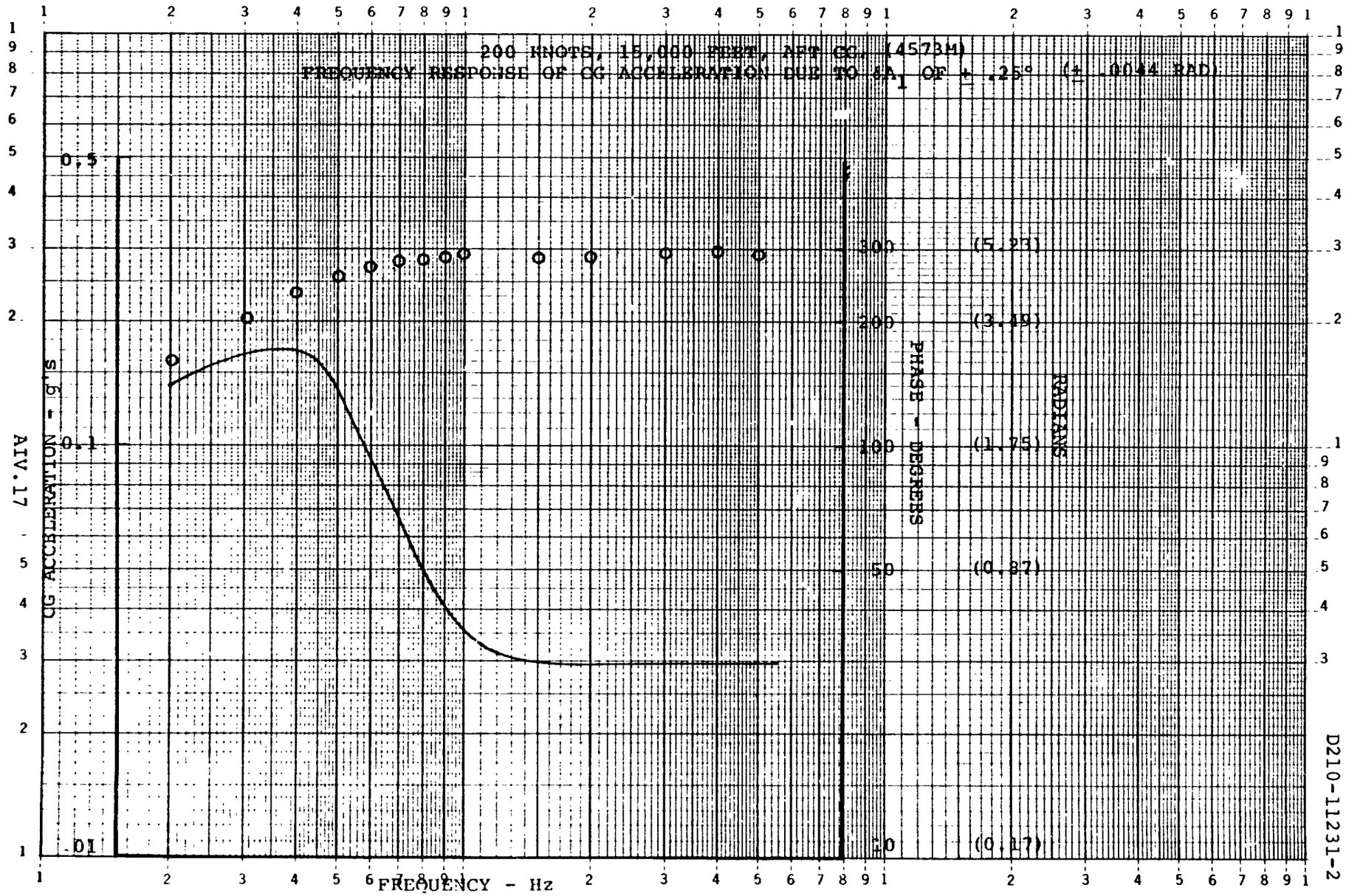

FIGURE 1.3.2.3.4.0

K•E LOGARITHMIC • 2 X 3 CYCLES
KEUFFEL & ESSER CO. MADE IN U.S.A.

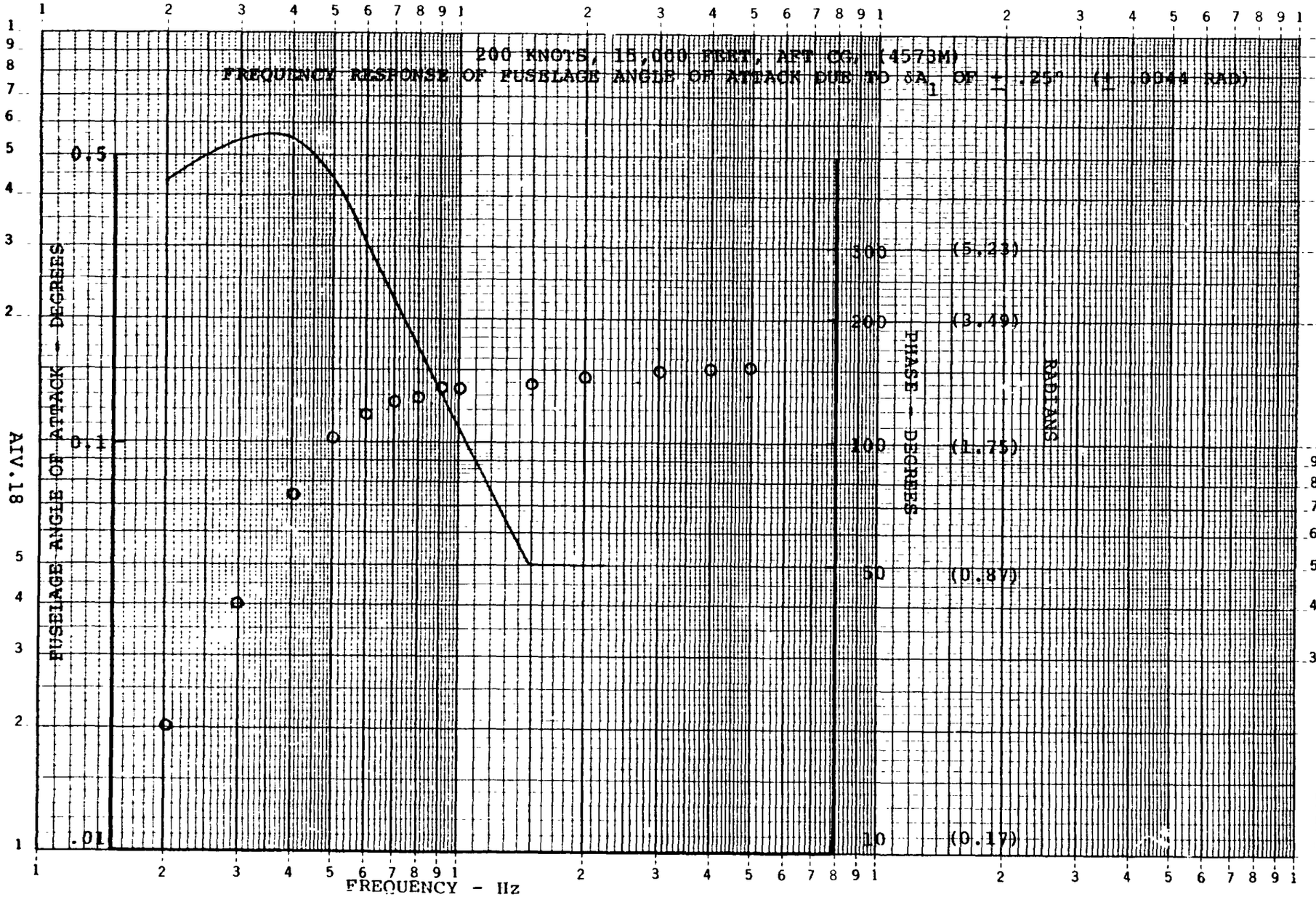

FIGURE 1.3.2.4.4.0

ORIGINAL PAGE IS
OF POOR QUALITY

K•E LOGARITHMIC • 2 X 3 CYCLES
KEUFFEL & ESSER CO MADE IN U.S.A.
46 7323

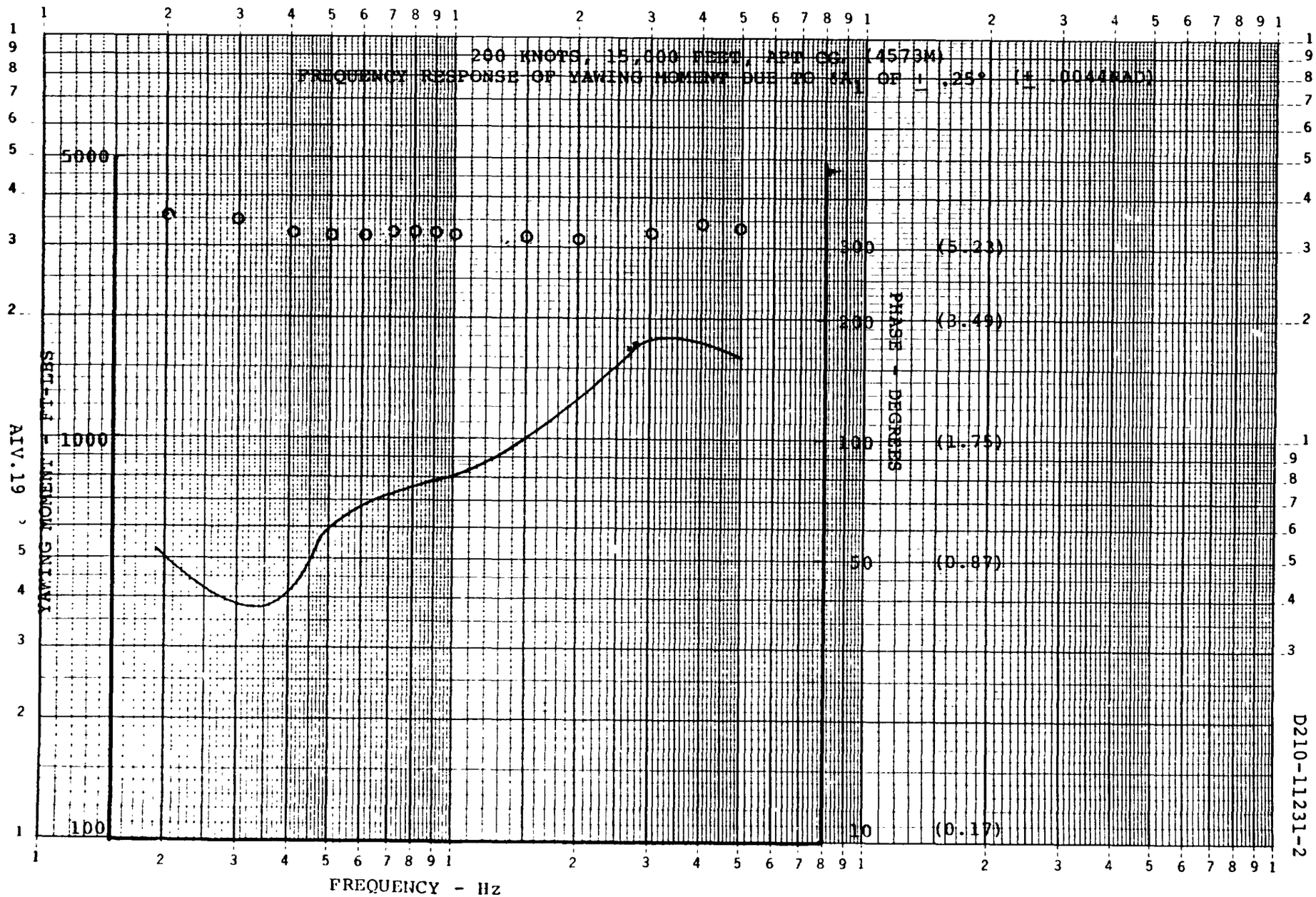

FIGURE 1.3.2.5.4.0

K·E LOGARITHMIC • 2 X 3 CYCLES
KEUFFEL & ESSER CO MADE IN U.S.A.

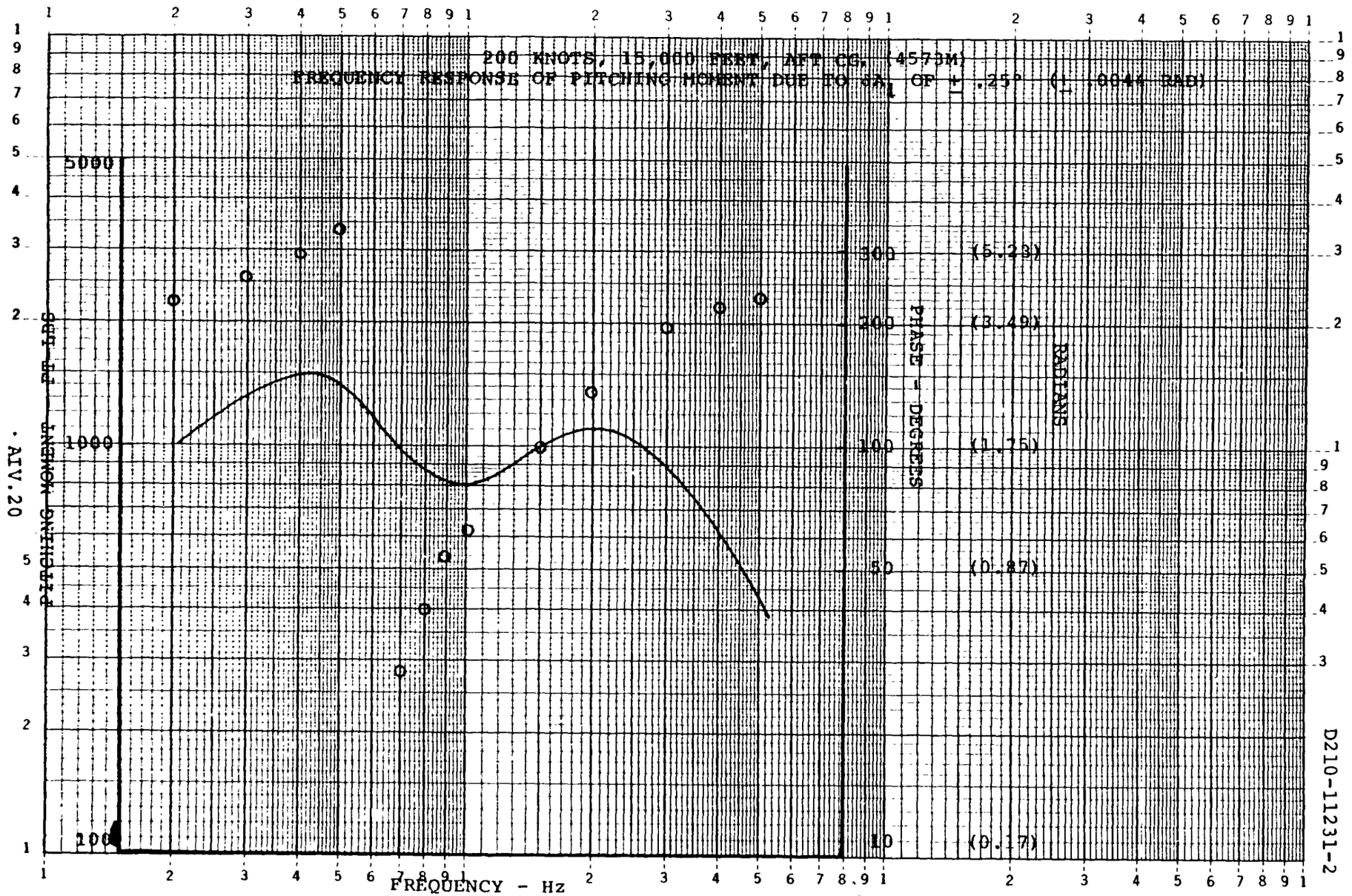

FIGURE 1.3.2.6.4.0

K•E LOGARITHMIC • 2 X 3 CYCLES
KEUFFEL & ESSER CO. MADE IN U.S.A.
46 7323

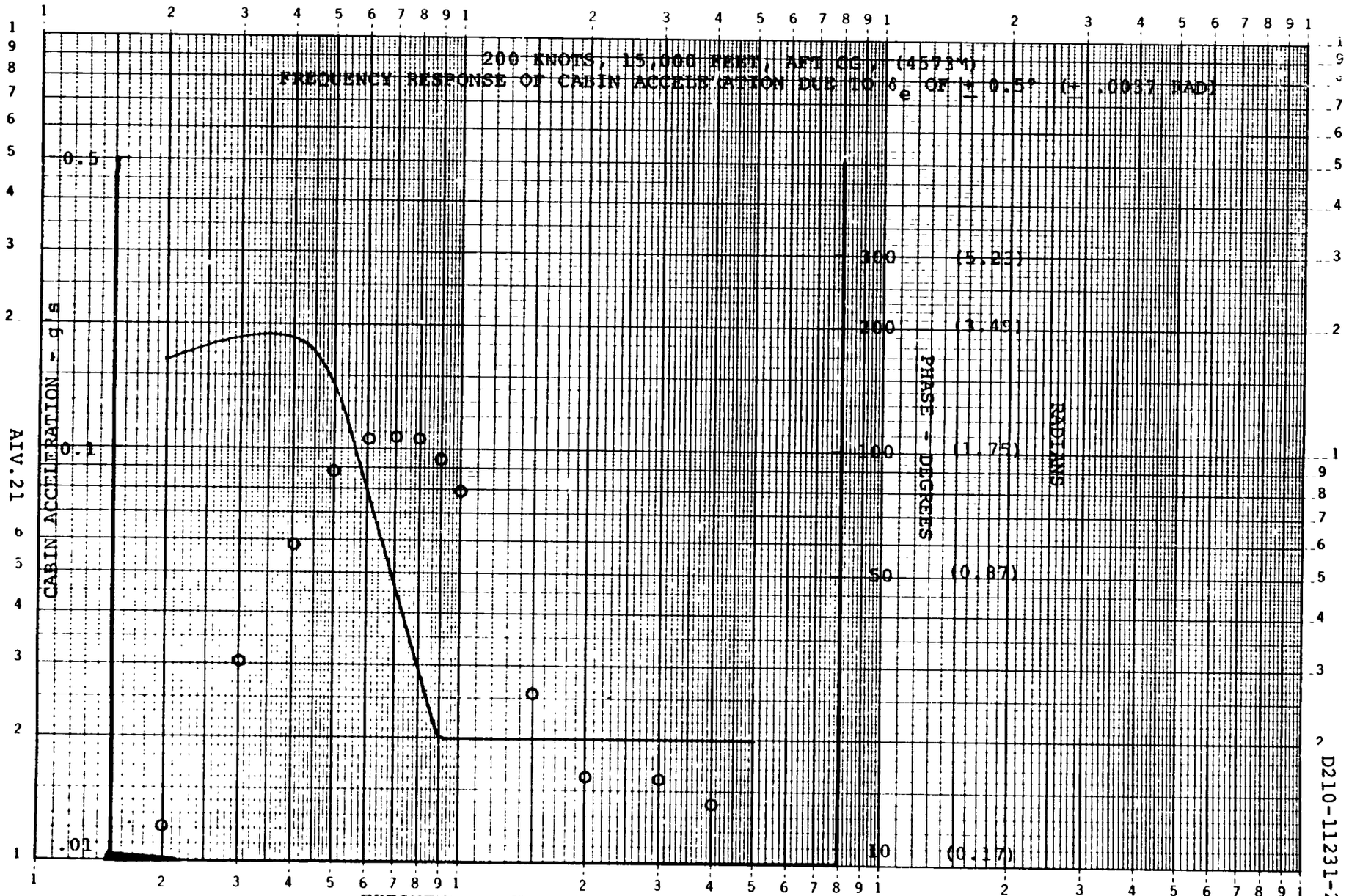

FIGURE 1.3.2.1.3.0

K•Σ LOGARITHMIC • 2 X 3 CYCLES
KEUFFEL & ESSER CO MADE IN U.S.A.

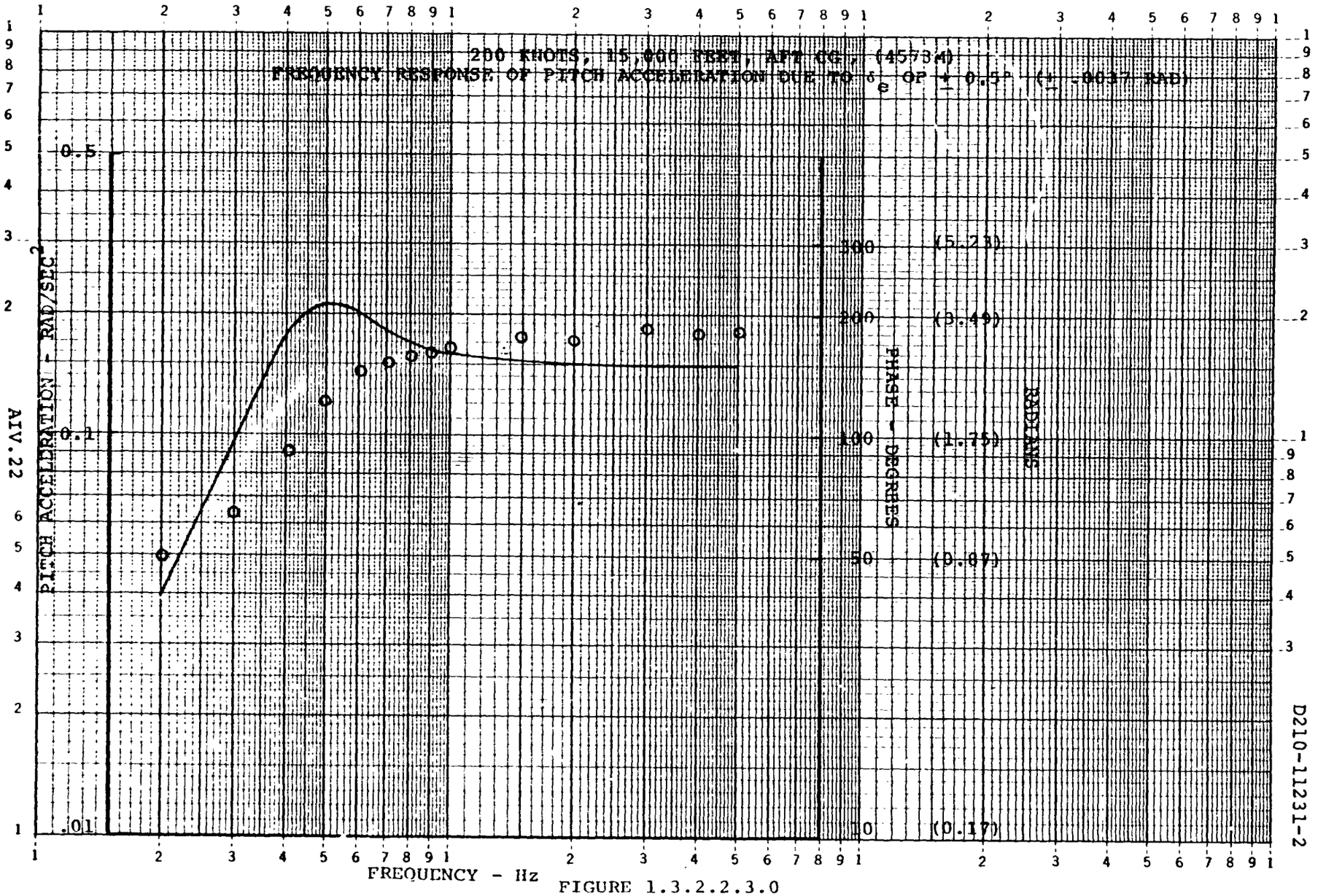

FIGURE 1.3.2.2.3.0

K·E LOGARITHMIC 2 X 3 CYCLES
KEUFFEL & ESSER CO MADE IN U.S.A.
46 7323

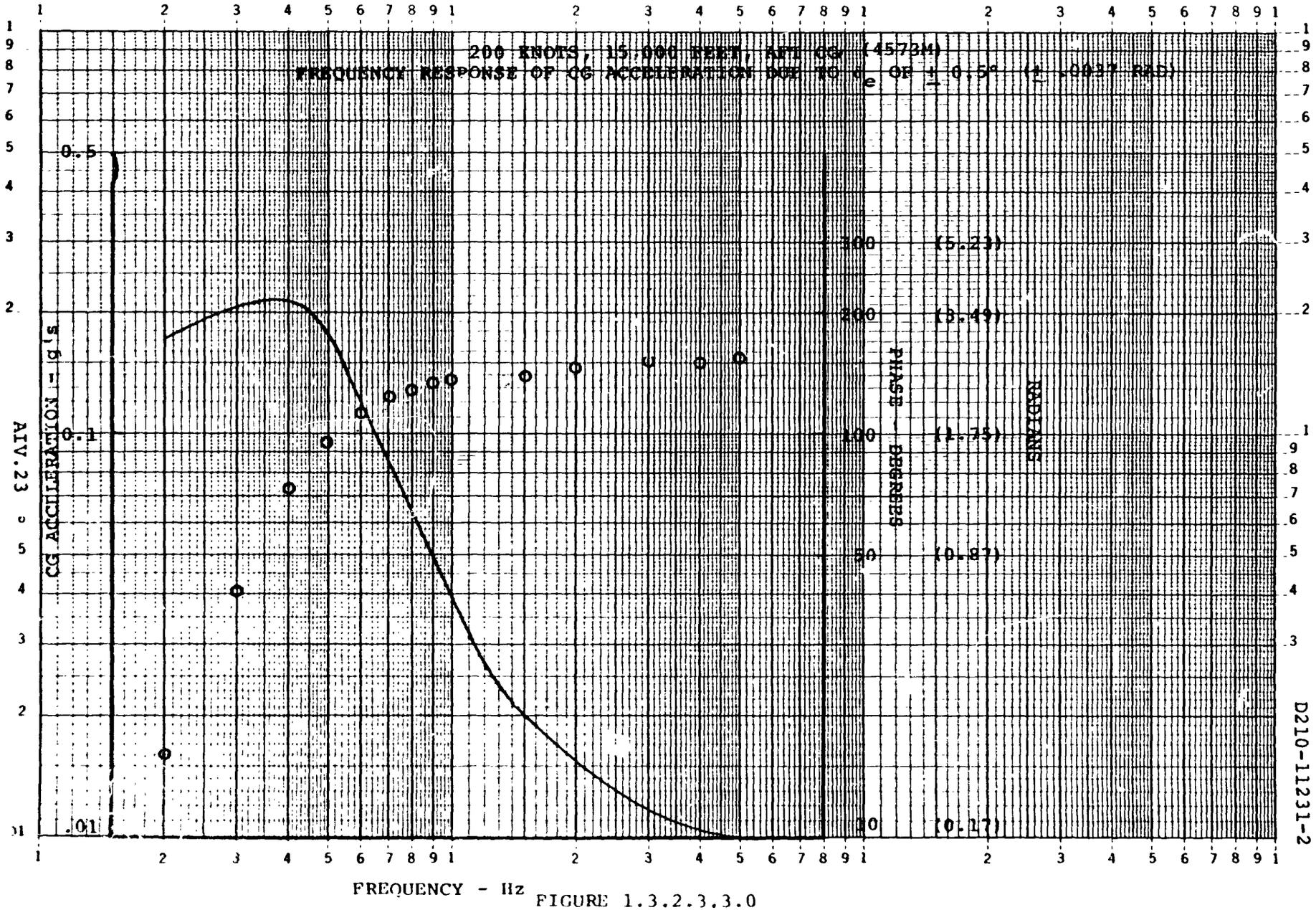

FIGURE 1.3.2.3.3.0

K·E LOGARITHMIC 2 X 3 CYCLES
KEUFFEL & ESSER CO. MADE IN U.S.A.

46 7323

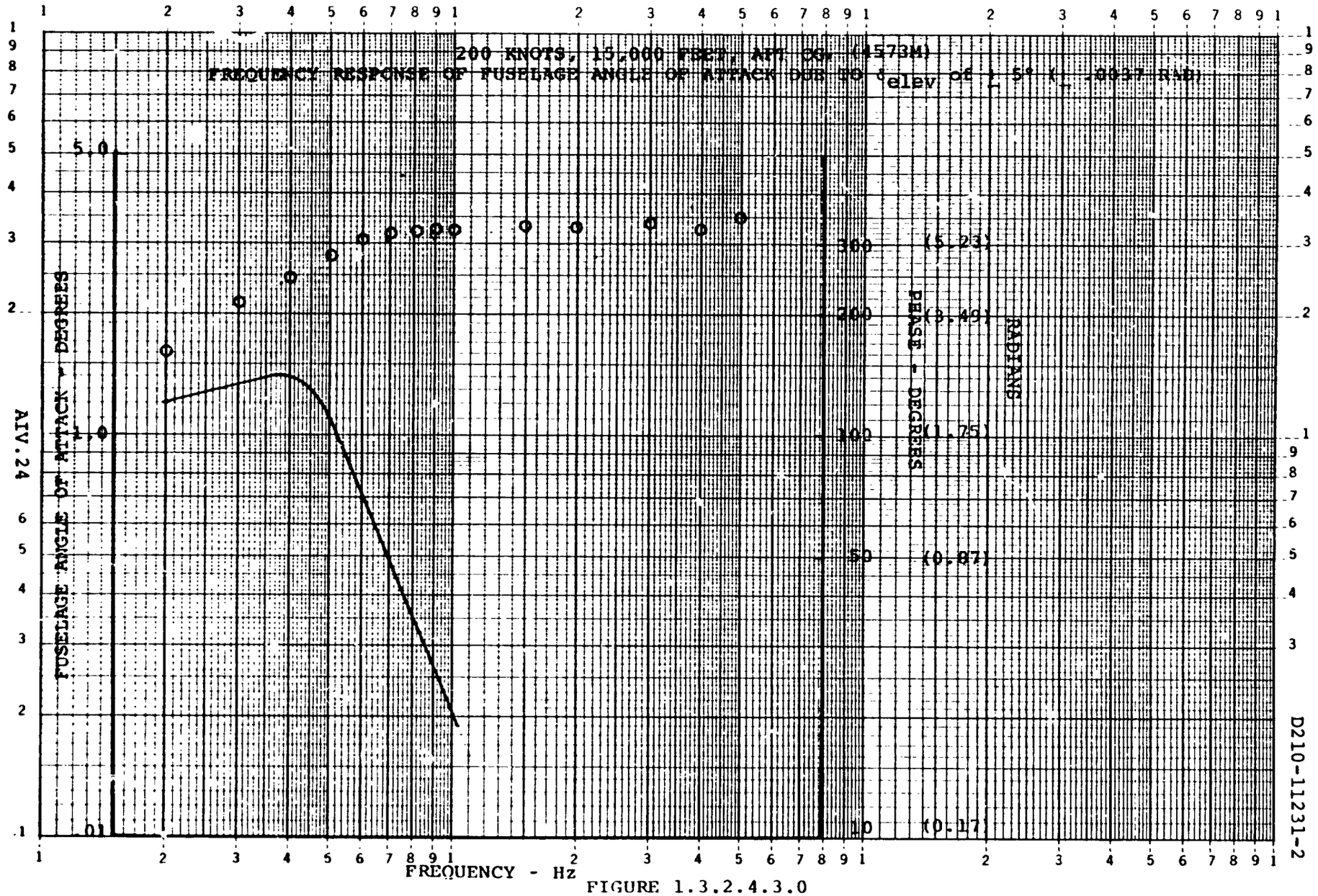

FIGURE 1.3.2.4.3.0

K·E LOGARITHMIC • 2 X 3 CYCLES
KEUFFEL & ESSER CO MADE IN U.S.A.
46 7323

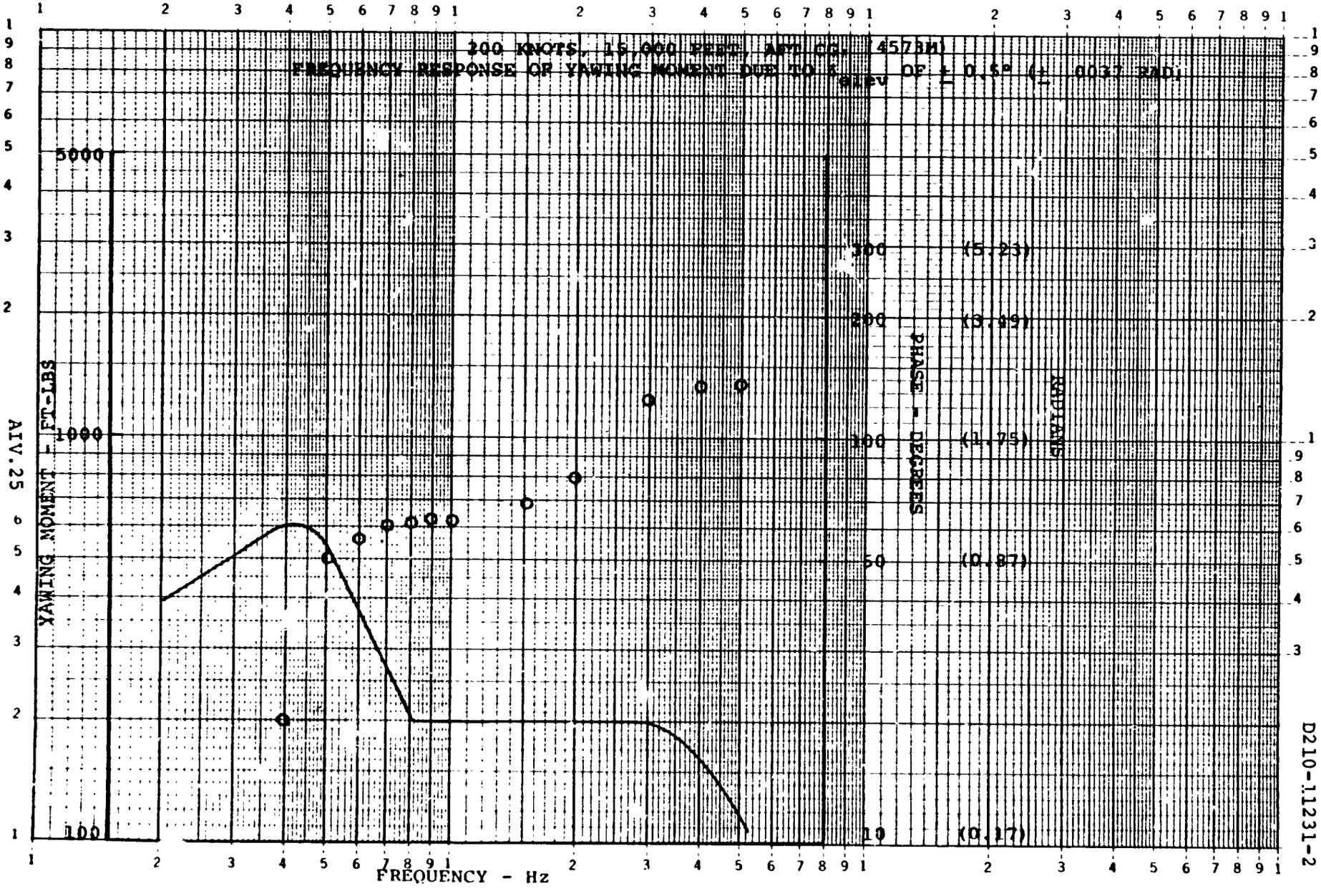

FIGURE 1.3.2.5.3.0

K•E LOGARITHMIC • 2 X 3 CYCLES
KEUFFEL & ESSER CO. MADE IN U.S.A.

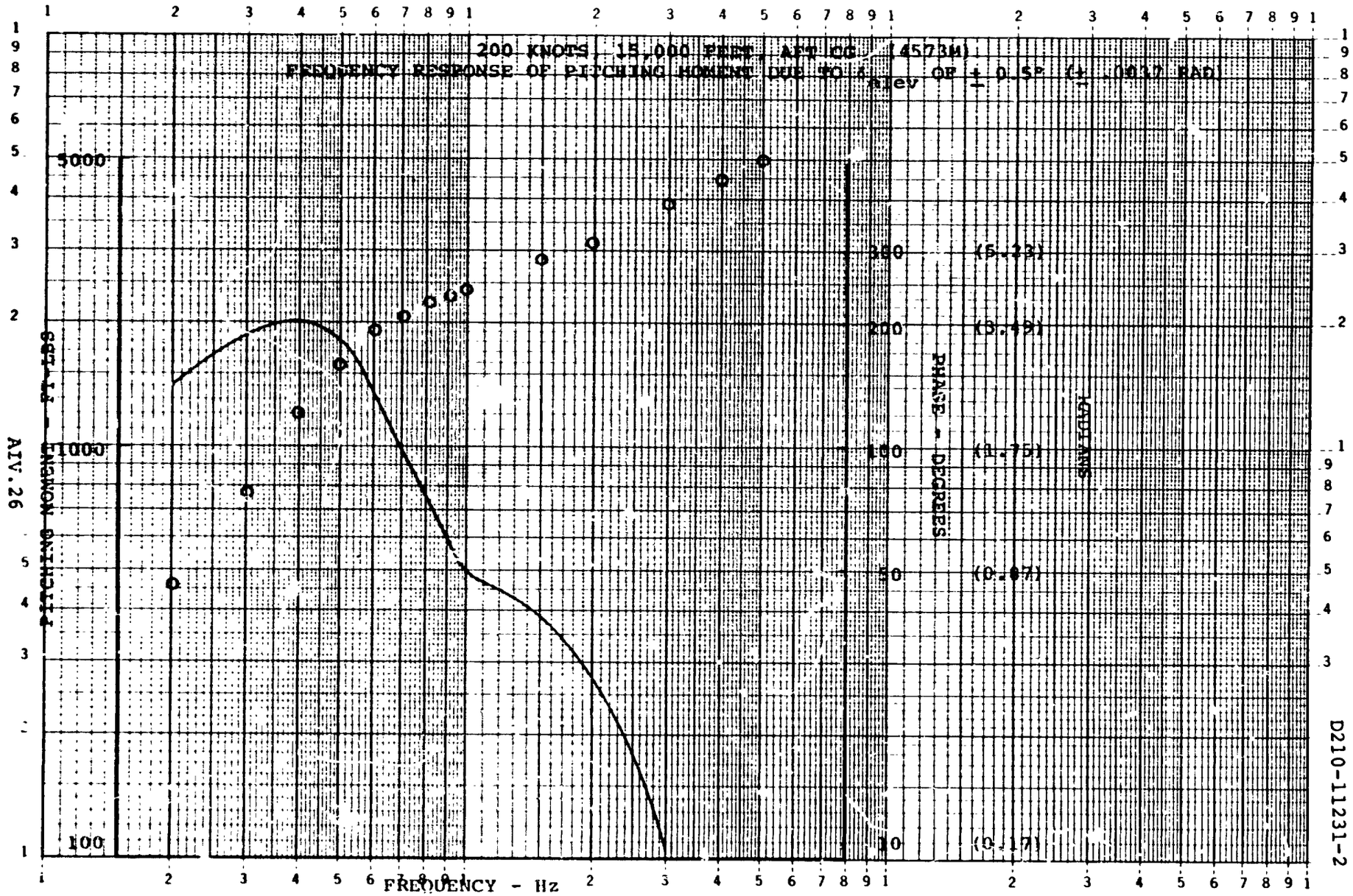

FIGURE 1.3.2.6.3.0

K+E LOGARITHMIC • 2 X 3 CYCLES
KEUFFEL & ESSER CO. MADE IN U.S.A.

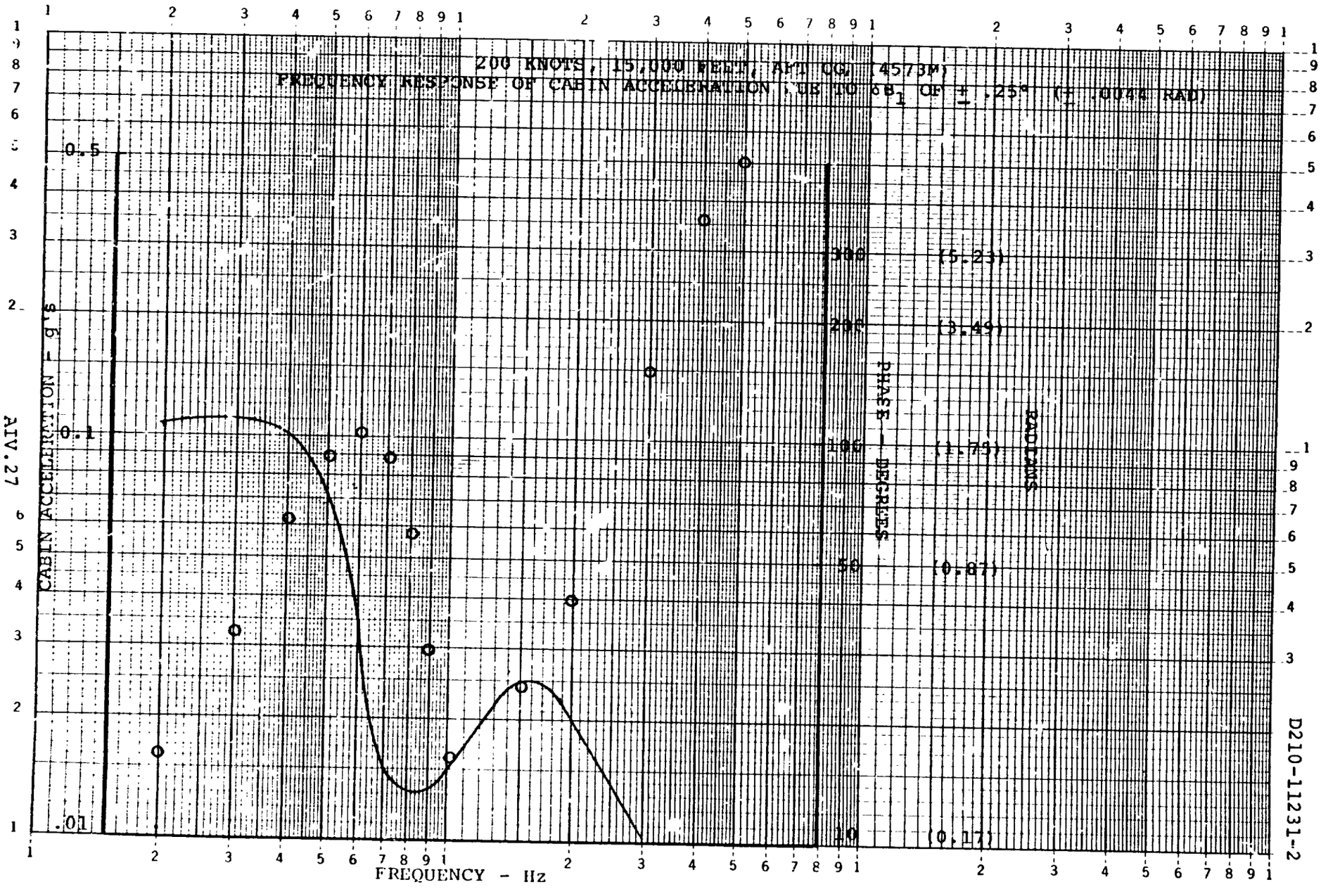

FIGURE 1.3.2.1.5.0

K•E LOGARITHMIC • 2 X 3 CYCLES
KEUFFEL & ESSER CO. MADE IN U.S.A.

46 7323

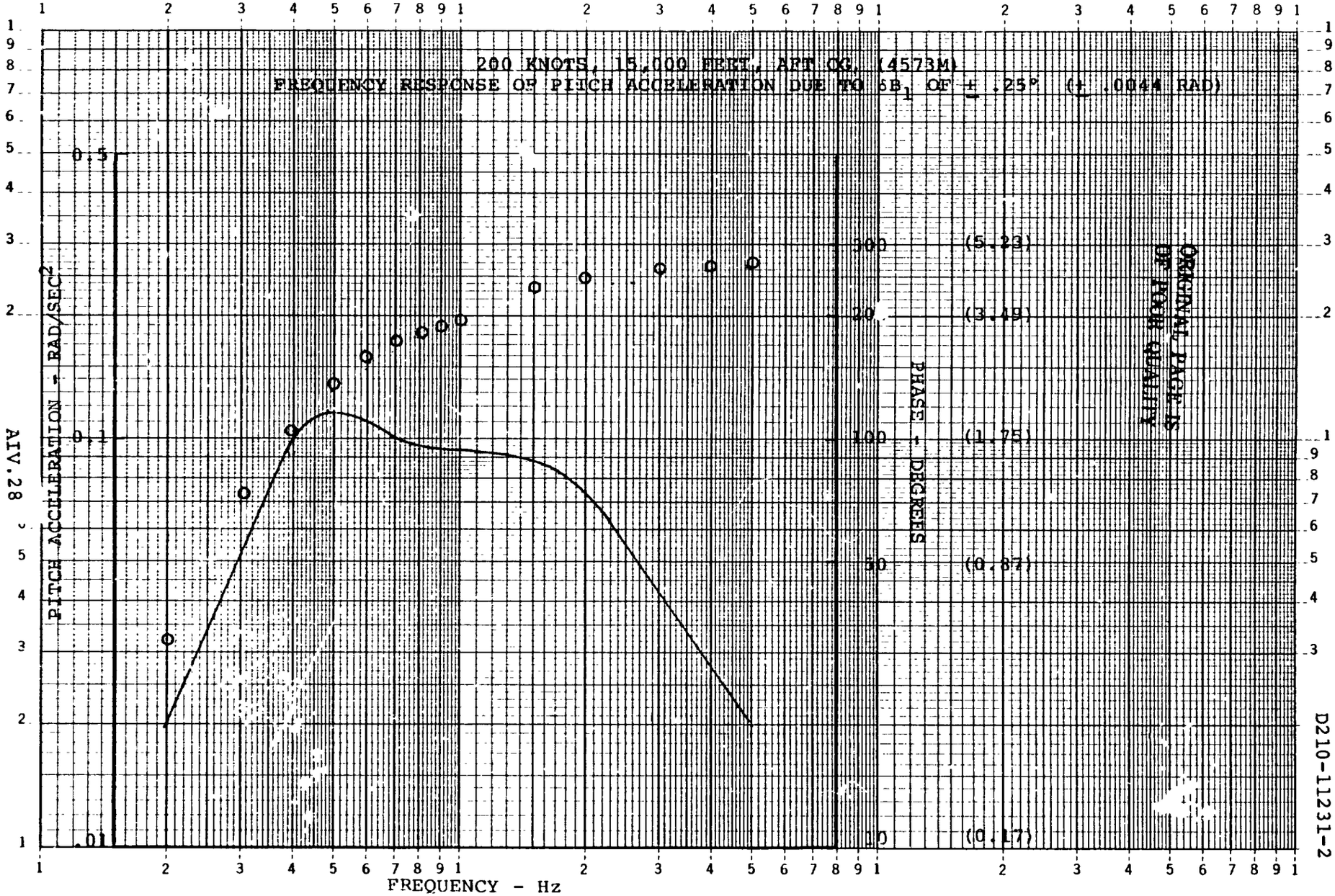

FIGURE 1.3.2.2.5.0

ORIGINAL PAGE IS
OF POOR QUALITY

K+E LOGARITHMIC 2 X 3 CYCLES
KEUFFEL & ESSER CO. MADE IN U.S.A.
46 7323

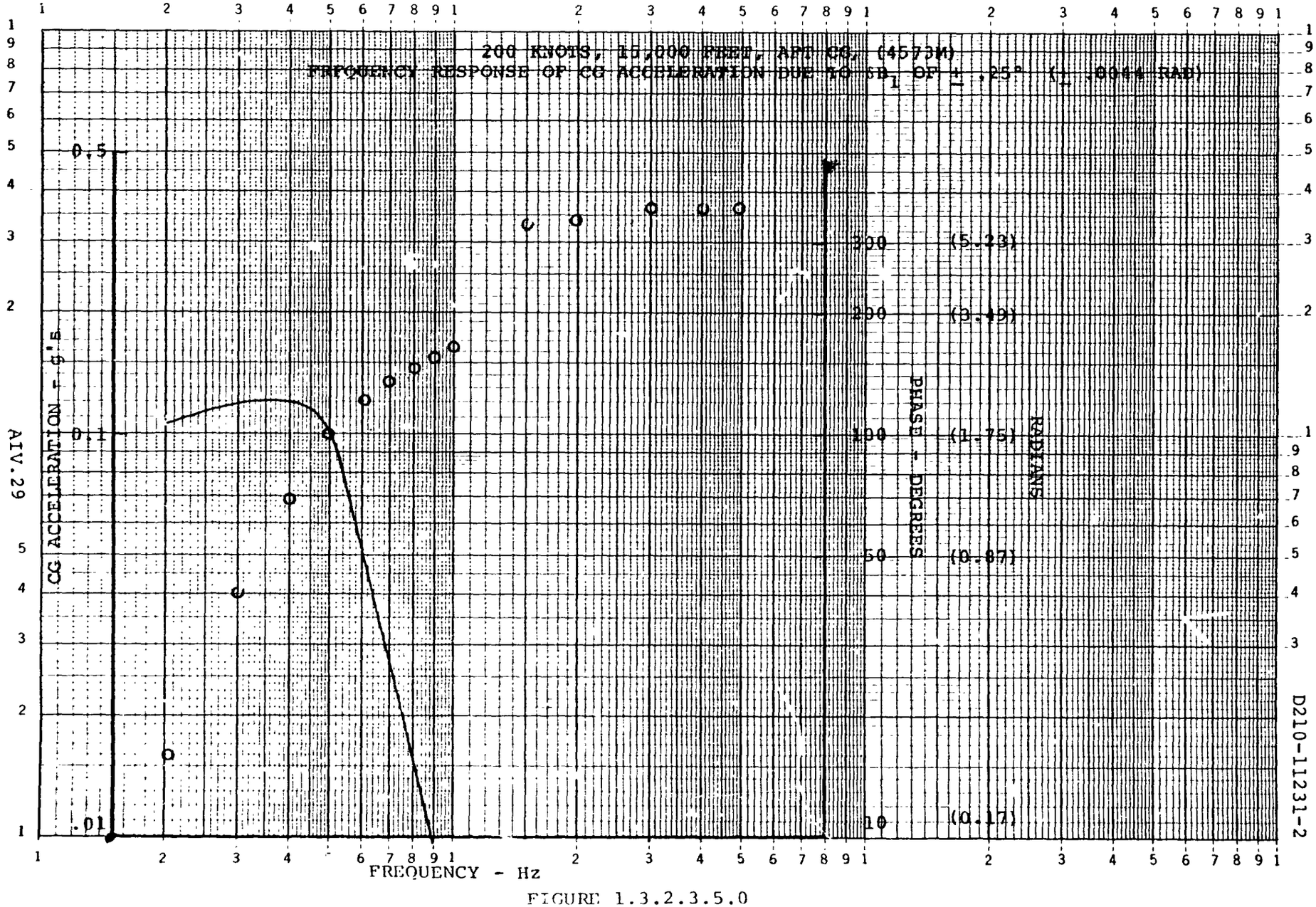

FIGURE 1.3.2.3.5.0

K·E LOGARITHMIC • 2 X 3 CYCLES
KEUFFEL & ESSER CO MADE IN U.S.A.

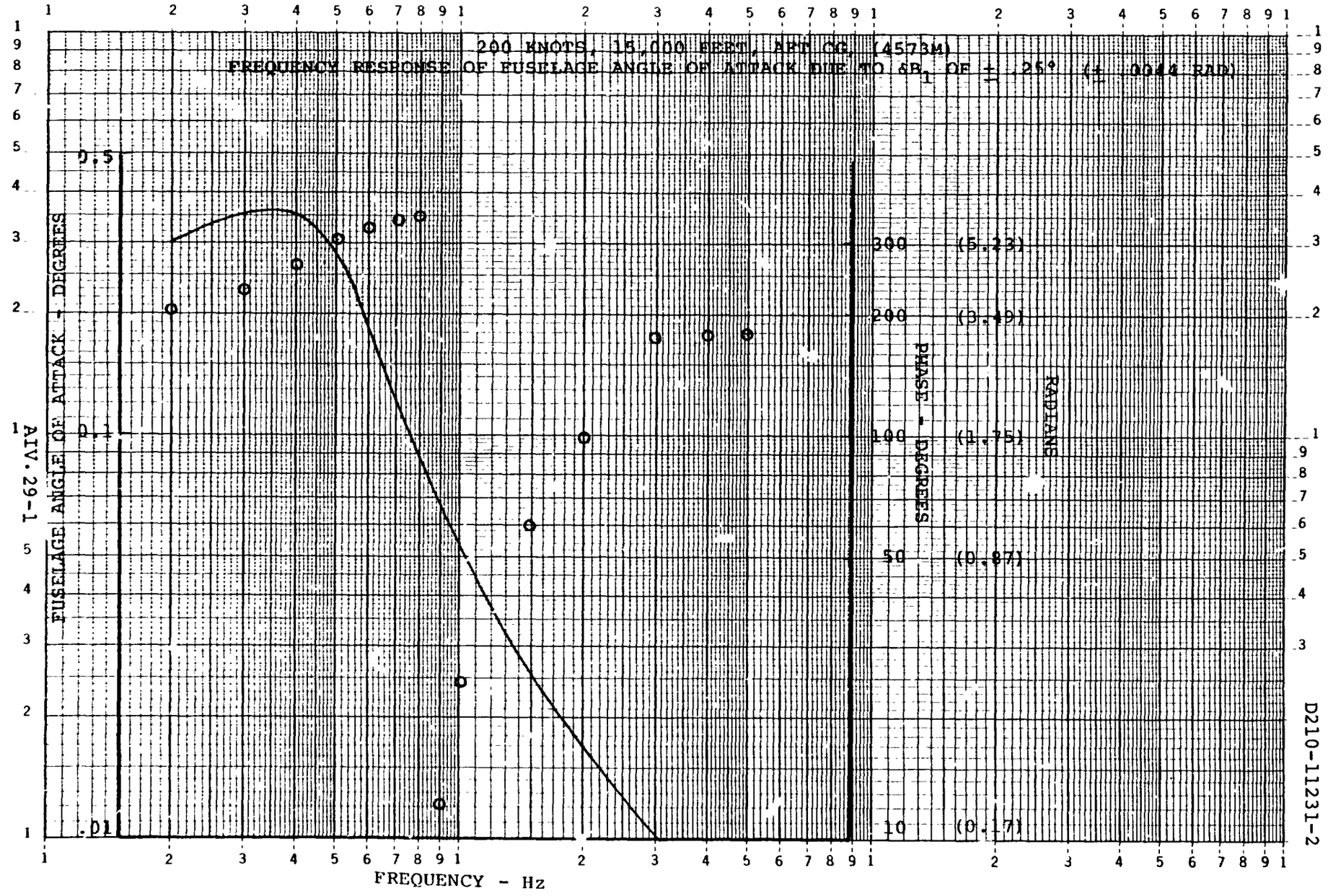

FIGURE 1.3.2.4.5.0

K•E LOGARITHMIC • 2 X 3 CYCLES
KEUFFEL & ESSER CO. MADE IN U.S.A.
46 7323

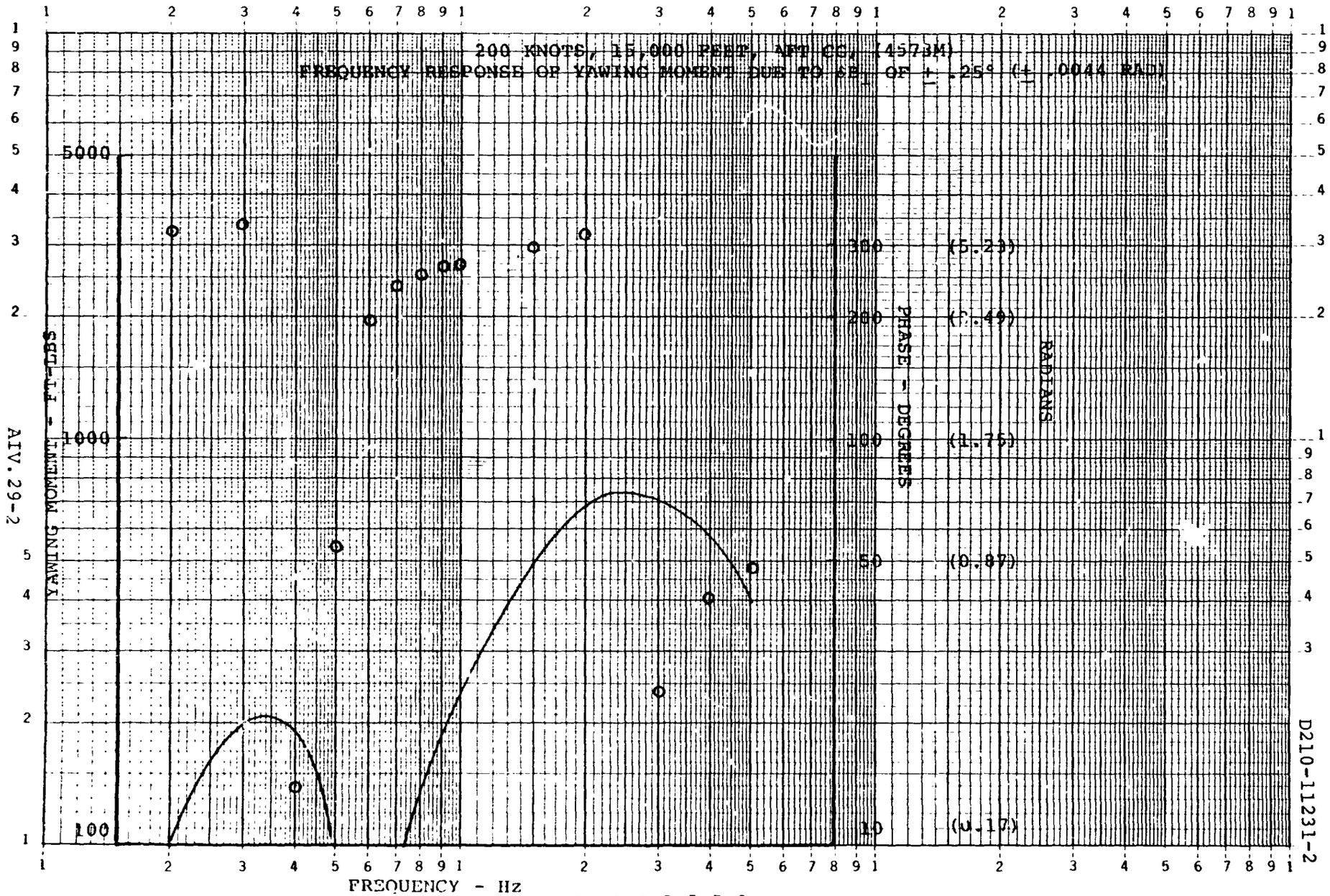

FIGURE 1.3.2.5.5.0

K+E LOGARITHMIC • 2 X 3 CYCLES
KEUFFEL & ESSER CO MADE IN U.S.A.

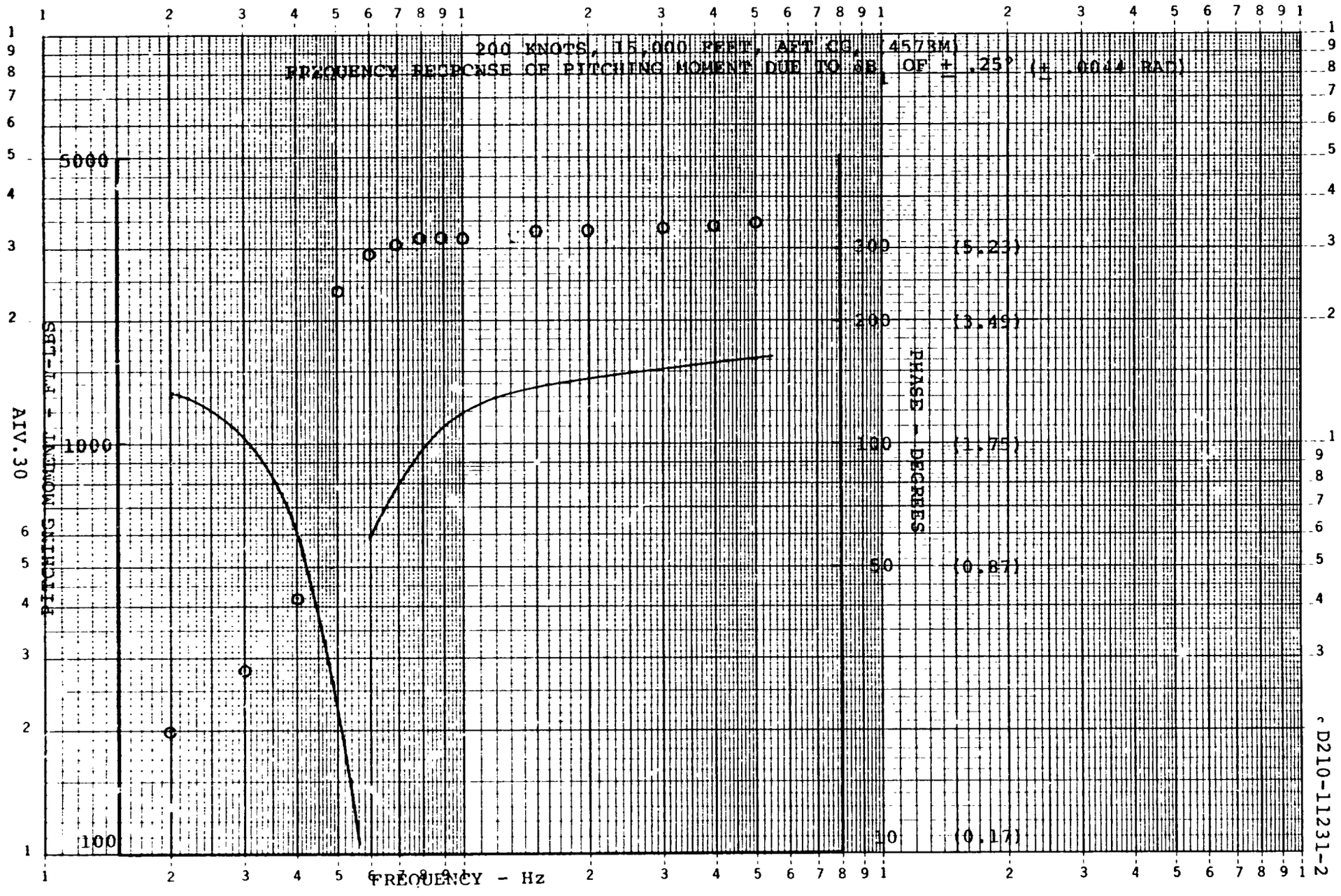

FIGURE 1.3.2.6.5.0

NO 340R-L410 DIETZGEN GRAPH PAPER
SEMI-LOGARITHMIC
4 CYCLES X 10 DIVISIONS PER INCH

EUGENE DIETZGEN CO.
MADE IN U.S.A.

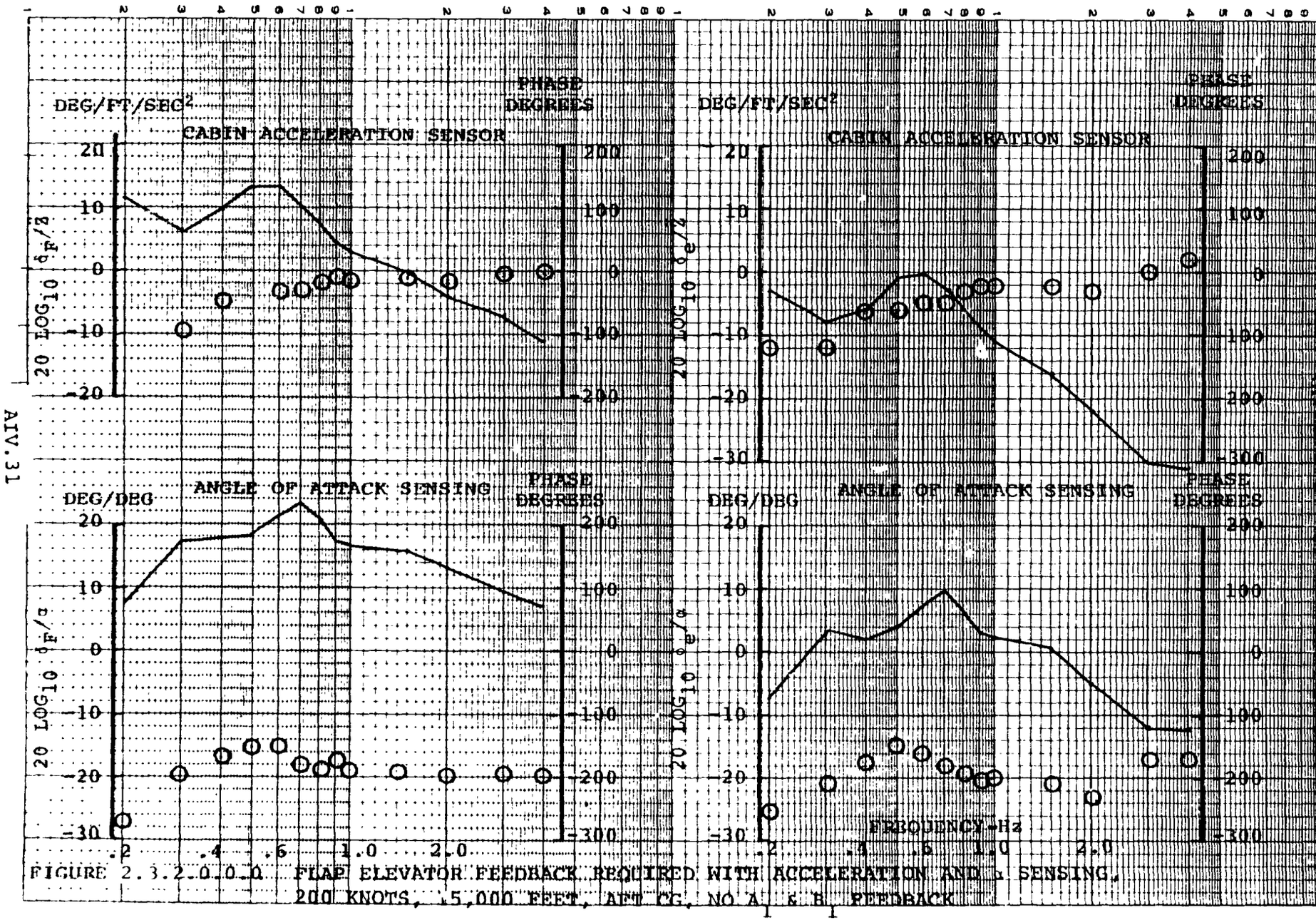

FIGURE 2.3.2.0.0.0 FLAP ELEVATOR FEEDBACK REQUIRED WITH ACCELERATION AND α SENSING.
200 KNOTS, 15,000 FEET, AFT CG, NO A & B FEEDBACK

ORIGINAL PAGE IS
OF POOR QUALITY

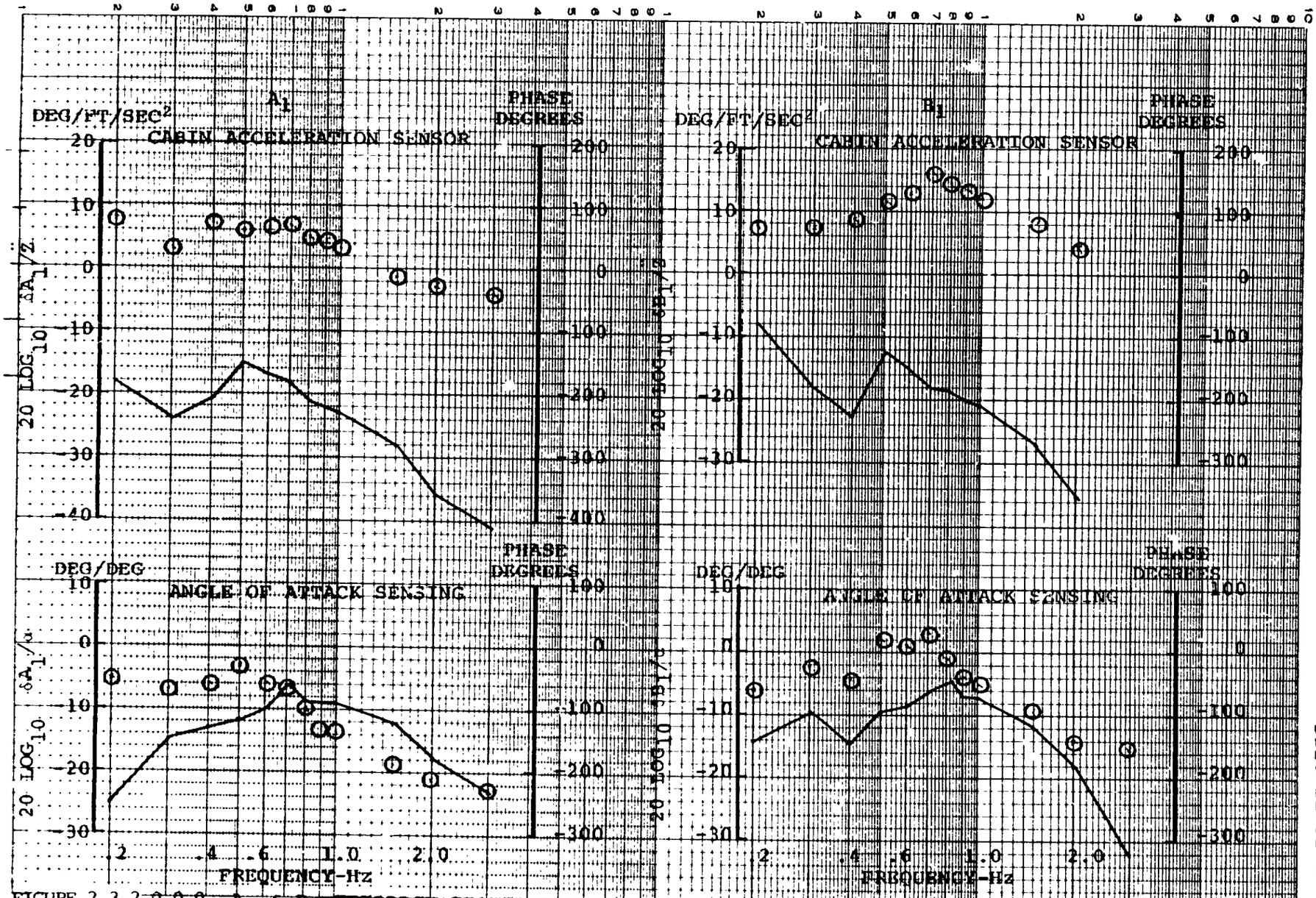

FIGURE 2.3.2.0.0.0. A_1 & B_1 FEEDBACK REQUIRED WITH ACCELERATION AND α SENSING RESPECTIVELY, 200 KNOTS, AFT CG, 15,000 FEET

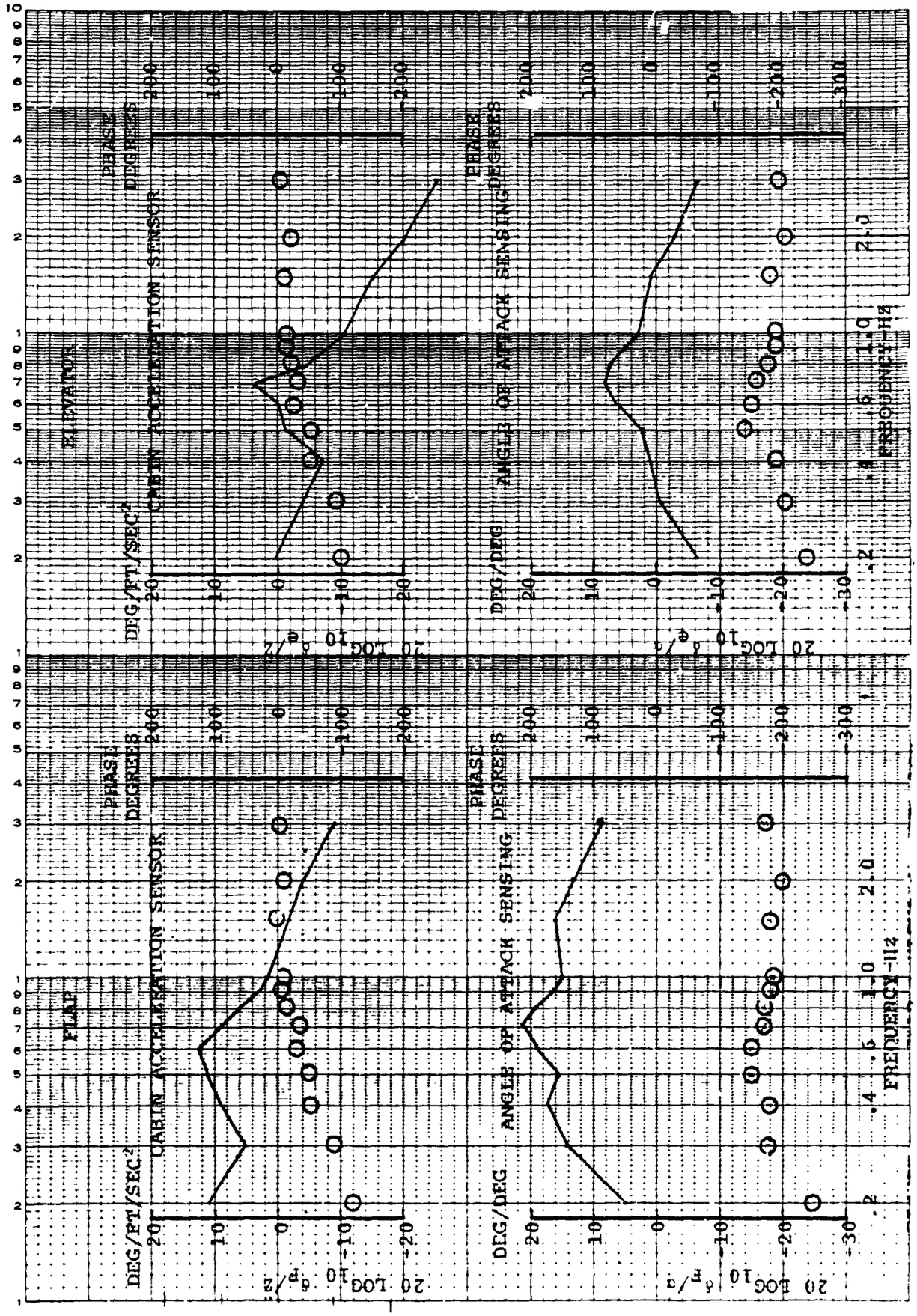

FIGURE 2.3.2.0.0.0. FLAP & ELEVATOR FEEDBACK REQUIRED WITH ACCELERATION AND α SENSING RESPECTIVELY, 200 KNOTS, AFT CG, 15,000 FEET, WITH A_1 & B_1 FEEDBACK

ORIGINAL PAGE IS
OF POOR QUALITY

FLIGHT CONDITION: 200 KNOTS, 5,000 FEET, (1,524m), FWD CG

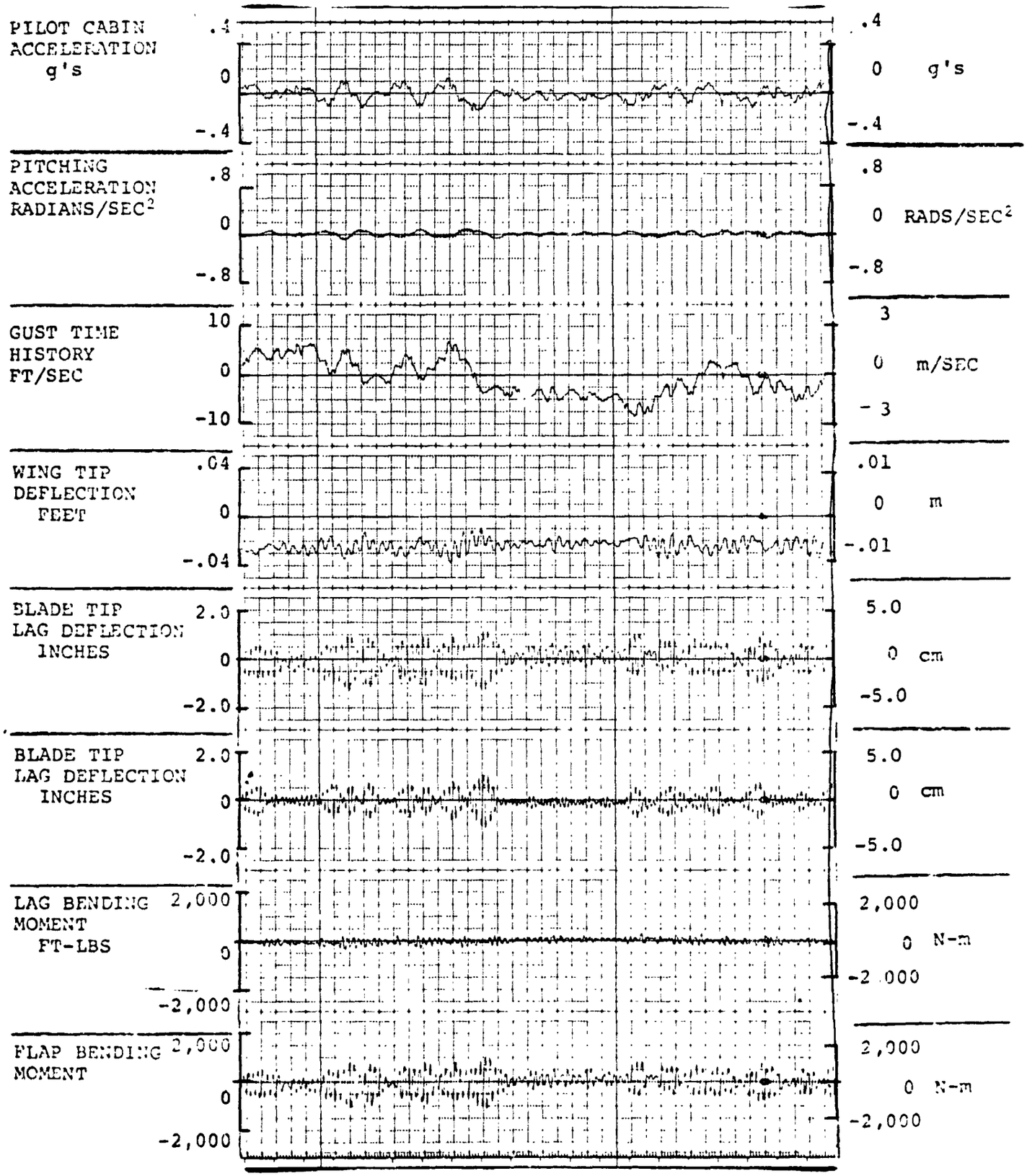

FIGURE 3.1.1.0.0.1. RESPONSES FOR GAIN F = 0, GAIN E = 0

FLIGHT CONDITION: 200 KNOTS, 5,000 FEET, (1,524m), FWD CG

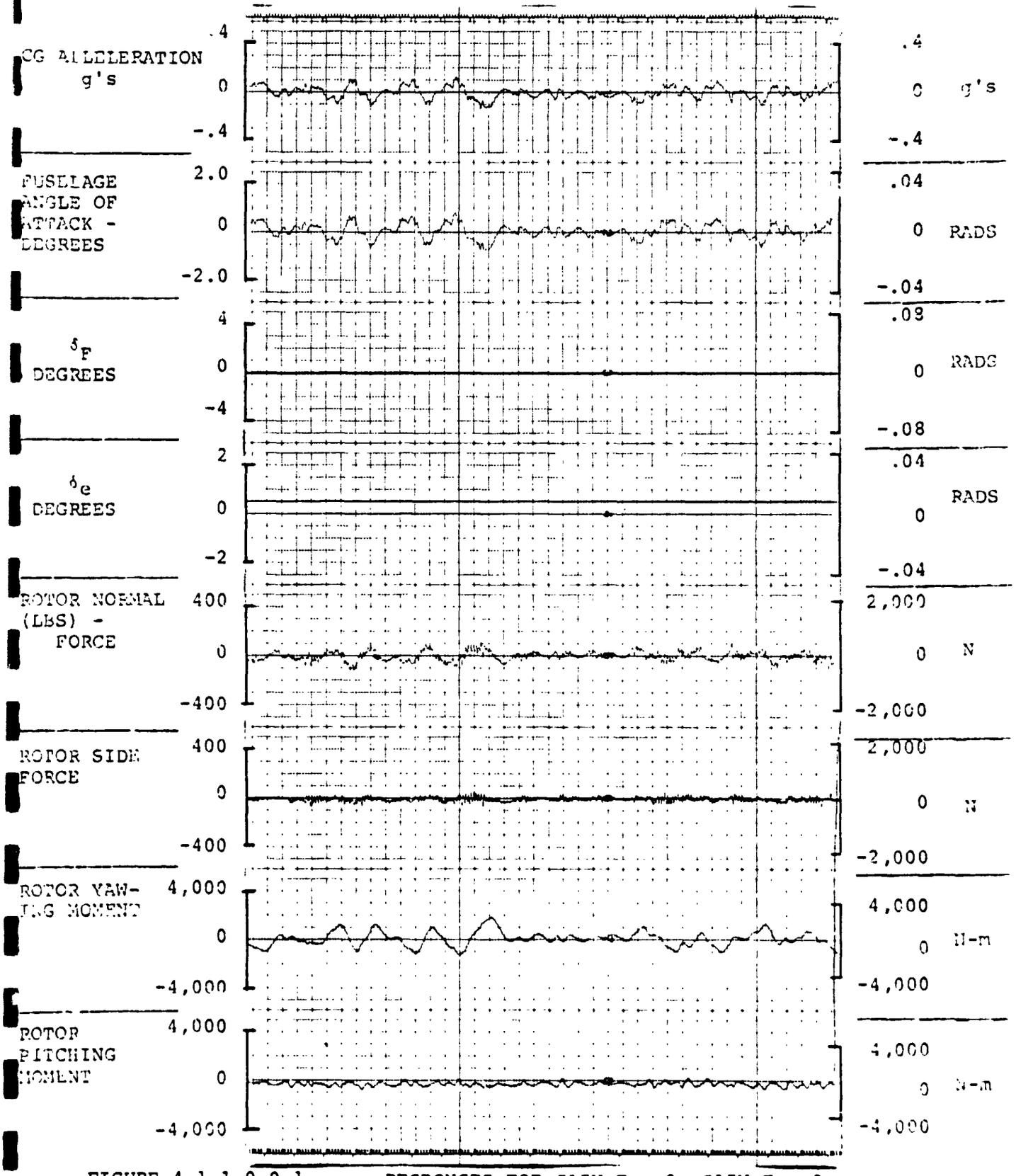

FIGURE 4.1.1.0.0.1. RESPONSES FOR GAIN F = 0, GAIN E = 0

FLIGHT CONDITION: 200 KNOTS, 5,000 FEET, (1,524m), CG

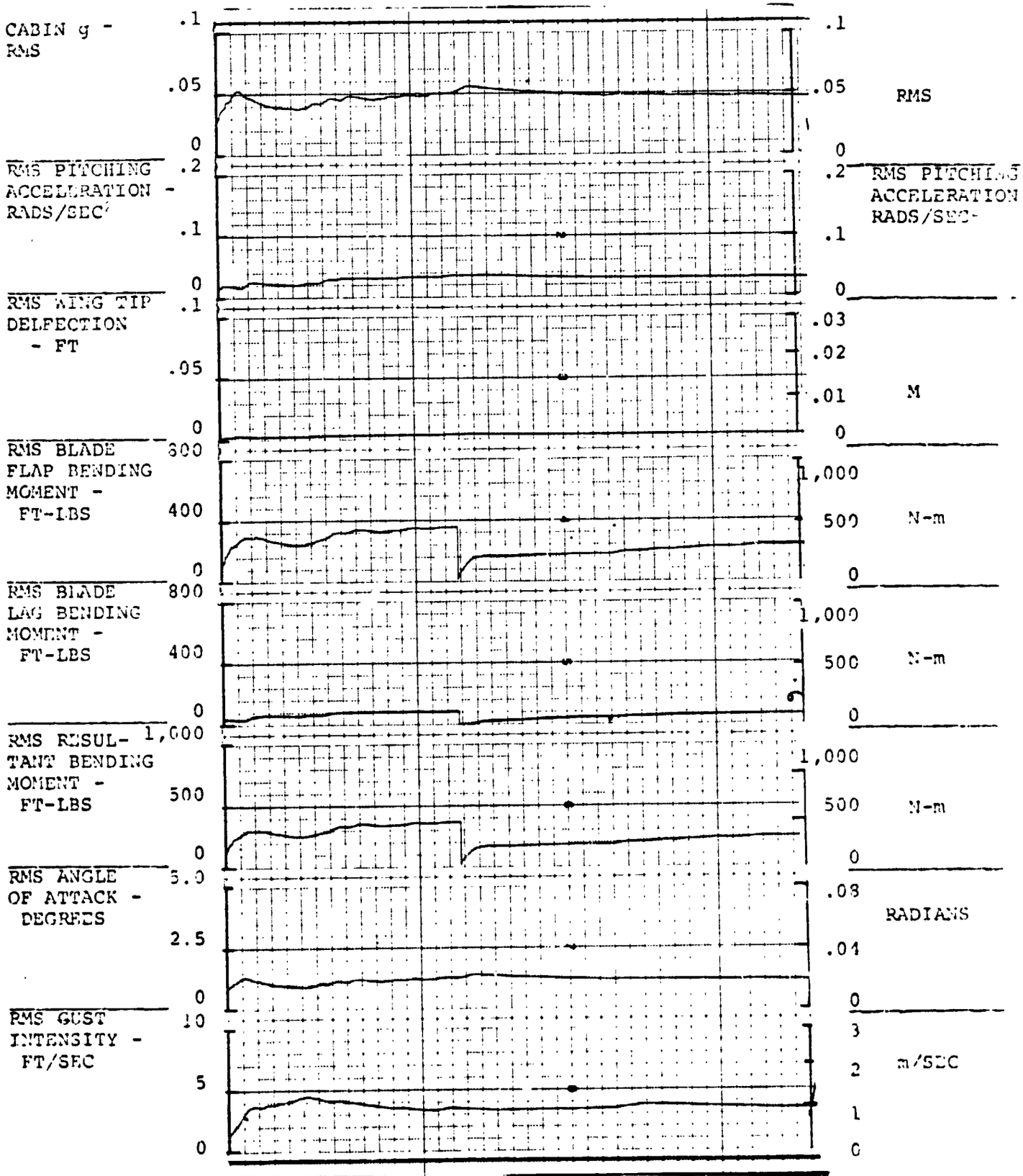

FIGURE 5.1.1.0.0.1. RESPONSES FOR GAIN F = 0, GAIN E = 0

FLIGHT CONDITION: 200 KNOTS, 5,000 FEET, (1,524m), FWD CG

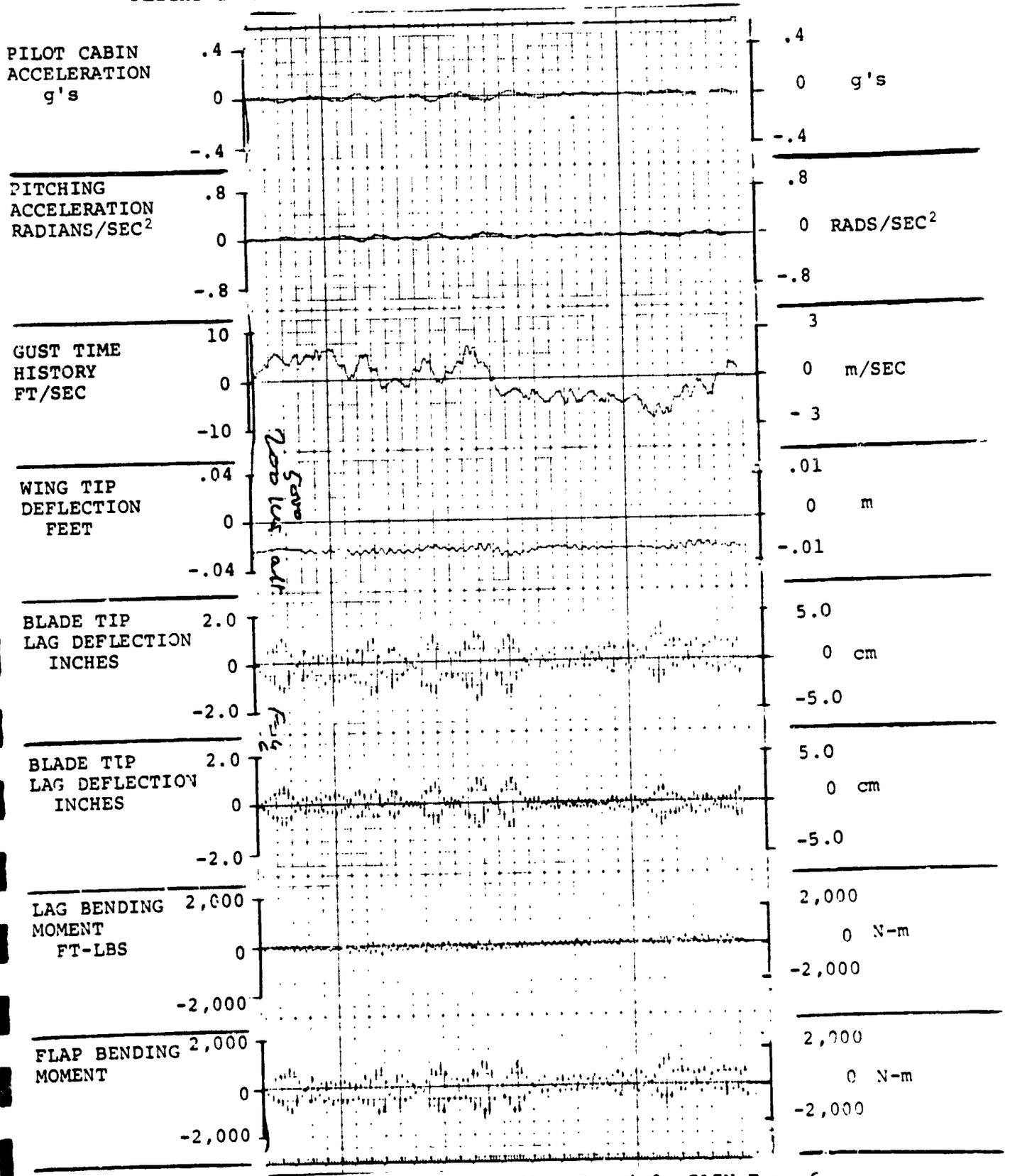

FIGURE 3.1.1.0.0.2. RESPONSES FOR GAIN F = 4.0, GAIN E = .6

FLIGHT CONDITION: 200 KNOTS, 5,000 FEET, (1,524m), FWD CG

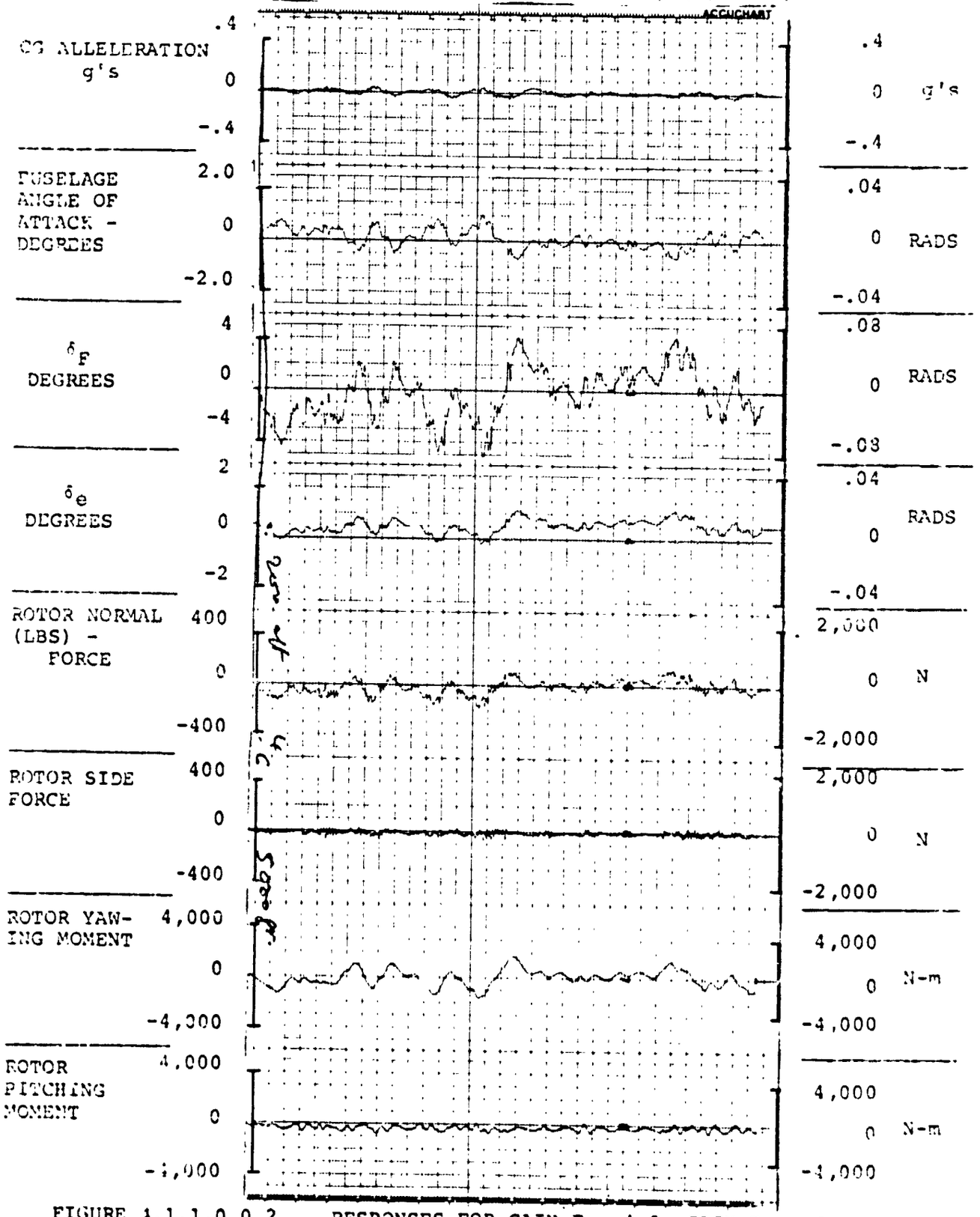

FIGURE 1.1.1.0.0.2. RESPONSES FOR GAIN F = 4.0, GAIN E = .6

ORIGINAL PAGE IS
OF POOR QUALITY

FLIGHT CONDITION: 200 KNOTS, 5,000 FEET, (1,524m), FWD CG

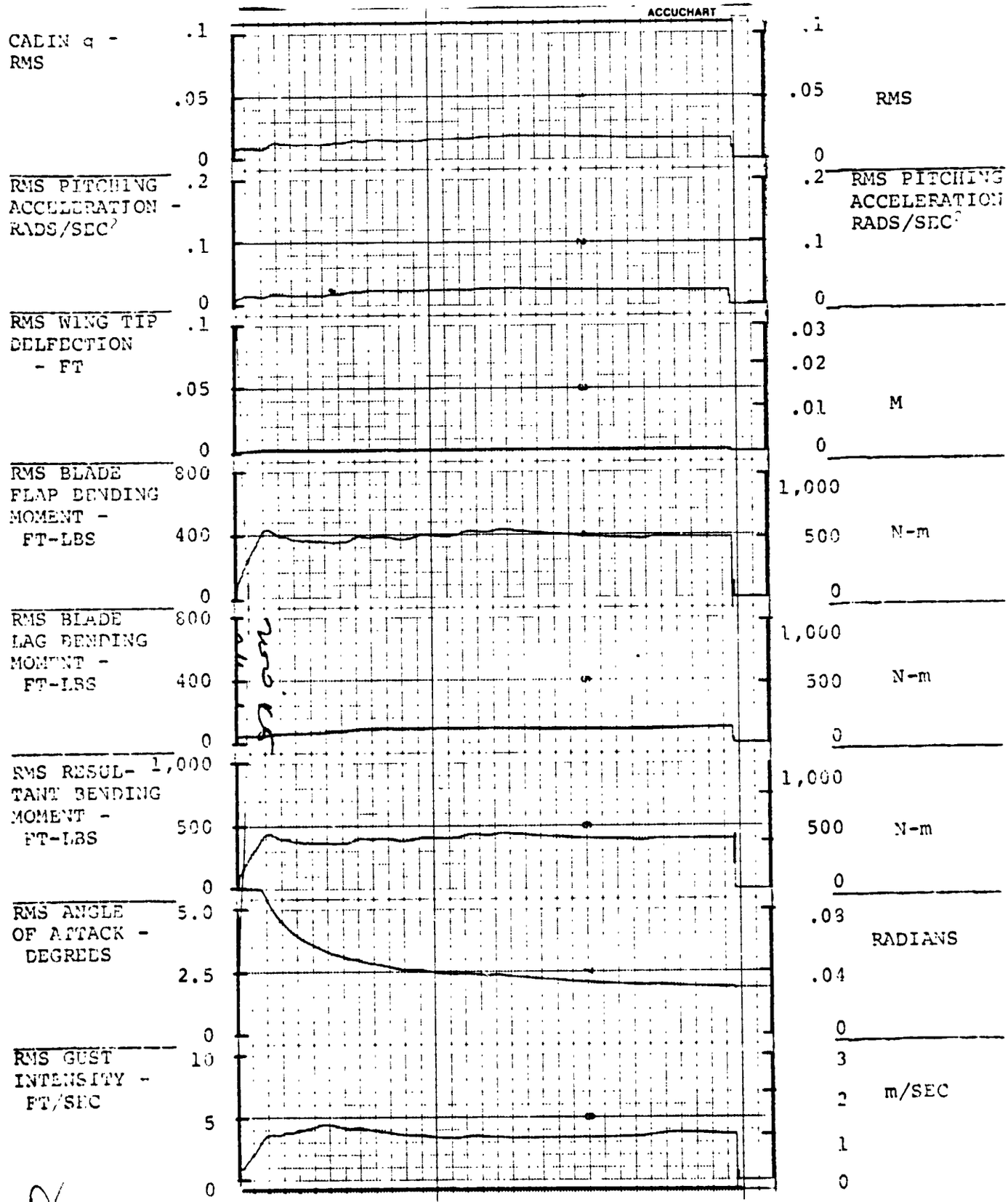

FIGURE 5.1.1.0.0.2. RESPONSES FOR GAIN F = 4.0, GAIN E = .6

FLIGHT CONDITION: 200 KNOTS, 5,000 FEET, (1,524m), FWD CG

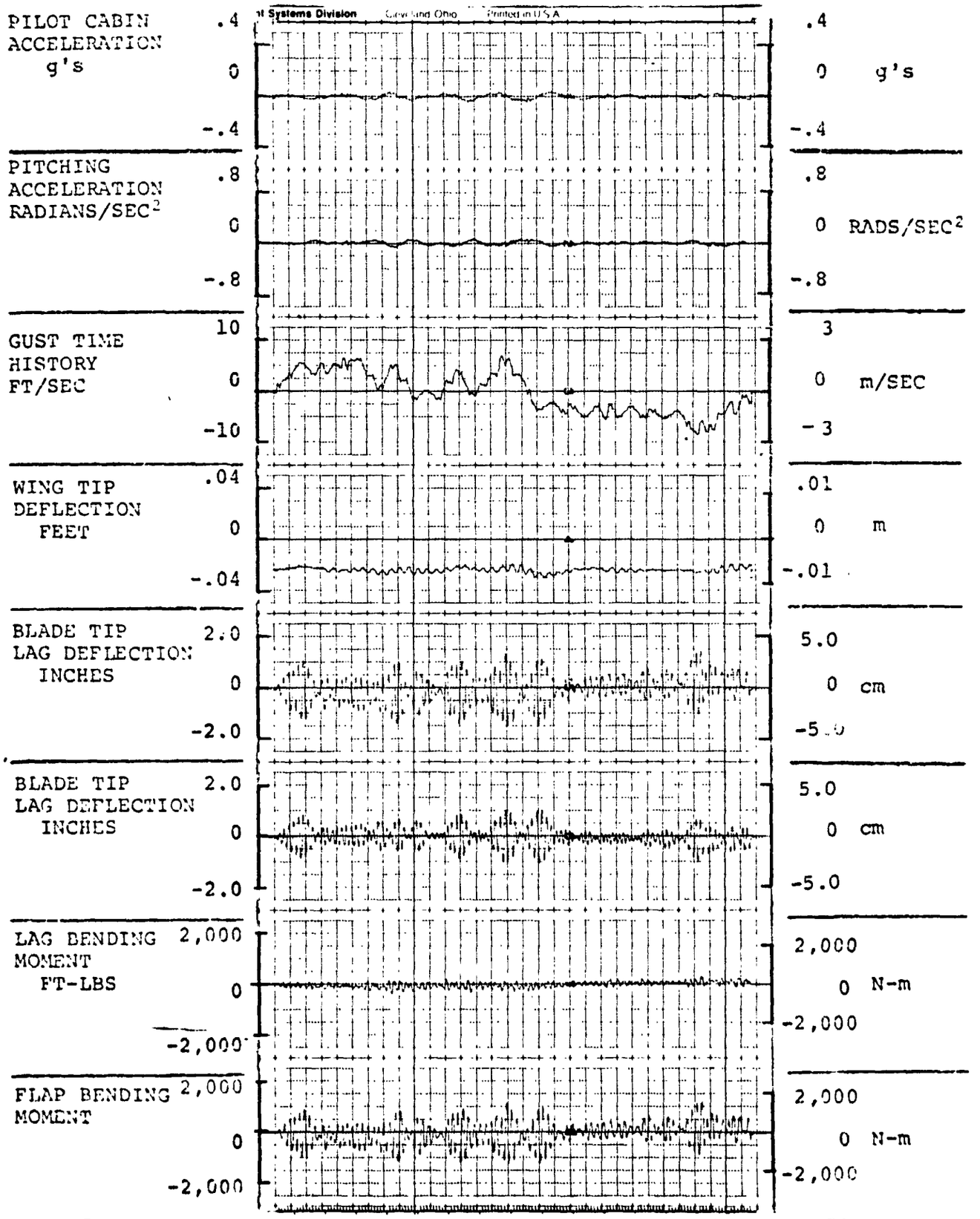

FIGURE 3.1.1.0.0.6. RESPONSES FOR GAIN F = 4.8, GAIN E = .72

FLIGHT CONDITION: 200 KNOTS, 5,000 FEET, (1,524m), FWD CG

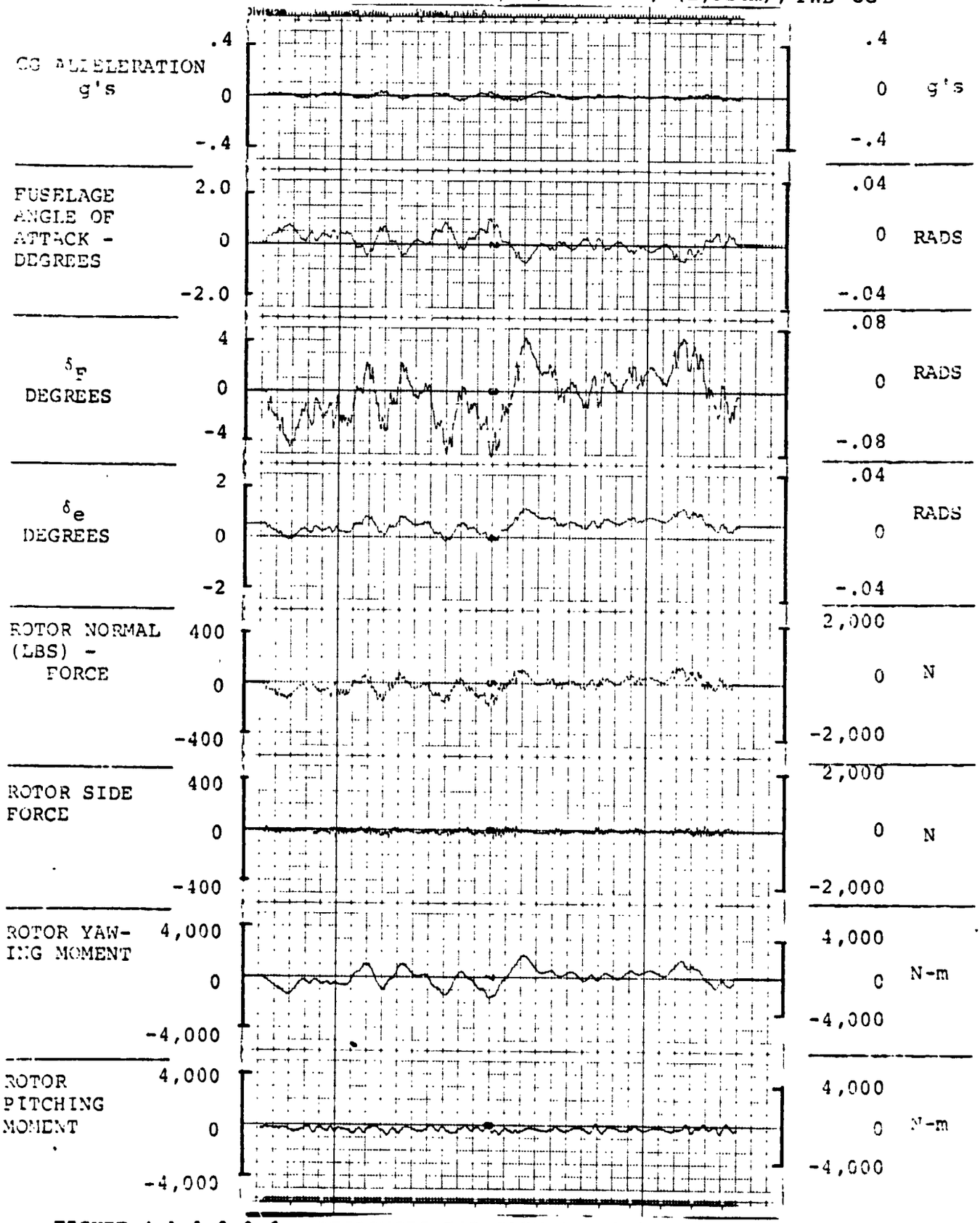

FIGURE 4.1.1.0.0.6. RESPONSES FOR GAIN F = 4.8, GAIN E = .72

FLIGHT CONDITION: 200 KNOTS, 5,000 FEET, (1,524m), FWD CG

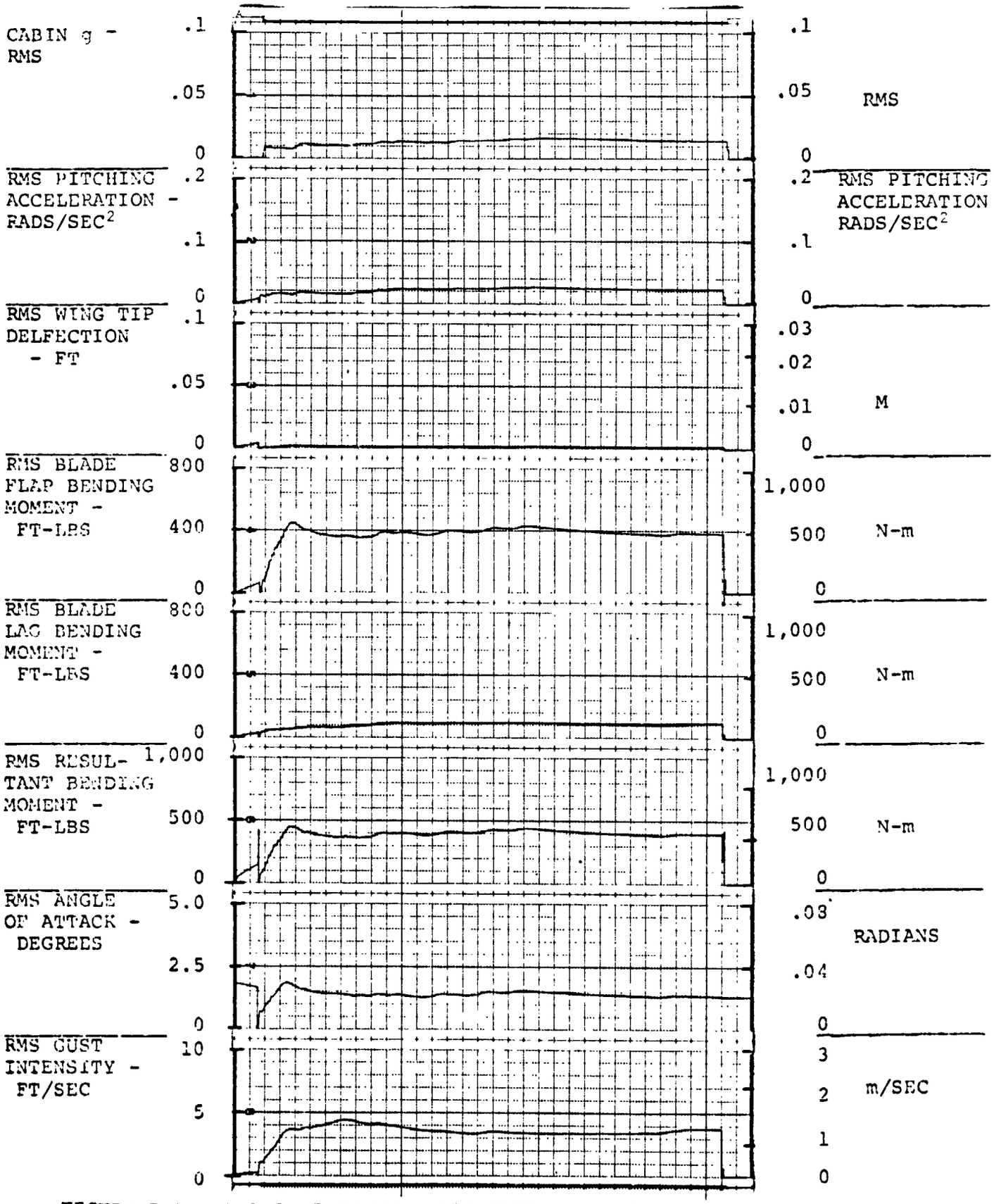

FIGURE 5.1.1.0.0.6. RESPONSES FOR GAIN F = 4.8, GAIN E = .72

FLIGHT CONDITION: 200 KNOTS, 10,000 FEET, (3,049m), FORWARD CG

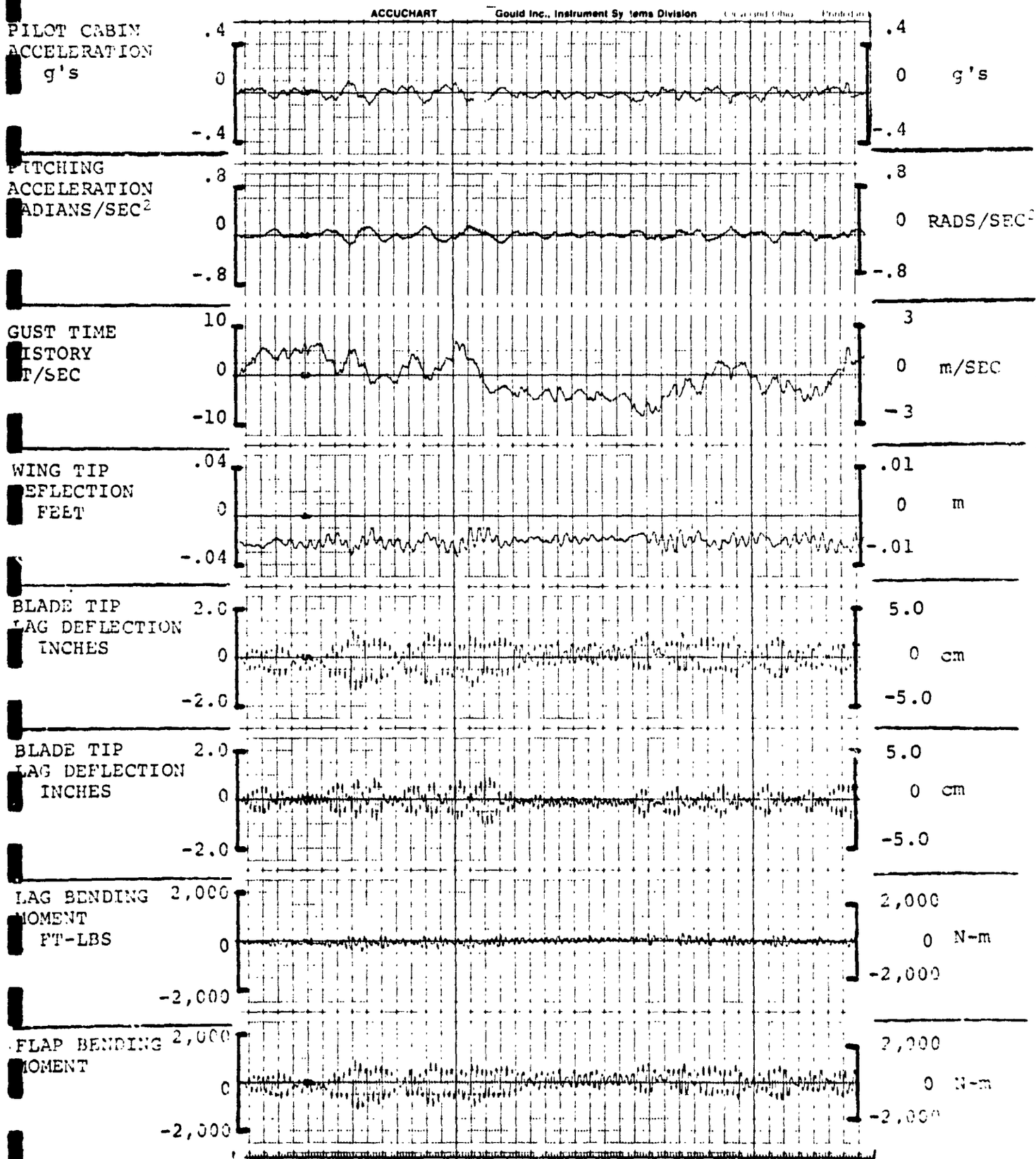

FIGUPE 3.2.1.0.0.1. RESPONSES FOR GAIN F = 0, GAIN E = 0

ORIGINAL PAGE IS
OF POOR QUALITY

FLIGHT CONDITION: 200 KNOTS, 10,000 FEET, (3,049m), FORWARD CG

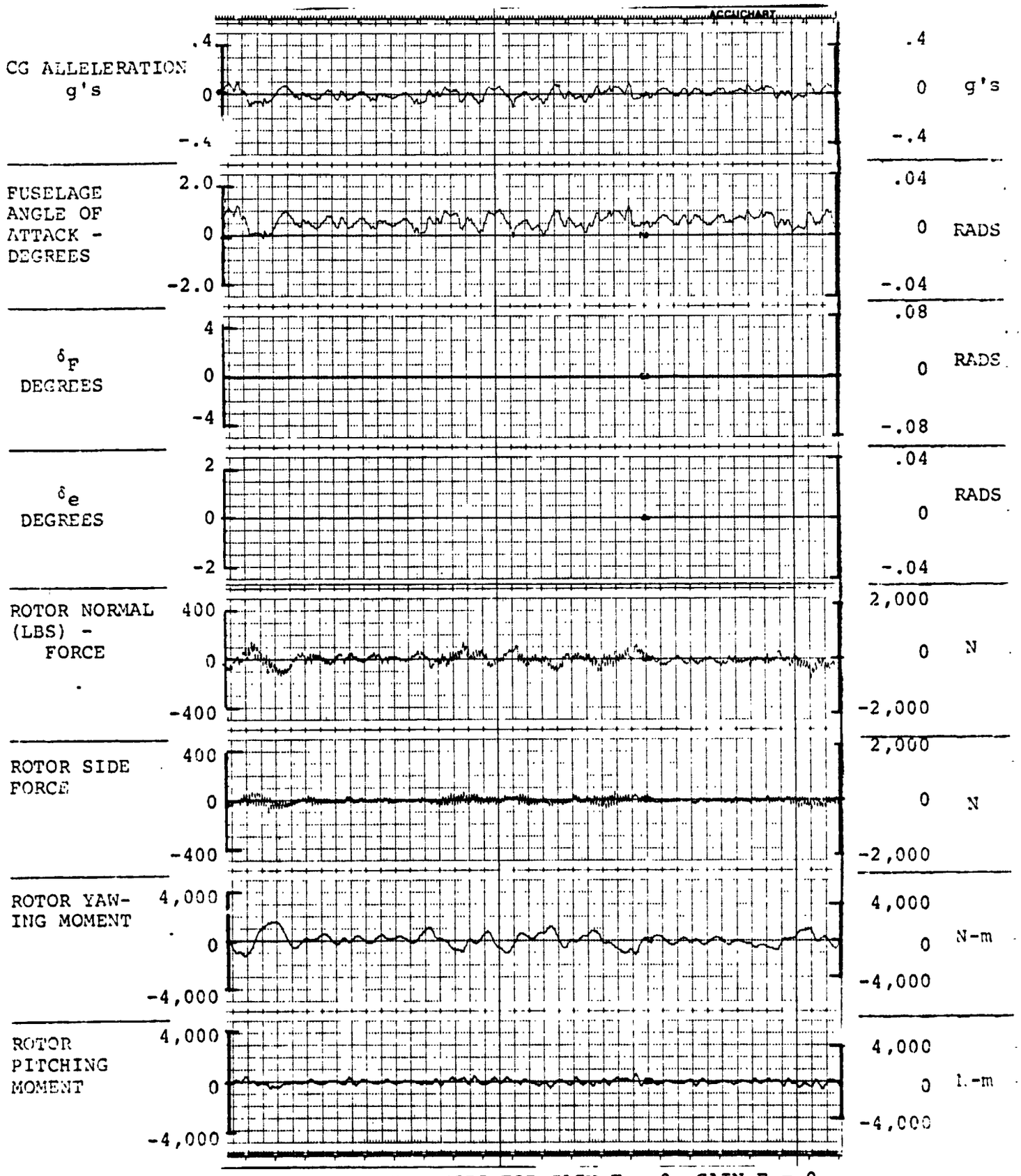

FIGURE 4.2.1.0.0.1. RESPONSES FOR GAIN F = 0, GAIN E = 0

ORIGINAL PAGE IS
OF POOR QUALITY

FLIGHT CONDITION: 200 KNOTS, 10,000 FEET, (3,049m), FORWARD CG

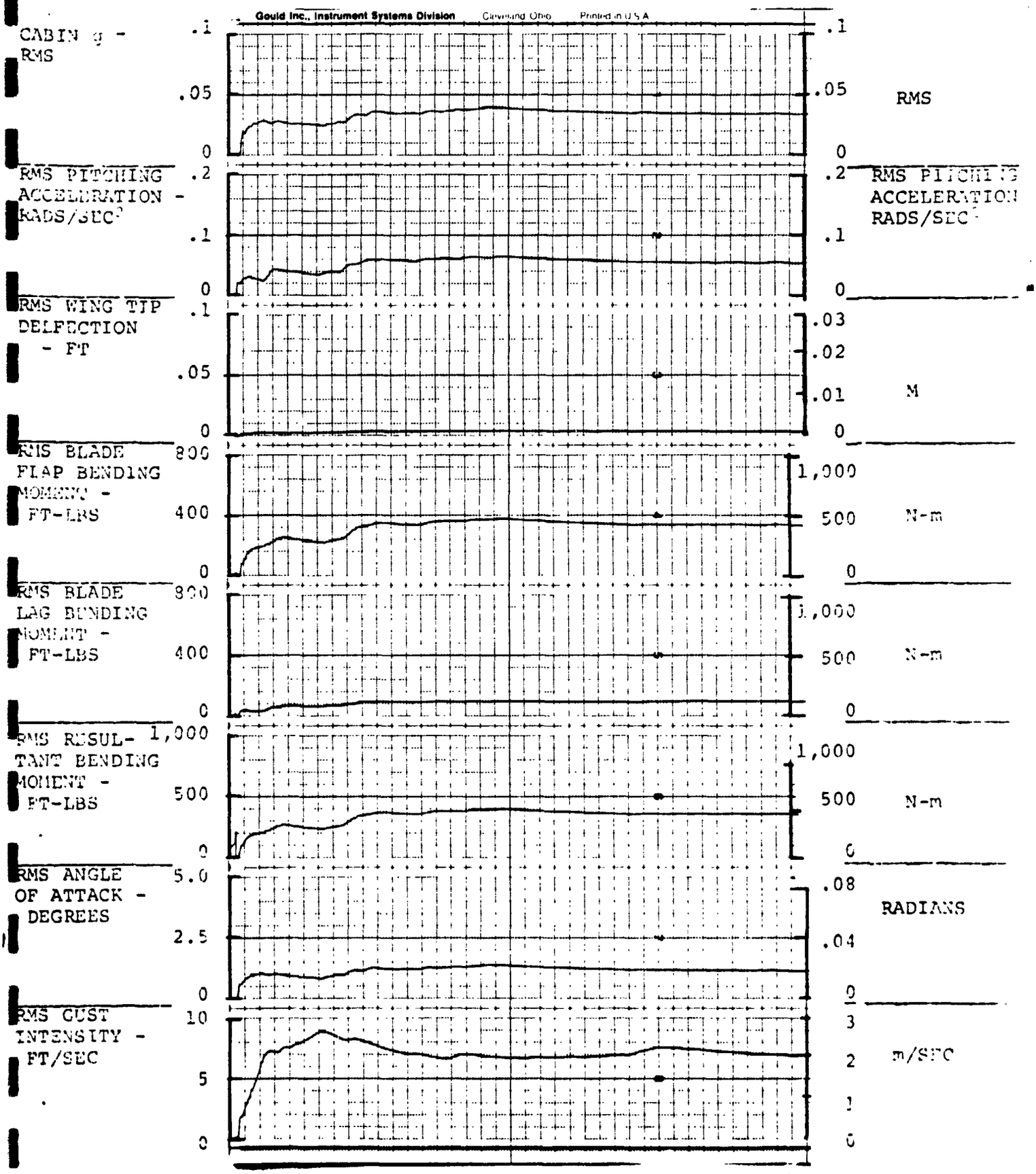

FIGURE 5.2.1.0.0.1. RESPONSES FOR GAIN F = 0, GAIN E = '

ORIGINAL PAGE IS
OF POOR QUALITY

FLIGHT CONDITION: 200 KNOTS, 10,000 FEET, (3,049m), FORWARD CG

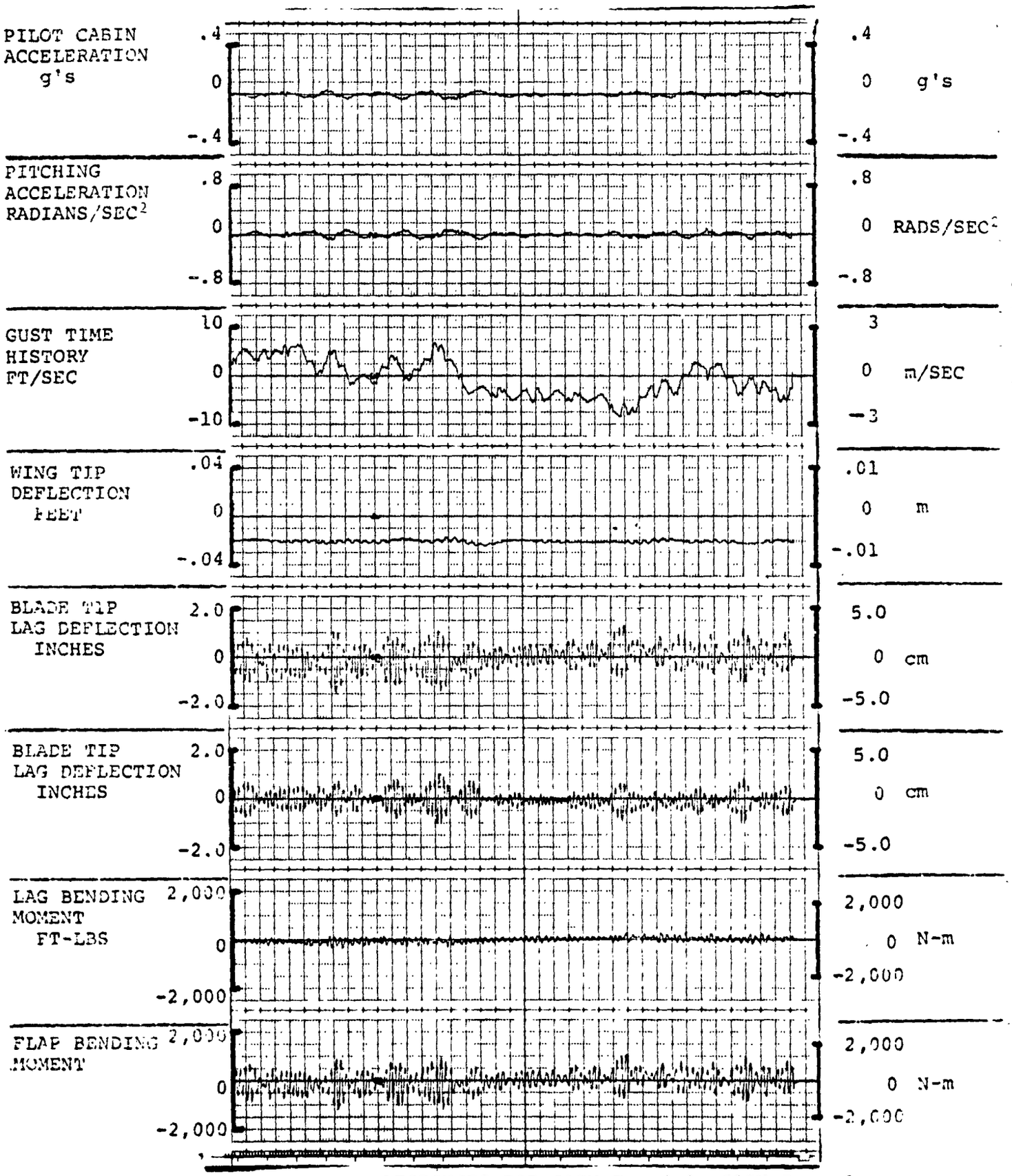

FIGURE 3.2.1.0.0.3. RESPONSES FOR GAIN F = 4.0, GAIN E = .6

FLIGHT CONDITION: 200 KNOTS, 10,000 FEET, (3,049m), FORWARD CG

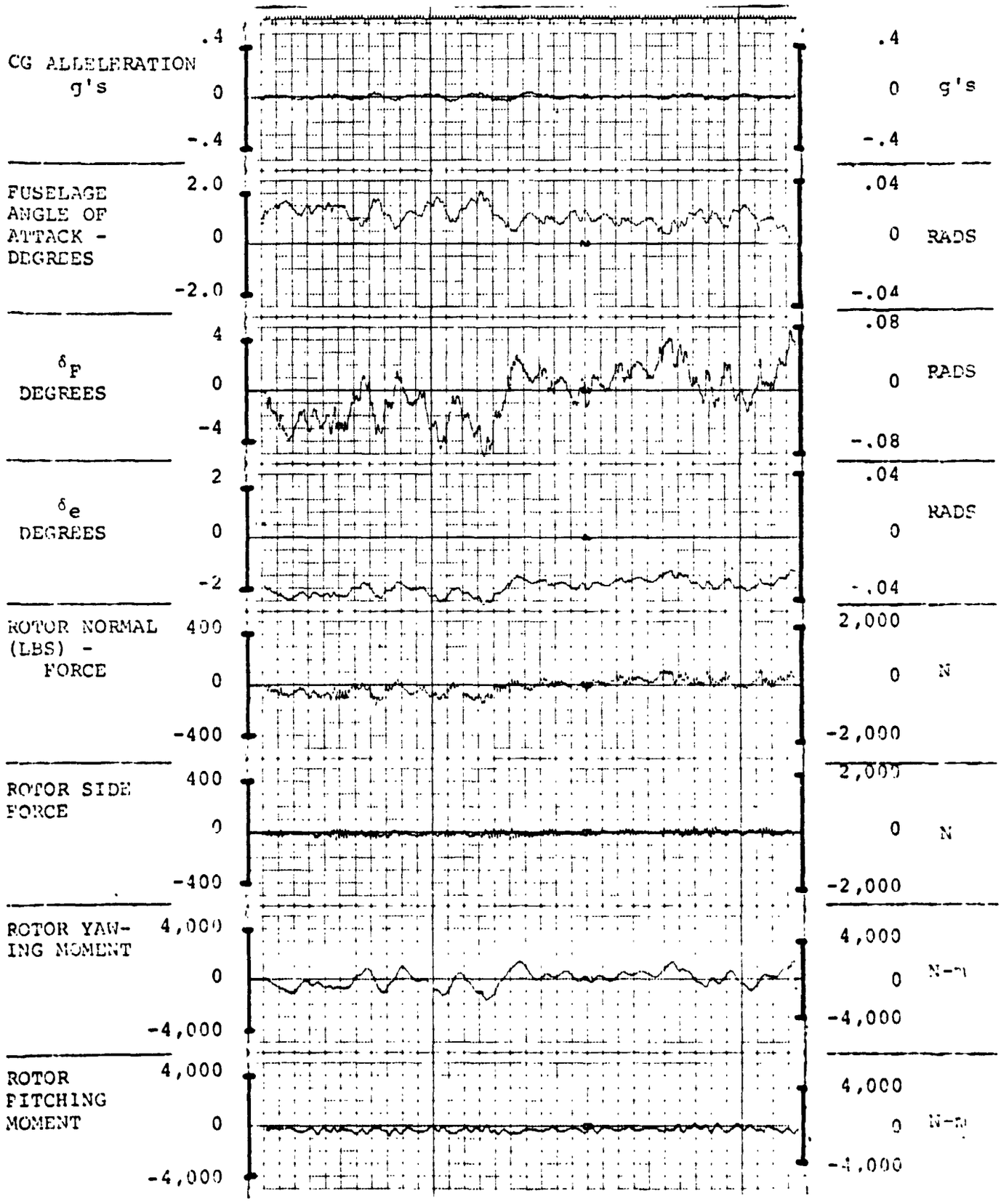

FIGURE 4.2.1.0.0.3. RESPONSES FOR GAIN F = 4.0, GAIN E = .6

FLIGHT CONDITION: 200 KNOTS, 10,000 FEET, (3,049m), FORWARD CG

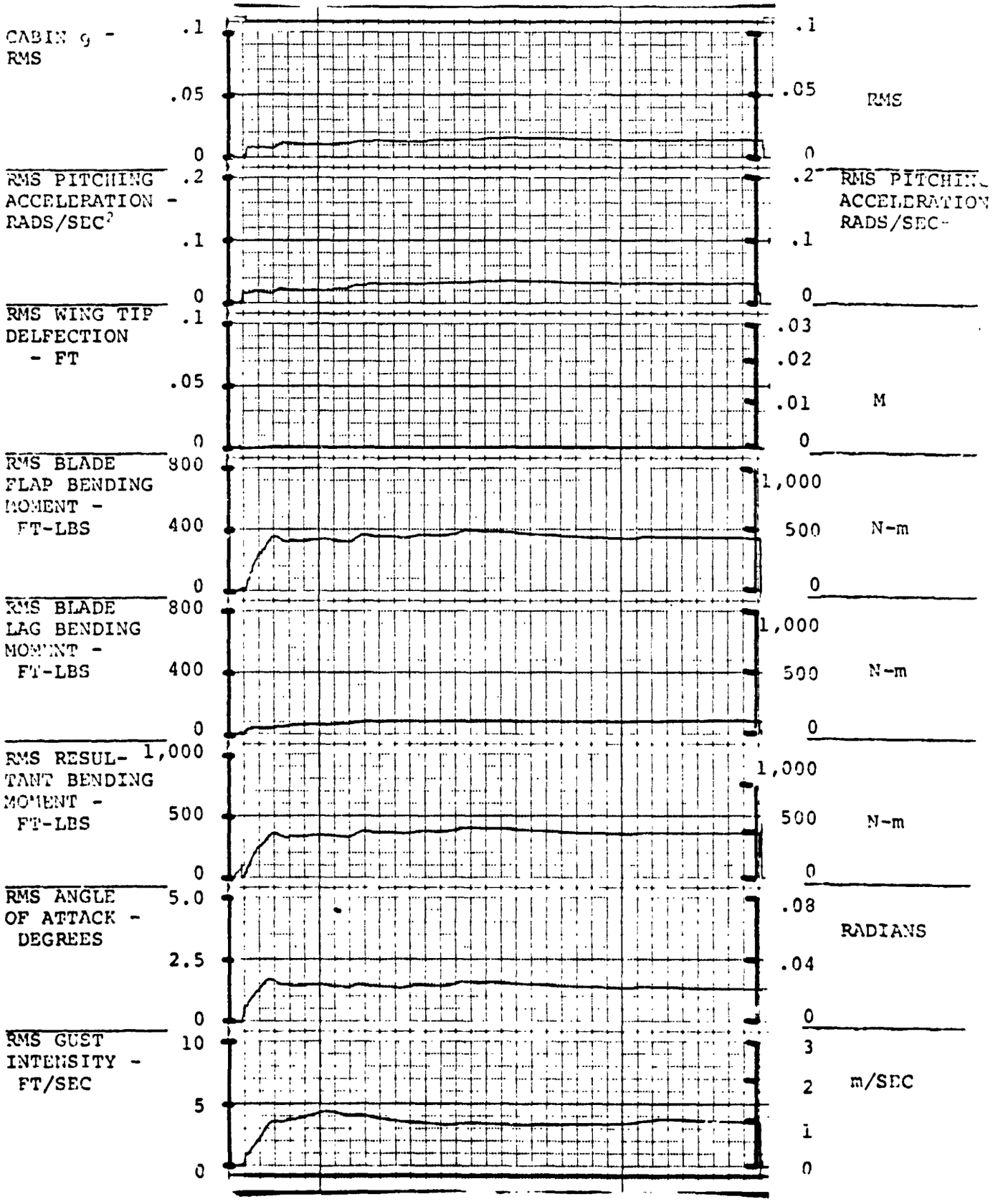

FIGURE 5.2.1.0.0.3. RESPONSES FOR GAIN F = 4.0, GAIN E = .6

FLIGHT CONDITION: 200 KNOTS, 10,000 FEET, (3,049m), FORWARD CG

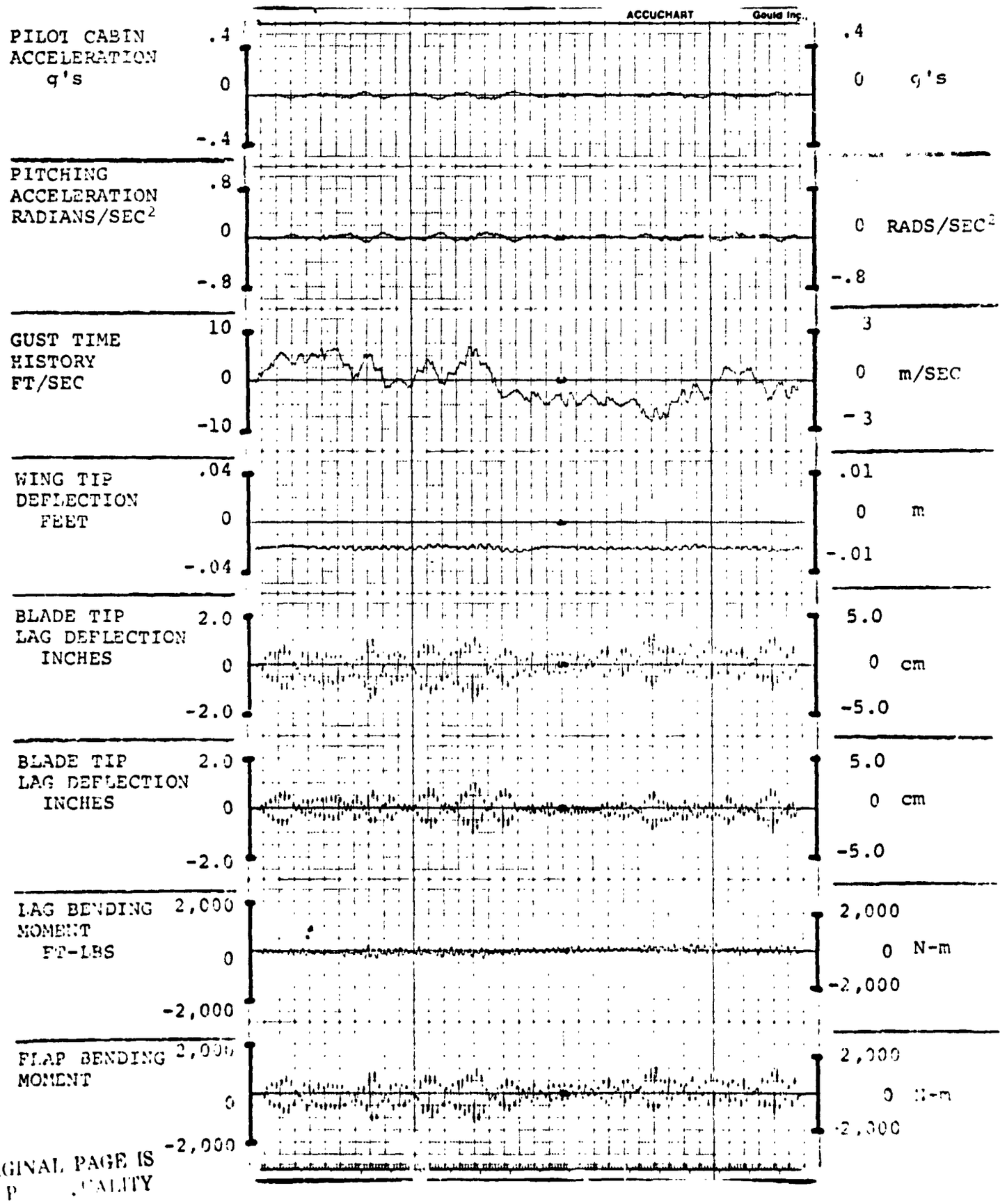

ORIGINAL PAGE IS
OF POOR QUALITY

FIGURE 3.2.1.0.0.6. RESPONSES FOR GAIN F = 4.8, GAIN E = .72

FLIGHT CONDITION: 200 KNOTS, 10,000 FEET, (3,049m), FORWARD CG

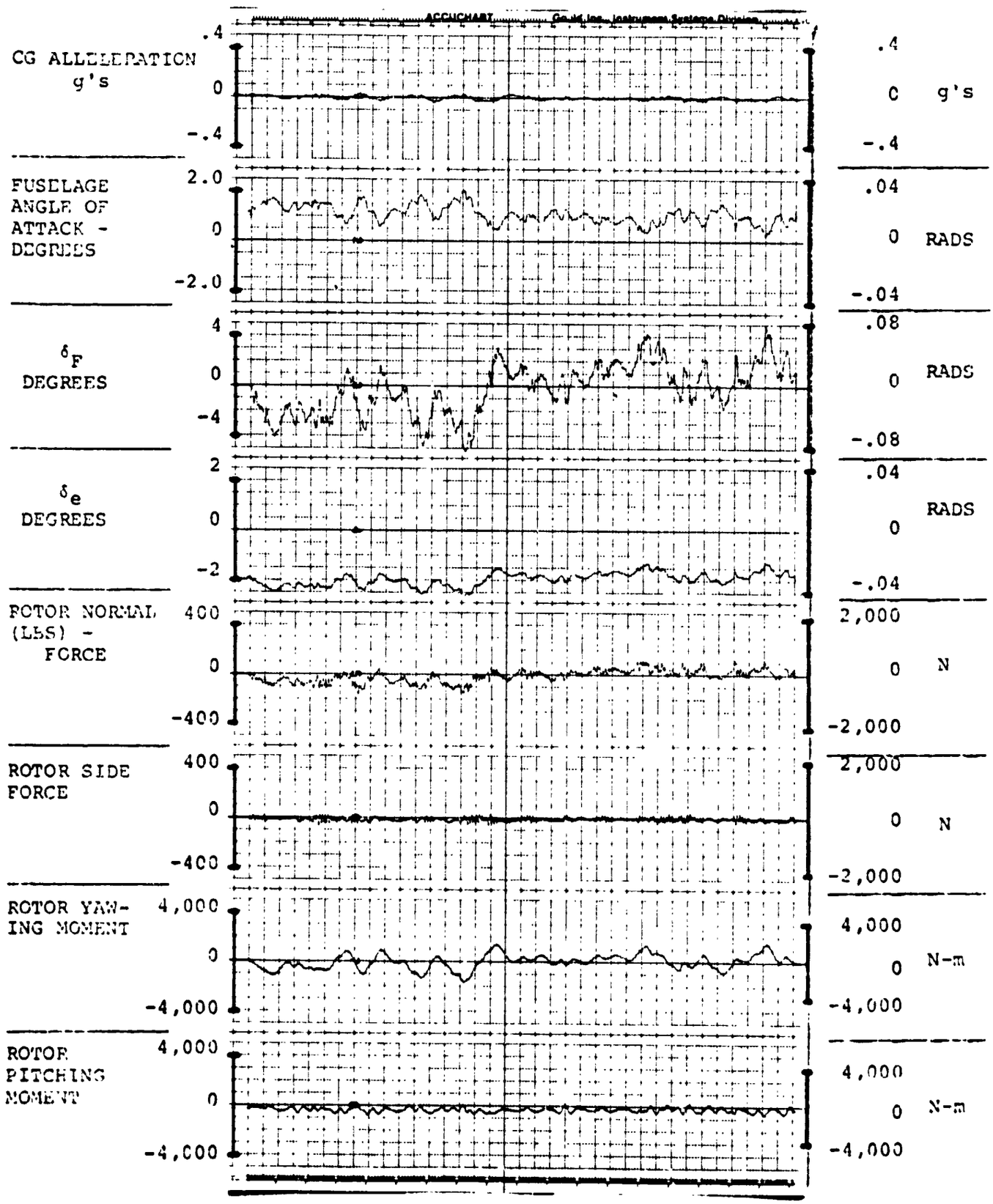

FIGURE 4.2.1.0.0.6. RESPONSES FOR GAIN F = 4.8, GAIN E = .72

FLIGHT CONDITION: 200 KNOTS, 10,000 FEET, (3,049m), FORWARD CG

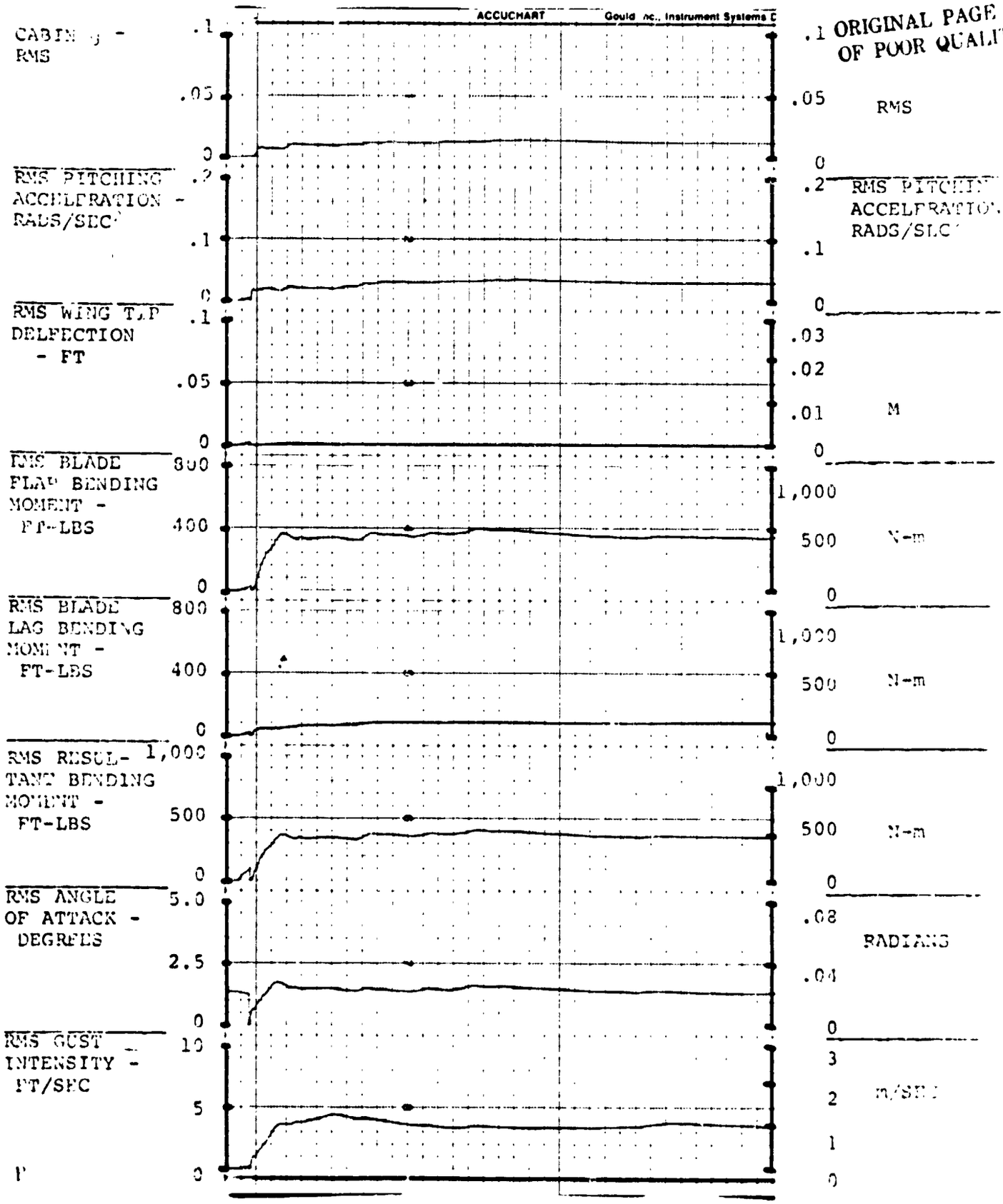

ORIGINAL PAGE IS OF POOR QUALITY

FIGURE 5.2.1.0.0.6. RESPONSES FOR GAIN F = 4.8, GAIN E = .72

FLIGHT CONDITION: 200 KNOTS, 15,000 FEET, (4,573m), FORWARD CG

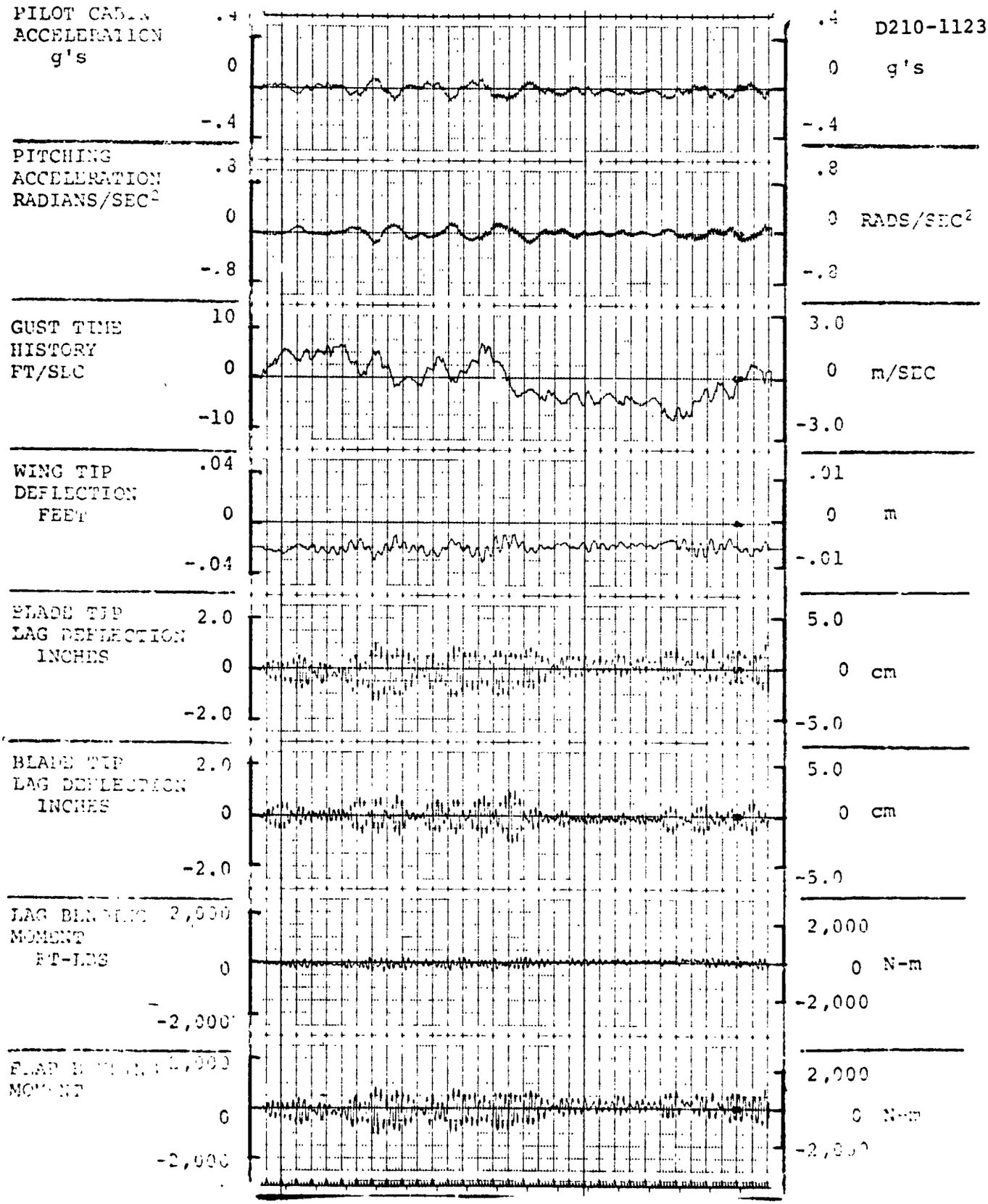

FIGURE 3.3.1.0.0.1. RESPONSES FOR GAIN F = 0, GAIN E = 0

ORIGINAL PAGE IS
OF POOR QUALITY

FLIGHT CONDITION: 200 KNOTS, 15,000 FEET, (4,573m), FORWARD CG

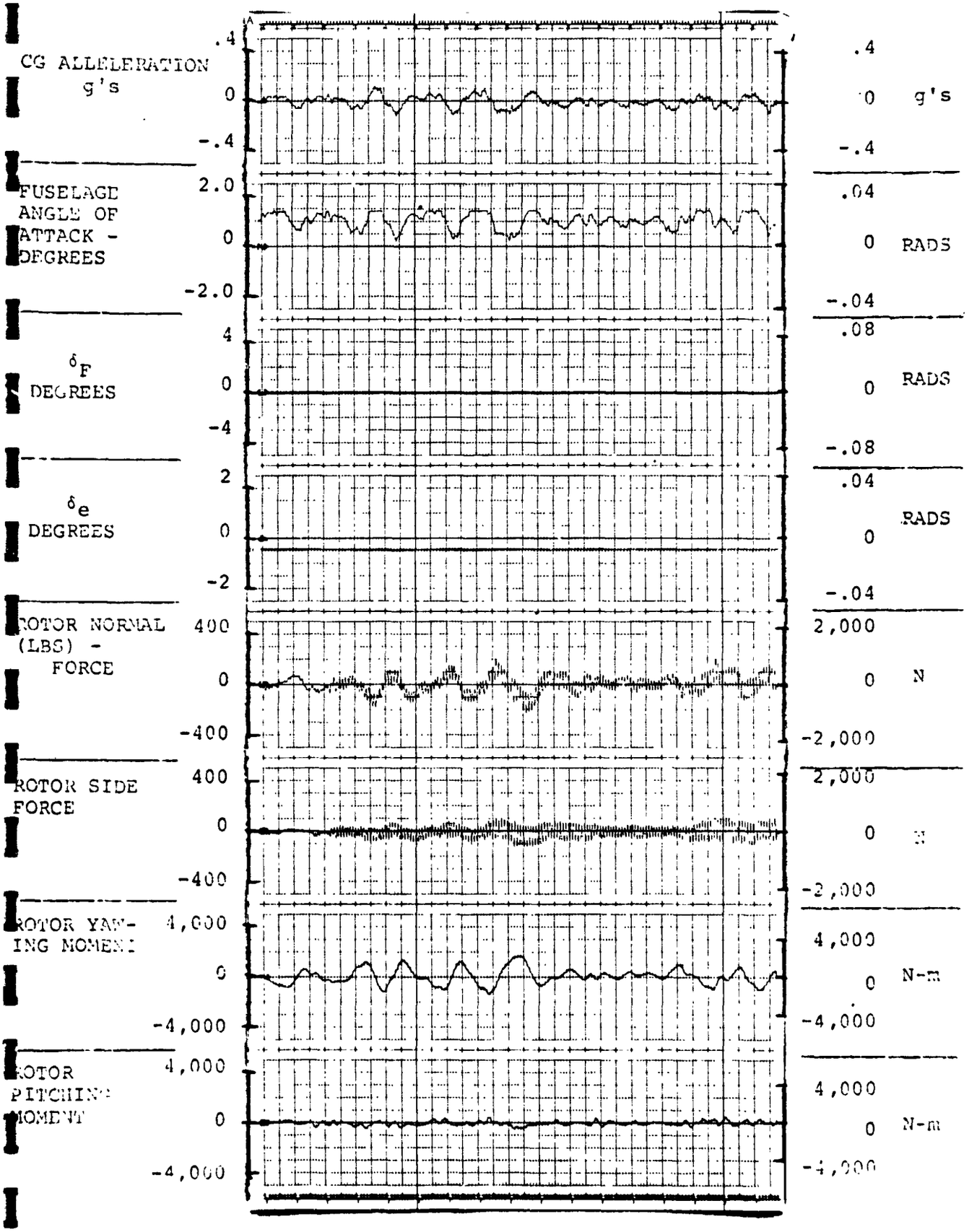

FIGURE 4.3.1.0.0.1. RESPONSES FOR GAIN F = 0, GAIN E = 0

ORIGINAL PAGE IS OF POOR QUALITY

FLIGHT CONDITION: 200 KNOTS, 15,000 FEET, (4,573m), FORWARD CG

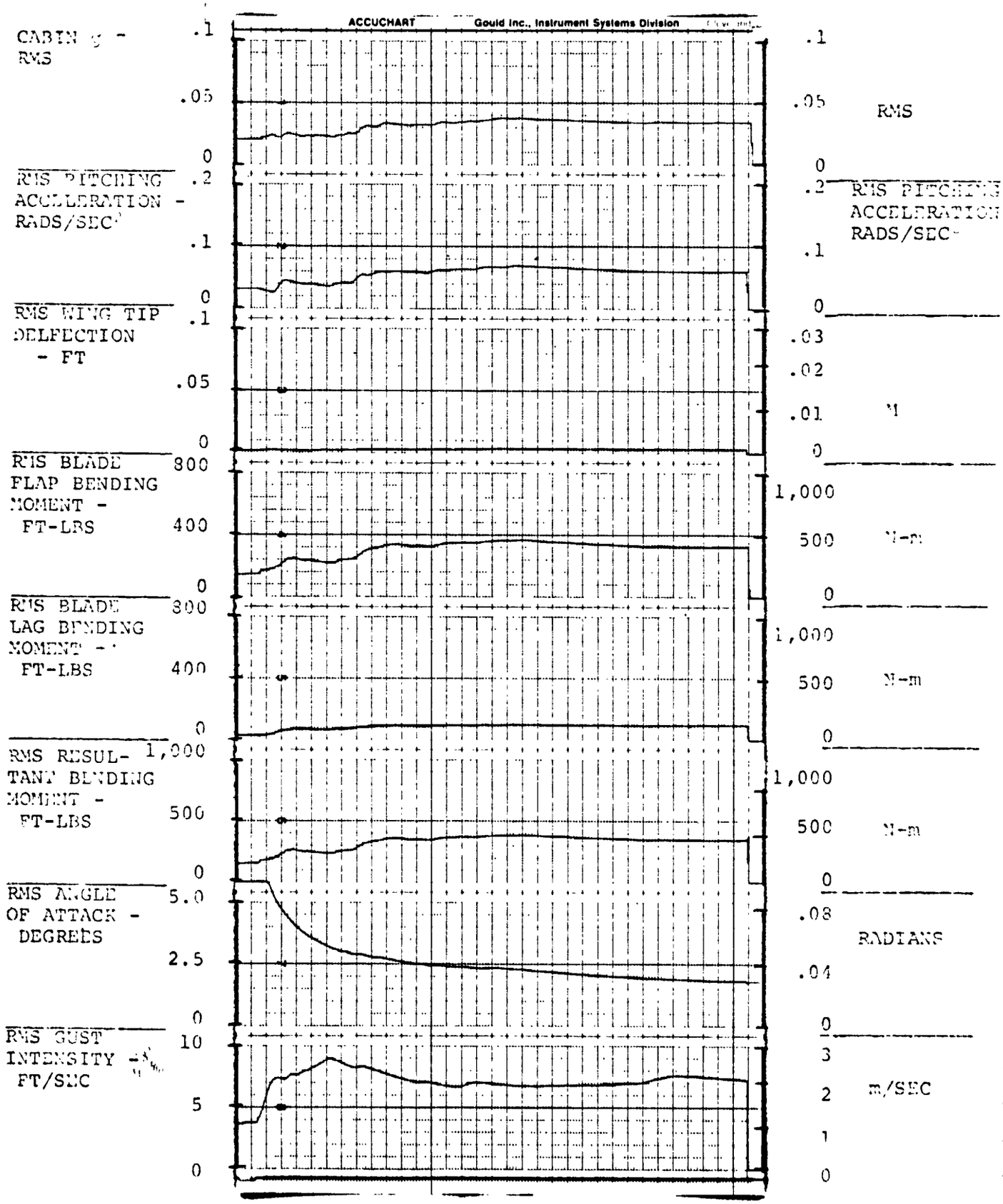

FIGURE 5.3.1.0.0.1. RESPONSES FOR GAIN F = 0, GAIN E = 0

FLIGHT CONDITION: 200 KNOTS, 15,000 FEET, (4,573m), FORWARD CG

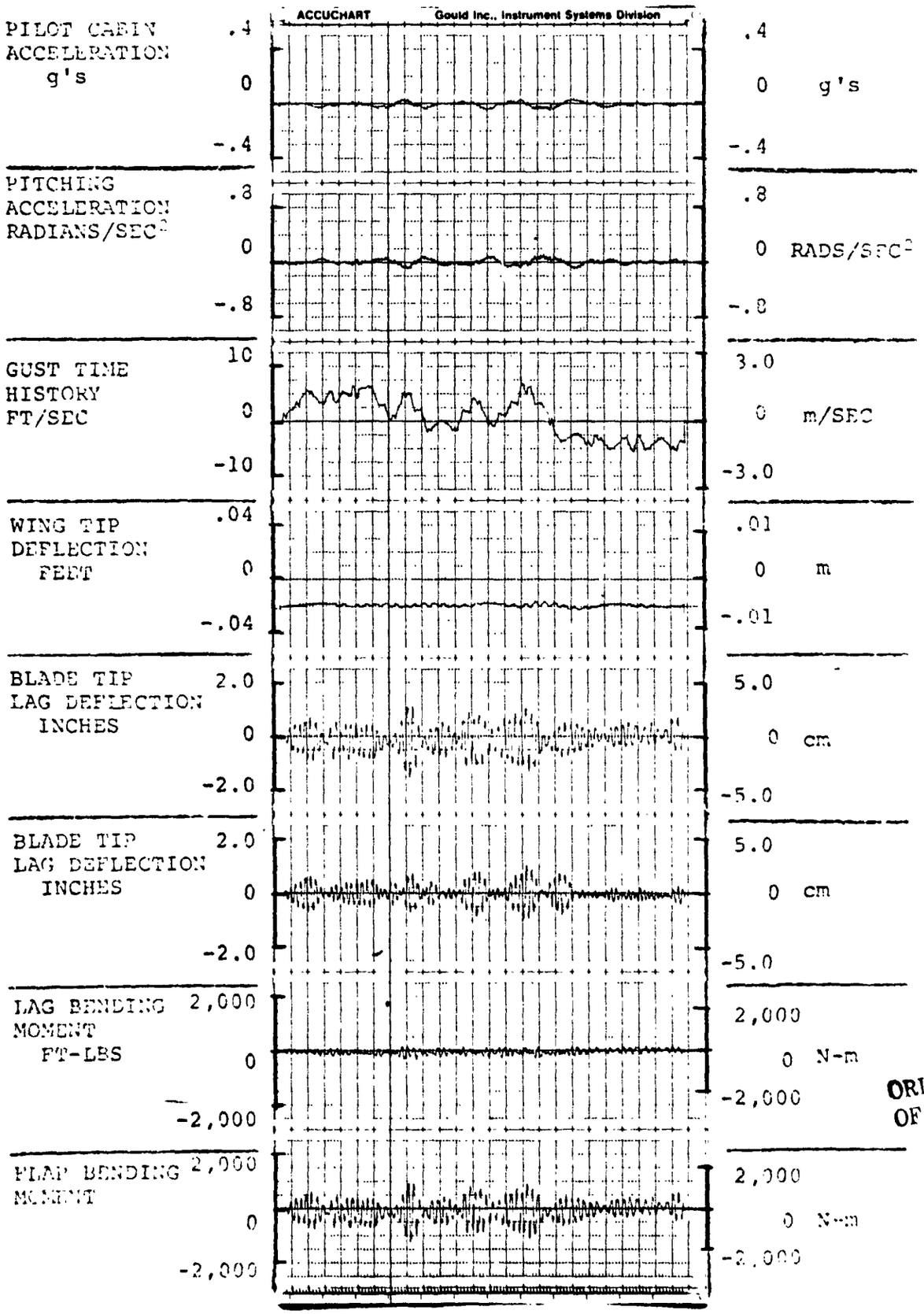

ORIGINAL PAGE IS OF POOR QUALITY

FIGURE 3.3.1.0.0.2. RESPONSES FOR GAIN F = 4.0, GAIN E = .6

FLIGHT CONDITION: 200 KNOTS, 15,000 FEET, (4,573m), FORWARD CG

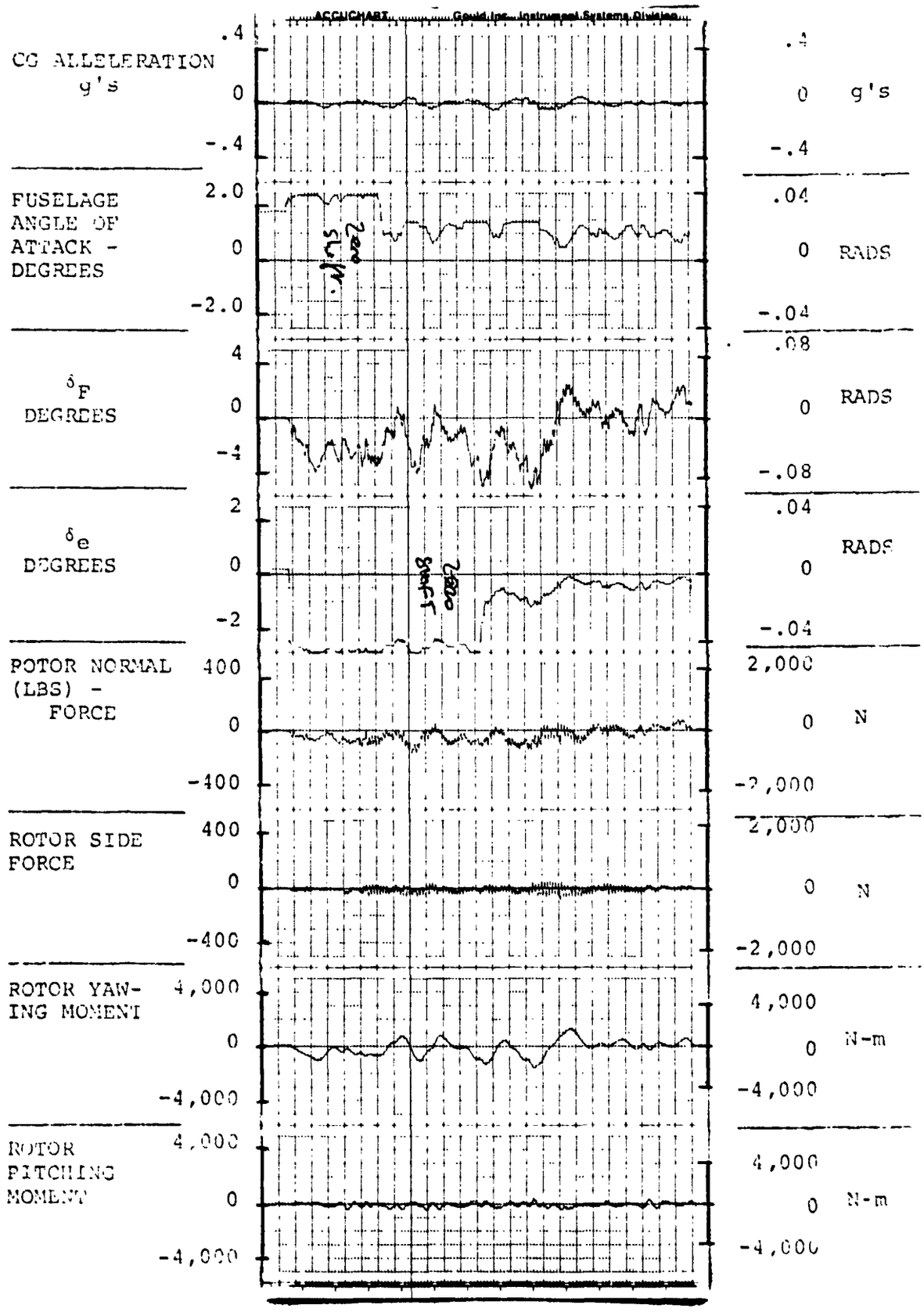

FIGURE 4.3.1.0.0.2. RESPONSES FOR GAIN F = 4.0, GAIN E = .6

FLIGHT CONDITION: 200 KNOTS, 15,000 FEET, (4,573m), FORWARD CG

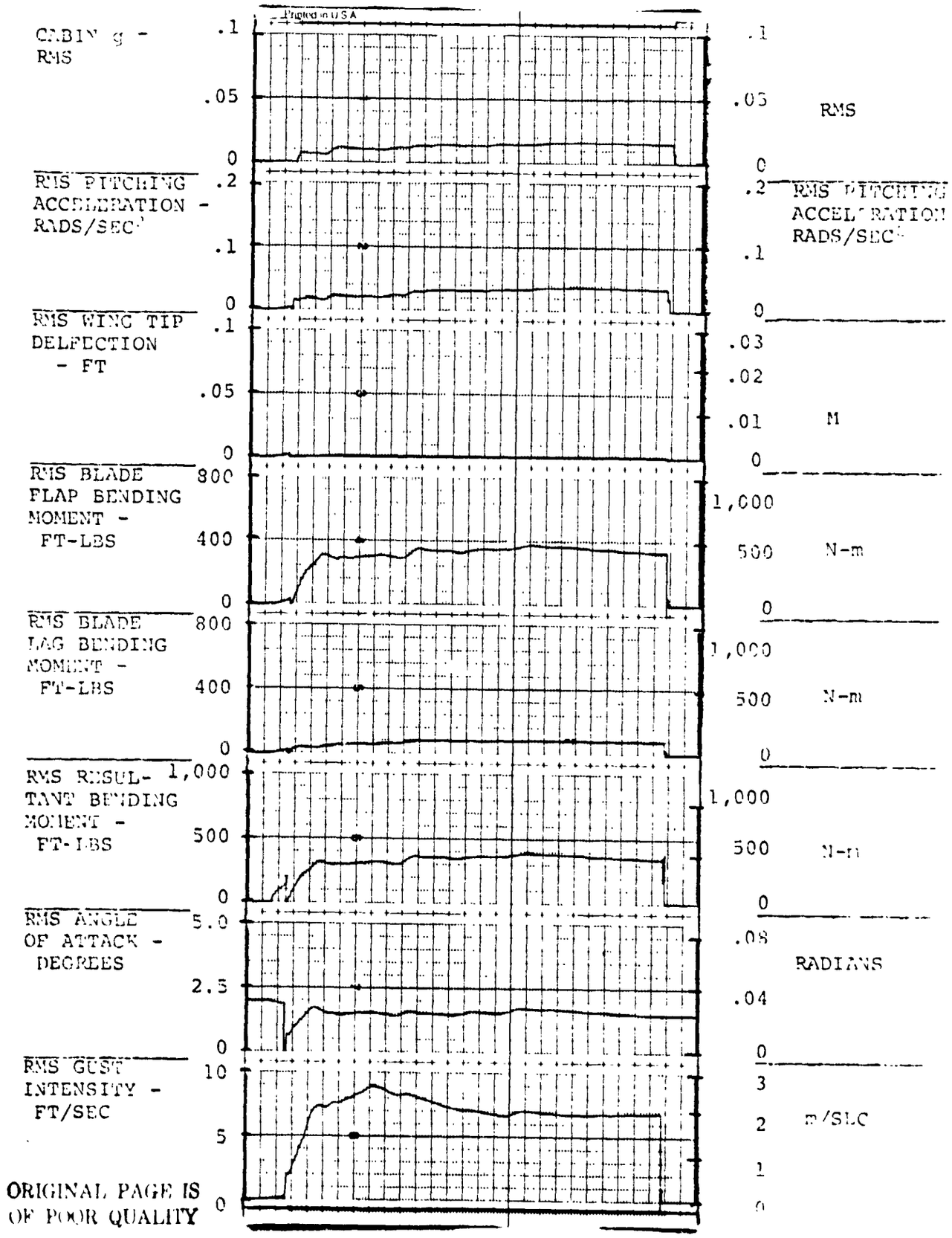

ORIGINAL PAGE IS OF POOR QUALITY

FIGURE 5.3.1.0.0.2. RESPONSES FOR GAIN F = 4.0, GAIN E = .6

FLIGHT CONDITION: 200 KNOTS, 5,000 FEET, (1,524m), AFT CG

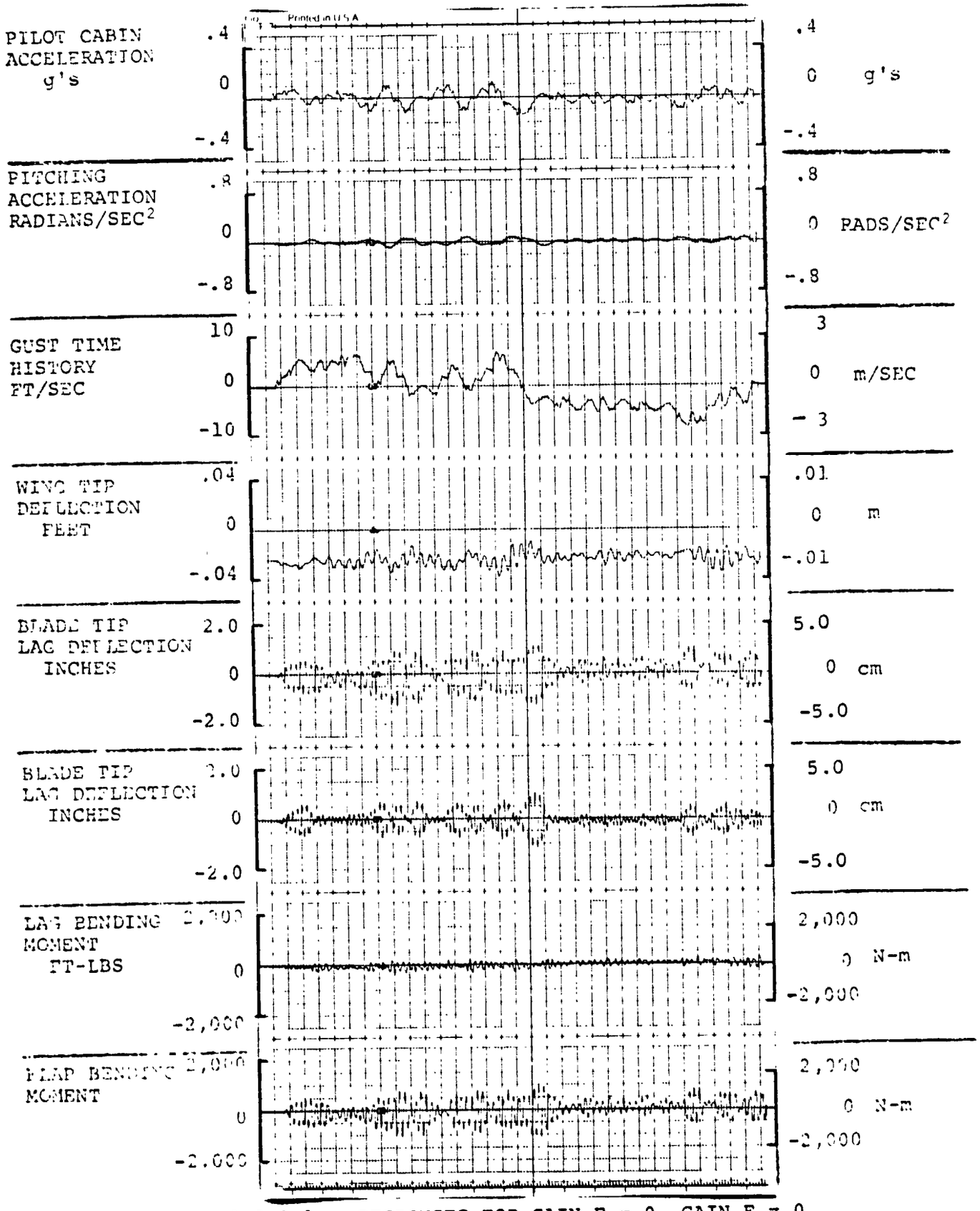

FIGURE 3.1.2.0.0.1. RESPONSES FOR GAIN F = 0, GAIN E = 0

ORIGINAL PAGE IS
OF POOR QUALITY

FLIGHT CONDITION: 200 KNOTS, 5,000 FEET, (1,524m), AFT CG

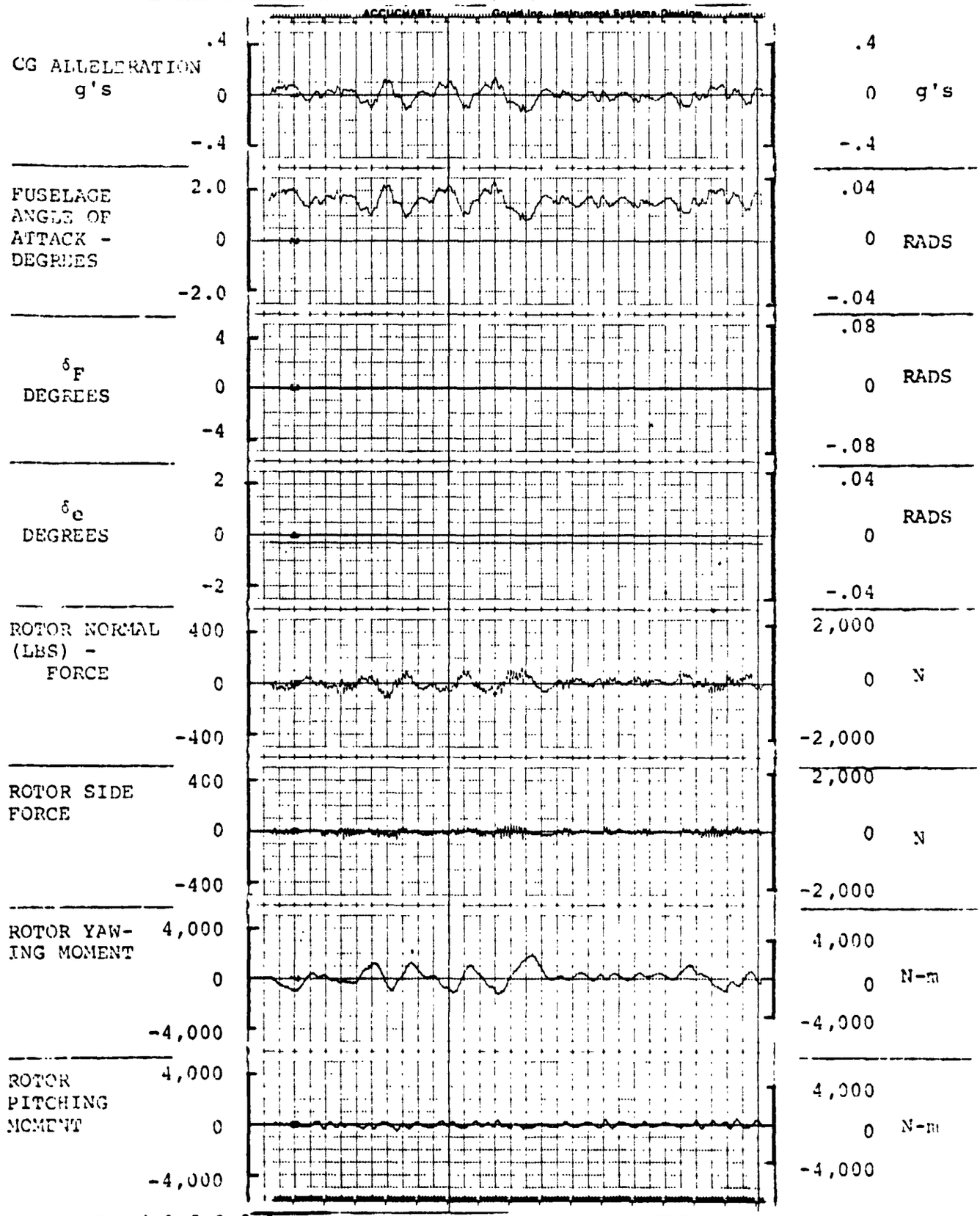

FIGURE 4.1.2.0.0.1. RESPONSES FOR GAIN F = 0, GAIN E = 0

ORIGINAL PAGE IS
OF POOR QUALITY

FLIGHT CONDITION: 200 KNOTS, 5,000 FEET, (1,524m), AFT CG

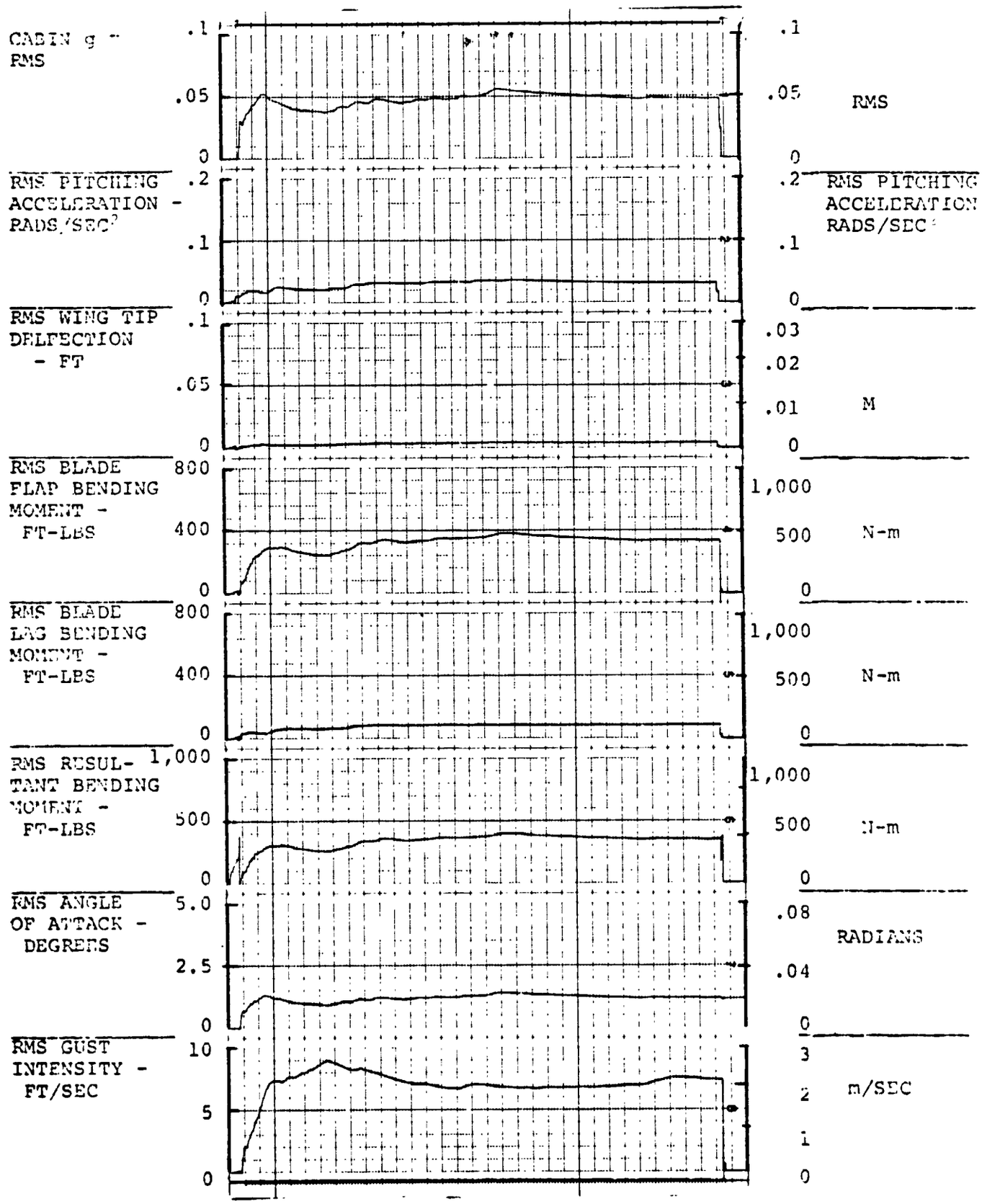

FIGURE 5.1.2.0.0.1. RESPONSES FOR GAIN F = 0, GAIN E = 0

FLIGHT CONDITION: 200 KNOTS, 5,000 FEET, (1,524m), AFT CG

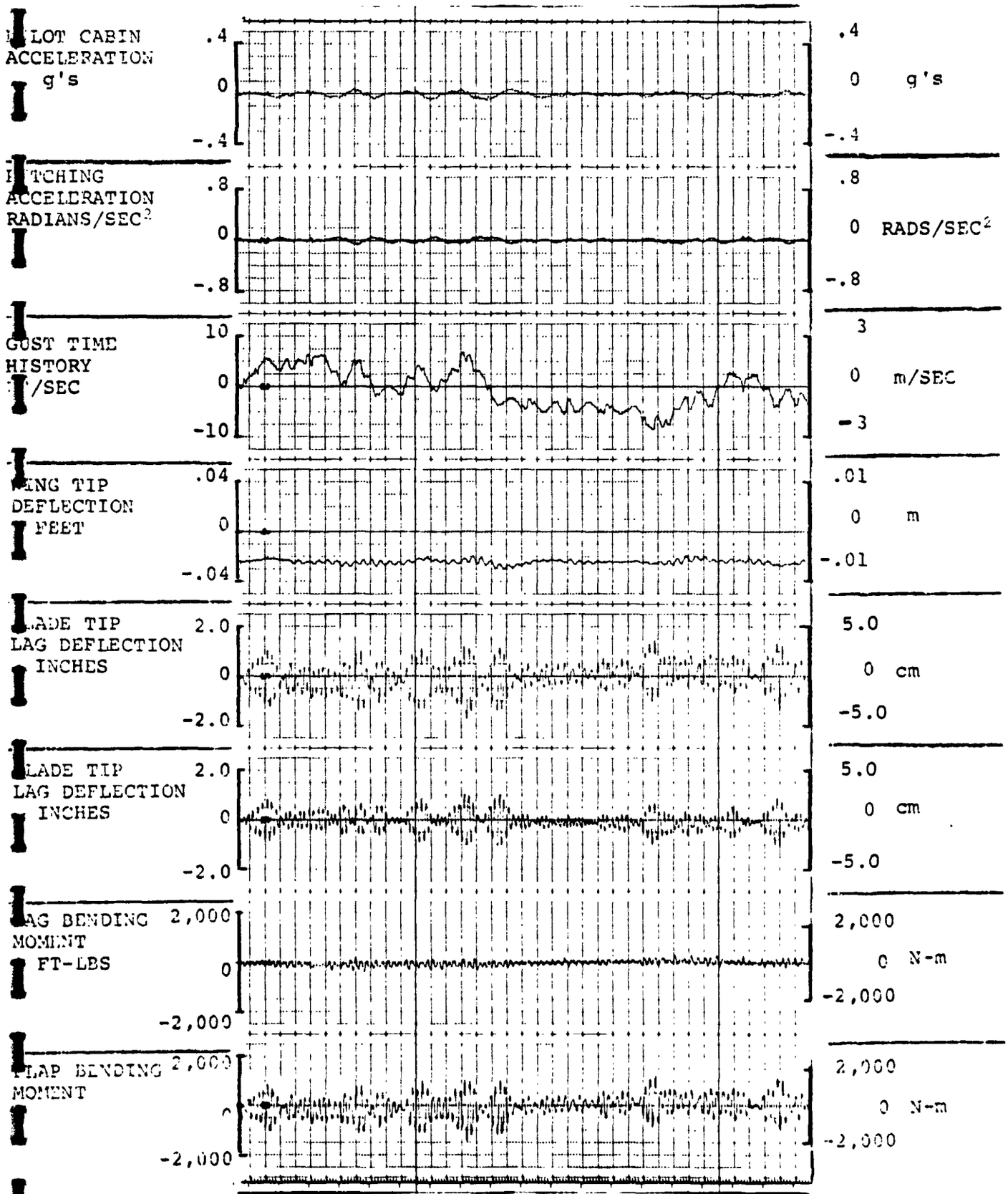

FIGURE 3.1.2.0.0.2. RESPONSES FOR GAIN F = 4.0, GAIN E = .6

FLIGHT CONDITION: 200 KNOTS, 5,000 FEET, (1,524m), AFT CG

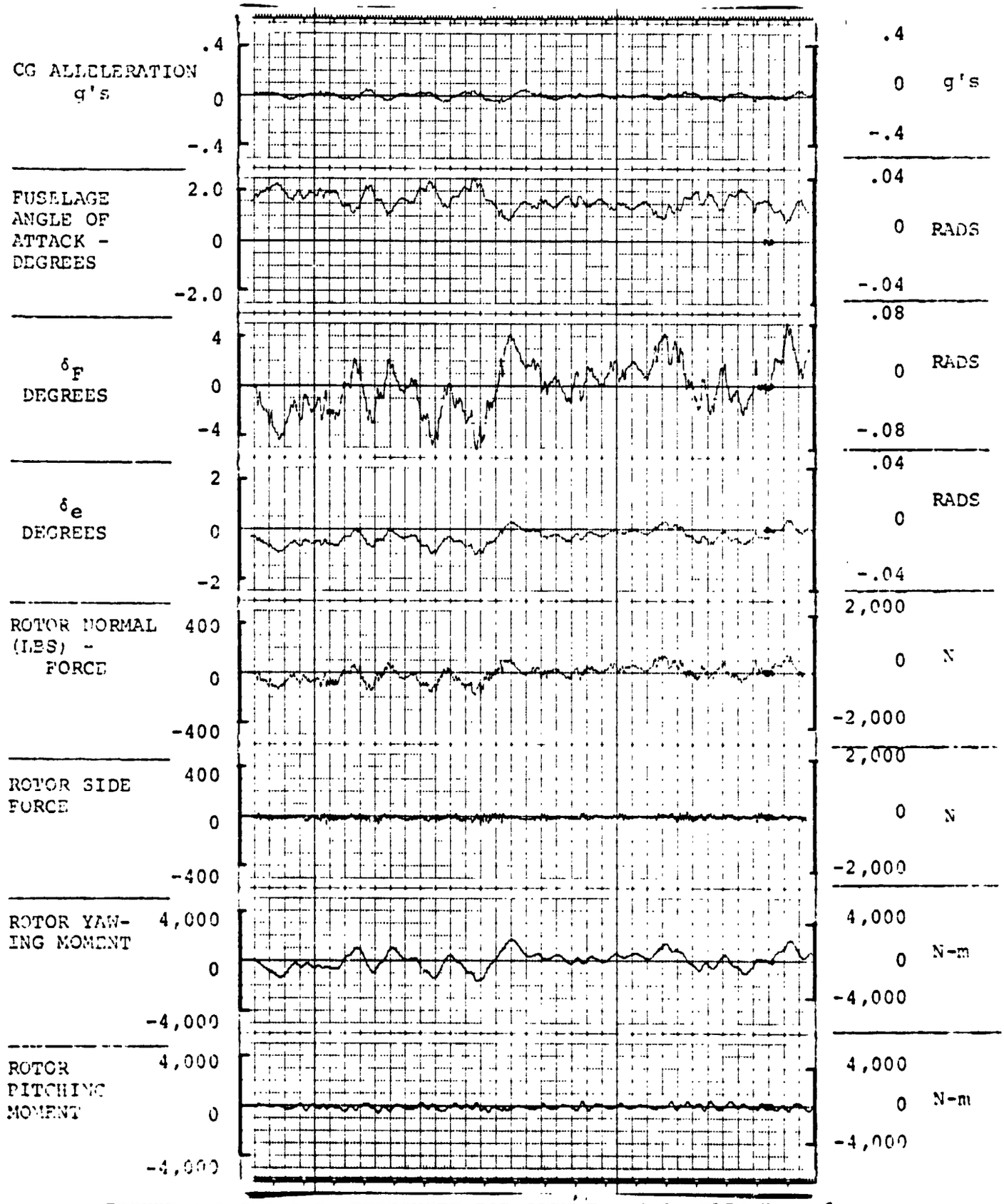

FIGURE 4.1.2.0.0.2. RESPONSES FOR GAIN F = 4.0, GAIN E = .6

FLIGHT CONDITION: 200 KNOTS, 5,000 FEET, (1,524m), AFT CG

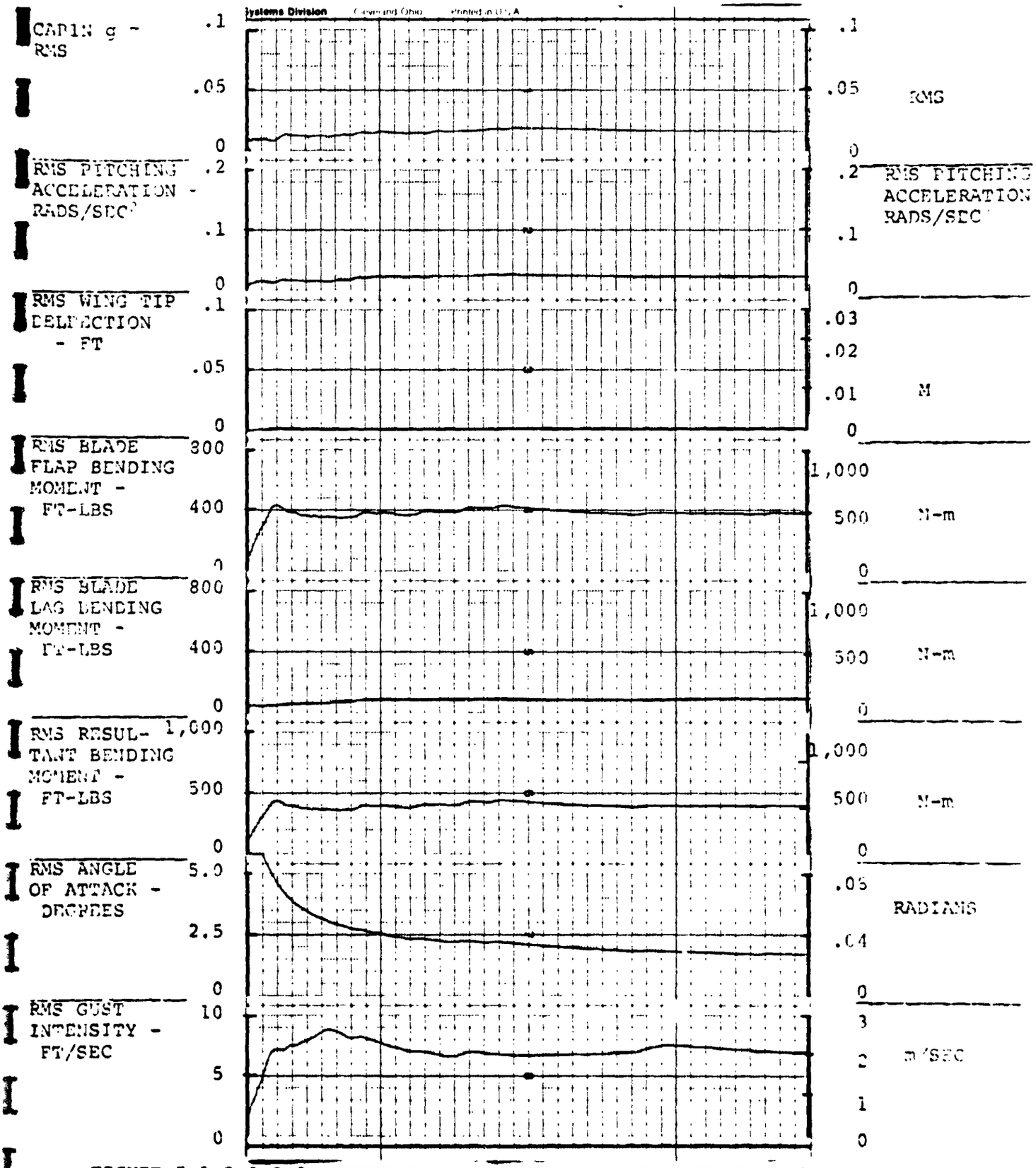

FIGURE 5.1.2.0.0.2. RESPONSES FOR GAIN F = 4.0, GAIN E = .6

ORIGINAL PAGE IS OF POOR QUALITY

FLIGHT CONDITION: 200 KNOTS, 5,000 FEET, (1,524m), AFT CG

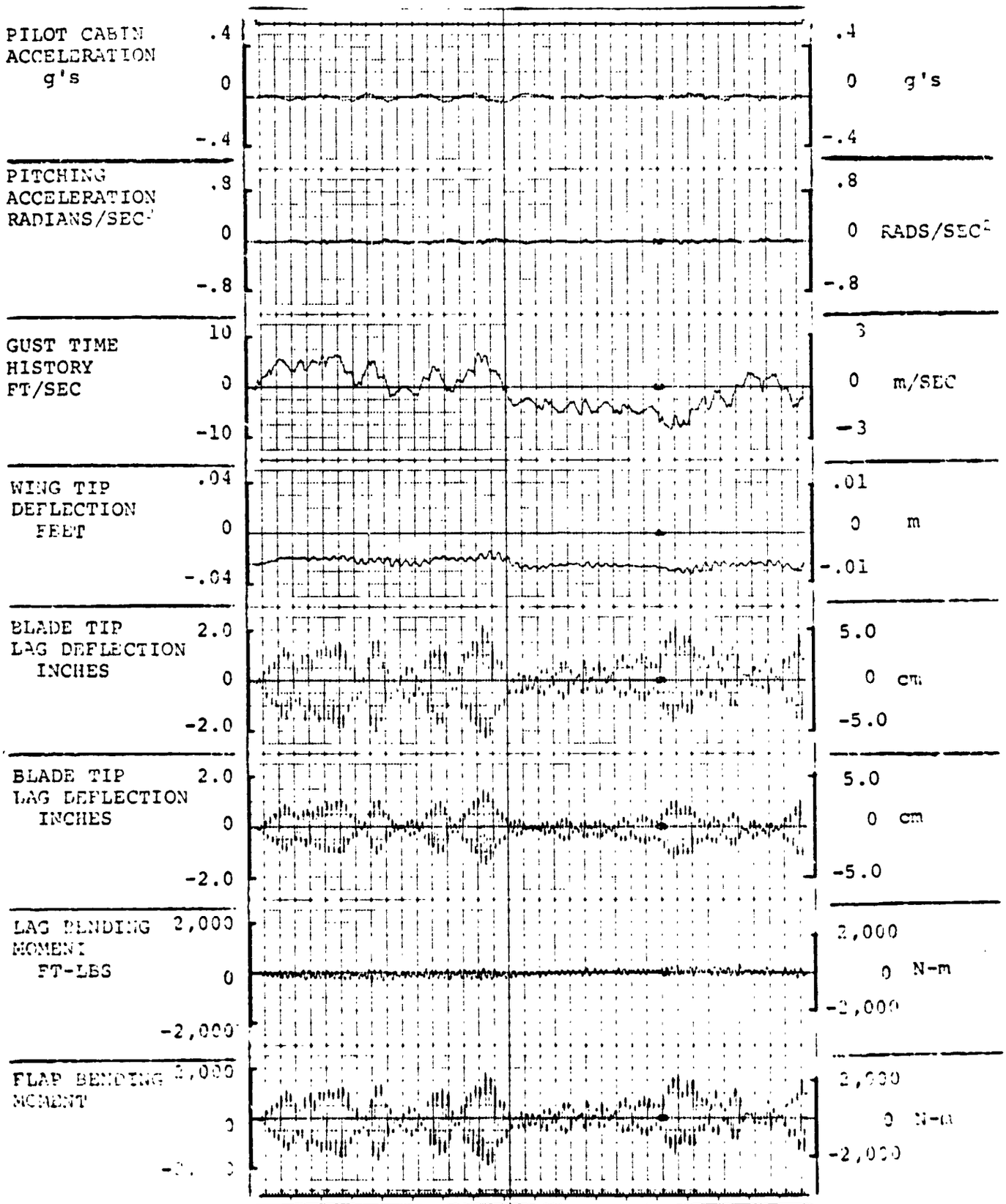

FIGURE 3.1.2.0.0.3. RESPONSES FOR GAIN F = 4.0, GAIN E = .7

ORIGINAL PAGE IS OF POOR QUALITY

FLIGHT CONDITION: 200 KNOTS, 5,000 FEET, (1,524m), AFT CG

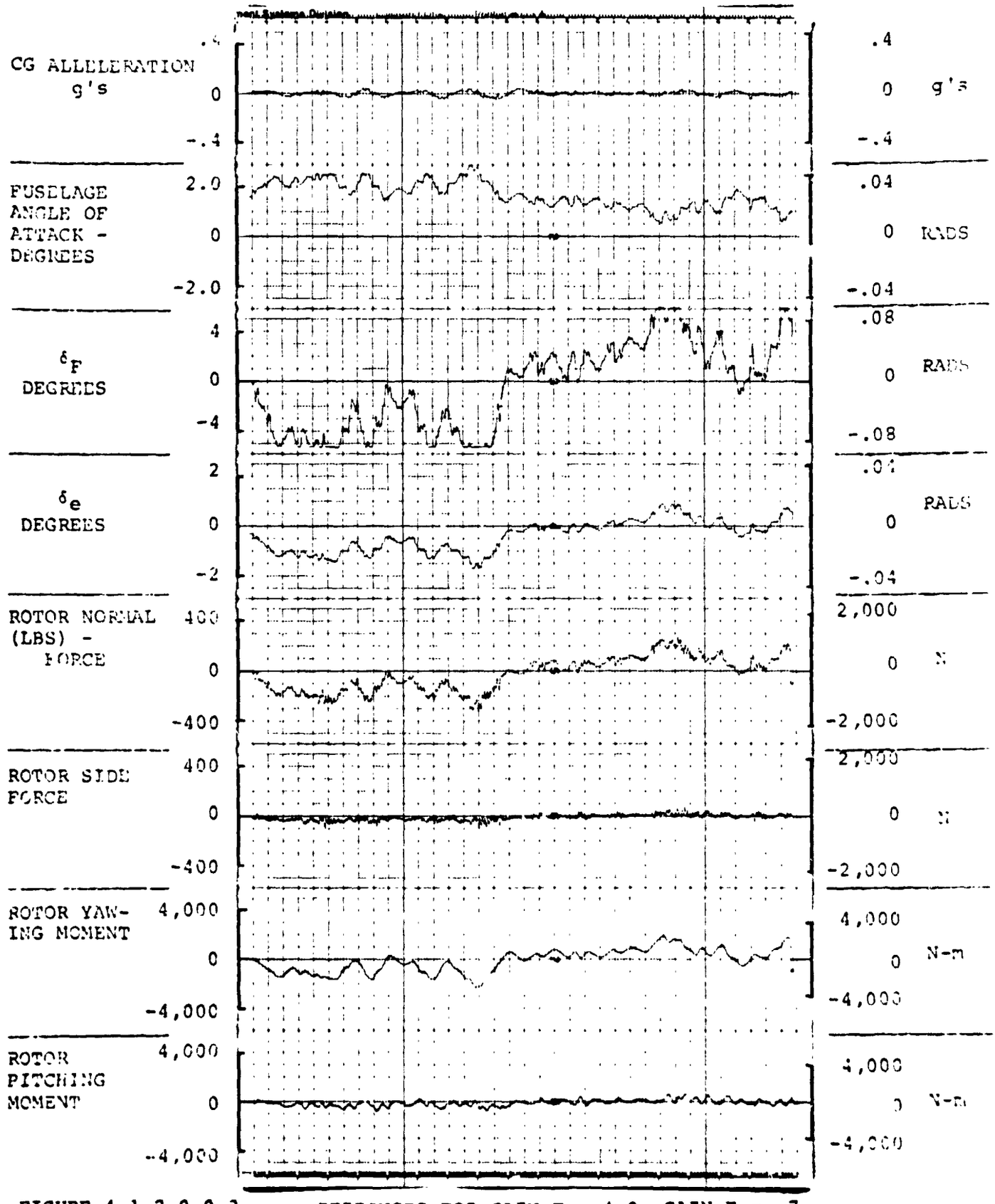

FIGURE 4.1.2.0.0.3. RESPONSES FOR GAIN F = 4.0, GAIN E = .7

ORIGINAL PAGE IS OF POOR QUALITY

FLIGHT CONDITION: 200 KNOTS, 5,000 FEET, (1,524m), AFT CG

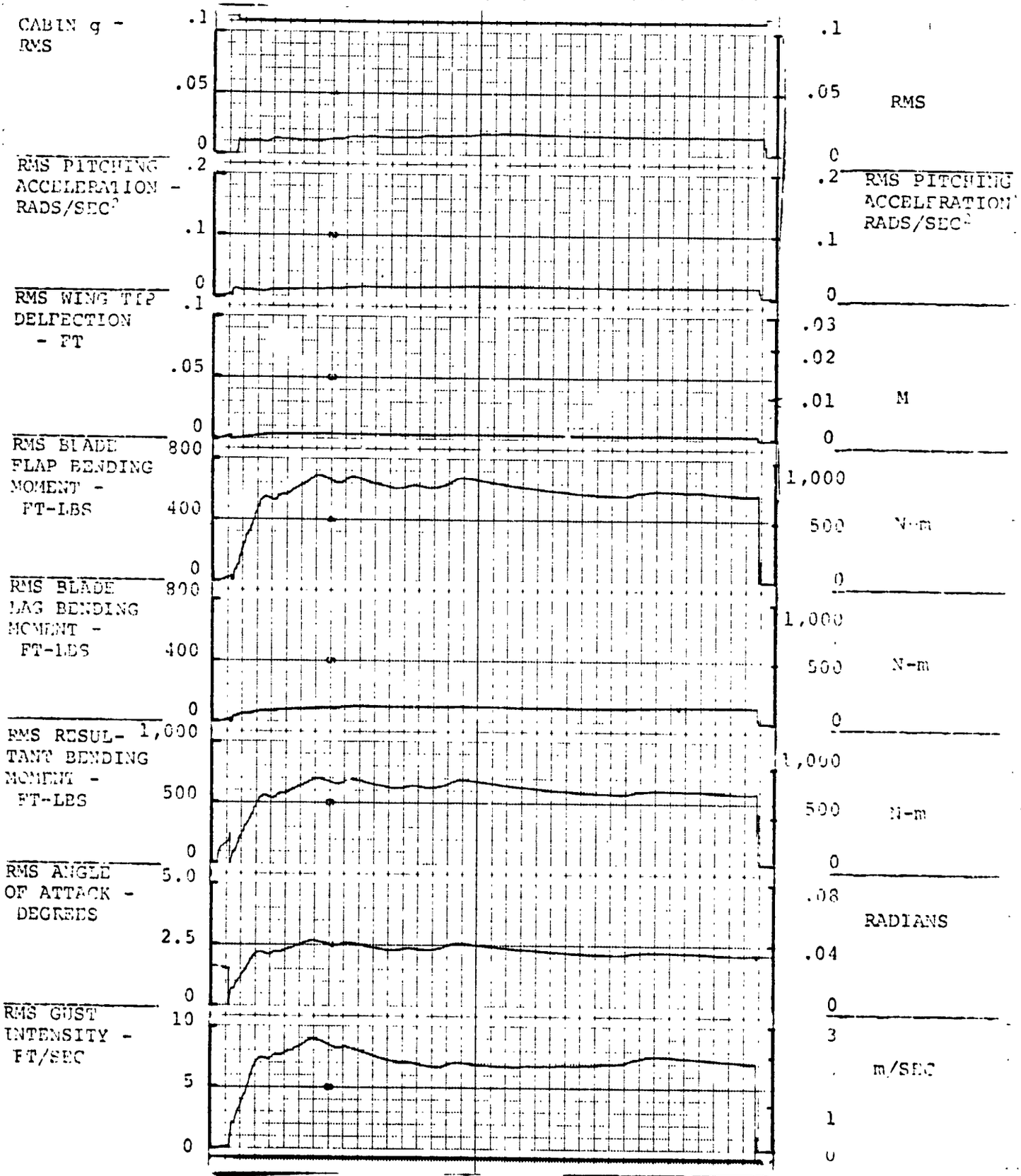

FIGURE 5.1.2.0.0.3. RESPONSES FOR GAIN F = 4.0, GAIN E = .7

FLIGHT CONDITION: 200 KNOTS, 10,000 FEET, (3,049m), AFT CG

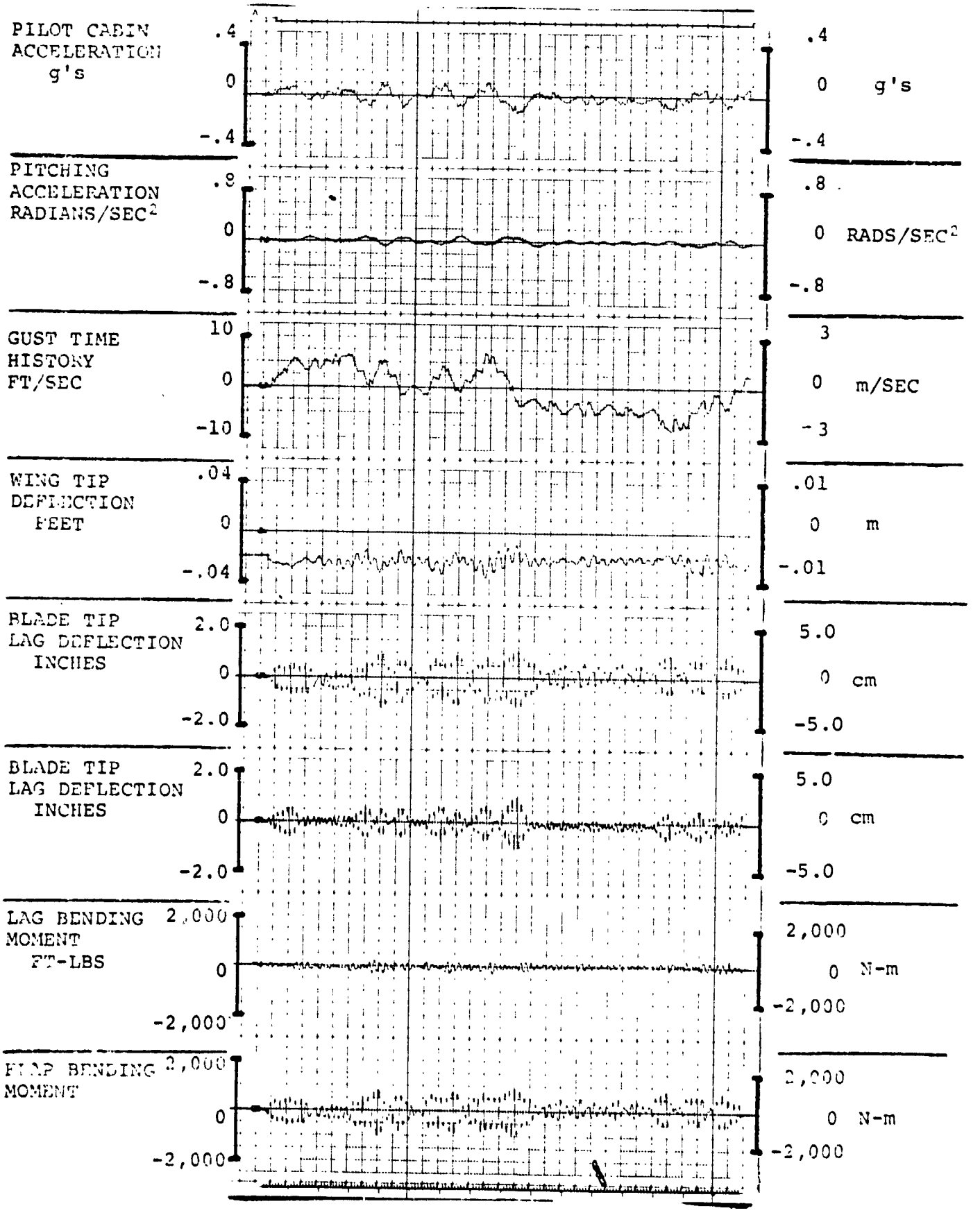

FIGURE 3.2.2.0.0.1. RESPONSES FOR GAIN F = 0, GAIN E = 0

FLIGHT CONDITION: 200 KNOTS, 10,000 FEET, (3,049m), AFT CG

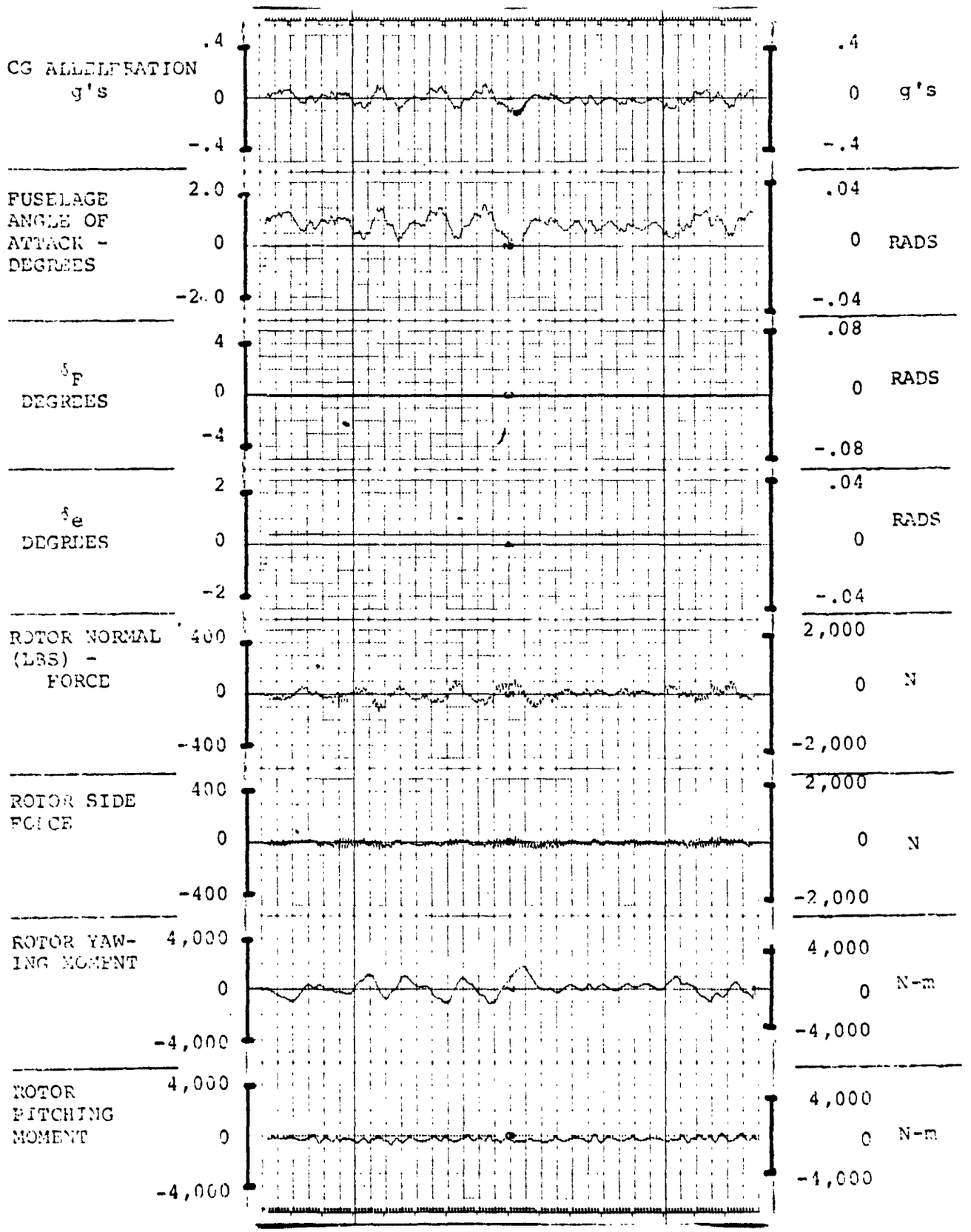

FIGURE 4.2.2.0.0.1. RESPONSES FOR GAIN F = 0, GAIN E = 0

FLIGHT CONDITION: 200 KNOTS, 10,000 FEET, (3,049m), AFT CG

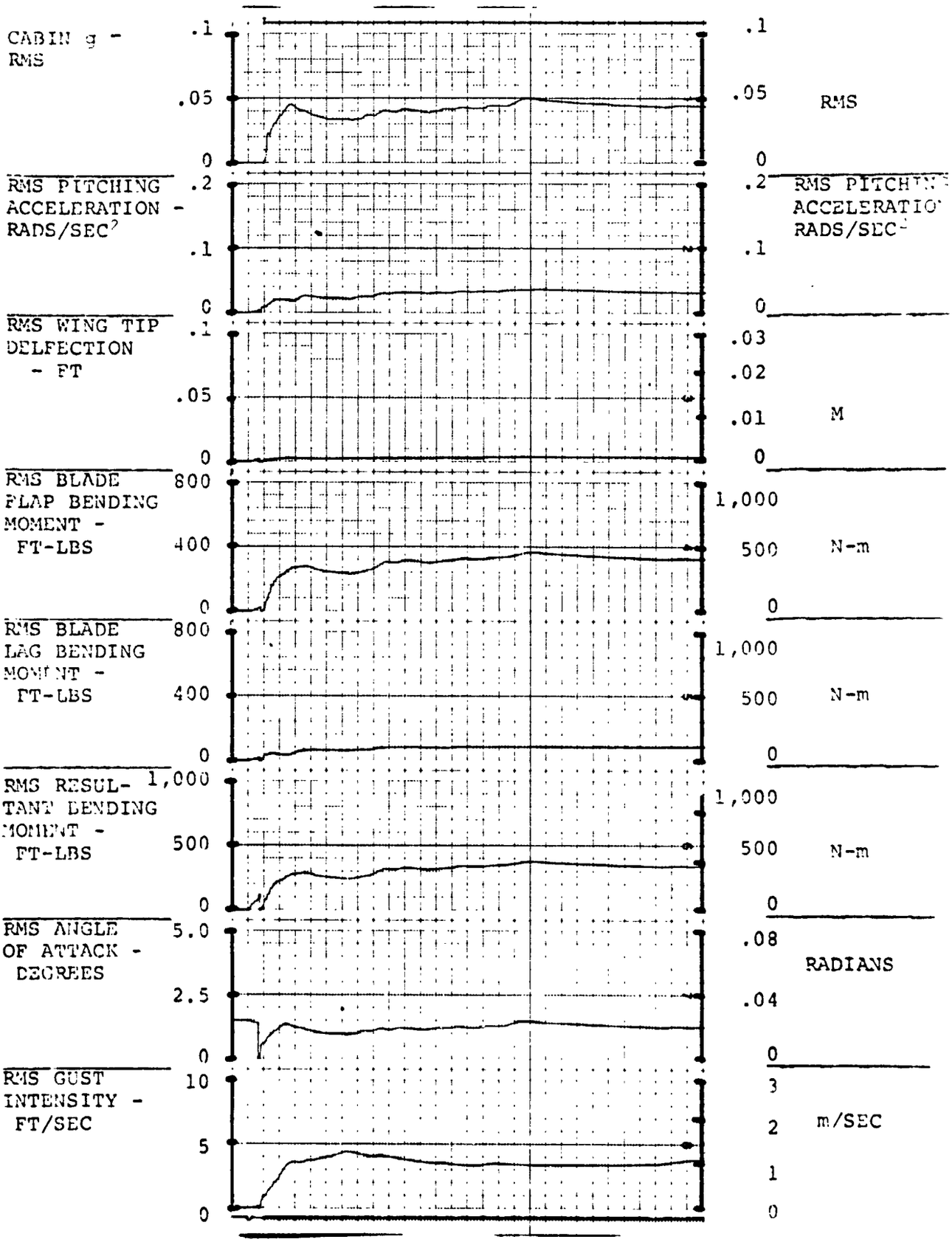

FIGURE 5.2.2.0.0.1. RESPONSES FOR GAIN F = 0, GAIN E = 0

FLIGHT CONDITION: 200 KNOTS, 10,000 FEET, (3,049m), AFT CG

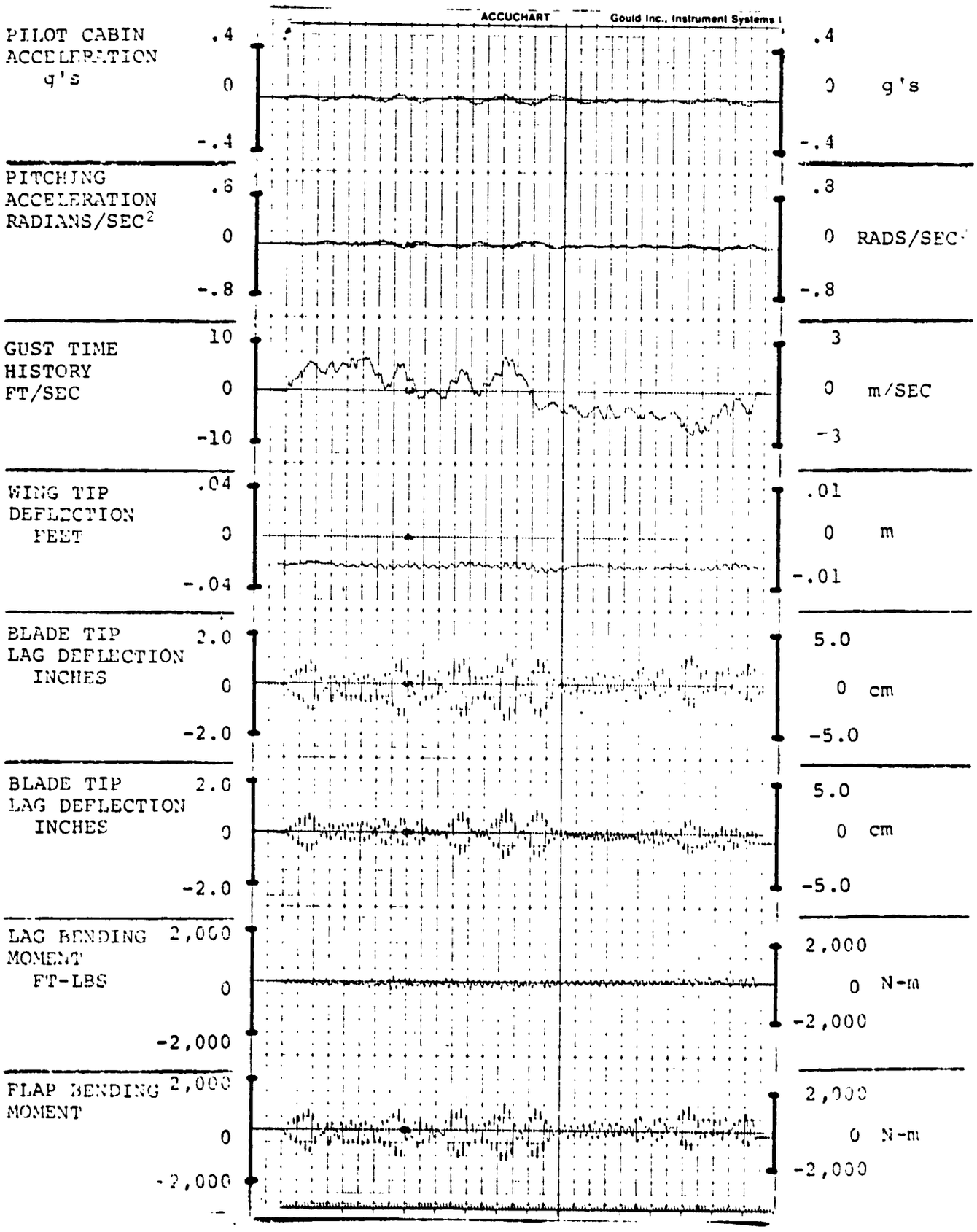

FIGURE 3.2.2.0.0.2. RESPONSES FOR GAIN F = 4.0, GAIN E = .6

FLIGHT CONDITION: 200 KNOTS, 10,000 FEET, (3,049m), AFT CG

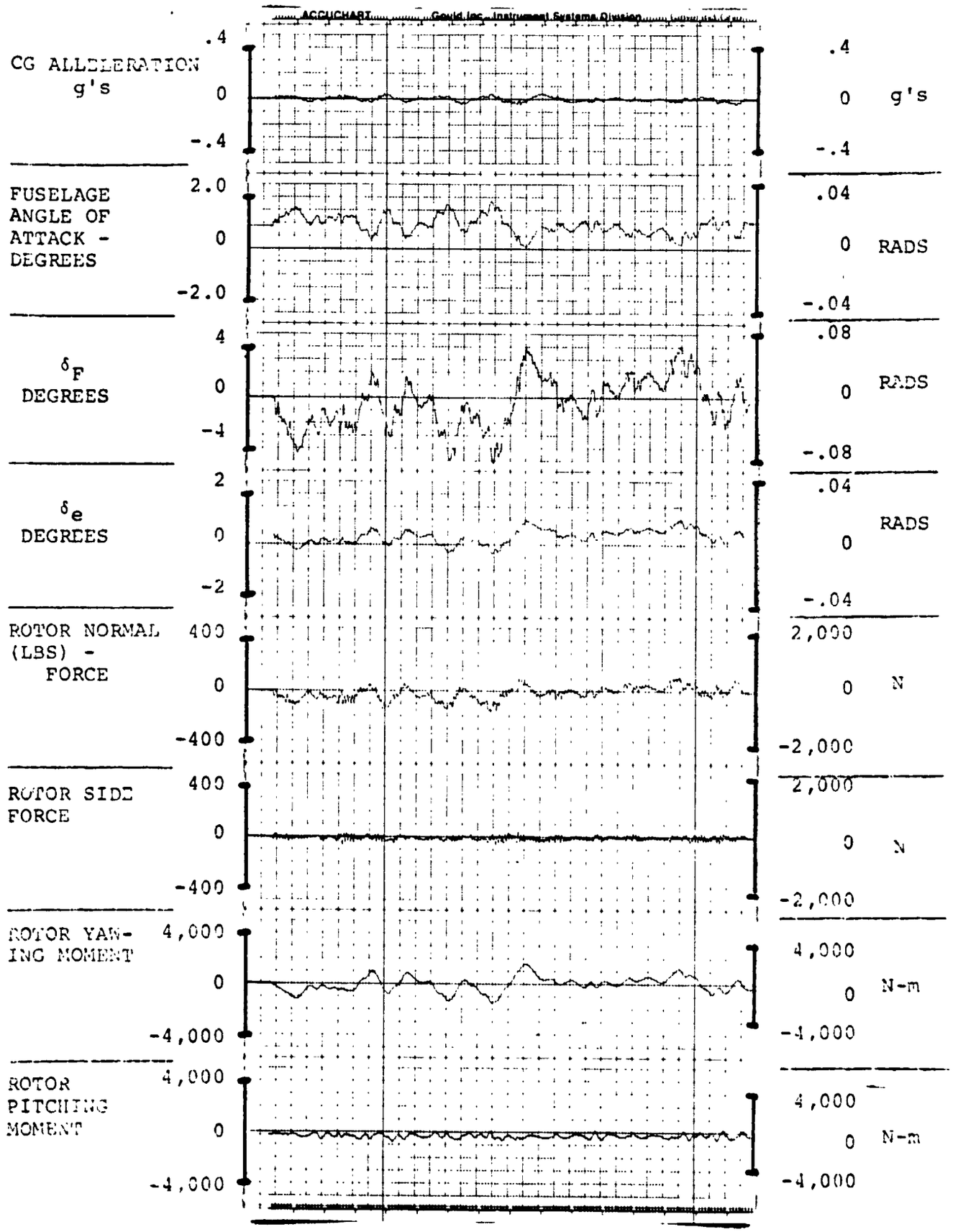

FIGURE 4.2.2.0.0.2. RESPONSES FOR GAIN F = 4.0, GAIN E = .6

FLIGHT CONDITION: 200 KNOTS, 10,000 FEET, (3,049m), AFT CG

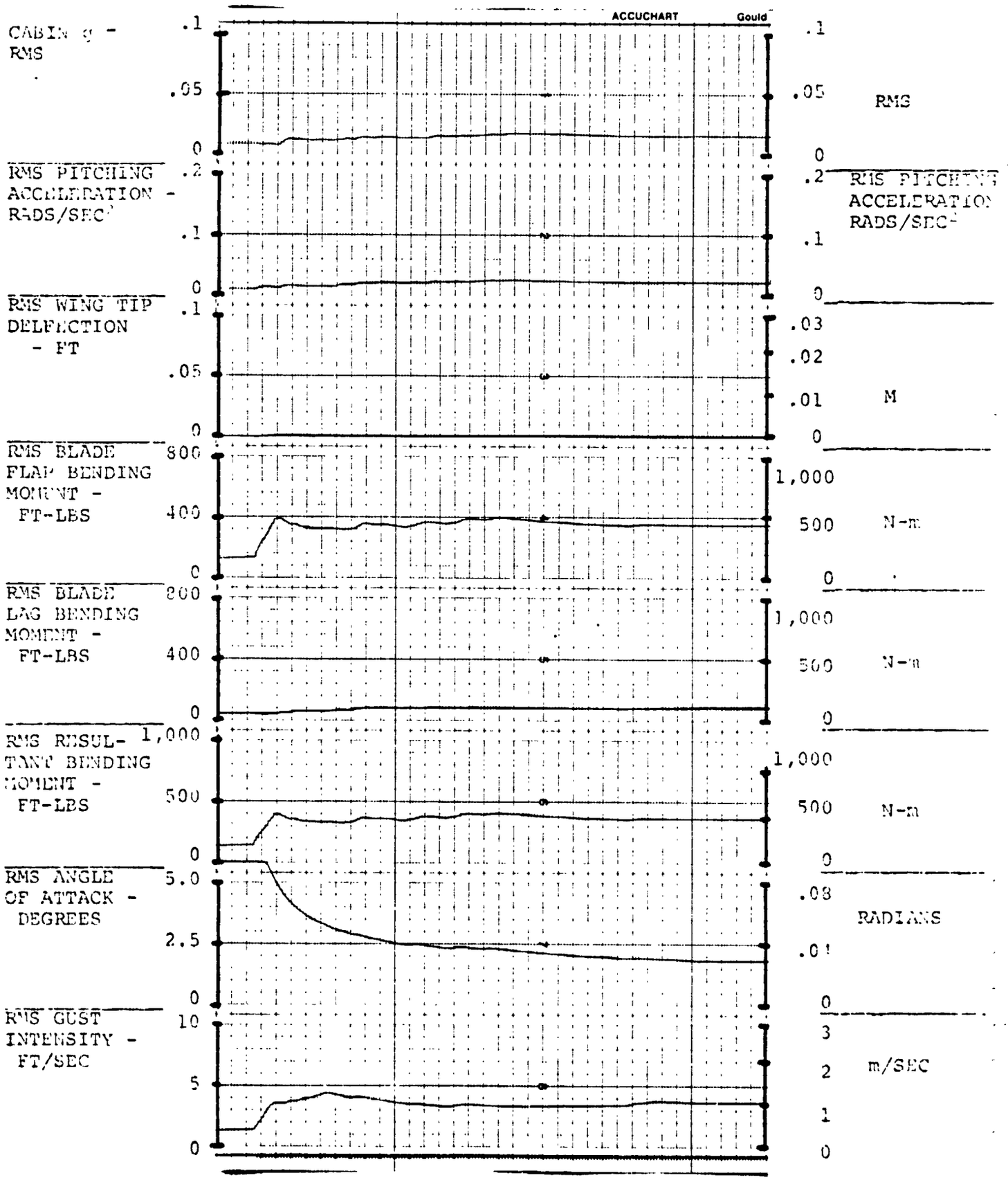

FIGURE 5.2.2.0.0.2. RESPONSES FOR GAIN F = 4.0, GAIN E = .6

FLIGHT CONDITION: 200 KNOTS, 15,000 FEET, (4,573m), AFT CG

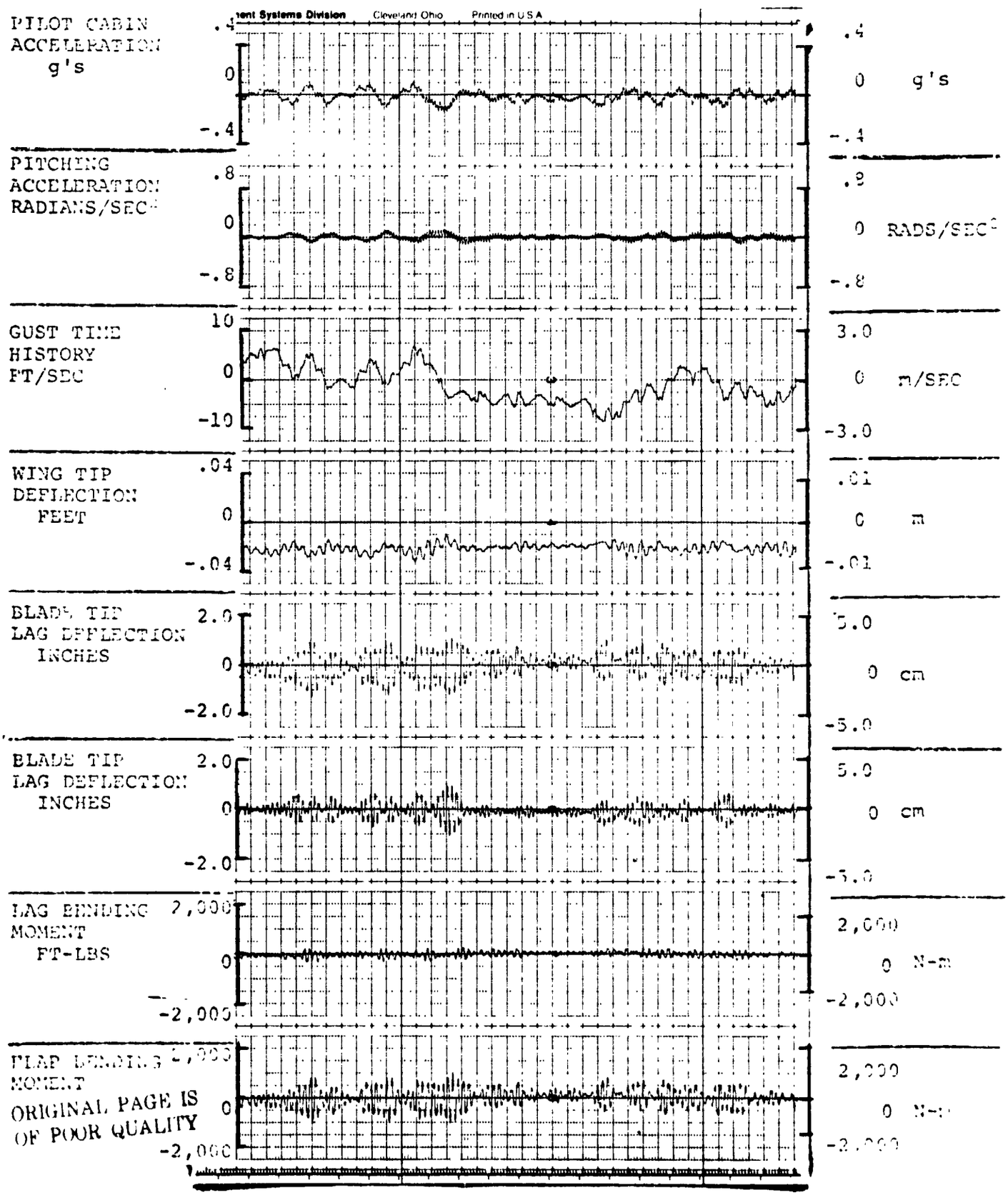

ORIGINAL PAGE IS OF POOR QUALITY

FIGURE 3.3.2.0.0.1. RESPONSES FOR GAIN F = 0, GAIN E = 0

FLIGHT CONDITION: 200 KNOTS, 15,000 FEET, (4,573m), AFT CG

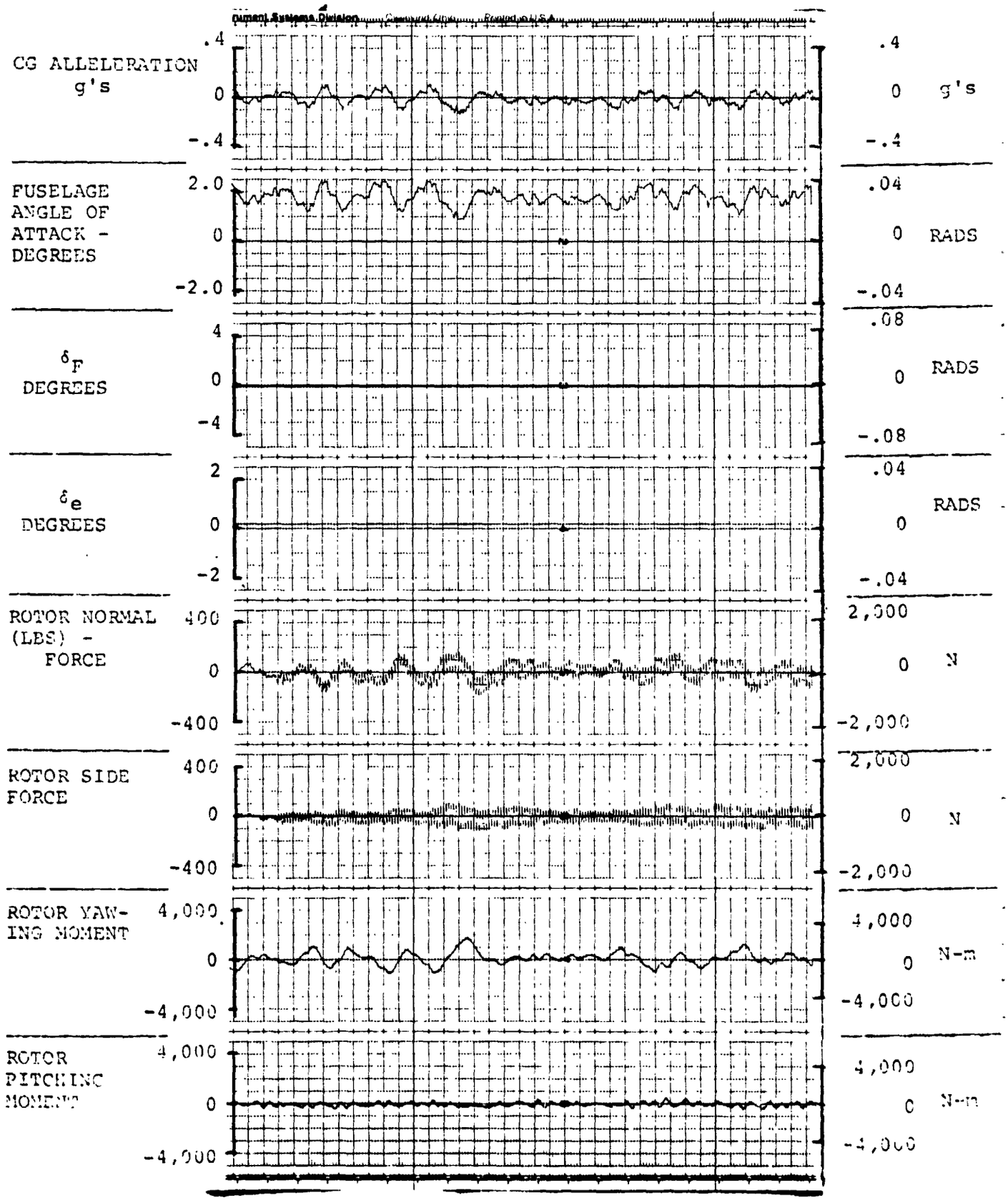

FIGURE 4.3.2.0.0.1. RESPONSES FOR GAIN F = 0, GAIN E = 0

FLIGHT CONDITION: 200 KNOTS, 15,000 FEET, (4,573m), AFT CG

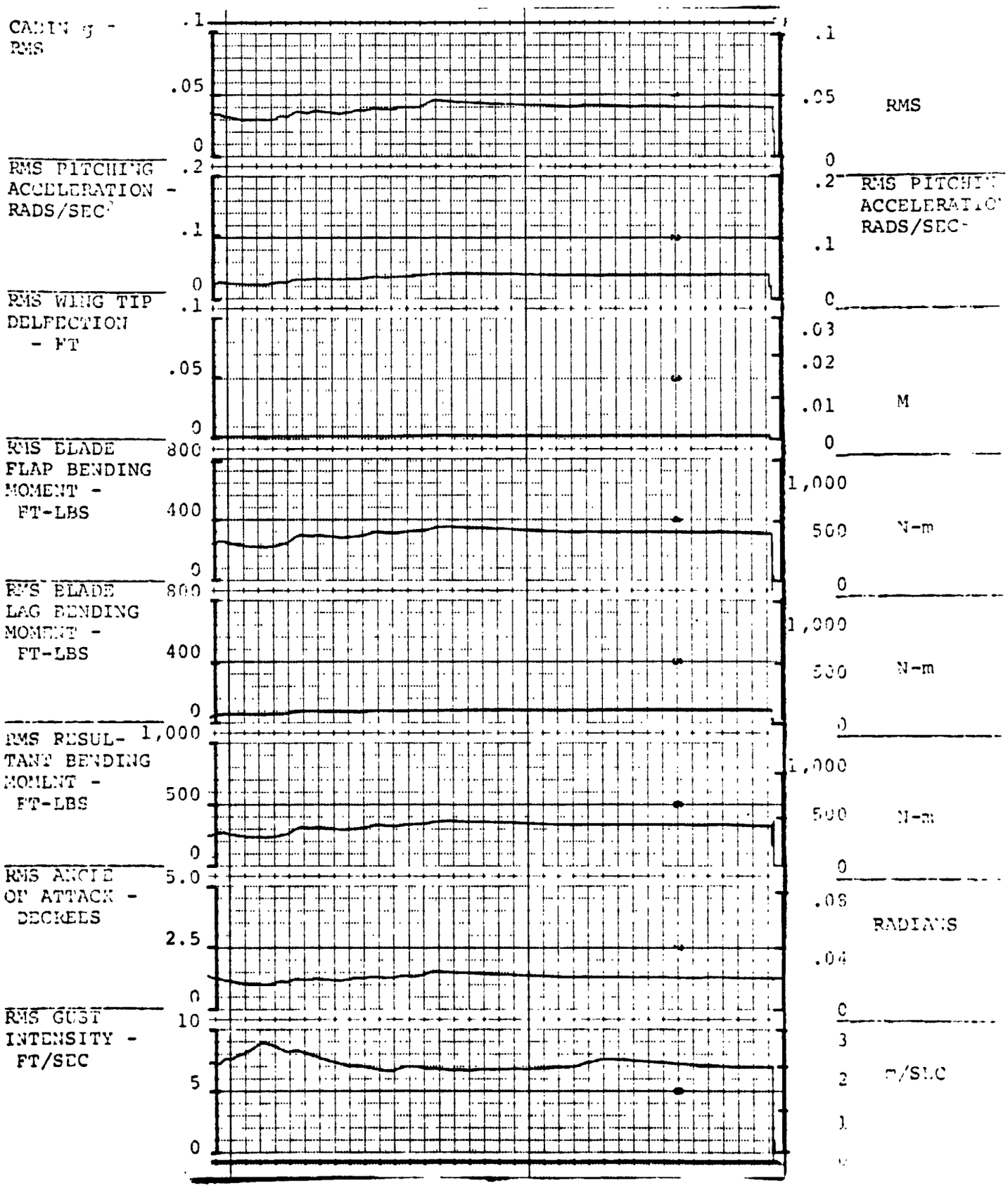

FIGURE 5.3.2.0.0.1. RESPONSES FOR GAIN F = 0, GAIN E = 0

FLIGHT CONDITION: 200 KNOTS, 15,000 FEET, (4,573m), AFT CG

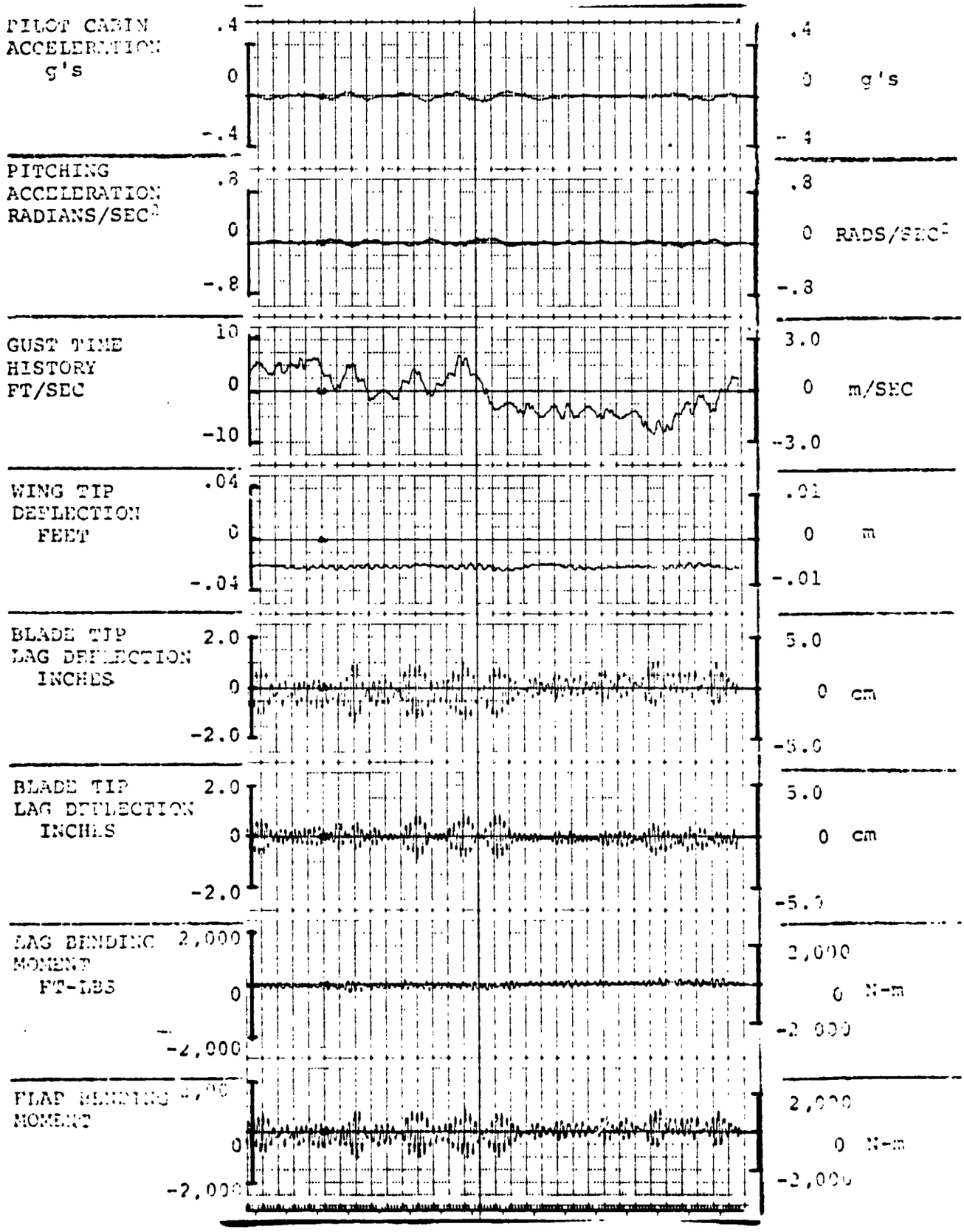

FIGURE 3.3.2.0.0.2. RESPONSES FOR GAIN F = 4.0, GAIN E = .6

FLIGHT CONDITION: 200 KNOTS, 15,000 FEET, (4,573m), AFT CG

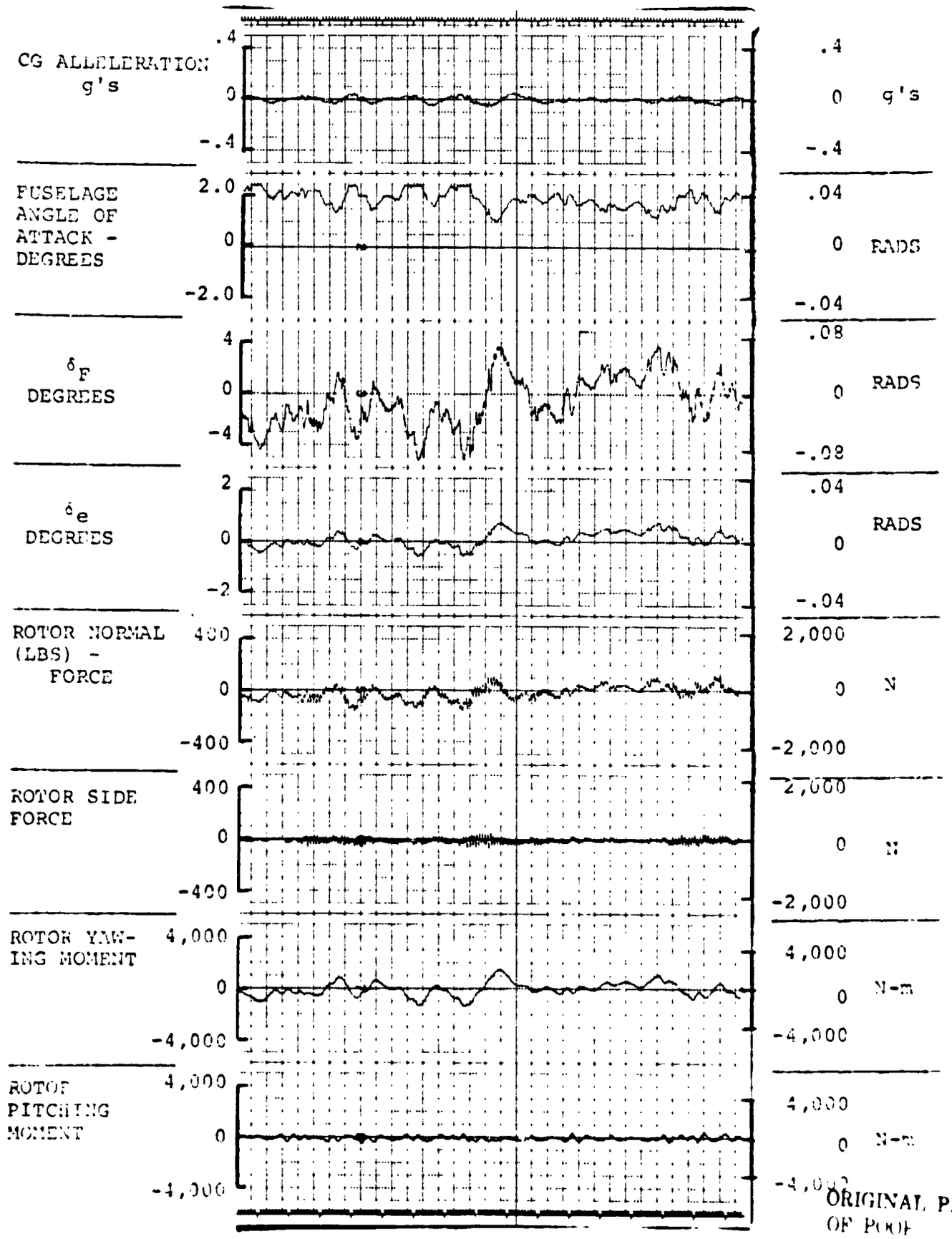

ORIGINAL PAGE IS OF POOR

FIGURE 4.3.2.0.0.2. RESPONSES FOR GAIN F = 4.0, GAIN E = .6

FLIGHT CONDITION: 200 KNOTS, 15,000 FEET, (4,573m), AFT CG

D210-11231-2

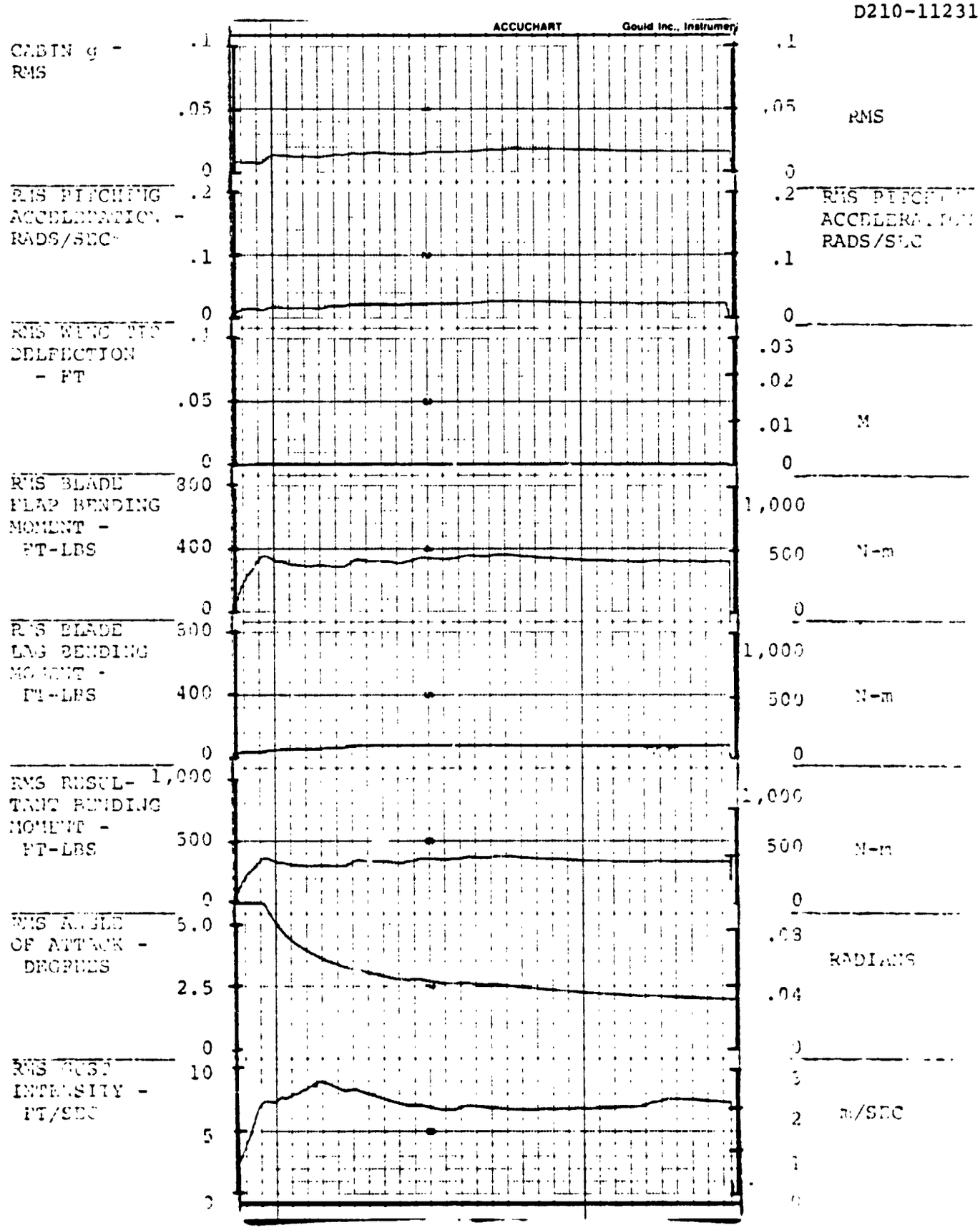

FIGURE 3. 0.0.2. RESPONSES FOR GAIN F = 4.0, GAIN E = .6

240 KNOTS, 3049M (10,000 FEET), FORWARD CG

$\omega_g = \pm 5$ FT/SEC

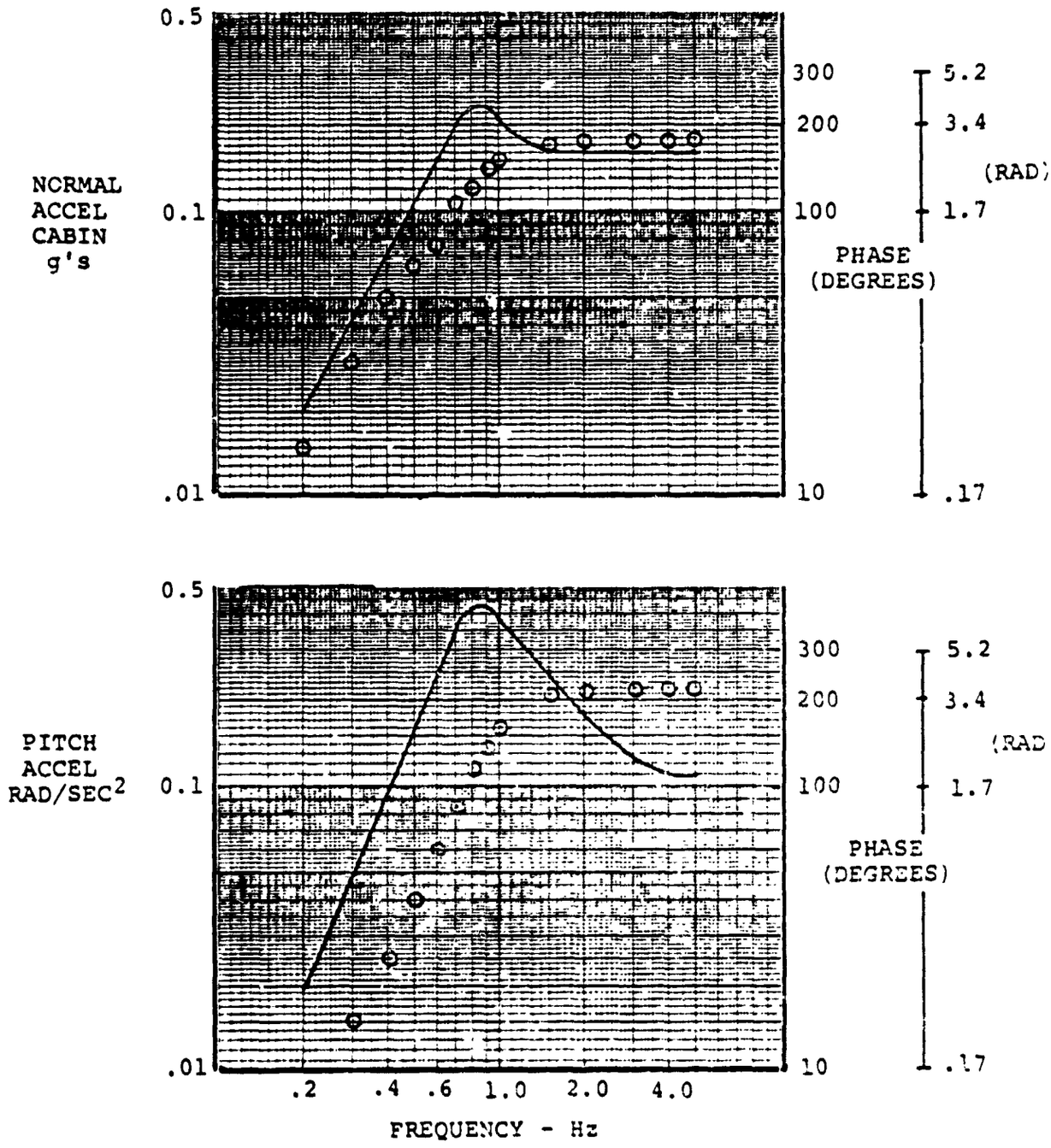

FREQUENCY RESPONSE OF CABIN NORMAL AND PITCH ACCELERATIONS DUE TO VERTICAL GUST (240 KNOTS, 3049 METERS, FORWARD CG)

FIGURE 1.5.1.1/2.1.0

240 KNOTS, 3049M (10,000 FEET), FORWARD CG

$\omega_g = \pm 5$ FT/SEC

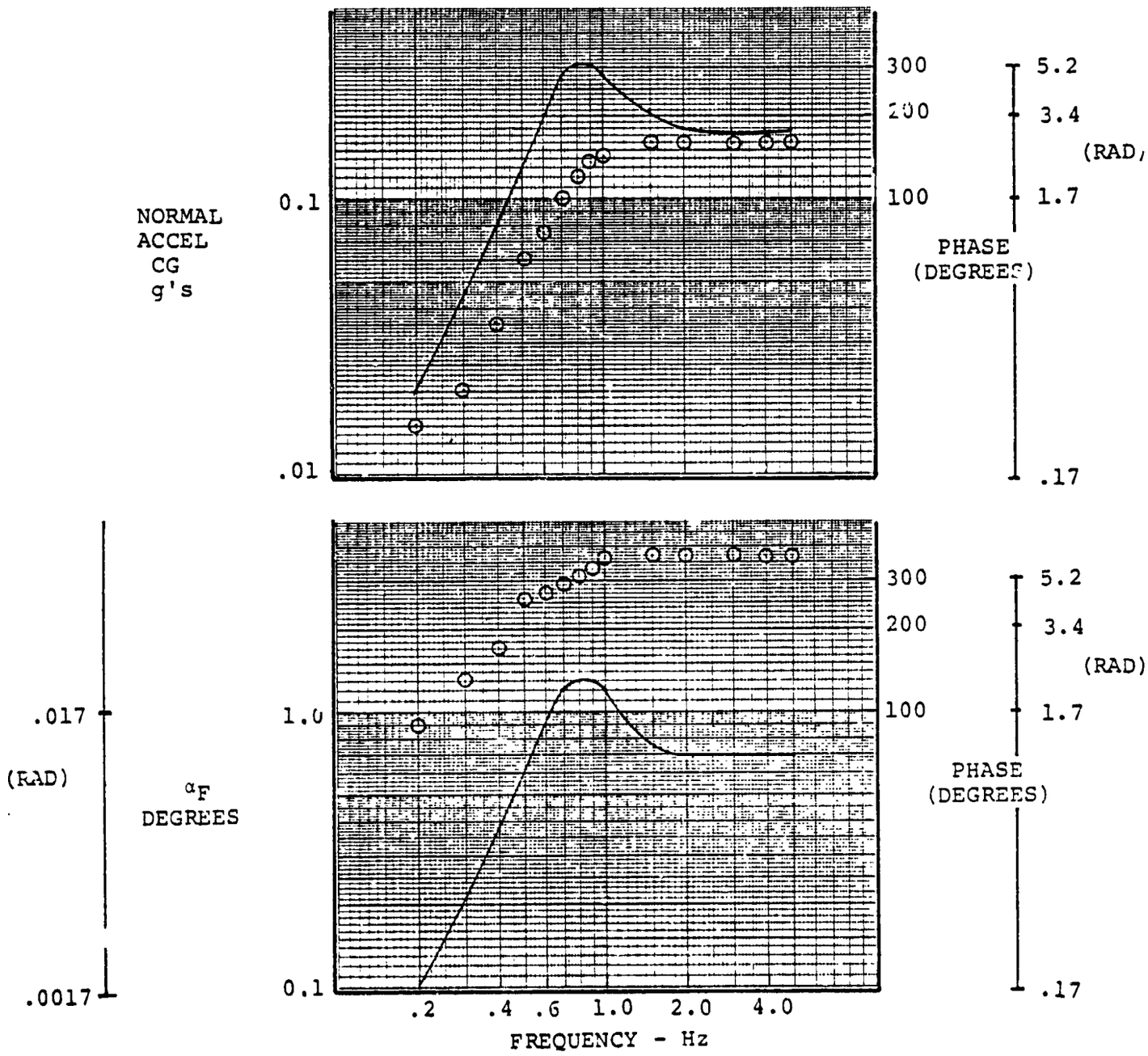

FREQUENCY RESPONSE OF NORMAL ACCELERATION AT CG AND FUSELAGE ANGLE OF ATTACK DUE TO VERTICAL GUSTS (240 KNOTS, 3049 METERS, FORWARD CG)

FIGURE 1.5.1.3/4.1.0

240 KNOTS, 3049M (10,000 FEET), FORWARD CG

ω_g = 5 FT/SEC

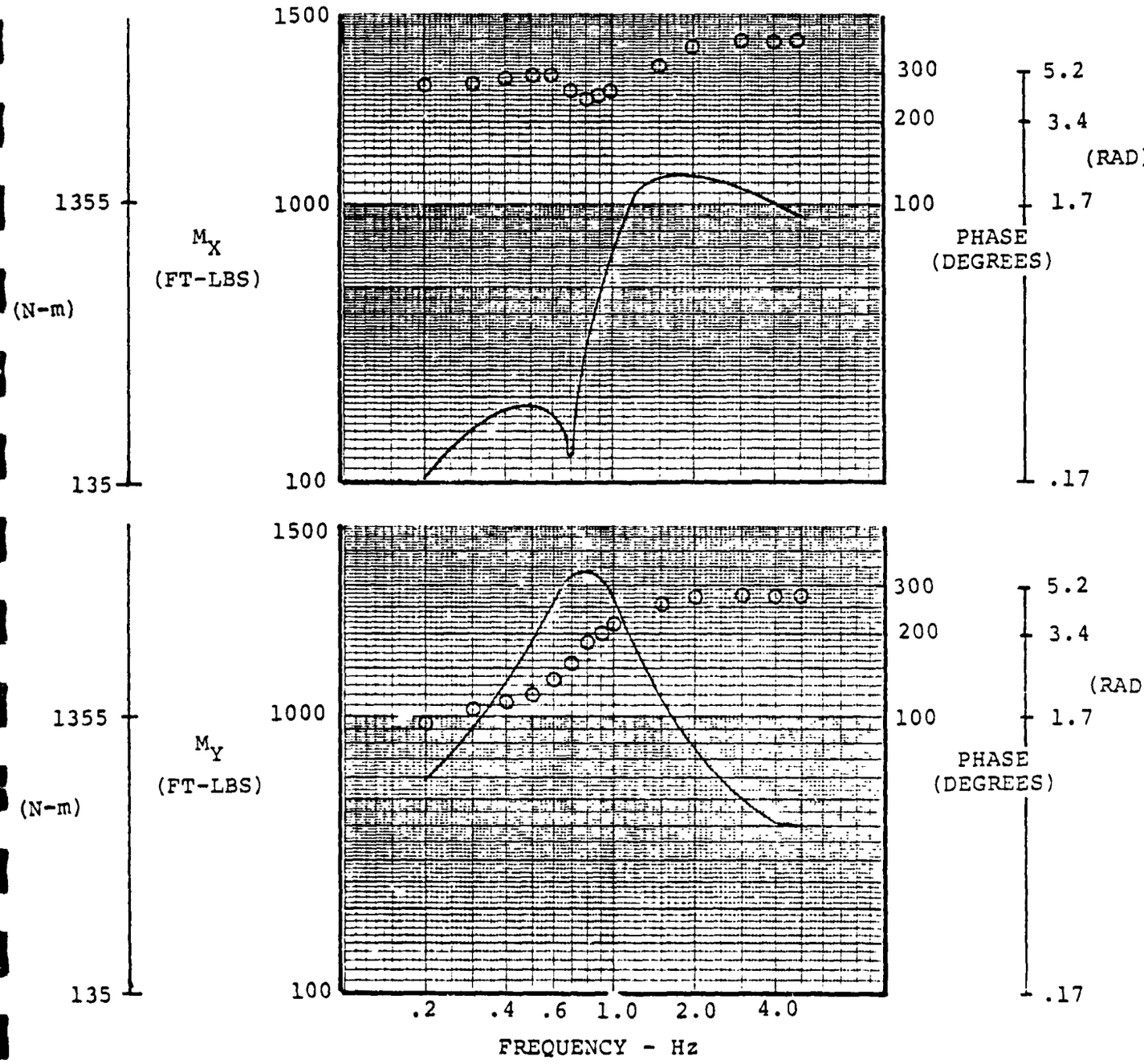

FREQUENCY RESPONSE OF ROTOR HUB MOMENTS DUE TO VERTICAL GUSTS (240 KNOTS, 3049 METERS, FORWARD CG)

FIGURE 1.5.1.5/6.1.0

240 KNOTS, 3049M (10,000 FEET), FORWARD CG

$\delta_F = \pm 1.0°$

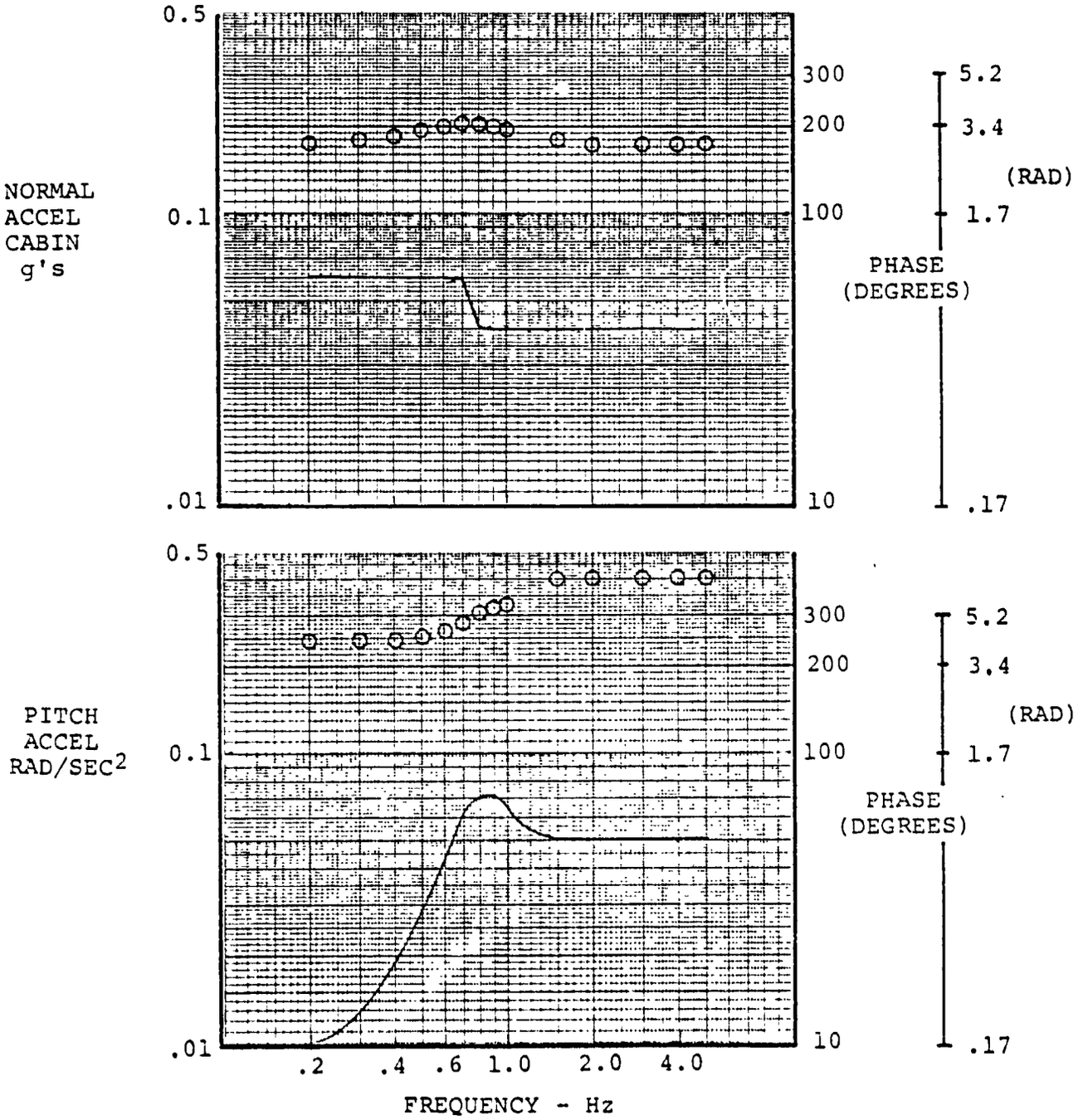

FREQUENCY RESPONSE OF CABIN NORMAL AND PITCH ACCELERATIONS DUE TO δ_F (240 KNOTS, 3049 METERS, FORWARD CG)

FIGURE 1.5.1.1/2.2.0

240 KNOTS, 3049M (10,000 FEET), FORWARD CG

$\delta_F = \pm 1°$

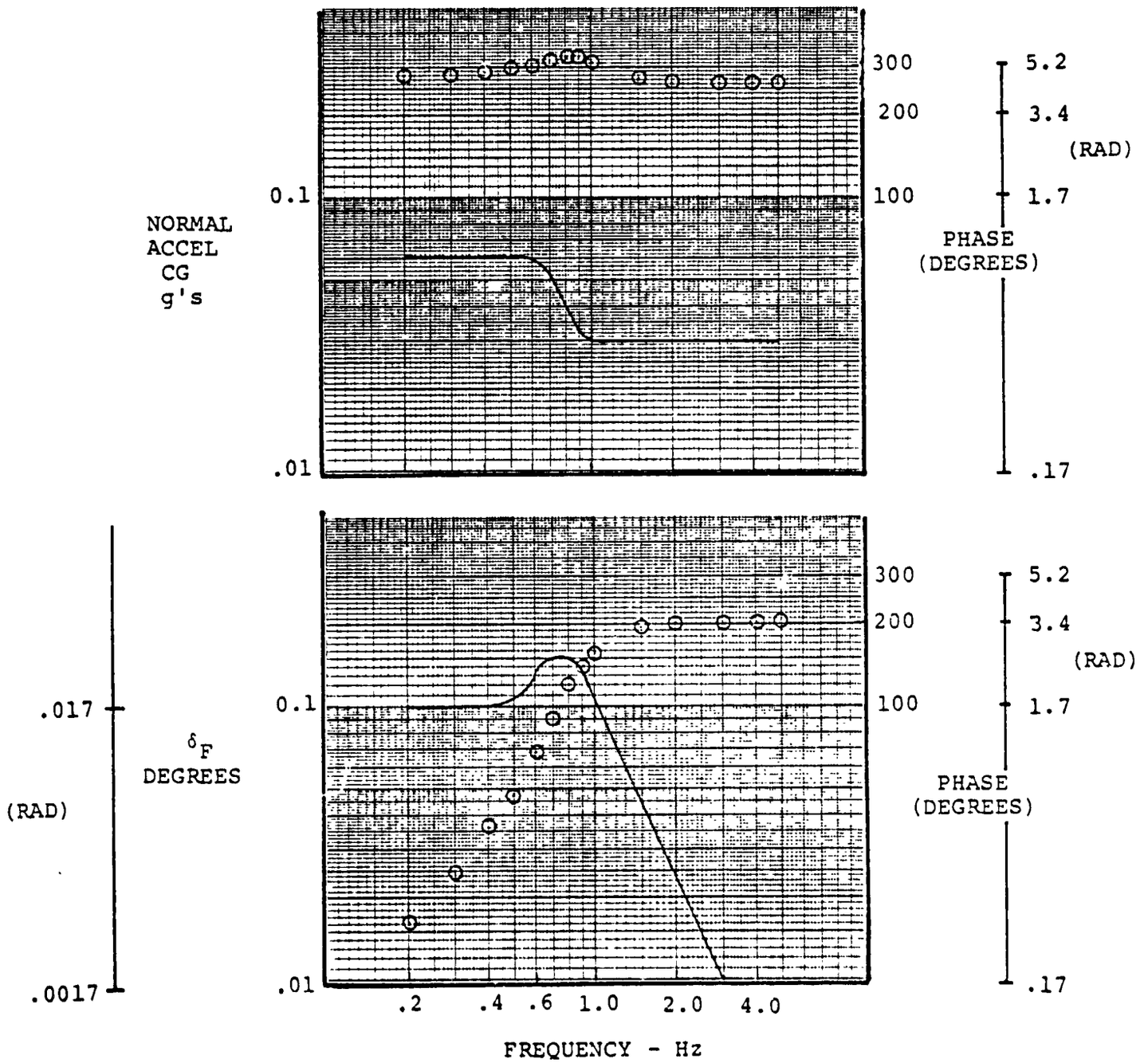

FREQUENCY RESPONSE AT NORMAL ACCELERATION AT CG AND FUSELAGE ANGLE OF ATTACK DUE TO δ_F
(240 KNOTS, 3049 METERS, FORWARD CG)

FIGURE 1.5.1.3/4.2.0

240 KNOTS, 3049M (10,000 FEET), FORWARD CG

$\delta_F = \pm 1.0°$

D210-11231-2

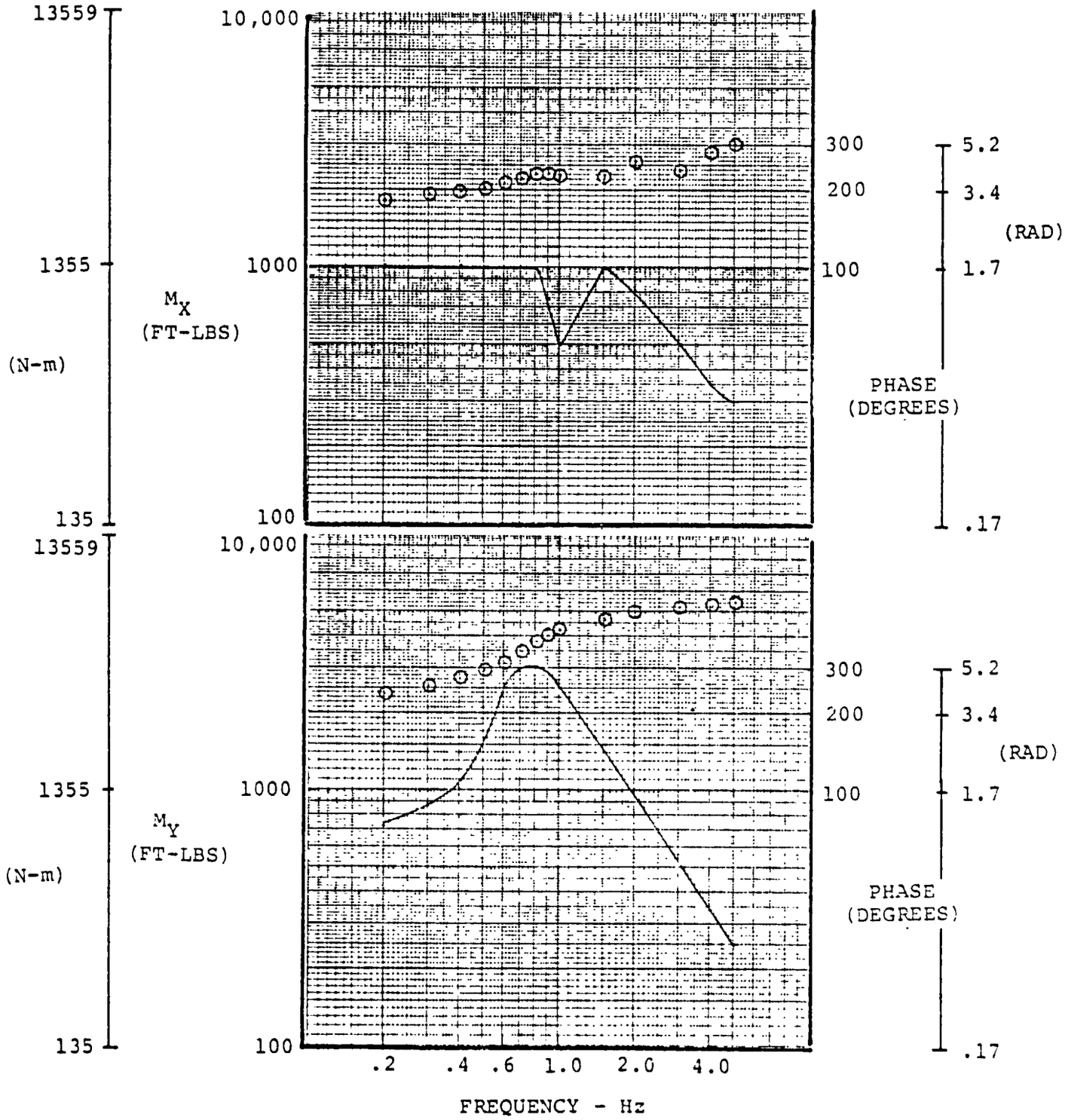

FREQUENCY RESPONSE OF ROTOR HUB MOMENTS DUE TO δ_F (240 KNOTS, 3049 METERS, FORWARD CG)

FIGURE 1.5.1.5/6.2.0

240 KNOTS, 3049M (10,000 FEET), FORWARD CG

$\delta_e = \pm .5°$

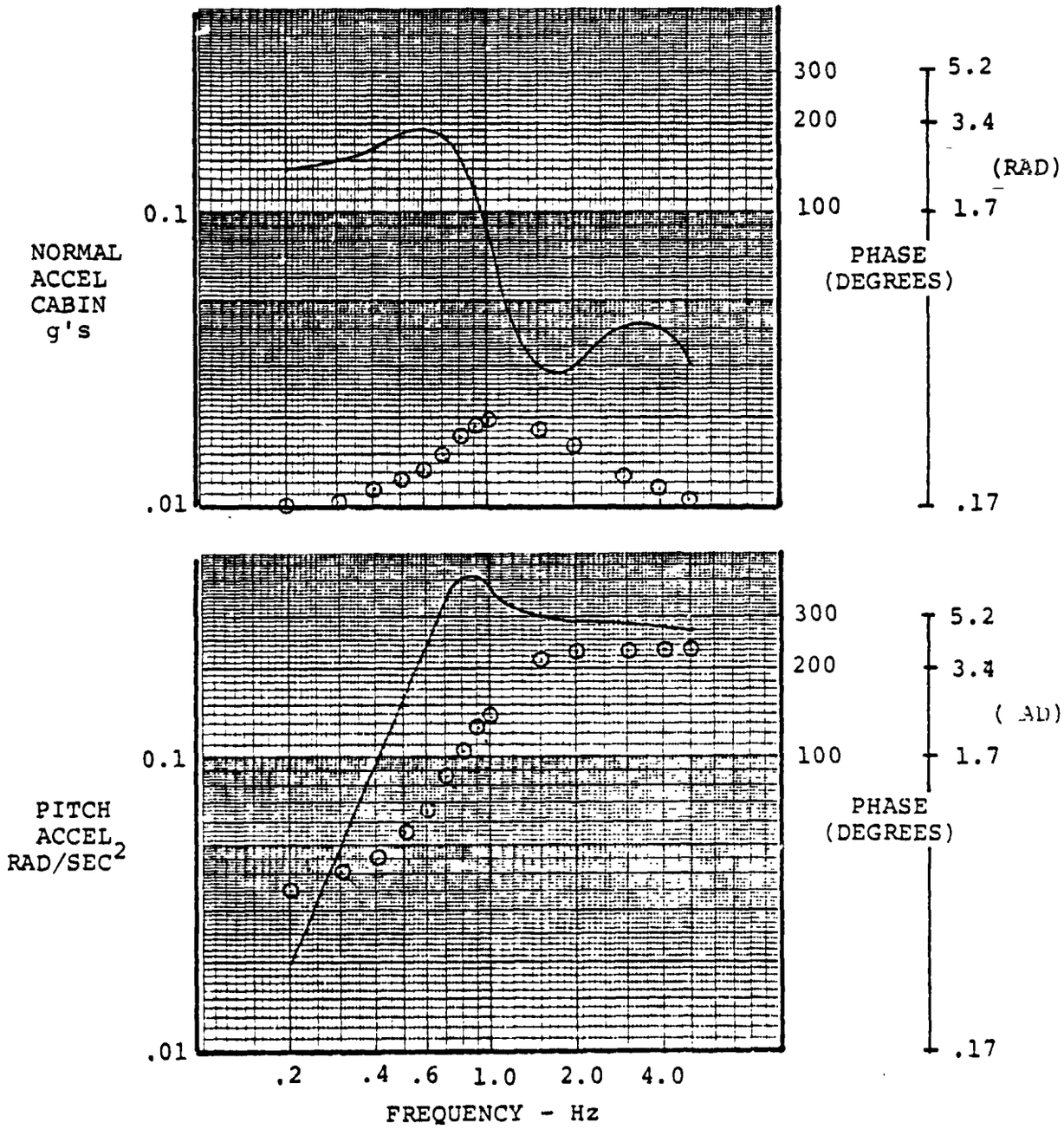

FREQUENCY RESPONSE OF CABIN NORMAL AND PITCH ACCELERATIONS DUE TO δ_e (240 KNOTS, 3049 METERS, FORWARD CG)

FIGURE 1.5.1.1/2.3.0

240 KNOTS, 3049M (10,000 FEET), FORWARD CG

$\delta_e = \pm .5°$

D210-11231-2

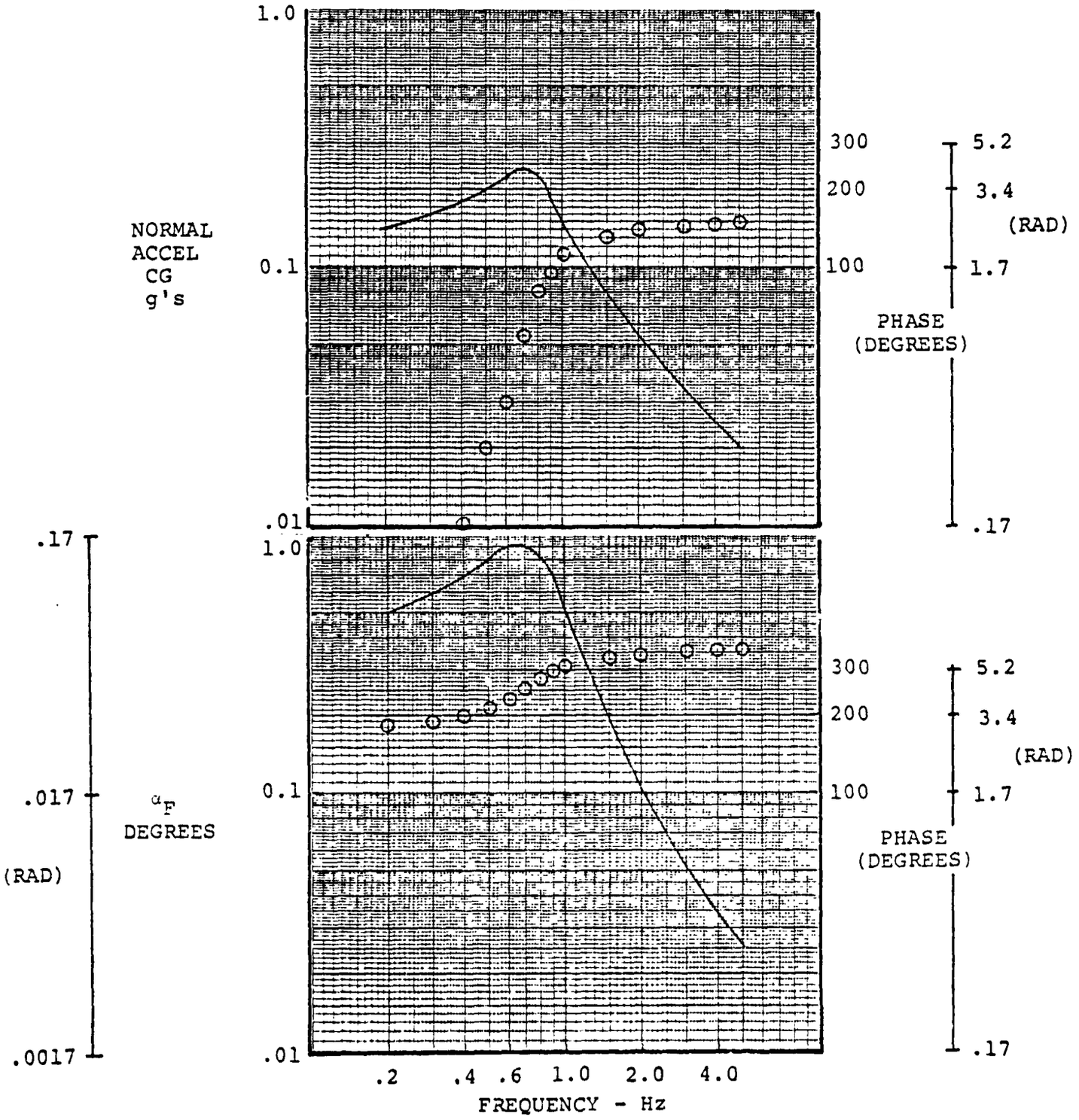

FREQUENCY RESPONSE OF NORMAL ACCELERATION AT CG AND FUSELAGE ANGLE OF ATTACK DUE TO δ_e (240 KNOTS, 3049 METERS, FORWARD CG)

FIGURE 1.5.1.3/4.3.0

240 KNOTS, 3049M (10,000 FEET), FORWARD CG

$\delta_e = \pm .5°$

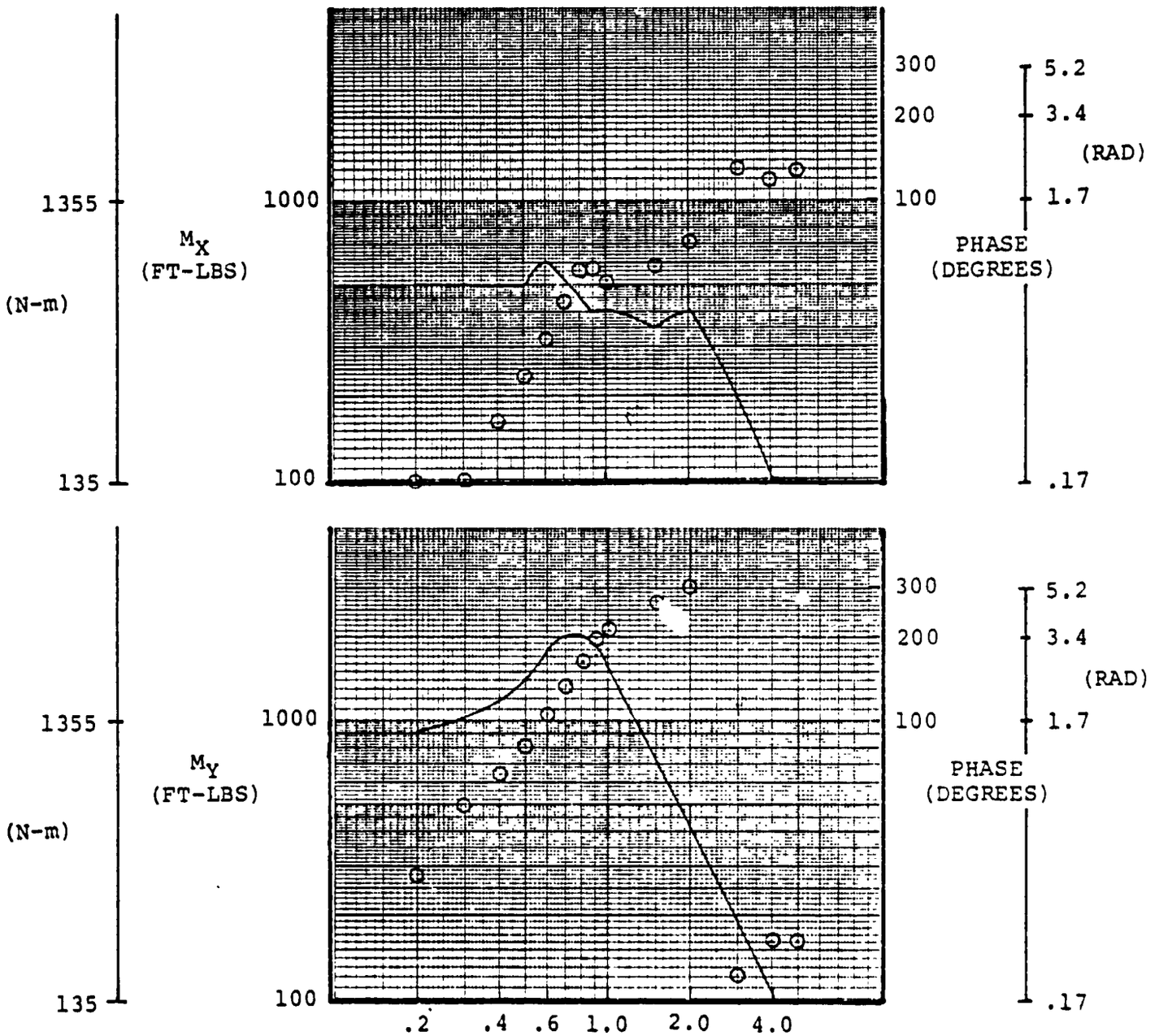

FREQUENCY RESPONSE OF ROTOR HUB MOMENTS DUE TO δ_e (240 KNOTS, 3049 METERS, FORWARD CG)

FIGURE 1.5.1.5/6.3.0

240 KNOTS, 3049M (10,000 FEET), FORWARD CG
$\delta A_1 = \pm .25°$

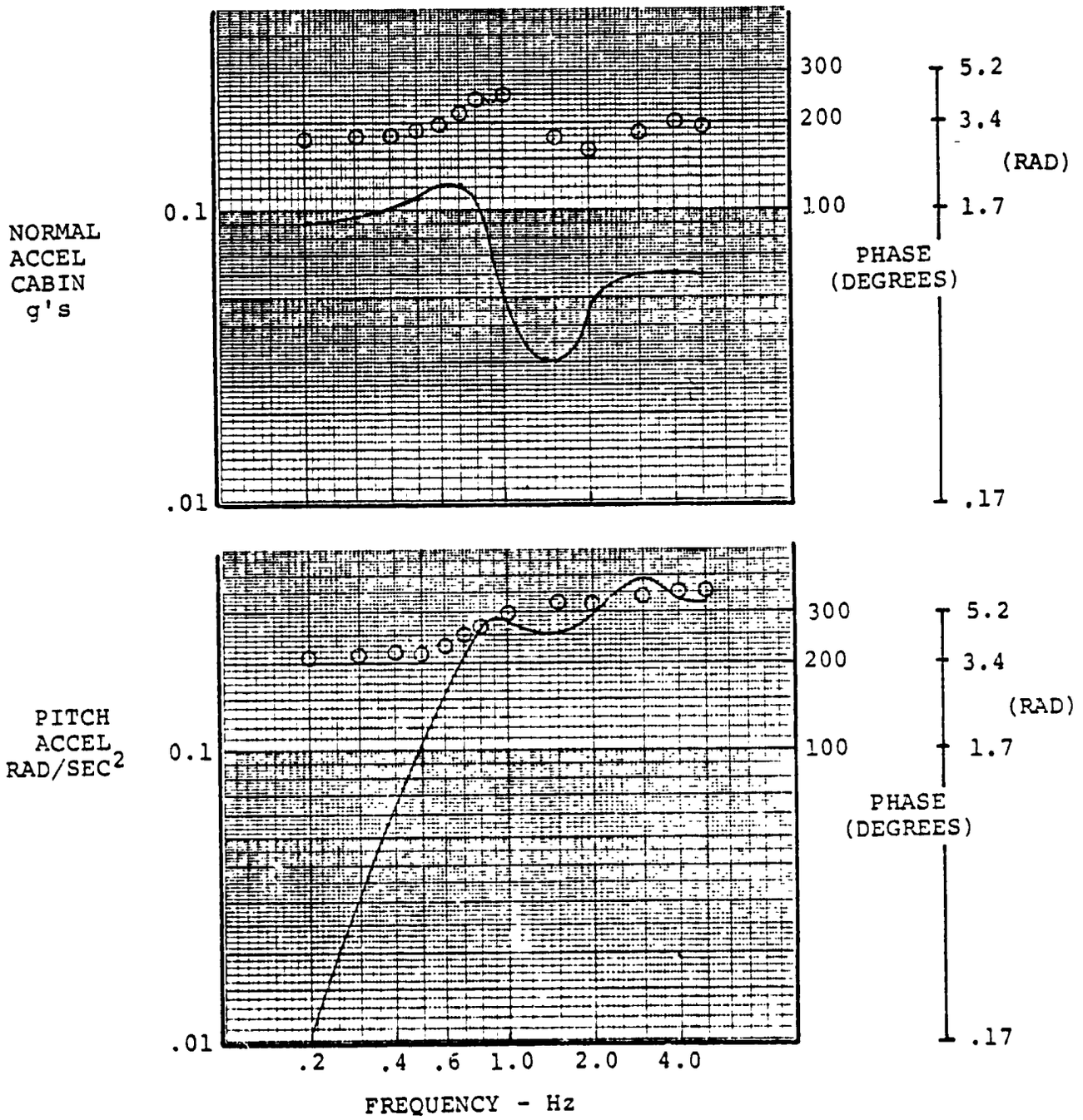

FREQUENCY RESPONSE OF CABIN NORMAL AND PITCH ACCELERATIONS DUE TO A_1 CYCLIC (240 KNOTS, 3049 METERS, FORWARD CG)

FIGURE 1.5.1.1/2.4/0

240 KNOTS, 3049M (10,000 FEET), FORWARD CG

$\delta A_1 = \pm .25°$

D210-11231-2

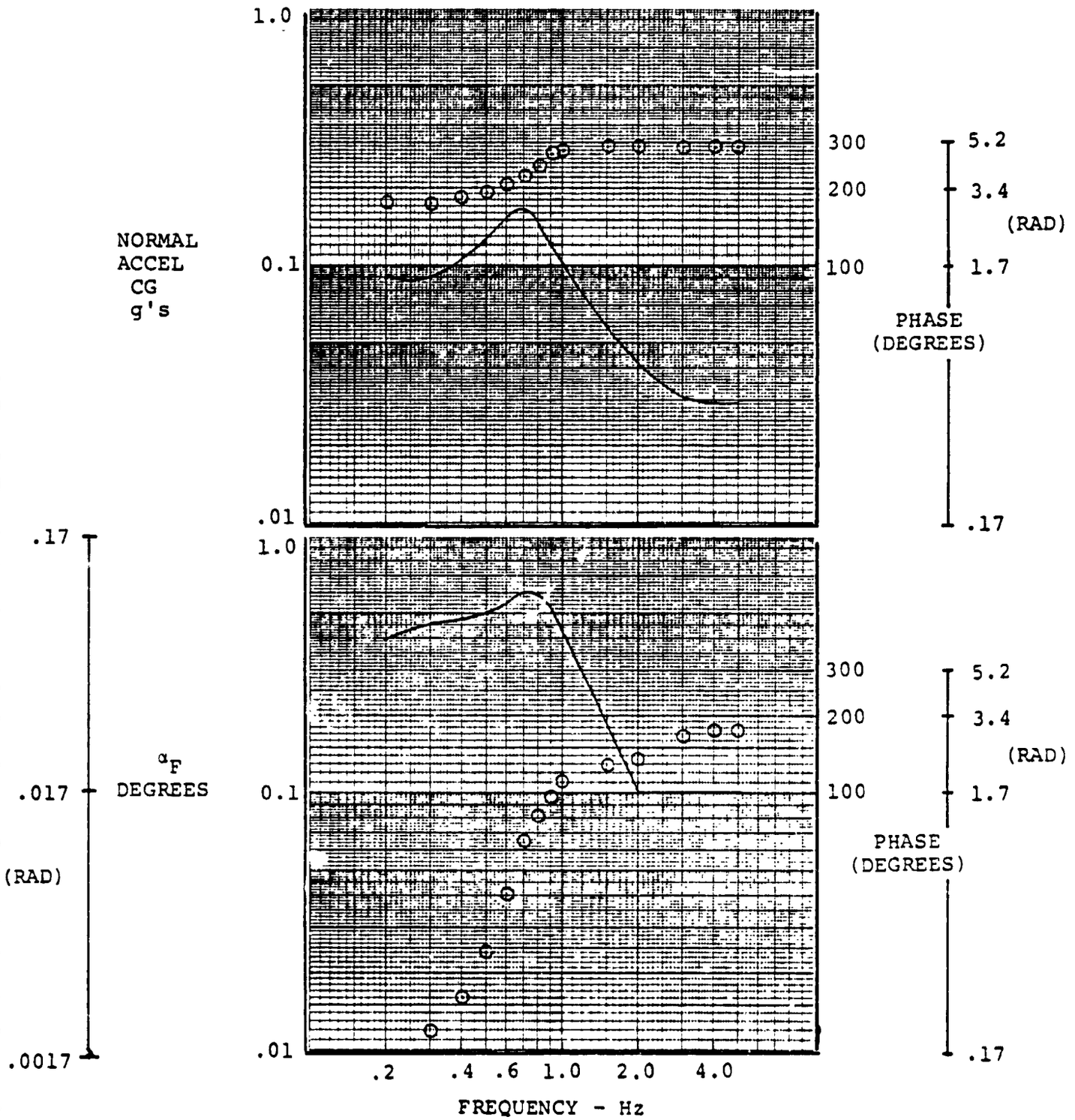

FREQUENCY RESPONSE OF NORMAL ACCELERATION AT CG AND FUSELAGE ANGLE OF ATTACK DUE TO A_1 CYCLIC (240 KNOTS, 3049 METERS, FORWARD CG)

FIGURE 1.5.1.3/4.4.0

240 KNOTS, 3049M (10,000 FEET), FORWARD CG

$\delta A_1 = \pm .25°$

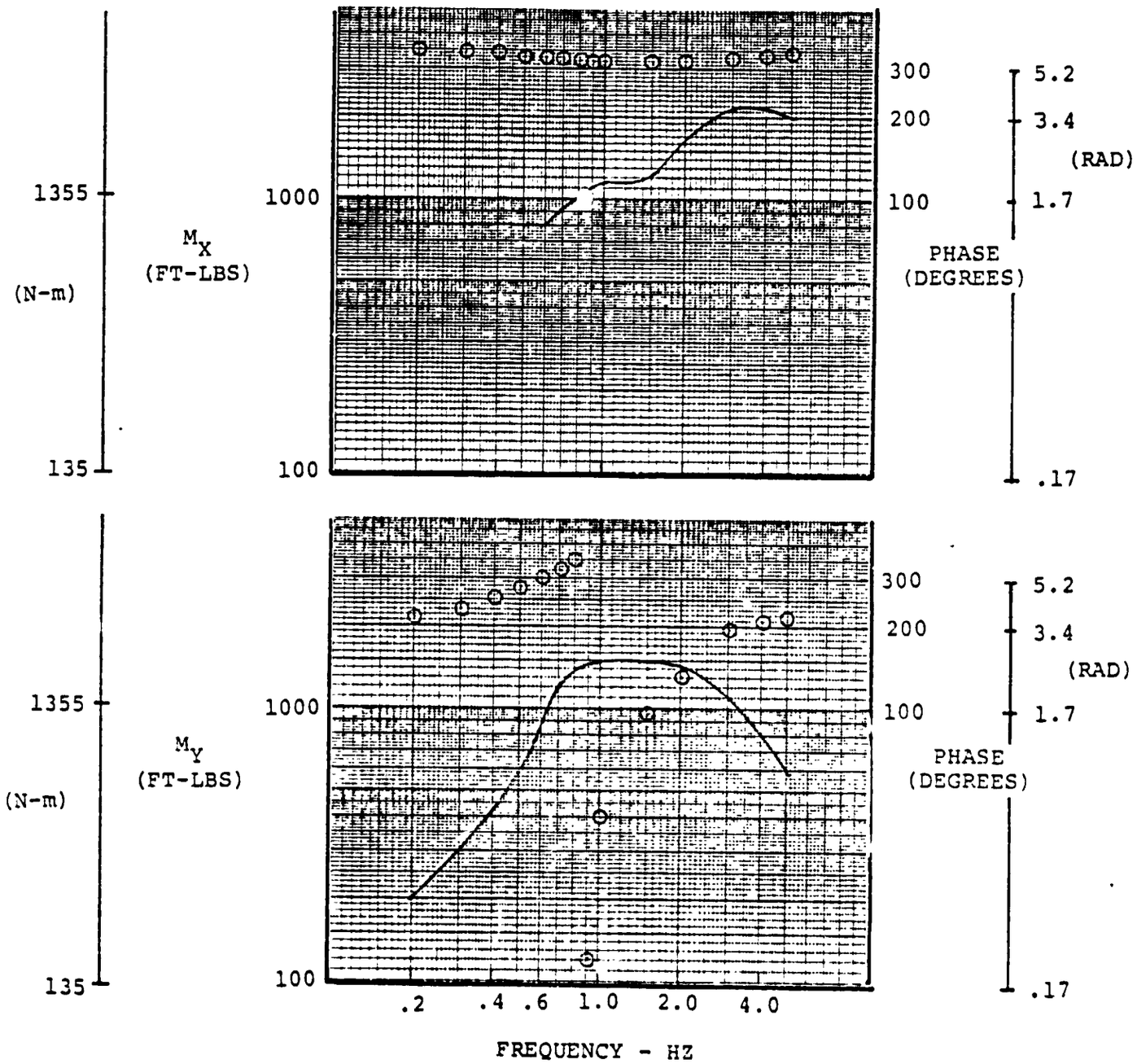

FREQUENCY RESPONSE OF ROTOR HUB MOMENTS DUE TO A_1 CYCLIC (240 KNOTS, 3049 METERS, FORWARD CG)

FIGURE 1.5.1.5/6.4.0

240 KNOTS, 3049M (10,000 FEET), FORWARD CG
$\delta B_1 = \pm .25°$

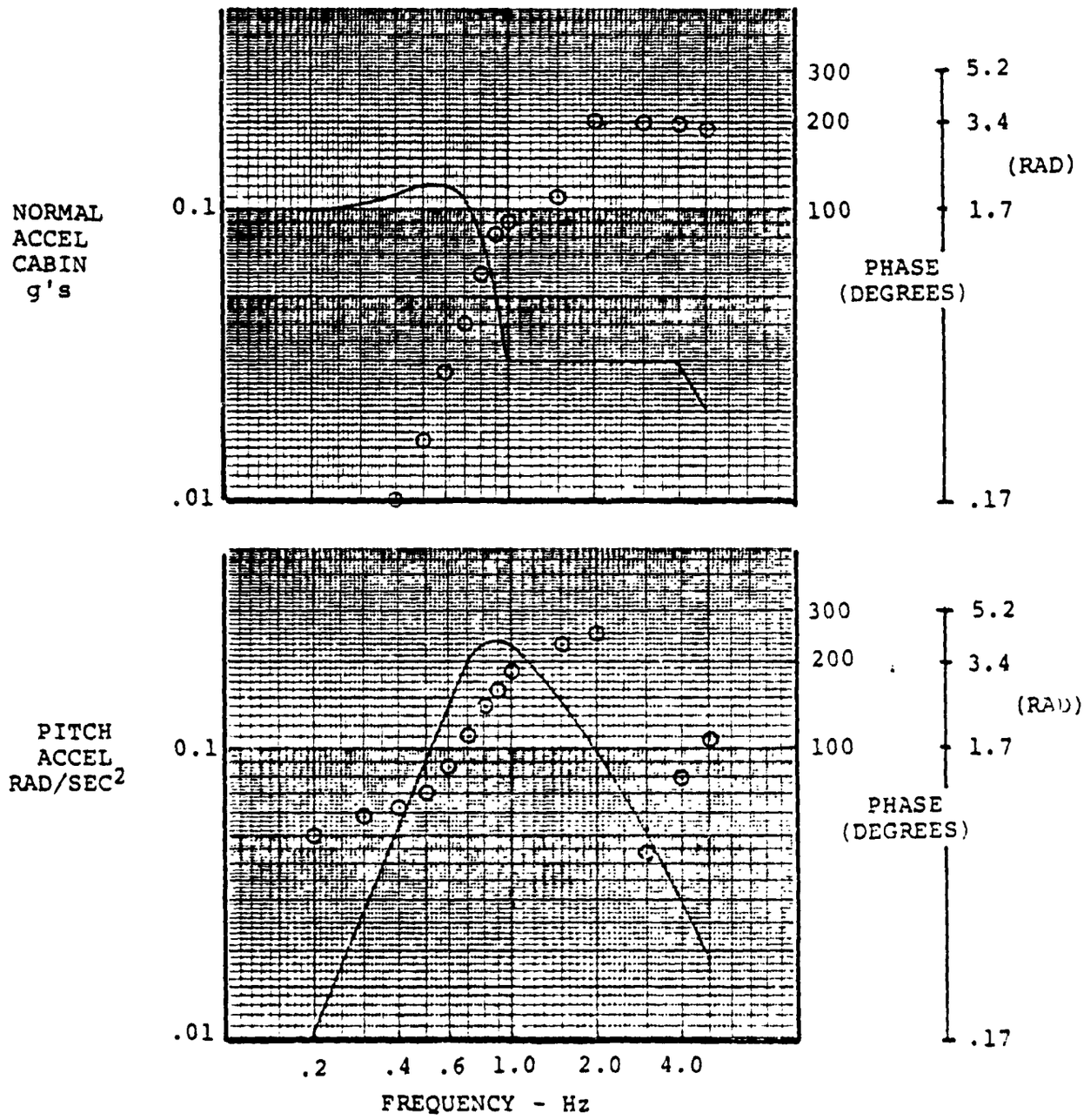

FREQUENCY RESPONSE OF CABIN NORMAL AND PITCH ACCELERATIONS DUE TO B_1 CYCLIC (240 KNOTS, 3049 METERS, FORWARD CG)

FIGURE 1.5.1.1/2.5.0

240 KNOTS, 3049M (10,000 FEET), FORWARD CG

$\delta B_1 \pm .25°$

D210-11231-2

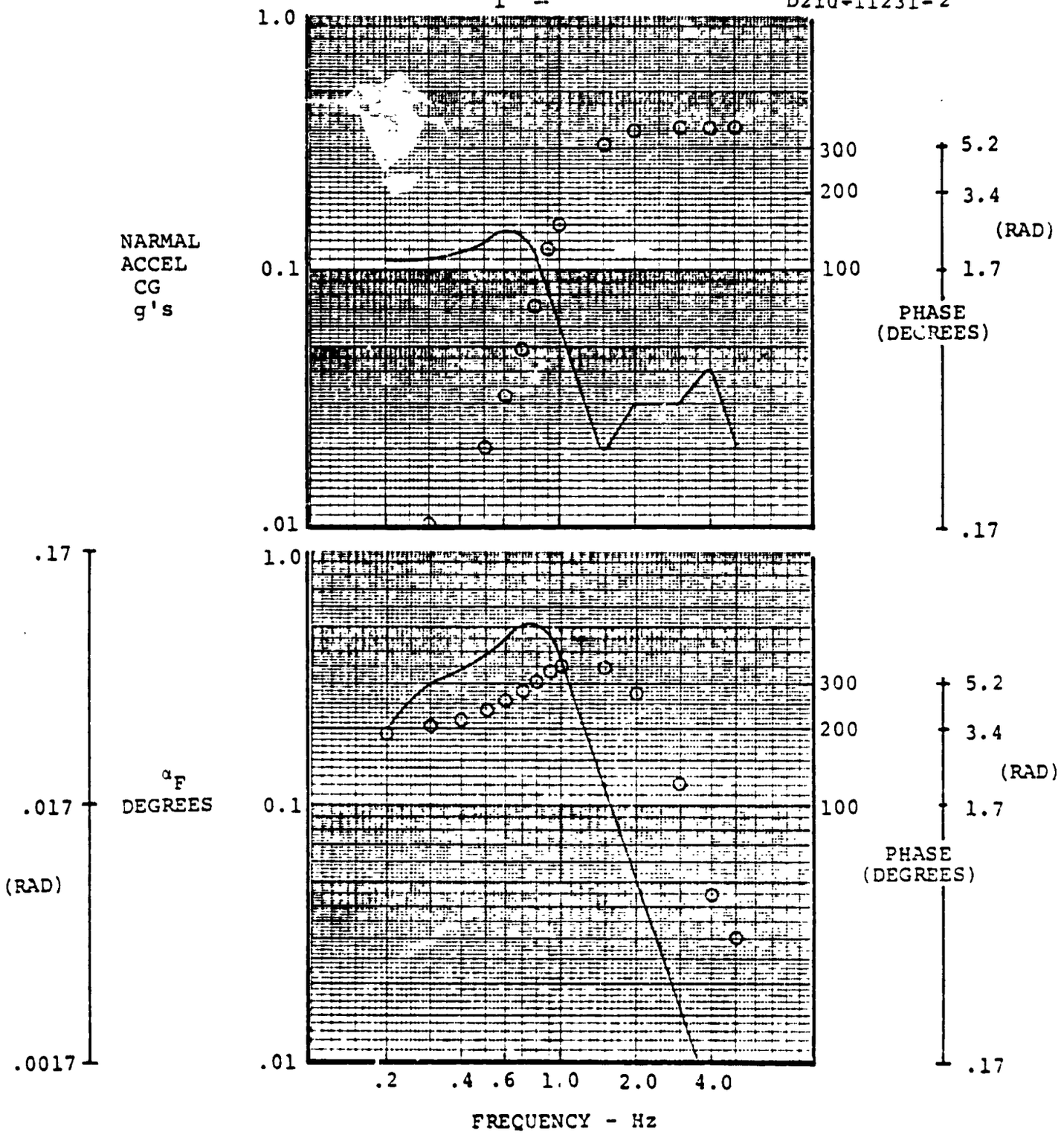

FREQUENCY RESPONSE OF NORMAL ACCELERATION AT CG AND FUSELAGE ANGLE OF ATTACK DUE TO B_1 CYCLIC (240 KNOTS, 3049 METERS, FORWARD CG)

FIGURE 1.5.1.3/4.5.0

240 KNOTS, 3049M (10,000 FEET), FORWARD CG

$\delta B_1 = \pm .25°$

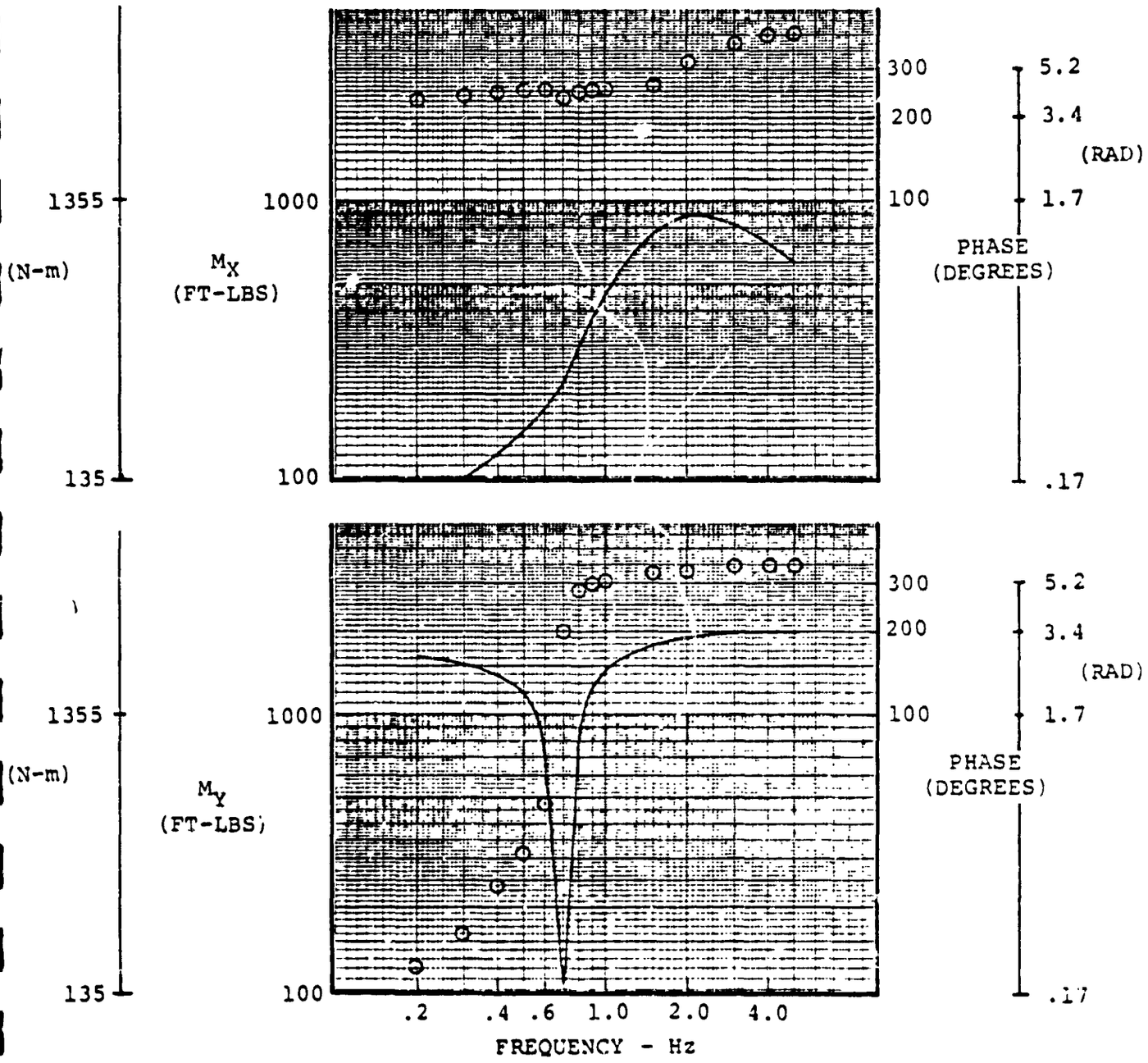

FREQUENCY RESPONSE OF ROTOR HUB MOMENTS DUE TO B_1 CYCLIC (240 KNOTS, 3049 METERS, FORWARD CG)

FIGURE 1.5.1.5/6.5.0

FEEDBACK REQUIRED FOR SPECIFIED ALLEVIATION IN CABIN

240 KNOTS, 10,000 FEET (3049M), FORWARD CG

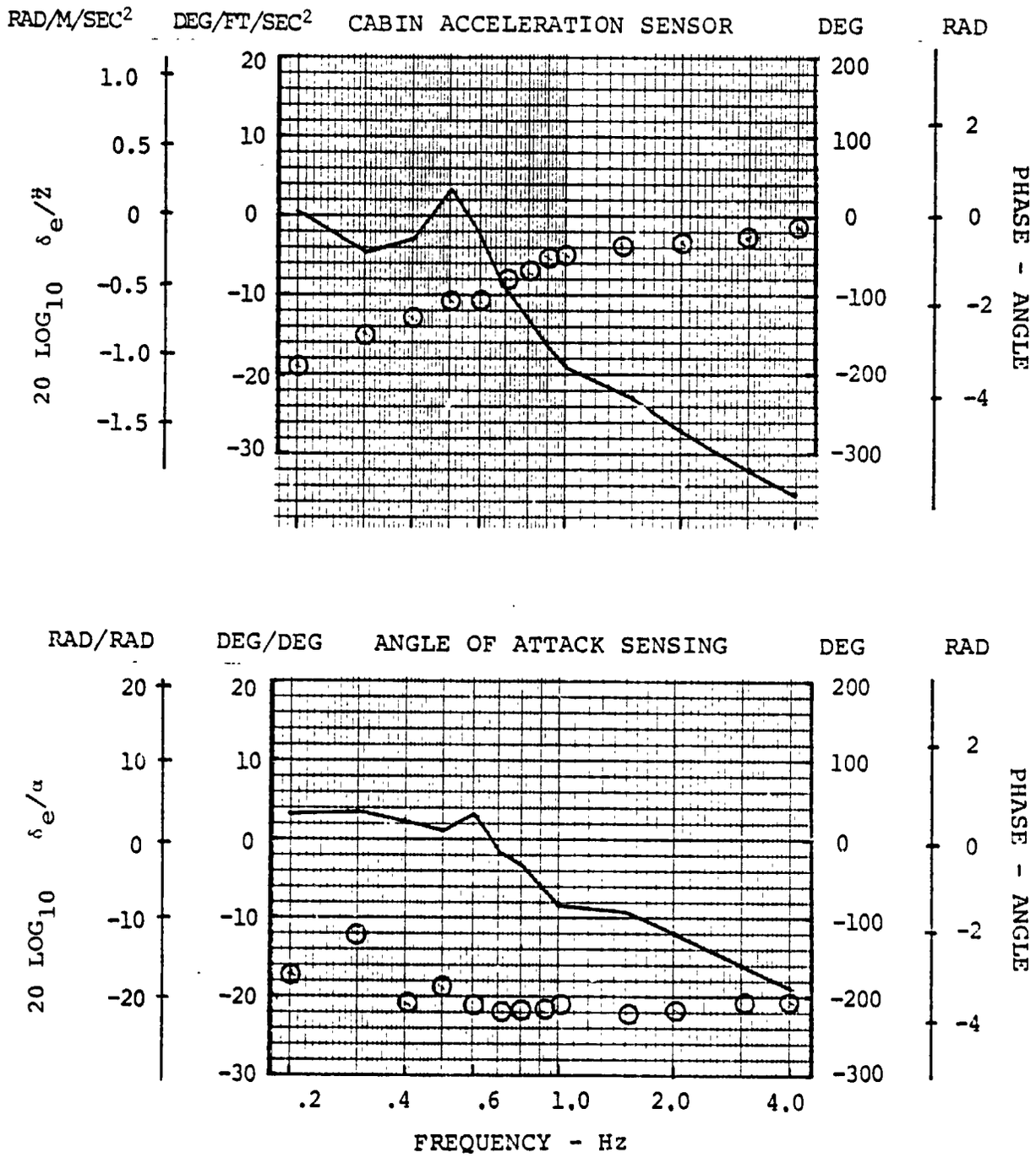

ELEVATOR FEEDBACK REQUIRED WITH ACCELERATION AND α SENSING RESPECTIVELY, 240 KNOTS, 3049 METERS, FORWARD CG, NO A_1, B_1 FEEDBACK

FIGURE 2.5.1.0.0.0

FEEDBACK REQUIRED FOR SPECIFIED ALLEVIATION IN CABIN

240 KNOTS, 10,000 FEET (3049M), FORWARD CG

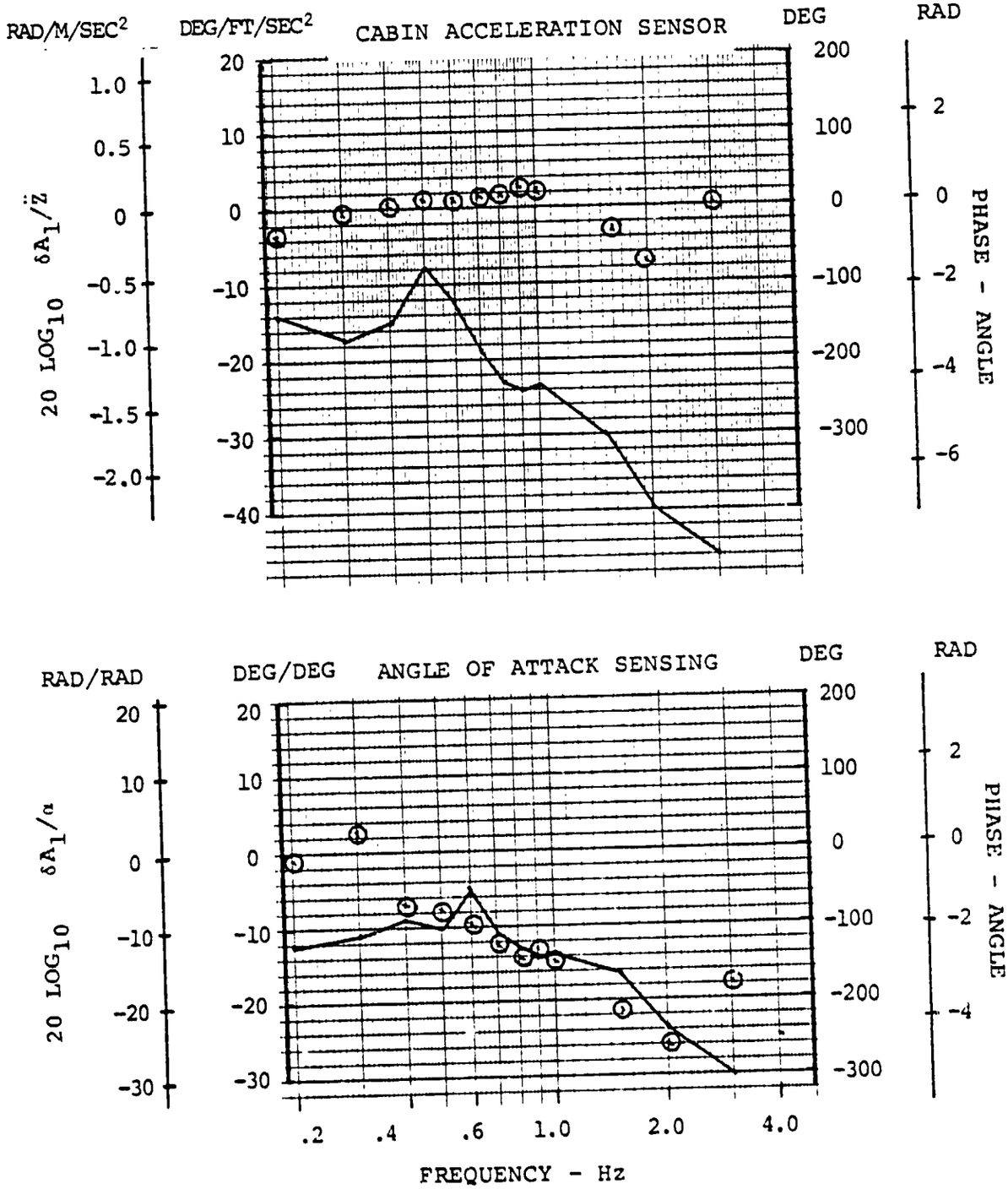

A_1 FEEDBACK REQUIRED WITH ACCELERATION AND α SENSING RESPECTIVELY, 240 KNOTS, 3049 METERS, FORWARD CG

FIGURE 2.5.1.0.0.0

FEEDBACK REQUIRED FOR SPECIFIED ALLEVIATION IN CABIN

240 KNOTS, 10,000 FEET (3049M), FORWARD CG

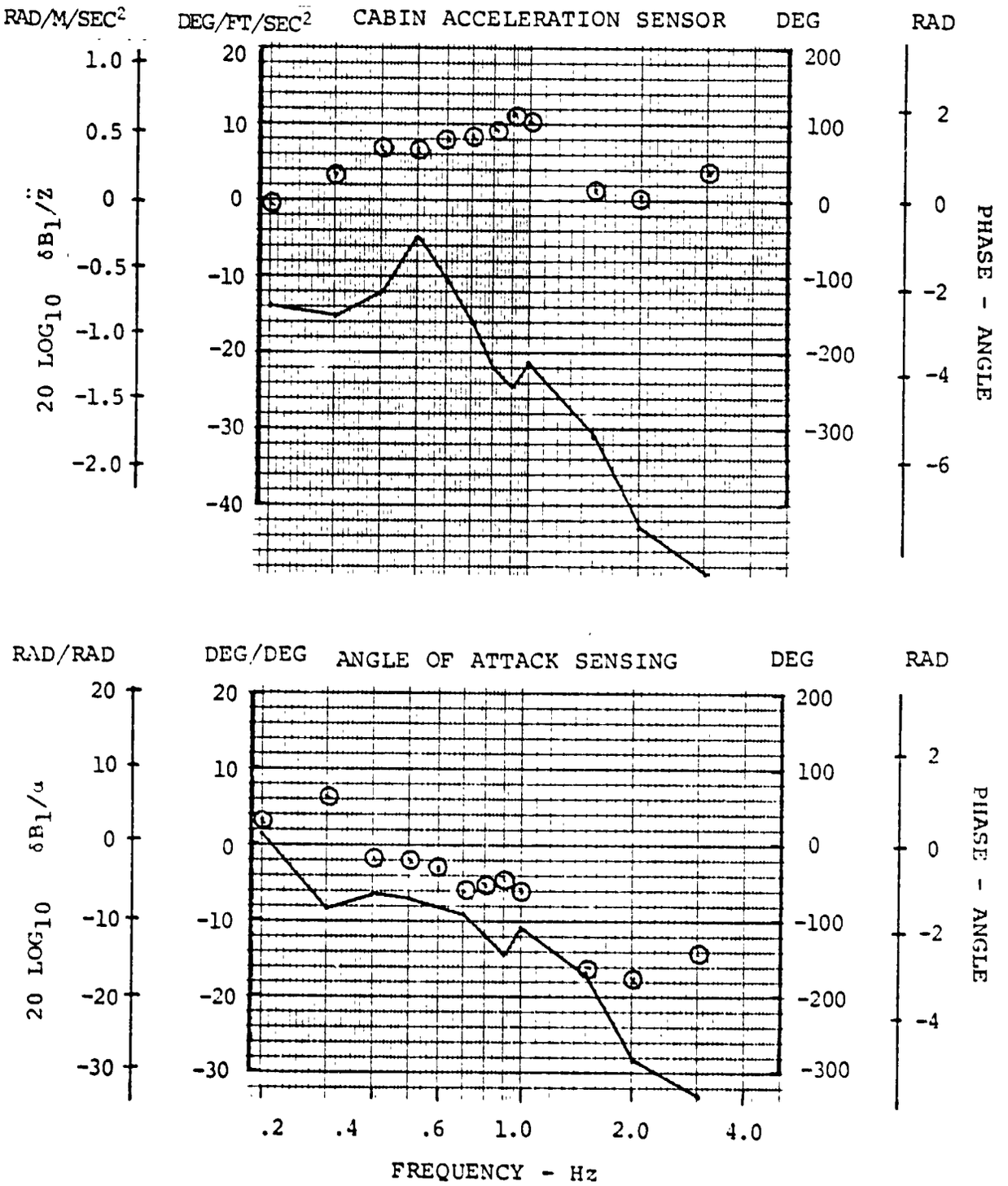

B_1 FEEDBACK REQUIRED WITH ACCELERATION AND α SENSING RESPECTIVELY, 240 KNOTS, 3049 METERS, FORWARD CG

FIGURE 2.5.1.0.0.0

FEEDBACK REQUIRED FOR SPECIFIED ALLEVIATION IN CABIN

240 KNOTS, 10,000 FEET (3049M), FORWARD CG

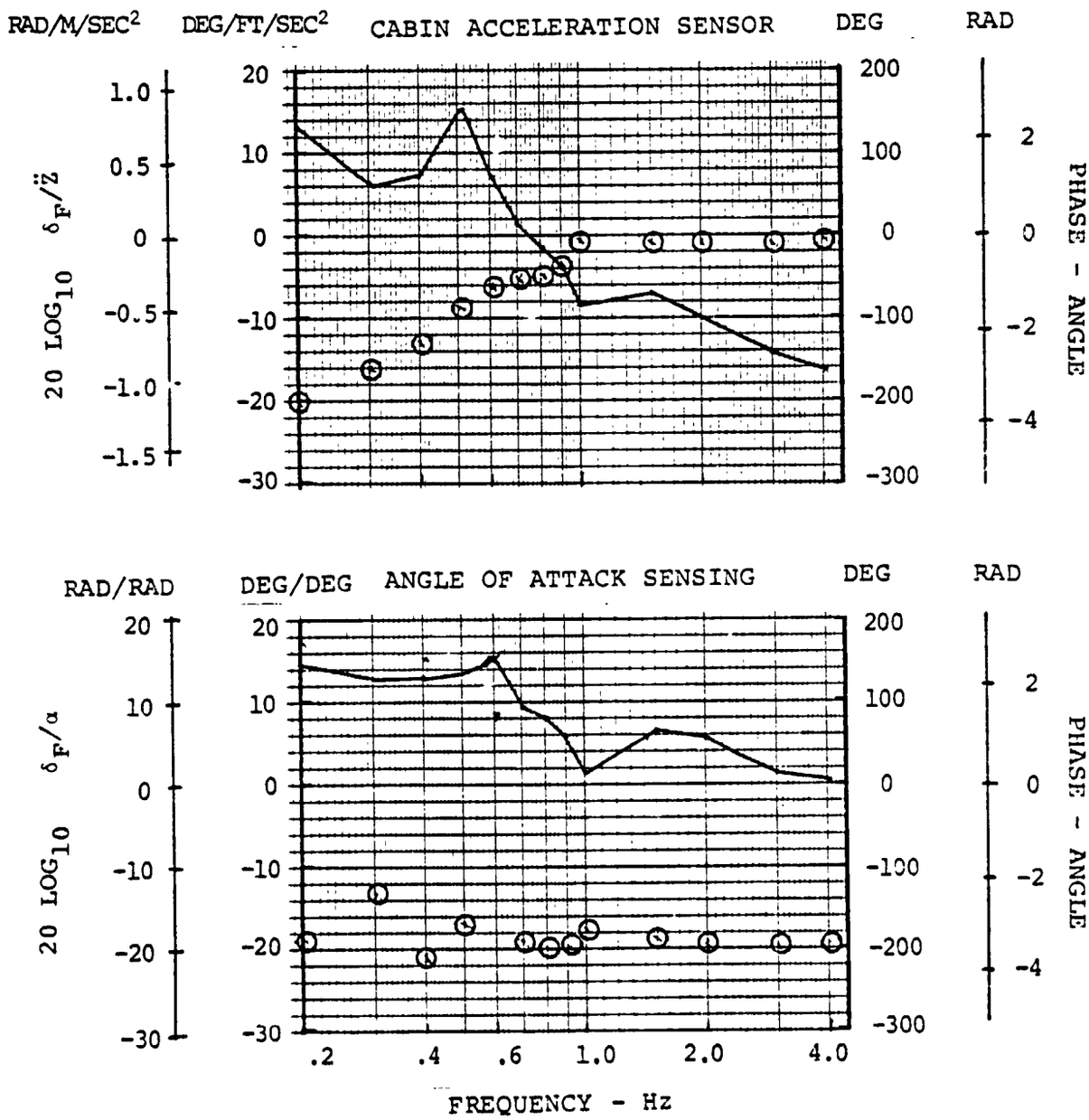

FLAP FEEDBACK REQUIRED WITH ACCELERATION AND α SENSING RESPECTIVELY, 240 KNOTS, 3049 METERS, FORWARD CG, A_1 & B_1 FEEDBACK INCLUDED

FIGURE 2.5.1.0.0.0

FEEDBACK REQUIRED FOR SPECIFIED ALLEVIATION IN CABIN

240 KNOTS, 10,000 FEET (3049M), FORWARD CG

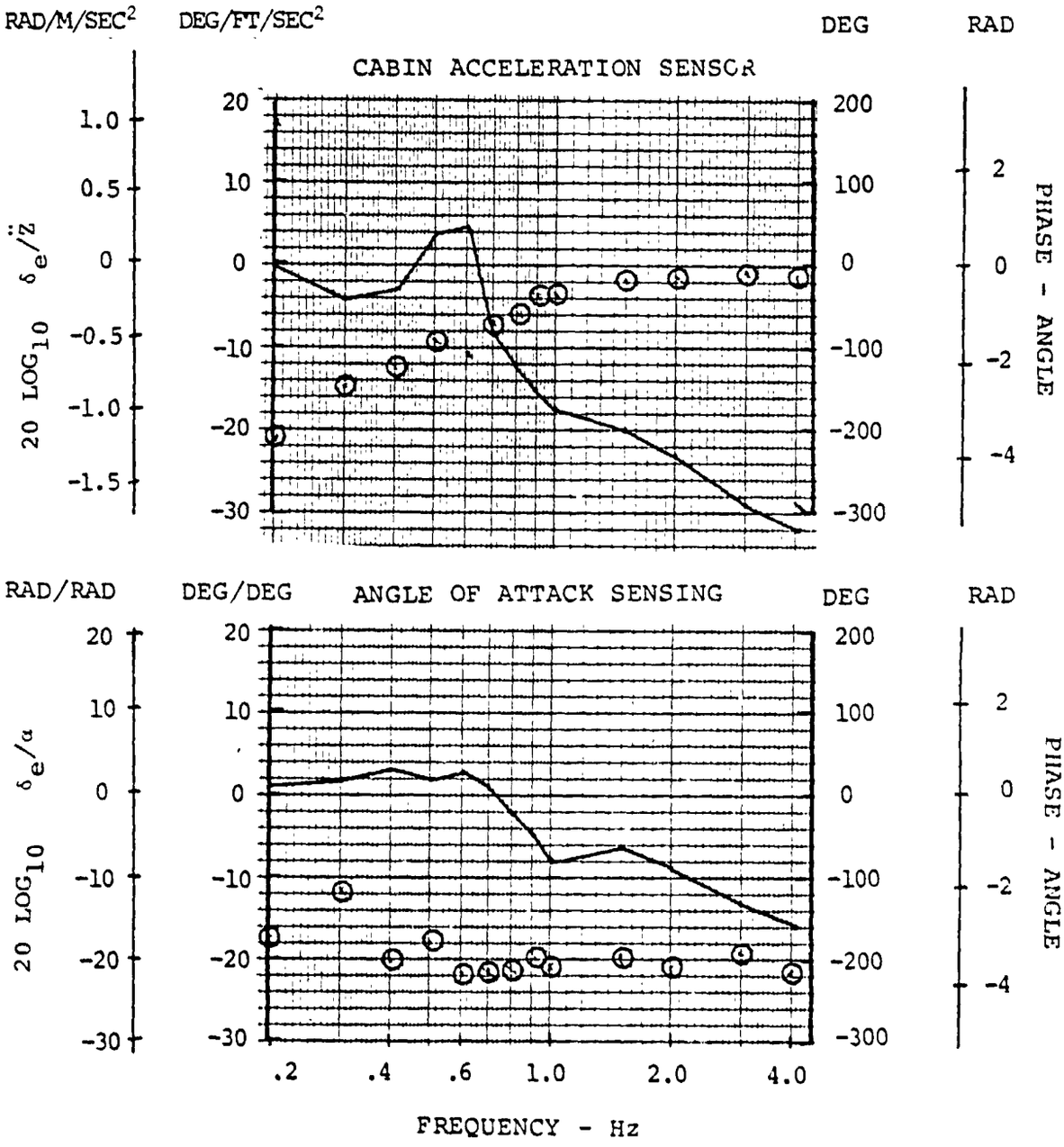

ELEVATOR FEEDBACK REQUIRED WITH ACCELERATION AND α SENSING RESPECTIVELY, 240 KNOTS, 3049 METERS, FORWARD CG, A_1 & B_1 FEEDBACK INCLUDED

FIGURE 2.5.1.0.0.0

FLIGHT CONDITION: 240 KNOTS, 5,000 FEET, (1,524m), FORWARD CG

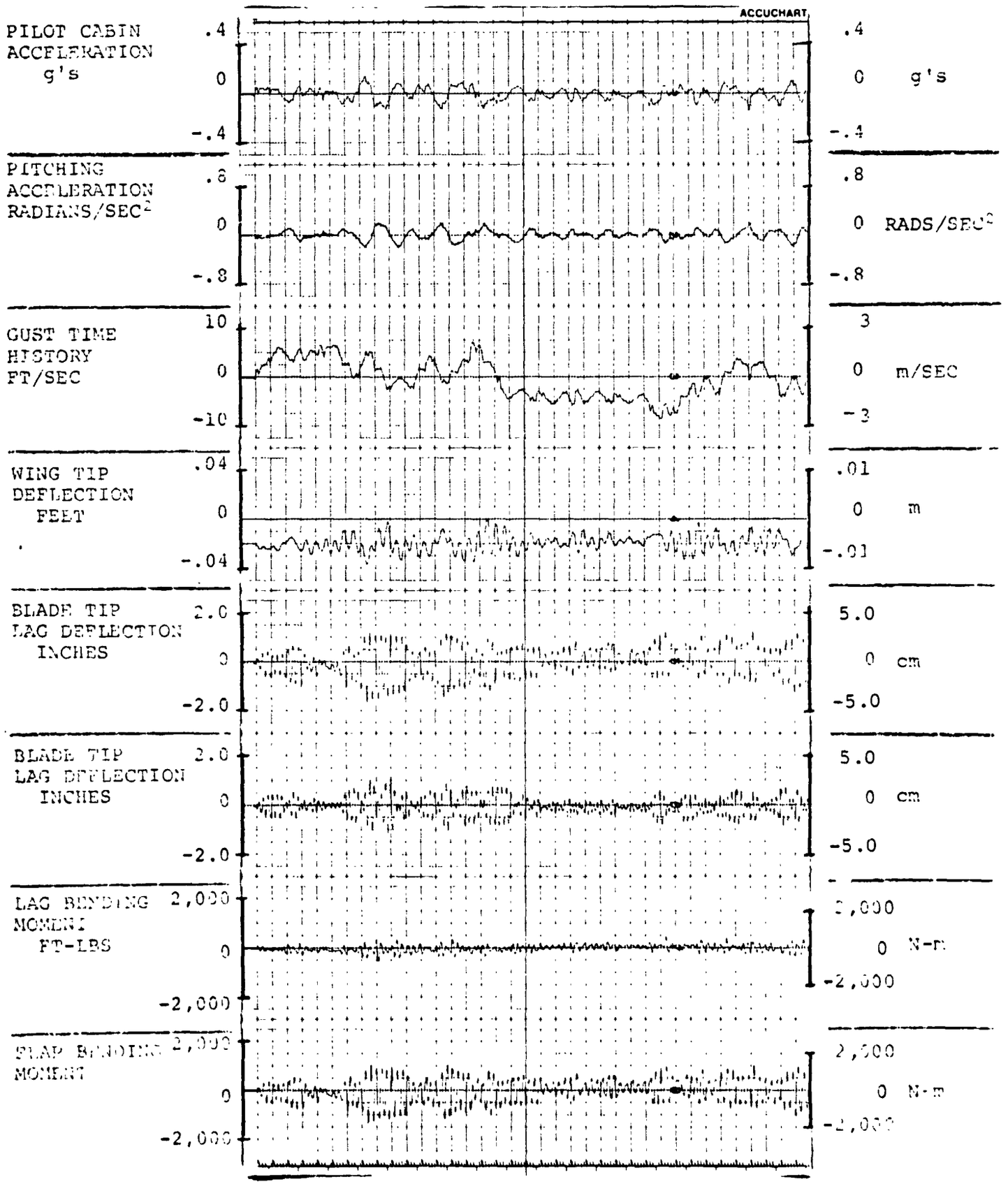

FIGURE 3.4.1.0.0.1. RESPONSES FOR GAIN F = 0, GAIN E = 0

FLIGHT CONDITION: 240 KNOTS, 5,000 FEET, (1,524m), FORWARD CG

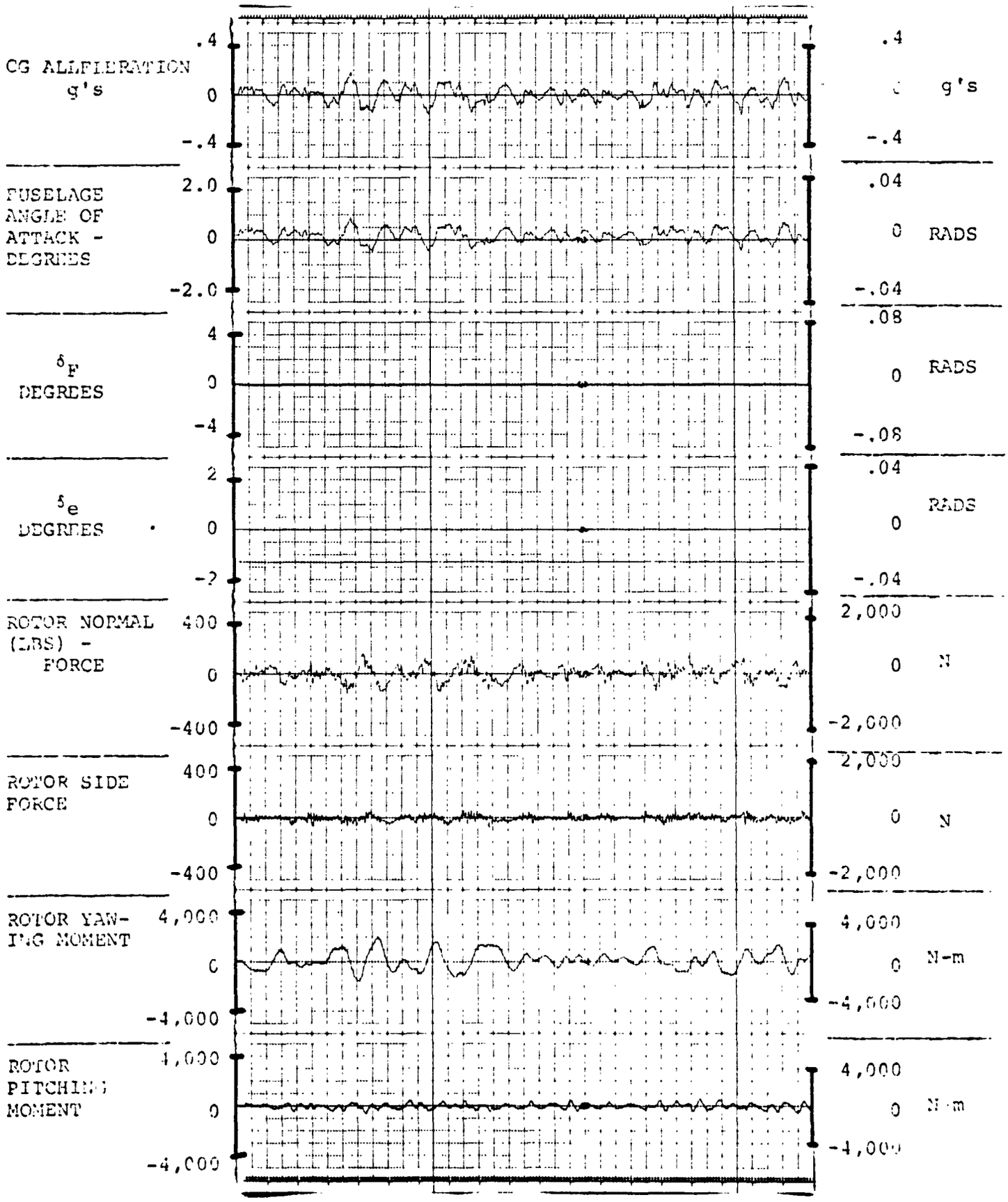

FIGURE 4.4.1.0.0.1. RESPONSES FOR GAIN F = 0, GAIN E = 0

AIV.100

FLIGHT CONDITION: 240 KNOTS, 5,000 FEET, (1,524m), FORWARD CG

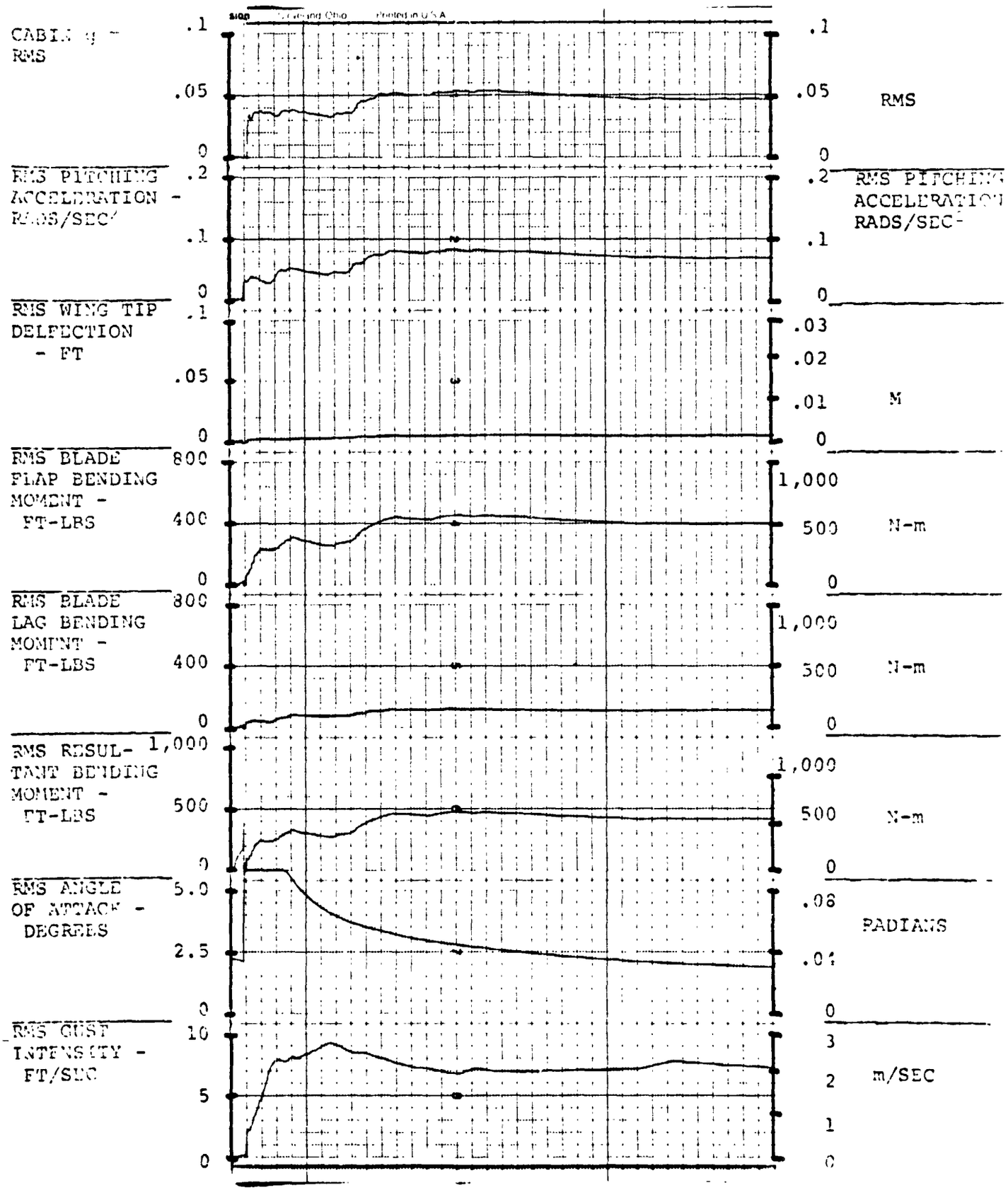

FIGURE 5.4.1.0.0.1. RESPONSES FOR GAIN F = 0, GAIN E = 0

FLIGHT CONDITION: 240 KNOTS, 5,000 FEET, (1,524m), FORWARD CG

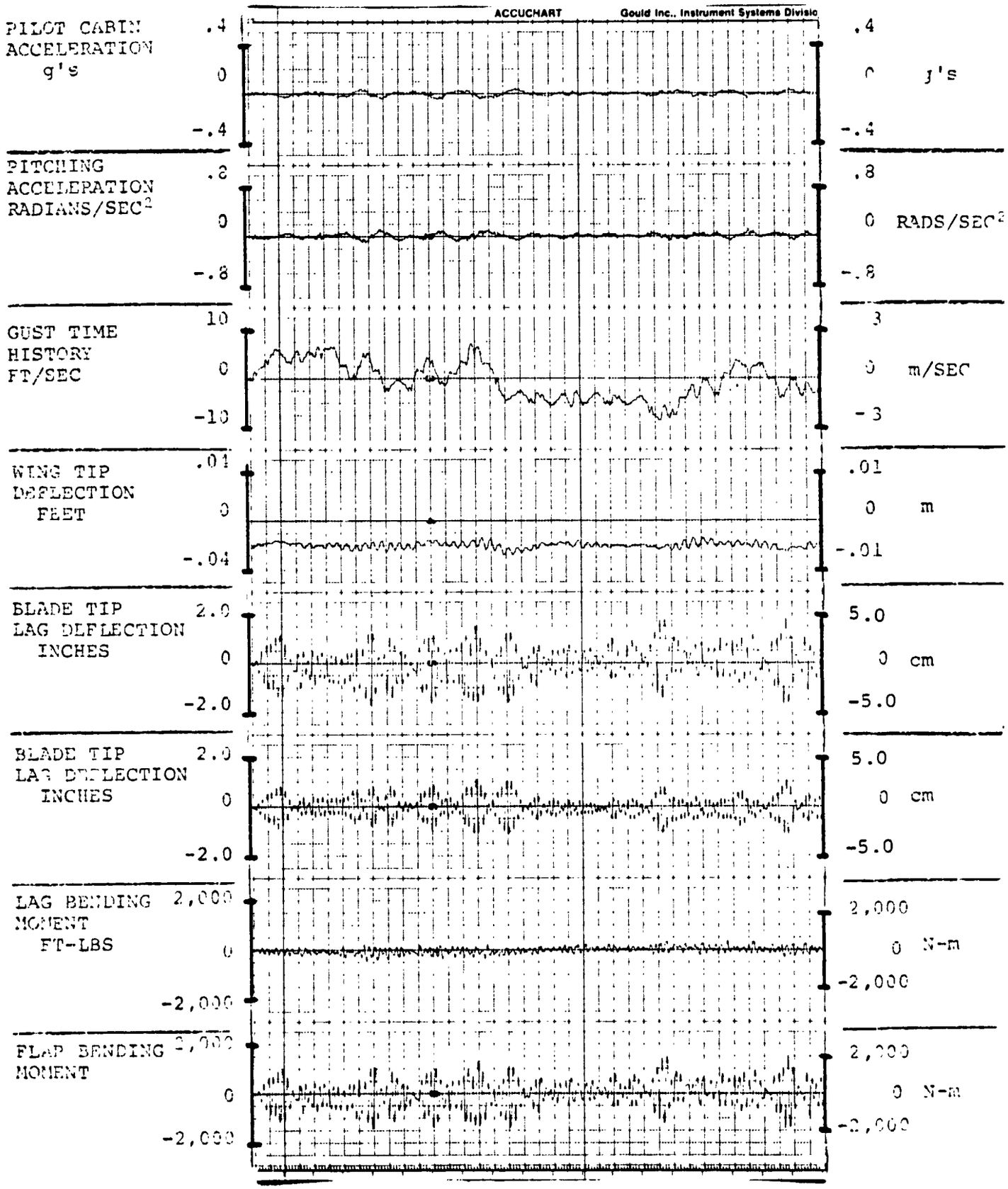

FIGURE 3.4.1.0.0.3. RESPONSES FOR GAIN F = 4.0, GAIN E = .7

FLIGHT CONDITION: 240 KNOTS, 5,000 FEET, (1,524m), FORWARD CG

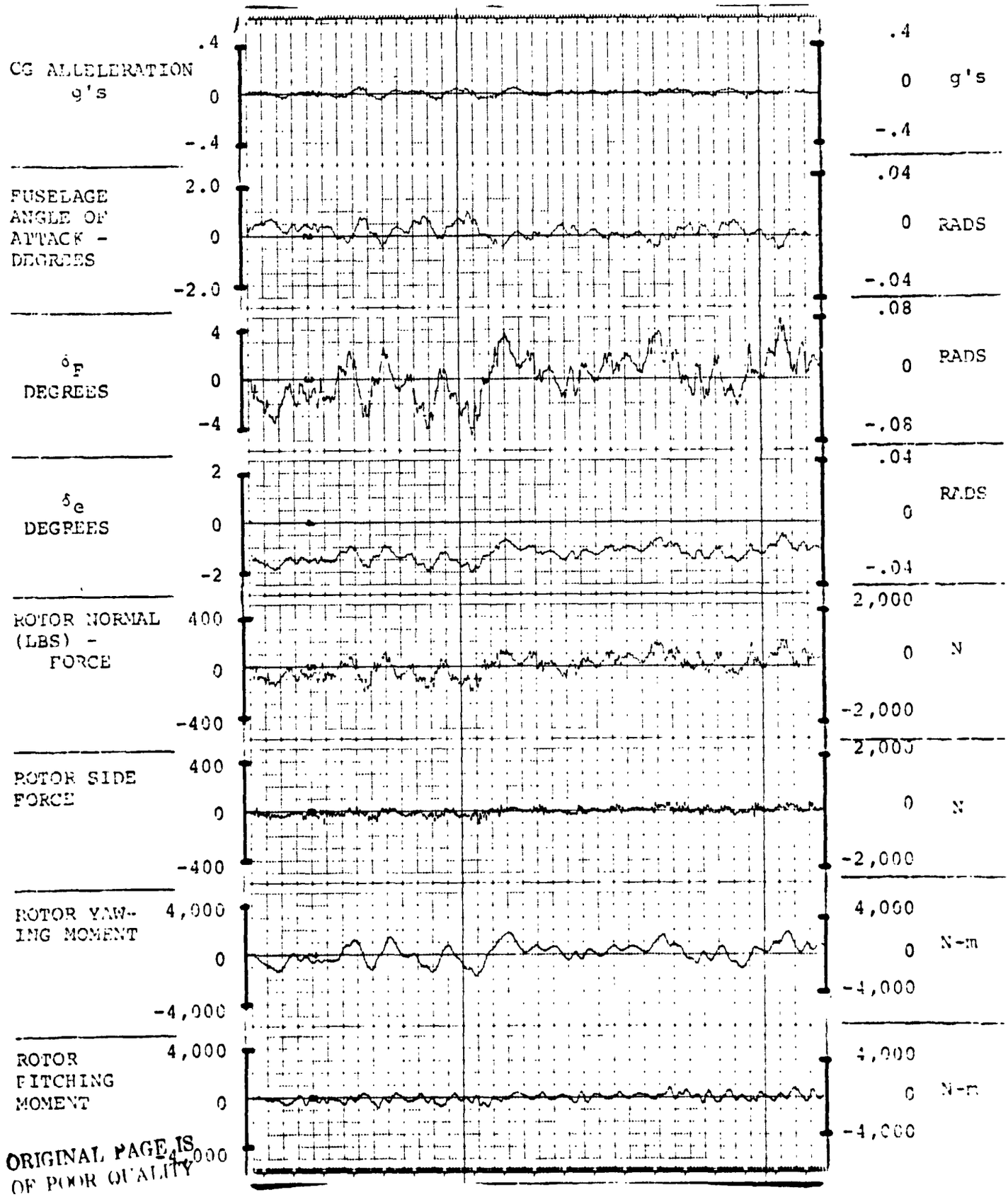

ORIGINAL PAGE IS
OF POOR QUALITY

FIGURE 4.4.1.0.0.3. RESPONSES FOR GAIN F = 4.0, GAIN E = .7

ORIGINAL PAGE IS
OF POOR QUALITY

FLIGHT CONDITION: 240 KNOTS, 5,000 FEET, (1,524m), FORWARD CG

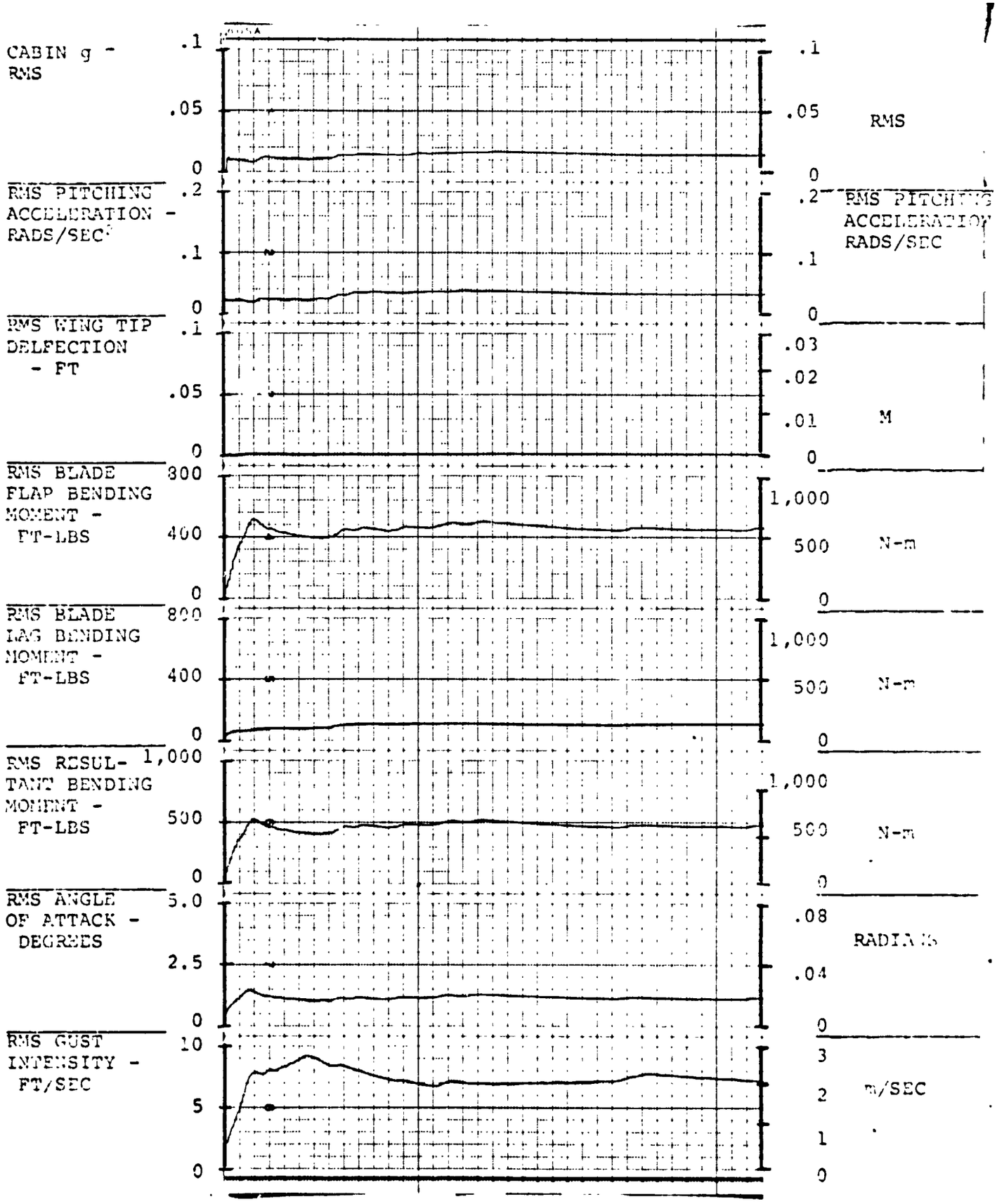

FIGURE 5.4.1.0.0.3. RESPONSES FOR GAIN F = 4.0, GAIN E= .7

FLIGHT CONDITION: 240 KNOTS, 10,000 FEET, (3,049m), FORWARD CG

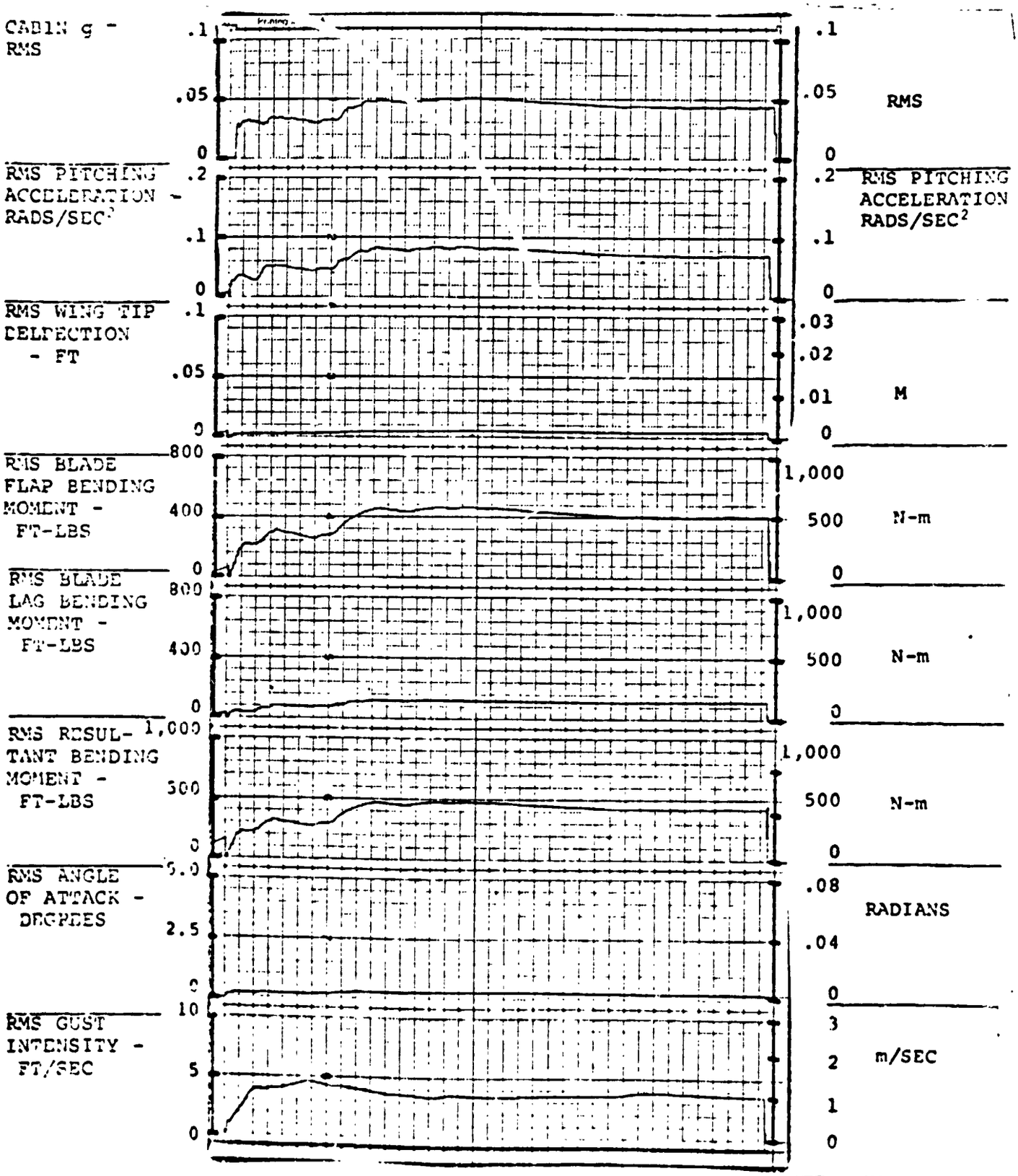

FIGURE 3.5.1.0.0.1. RESPONSES FOR GAIN F = 0, GAIN E = 0

FLIGHT CONDITION: 240 KNOTS, 10,000 FEET, (3,049m), FORWARD CG

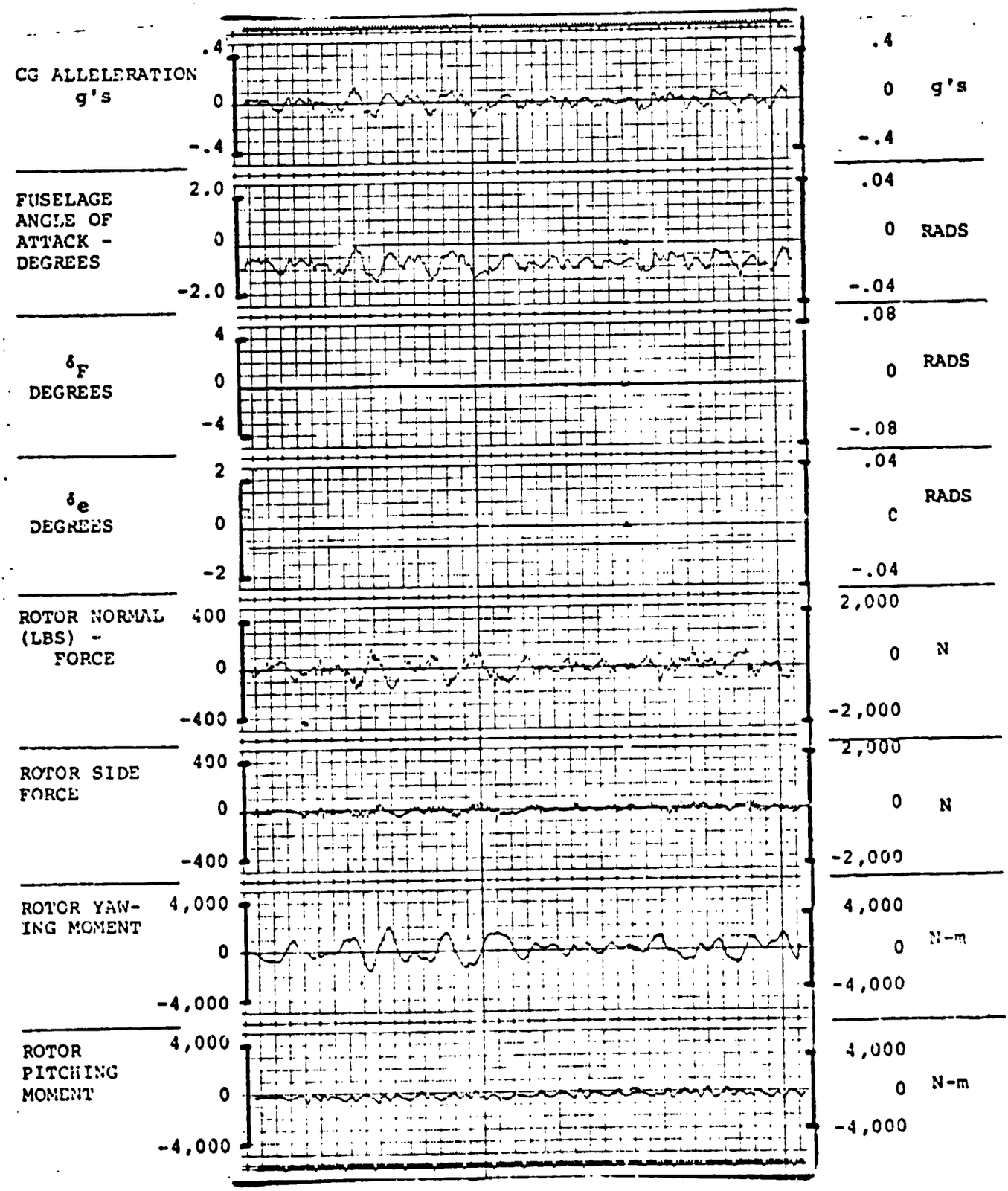

FIGURE 4.5.1.0.0.1. RESPONSES FOR GAIN F = 0, GAIN E = 0

ORIGINAL PAGE IS
OF POOR QUALITY

FLIGHT CONDITION: 240 KNOTS, 10,000 FEET, (3,049m), FORWARD CG

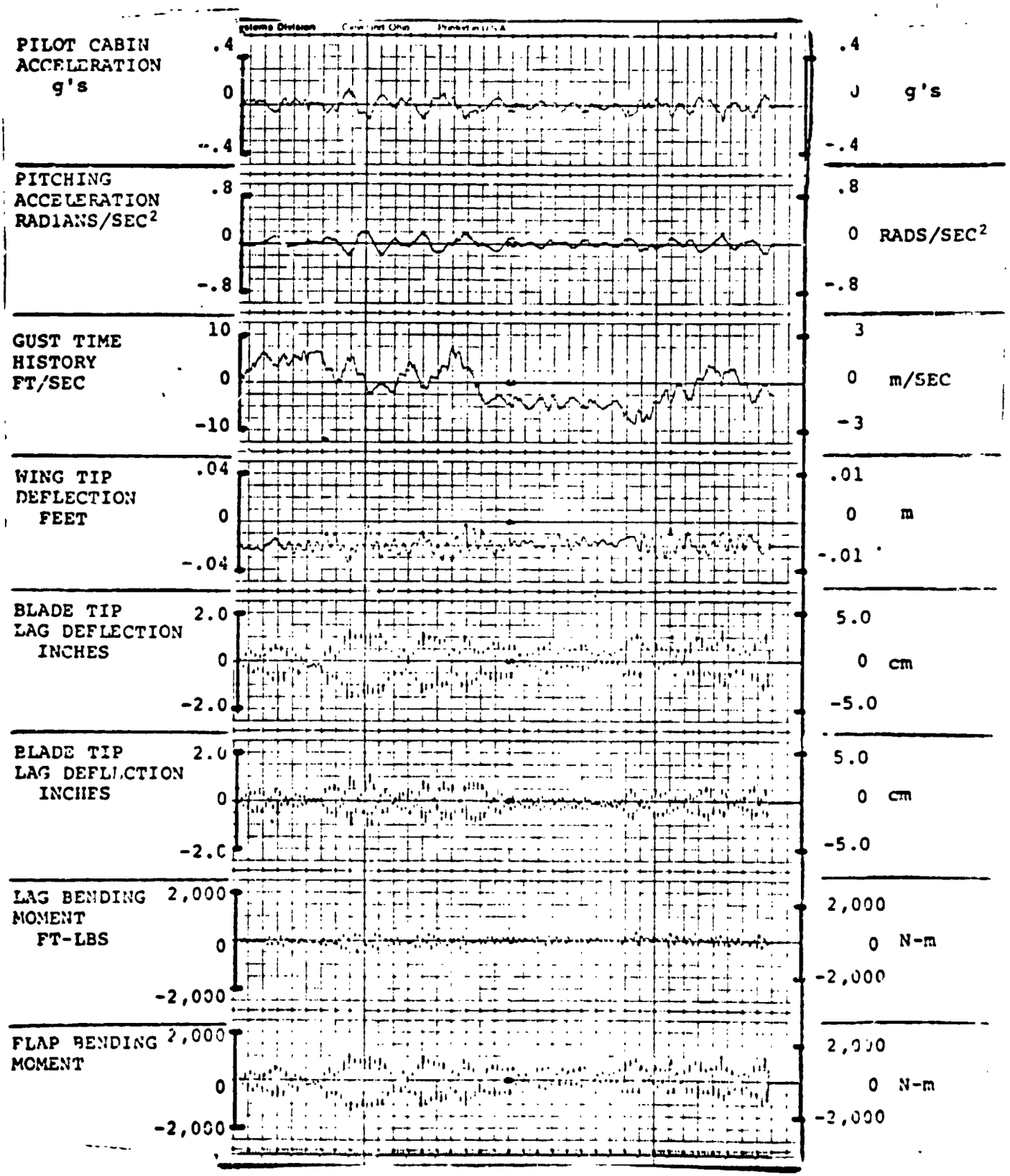

FIGURE 5.5.1.0.0.1. RESPONSES FOR GAIN F = 0, GAIN E = 0

ORIGINAL PAGE IS
OF POOR QUALITY

FLIGHT CONDITION: 240 KNOTS, 10,000 FEET, (3,048m), FORWARD CG

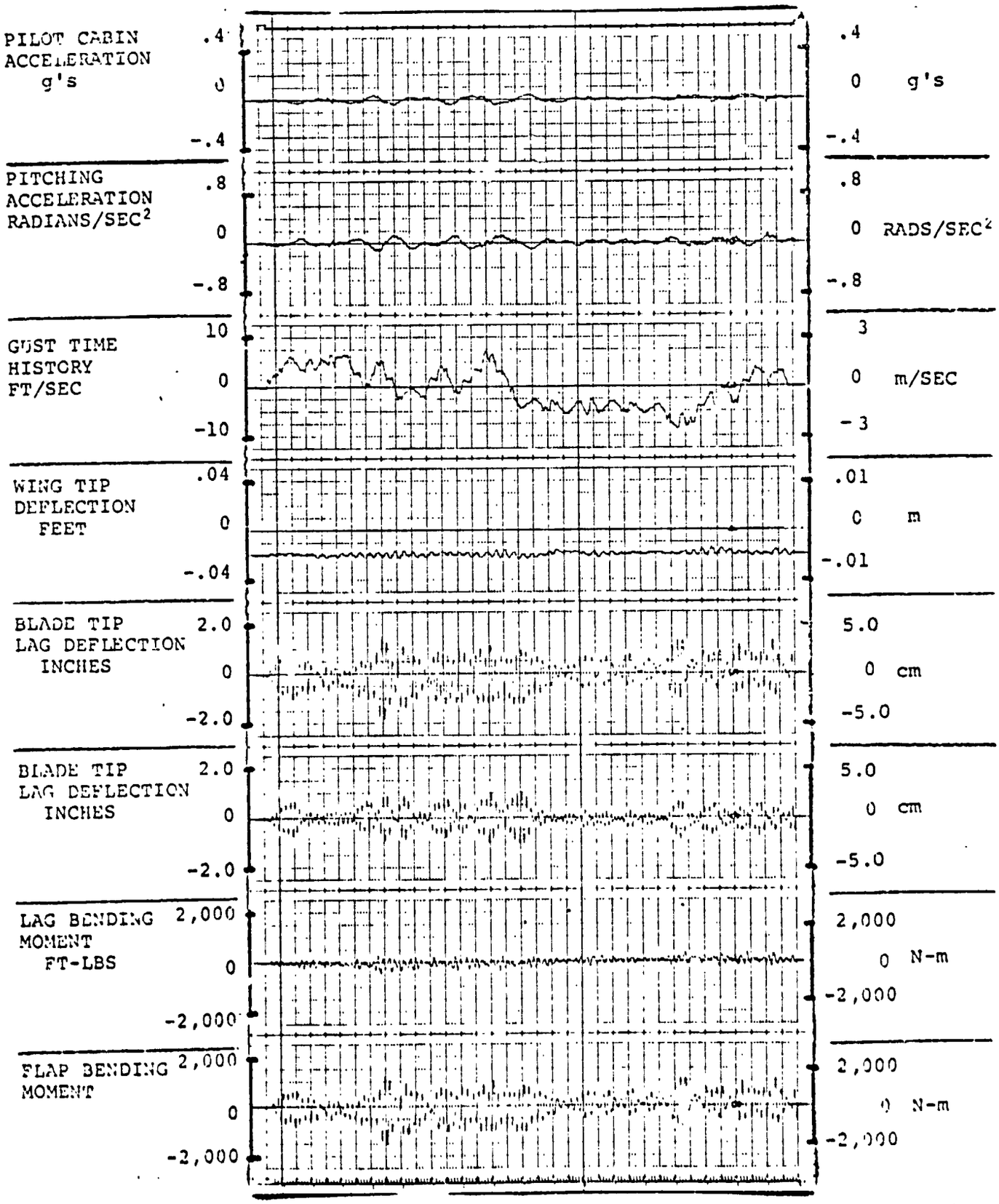

FIGURE 3.5.1.0.0.2. RESPONSES FOR GAIN F = 4.0, GAIN E = .6

FLIGHT CONDITION: 240 KNOTS, 10,000 FEET, (3,049m), FORWARD CG

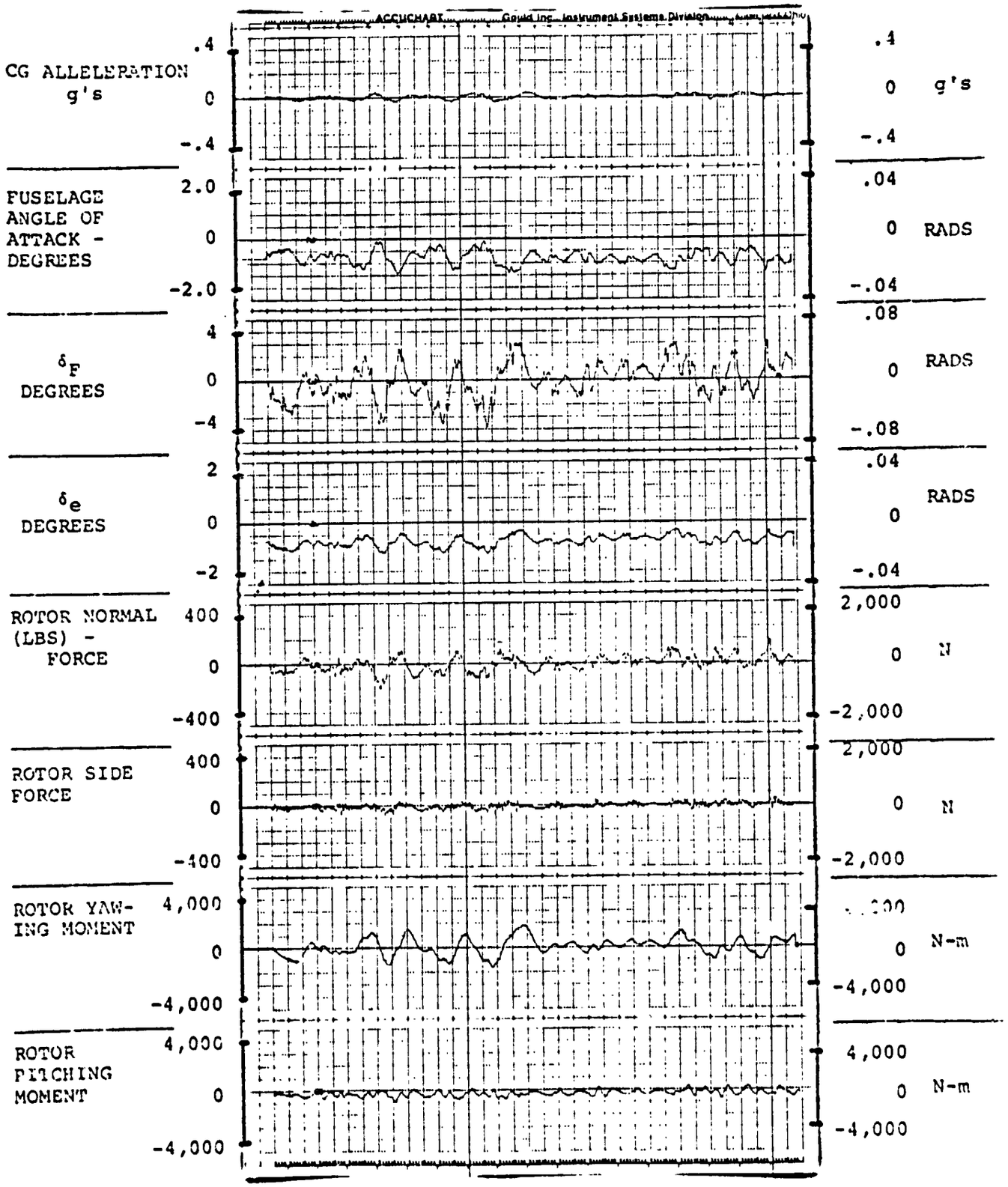

FIGURE 4.5.1.0.0.2. RESPONSES FOR GAIN F = 4.0, GAIN E = .6

ORIGINAL PAGE IS
OF POOR QUALITY

FLIGHT CONDITION: 240 KNOTS, 10,000 FEET,(3,049m), FORWARD CG

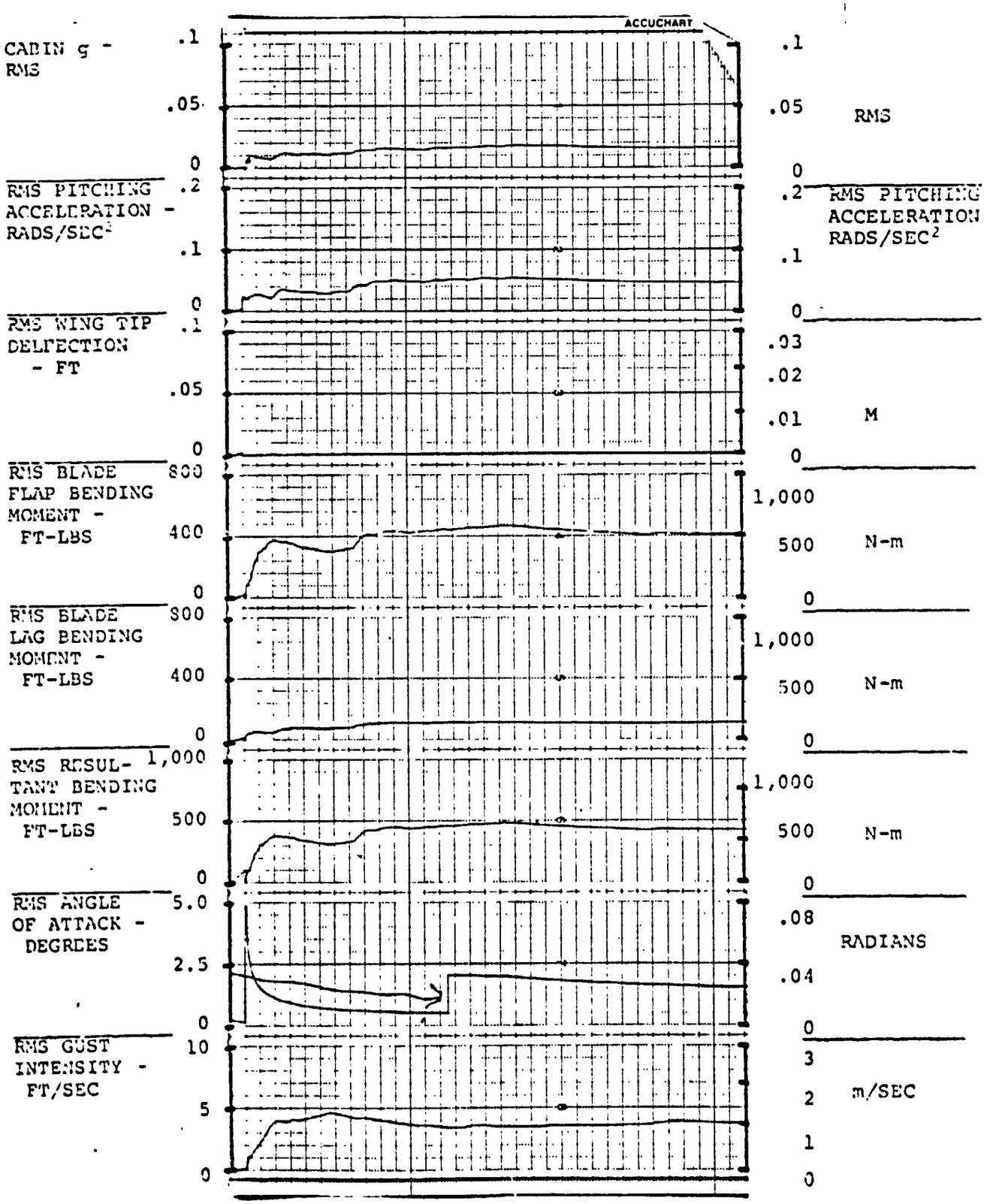

FIGURE 5.5.1.0.0.2. RESPONSES FOR GAIN F = 4.0, GAIN E = .6

FLIGHT CONDITION: 240 KNOTS, 10,000 FEET, (3,049m), FORWARD CG
α FEEDBACK

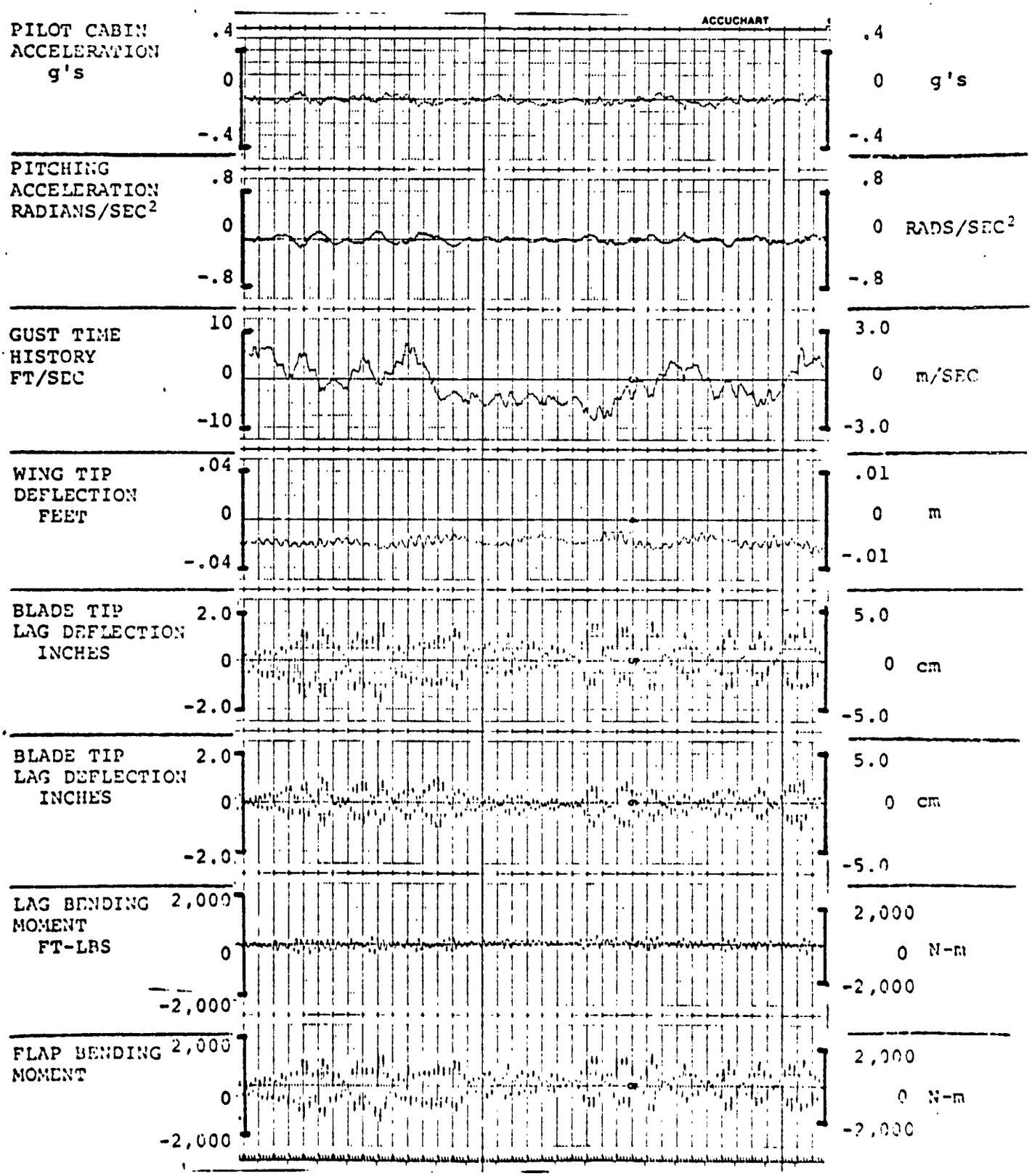

FIGURE 3.5.1.0.0.5.RESPONSES FOR GAIN F = 4.0, GAIN E = .6

ORIGINAL PAGE IS
OF POOR QUALITY

FLIGHT CONDITION: 240 KNOTS, 10,000 FEET, (3,049m), FORWARD CG
α FEEDBACK

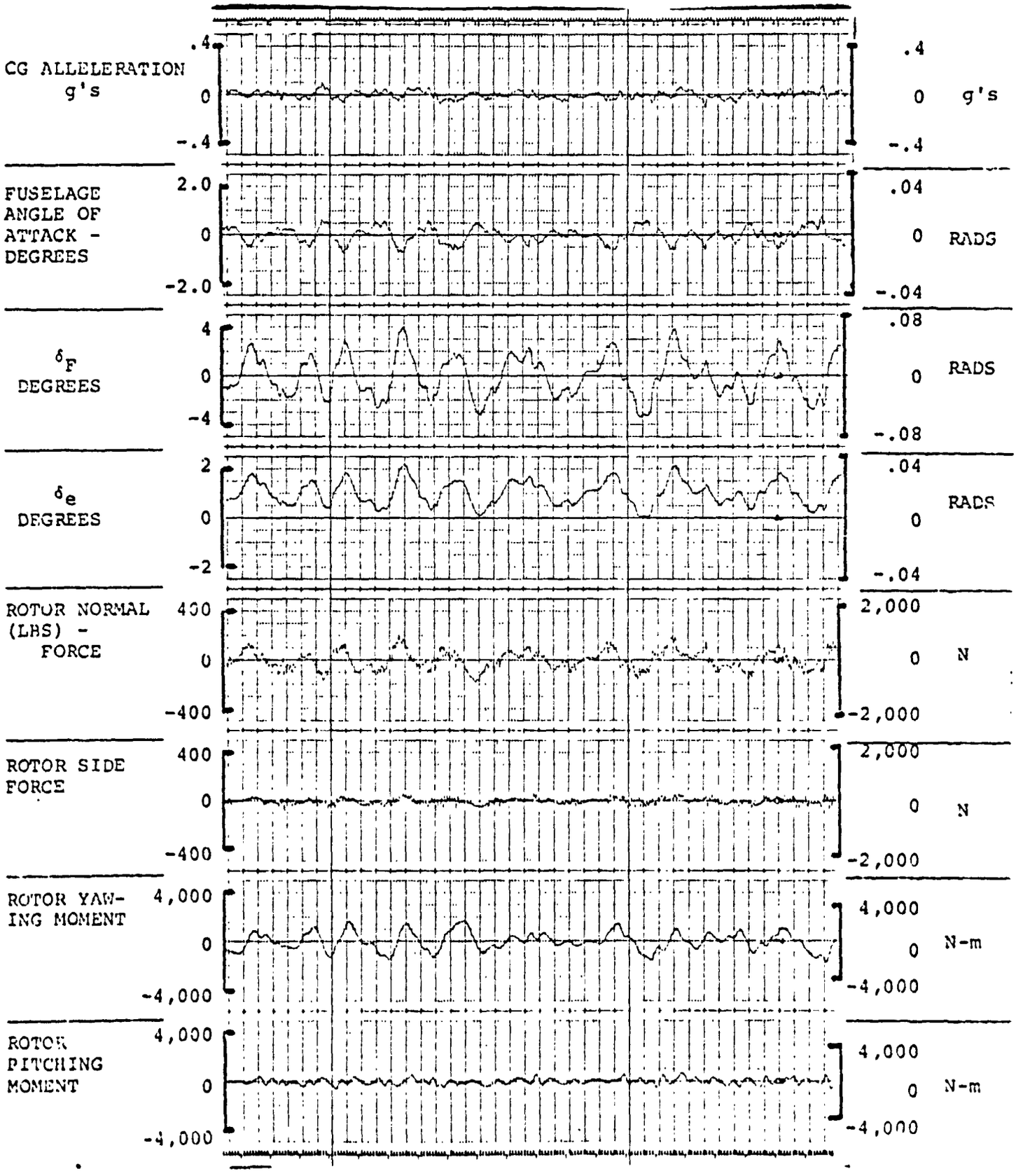

FIGURE 4.5.1.0.0.5. RESPONSES FOR GAIN F = 4.0, GAIN E = .6

FLIGHT CONDITION: 240 KNOTS, 10,000 FEET, (3,049m), FORWARD CG, α FEEDBACK

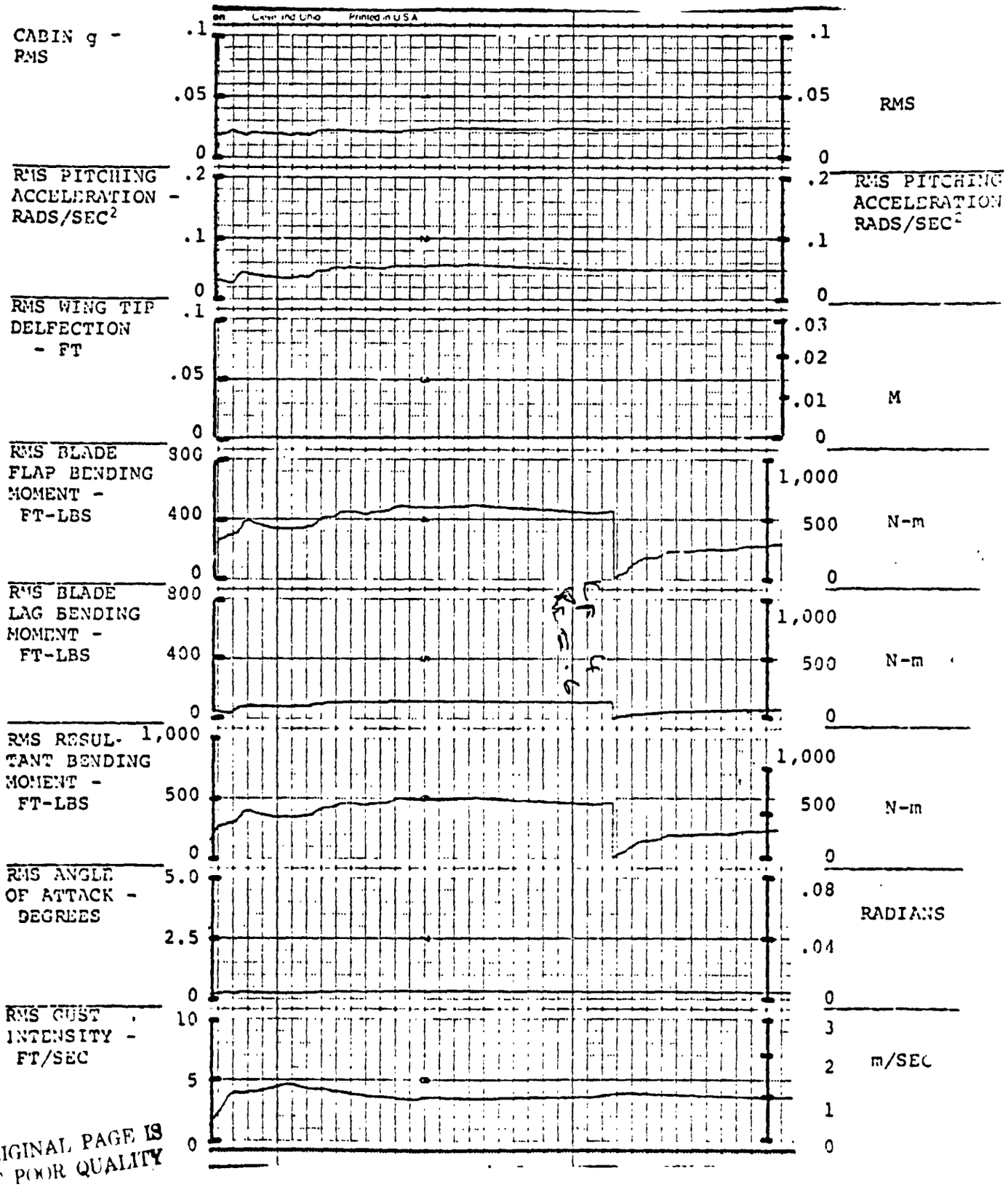

ORIGINAL PAGE IS OF POOR QUALITY

FIGURE 5.5.1.0.0.5. RESPONSES FOR GAIN F = 4.0, GAIN E = .6

FLIGHT CONDITION: 240 KNOTS, 15,000 FEET, (4,573m), FORWARD CG

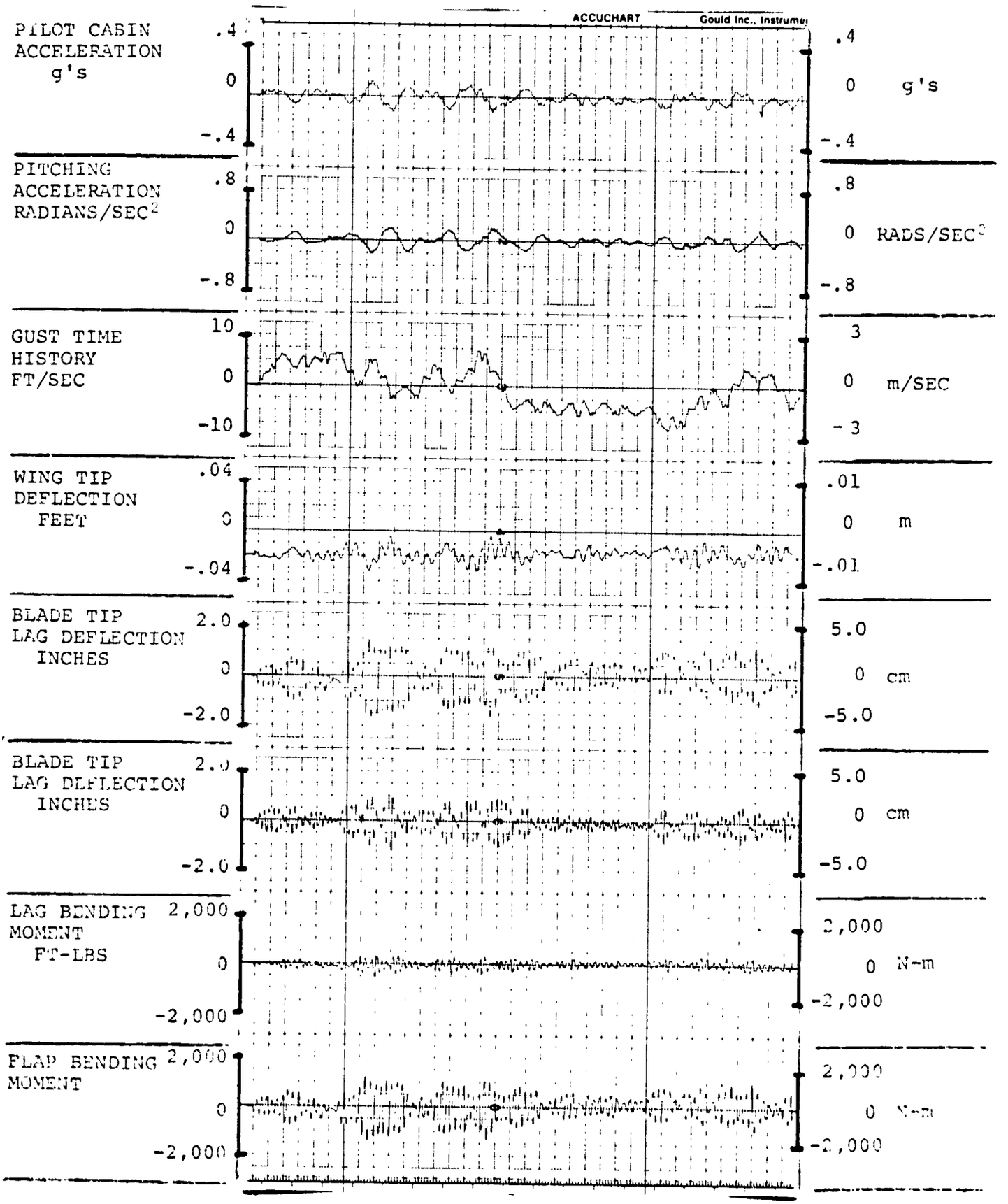

FIGURE 3.6.1.0.0.1. RESPONSES FOR GAIN F = 0, GAIN E = 0

ORIGINAL PAGE IS
OF POOR QUALITY

FLIGHT CONDITION: 240 KNOTS, 15,000 FEET, (4,573m), FORWARD CG

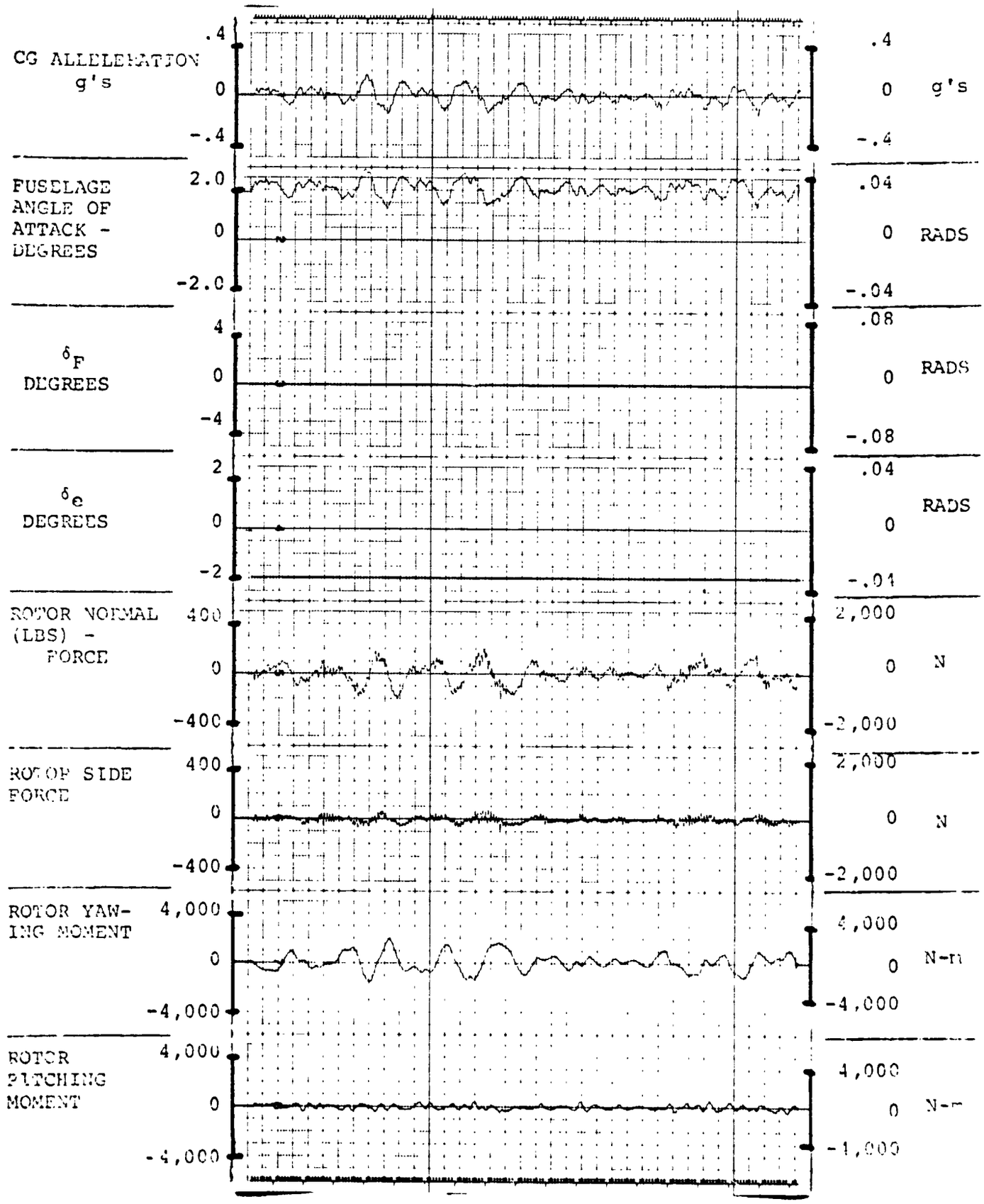

FIGURE 4.6.1.0.0.1. RESPONSES FOR GAIN F = 0, GAIN E = 0

FLIGHT CONDITION: 240 KNOTS, 15,000 FEET, (4,573m), FORWARD CG

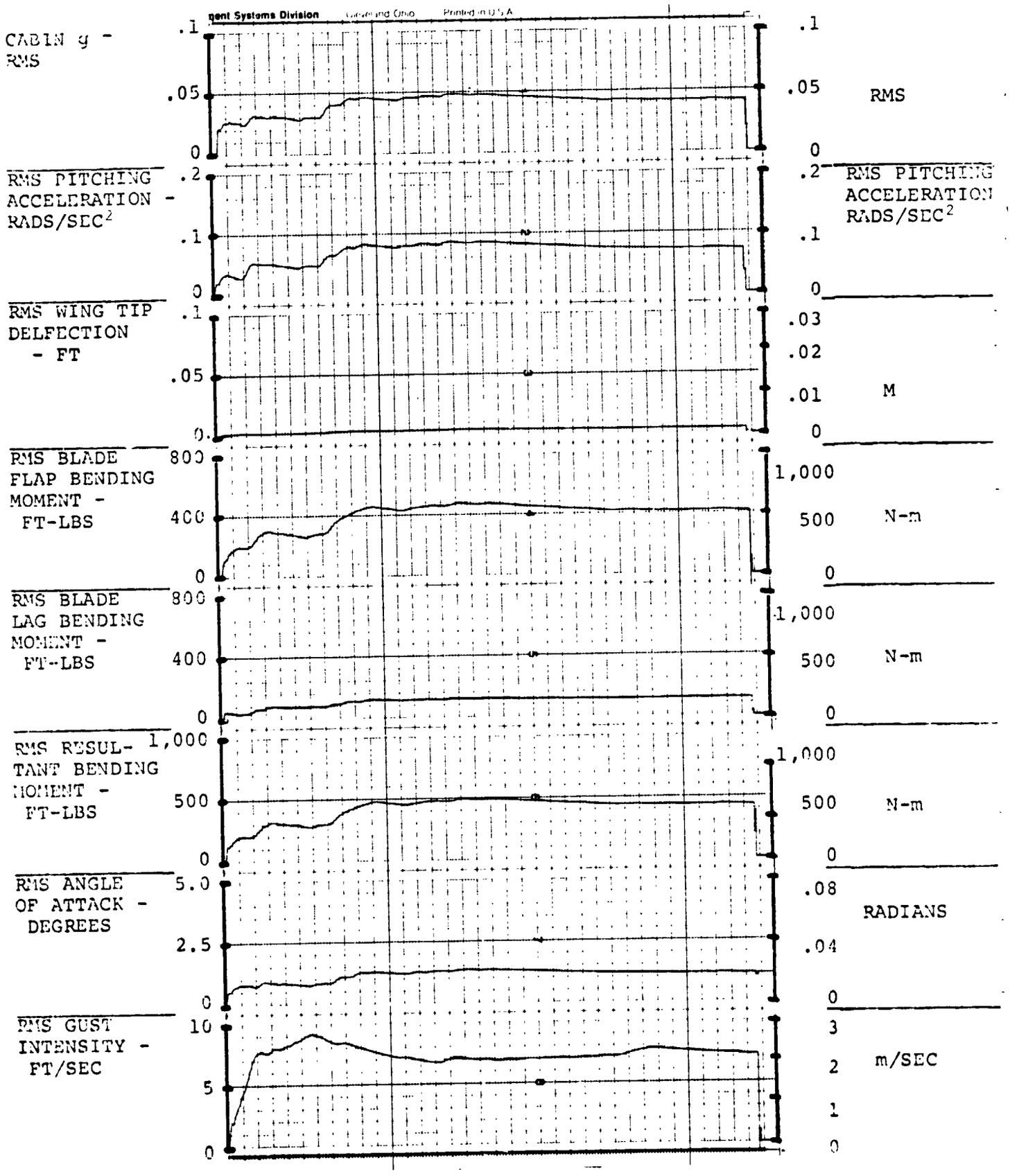

FIGURE 5.6.1.0.0.1. RESPONSES FOR GAIN F = 0, GAIN E = 0

FLIGHT CONDITION: 240 KNOTS, 15,000 FEET, (4,573m), FORWARD CG

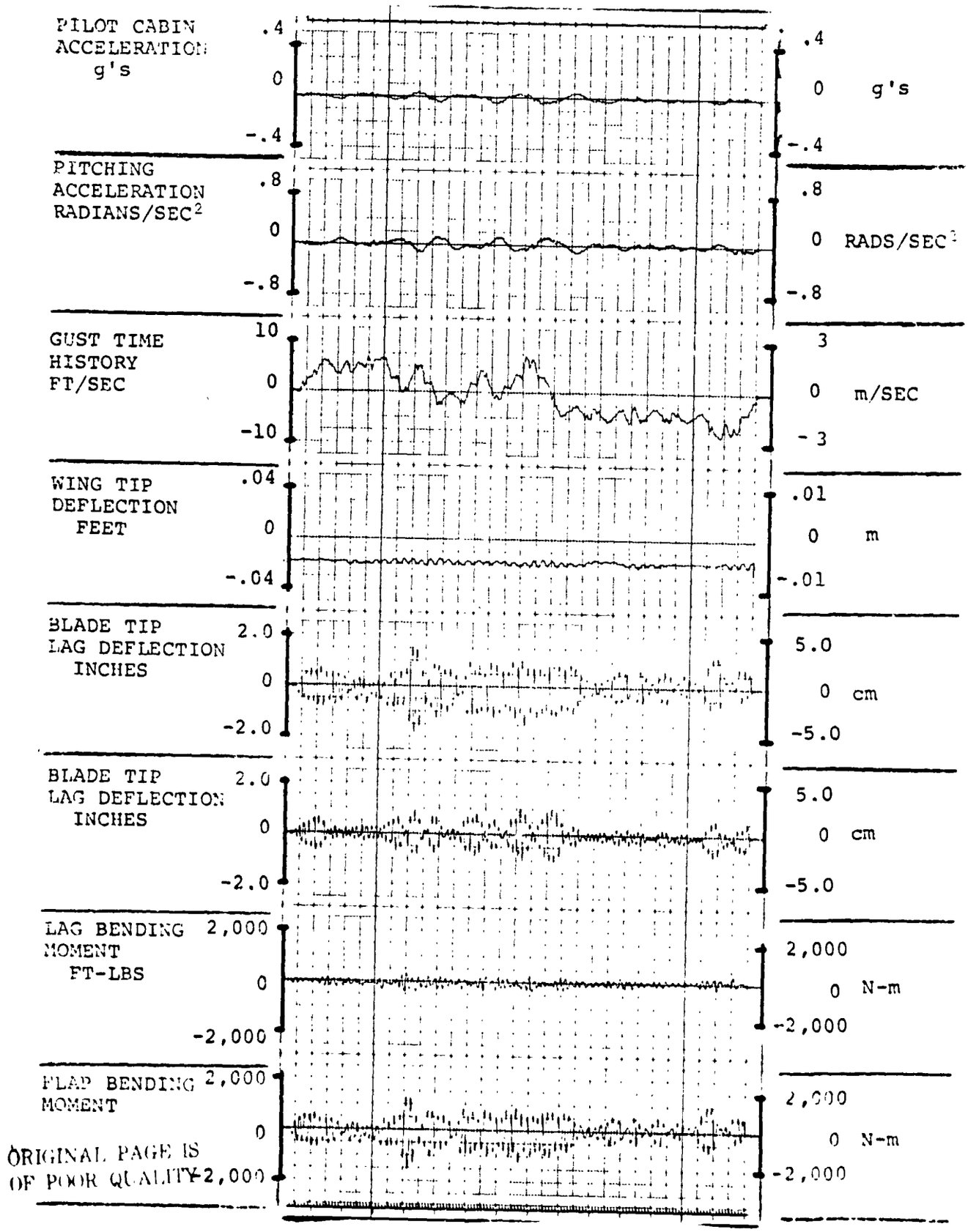

ORIGINAL PAGE IS
OF POOR QUALITY

FIGURE 3.6.1.0.0.2. RESPONSES FOR GAIN F = 4.0, GAIN E = .6

FLIGHT CONDITION: 240 KNOTS, 15,000 FEET, (4,573m), FORWARD CG

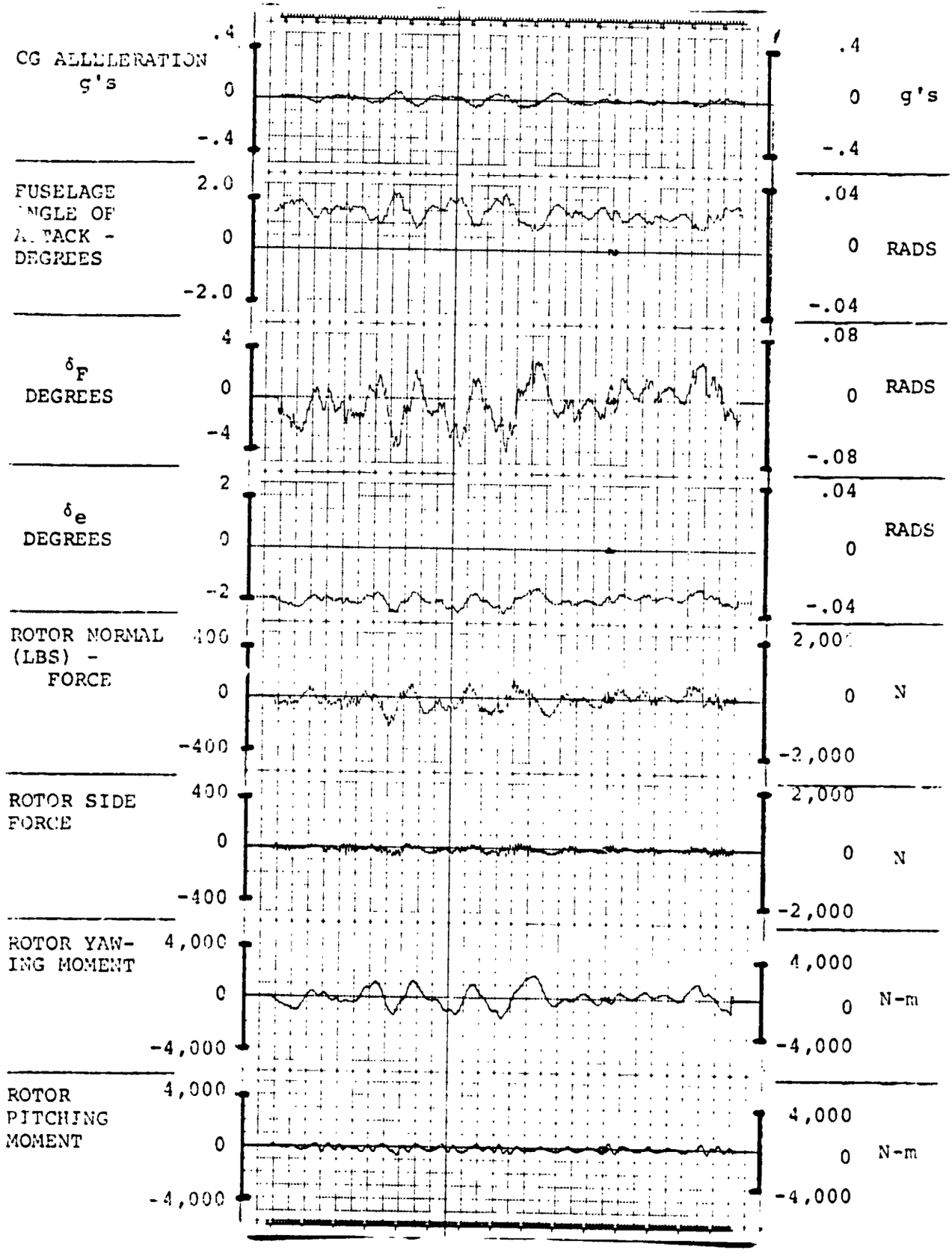

FIGURE 4.6.1.0.0.2. RESPONSES FOR GAIN F = 4.0, GAIN E = .6

FLIGHT CONDITION: 240 KNOTS, 15,000 FEET, (4,573m), FORWARD CG

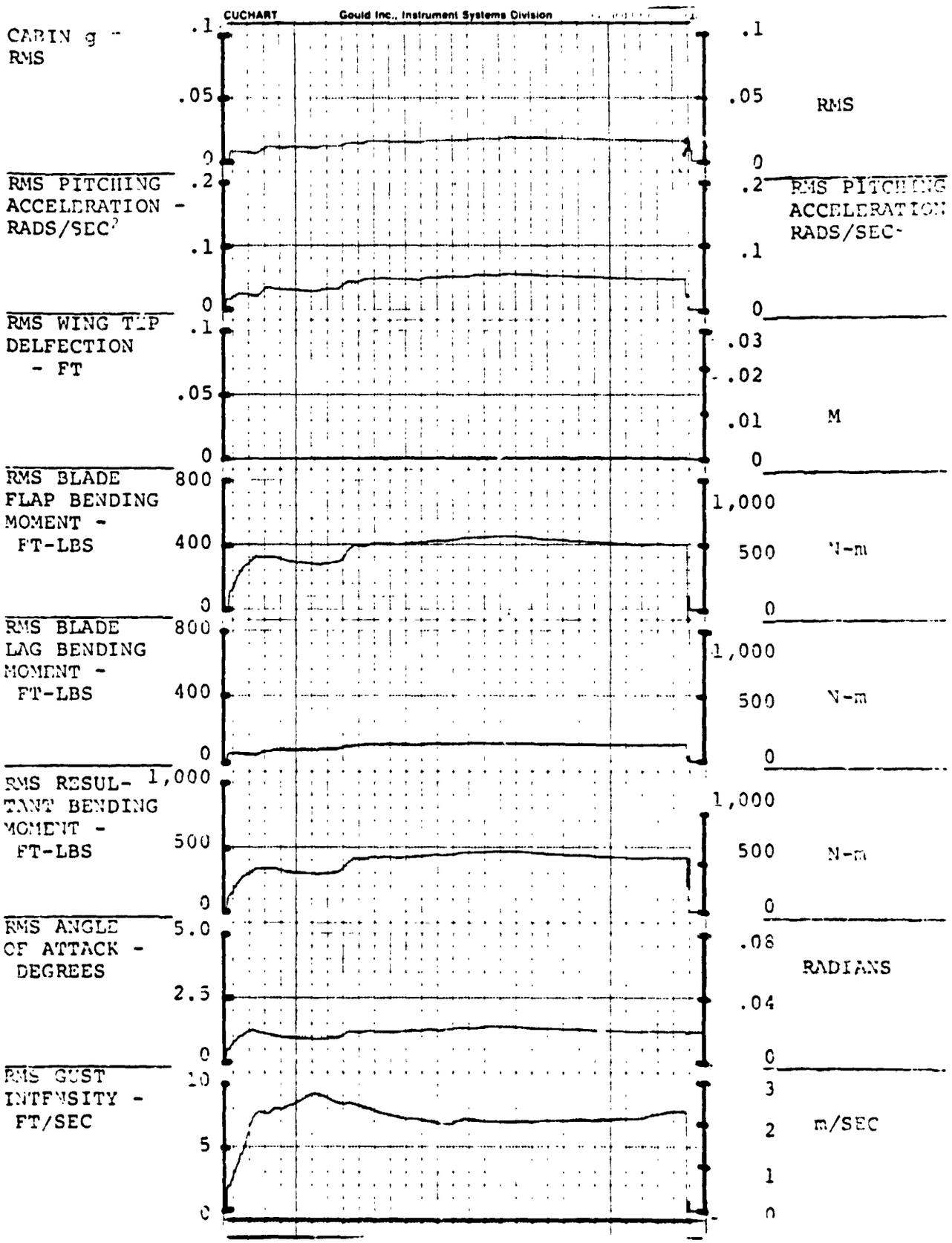

FIGURE 5.6.1.0.0.2. RESPONSES FOR GAIN F = 4.0, GAIN E = .6

FLIGHT CONDITION: 240 KNOTS, 15,000 FEET, (4,573m), FORWARD CG

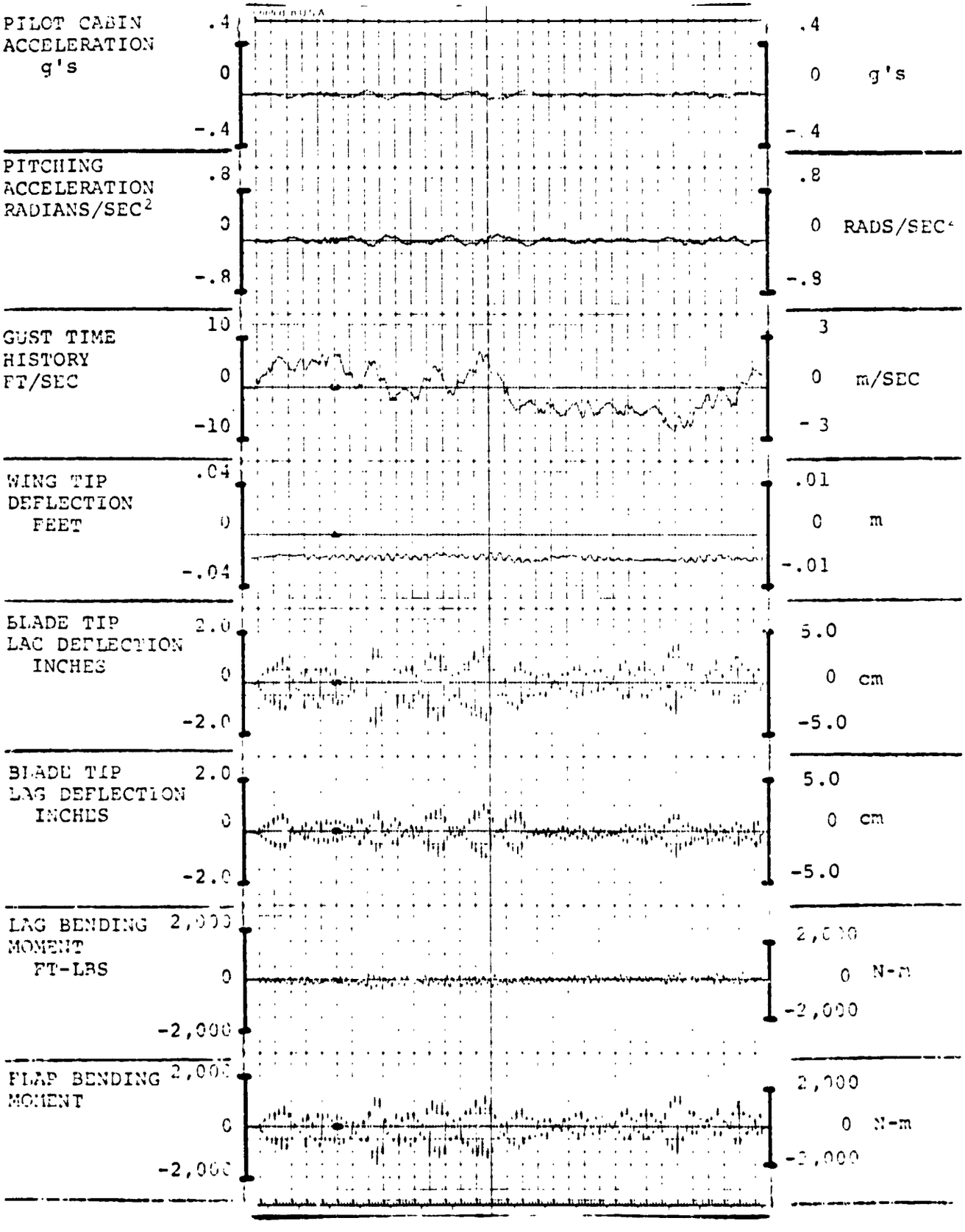

FIGURE 3.6.1.0.0.3. RESPONSES FOR GAIN F = 4.0, GAIN E = .7

FLIGHT CONDITION: 240 KNOTS, 15,000 FEET, (4,573m), FORWARD CG

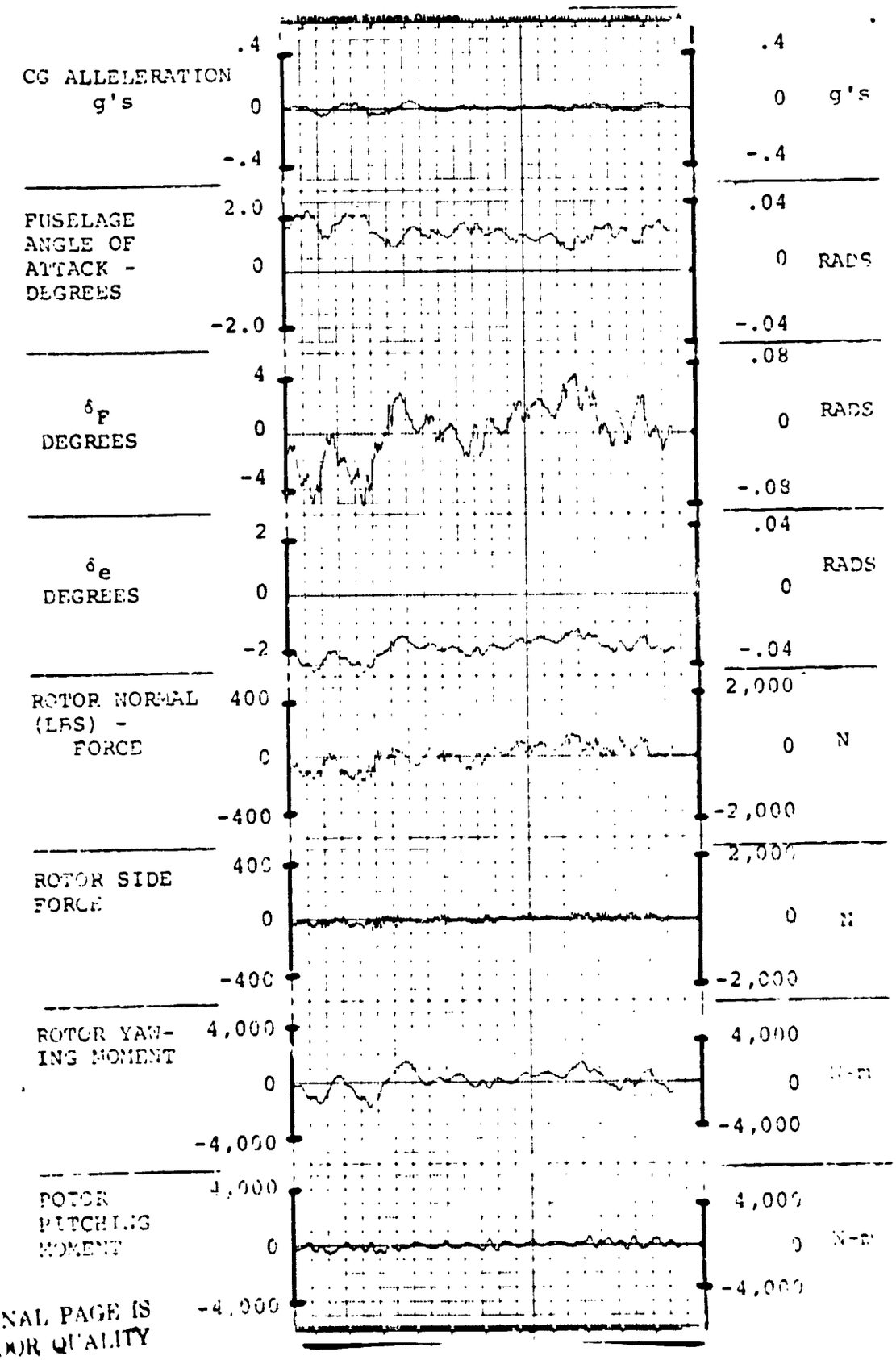

ORIGINAL PAGE IS OF POOR QUALITY

FIGURE 4.6.1.0.0.3. RESPONSES FOR GAIN F = 4.0, GAIN E = .7

FLIGHT CONDITION: 240 KNOTS, 15,000 FEET, (4,573m), FORWARD CG

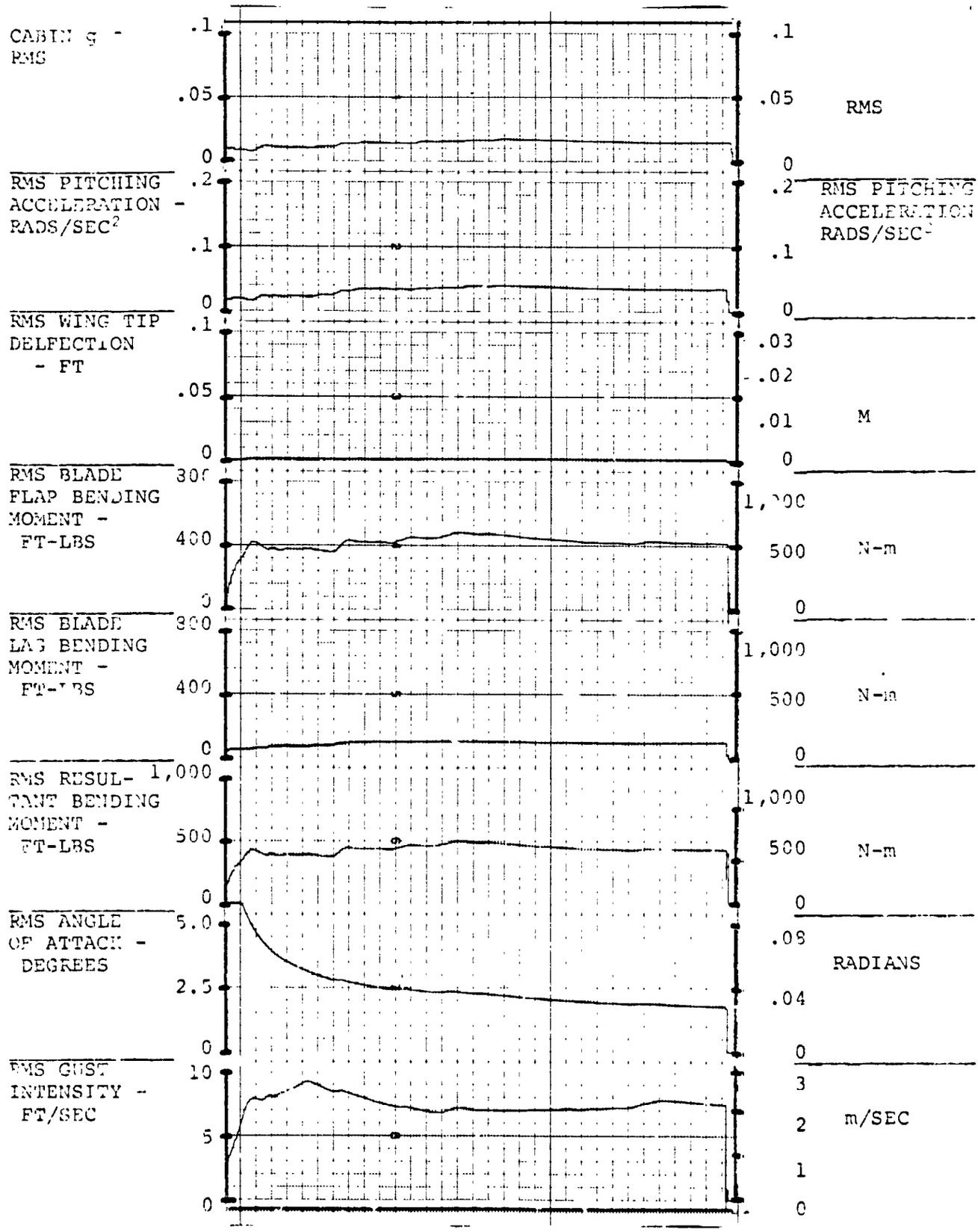

FIGURE 5.6.1.0.0.3. RESPONSES FOR GAIN F = 4.0, GAIN E = .7

FLIGHT CONDITION: 240 KNOTS, 15,000 FEET, (4,573m), FORWARD CG

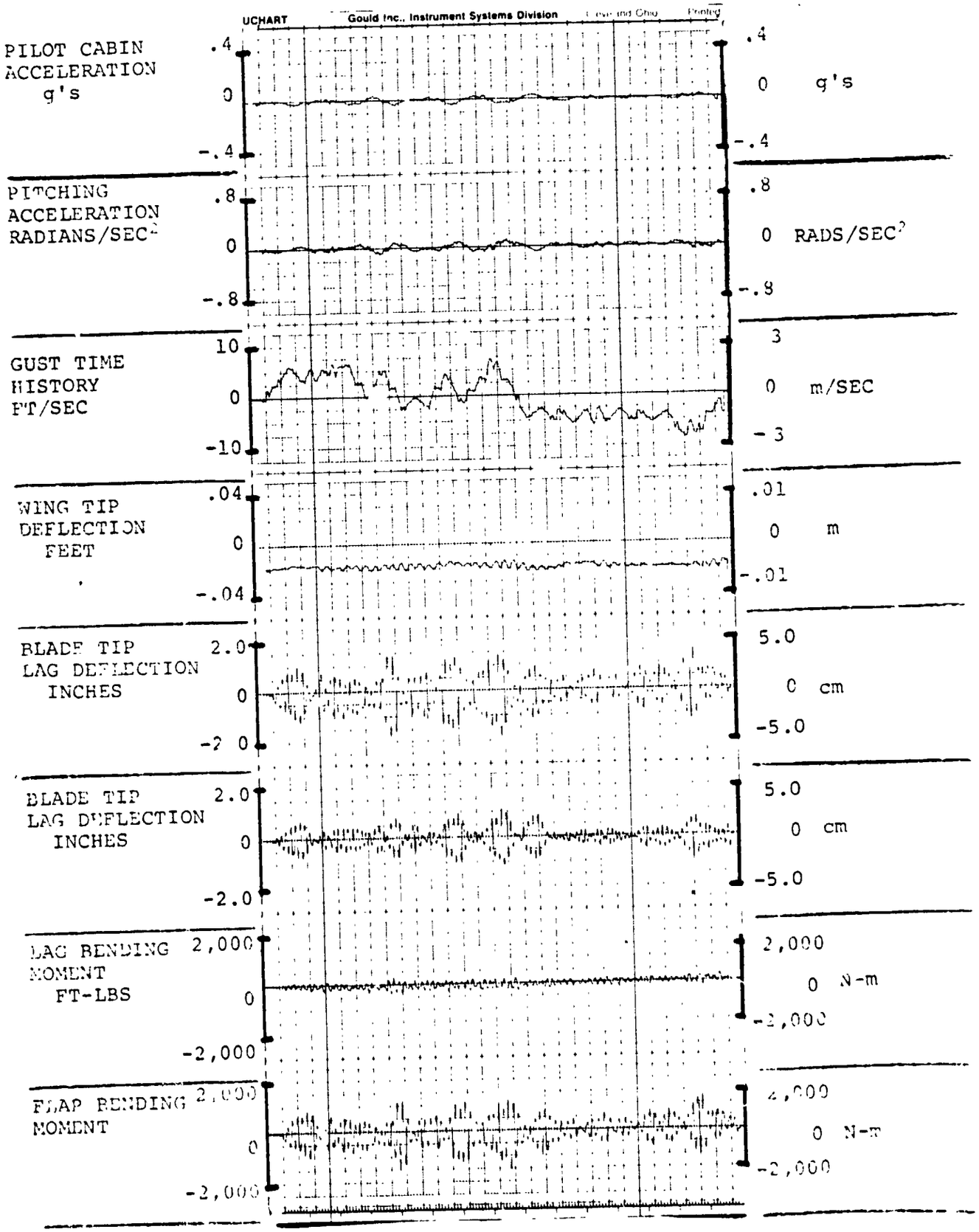

FIGURE 3.6.1.0.0.7. RESPONSES FOR GAIN F = 4.4, GAIN E = .77

FLIGHT CONDITION: 240 KNOTS, 15,000 FEET, (4,573m), FORWARD CG

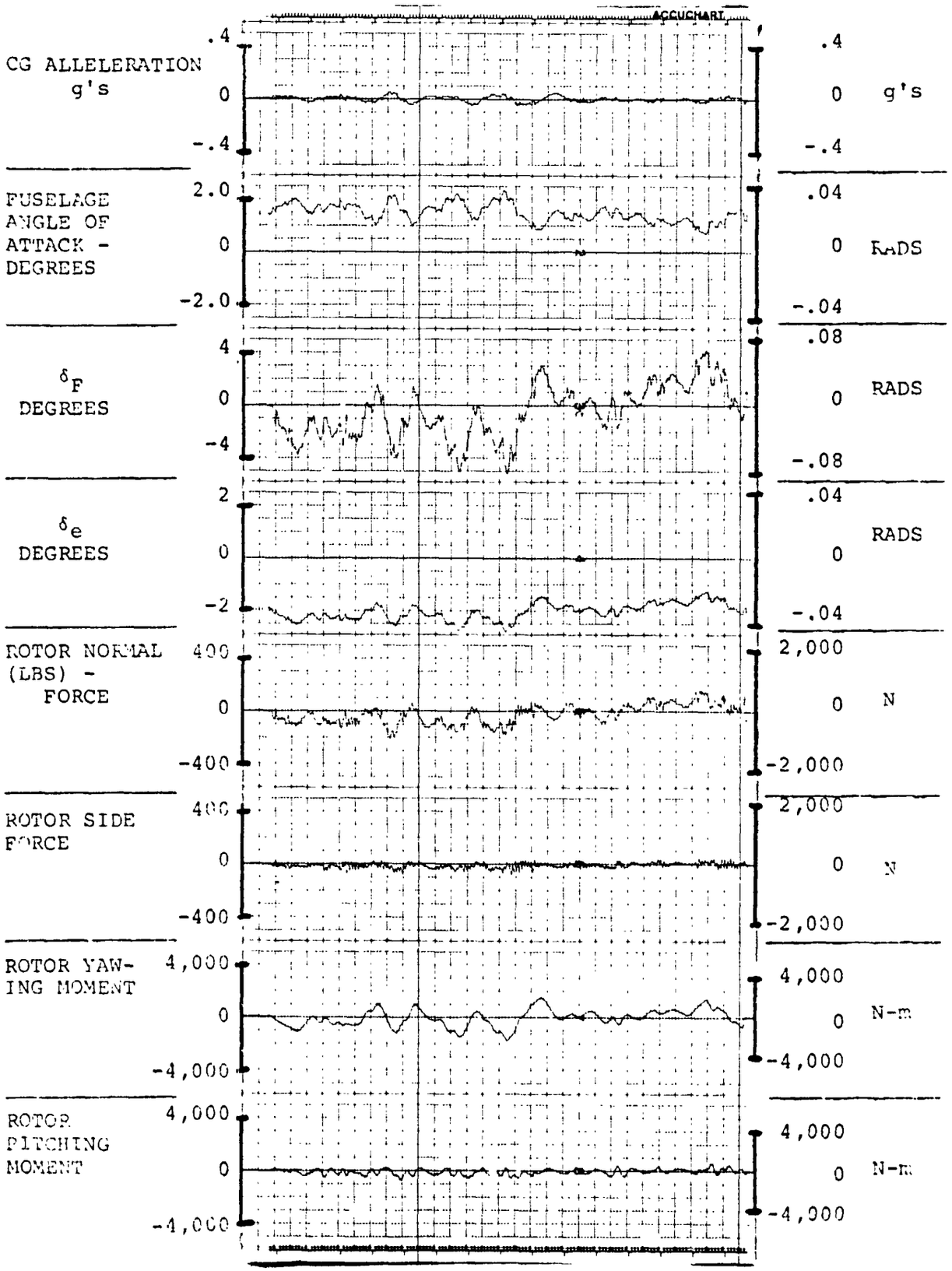

FIGURE 4.6.1.0.0.7. RESPONSES FOR GAIN F = 4.4, GAIN E = .77

FLIGHT CONDITION: 240 KNOTS, 15,000 FEET, (4,573m); FORWARD CG

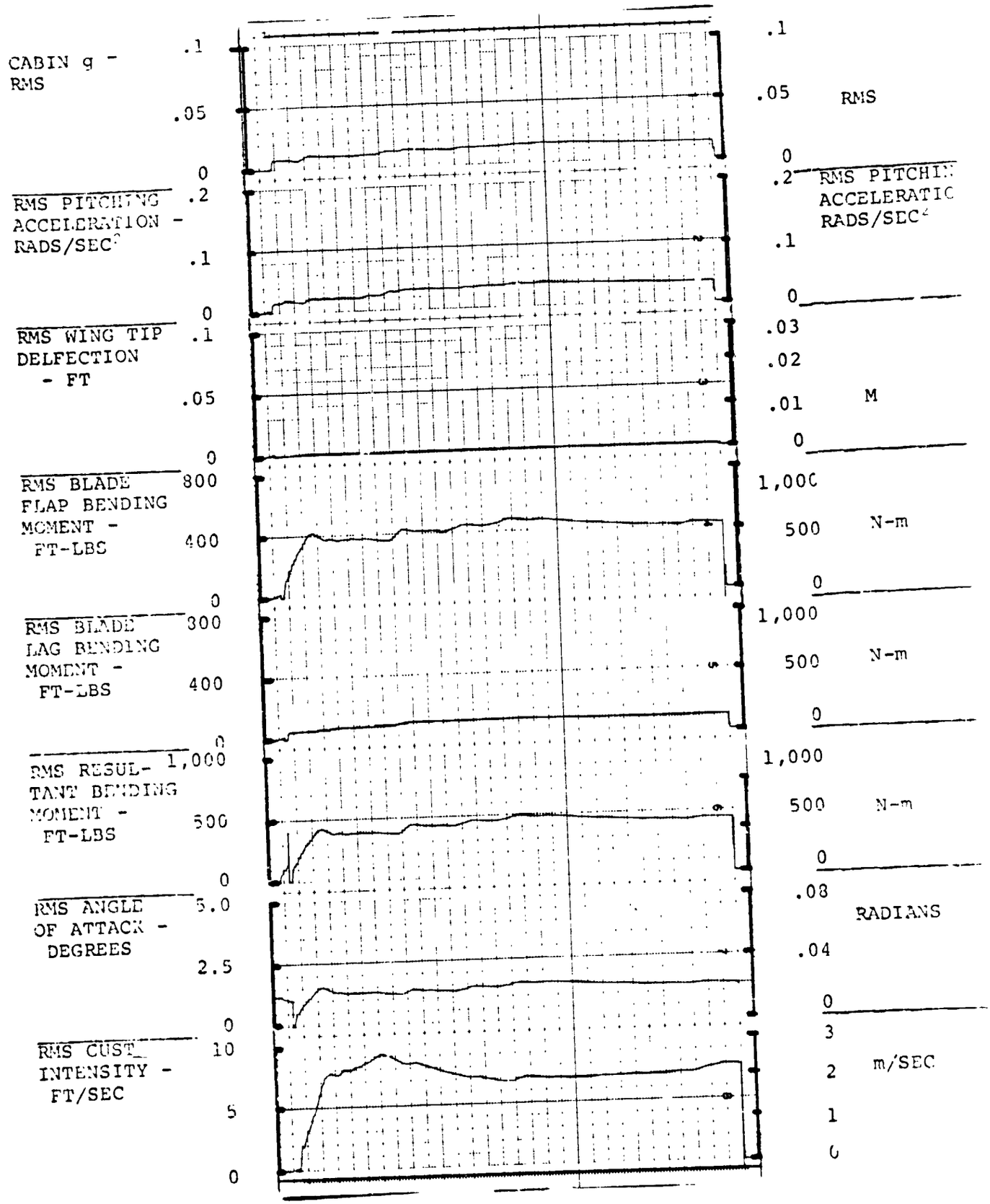

FIGURE 5.6.1.0.0.7. RESPONSES FOR GAIN F = 4.4, GAIN E = .77

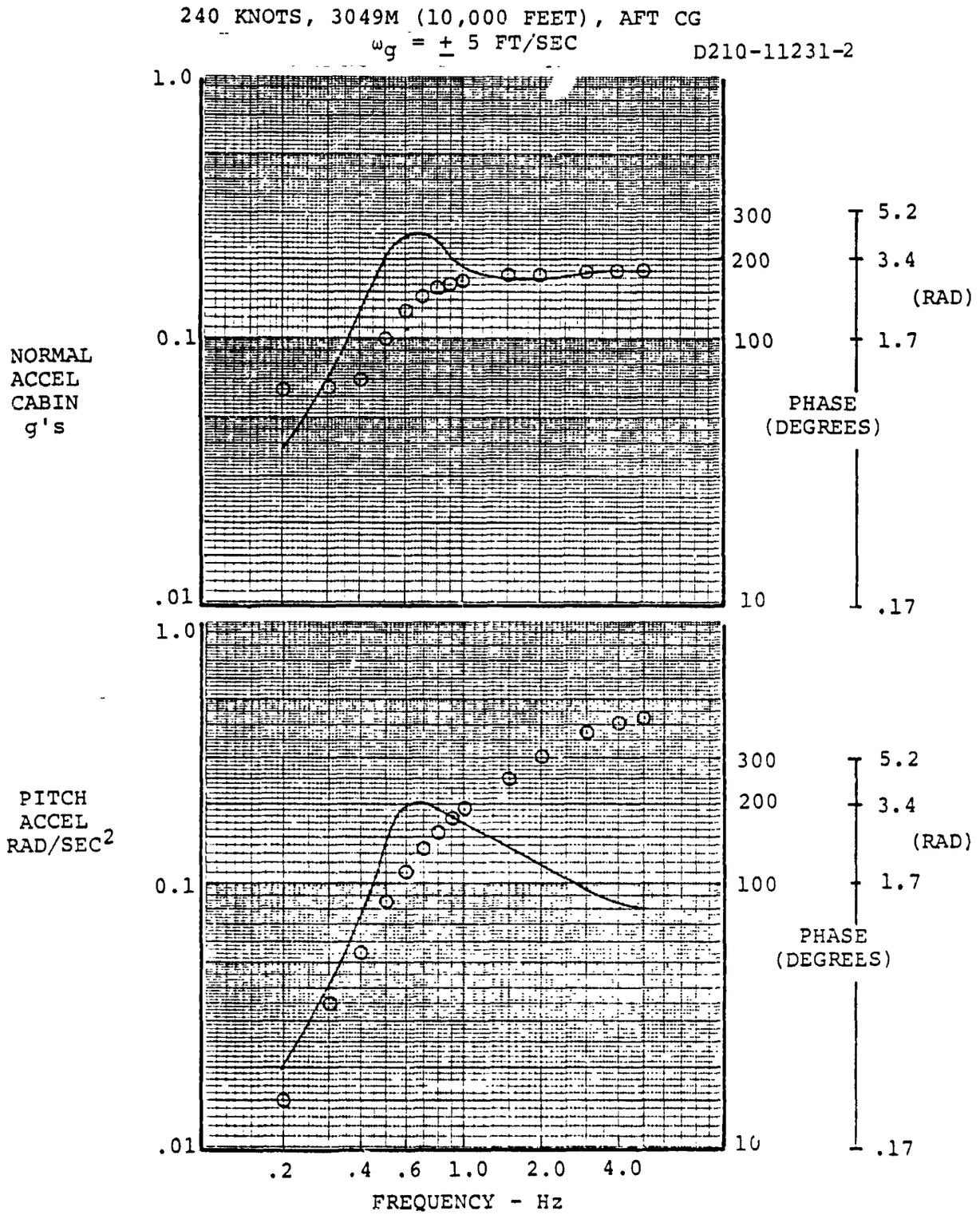

FREQUENCY RESPONSE OF NORMAL AND PITCH ACCELERATION DUE TO VERTICAL GUST (240 KNOTS, 3049 METERS, AFT CG)

FIGURE 1.5.2.1/2.1.0

240 KNOTS, 3049M (10,000 FEET), AFT CG

$\omega_g = \pm 5$ FT/SEC D210-11231-2

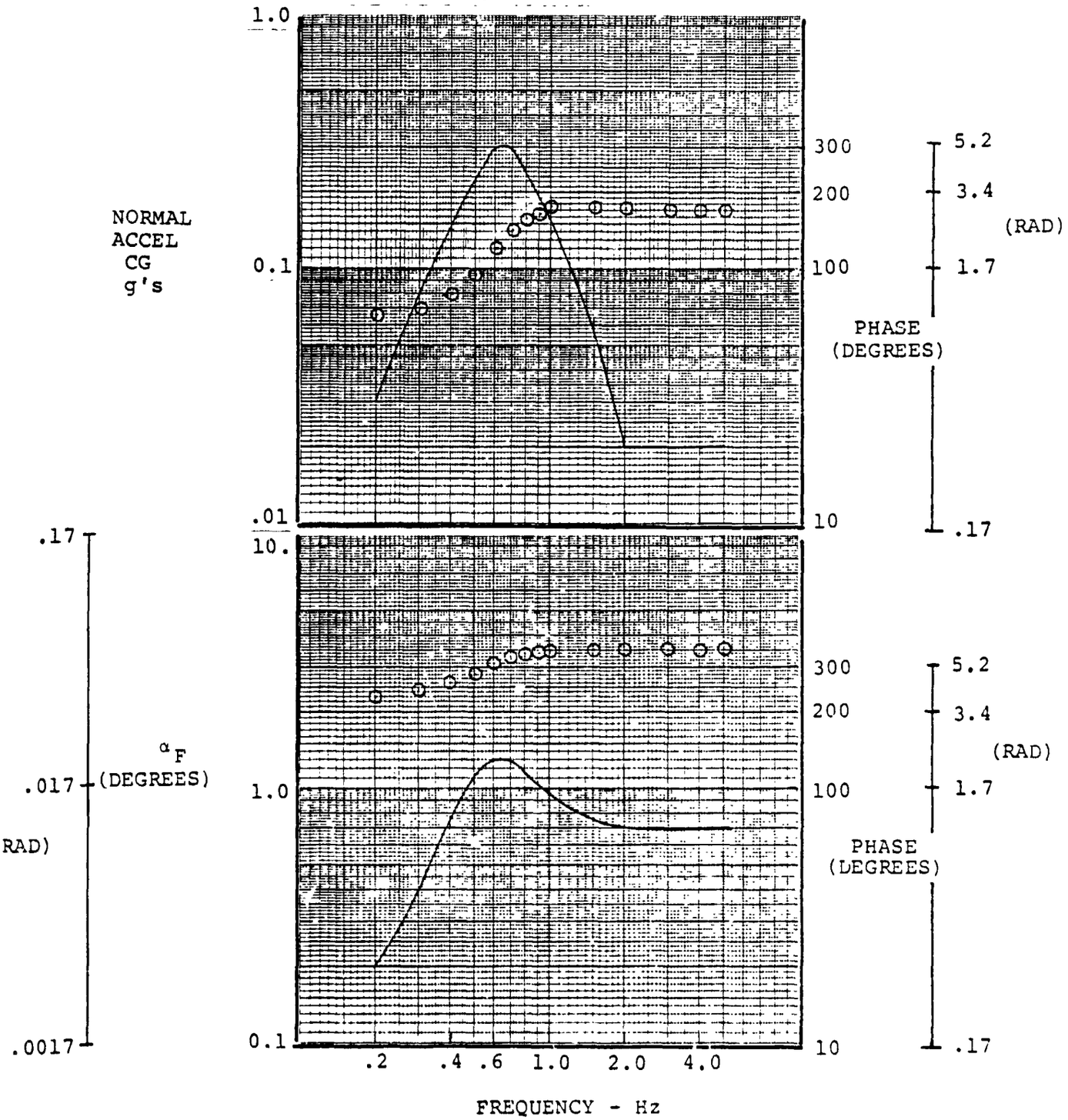

FREQUENCY RESPONSE OF NORMAL ACCELERATION AT CG AND FUSELAGE ANGLE OF ATTACK DUE TO VERTICAL GUSTS (240 KNOTS, 3049 METERS, AFT CG)

FIGURE 1.5.2.3/4.1.0

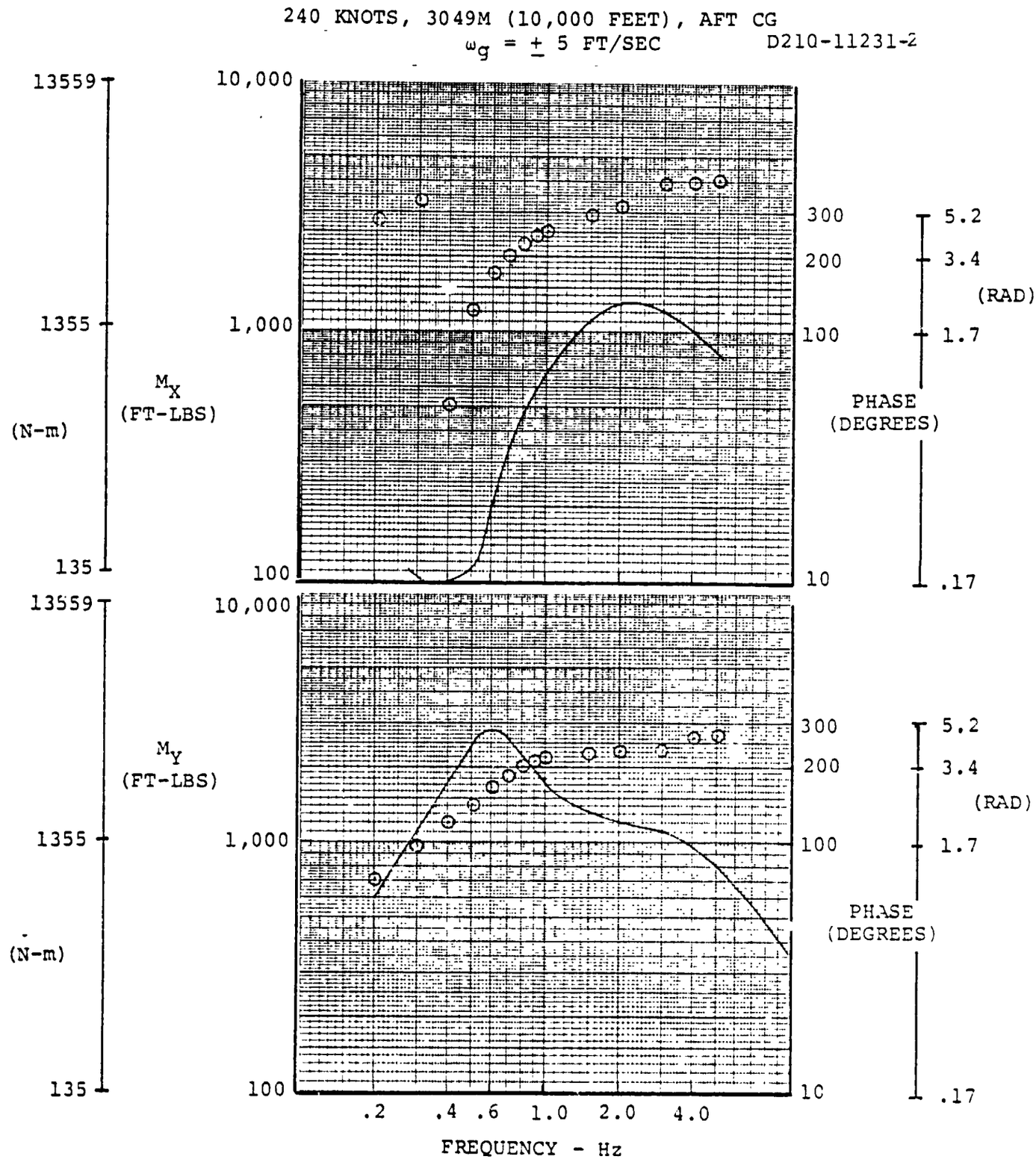

FREQUENCY RESPONSE OF HUB MOMENTS DUE TO VERTICAL GUSTS (240 KNOTS, 3049 METERS, AFT CG)

FIGURE 1.5.2.5/6.1.0

240 KNOTS, 3049M (10,000 FEET), AFT CG

$\delta_F = \pm 1.0°$ D210-11231-2

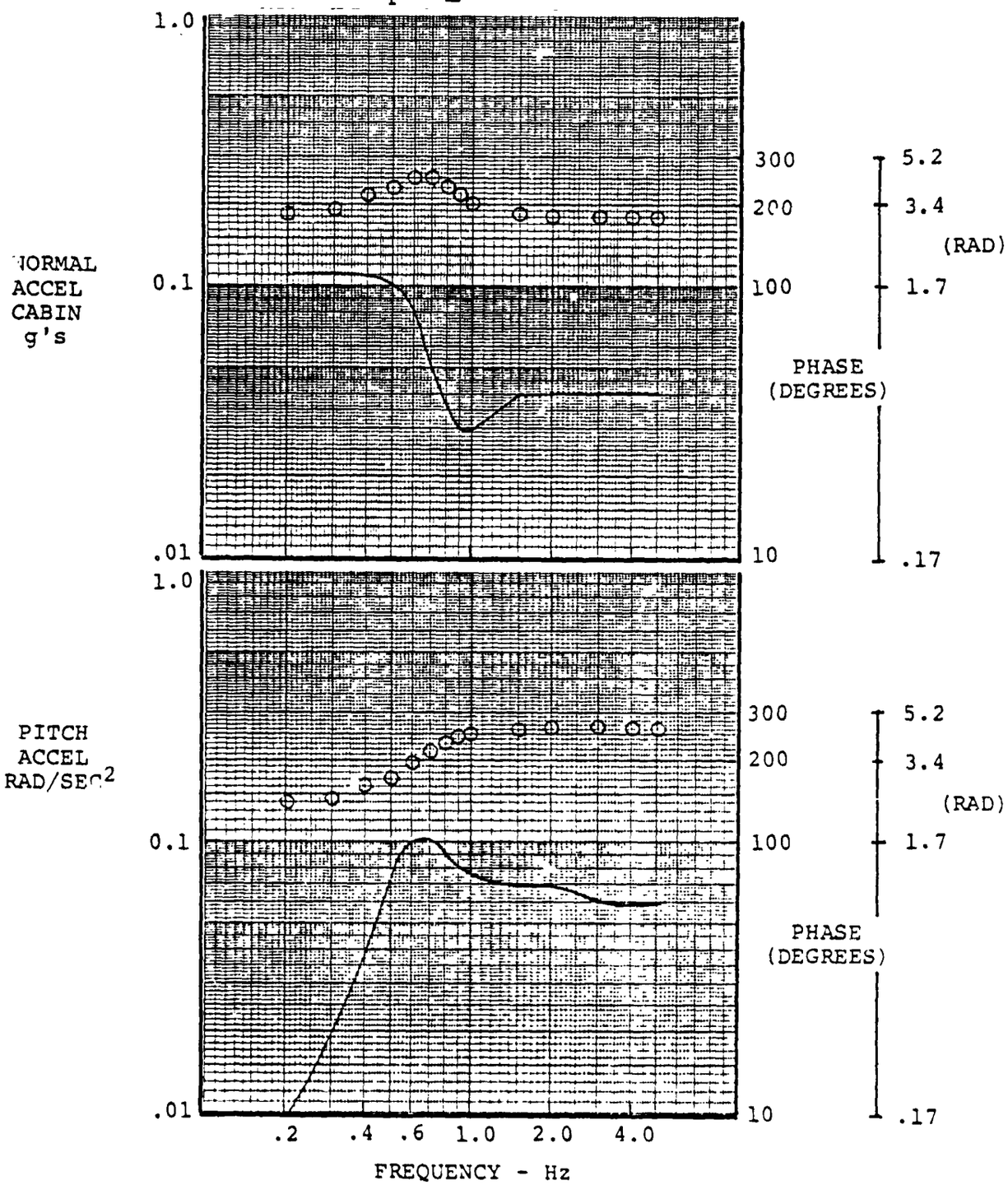

FREQUENCY RESPONSE OF NORMAL AND PITCH ACCELERATION DUE TO δ_F (240 KNOTS, 3049 METERS, AFT CG)

FIGURE 1.5.2.1/2.2.0

240 KNOTS, 3049M (10,000 FEET), AFT CG

$\delta_F = \pm 1.0°$

D210-11231-2

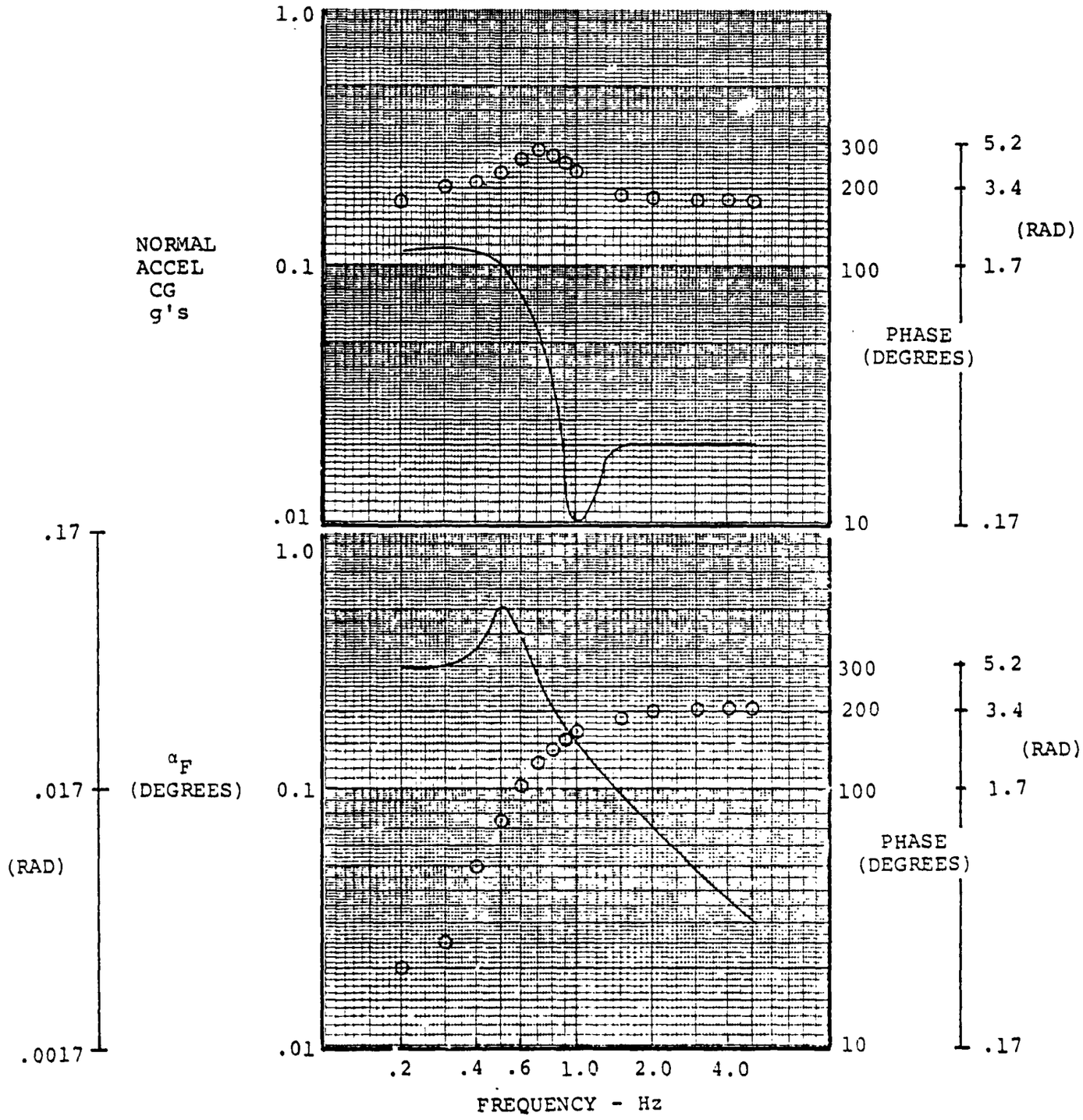

FREQUENCY RESPONSE OF NORMAL ACCELERATION AT CG AND FUSELAGE ANGLE OF ATTACK DUE TO δ_F (240 KNOTS, 3049 METERS, AFT CG)

FIGURE 1.5.2.3/4.2.0

240 KNOTS, 3049M (10,000 FEET), AFT CG

$\delta_F = \pm 1.0°$

D210-11231-2

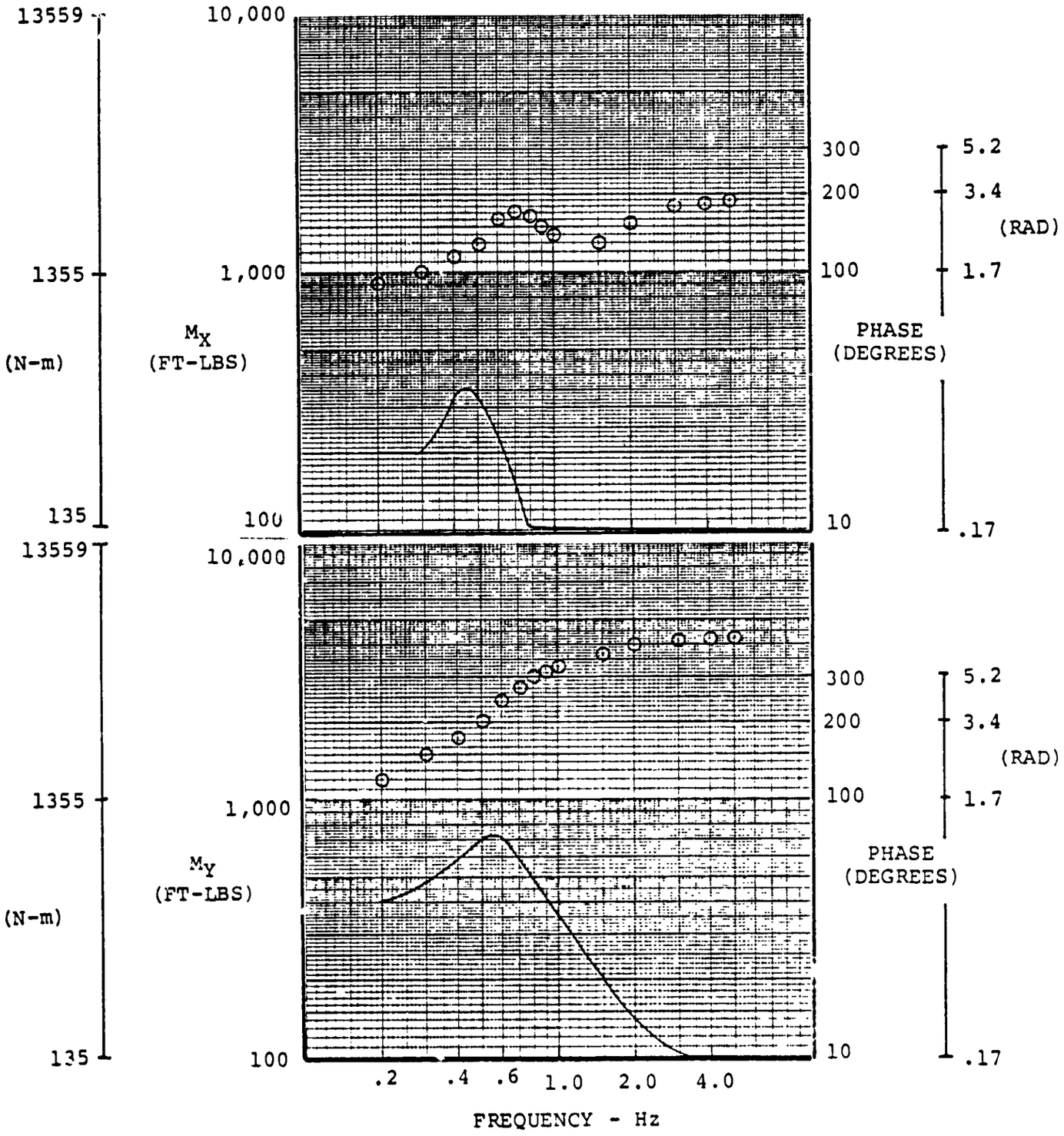

FREQUENCY RESPONSE OF HUB MOMENTS DUE TO δ_F (240 KNOTS, 3049 METERS, AFT CG)

FIGURE 1.5.2.5/6.2.0

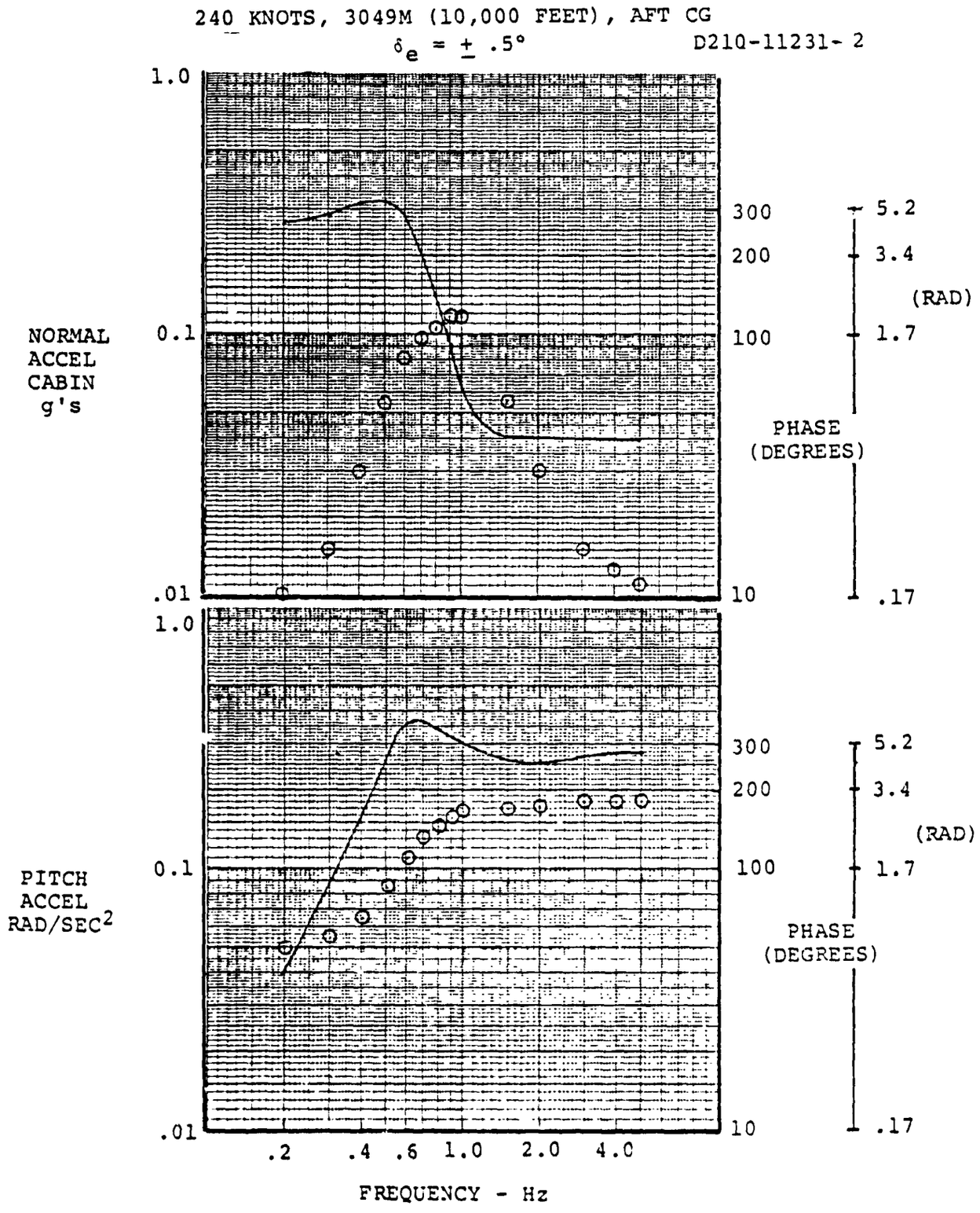

FREQUENCY RESPONSE OF NORMAL AND PITCH ACCELERATION DUE TO δ_e (240 KNOTS, 3049 METERS, AFT CG)

FIGURE 1.5.2.1/2.3.0

240 KNOTS, 3049M (10,000 FEET), AFT CG

$\delta_e = \pm .5°$ D210-11231-2

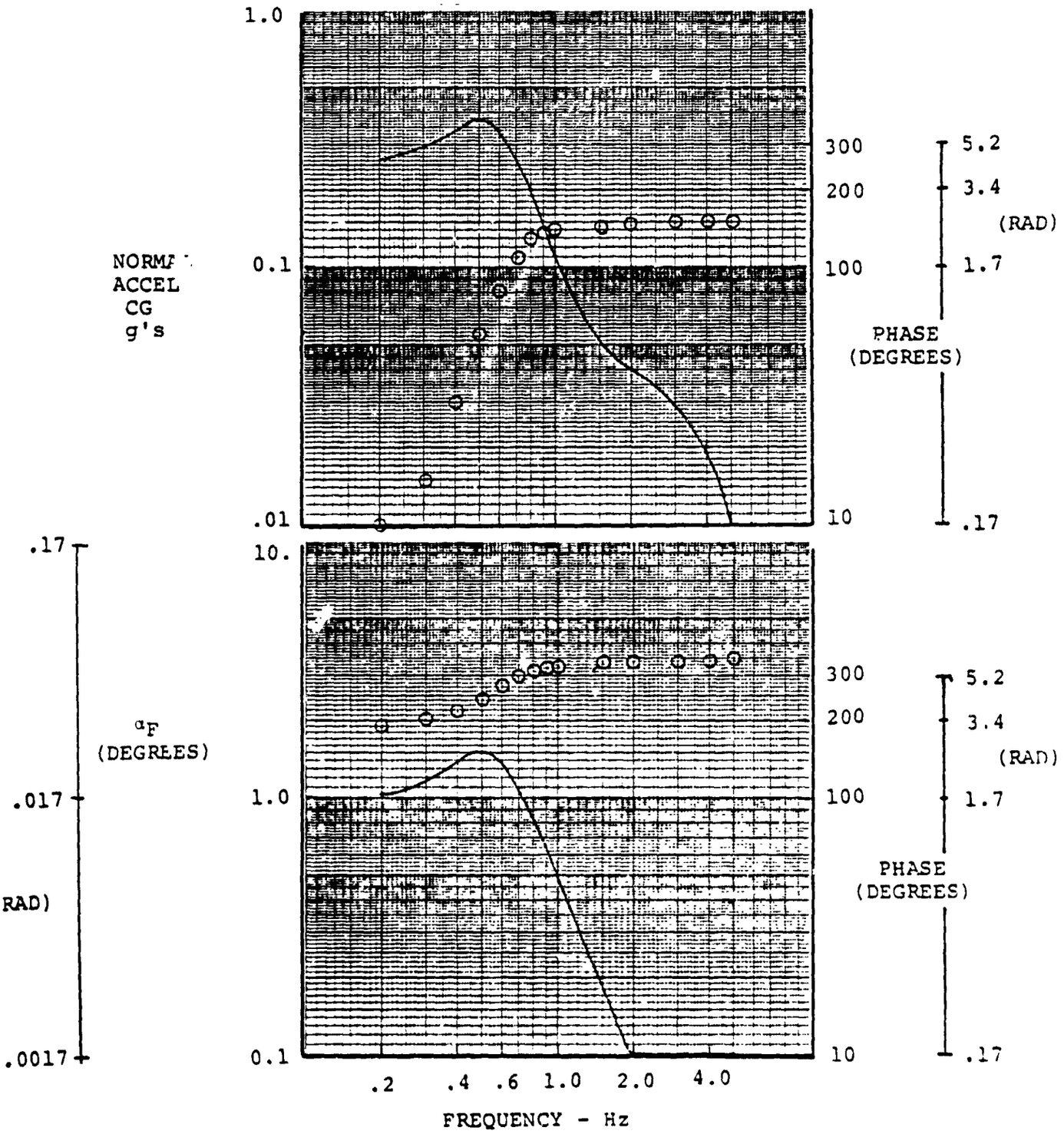

FREQUENCY RESPONSE OF NORMAL ACCELERATION AT CG AND FUSELAGE ANGLE OF ATTACK DUE TO δ_e (240 KNOTS, 3049 METERS, AFT CG)

FIGURE 1.5.2.3/4.3.0

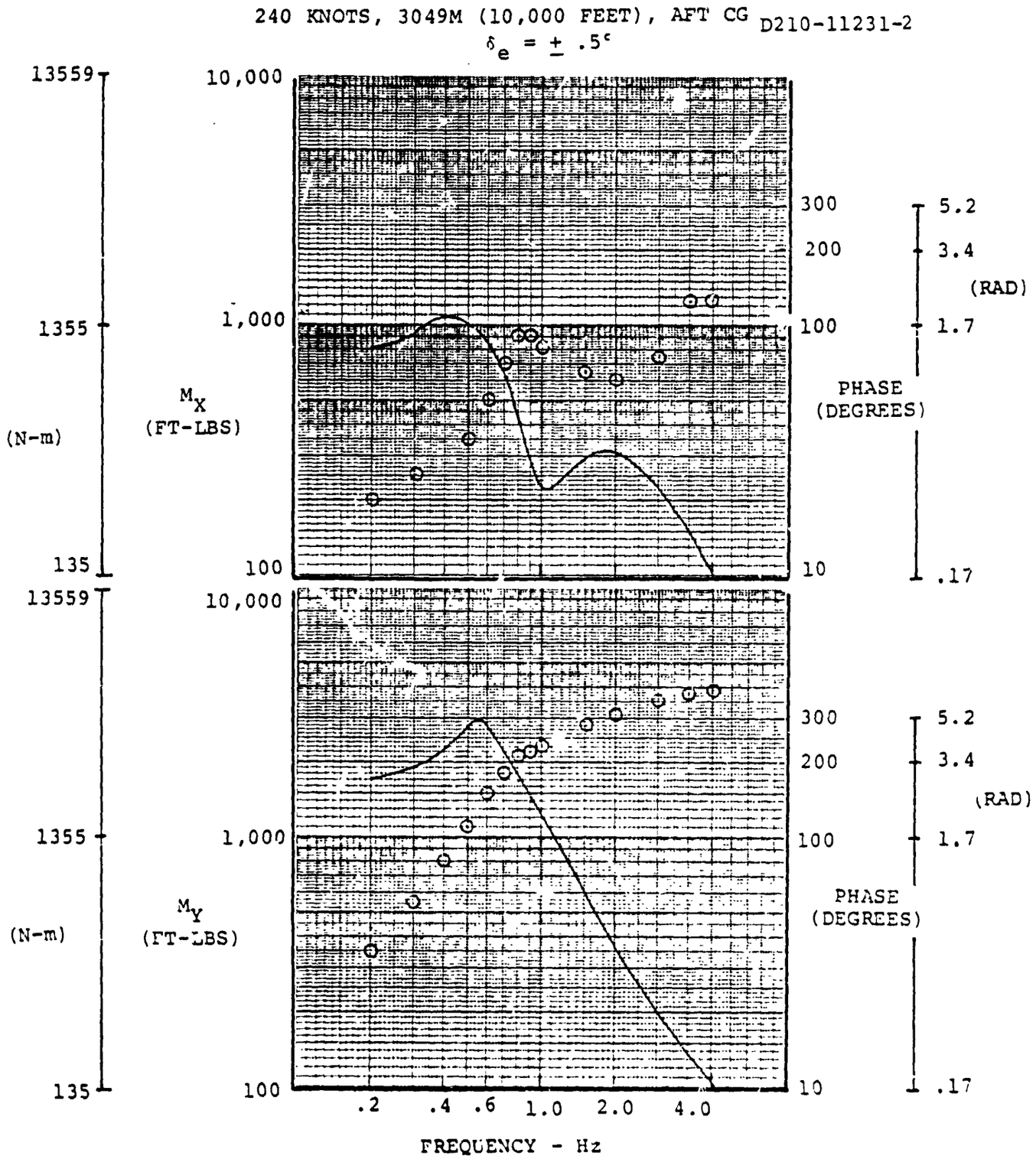

FREQUENCY RESPONSE OF HUB MOMENTS DUE TO δ_e (240 KNOTS, 3049 METERS, AFT CG)

FIGURE 1.5.2.5/6.3.0

240 KNOTS, 3049M (10,000 FEET), AFT CG

$\delta A_1 = \pm .25°$

D210-11231-2

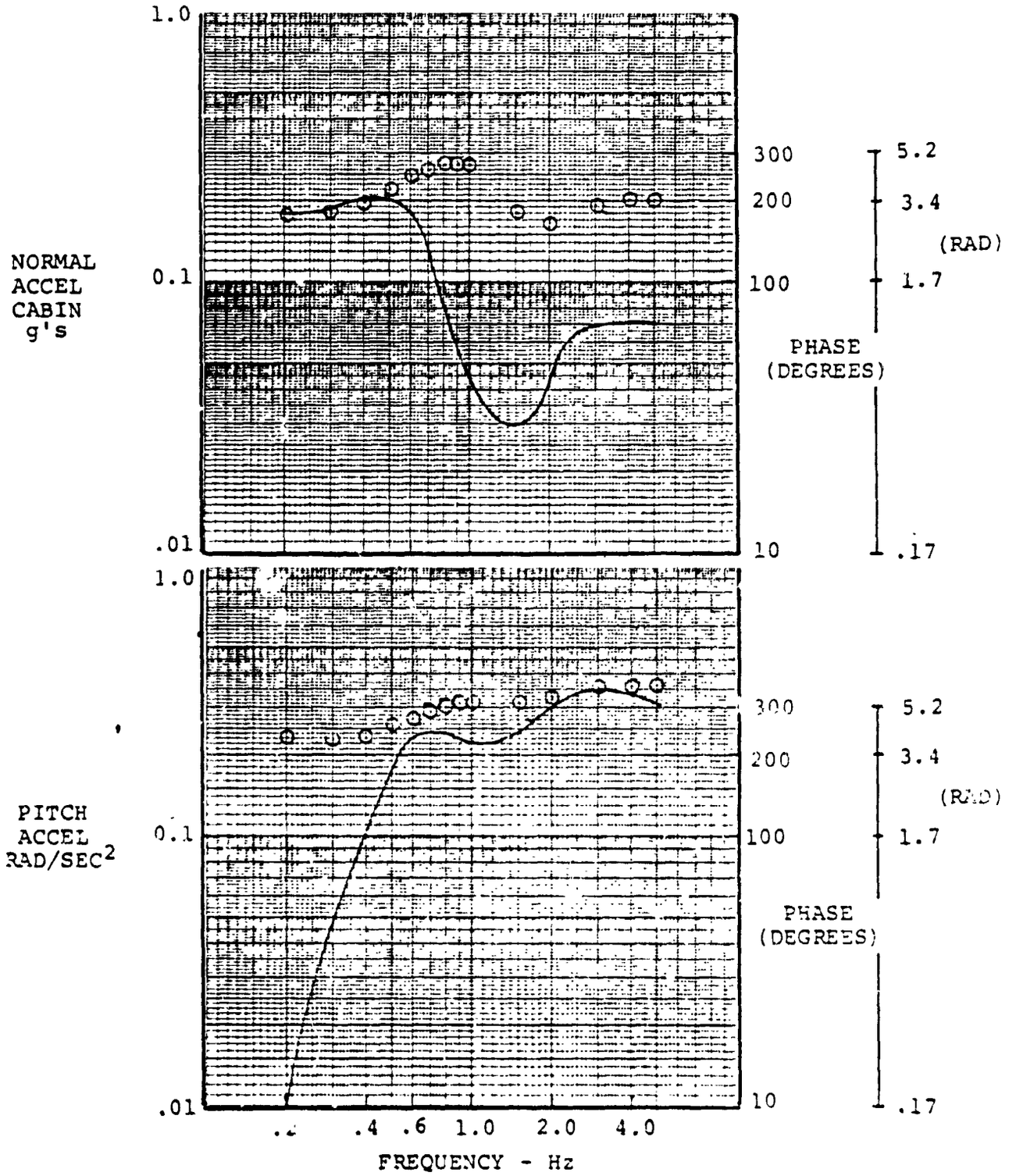

FREQUENCY RESPONSE OF NORMAL AND PITCH ACCELERATION DUE TO A_1 CYCLIC (240 KNOTS, 3049 METERS, AFT CG)

FIGURE 1.5.2.1/2.4.0

240 KNOTS, 3049M (10,000 FEET), AFT CG

$\delta A_1 = \pm .25°$

D210-11231-2

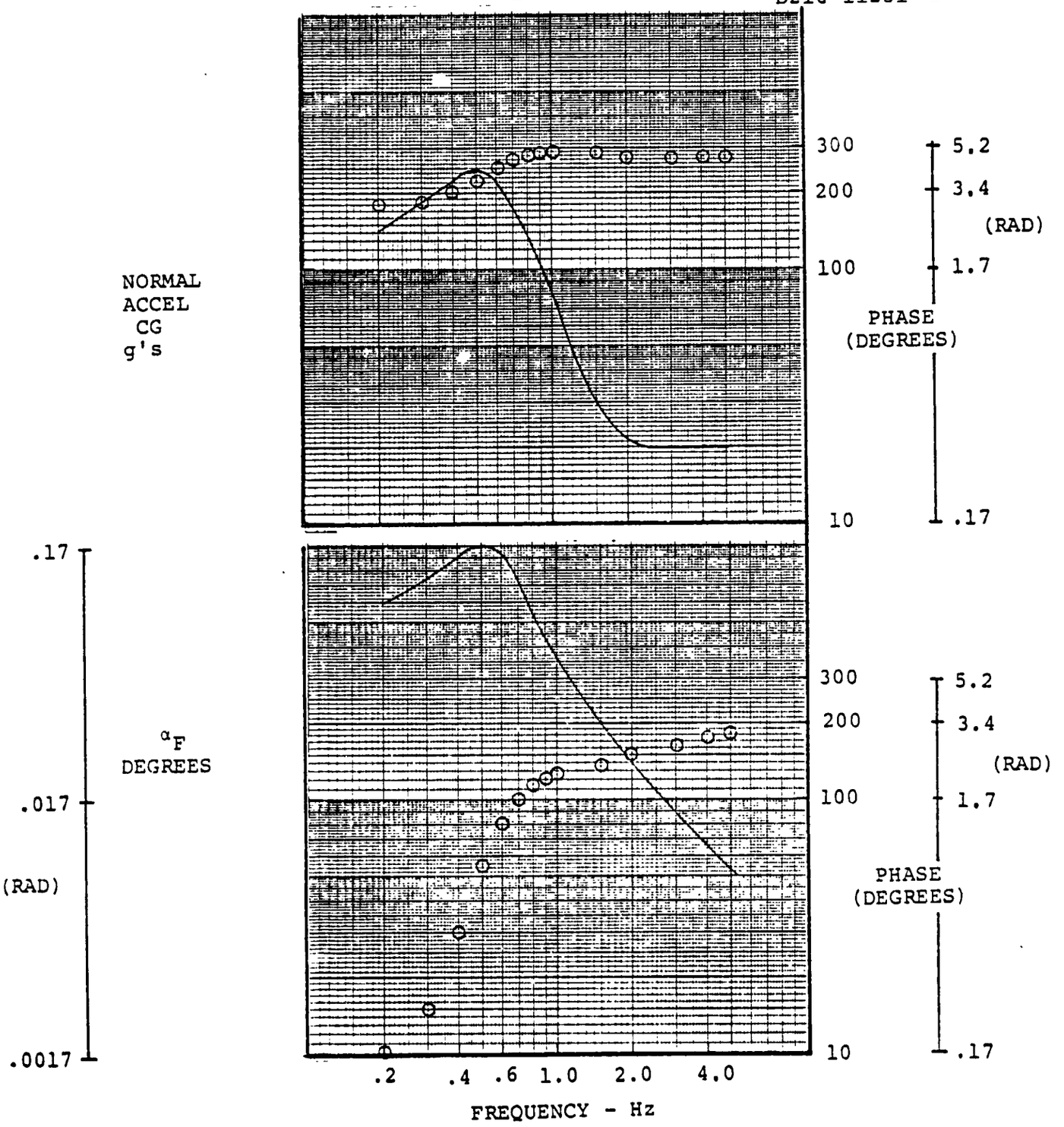

FREQUENCY RESPONSE OF NORMAL ACCELERATION A. CG AND FUSELAGE ANGLE OF ATTACK DUE TO A_1 CYCLIC (240 KNOTS, 3049 METERS, AFT CG)

FIGURE 1.5.2.3/4.4.0

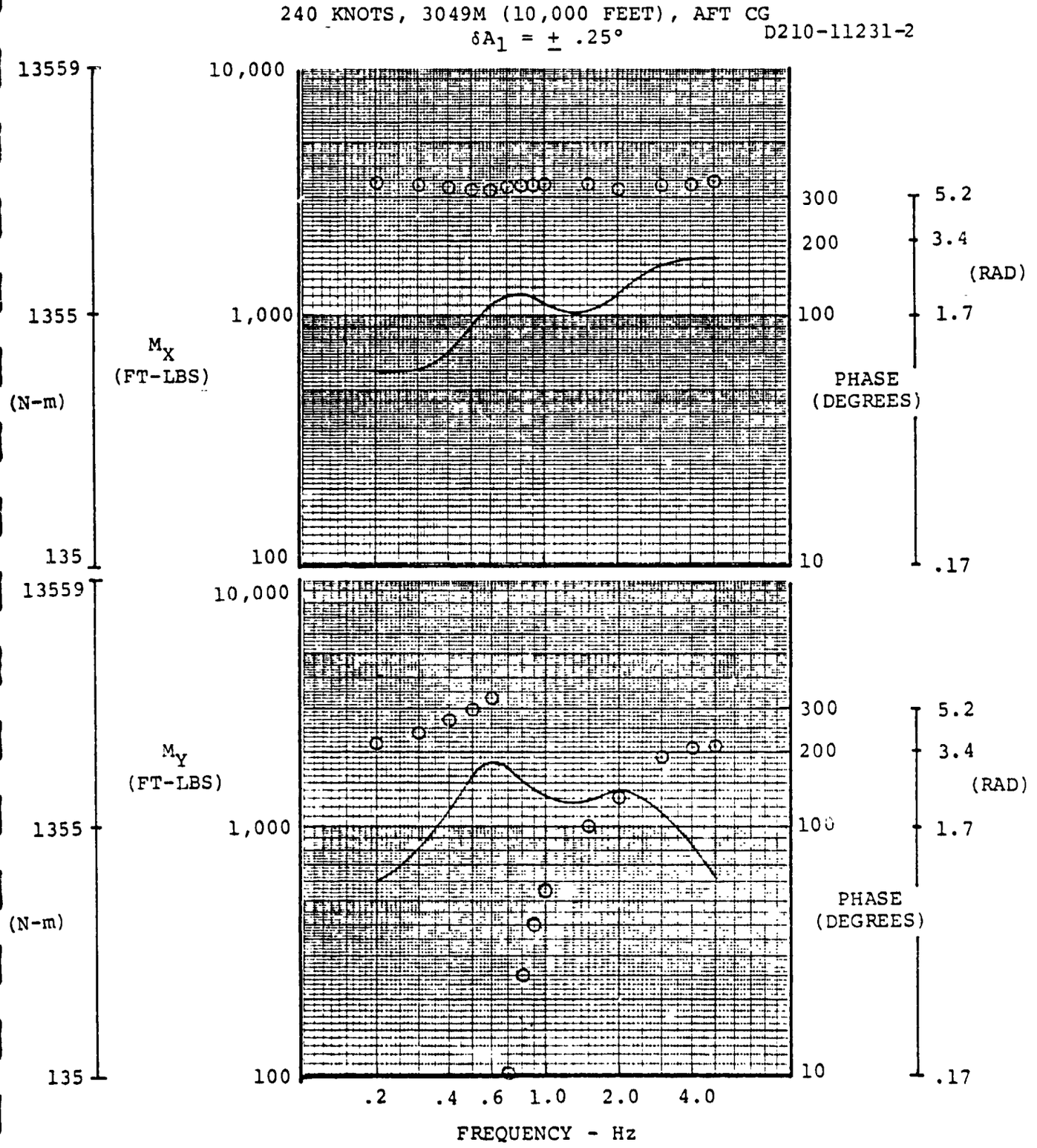

FREQUENCY RESPONSE OF ROTOR HUB MOMENTS DUE TO A_1 CYCLIC (240 KNOTS, 3049 METERS, AFT CG)

FIGURE 1.5.2.5/6.4.0

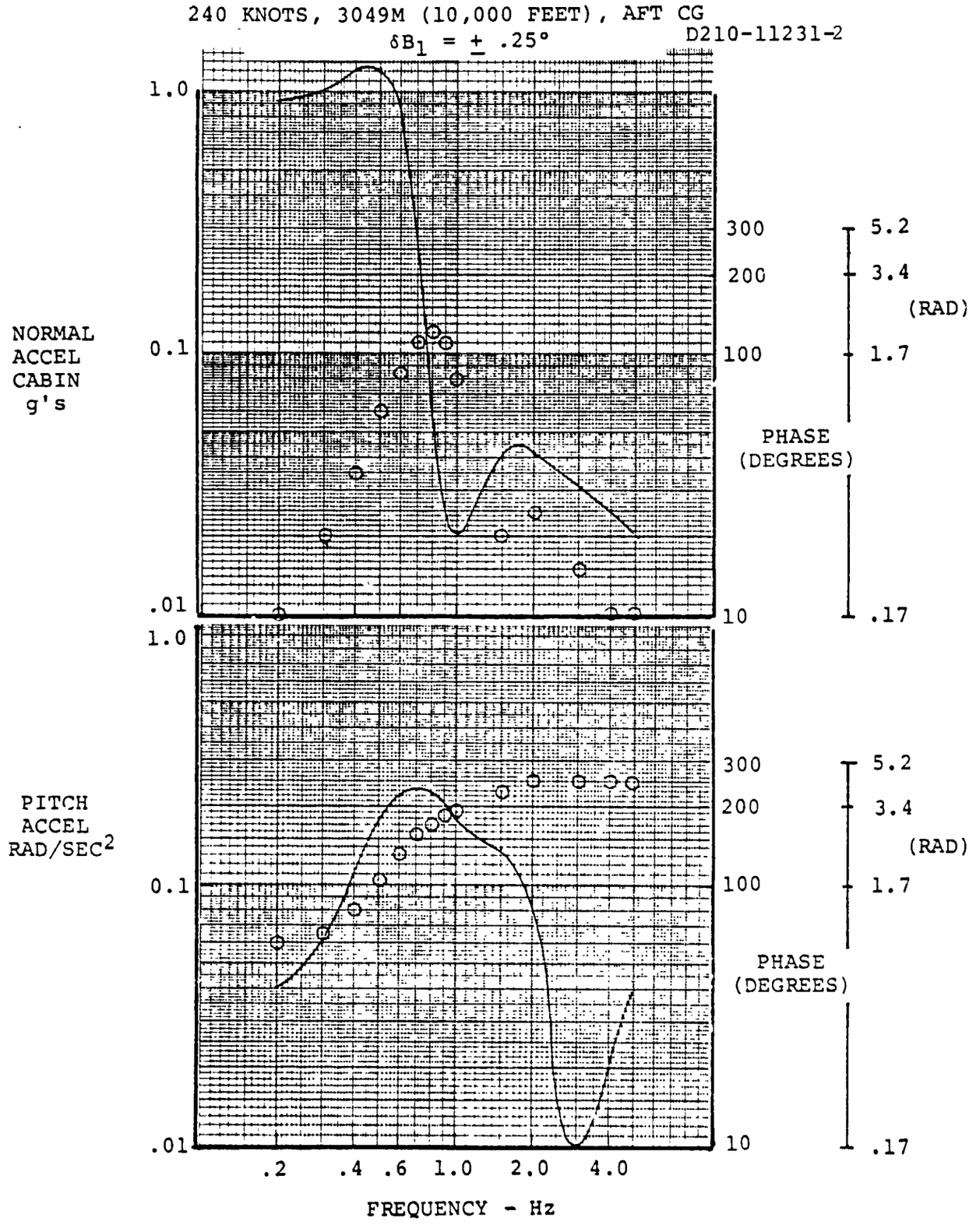

FREQUENCY RESPONSE OF NORMAL AND PITCH ACCELERATION DUE TO B_1 CYCLIC (240 KNOTS, 3049 METERS, AFT CG)

FIGURE 1.5.2.1/2.5.0

240 KNOTS, 3049M (10,000 FEET), AFT CG

$\delta B_1 = \pm .25°$ D210-11231-2

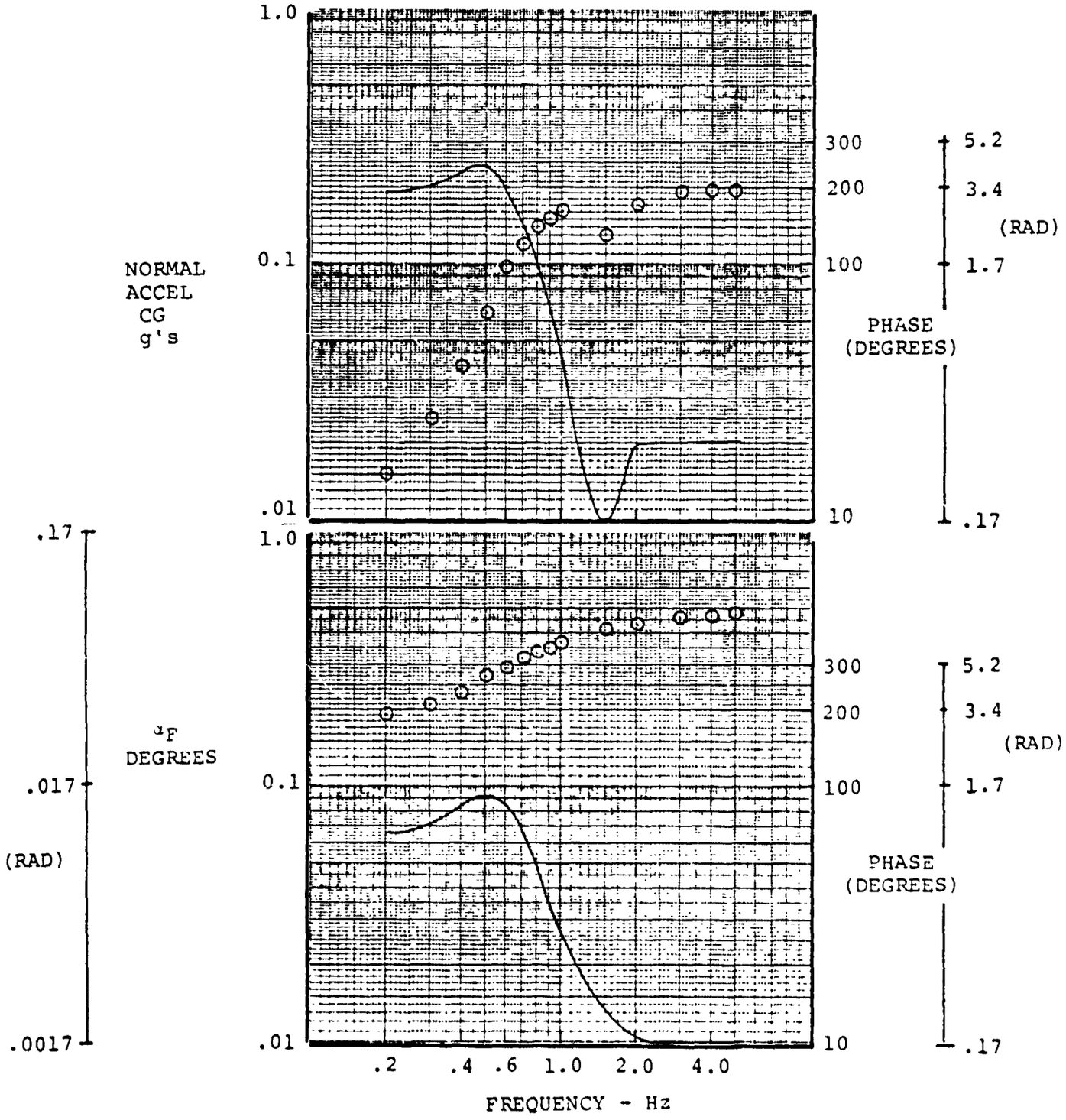

FREQUENCY RESPONSE OF NORMAL ACCELERATION AT CG AND FUSELAGE ANGLE OF ATTACK DUE TO B_1 CYCLIC (240 KNOTS, 3049 METERS, AFT CG)

FIGURE 1.5.2.3/4.5.0

240 KNOTS, 3049M (10,000 FEET), AFT CG

$\delta B_1 = \pm .25°$

D210-11231-2

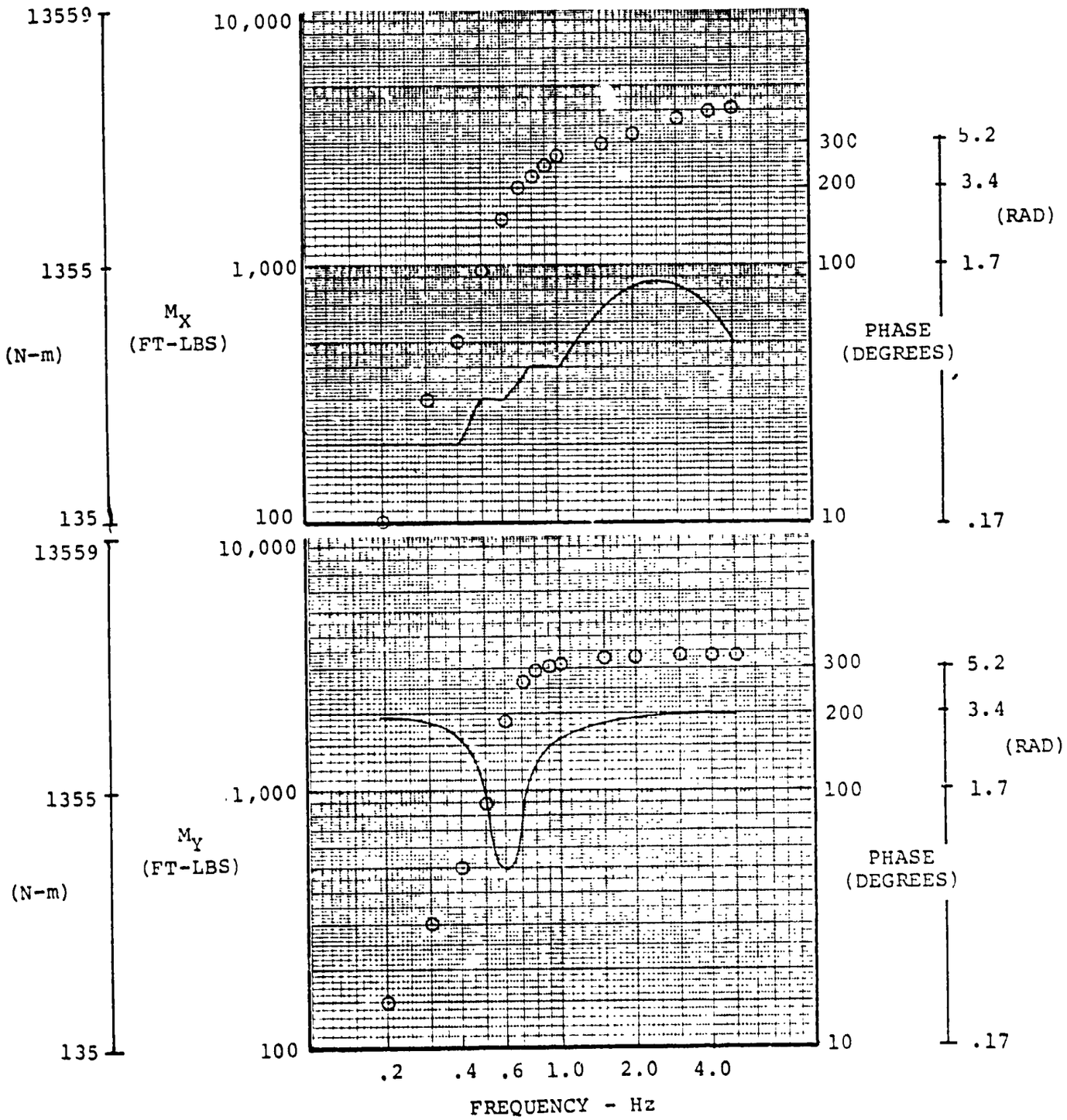

FREQUENCY RESPONSE OF ROTOR HUB MOMENTS DUE TO B_1 CYCLIC (240 KNOTS, 3049 METERS, AFT CG)

FIGURE 1.5.2.5/6.5.0

FEEDBACK REQUIRED FOR SPECIFIED ALLEVIATION IN CABIN

240 KNOTS, 10,000 FEET (3049M), FOREWARD CG

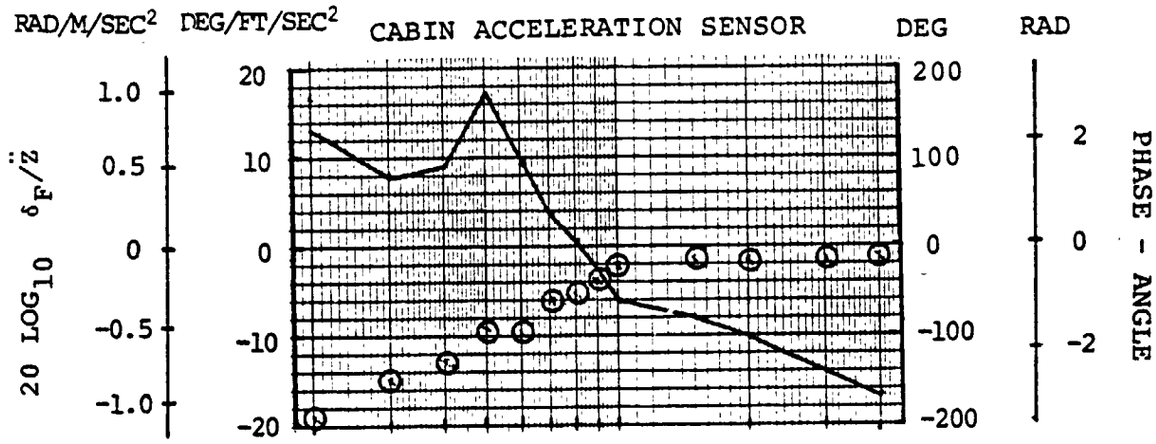

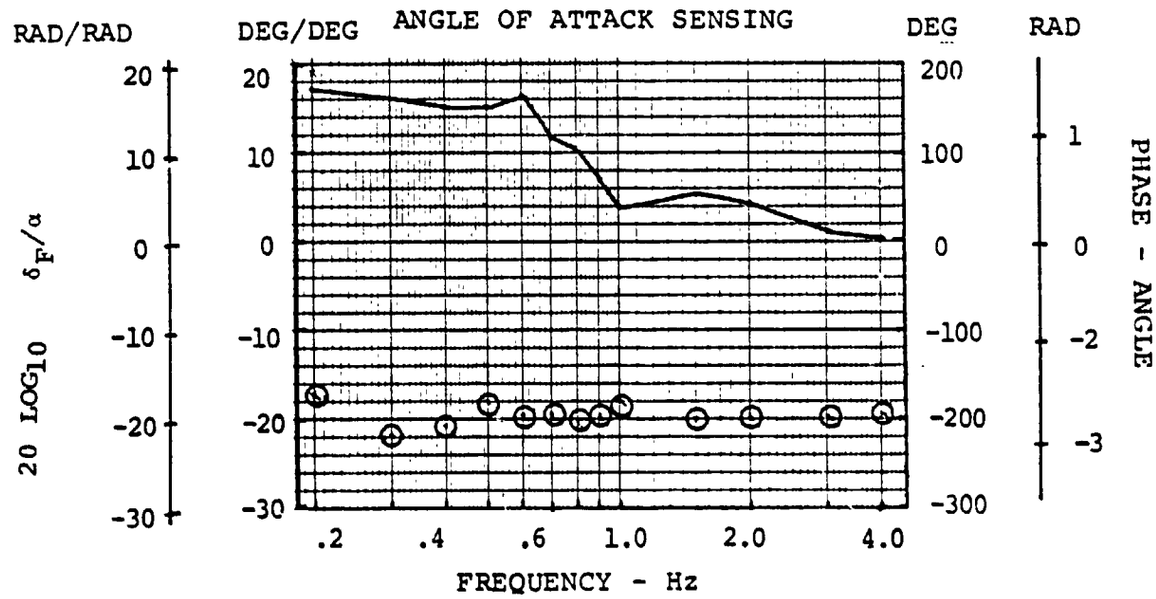

FLAP FEEDBACK REQUIRED WITH ACCELERATION AND α SENSING RESPECTIVELY, 240 KNOTS, 3049 METERS, FORWARD CG, NO A_1, B_1 FEEDBACK

FIGURE 2.5.1.0.0.0

FEEDBACK REQUIRED FOR SPECIFIED ALLEVIATION IN CABIN

240 KNOTS, 10,000 FEET (3049M), AFT CG

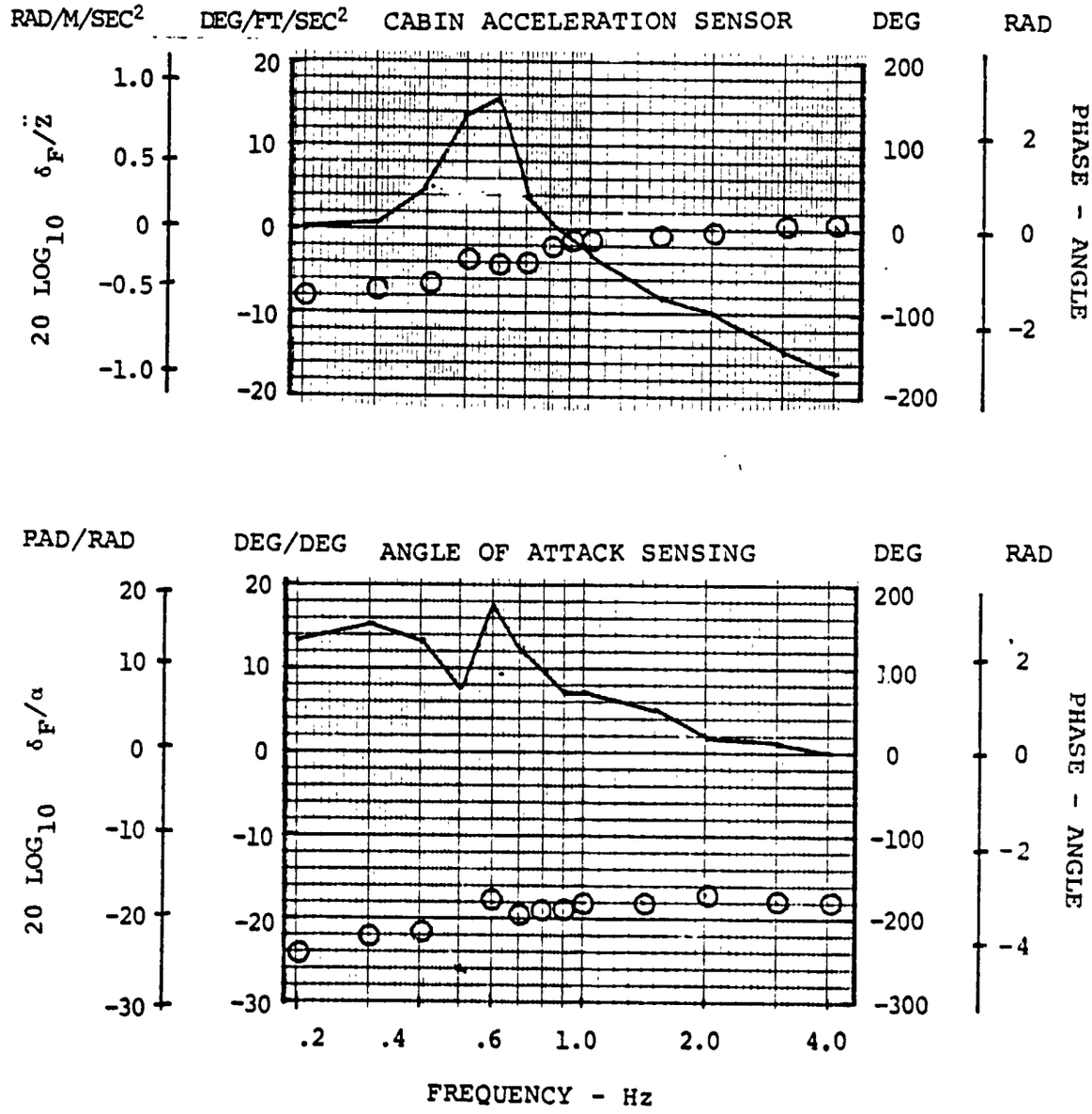

FLAP FEEDBACK REQUIRED WITH ACCELERATION AND α SENSING RESPECTIVELY, 240 KNOTS, 3049 METERS, AFT CG, NO A_1, B_1 FEEDBACK

FIGURE 2.5.2.0.0.0

FEEDBACK REQUIRED FOR SPECIFIED ALLEVIATION IN CABIN

240 KNOTS, 10,000 FEET (3049M), AFT CG

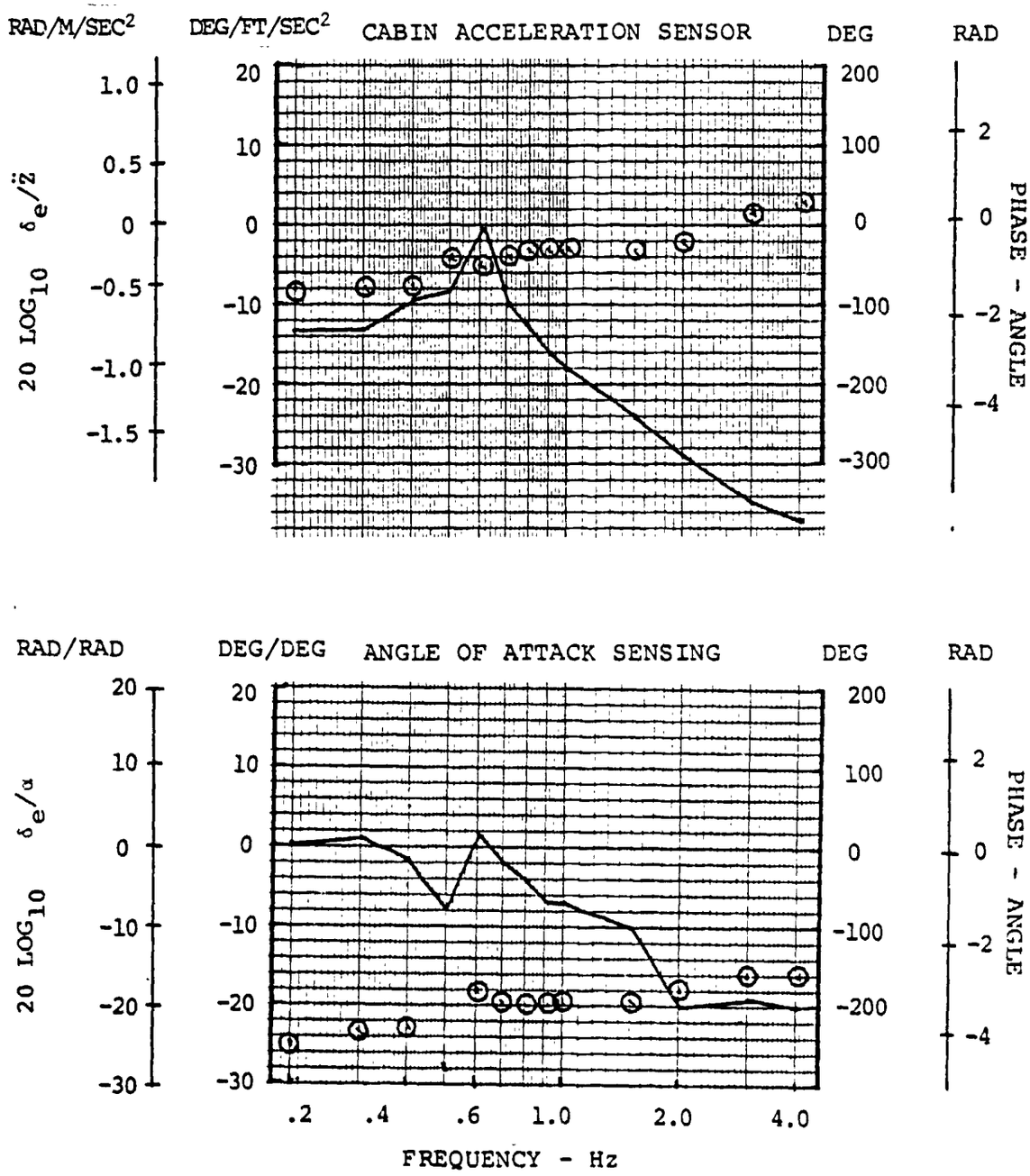

ELEVATOR FEEDBACK REQUIRED WITH ACCELERATION AND α SENSING RESPECTIVELY, 240 KNOTS, 3049 METERS, AFT CG, NO A_1, B_1 FEEDBACK

FIGURE 2.5.2.0.0.0

FEEDBACK REQUIRED FOR SPECIFIED ALLEVIATION IN CABIN

240 KNOTS, 10,000 FEET (3049M), AFT CG

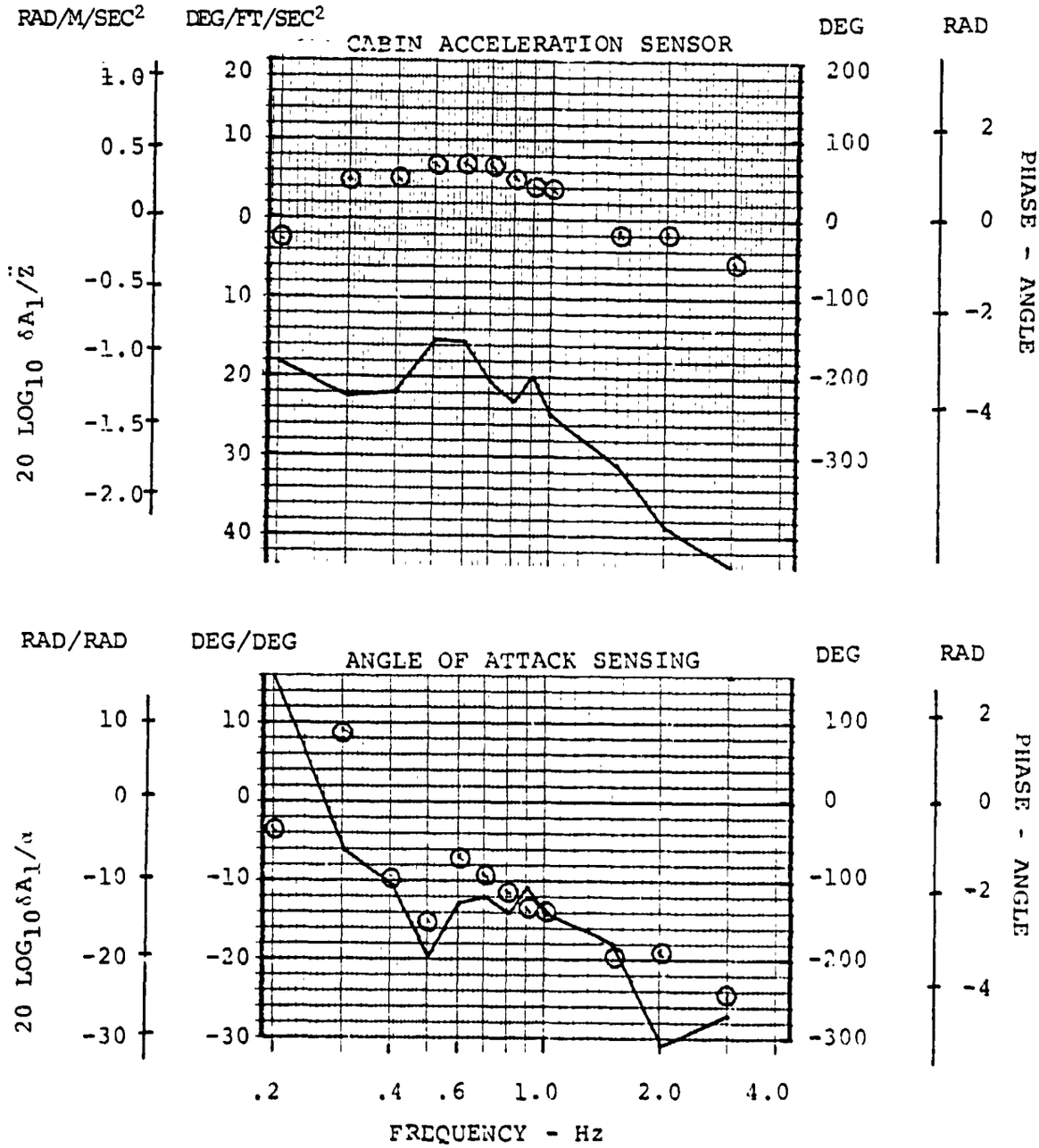

A_1 FEEDBACK REQUIRED WITH ACCELERATION AND α SENSING RESPECTIVELY, 240 KNOTS, 3049 METERS, AFT CG

FIGURE 2.5.2.0.0.0

FEEDBACK REQUIRED FOR SPECIFIED ALLEVIATION IN CABIN

240 KNOTS, 10,000 FEET (3049M), AFT CG

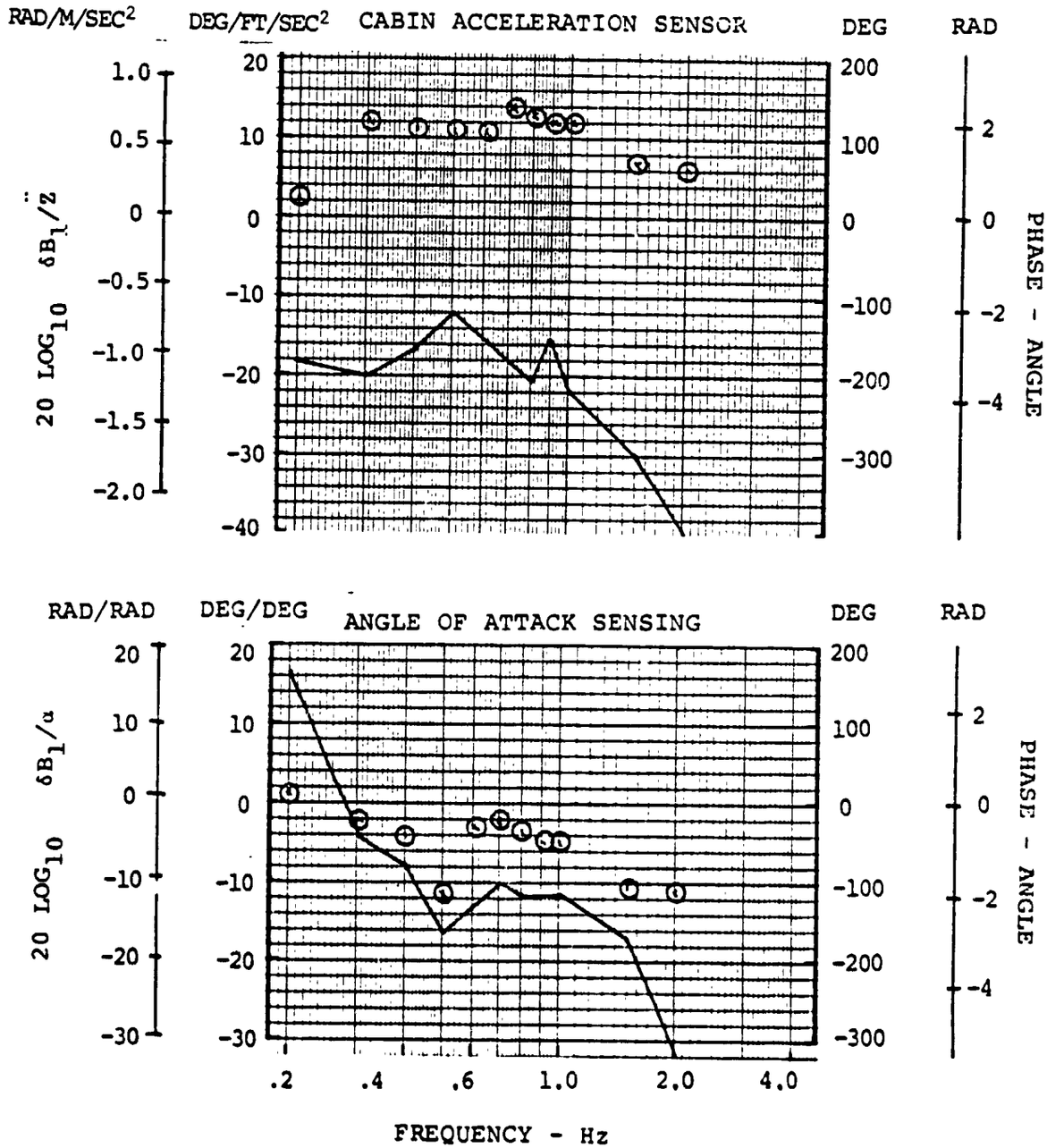

B_1 FEEDBACK REQUIRED WITH ACCELERATION AND α SENSING RESPECTIVELY, 240 KNOTS, 3049 METERS, AFT CG

FIGURE 2.5.2.0.0.0

FEEDBACK REQUIRED FOR SPECIFIED ALLEVIATION IN CABIN

240 KNOTS, 10,000 FEET (3049M), AFT CG

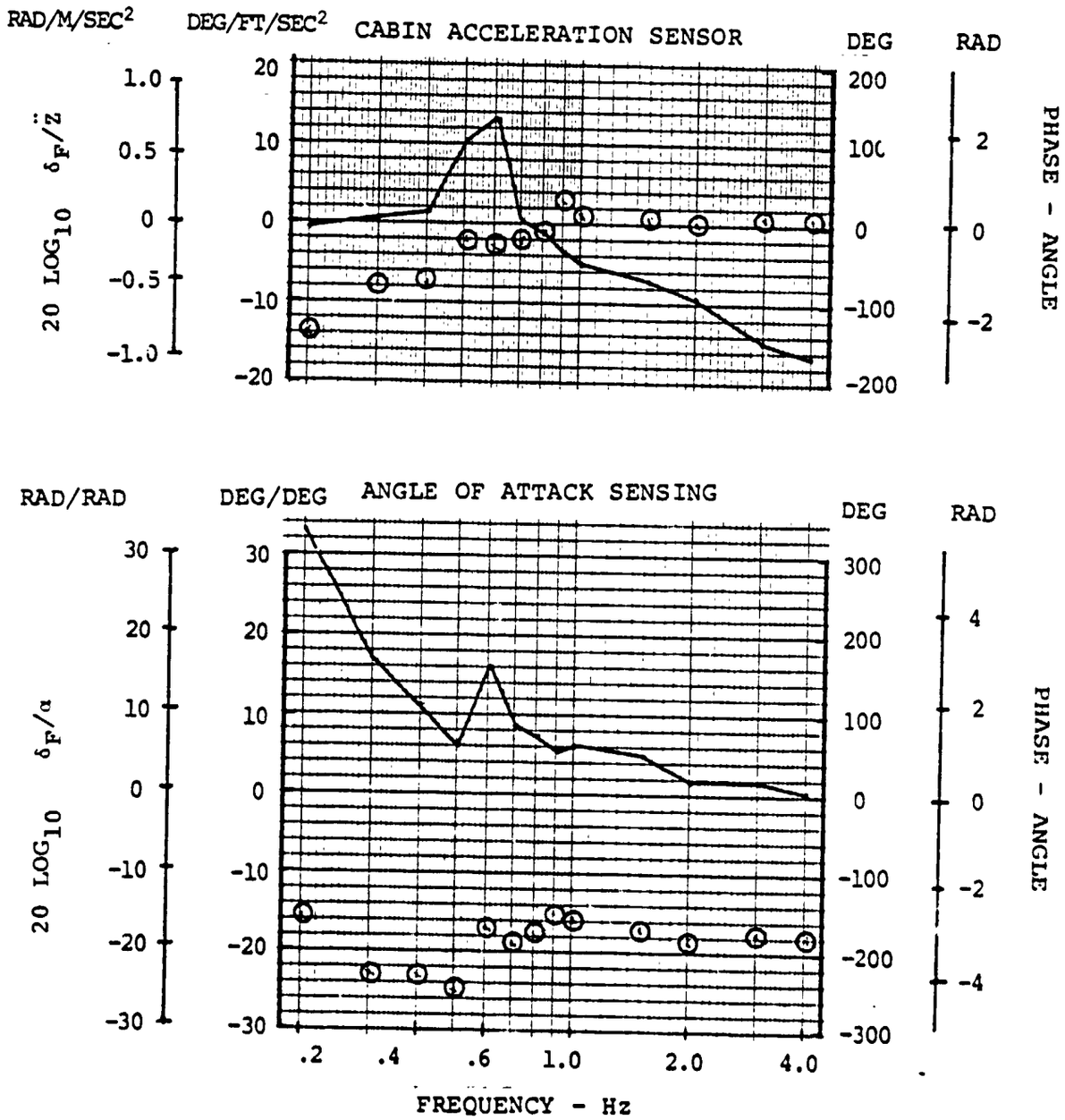

FLAP FEEDBACK REQUIRED WITH ACCELERATION AND α SENSING RESPECTIVELY, 240 KNOTS, 3049 METERS, AFT CG, A_1 & B_1 FEEDBACK

FIGURE 2.5.2.0.0.0

FEEDBACK REQUIRED FOR SPECIFIED ALLEVIATION IN CABIN

240 KNOTS, 10,000 FEET (3049M), AFT CG

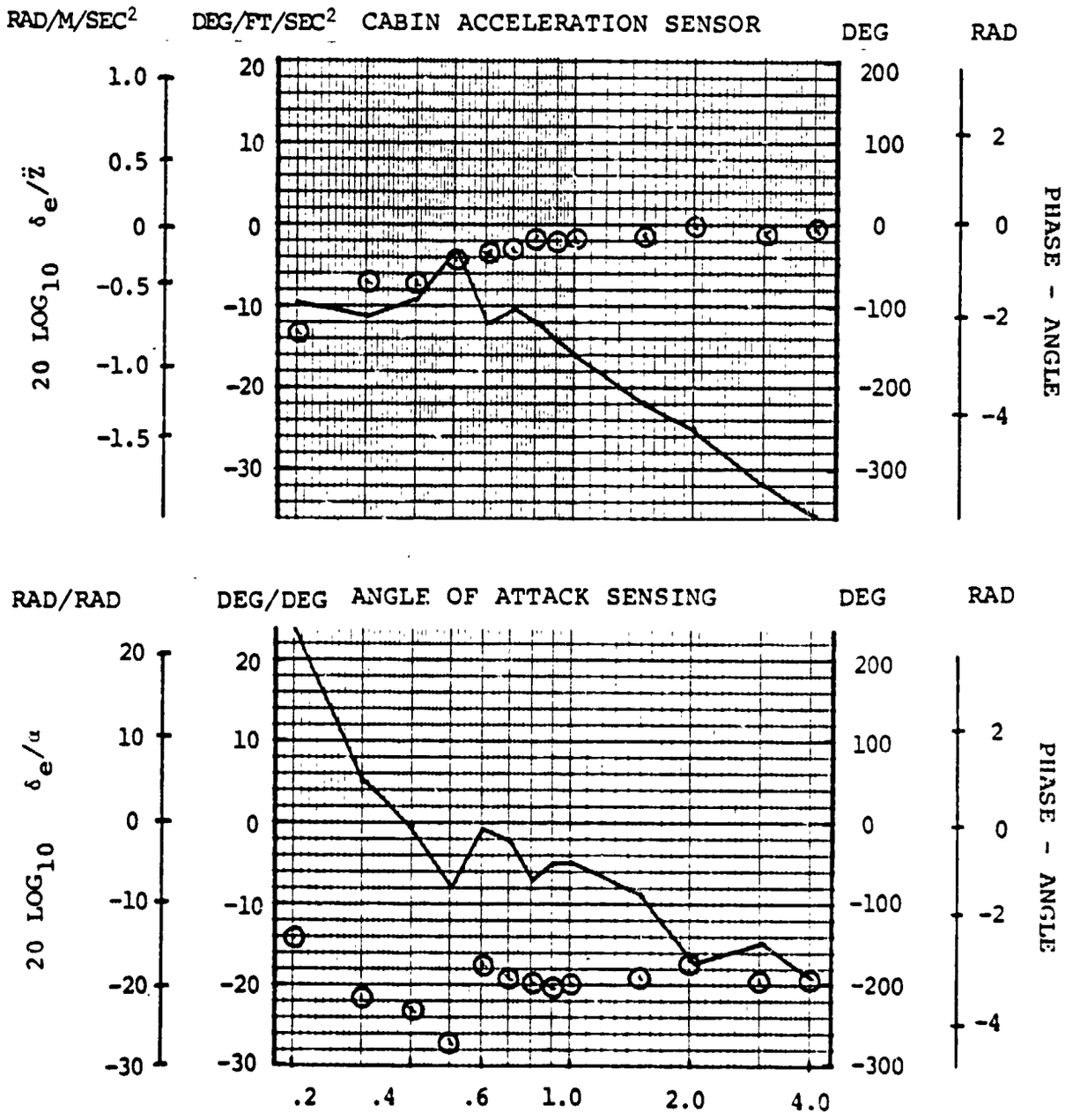

ELEVATOR FEEDBACK REQUIRED WITH ACCELERATION AND α SENSING RESPECTIVELY, 240 KNOTS, 3049 METERS, AFT CG, A_1 & B_1 FEEDBACK

FIGURE 2.5.2.0.0.0

FLIGHT CONDITION: 240 KNOTS, 5,000 FEET, (1,524m), AFT CG

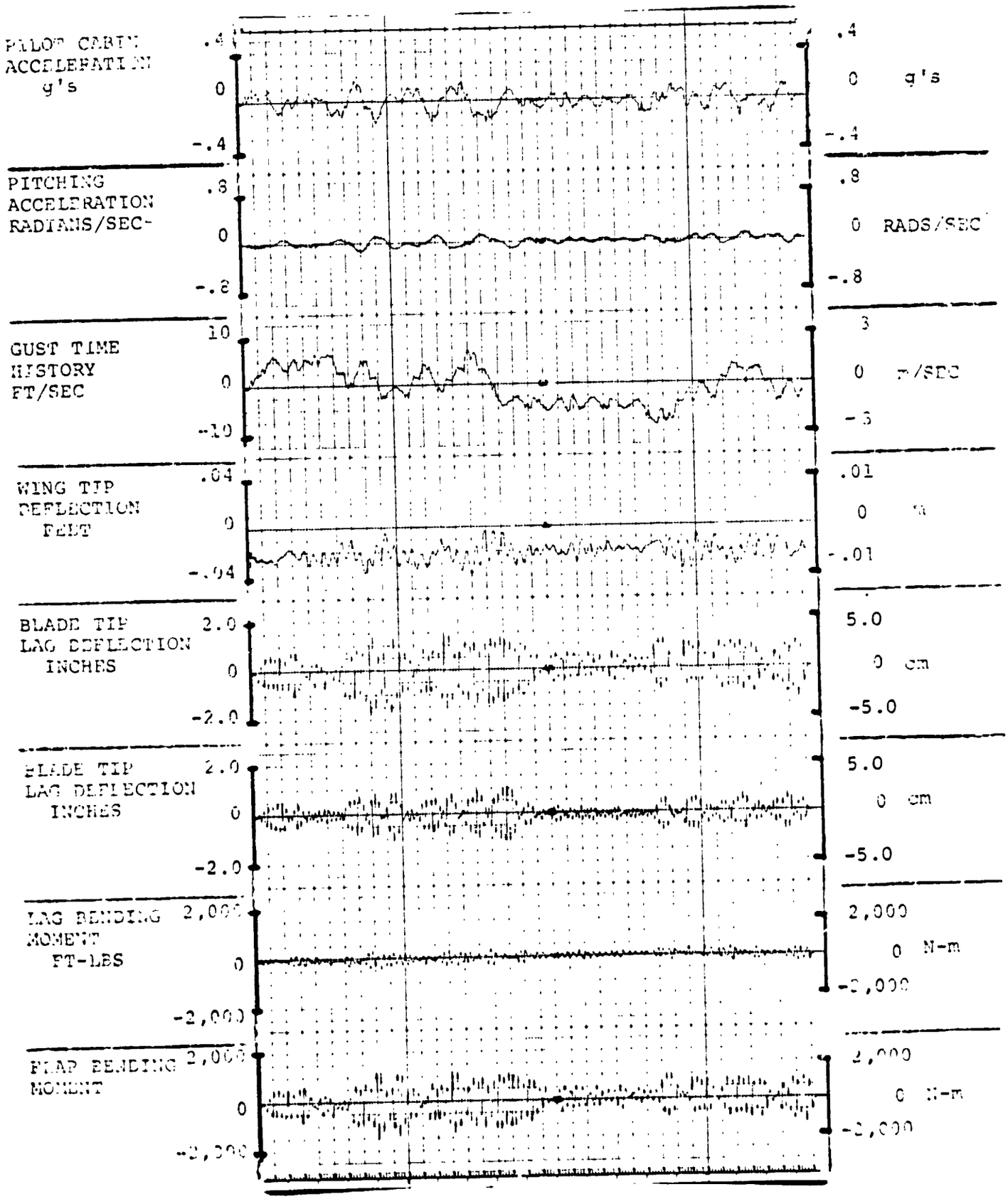

FIGURE 3.4.2.0.0.1. RESPONSES FOR GAIN F = 0, GAIN E = 0

FLIGHT CONDITION: 240 KNOTS, 5,000 FEET, (1,524m), AFT CG

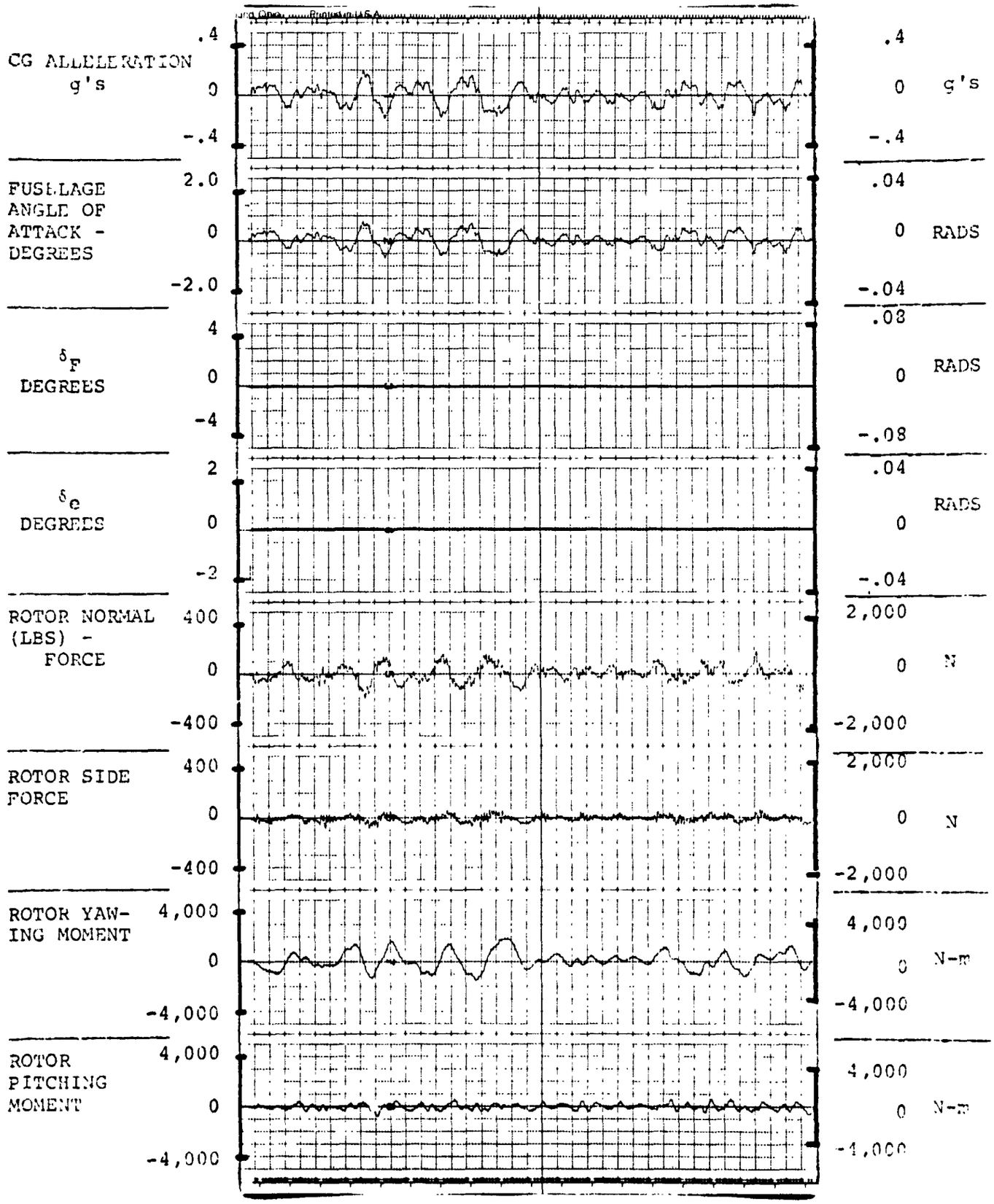

FIGURE 4.4.2.0.0.1. RESPONSES FOR GAIN F = 0, GAIN E = 0

FLIGHT CONDITION: 240 KNOTS, 5,000 FEET, (1,524m), AFT CG

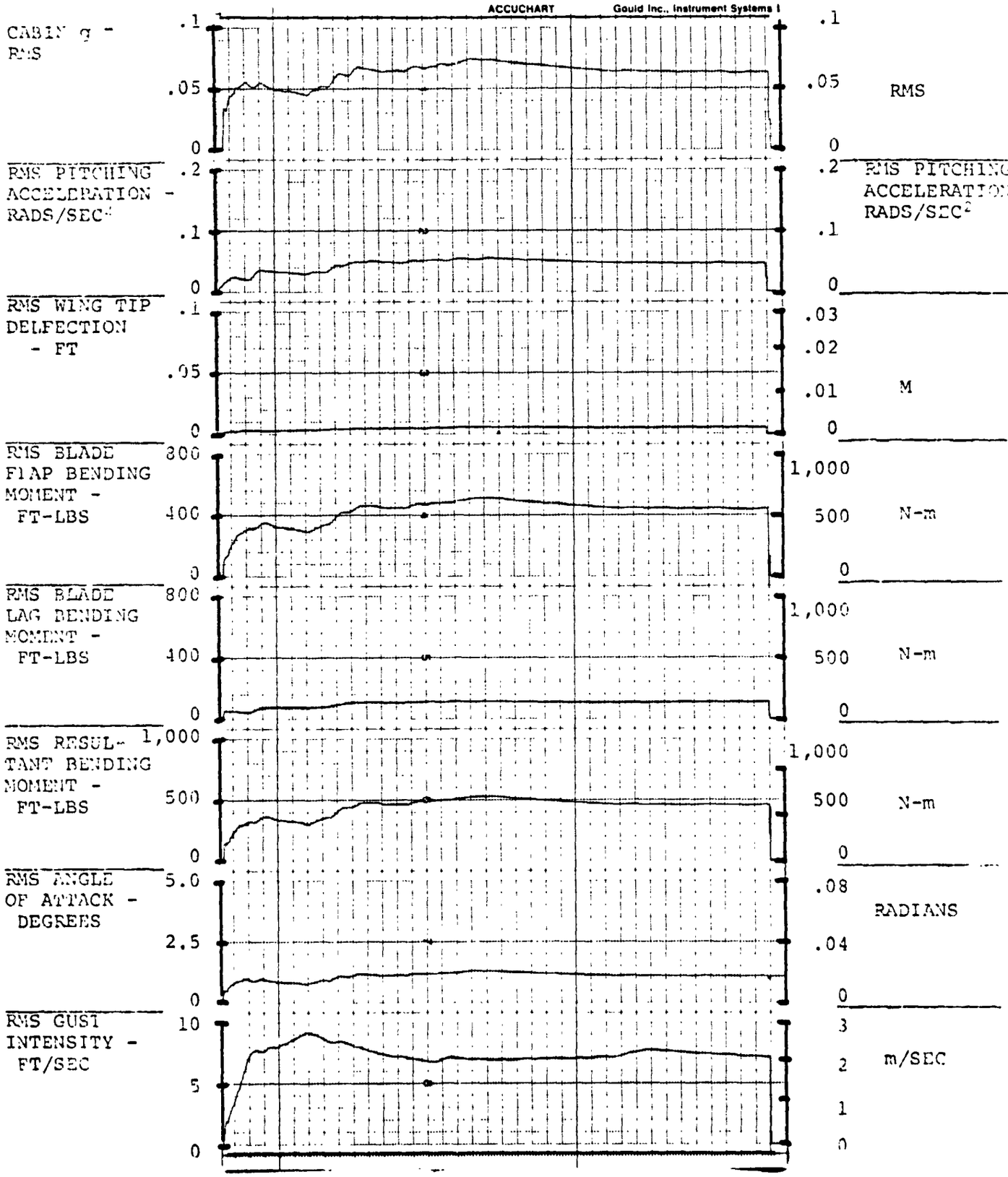

FIGURE 5.4.2.0.0.1. RESPONSES FOR GAIN F = 0, GAIN E = 0

ORIGINAL PAGE IS
OF POOR QUALITY

FLIGHT CONDITION: 240 KNOTS, 5,000 FEET, (1,524m), AFT CG

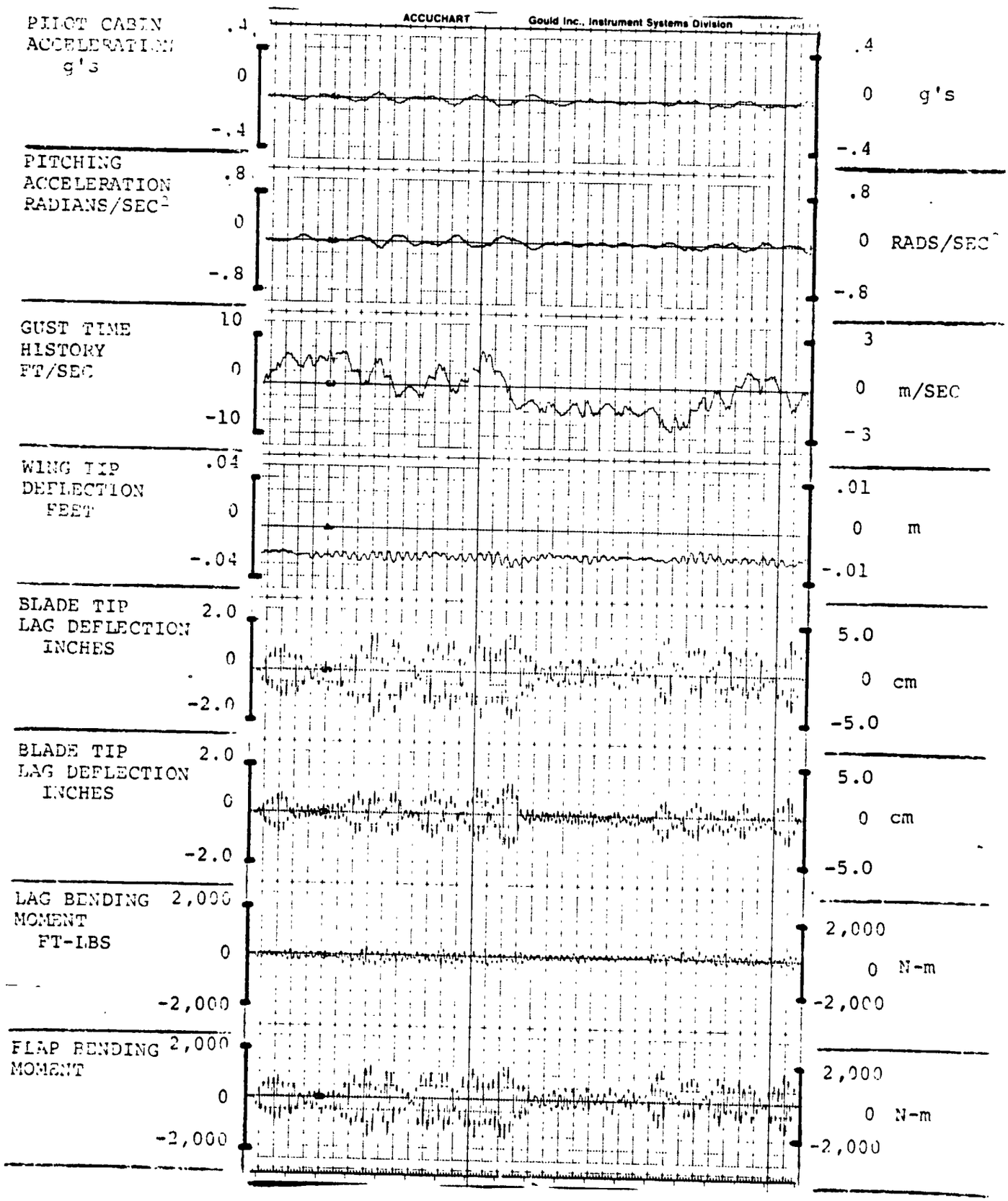

FIGURE 3.4.2.0.0.2. RESPONSES FOR GAIN F = 4.0, GAIN E = .6

FLIGHT CONDITION: 240 KNOTS, 5,000 FEET, (1,524m), AFT CG

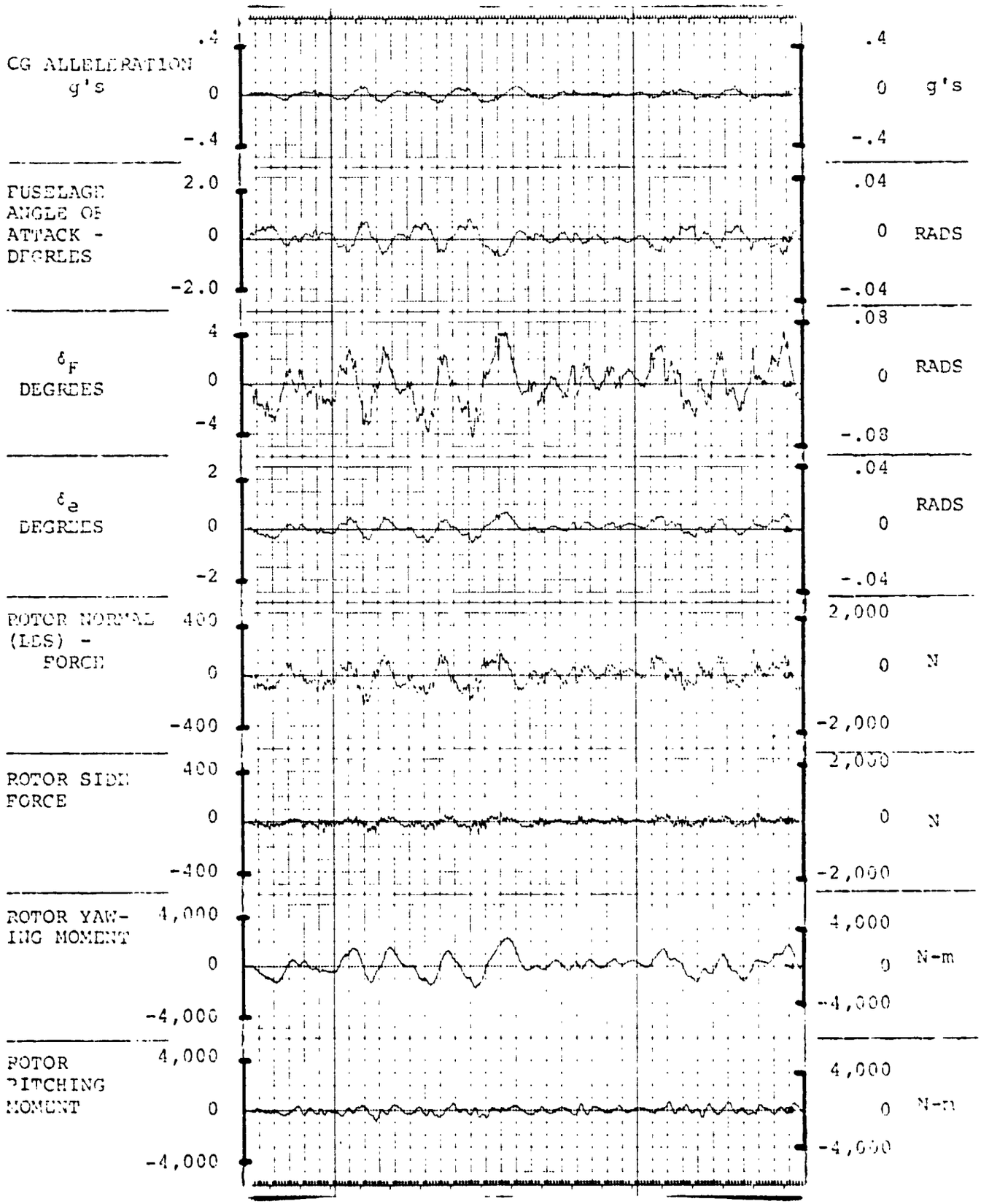

FIGURE 4.4.2.0.0.2. RESPONSES FOR GAIN F = 4.0, GAIN E = .6

FLIGHT CONDITION: 240 KNOTS, 5,000 FEET, (1,524m), AFT CG

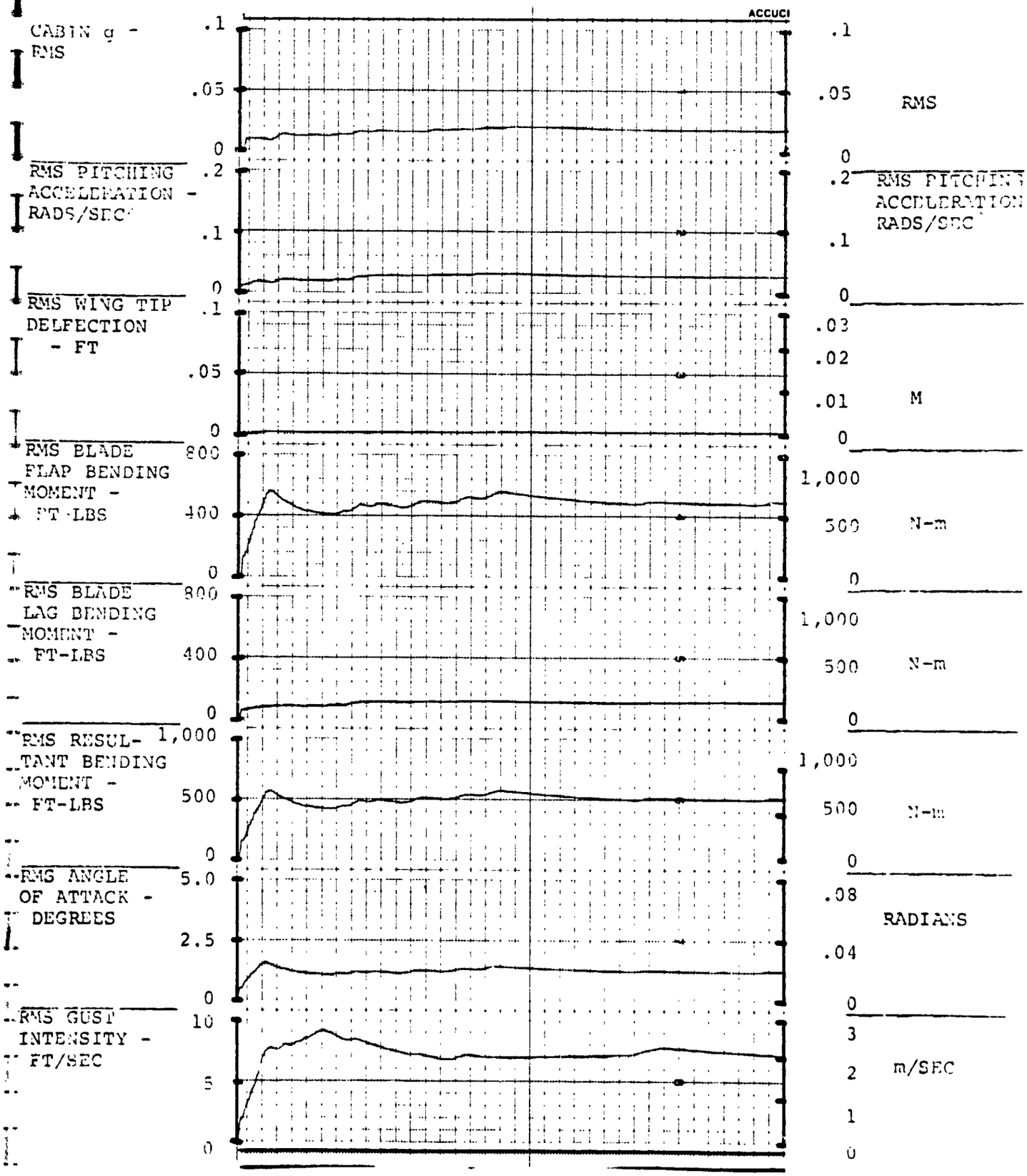

FIGURE 5.4.2.0.0.2. RESPONSES FOR GAIN F = 4.0, GAIN E = .6

FLIGHT CONDITION: 240 KNOTS, 10,000 FEET, (3,049m), AFT CG

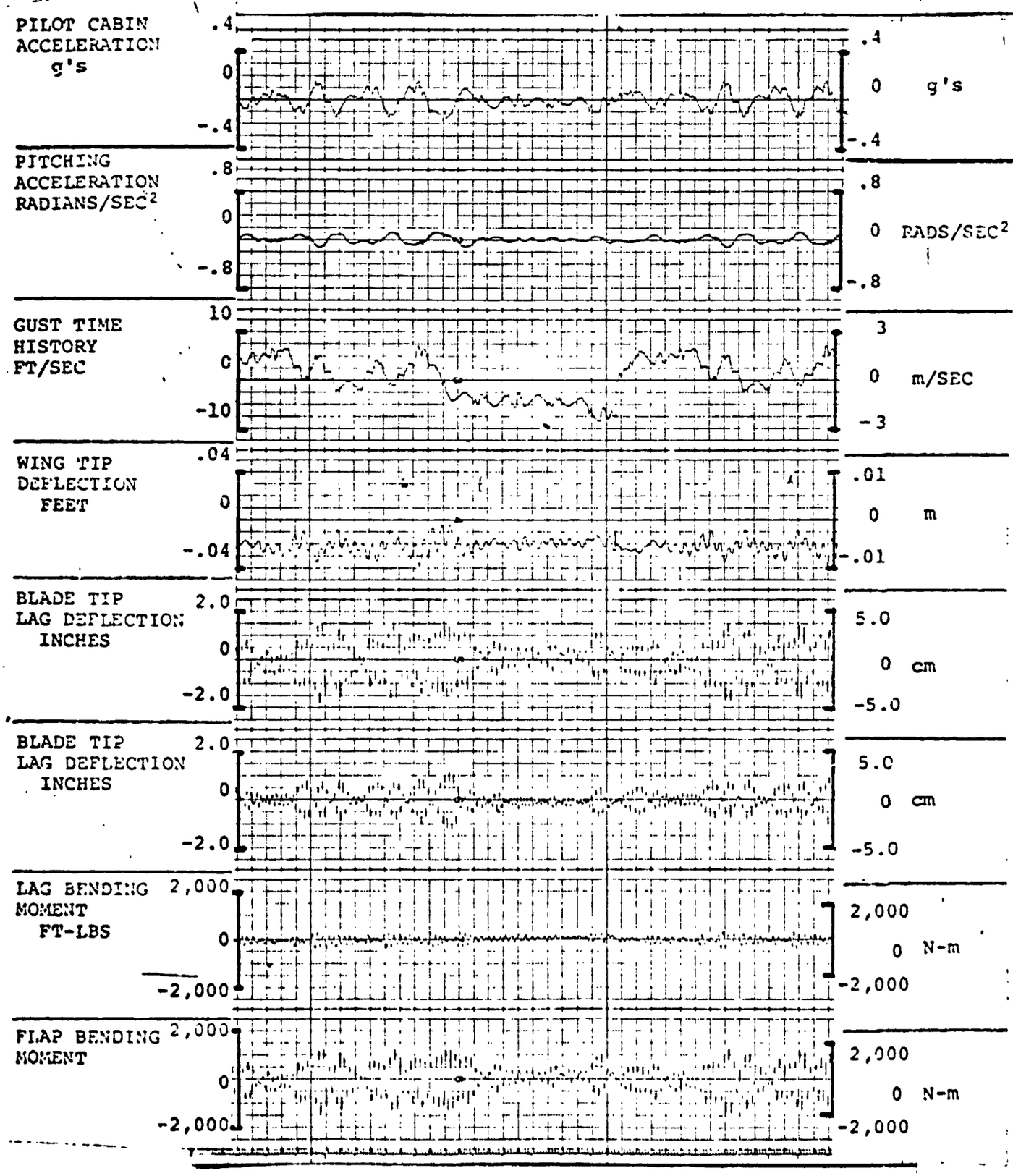

FIGURE 3.5.2.0.0.1. RESPONSES FOR GAIN F = 0, GAIN E = 0

FLIGHT CONDITION: 240 KNOTS, 10,000 FEET, (3,049m), AFT CG

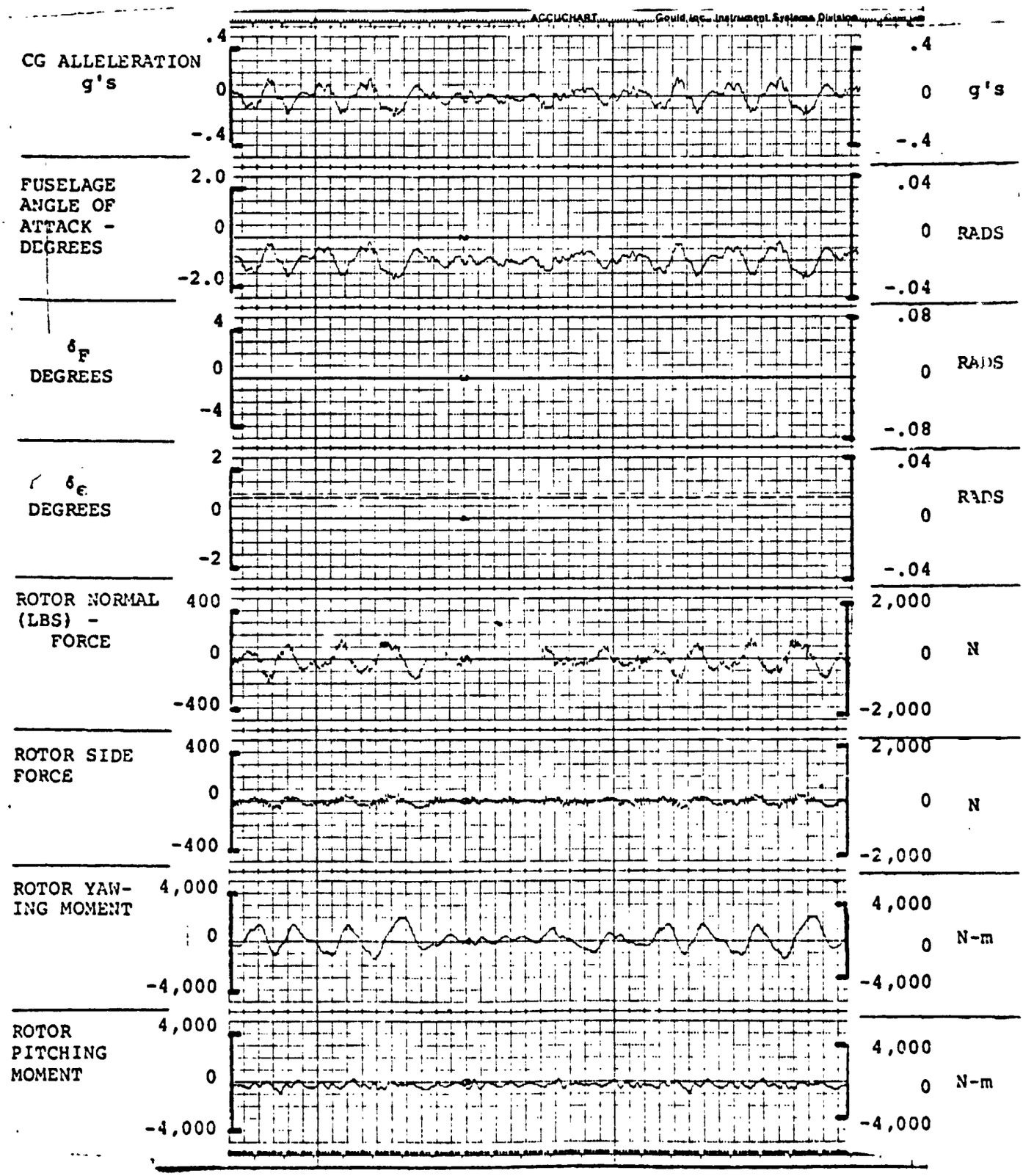

FIGURE 4.5.2.0.0.1. RESPONSES FOR GAIN F = 0, GAIN E = 0

FLIGHT CONDITION: 240 KNOTS, 10,000 FEET, (3,049m), AFT CG

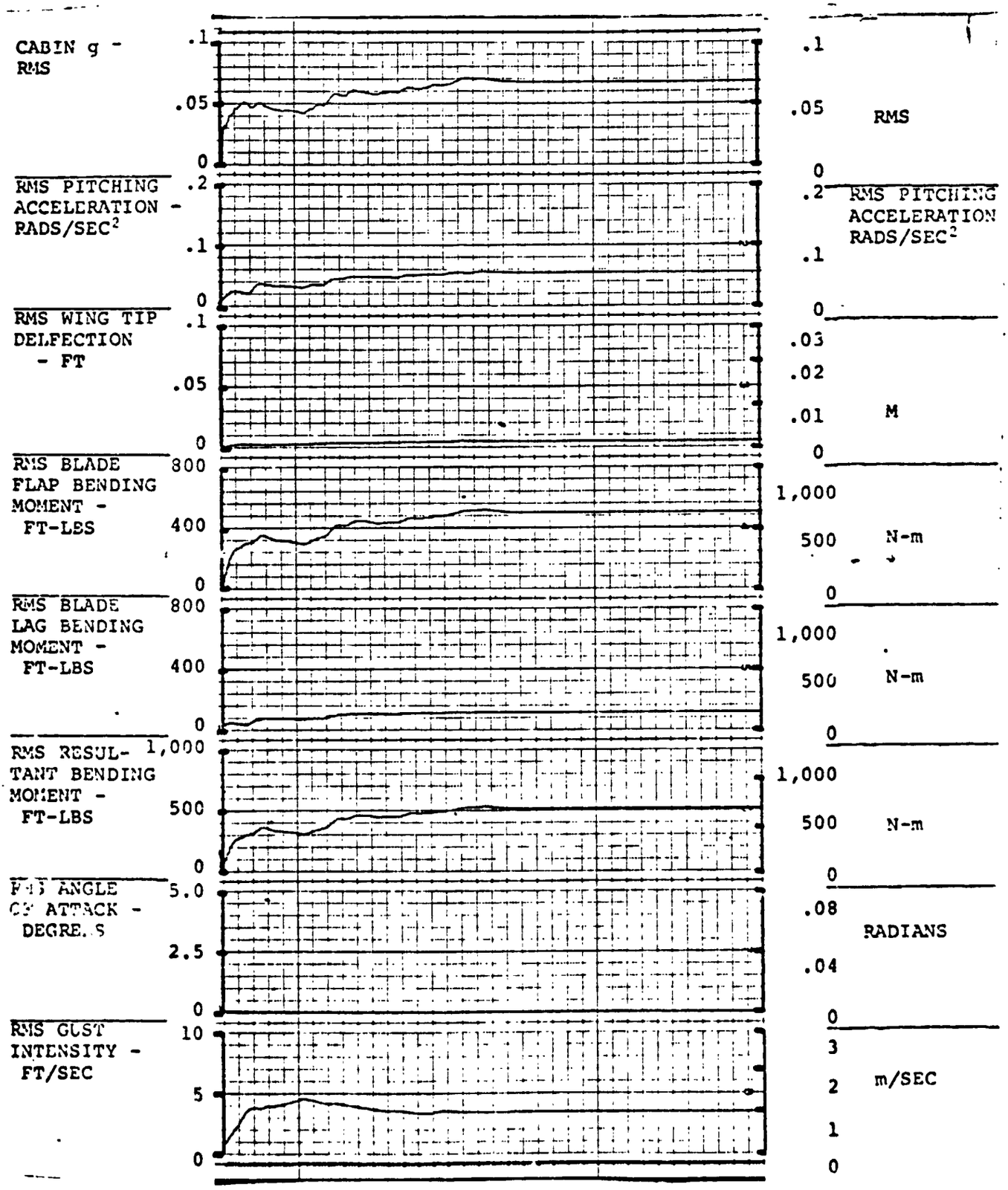

FIGURE 5.5.2.0.0.1.RESPONSES FOR GAIN F = 0, GAIN E = 0

FLIGHT CONDITION: 240 KNOTS, 10,000 FEET, (3,049m), AFT CG

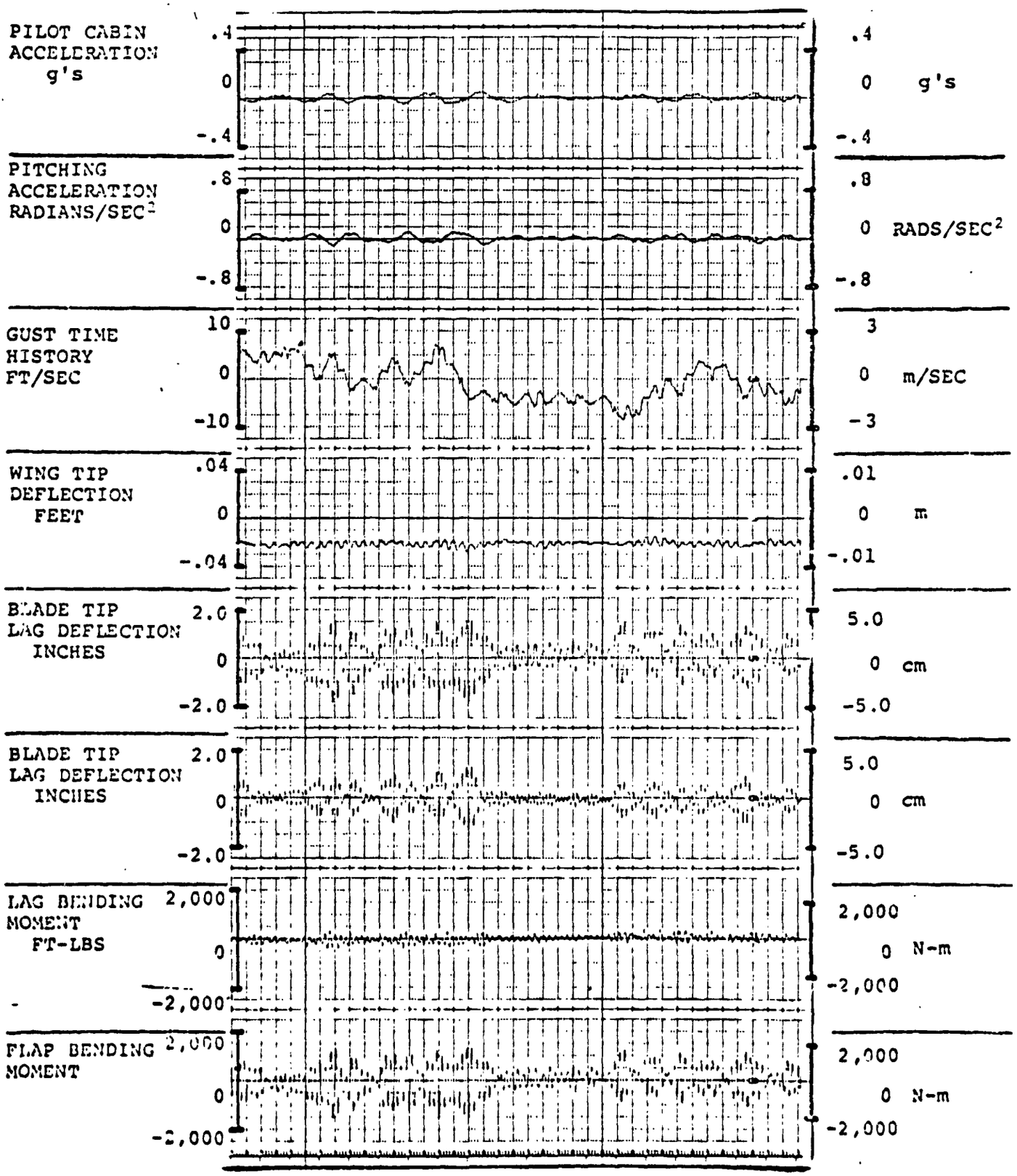

FIGURE 3.5.2.0.0.2. RESPONSES FOR GAIN F = 4.0, GAIN E = .6

FLIGHT CONDITION: 240 KNOTS, 10,000 FEET, (3,049m), AFT CG

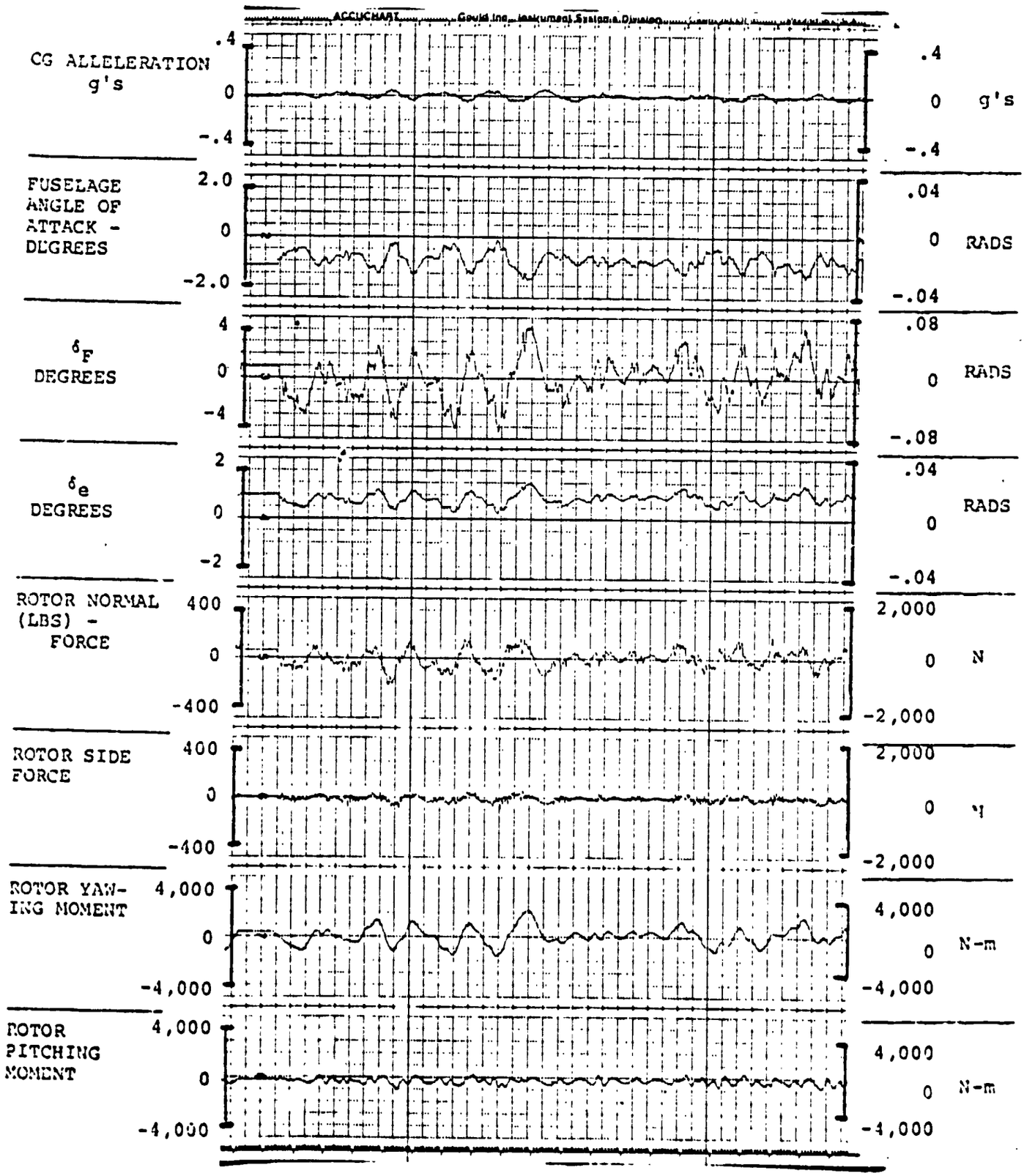

FIGURE 4.5.2.0.0.2. RESPONSES FOR GAIN F = 4.0, GAIN E = .6

FLIGHT CONDITION: 240 KNOTS, 10,000 FEET, (3,049m), AFT CG

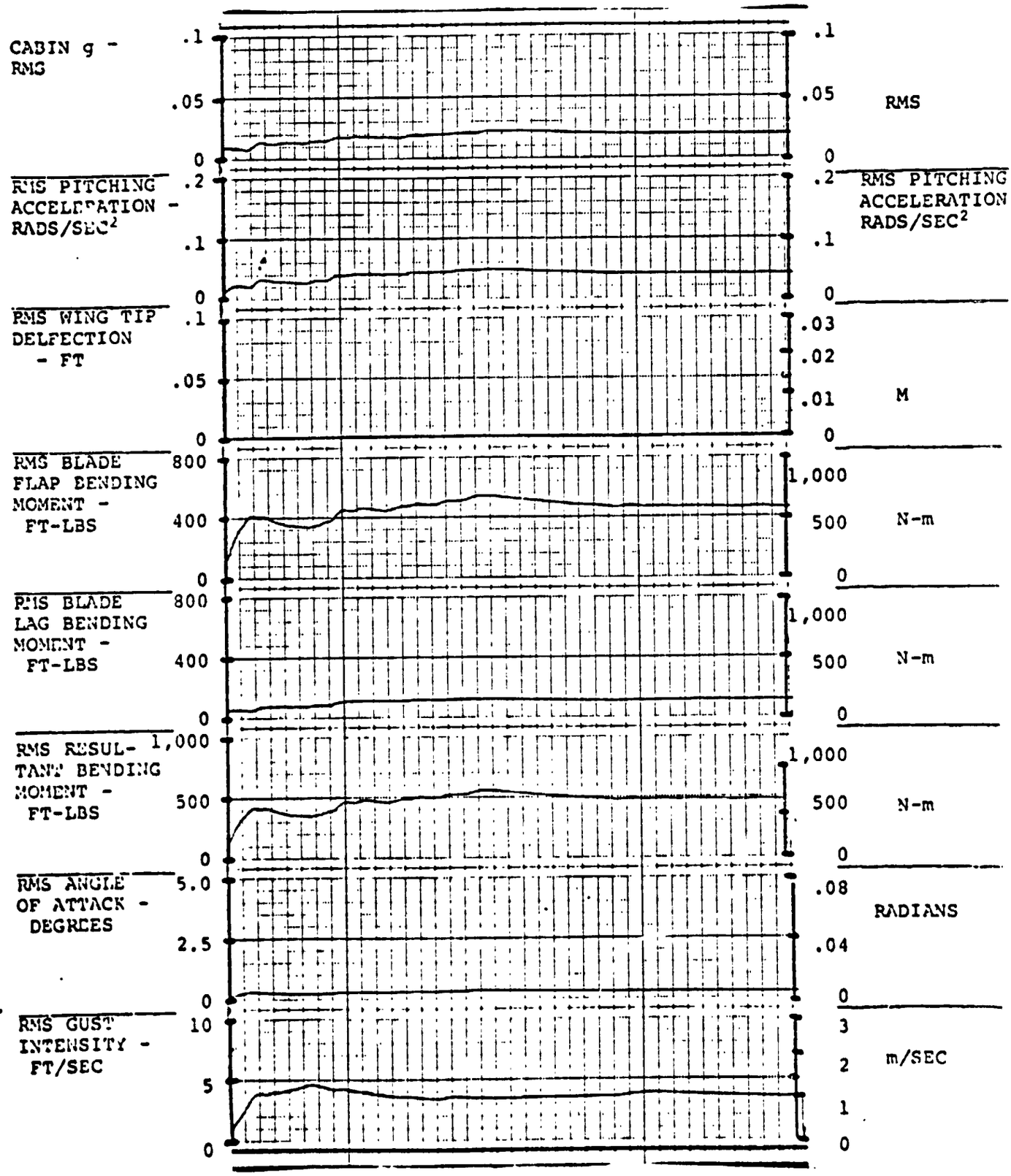

FIGURE 5.5.2.0.0.2. RESPONSES FOR GAIN F = 4.0, GAIN E = .6

FLIGHT CONDITION: 240 KNOTS, 15,000 FEET, (4,573m), AFT CG

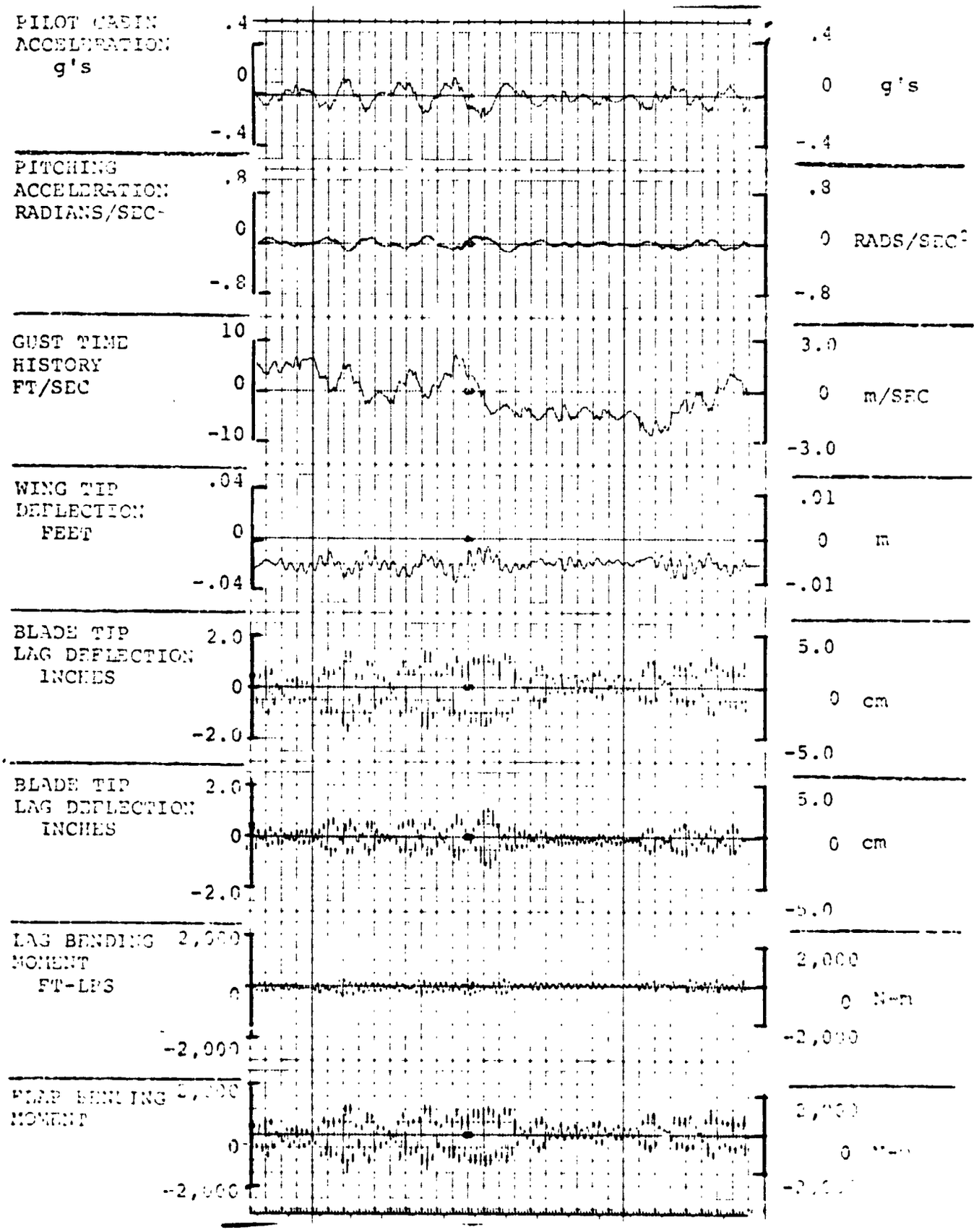

FIGURE 3.6.2.0.0.1. RESPONSES FOR GAIN F = 0, GAIN E = 0

FLIGHT CONDITION: 240 KNOTS, 15,000 FEET, (4,573m), AFT CG

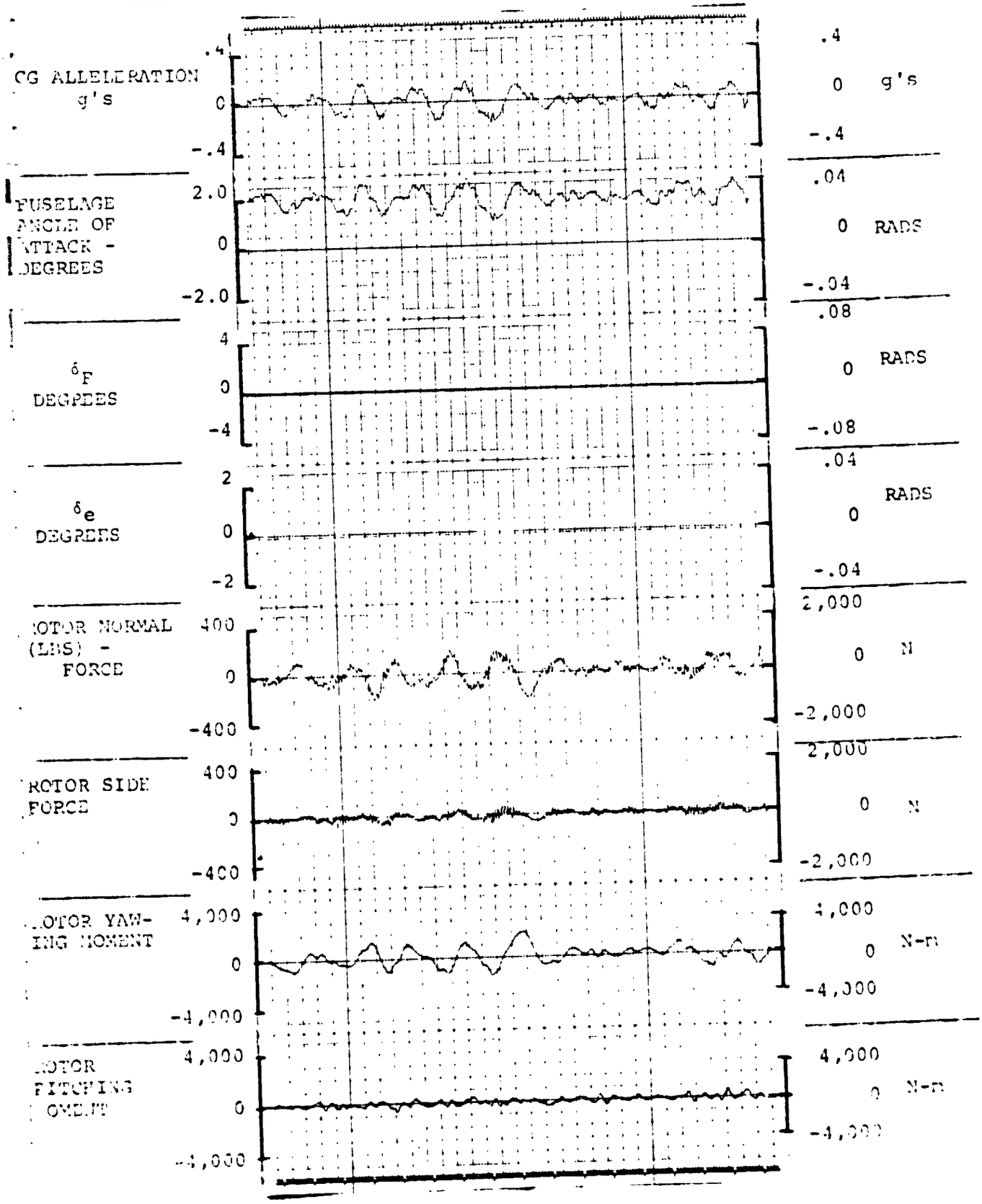

FIGURE 4.6.2.0.0.1. RESPONSES FOR GAIN F = 0, GAIN E = 0

FLIGHT CONDITION: 240 KNOTS, 15,000 FEET, (4,573m), AFT CG

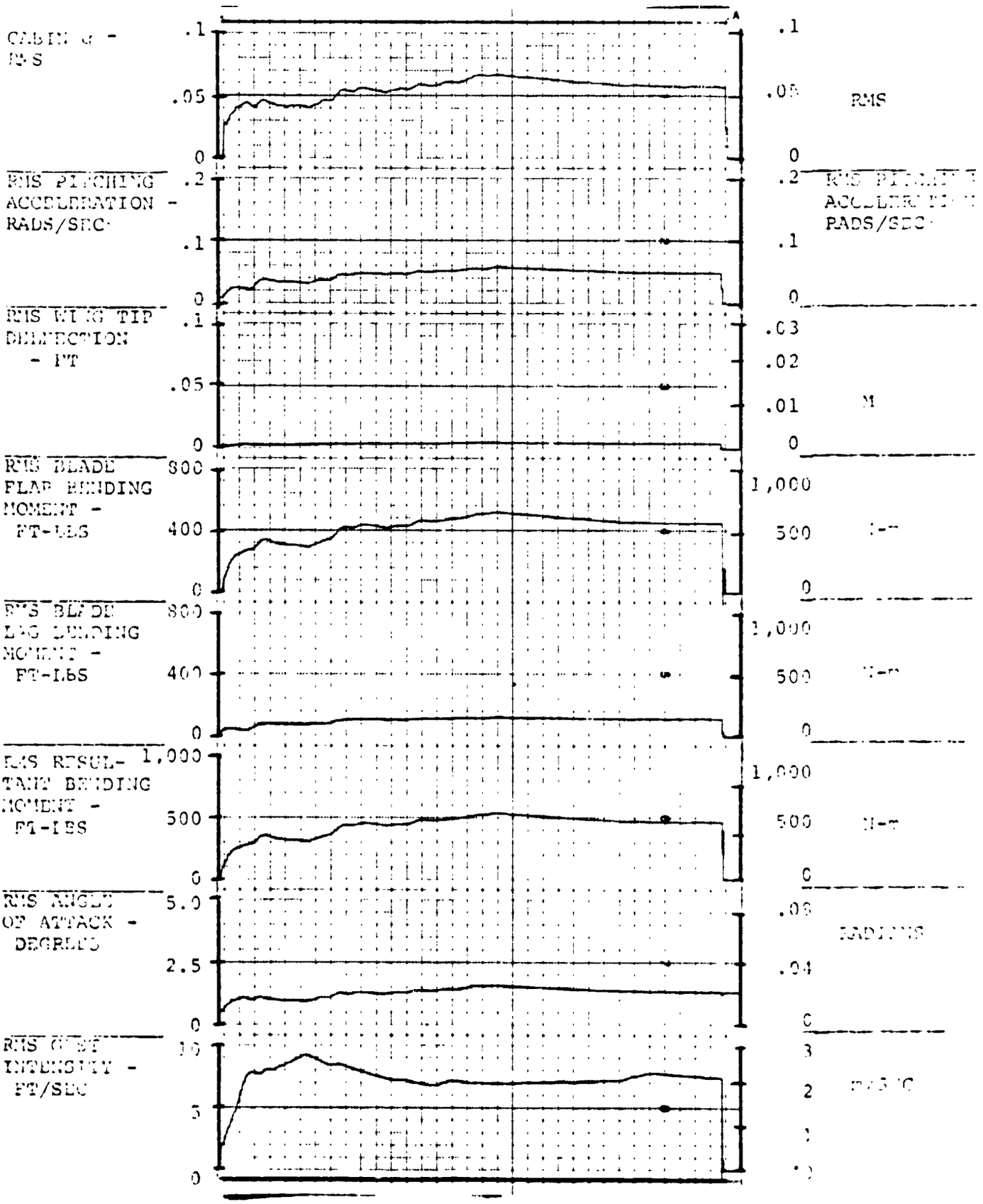

FIGURE 5.6.2.0.0.1. RESPONSES FOR GAIN F = 0, GAIN E = 0

ORIGINAL PAGE IS
OF POOR QUALITY

FLIGHT CONDITION: 240 KNOTS, 15,000 FEET, (4,573m), AFT CG

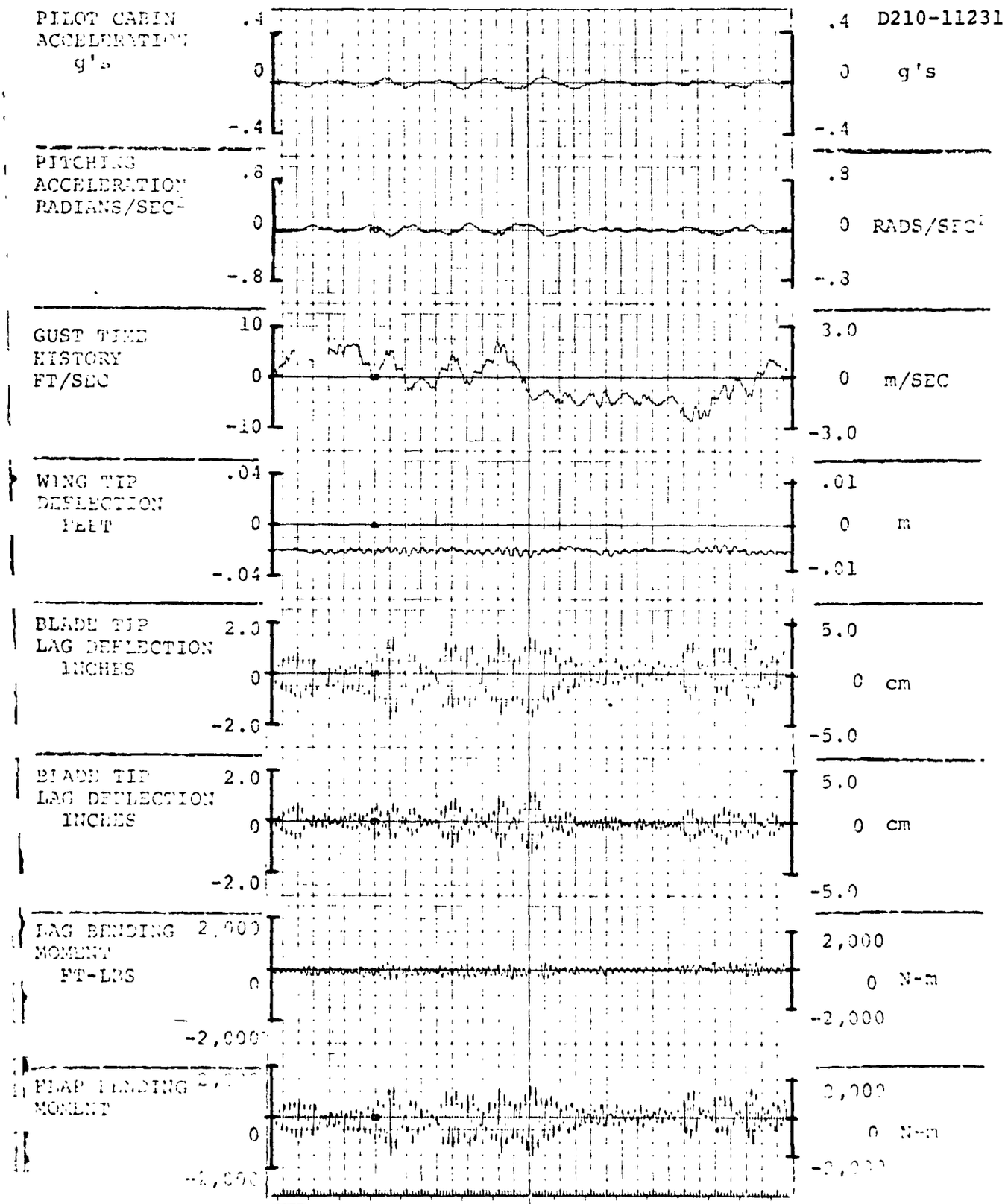

FIGURE 3.6.2.0.0.2. RESPONSES FOR GAIN F = 4.0, GAIN E = .6

FLIGHT CONDITION: 240 KNOTS, 15,000 FEET, (4,573m), AFT CG

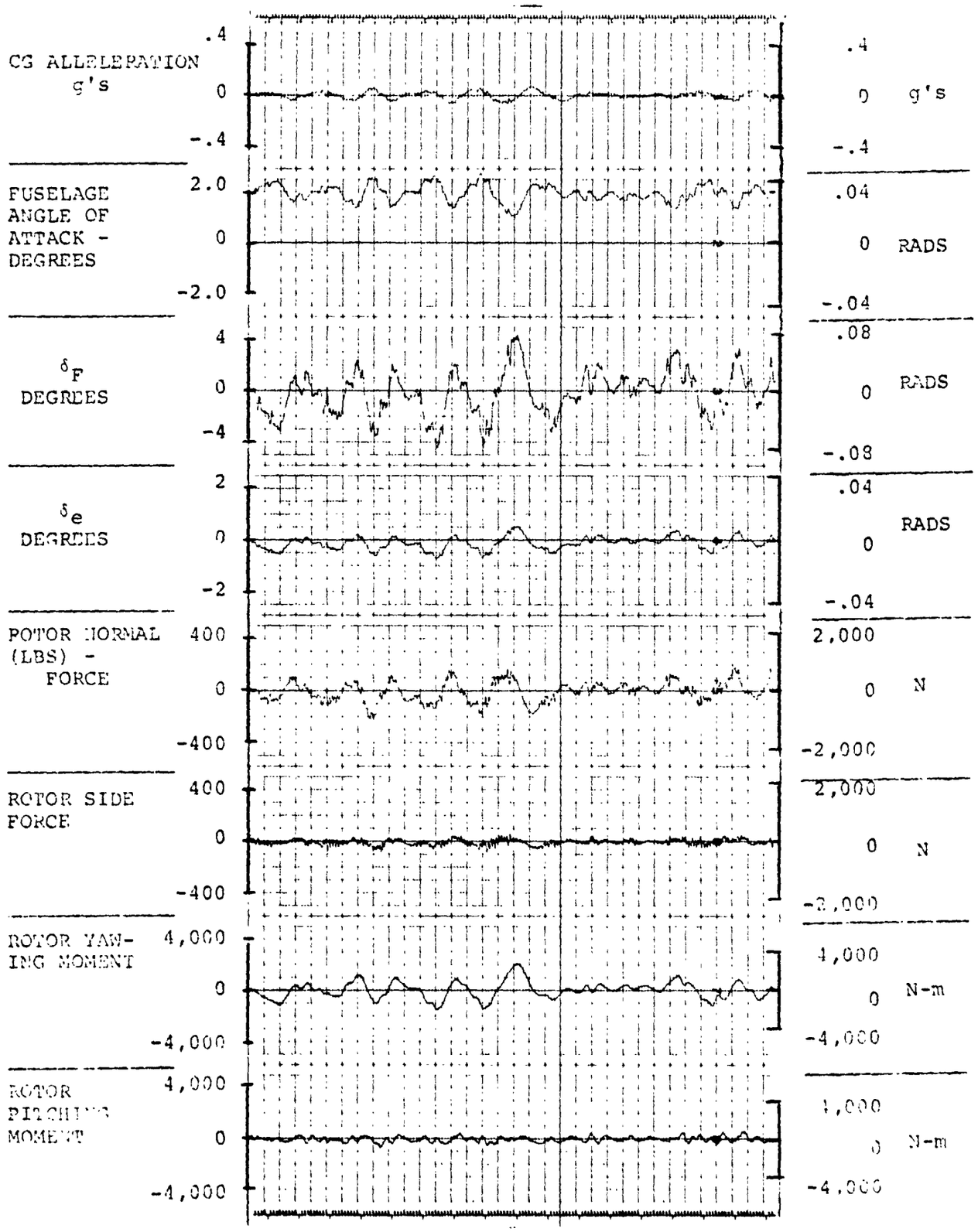

FIGURE 4.6.2.0.0.2. RESPONSES FOR GAIN F = 4.0, GAIN E = .6

FLIGHT CONDITION: 240 KNOTS, 15,000 FEET, (4,573m), AFT CG

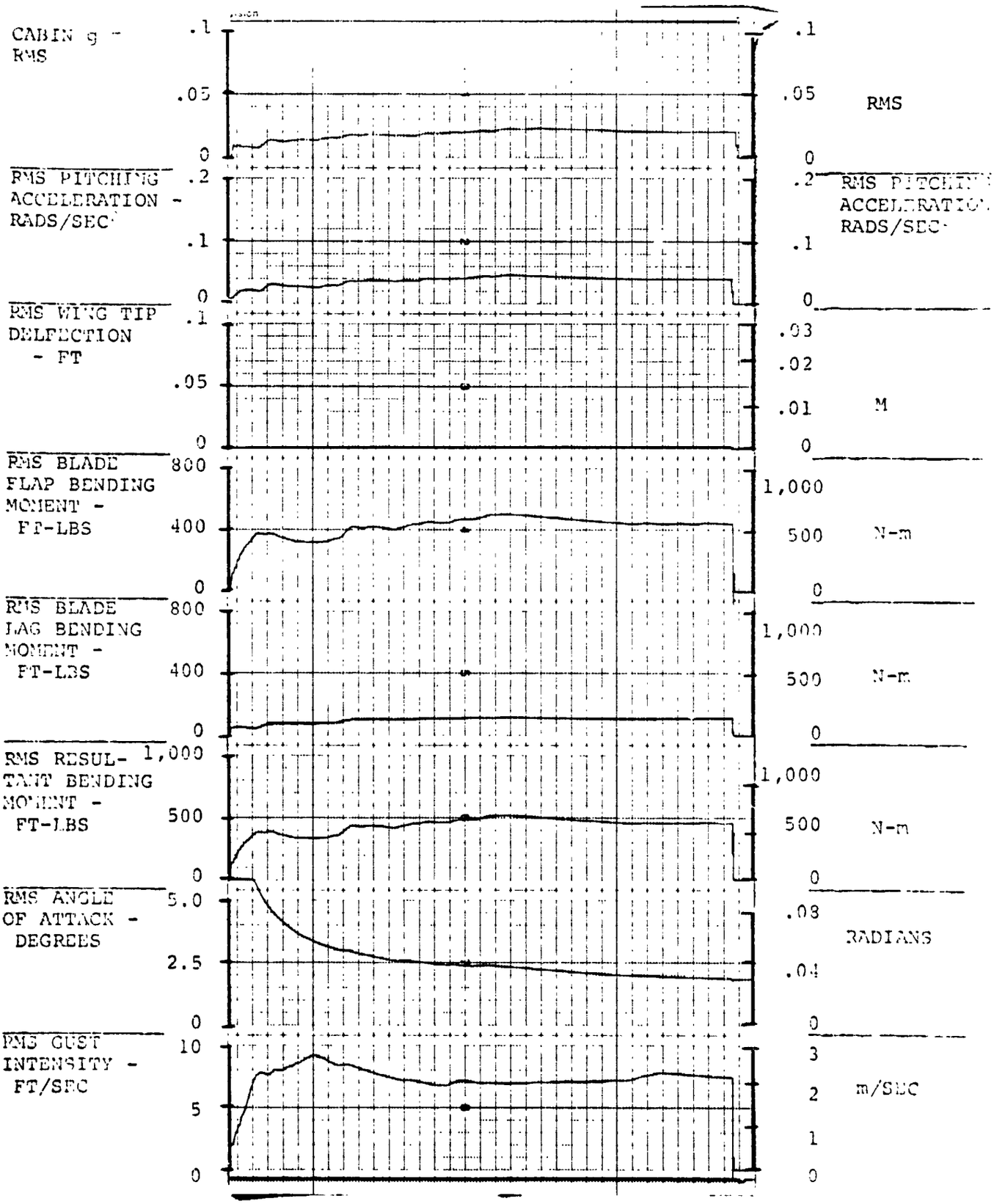

FIGURE 5.6.2.0.0.2. RESPONSES FOR GAIN F = 4.0, GAIN E = .6

ORIGINAL PAGE IS OF POOR QUALITY

FLIGHT CONDITION: 240 KNOTS, 15,000 FEET, (4,573m), AFT CG

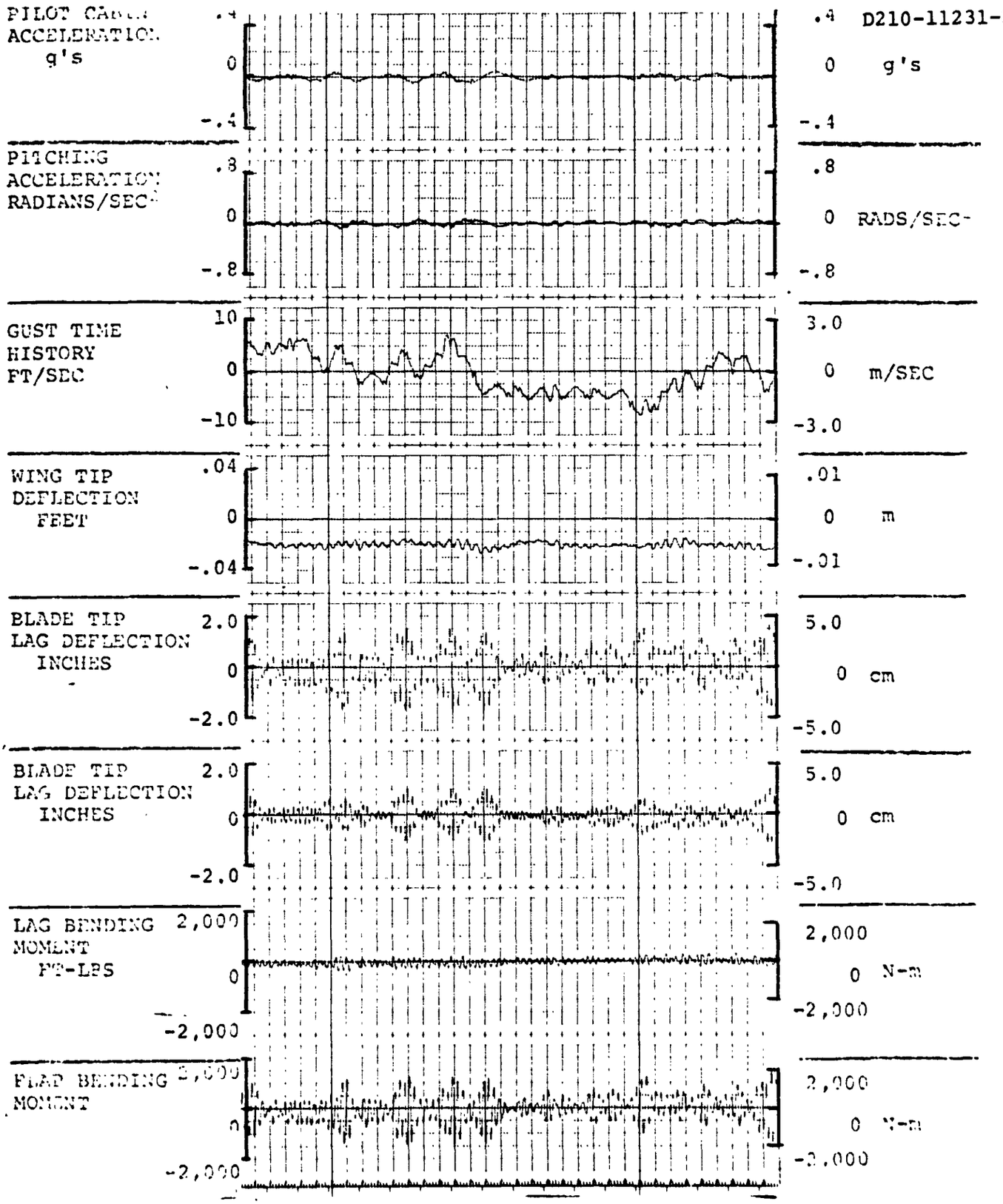

FIGURE 3.6.2.0.0.3. RESPONSES FOR GAIN F = 4.0, GAIN E = .7

FLIGHT CONDITION: 240 KNOTS, 15,000 FEET, (4,573m), AFT CG

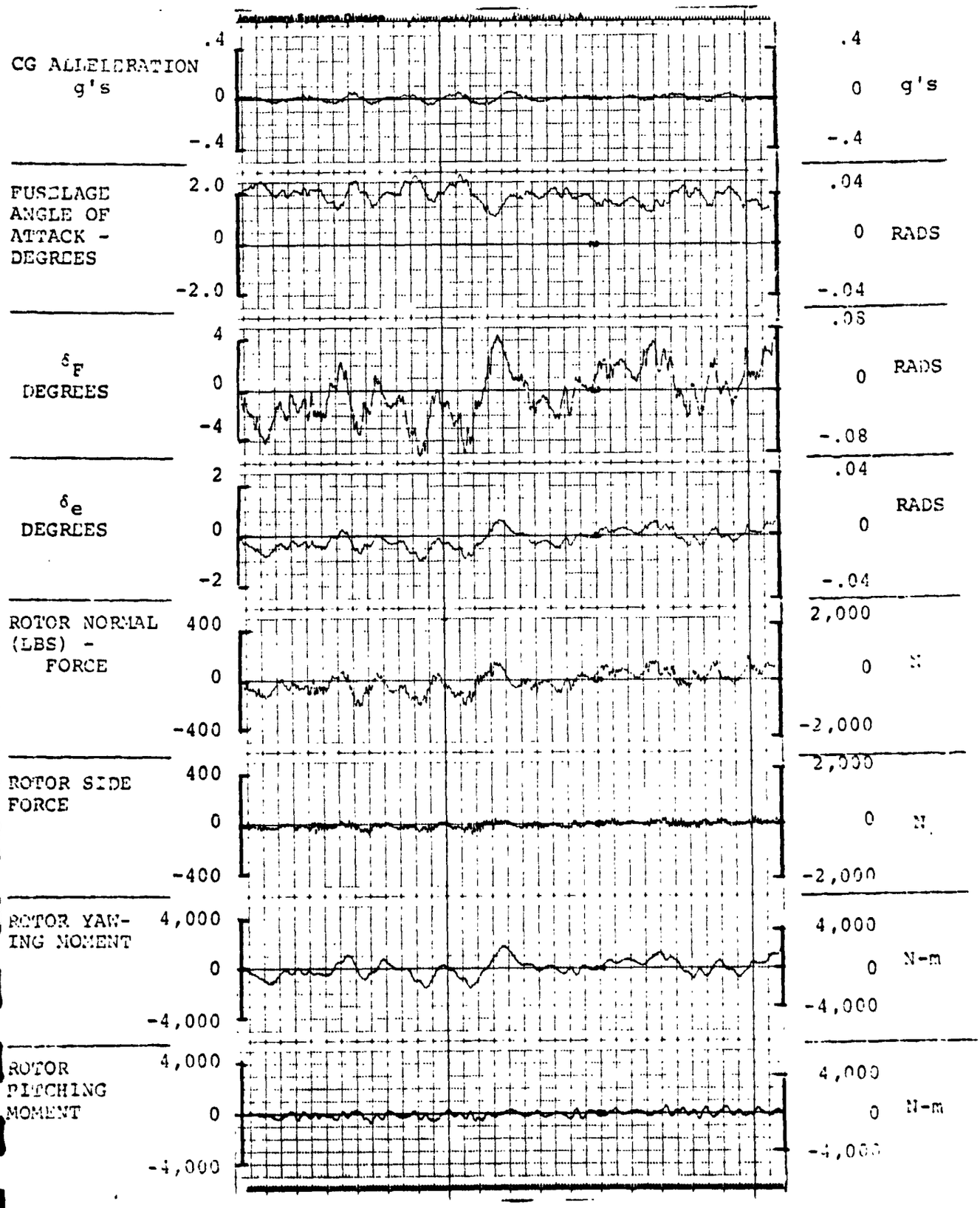

FIGURE 4.6.2.0.0.3. RESPONSES FOR GAIN F = 4.0, GAIN E = .7

FLIGHT CONDITION: 240 KNOTS, 15,000 FEET, (4,573m), AFT CG

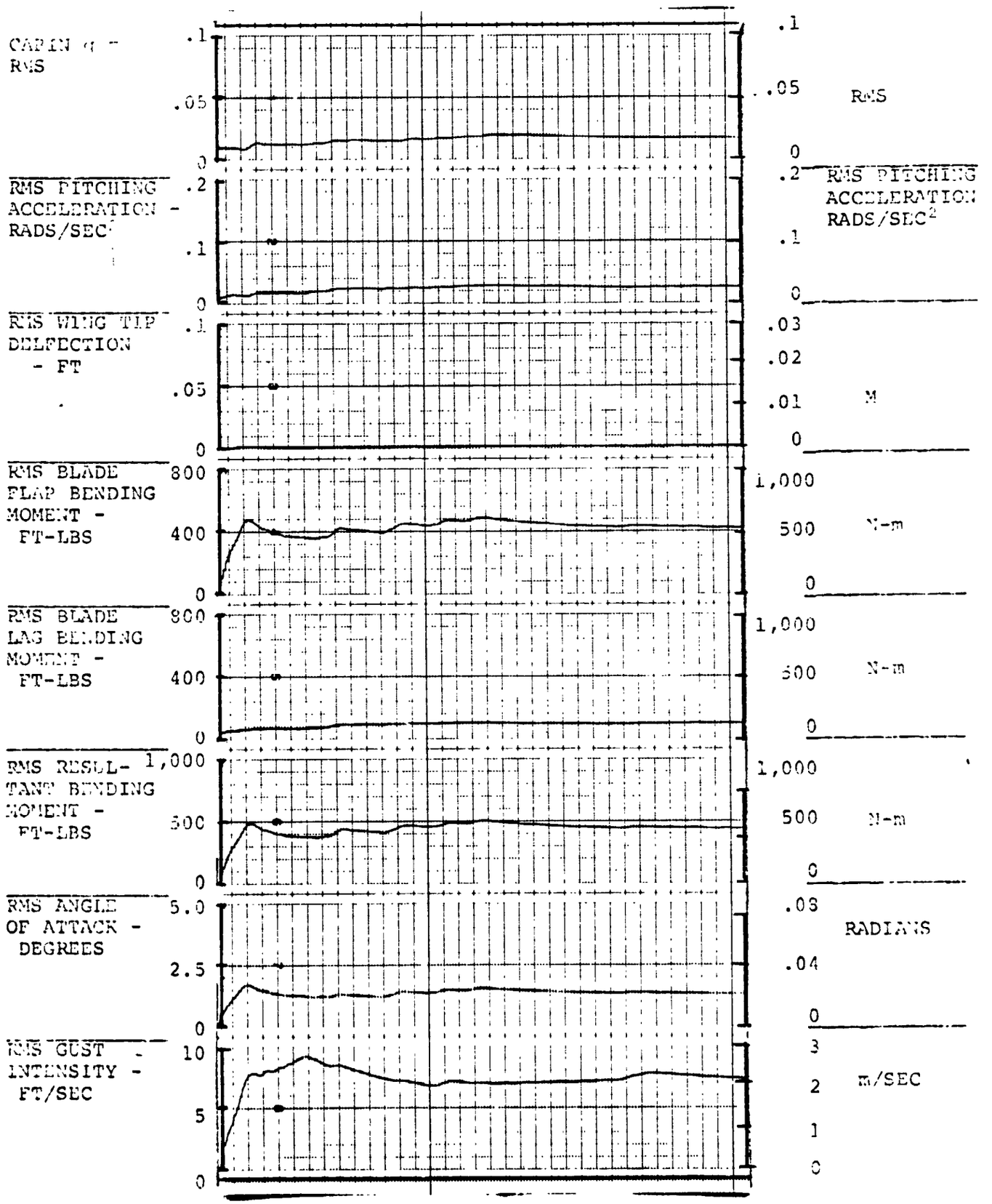

FIGURE 5.6.2.0.0.3. RESPONSES FOR GAIN F = 4.0, GAIN E = .7

ORIGINAL PAGE IS
OF POOR QUALITY

K+E LOGARITHMIC • 2 X 3 CYCLES
KEUFFEL & ESSER CO. MADE IN U.S.A.
46 7323

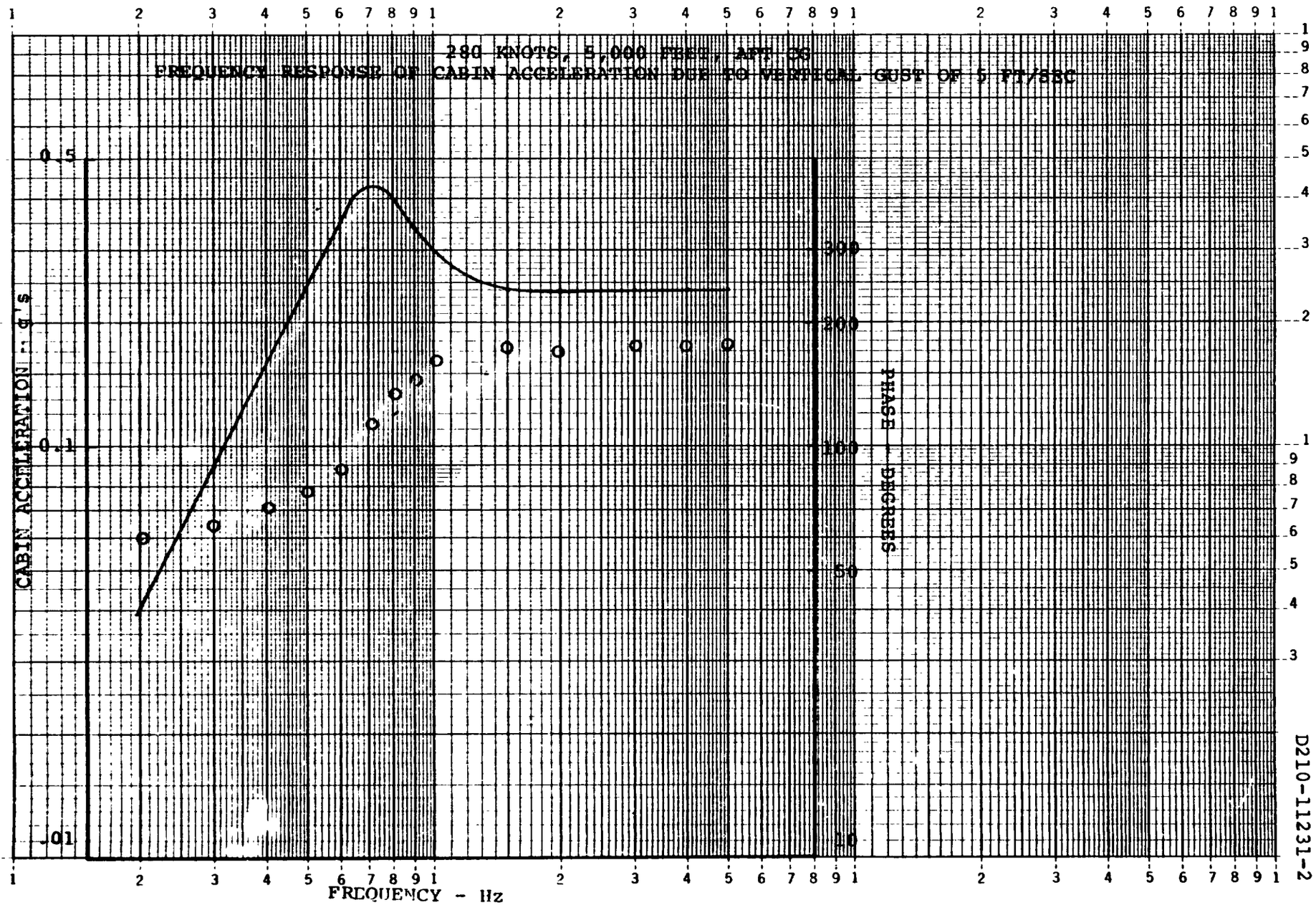

FIGURE 1.7.2.1.1.0

AIV.169
ORIGINAL PAGE IS
OF POOR QUALITY
D210-11231-2

K•Σ LOGARITHMIC • 2 X 3 CYCLES
KEUFFEL & ESSER CO MADE IN U.S.A.

46 7323

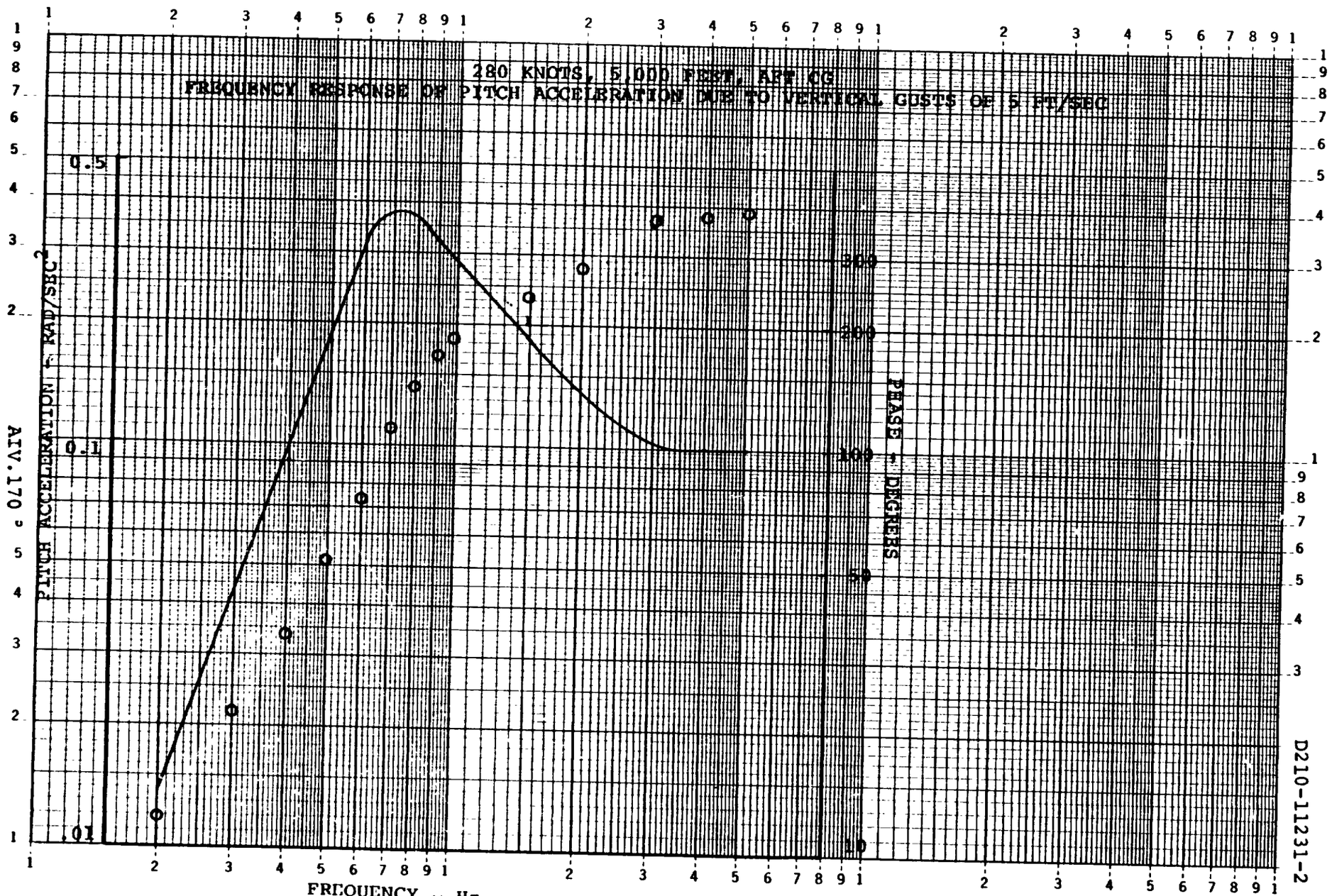

FIGURE 1.7.2.2.1.0

K·E LOGARITHMIC • 2 X 3 CYCLES
KEUFFEL & ESSER CO. MADE IN U.S.A.
46 7323

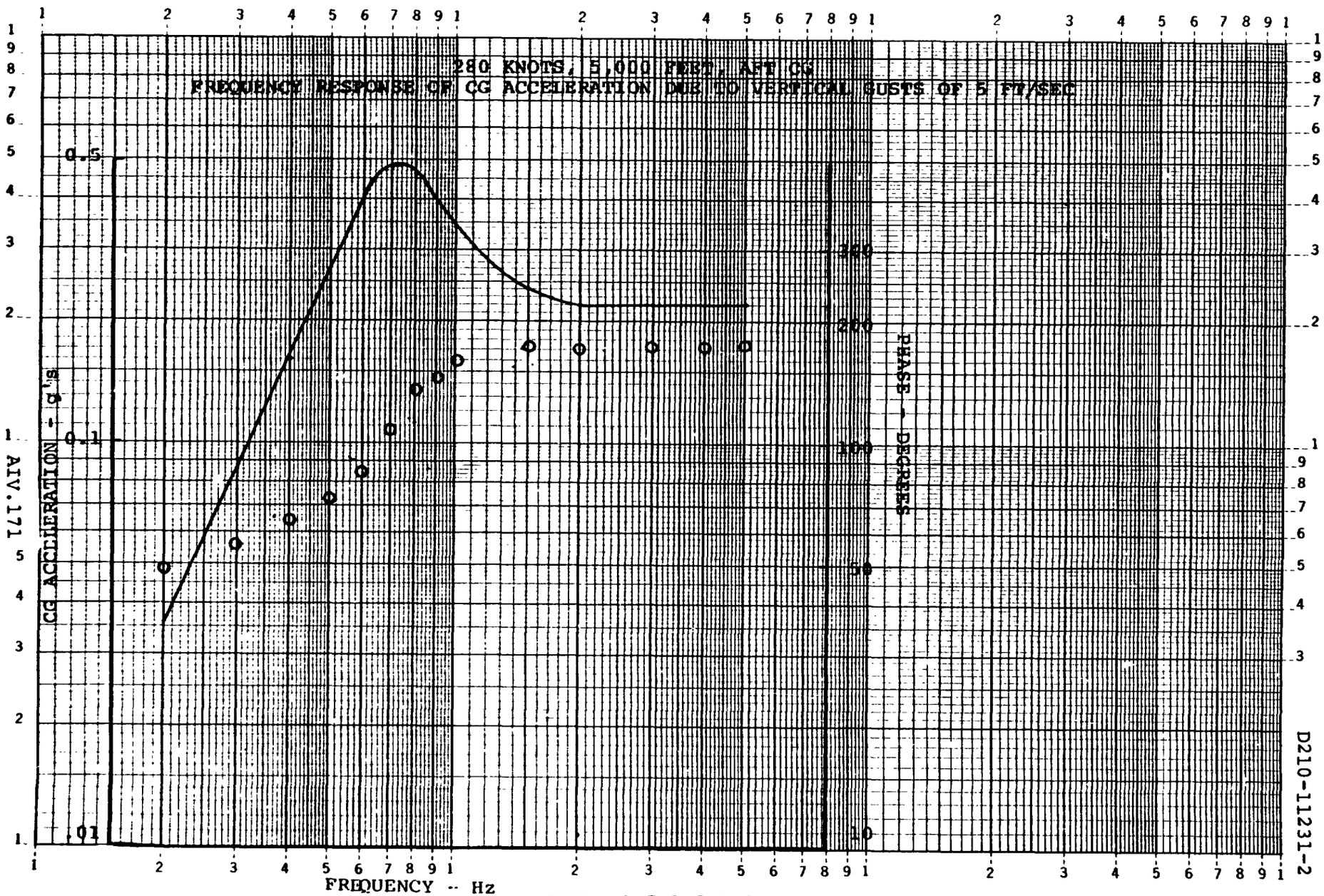

FIGURE 1.7.2.3.1.0

K·E LOGARITHMIC • 2 X 3 CYCLES
KEUFFEL & ESSER CO MADE IN U.S.A.

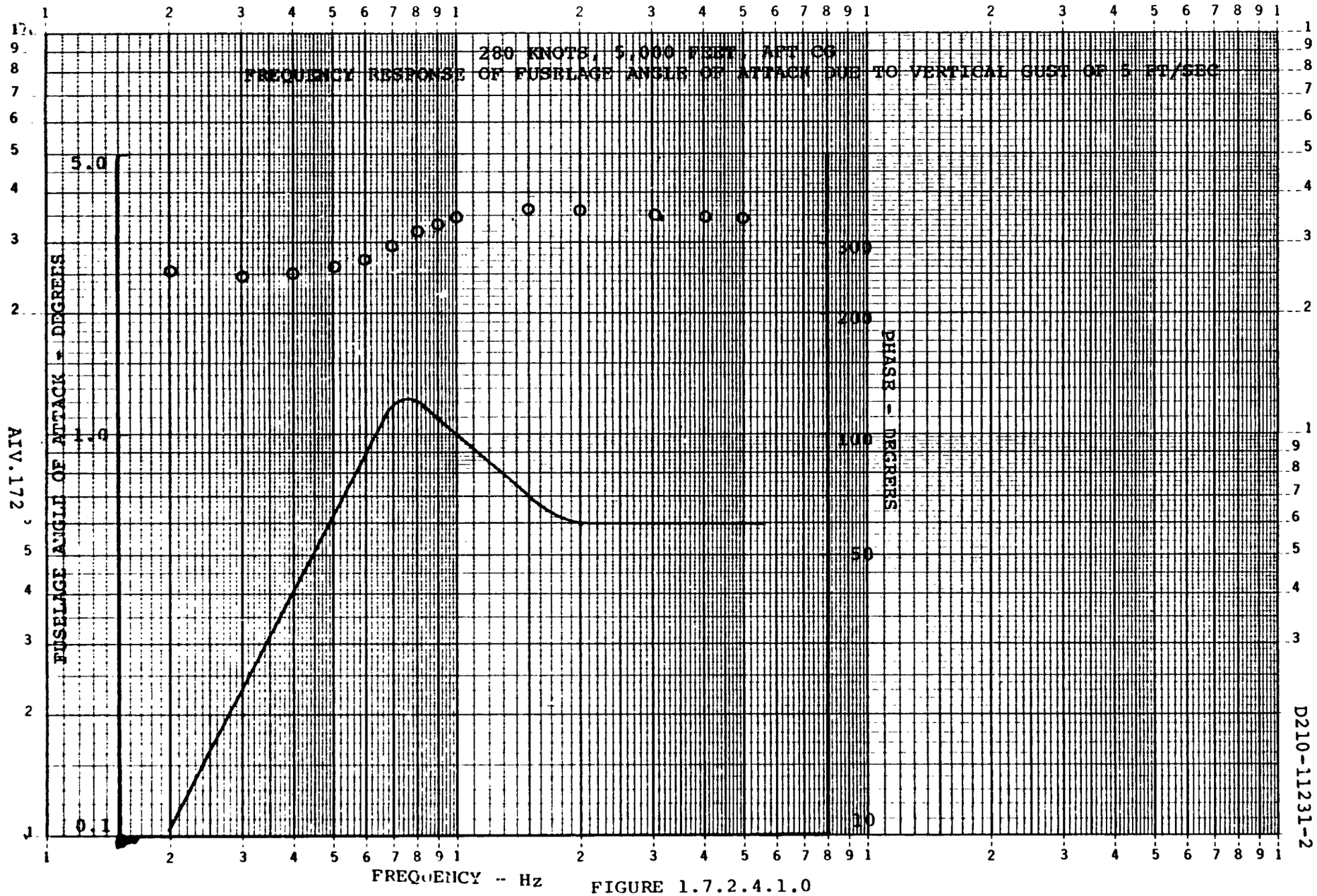

FIGURE 1.7.2.4.1.0

K•E LOGARITHMIC 2 X 3 CYCLES KEUFFEL & ESSER CO. MADE IN U.S.A.
46 7323

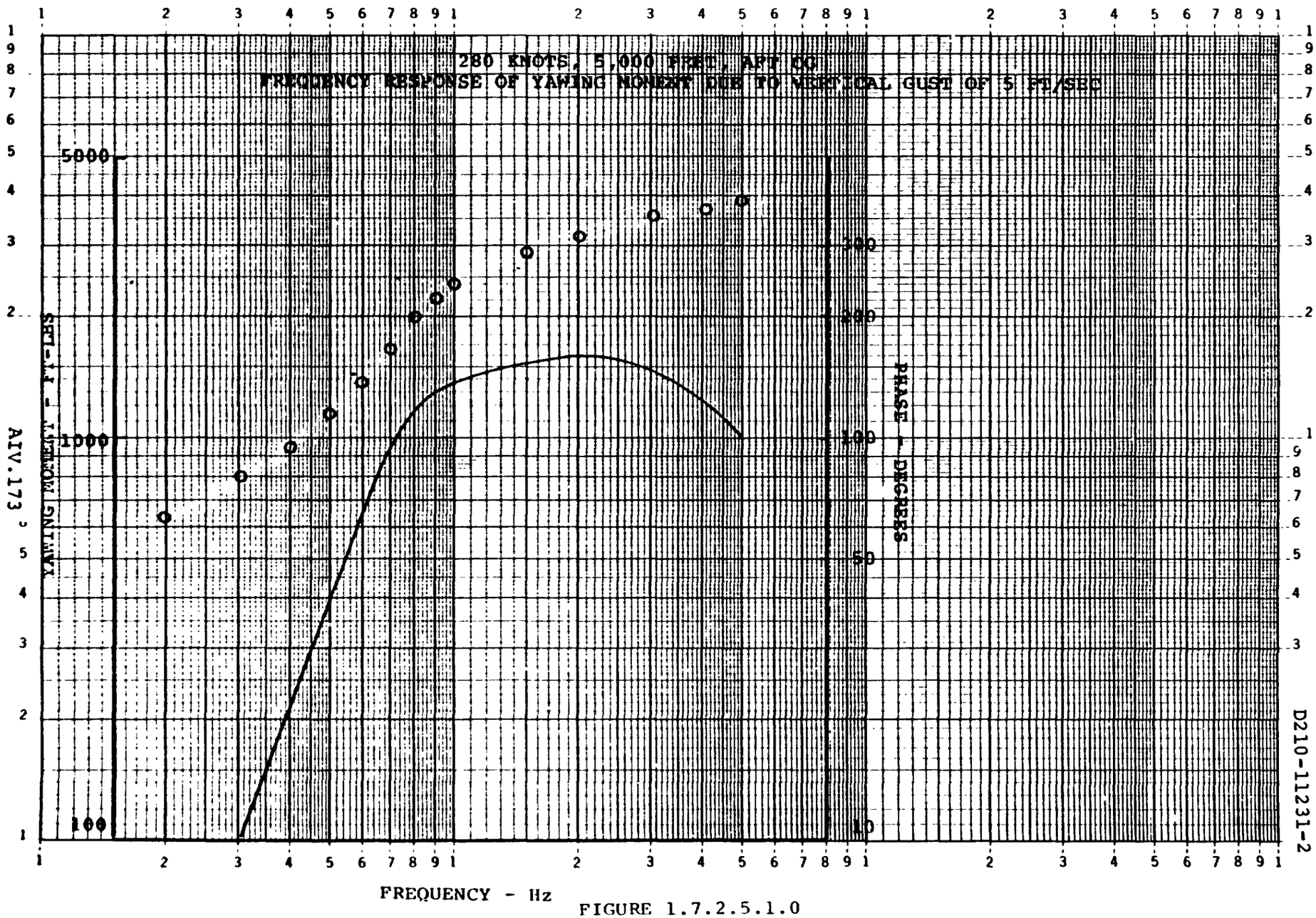

FIGURE 1.7.2.5.1.0

K•E LOGARITHMIC • 2 X 3 CYCLES
KEUFFEL & ESSER CO MADE IN U.S.A.

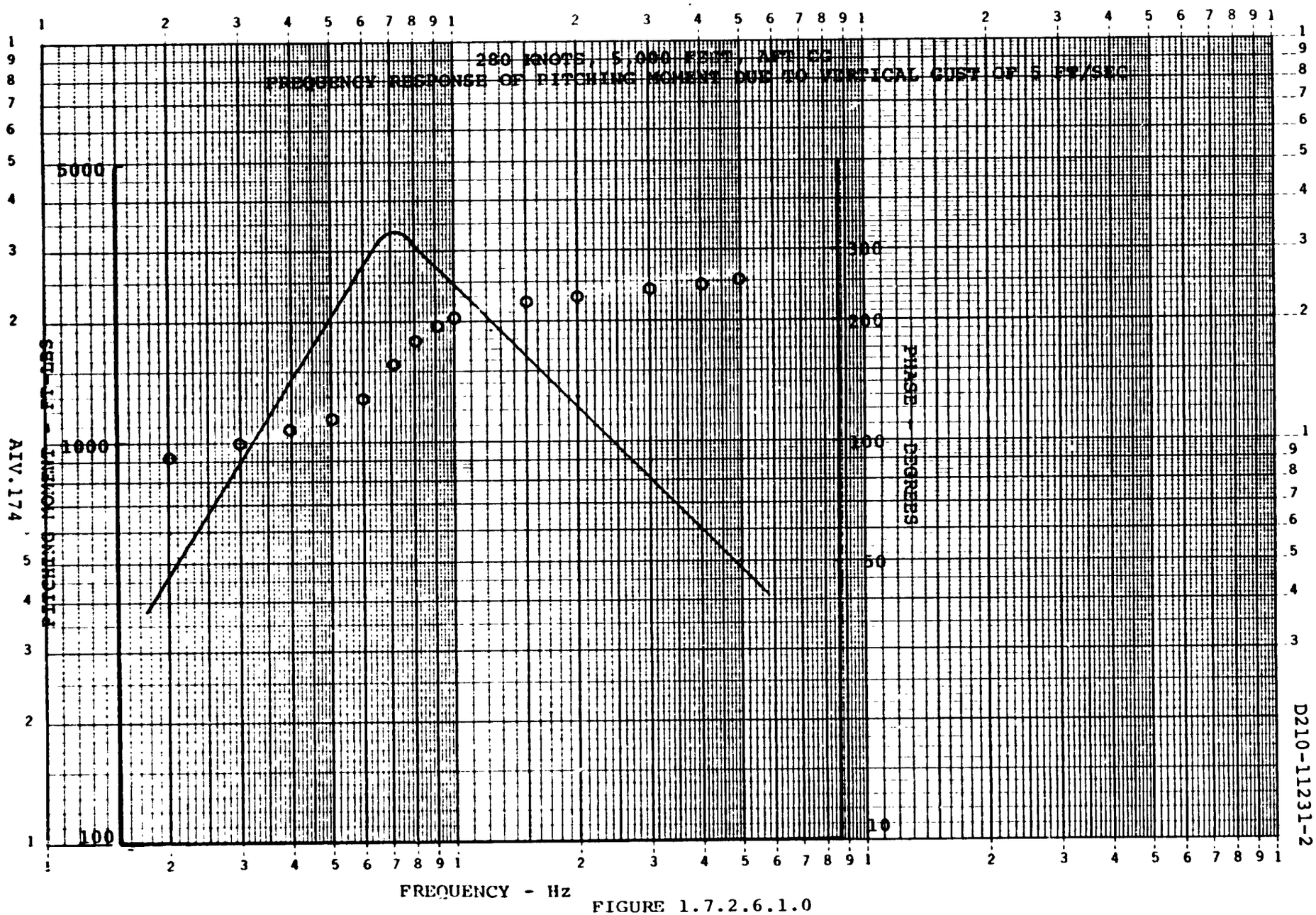

FIGURE 1.7.2.6.1.0

K•E LOGARITHMIC • 2 X 3 CYCLES
KEUFFEL & ESSER CO. MADE IN U.S.A.
46 7323

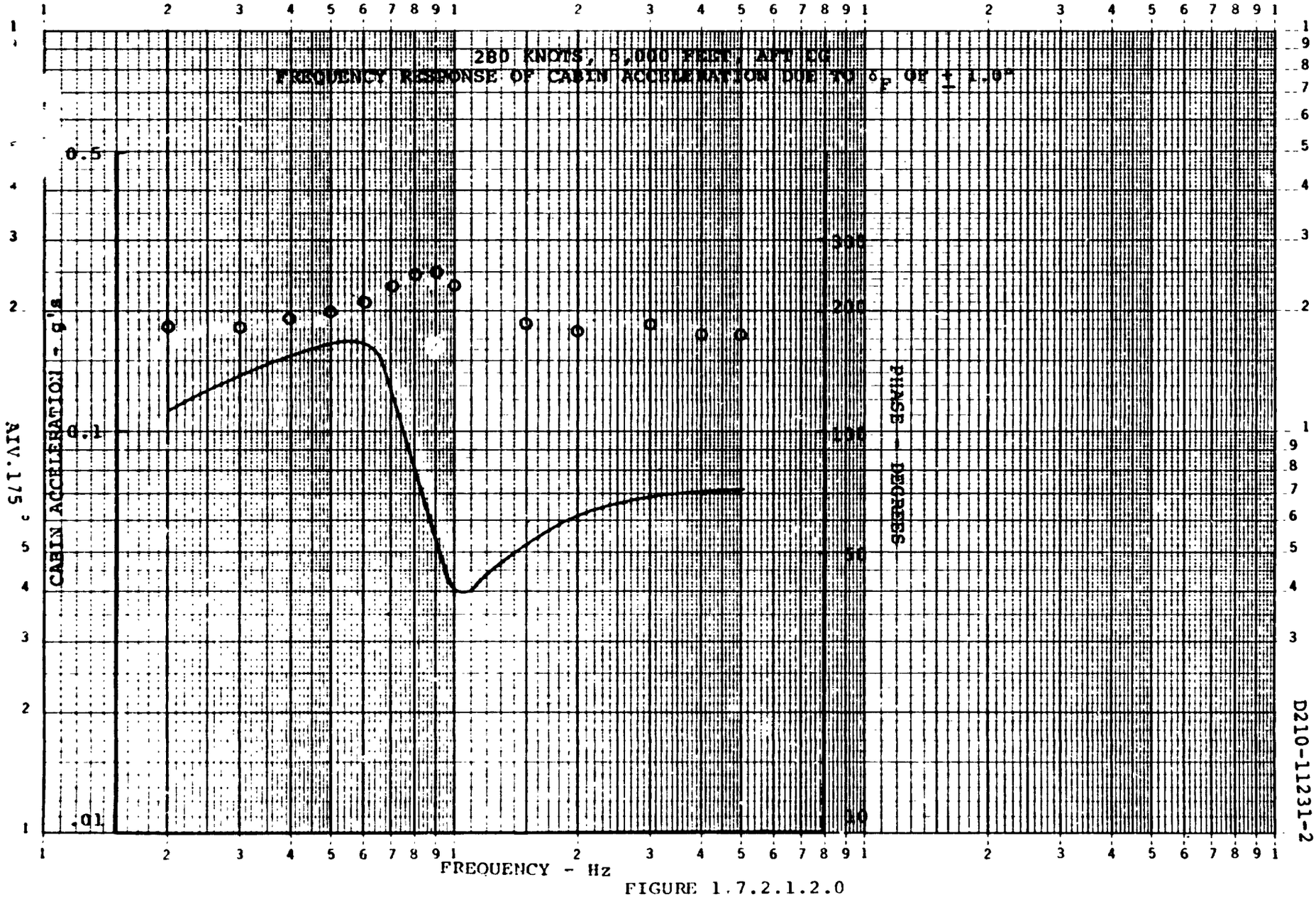

FIGURE 1.7.2.1.2.0

K·E LOGARITHMIC • 2 X 3 CYCLES
KEUFFEL & ESSER CO. MADE IN U.S.A.

46 7323

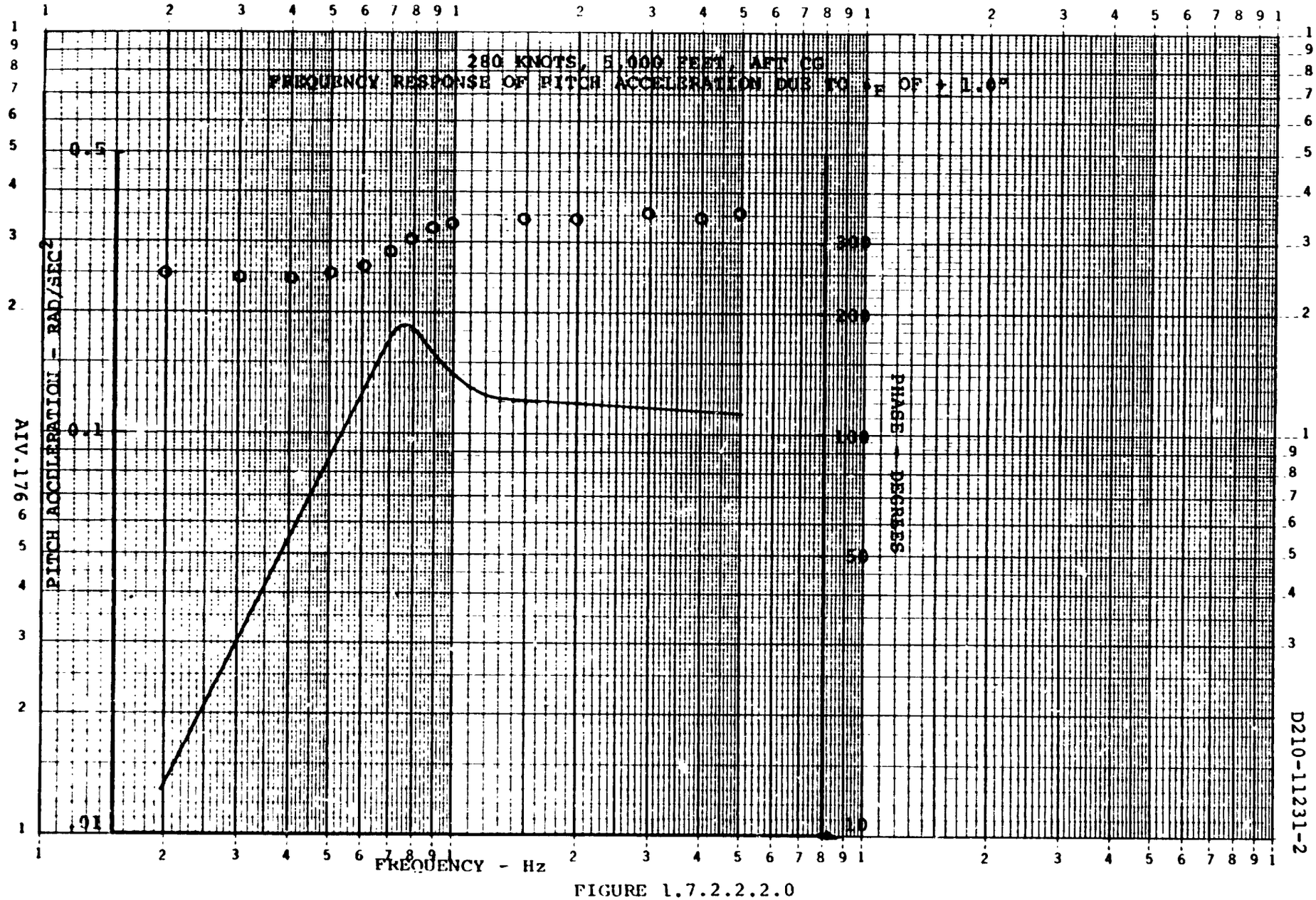

FIGURE 1.7.2.2.2.0

AIV.176

D210-11231-2

K•E LOGARITHMIC • 2 X 3 CYCLES
KEUFFEL & ESSER CO MADE IN U.S.A.
46 7323

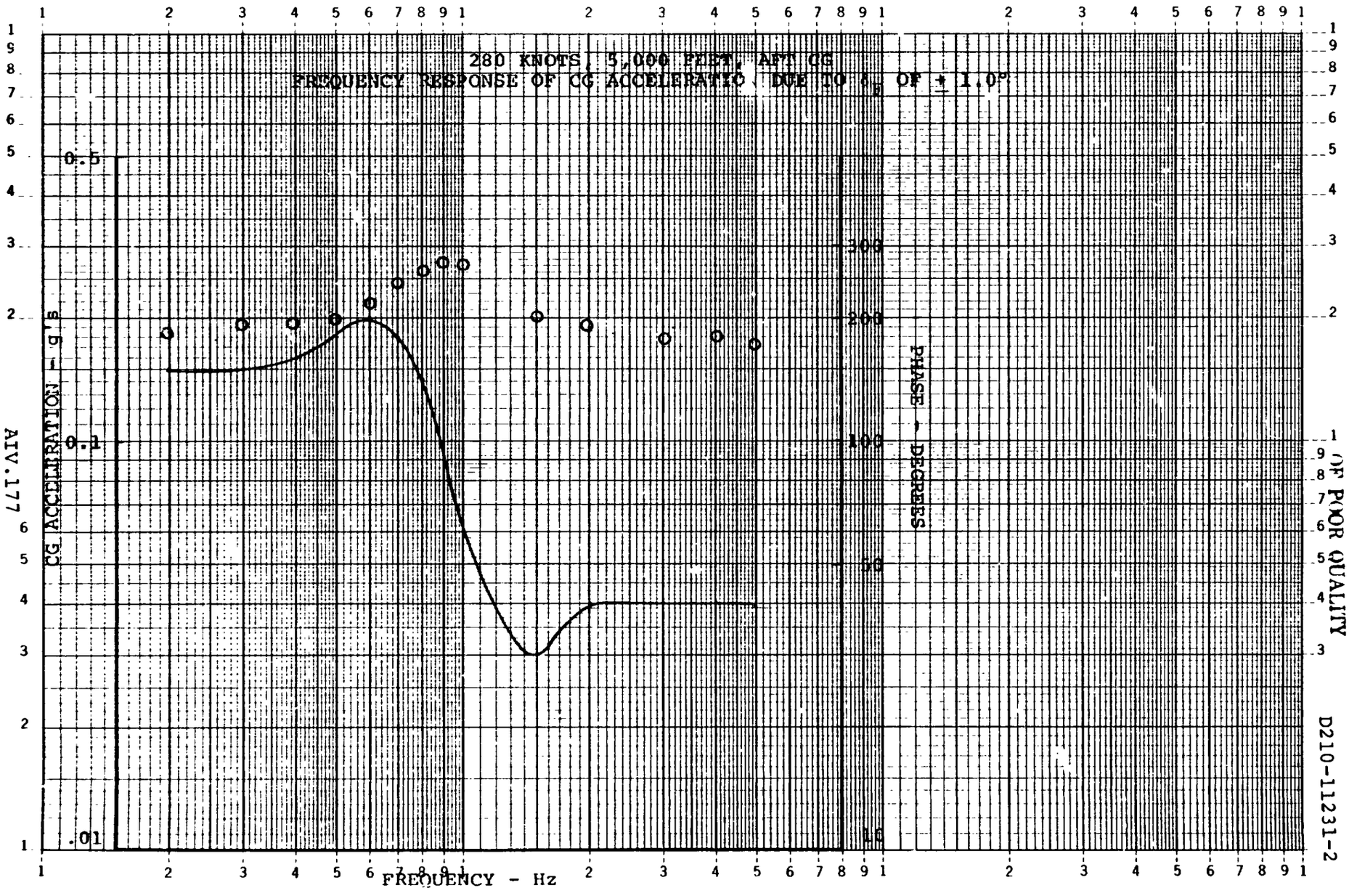

FIGURE 1.7.2.3.2.0

ORIGINAL PAGE IS
OF POOR QUALITY

K•E LOGARITHMIC • 2 X 3 CYCLES
KEUFFEL & ESSER CO MADE IN U.S.A.

46 7323

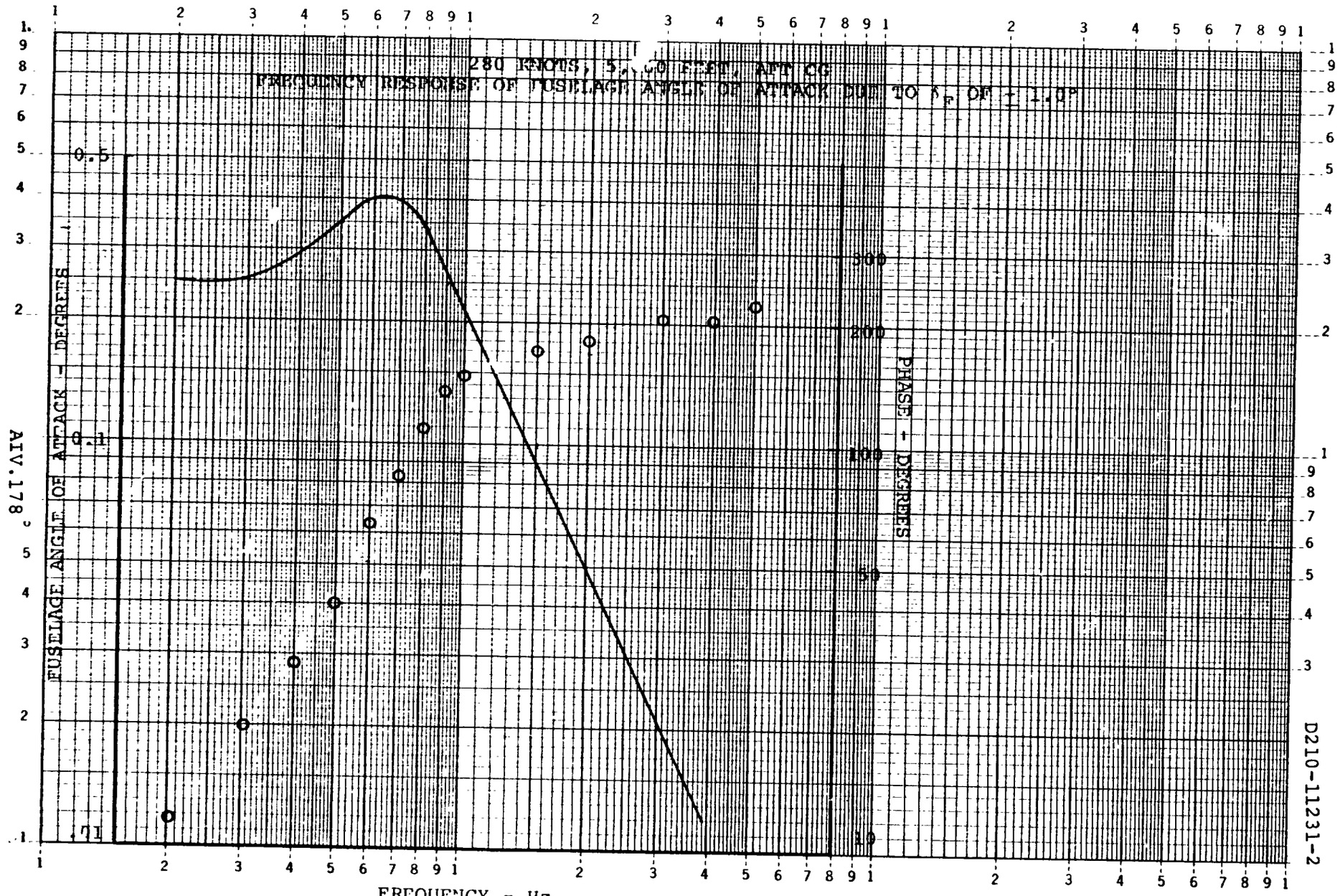

FIGURE 1.7.2.4.2.0

AIV.178

D210-11231-2

K+E LOGARITHMIC 2 X 3 CYCLES KEUFFEL & ESSER CO. MADE IN U.S.A.
46 7323

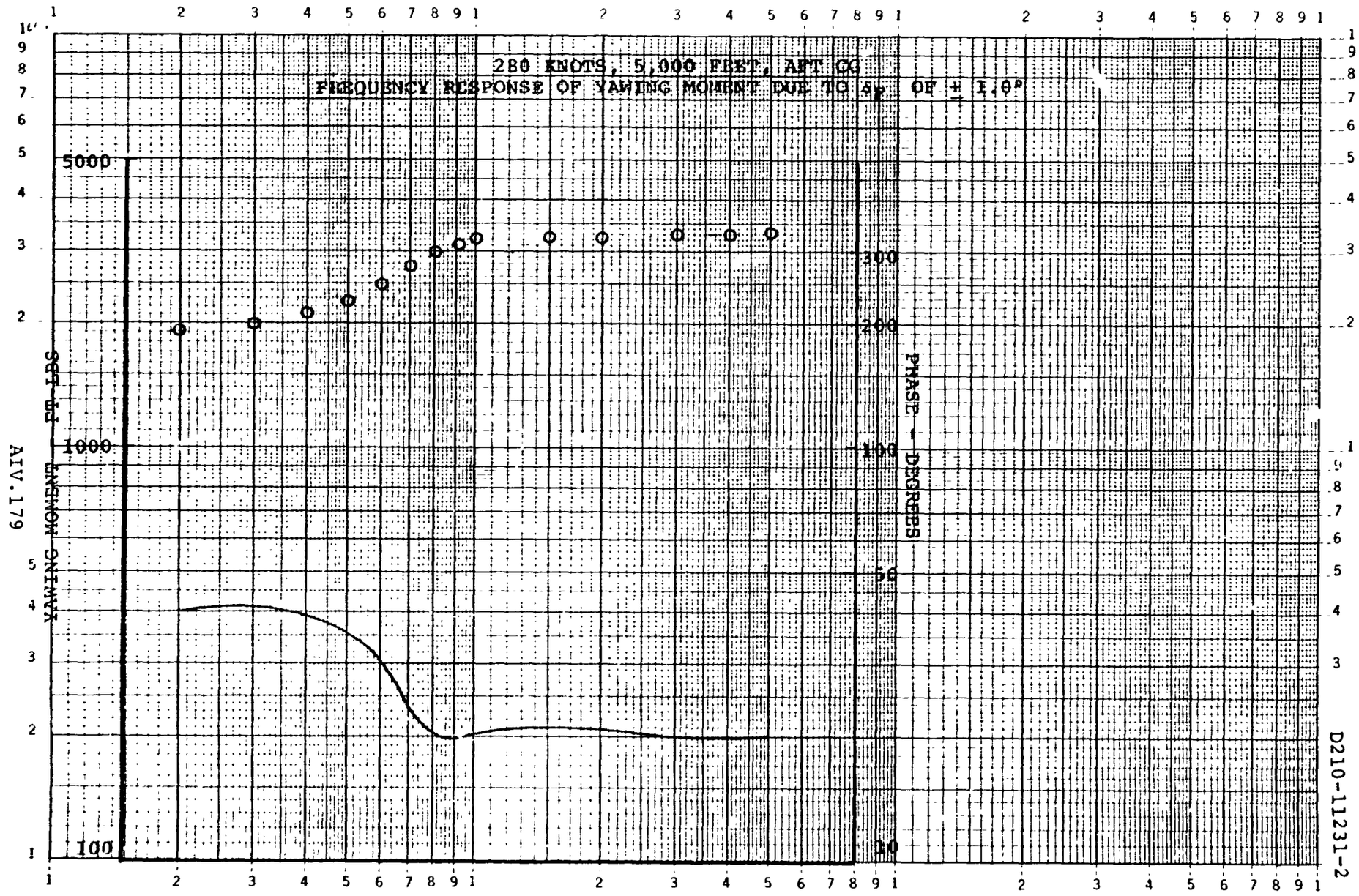

FIGURE 1.7.2.5.2.0

K•Σ LOGARITHMIC • 2 X 3 CYCLES
KEUFFEL & ESSER CO MADE IN U.S.A.

46 7323

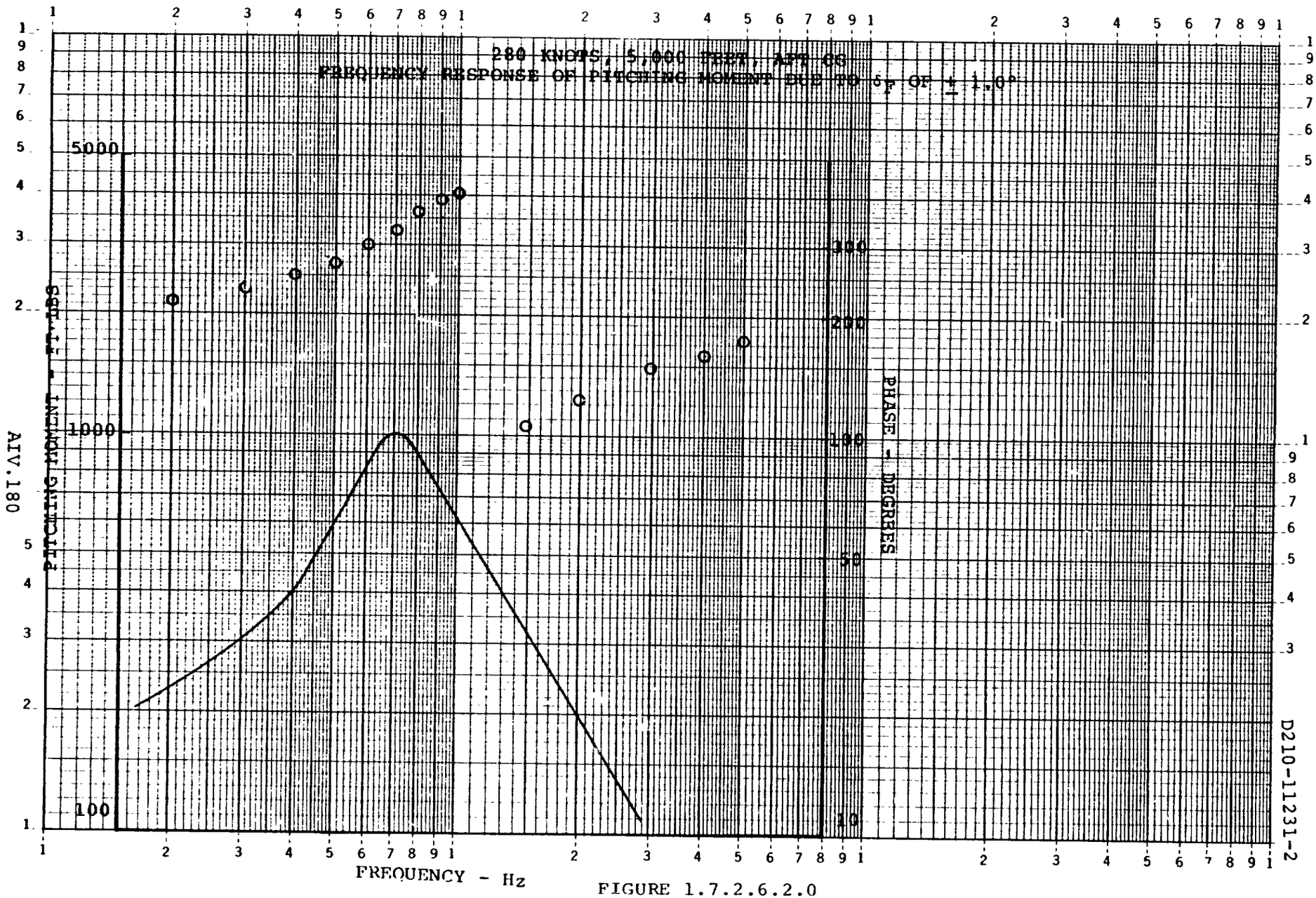

FIGURE 1.7.2.6.2.0

K•E LOGARITHMIC •2 X 3 CYCLES
KEUFFEL & ESSER CO. MADE IN U.S.A.
46 7323

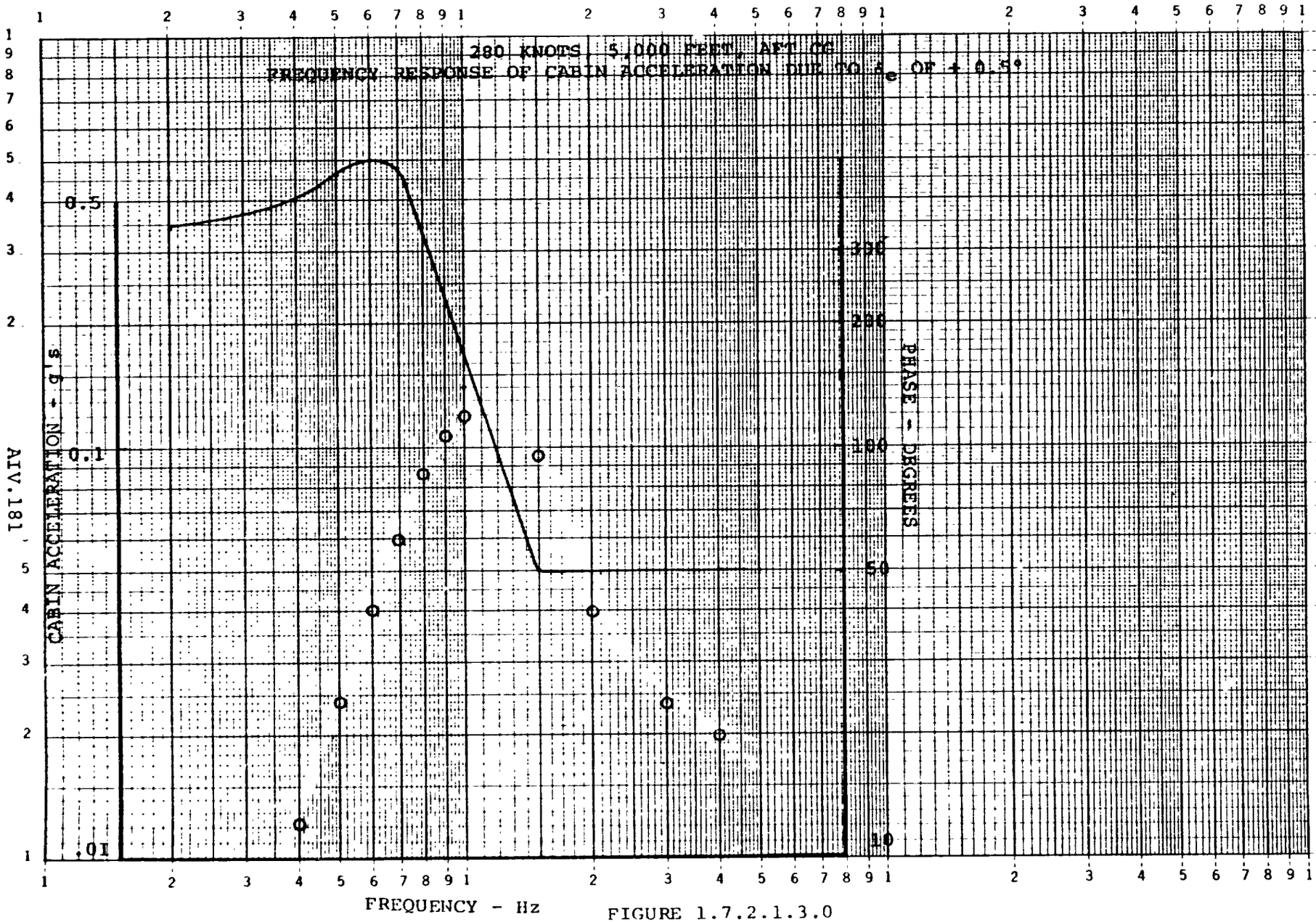

FIGURE 1.7.2.1.3.0

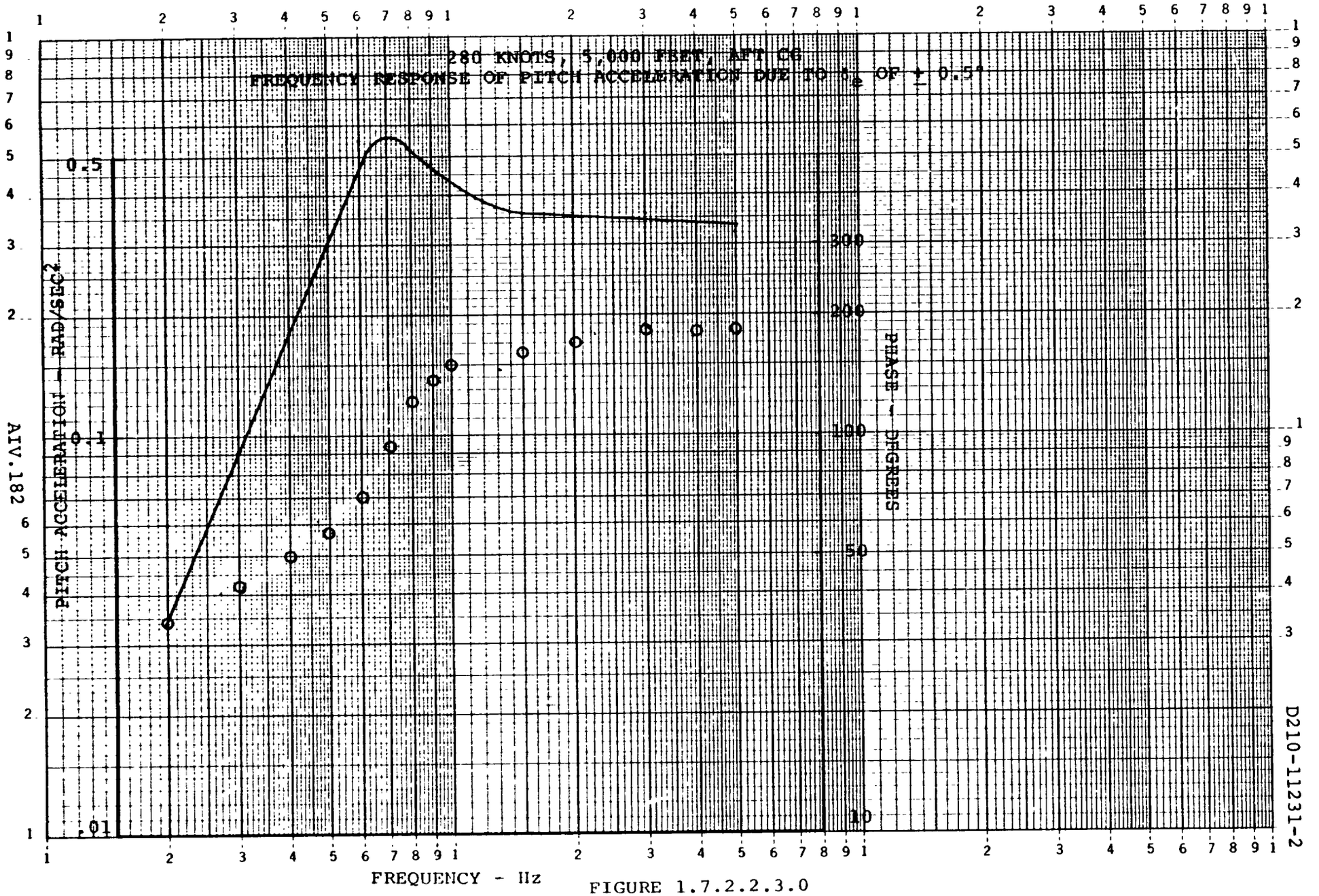

FIGURE 1.7.2.2.3.0

K+E LOGARITHMIC 2 X 3 CYCLES KEUFFEL & ESSER CO MADE IN U.S.A.
46 7323

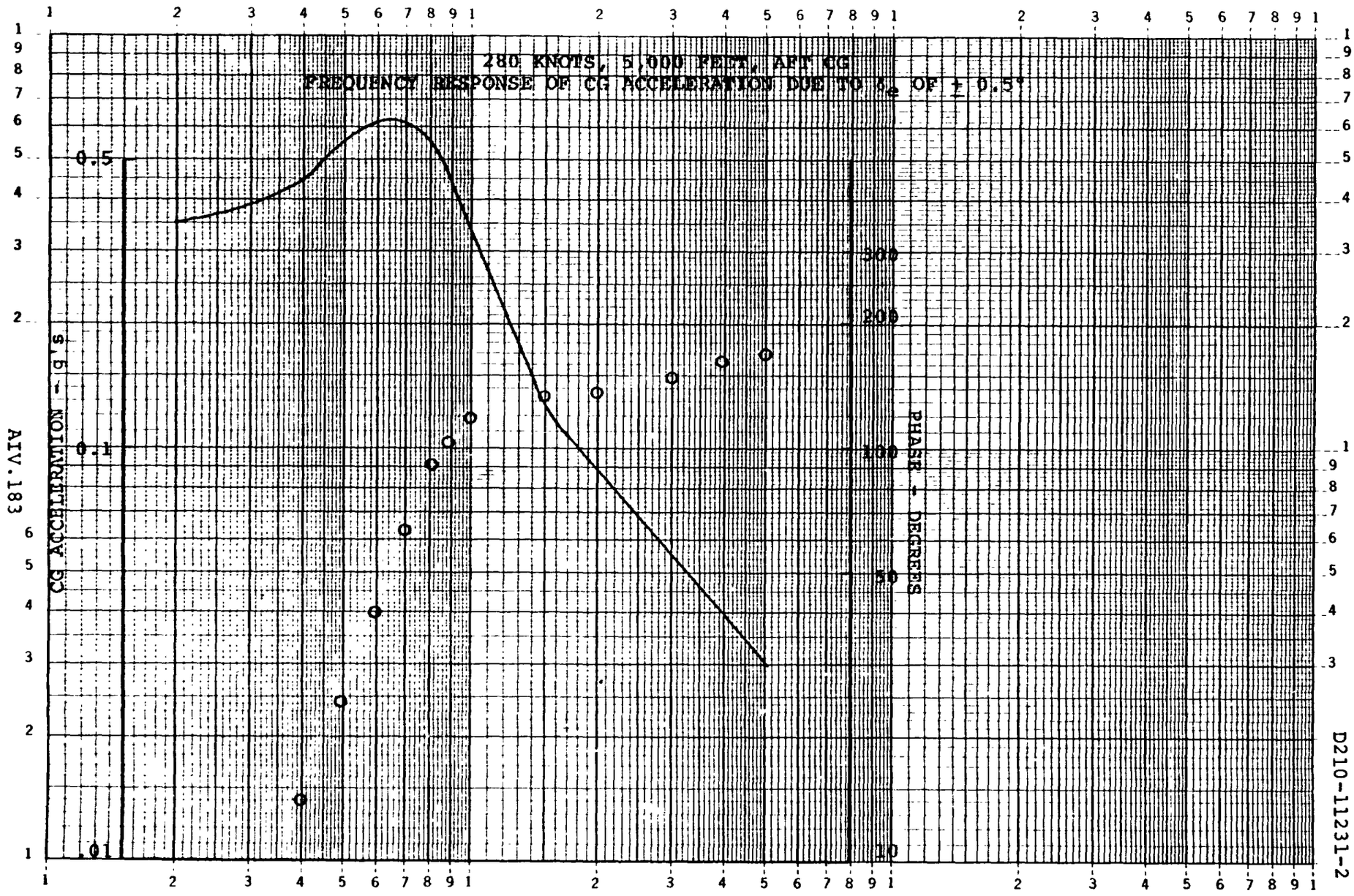

FIGURE 1.7.2.3.3.0

K+E LOGARITHMIC • 2 X 3 CYCLES
KEUFFEL & ESSER CO. MADE IN U.S.A.

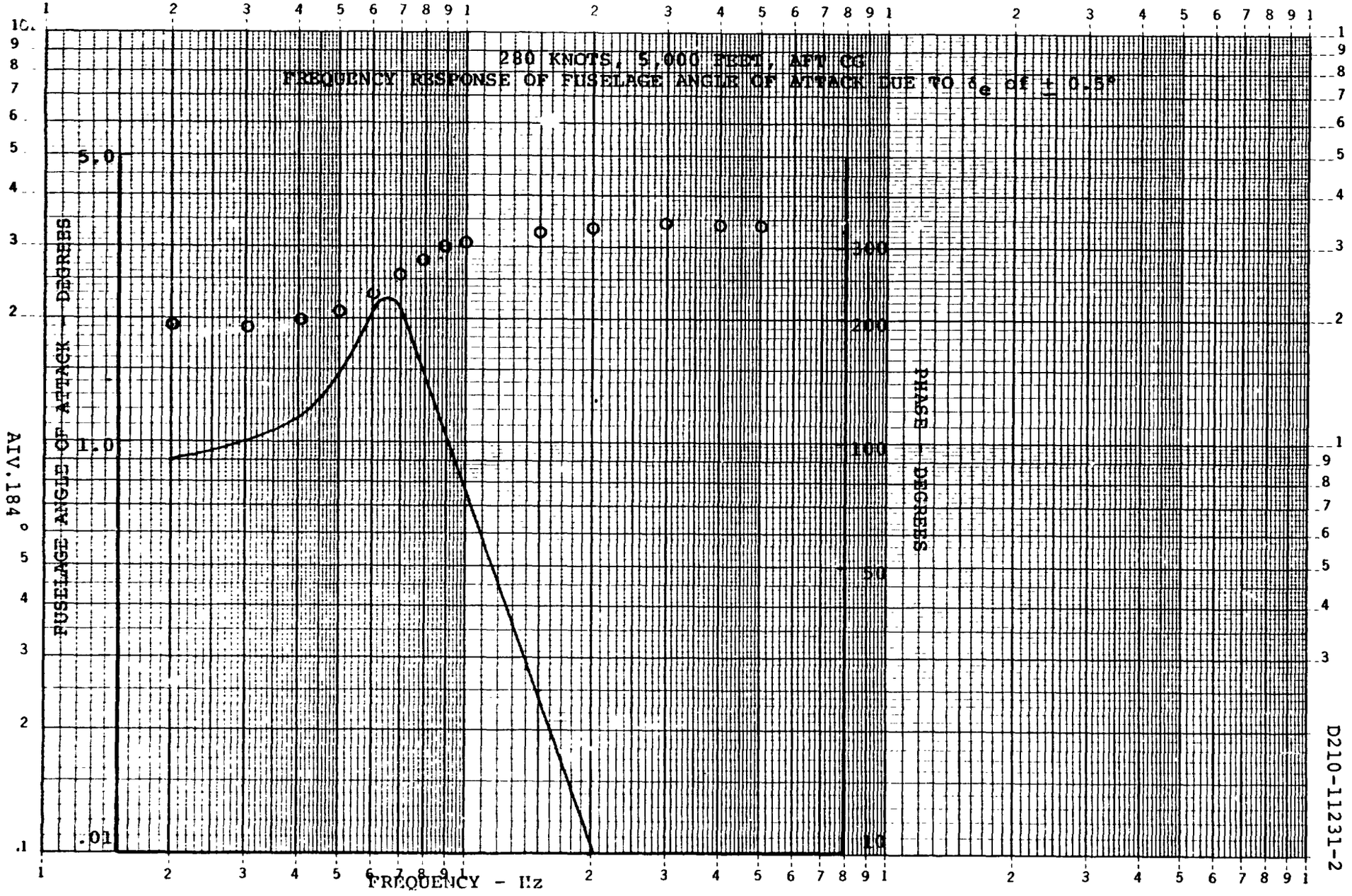

FIGURE 1.7.2.4.3.0

K·E LOGARITHMIC • 2 X 3 CYCLES
KEUFFEL & ESSER CO. MADE IN U.S.A.
46 7323

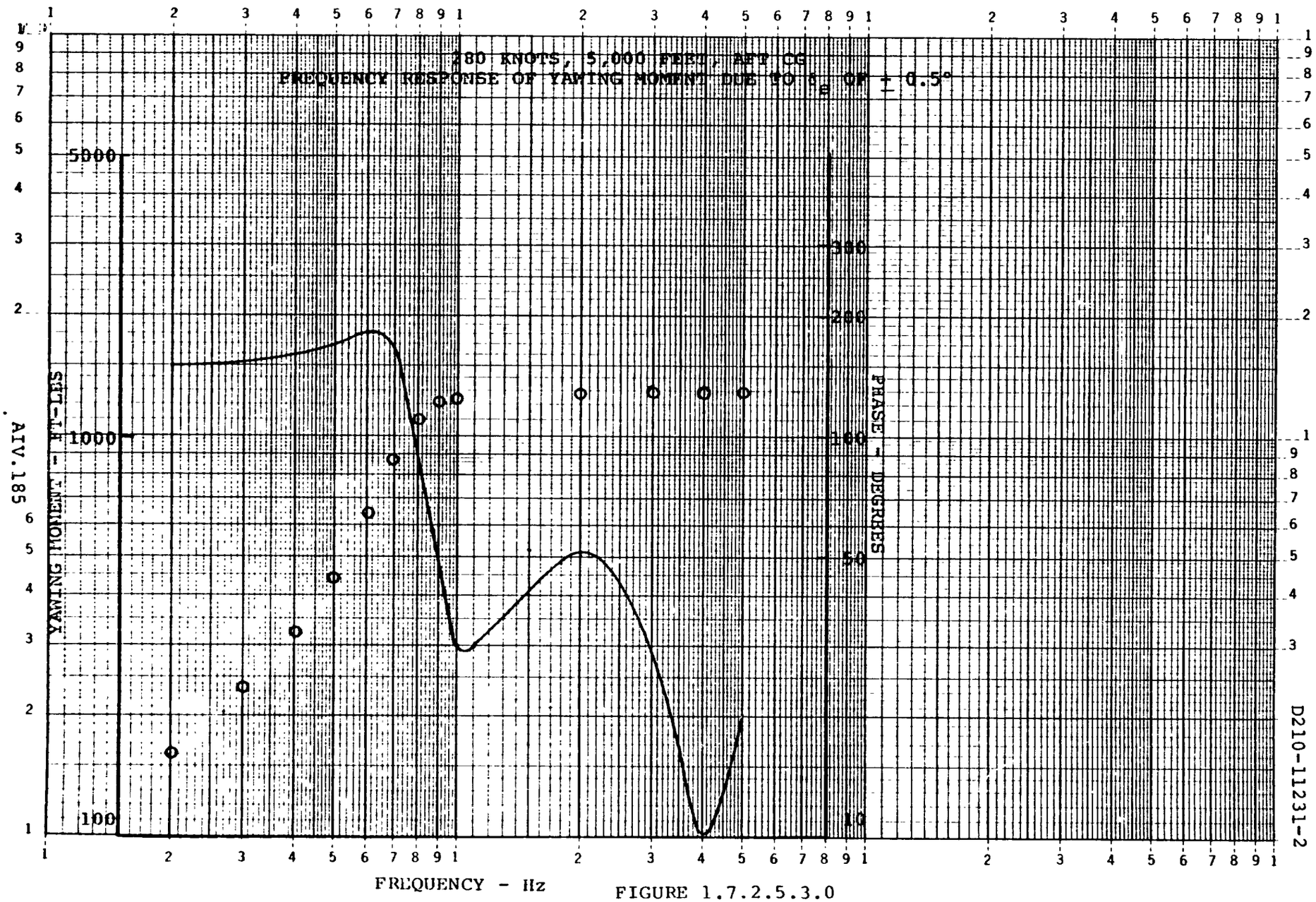

FIGURE 1.7.2.5.3.0

K•E LOGARITHMIC • 2 X 3 CYCLES
KEUFFEL & ESSER CO. MADE IN U.S.A.

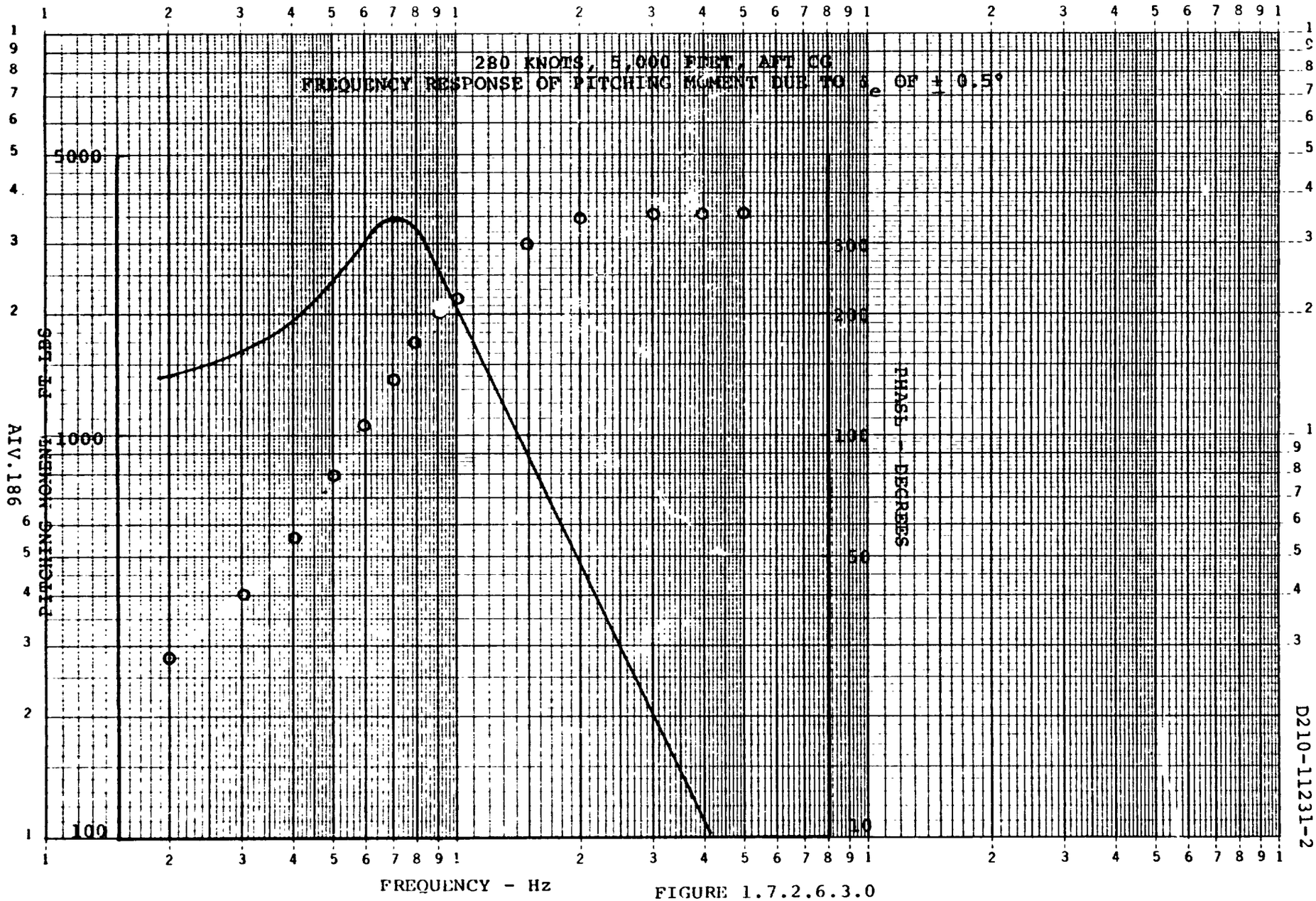

FIGURE 1.7.2.6.3.0

K·E LOGARITHMIC • 2 X 3 CYCLES
KEUFFEL & ESSER CO. MADE IN U.S.A.
46 7323

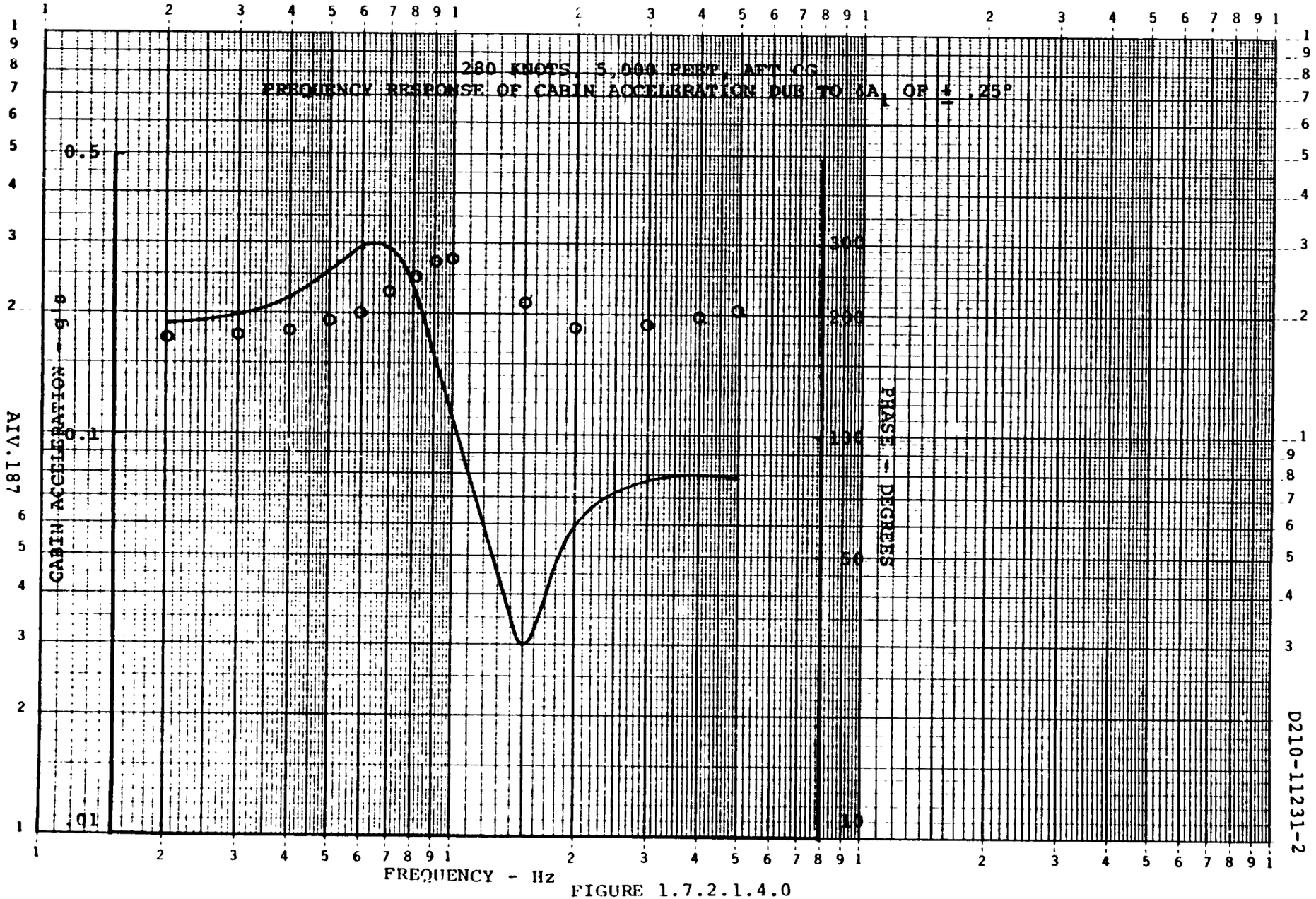

FIGURE 1.7.2.1.4.0

K·E LOGARITHMIC • 2 X 3 CYCLES
KEUFFEL & ESSER CO MADE IN U.S.A.

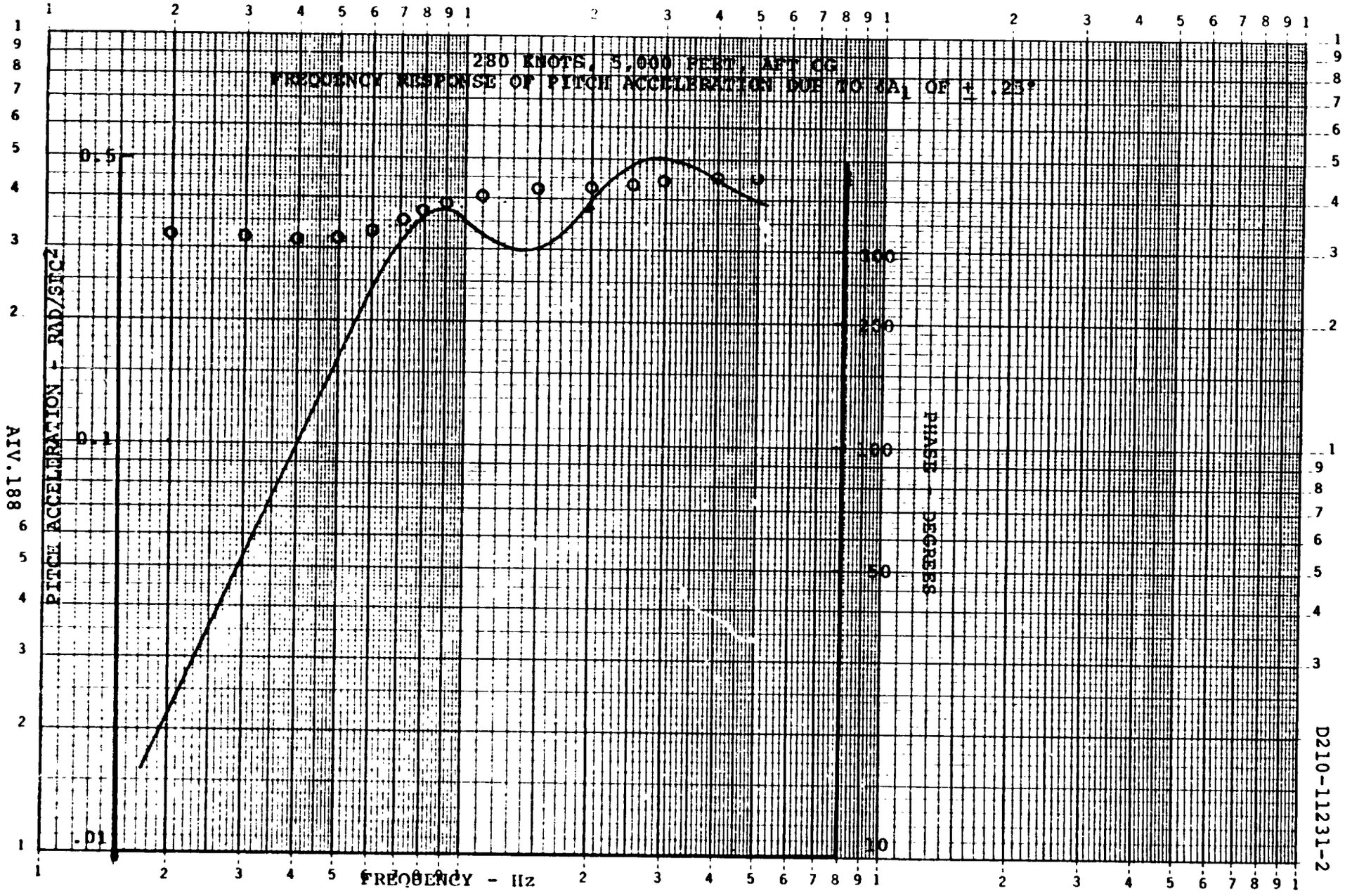

FIGURE 1.7.2.2.4.0

K+E LOGARITHMIC 2 X 3 CYCLES KEUFFEL & ESSER CO. MADE IN U.S.A.

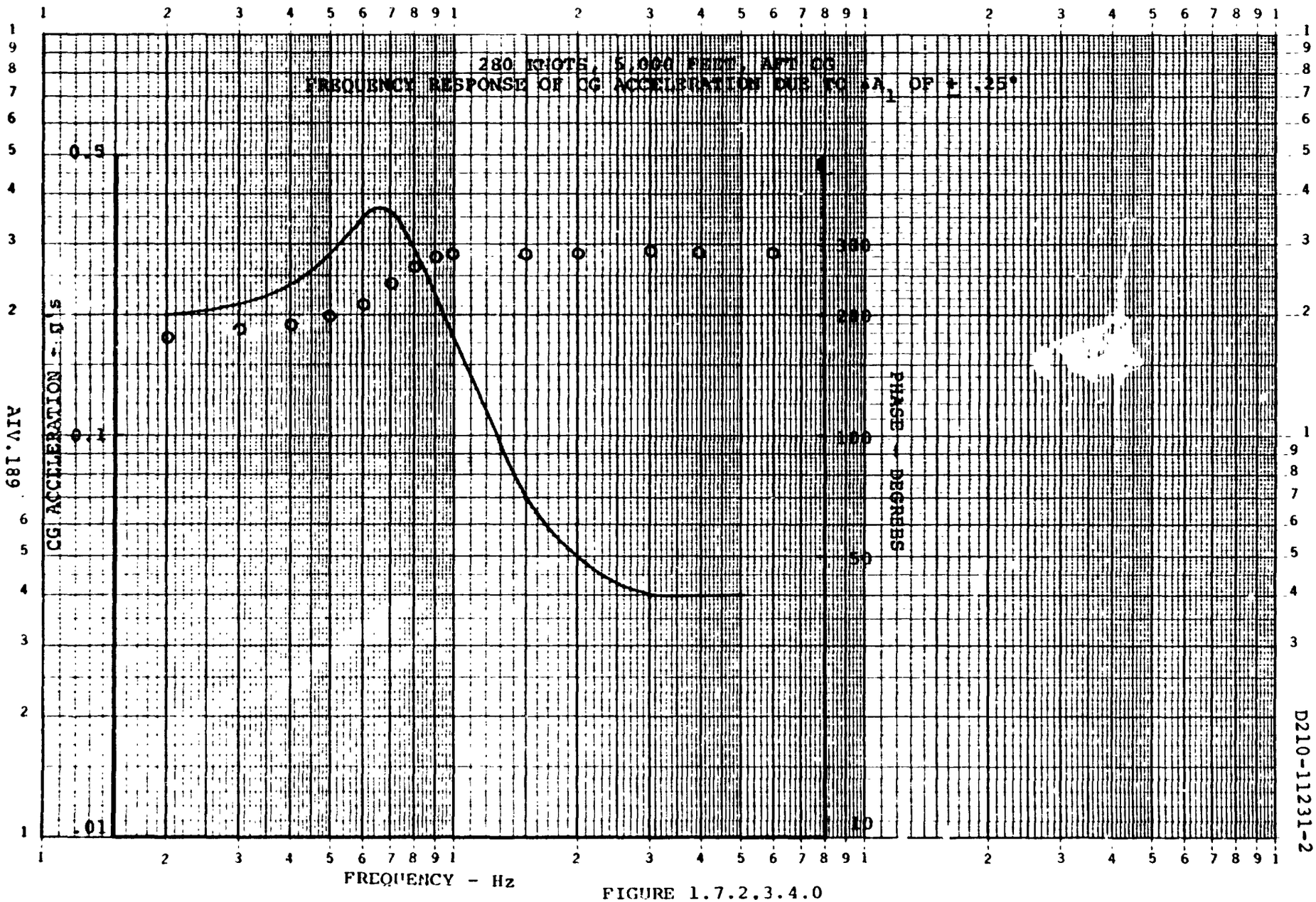

FIGURE 1.7.2.3.4.0

K·E LOGARITHMIC 2 X 3 CYCLES KEUFFEL & ESSER CO. MADE IN U.S.A.

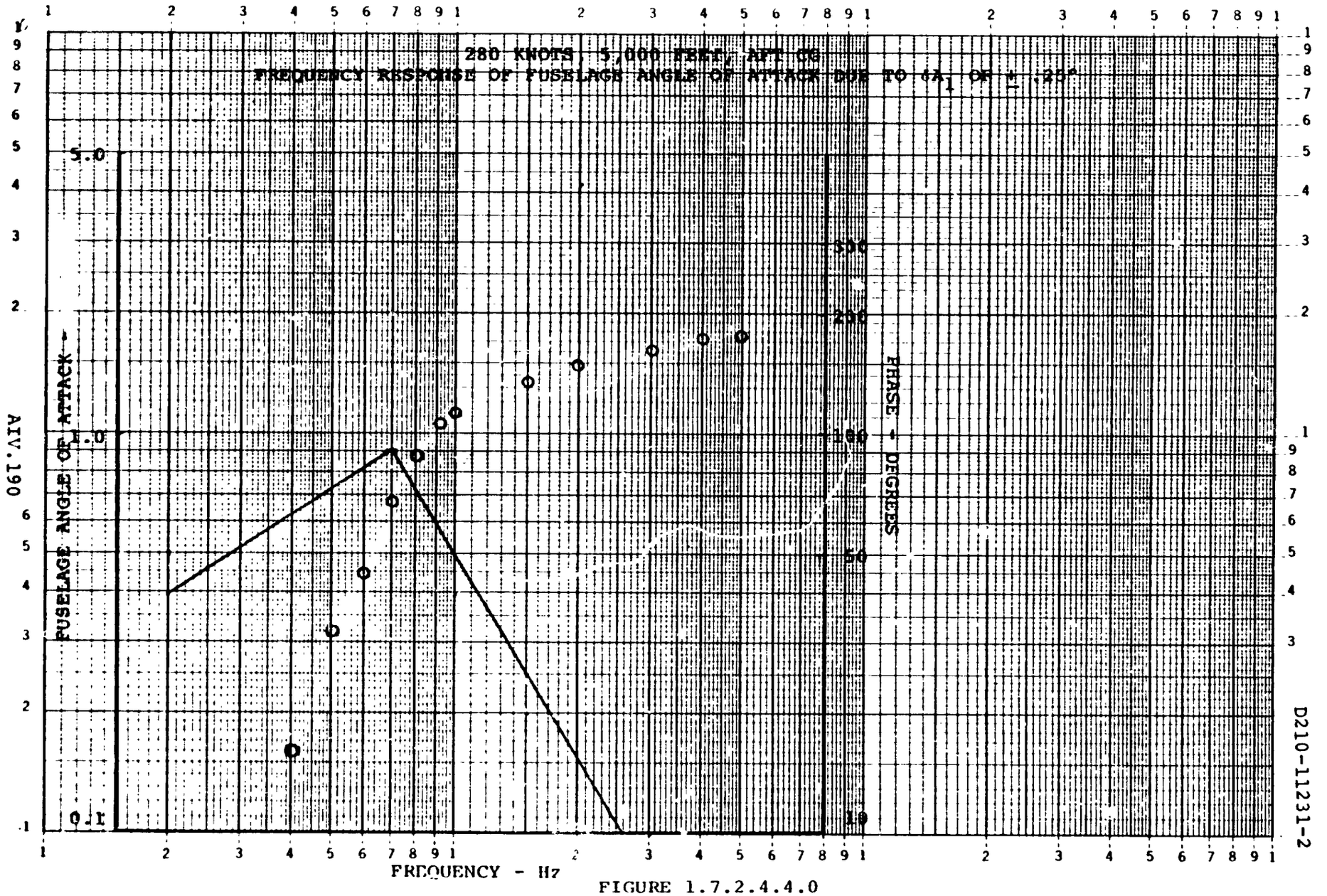

FIGURE 1.7.2.4.4.0

K•E LOGARITHMIC • 2 X 3 CYCLES
KEUFFEL & ESSER CO. MADE IN U.S.A.
46 7323

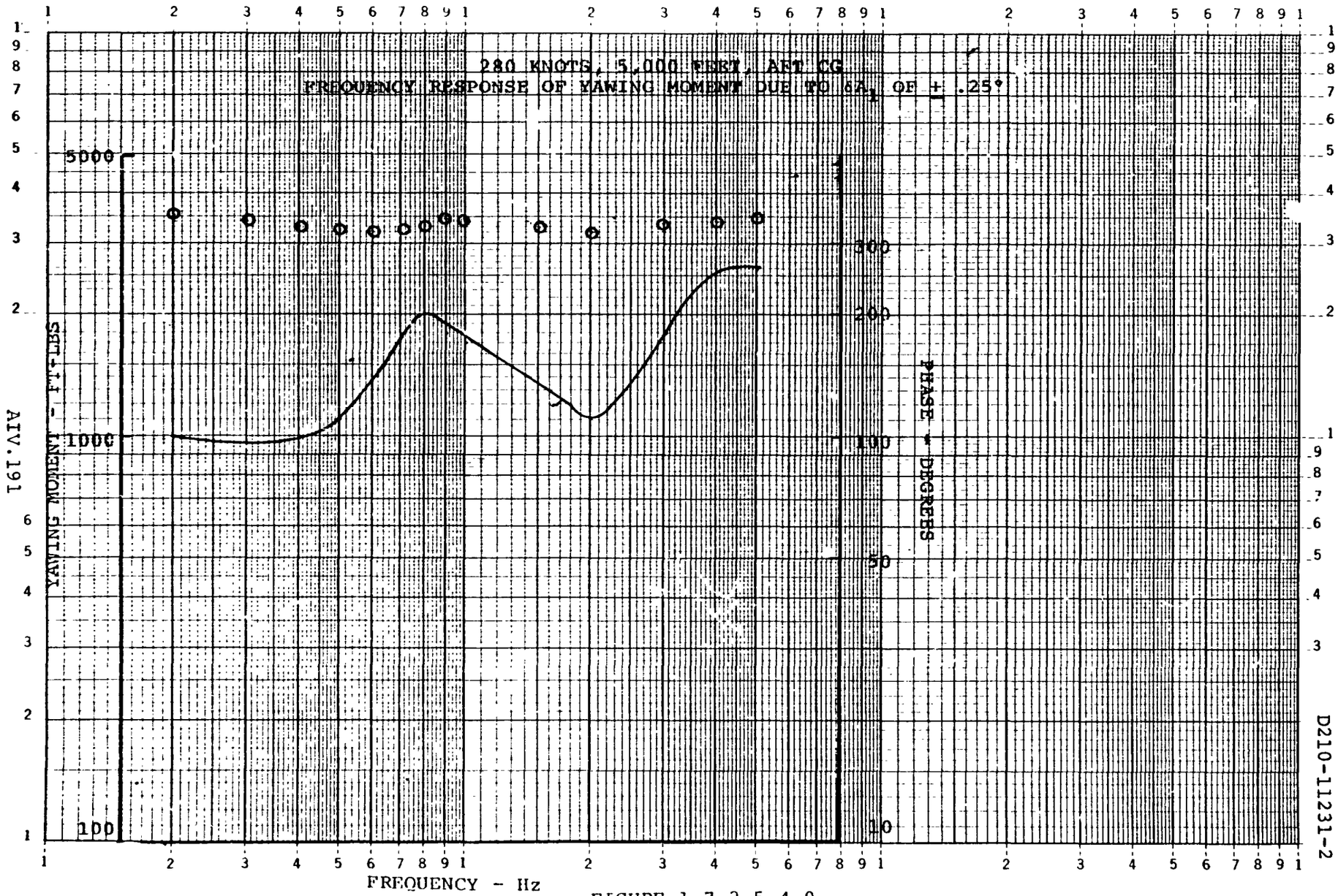

FIGURE 1.7.2.5.4.0

K·E LOGARITHMIC • 2 X 3 CYCLES
KEUFFEL & ESSER CO MADE IN U.S.A.

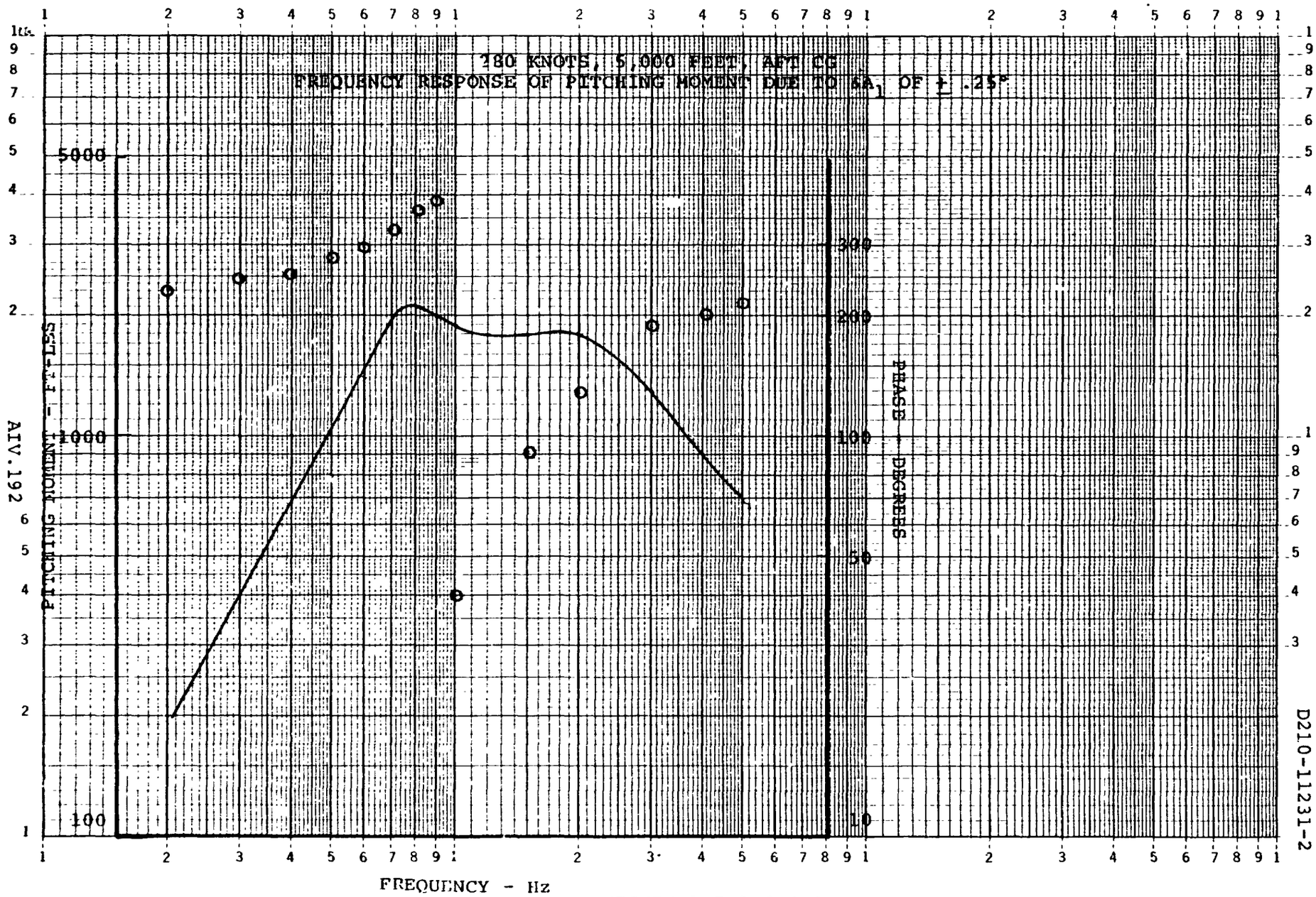

FIGURE 1.7.2.6.4.0

K·E LOGARITHMIC • 2 X 3 CYCLES
KEUFFEL & ESSER CO. MADE IN U.S.A.
46 7323

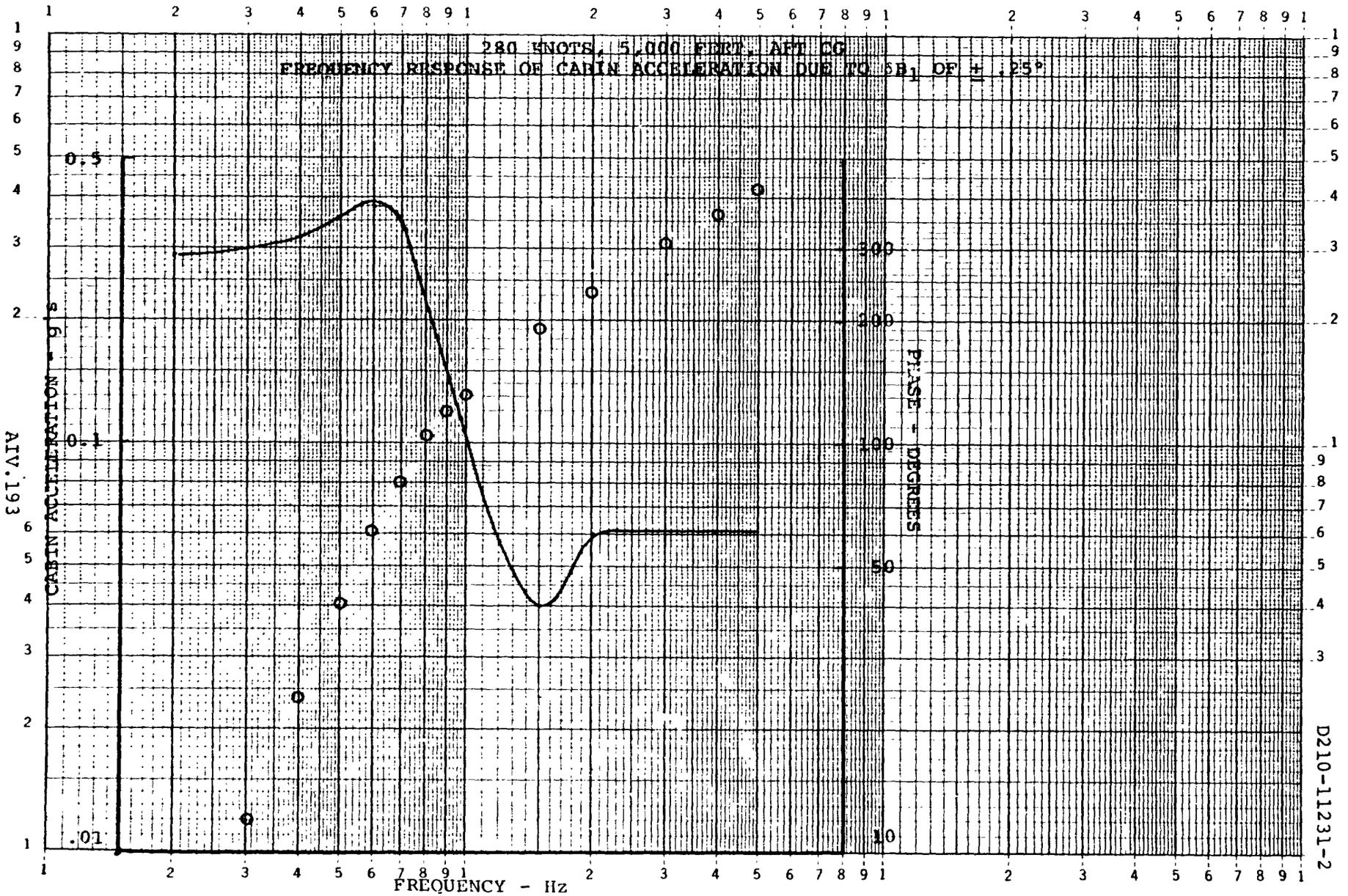

FIGURE 1.7.2.1.5.0

K+E LOGARITHMIC • 2 X 3 CYCLES
KEUFFEL & ESSER CO. MADE IN U.S.A.

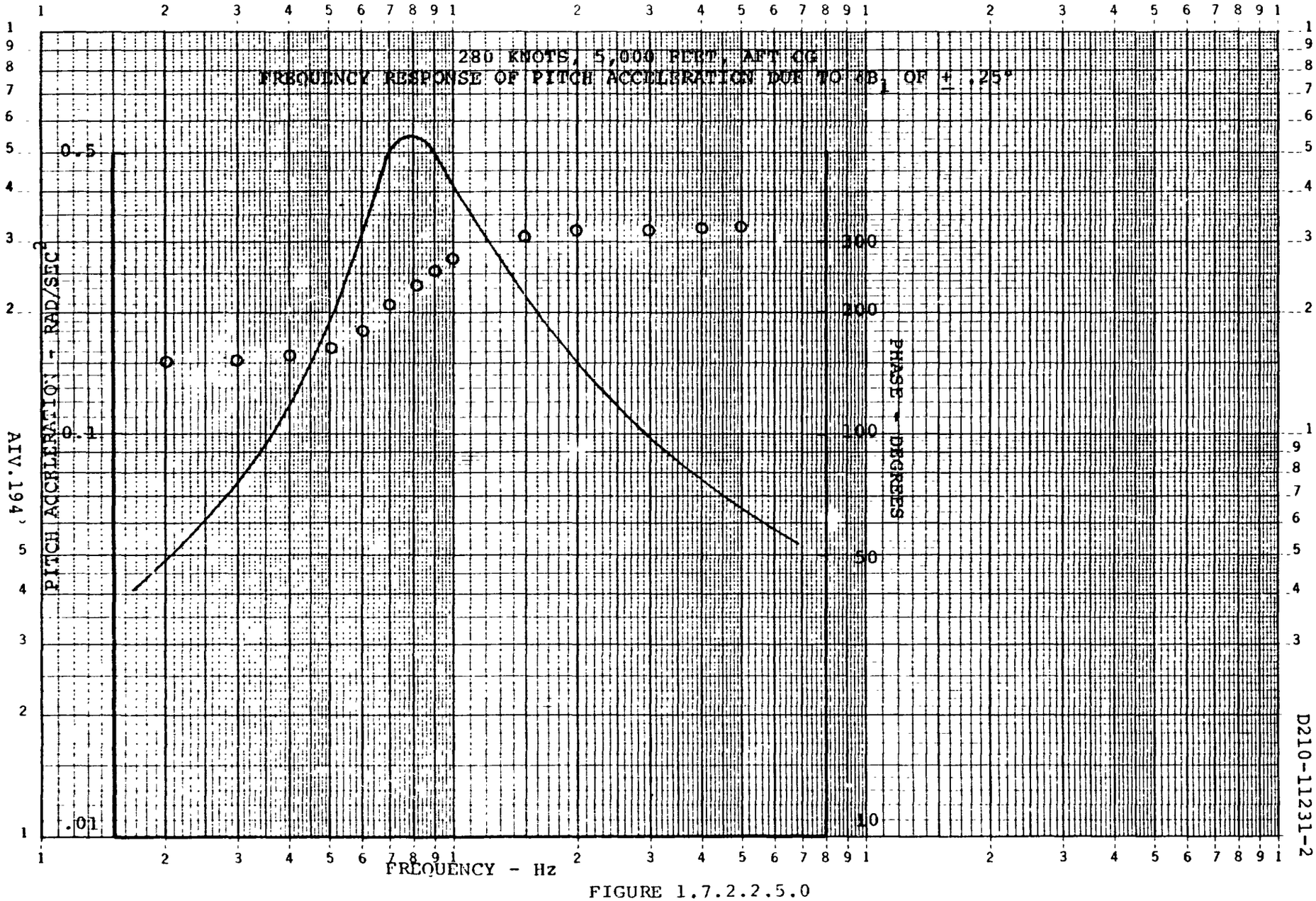

FIGURE 1.7.2.2.5.0

K+E LOGARITHMIC • 2 X 3 CYCLES
KEUFFEL & ESSER CO. MADE IN U.S.A.
46 7323

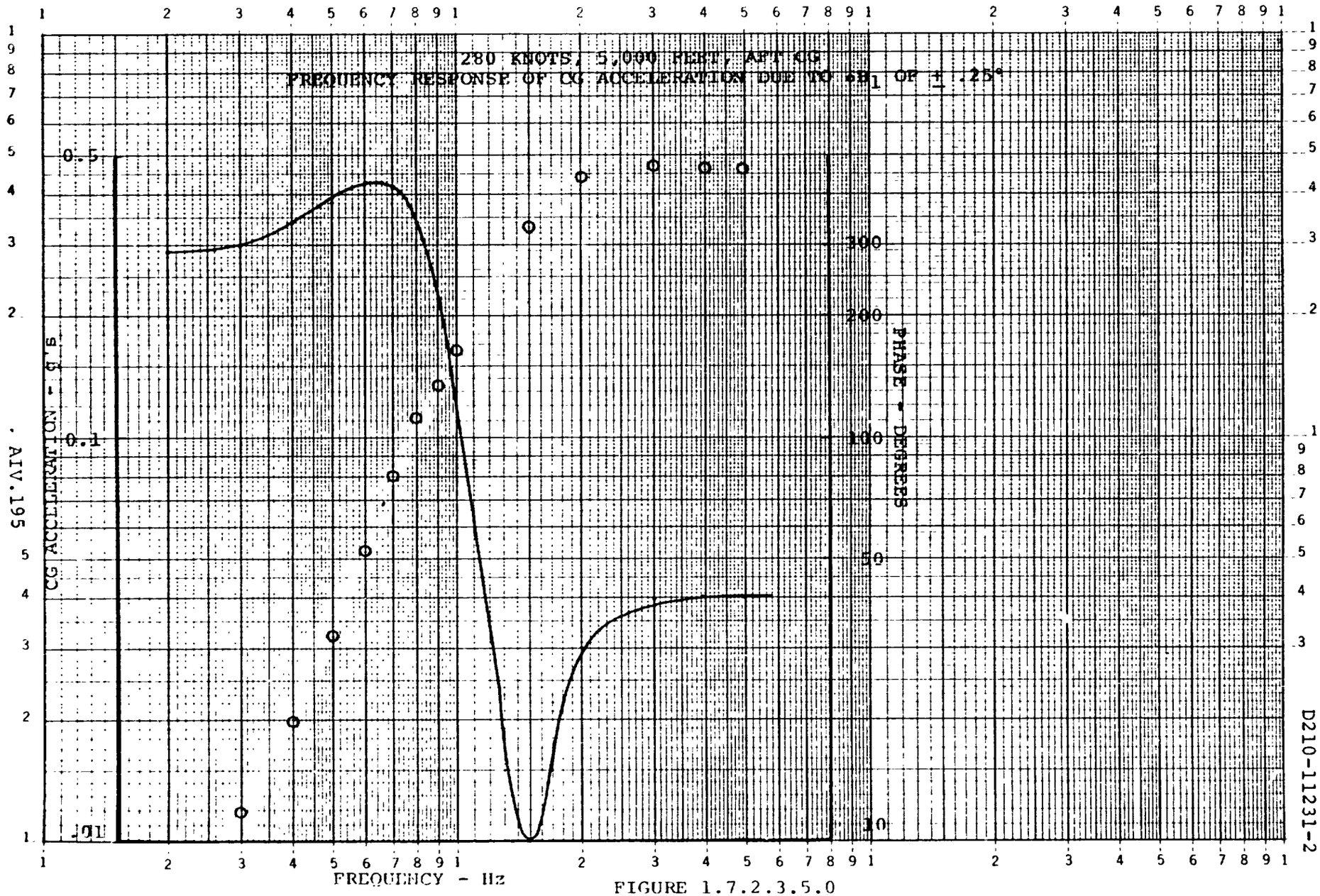

FIGURE 1.7.2.3.5.0

K•E LOGARITHMIC • 2 X 3 CYCLES
KEUFFEL & ESSER CO. MADE IN U.S.A.

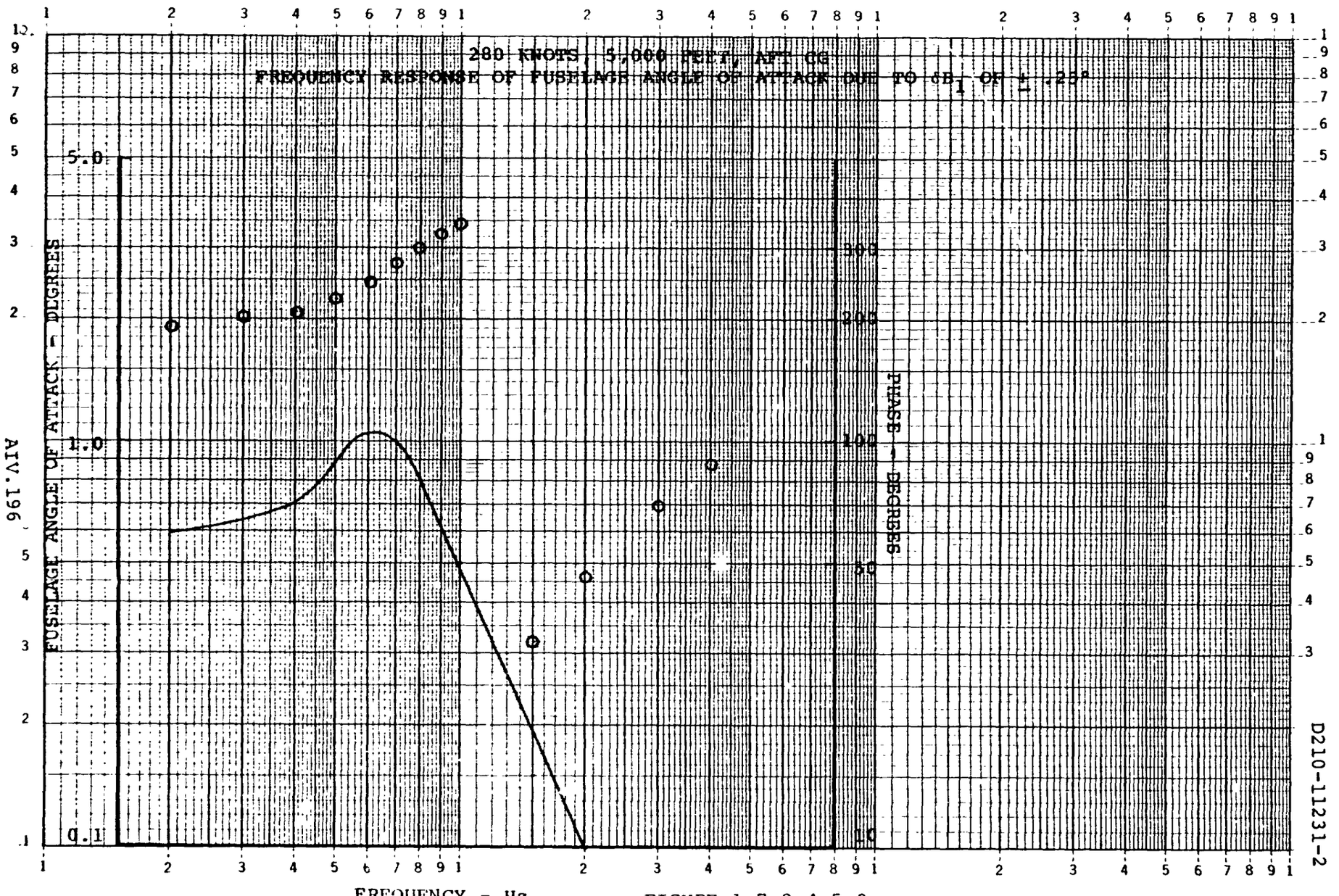

FIGURE 1.7.2.4.5.0

K+E LOGARITHMIC • 2 X 3 CYCLES
KEUFFEL & ESSER CO MADE IN U.S.A.
46 7323

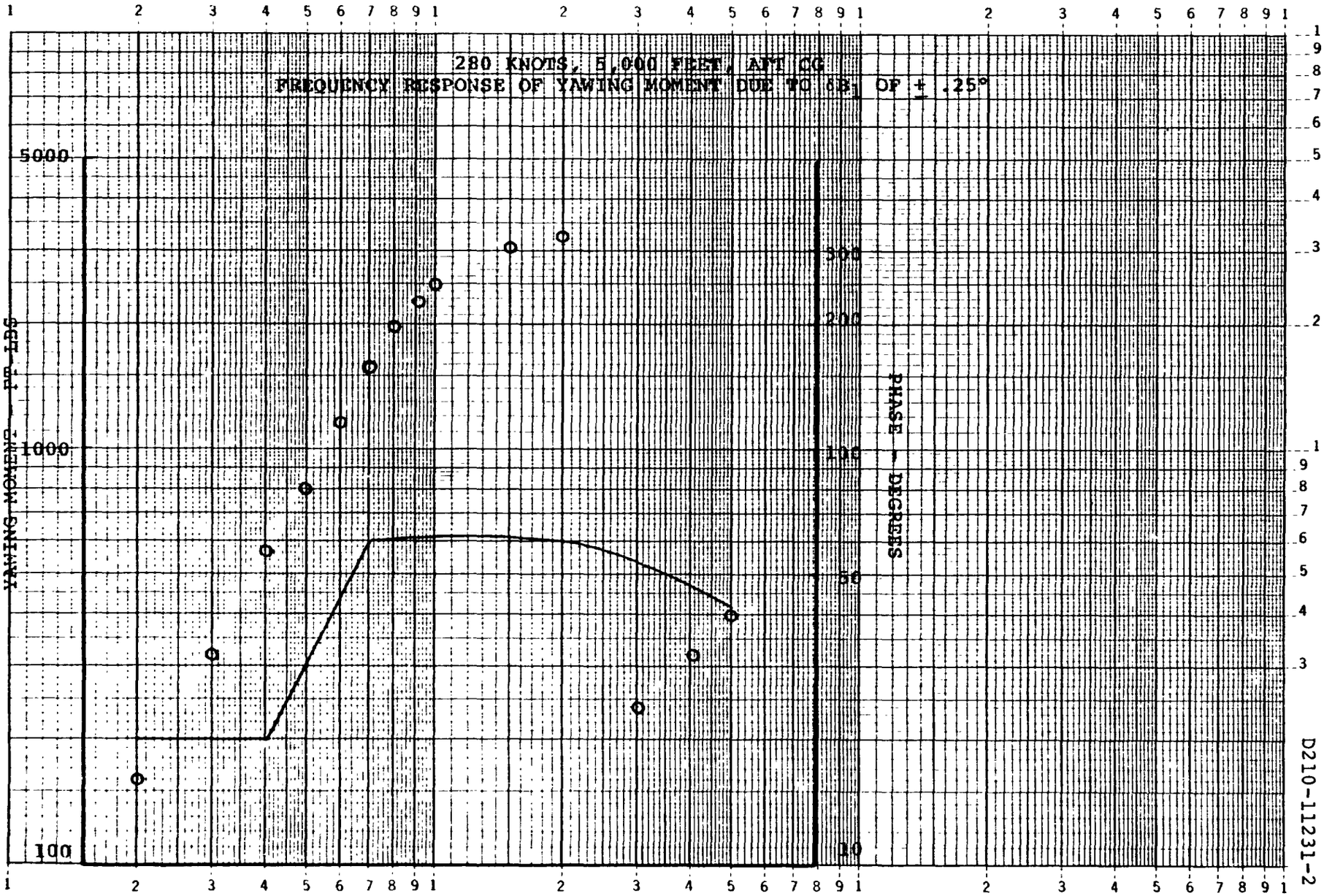

FIGURE 1.7.2.5.5.0

K·E LOGARITHMIC • 2 X 3 CYCLES
KEUFFEL & ESSER CO MADE IN U.S.A.

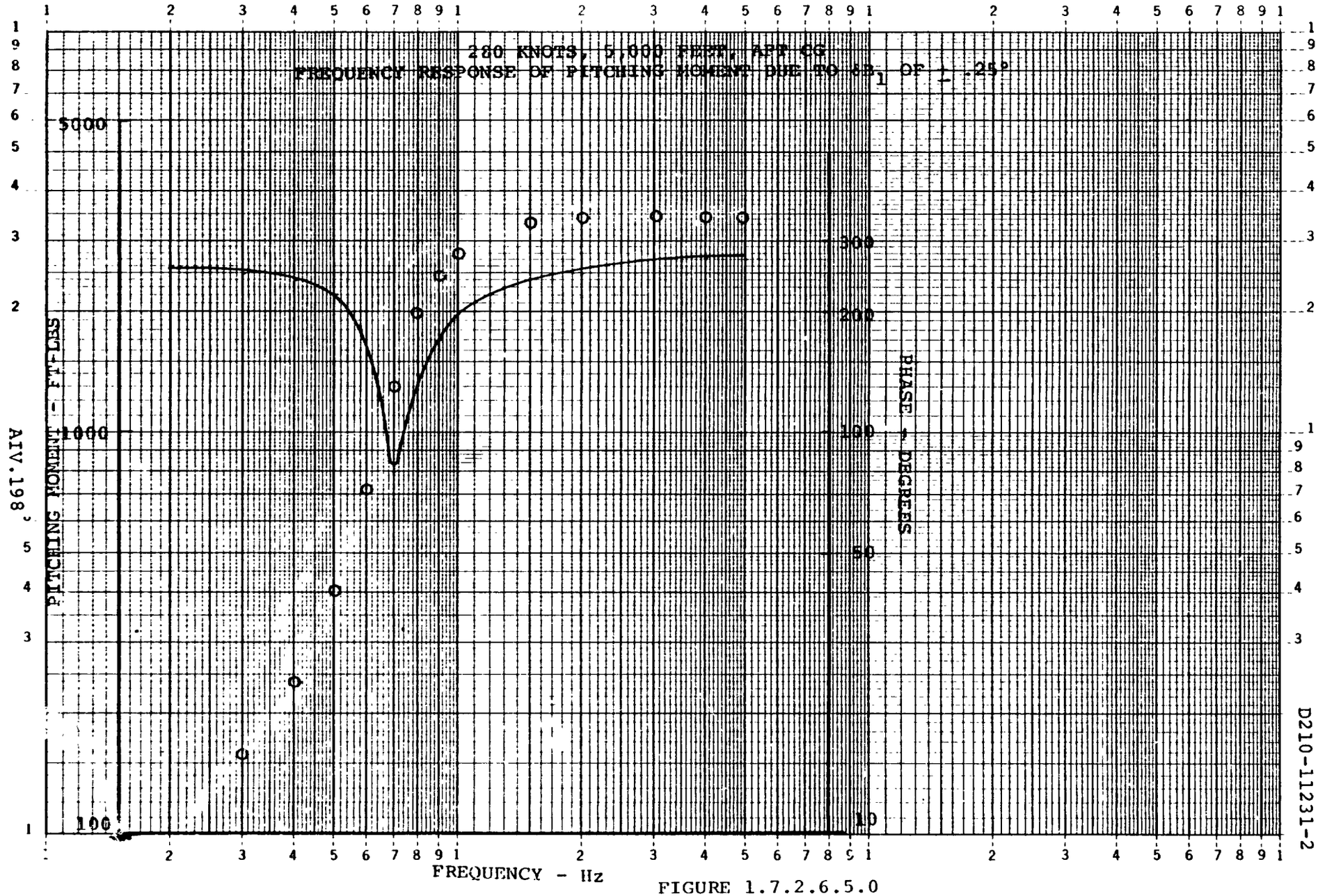

FIGURE 1.7.2.6.5.0

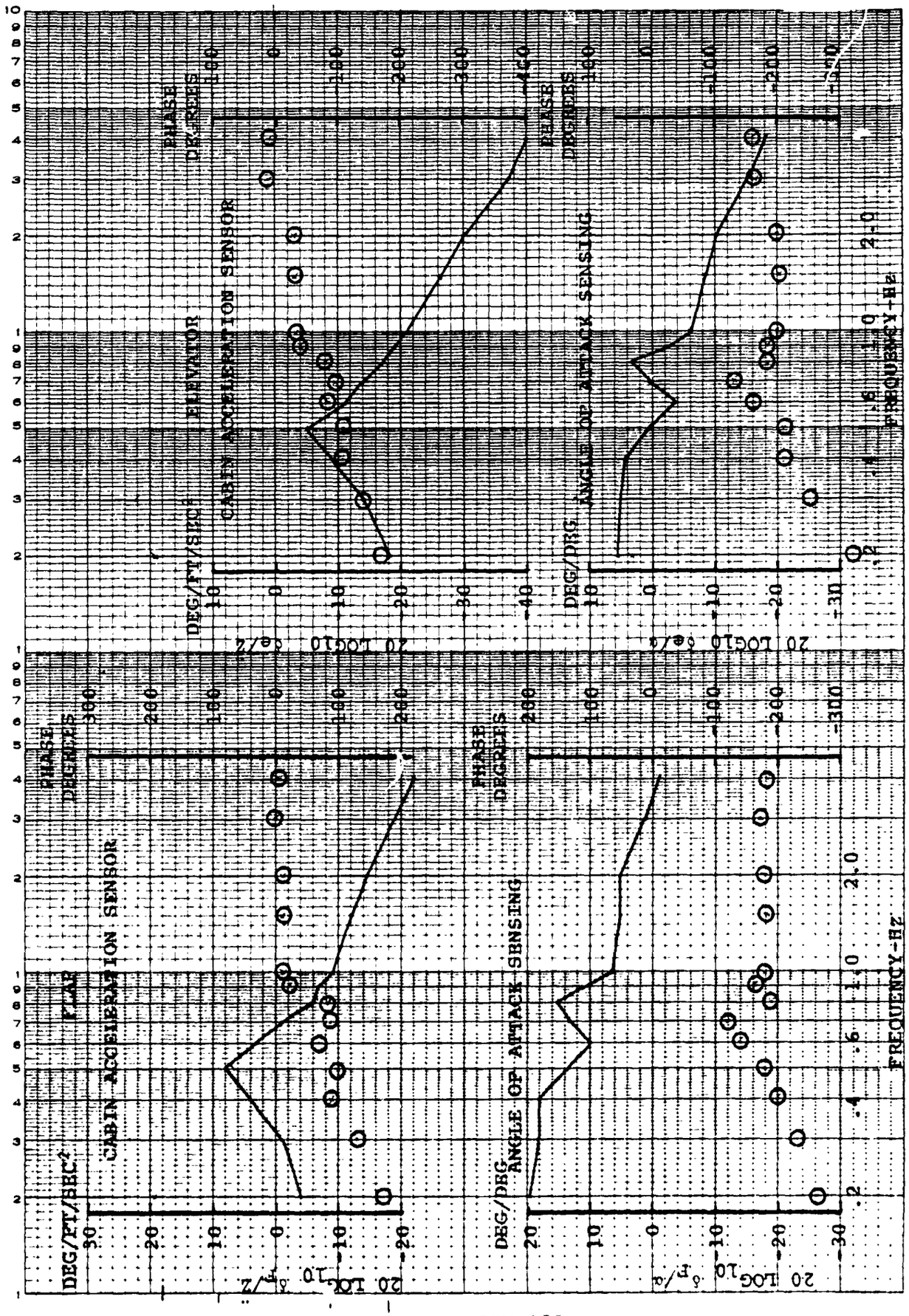

FIGURE 2.7.2.0.0.0. FLAP & ELEVATOR REQUIRED WITH ACCELERATION AND α SENSING, 280 KNOTS, 5,000 FEET, AFT CG, NO A_1 & B_1 FEEDBACK

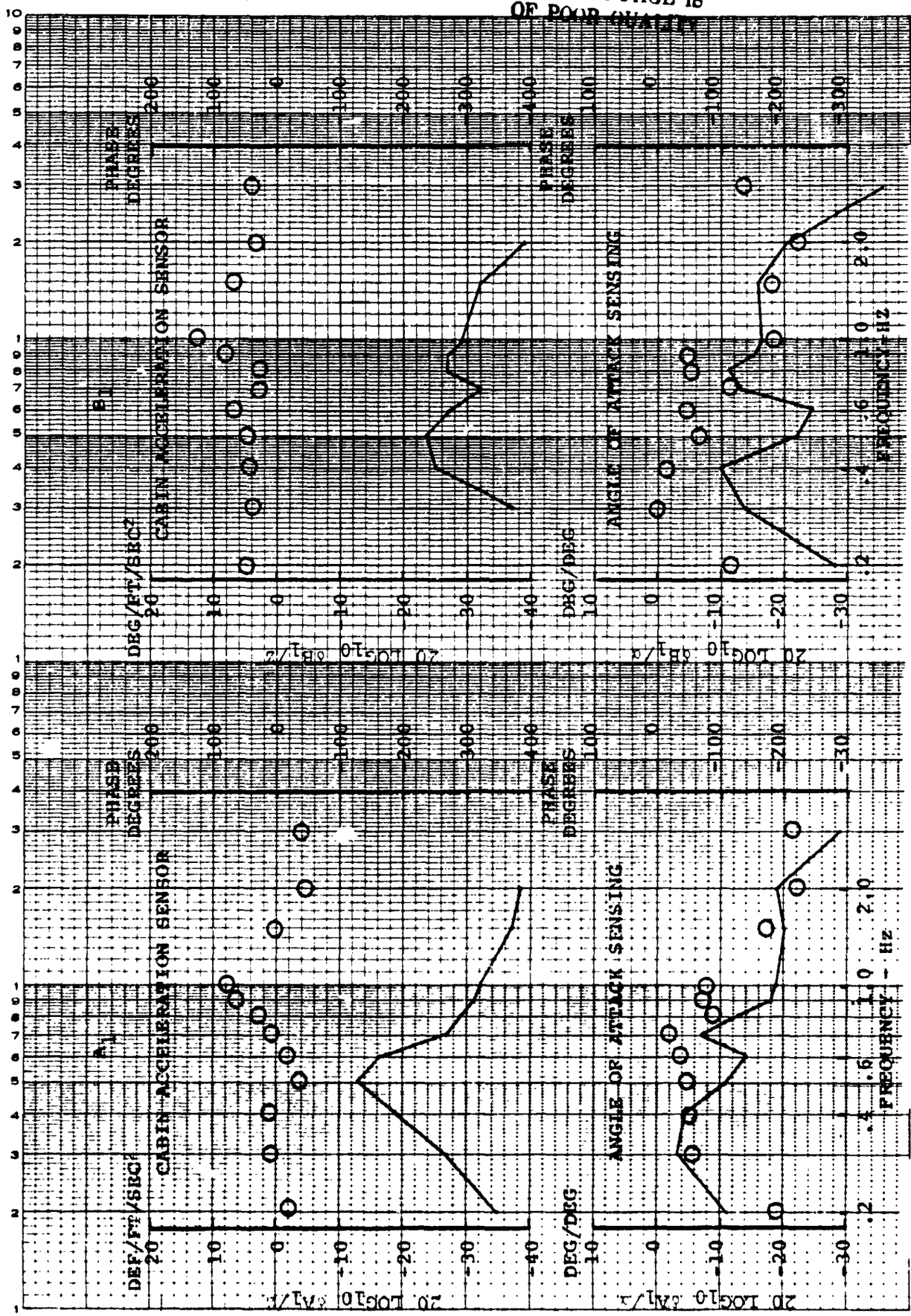

FIGURE 2.7.2.0.0.0. A_1 & B_1 FEEDBACK REQUIRED WITH ACCELERATION & α SENSING RESPECTIVELY, 280 KNOTS, 5,000 FEET, AFT CG

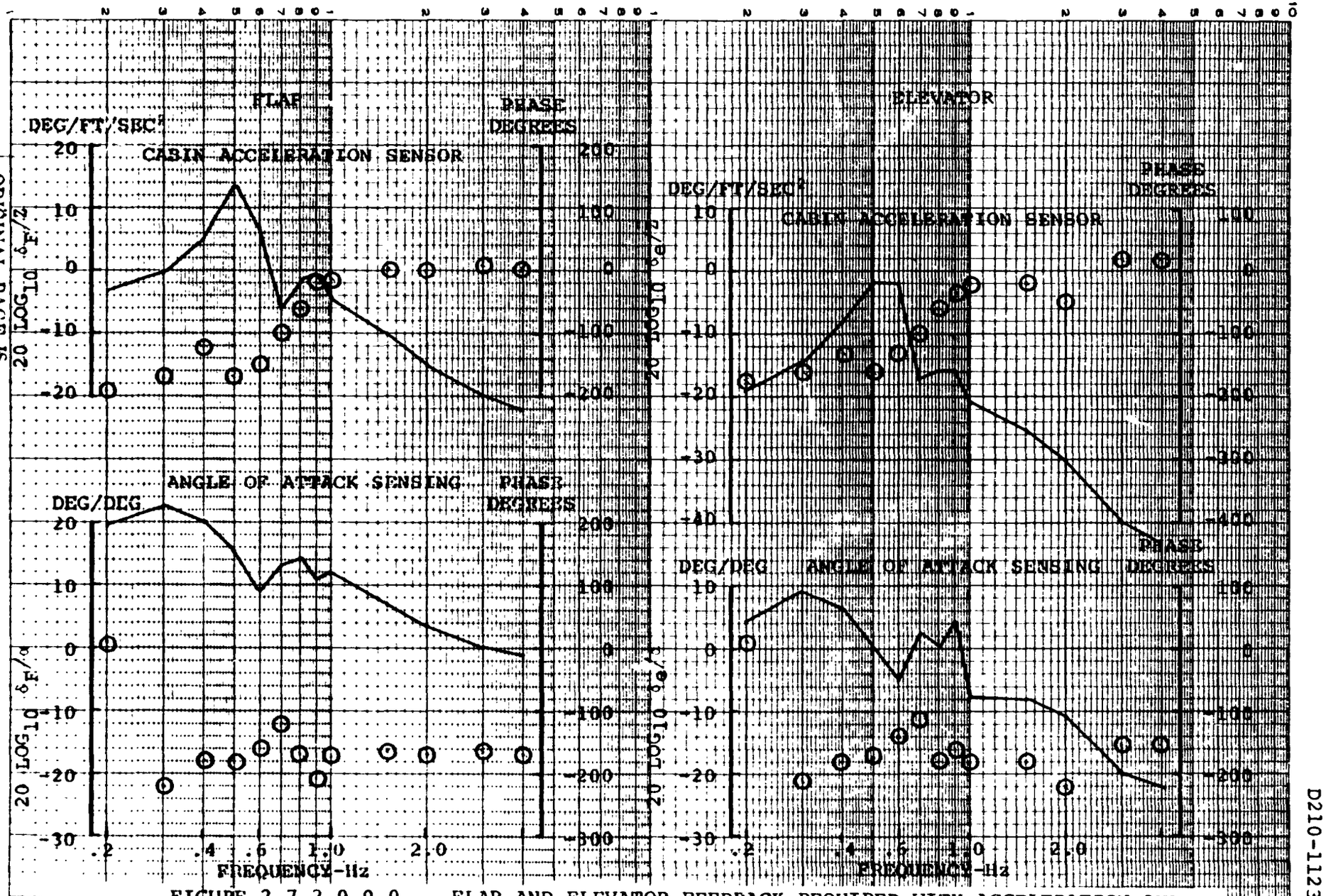

FIGURE 2.7.2.0.0.0. FLAP AND ELEVATOR FEEDBACK REQUIRED WITH ACCELERATION AND α SENSING RESPECTIVELY, 280 KNOTS, 5,000 FEET, AFT CG WITH A_1 & B_1 FEEDBACK

ORIGINAL PAGE IS
OF POOR QUALITY

FLIGHT CONDITION: 280 KNOTS, 5,000 FEET, (1,524m), AFT CG

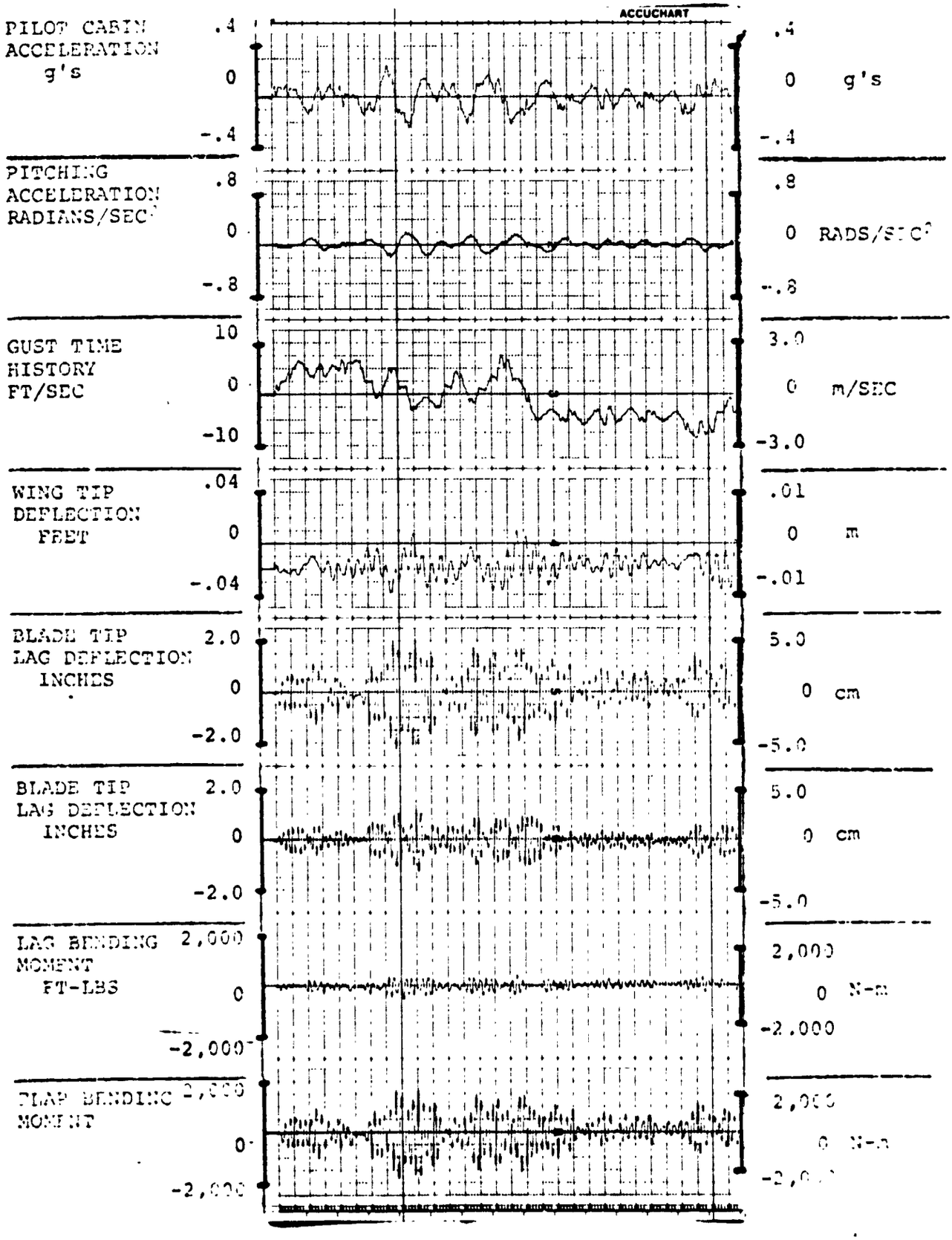

FIGURE 3.7.2.0.0.1. RESPONSES FOR GAIN F = 0, GAIN E = 0

ORIGINAL PAGE IS
OF POOR QUALITY

FLIGHT CONDITION: 280 KNOTS, 5,000 FEET, (1,524m), AFT CG

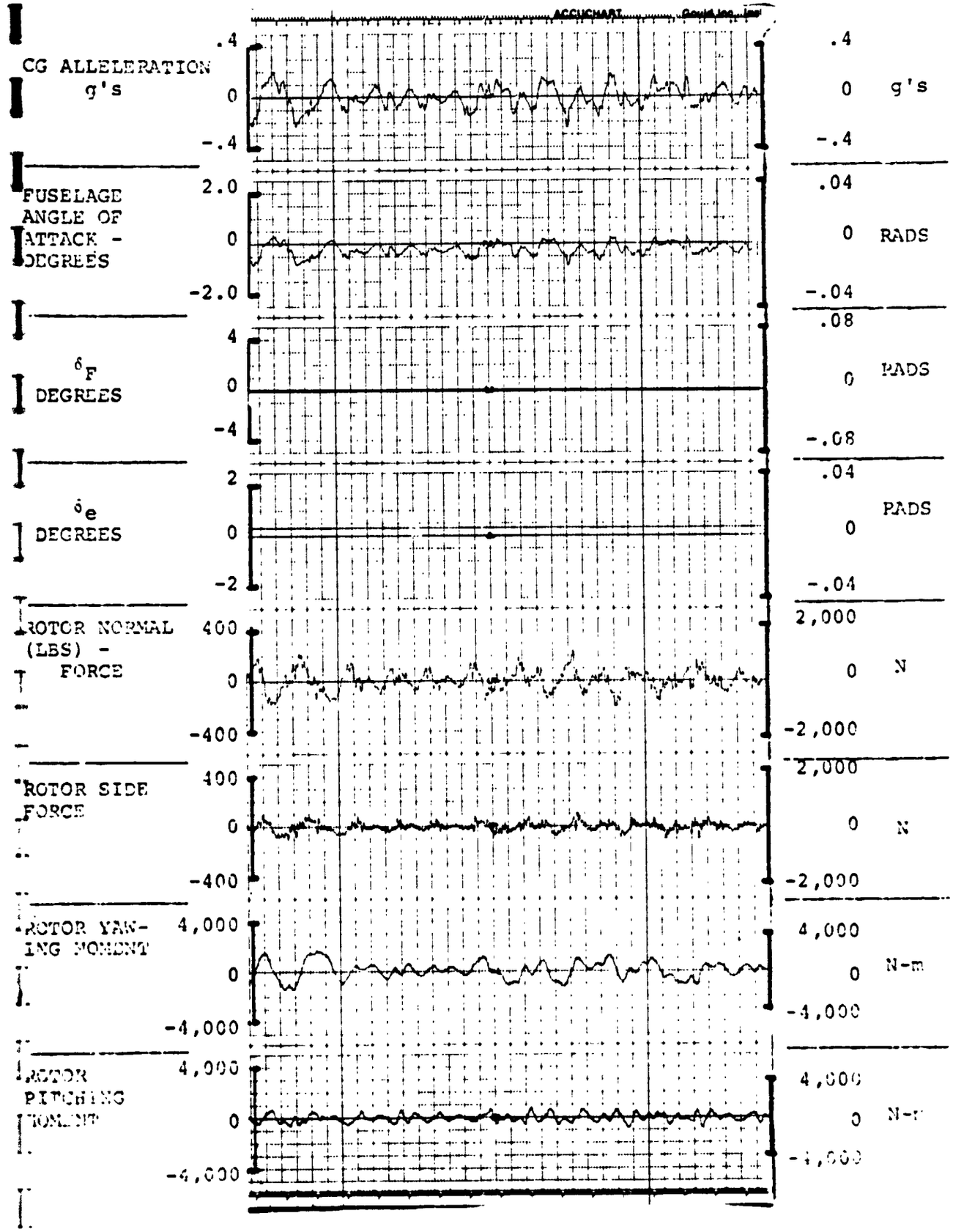

FIGURE 4.7.2.0.0.1. RESPONSES FOR GAIN F = 0, GAIN E = 0

FLIGHT CONDITION: 280 KNOTS, 5,000 FEET, (1,524m), AFT CG

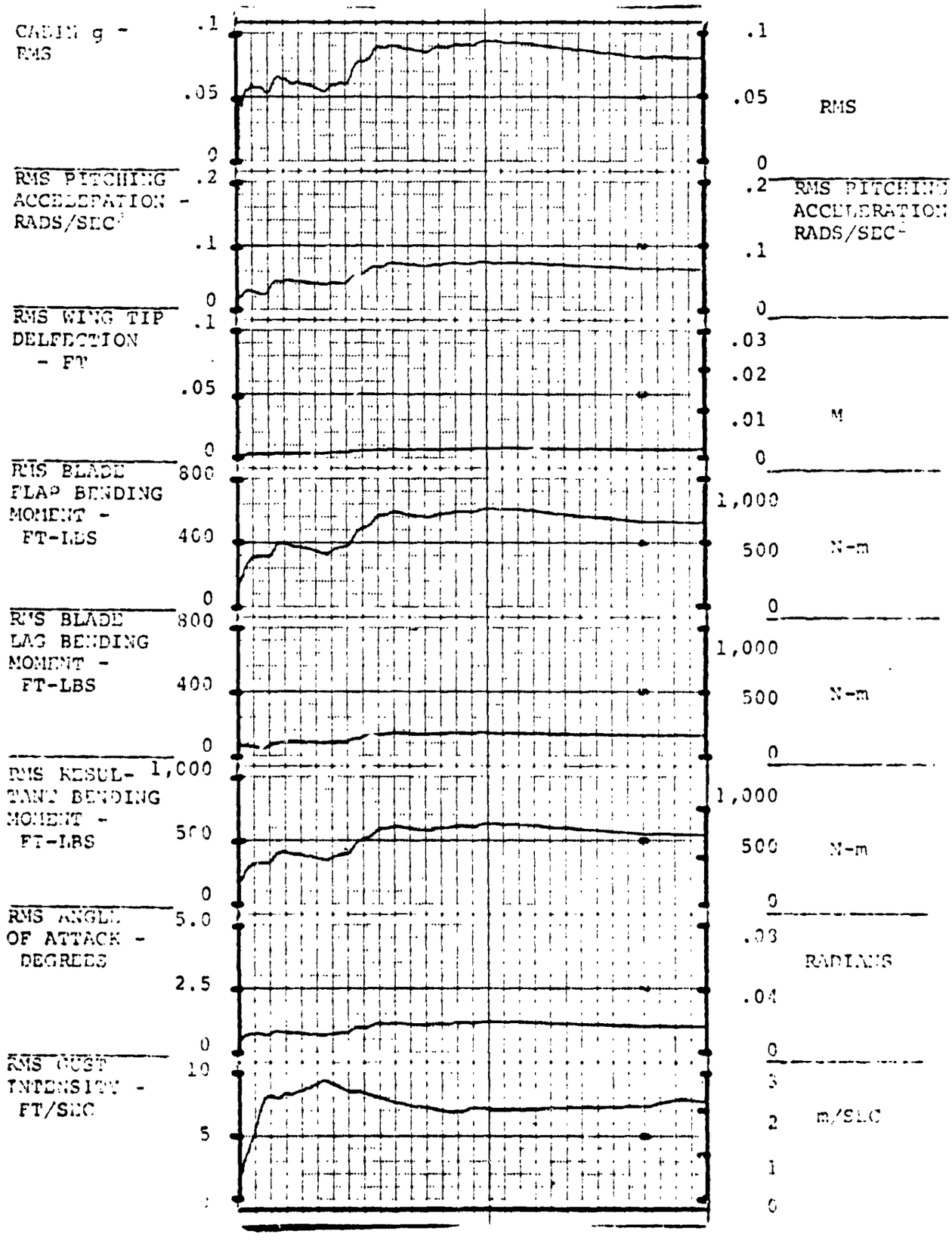

FIGURE 5.7.2.0.0.1. RESPONSES FOR GAIN F = 0, GAIN E = 0

FLIGHT CONDITION: 280 KNOTS, 5,000 FEET, (1,524m), AFT CG

ORIGINAL PAGE IS
OF POOR QUALITY

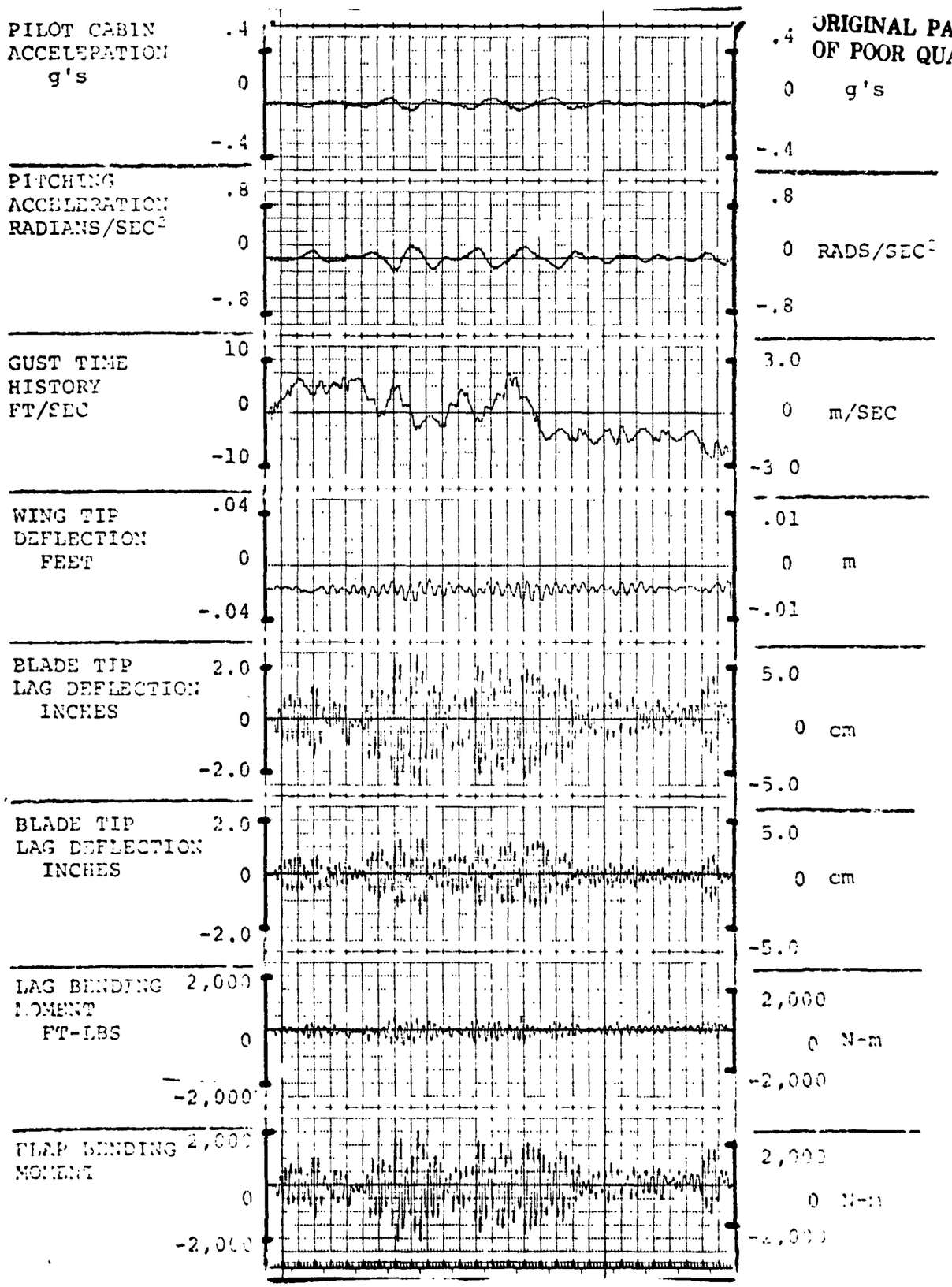

FIGURE 3.7.2.0.0.2. RESPONSES FOR GAIN F = 4.0, GAIN E = .6

FLIGHT CONDITION: 280 KNOTS, 5,000 FEET, (1,524m), AFT CG

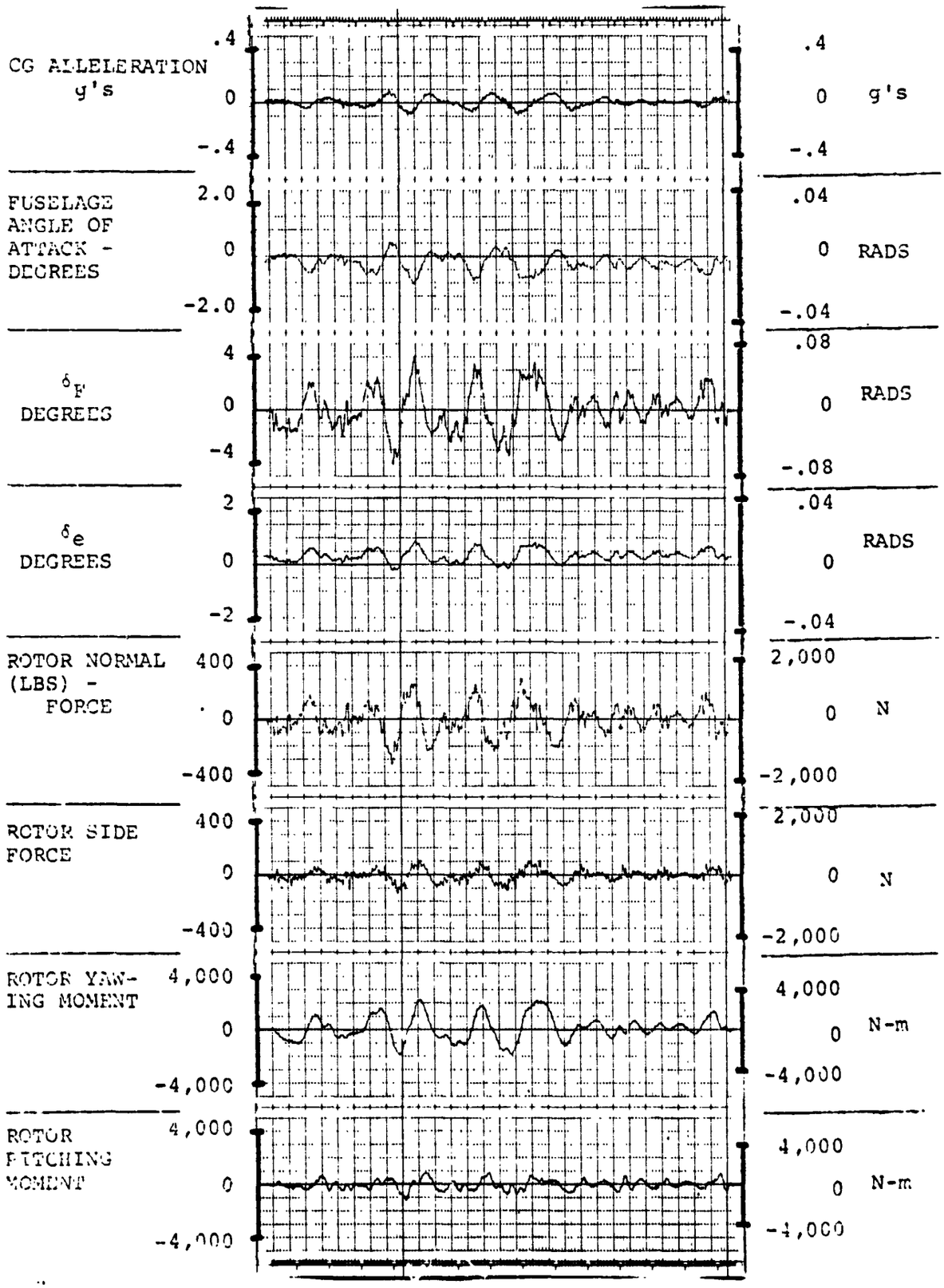

FIGURE 4.7.2.0.0.2. RESPONSES FOR GAIN F = 4.0, GAIN E = .6

FLIGHT CONDITION: 280 KNOTS, 5,000 FEET, (1,524m), AFT CG

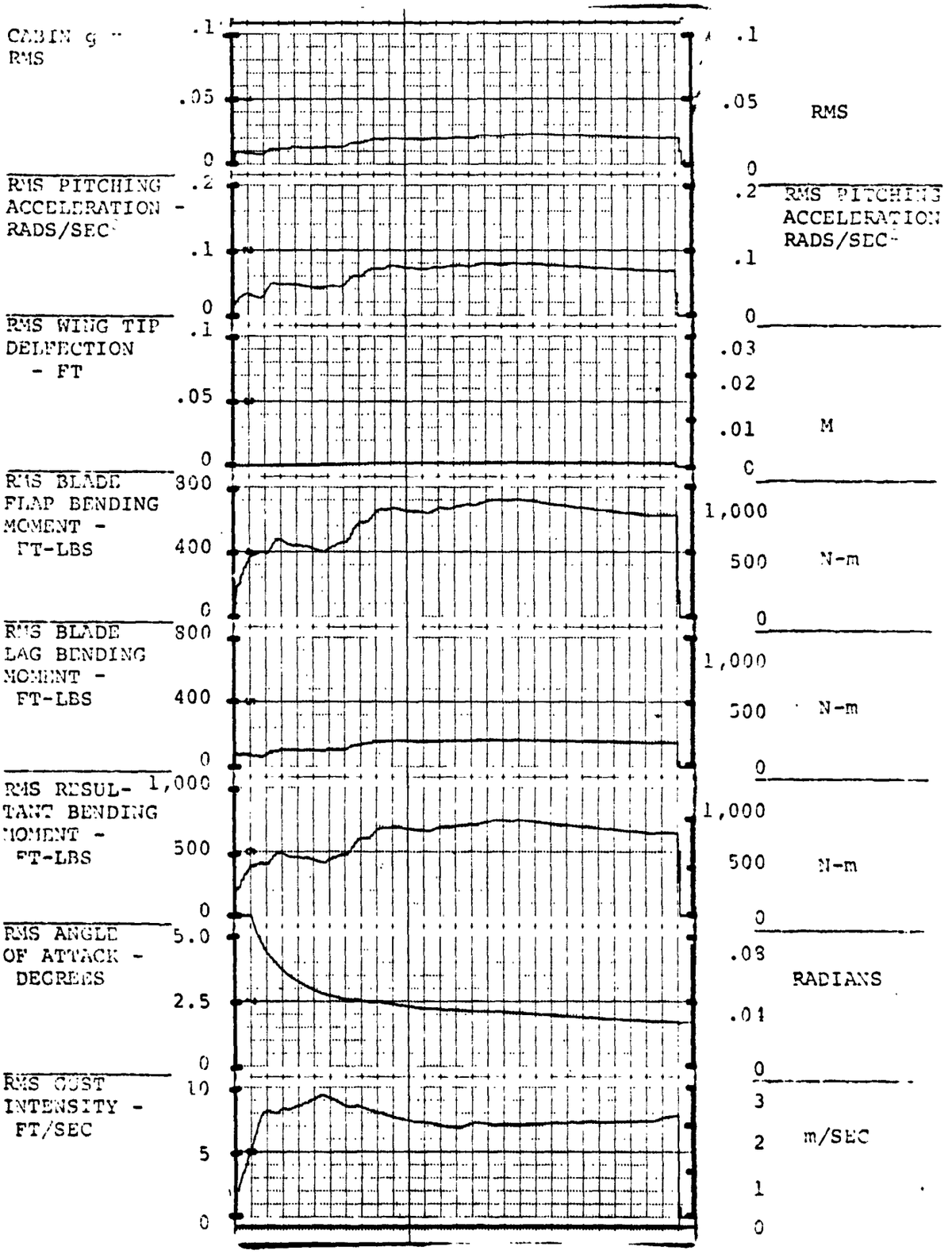

FIGURE 5.7.2.0.0.2. RESPONSES FOR GAIN F = 4.0, GAIN E = .6

FLIGHT CONDITION: 280 KNOTS, 5,000 FEET, (1,524m), AFT CG

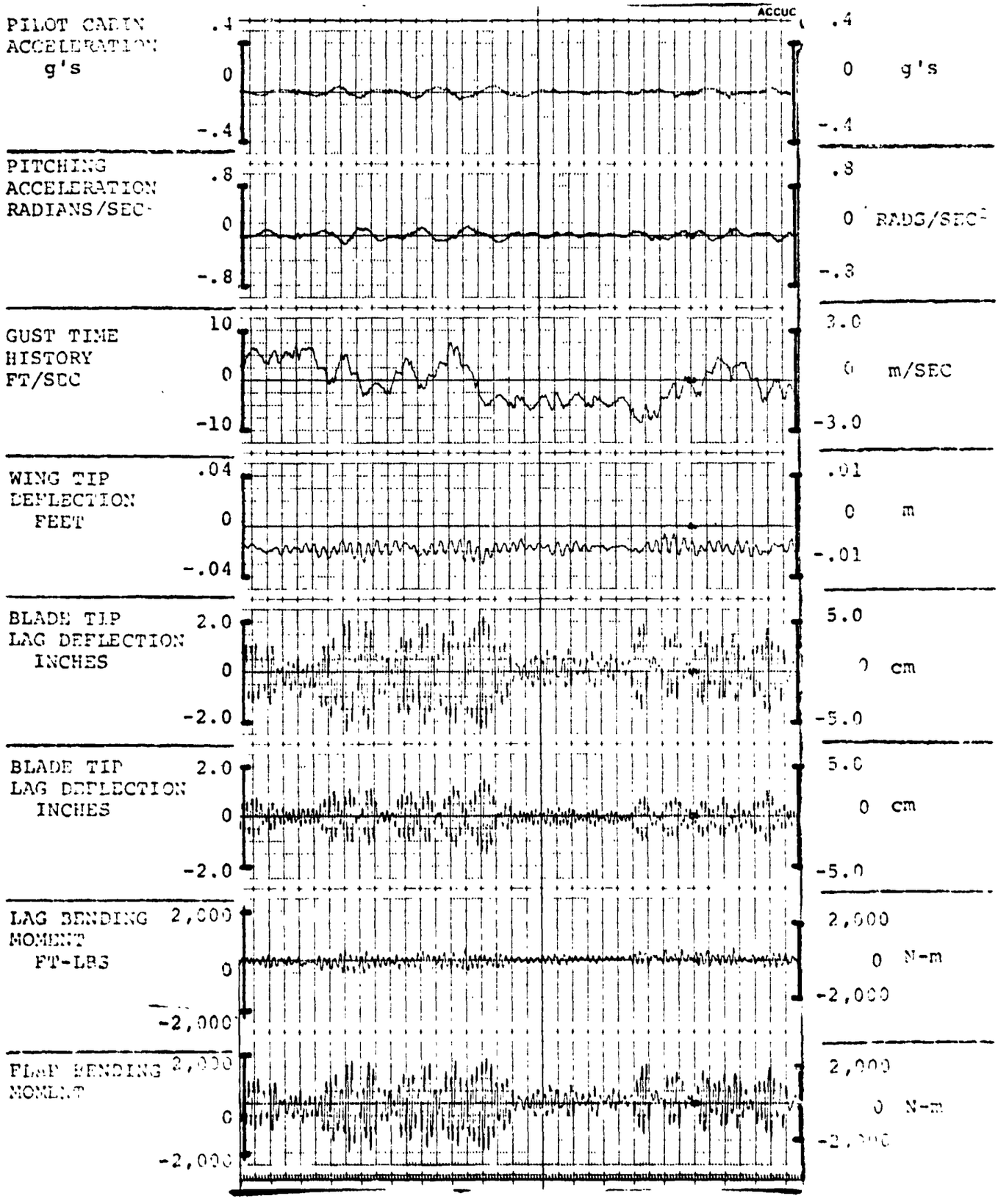

FIGURE 3.7.2.0.0.3. RESPONSES FOR GAIN F = 4.0, GAIN E = .7

FLIGHT CONDITION: 280 KNOTS, 5,000 FEET, (1,524m), AFT CG

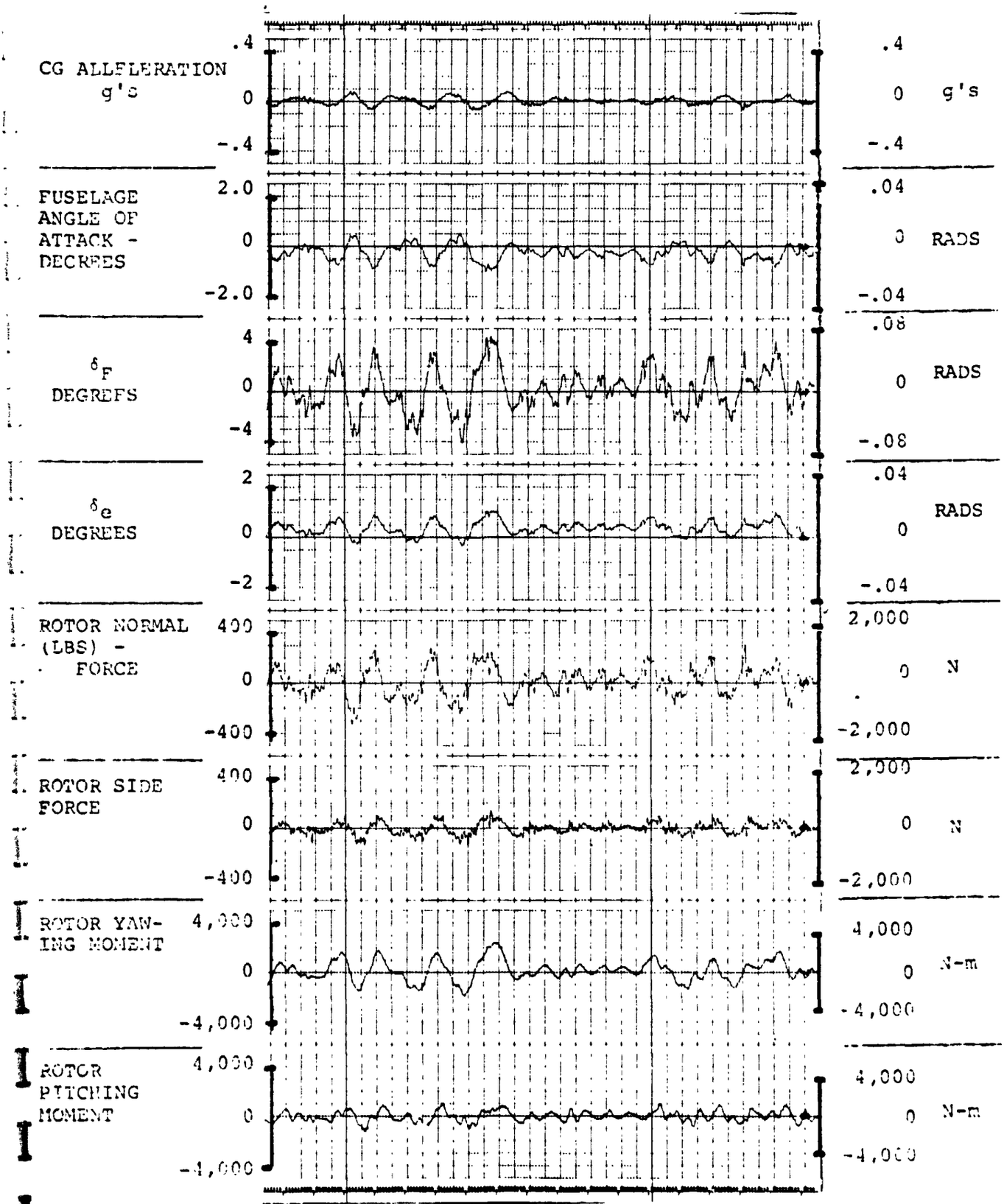

FIGURE 4.7.2.0.0.3. RESPONSES FOR GAIN F = 4.0, GAIN E = .7

FLIGHT CONDITION: 280 KNOTS, 5,000 FEET, (1,524m), AFT CG

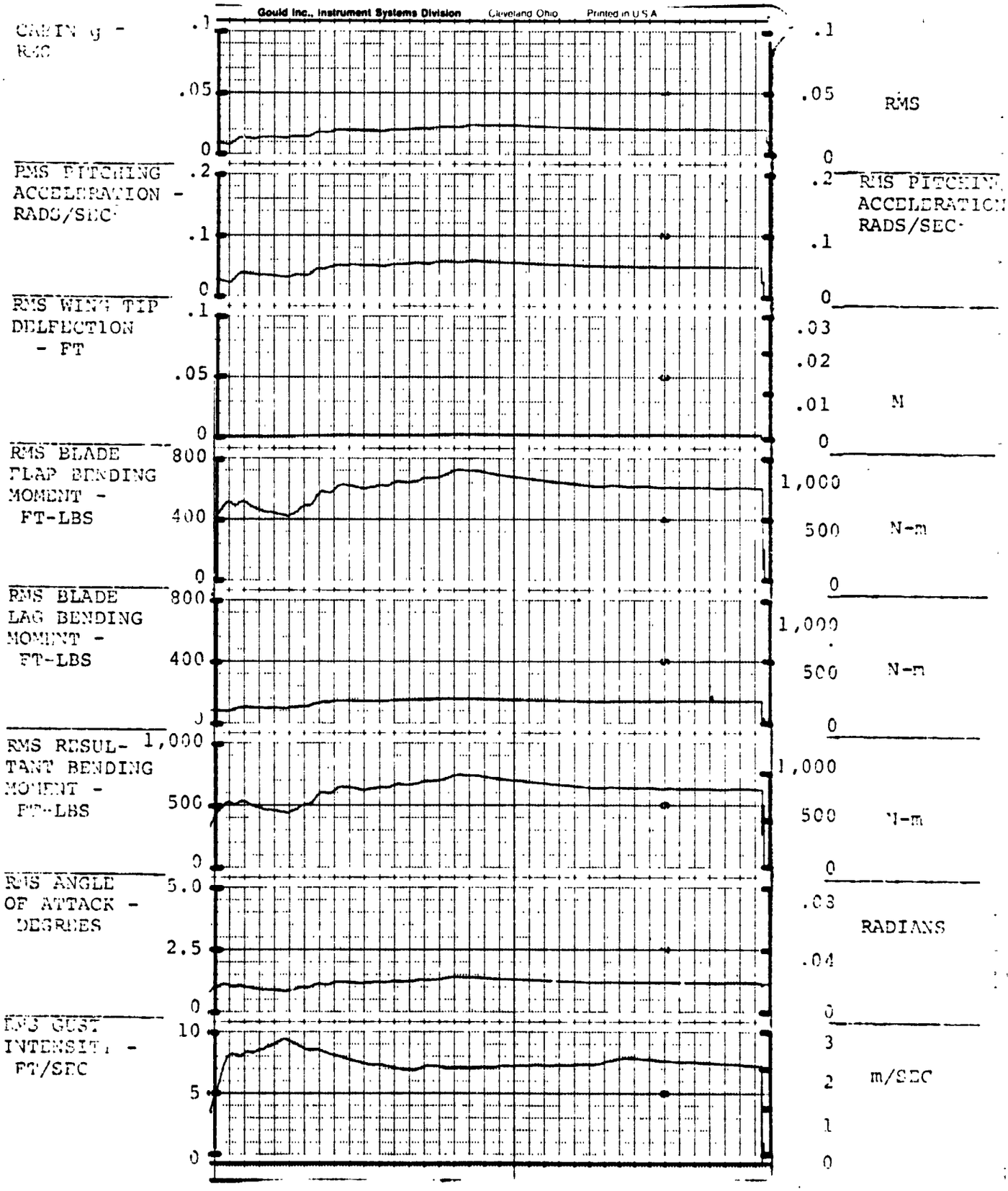

FIGURE 5.7.2.0.0.3. RESPONSES FOR GAIN F = 4.0, GAIN E = .7

AIV.210

FLIGHT CONDITION: 280 KNOTS, 5,000 FEET, (1,524m), FORWARD CG

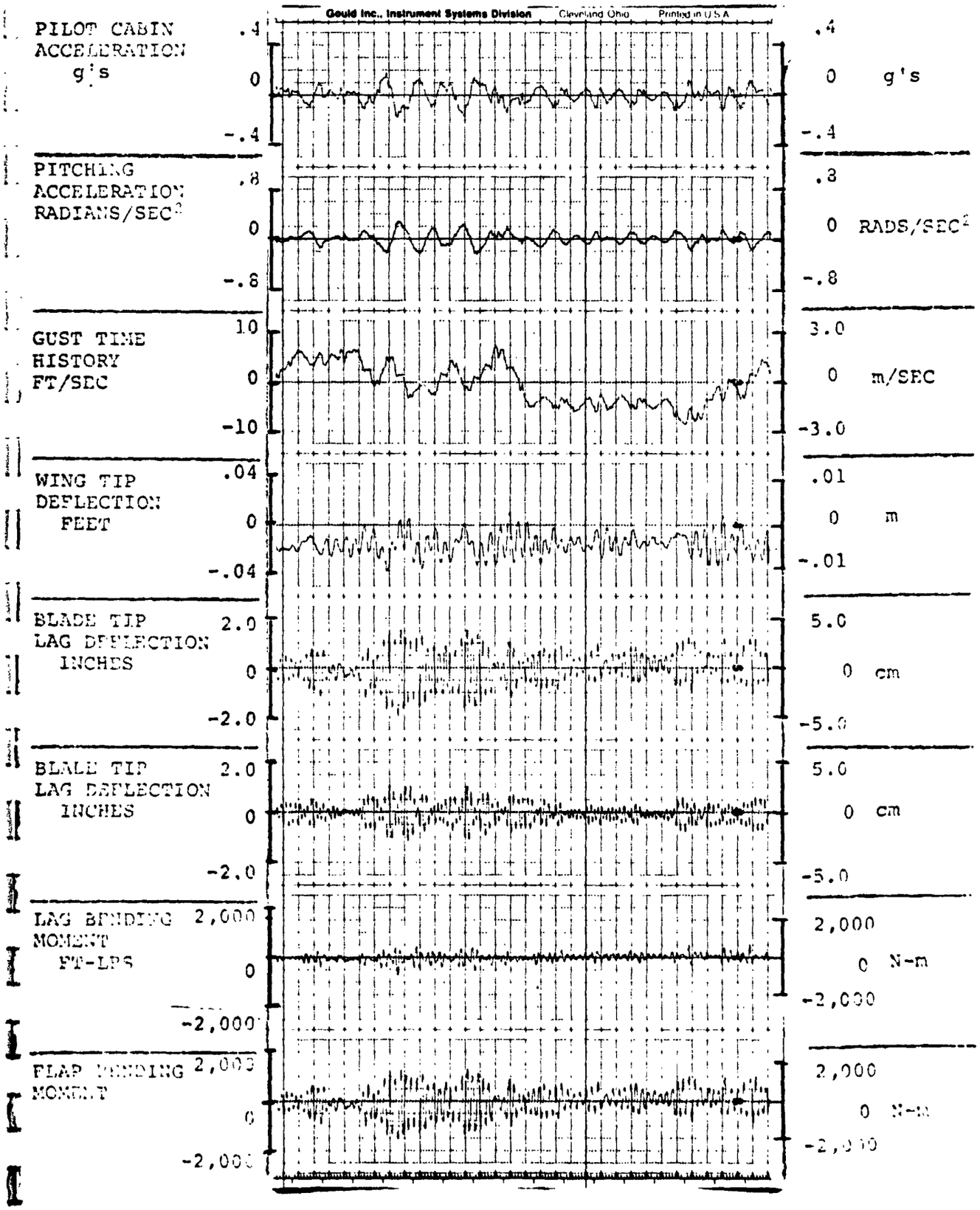

FIGURE 3.7.1.0.0.1. RESPONSES FOR GAIN F = 0, GAIN E = 0

FLIGHT CONDITION: 280 KNOTS, 5,000 FEET, (1,524m), FORWARD CG

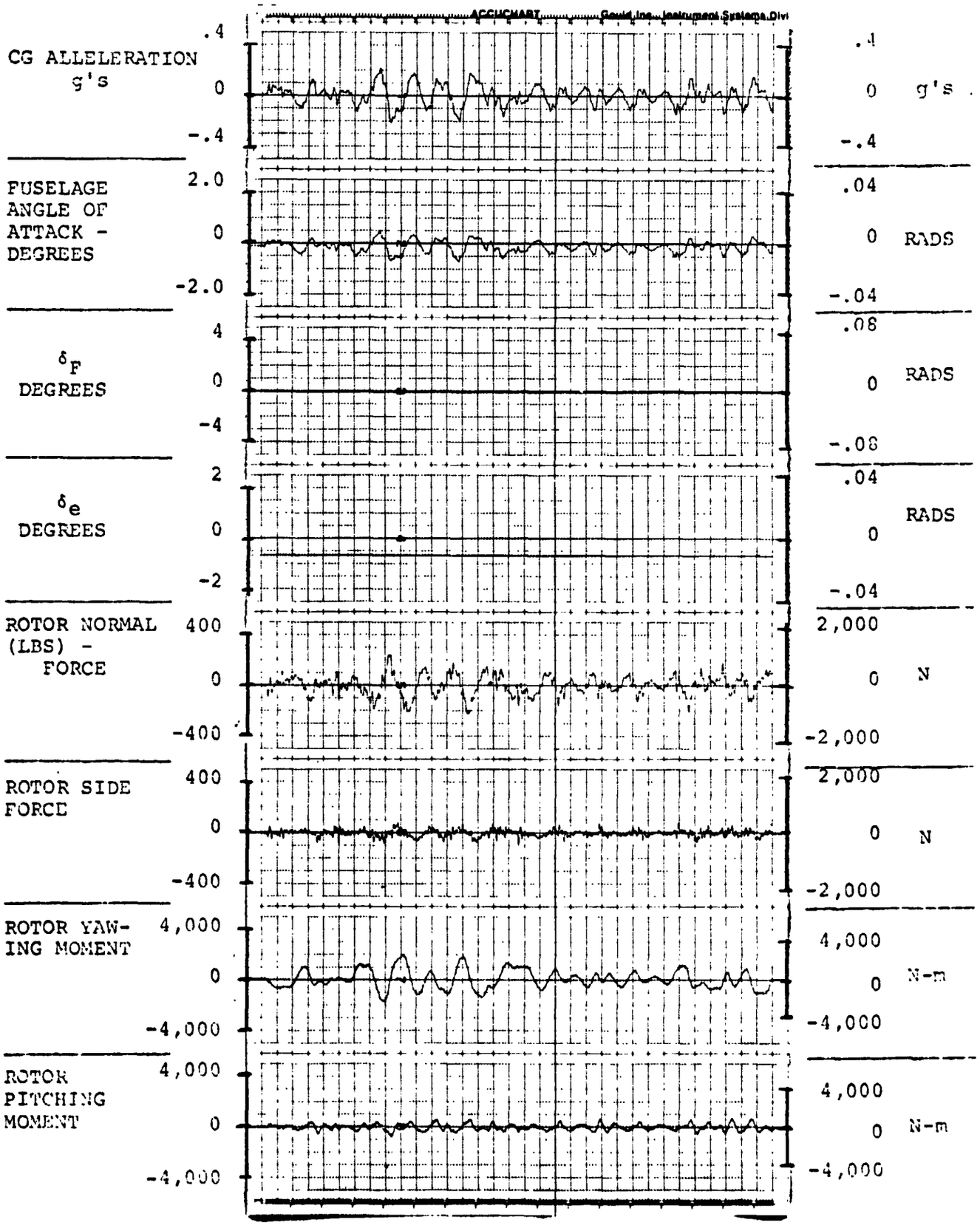

FIGURE 4.7.1.0.0.1. RESPONSES FOR GAIN F = 0, GAIN E = 0

ORIGINAL PAGE IS OF POOR QUALITY

FLIGHT CONDITION: 280 KNOTS, 5,000 FEET, (1,524m), FORWARD CG

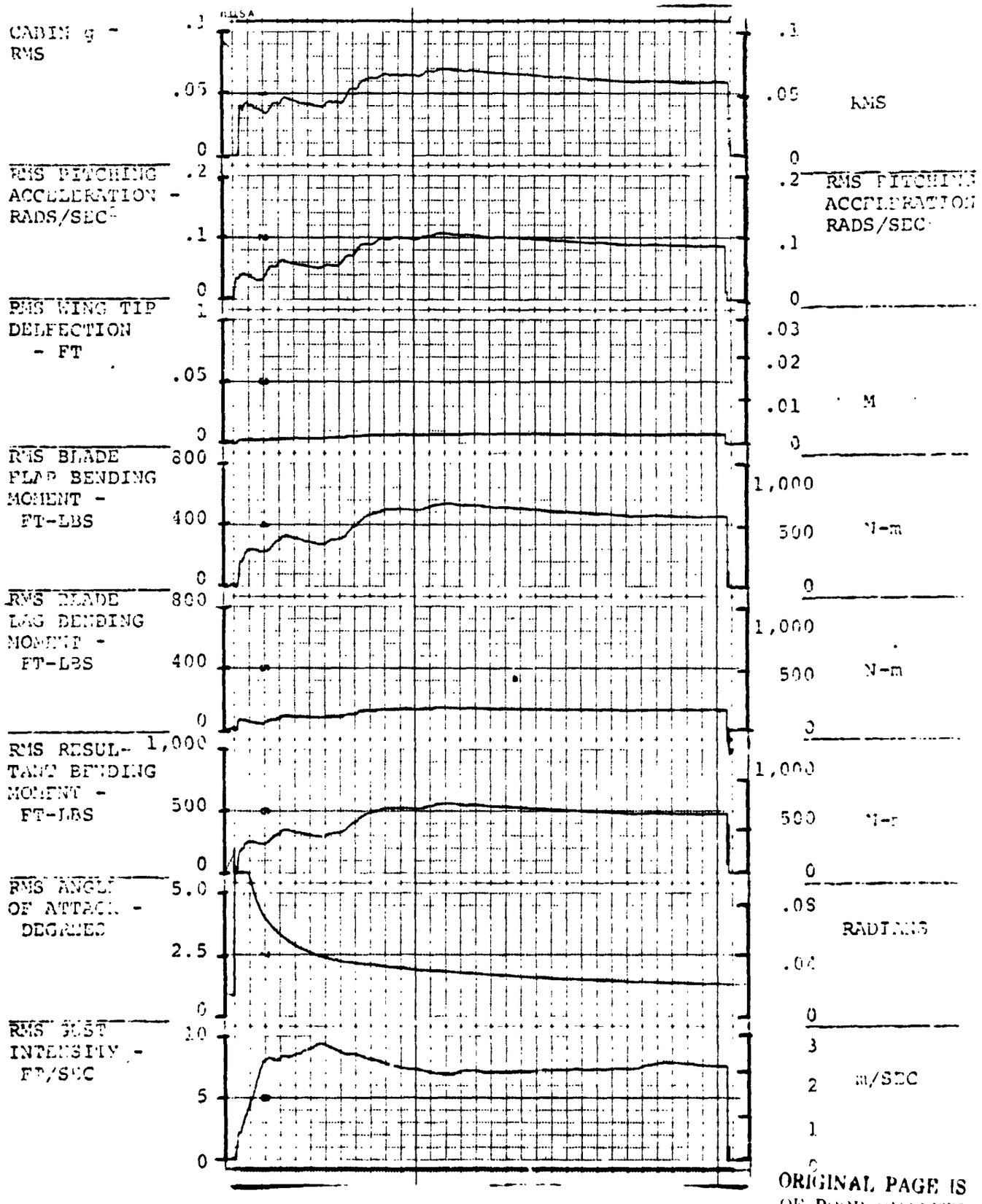

ORIGINAL PAGE IS OF POOR QUALITY

FIGURE 5.7.1.0.0.1. RESPONSES FOR GAIN F = 0, GAIN E = 0

FLIGHT CONDITION: 280 KNOTS, 5,000 FEET, (1,524m), FORWARD CG

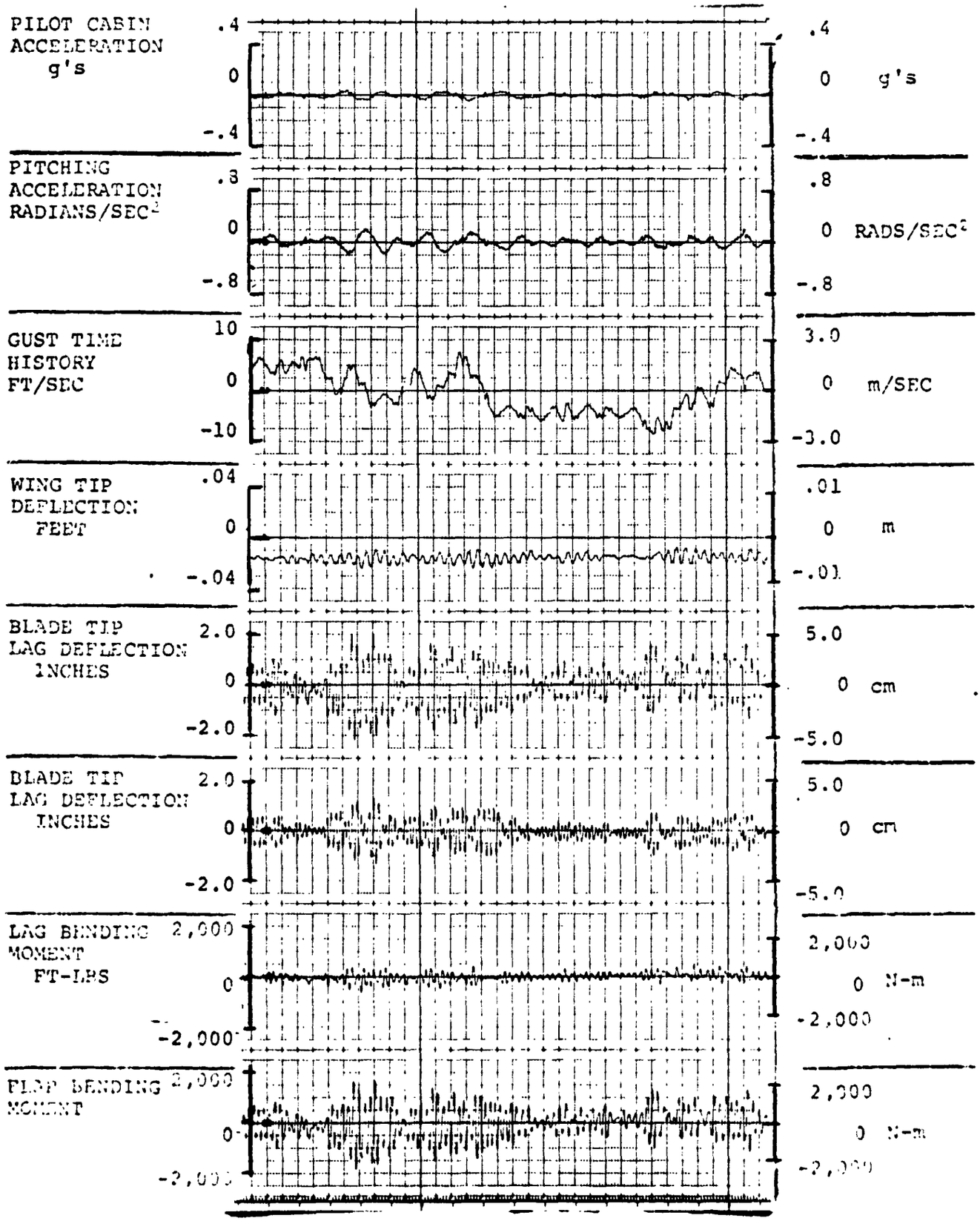

FIGURE 3.7.1.0.0.2. RESPONSES FOR GAIN F = 4.0, GAIN E = .6

FLIGHT CONDITION: 280 KNOTS, 5,000 FEET, (1,524m), FORWARD CG

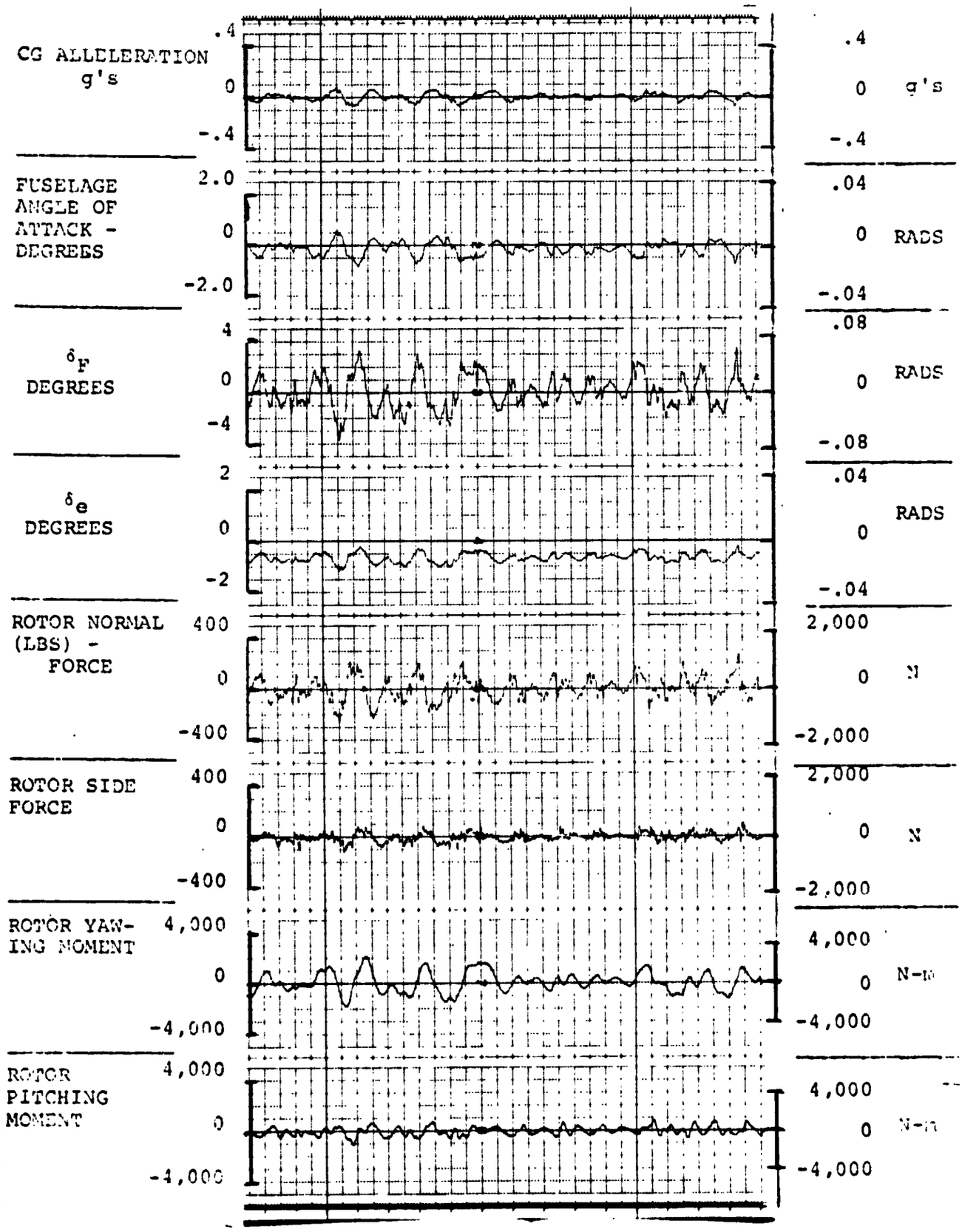

FIGURE 4.7.1.0.0.2. RESPONSES FOR GAIN F = 4.0, GAIN E = .6

FLIGHT CONDITION: 280 KNOTS, 5,000 FEET, (1,524m), FORWARD CG

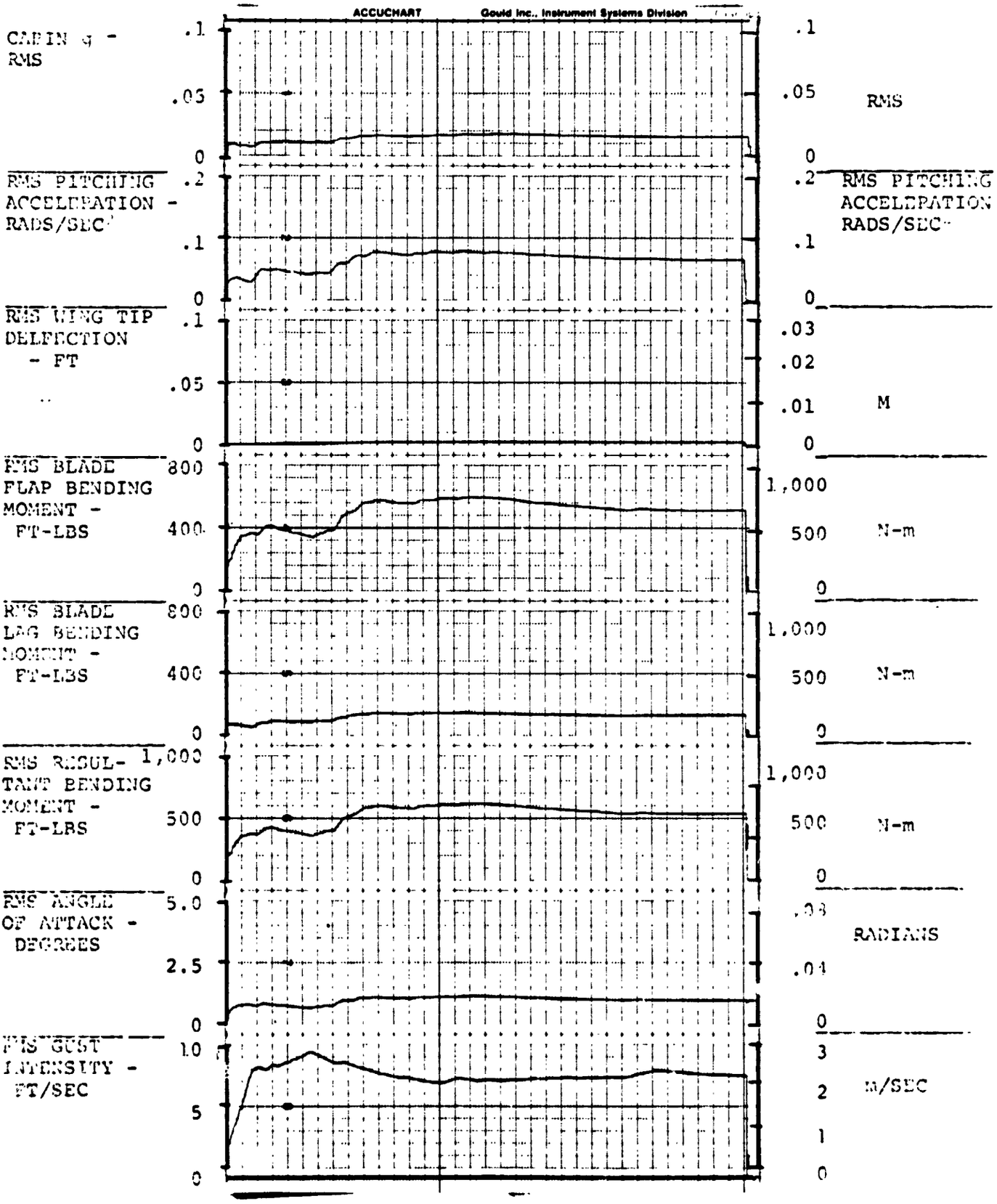

FIGURE 5.7.1.0.0.2. RESPONSES FOR GAIN F = 4.0, GAIN E = .6

FLIGHT CONDITION: 280 KNOTS, 5,000 FEET, (1,524m), FORWARD CG

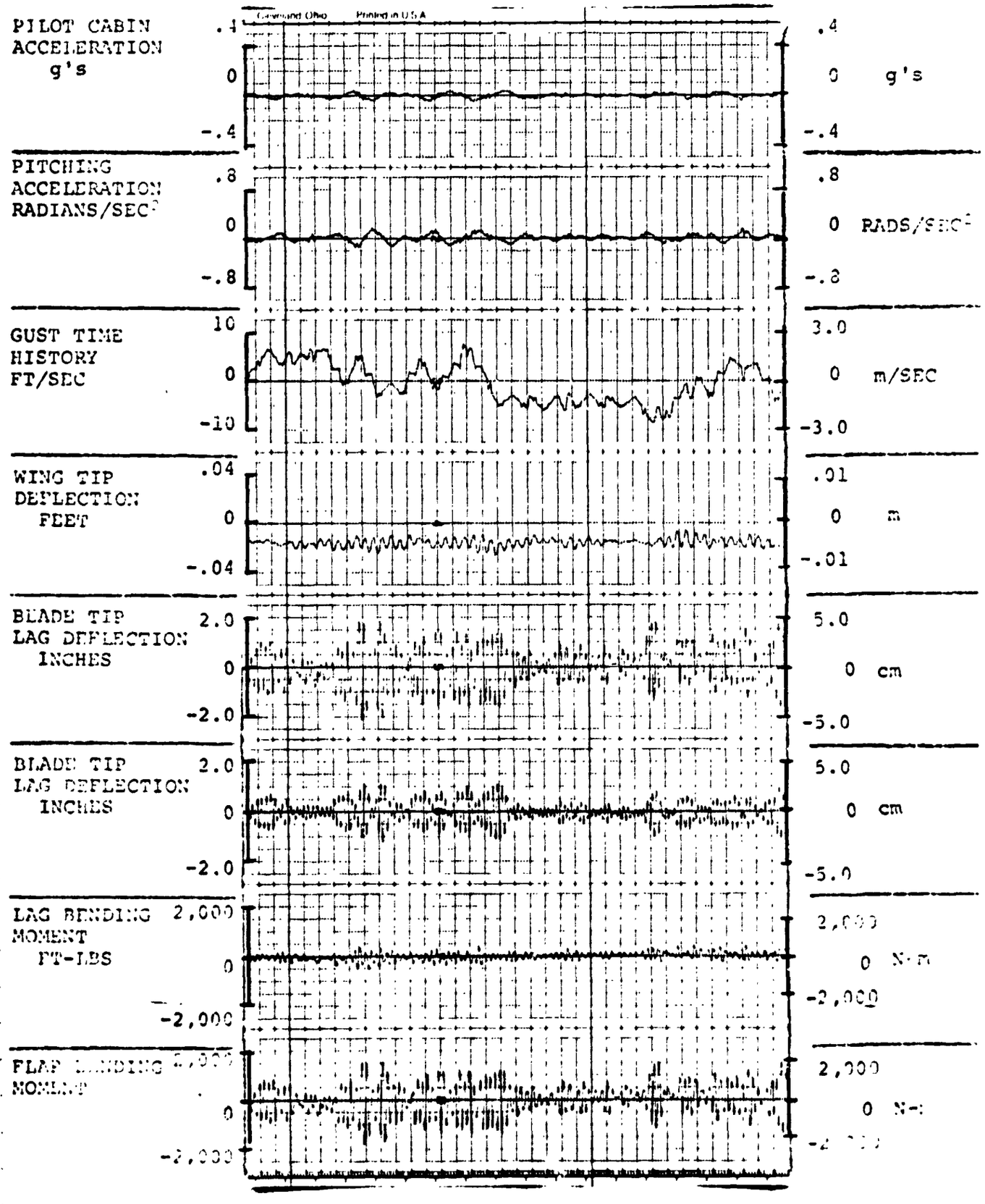

FIGURE 3.7.1.0.0.3. RESPONSES FOR GAIN F = 4.0, GAIN E = .7

FLIGHT CONDITION: 280 KNOTS, 5,000 FEET, (1,524m), FORWARD CG

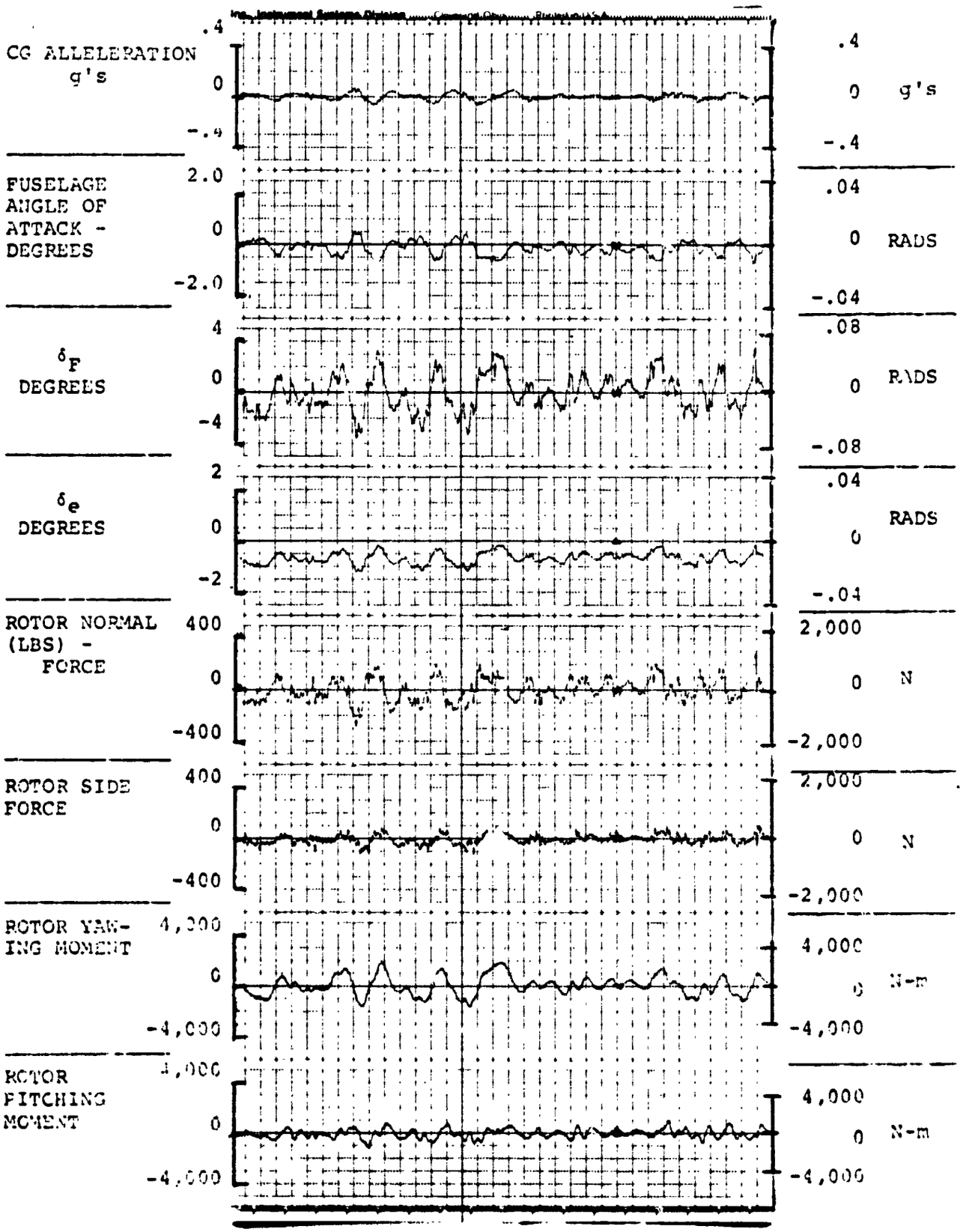

FIGURE 4.7...0.0.3. RESPONSES FOR GAIN F = 4.0, GAIN E = .7

FLIGHT CONDITION: 280 KNOTS, 5,000 FEET, (1,524m), FORWARD CG

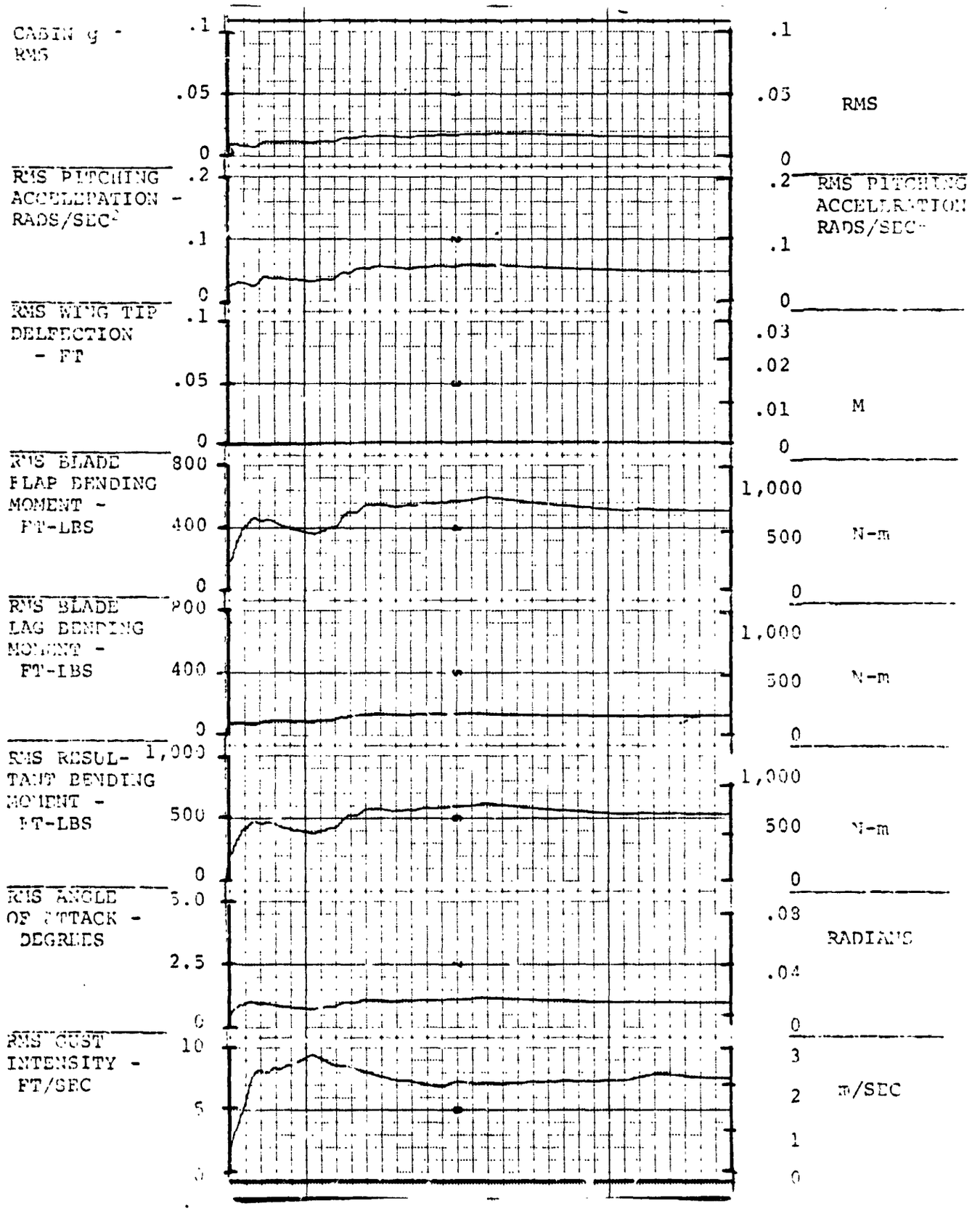

FIGURE 5.7.1.0.0.3. RESPONSES FOR GAIN F = 4.0, GAIN E = .7

ORIGINAL PAGE IS OF POOR QUALITY

FLIGHT CONDITION: 280 KNOTS, 10,000 FEET, (3,049m), FORWARD CG

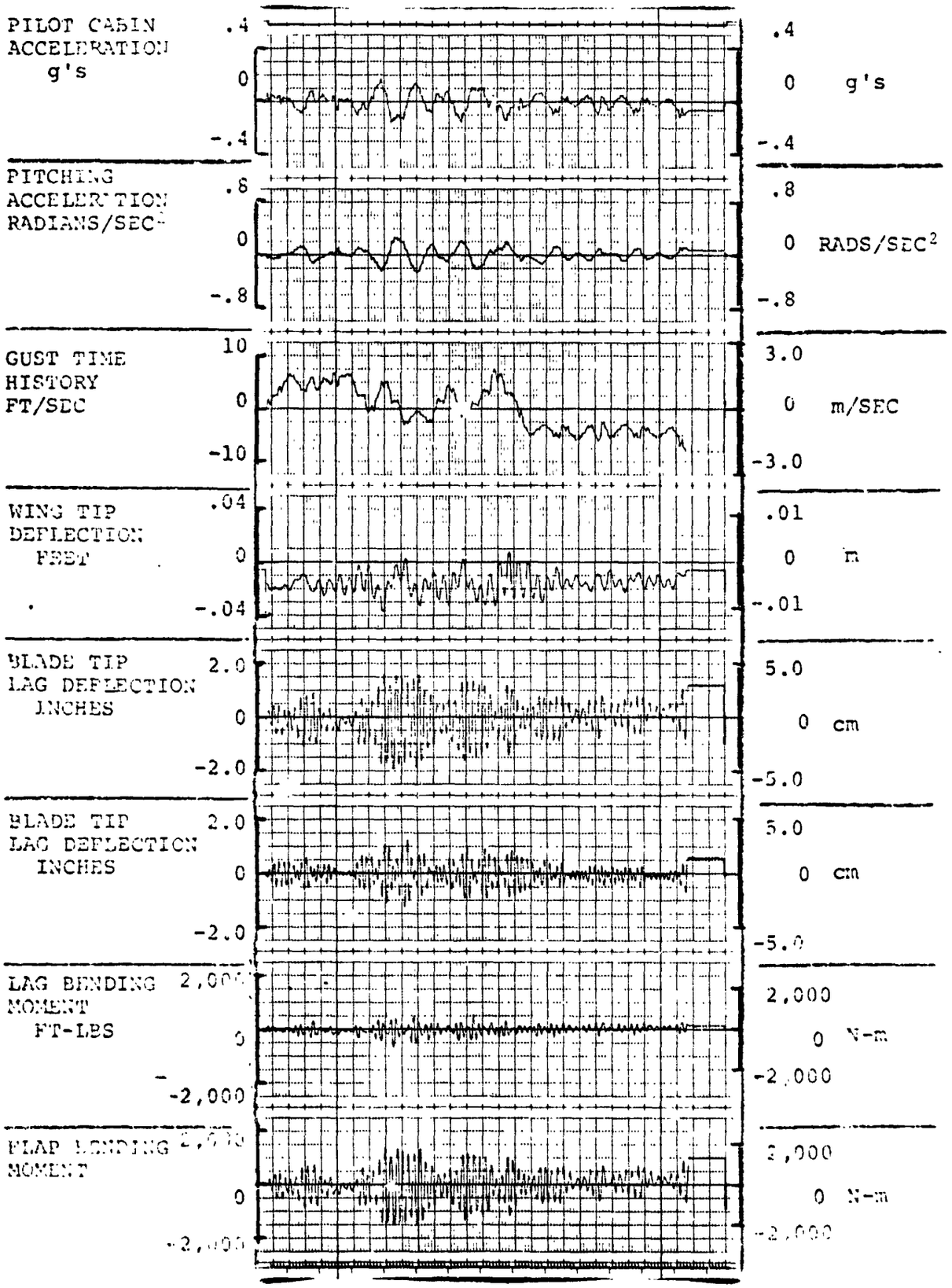

FIGURE 3.8.1.0.0.1. RESPONSES FOR GAIN F = 0, GAIN E = 0

FLIGHT CONDITION: 280 KNOTS, 10,000 FEET, (3,049m), FORWARD CG

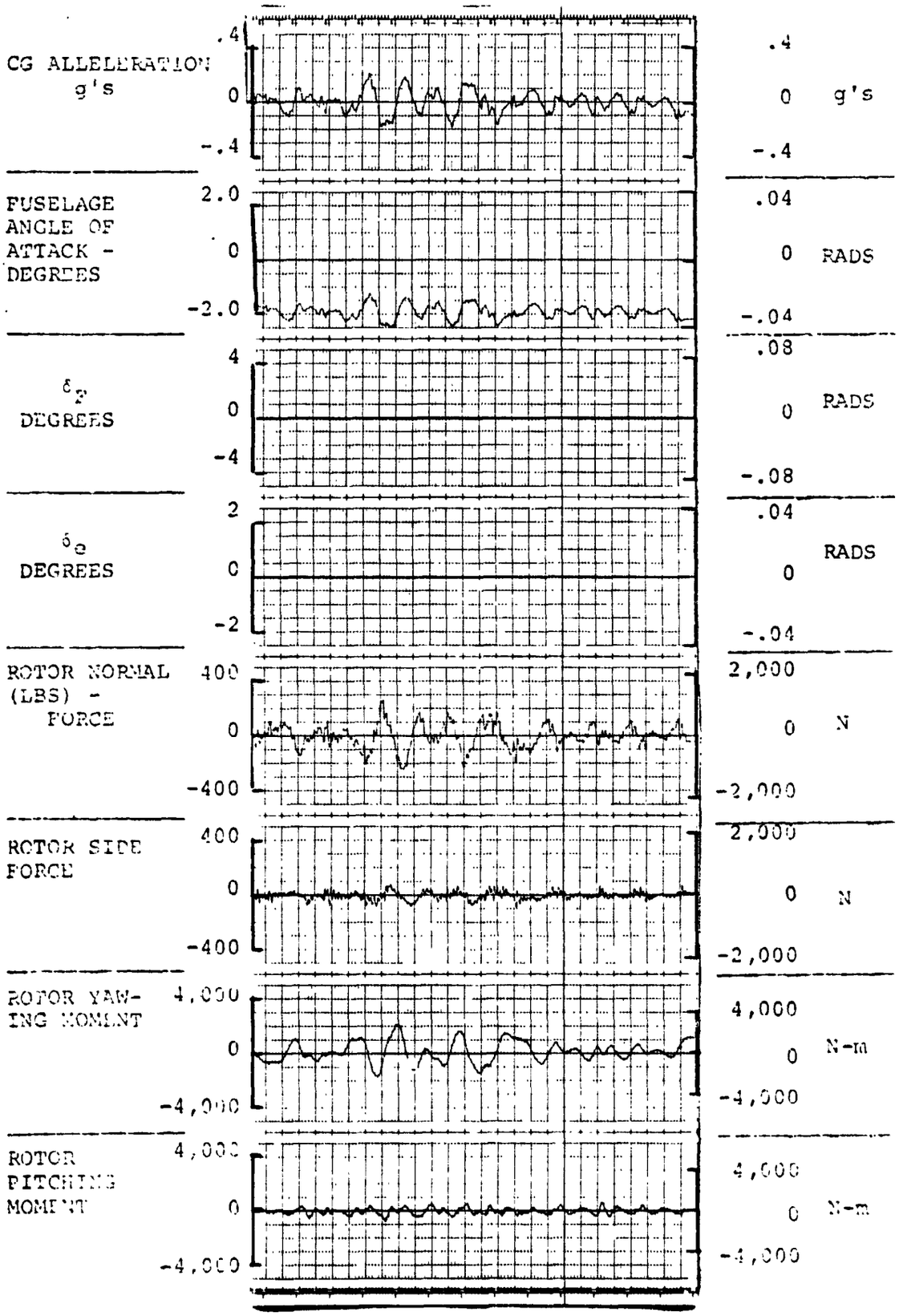

FIGURE 4.8.1.0.0.1. RESPONSES FOR GAIN F = 0, GAIN E = 0

FLIGHT CONDITION: 280 KNOTS, 10,000 FEET, (3,049m), FORWARD CG

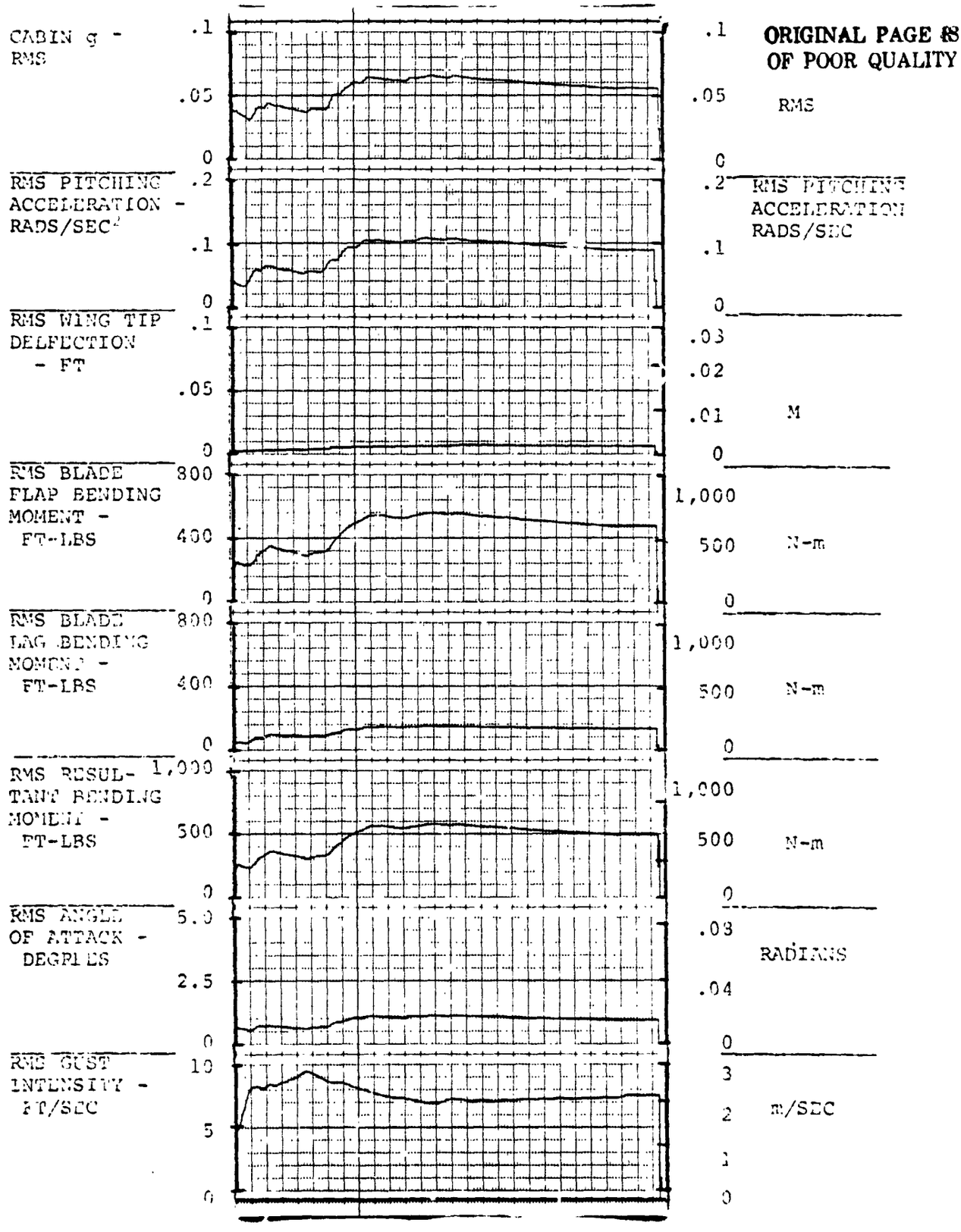

ORIGINAL PAGE IS OF POOR QUALITY

FIGURE 5.8.1.0.0.1. RESPONSES FOR GAIN F = 0, GAIN E = 0

FLIGHT CONDITION: 280 KNOTS, 10,000 FEET, (3,049m), FORWARD CG

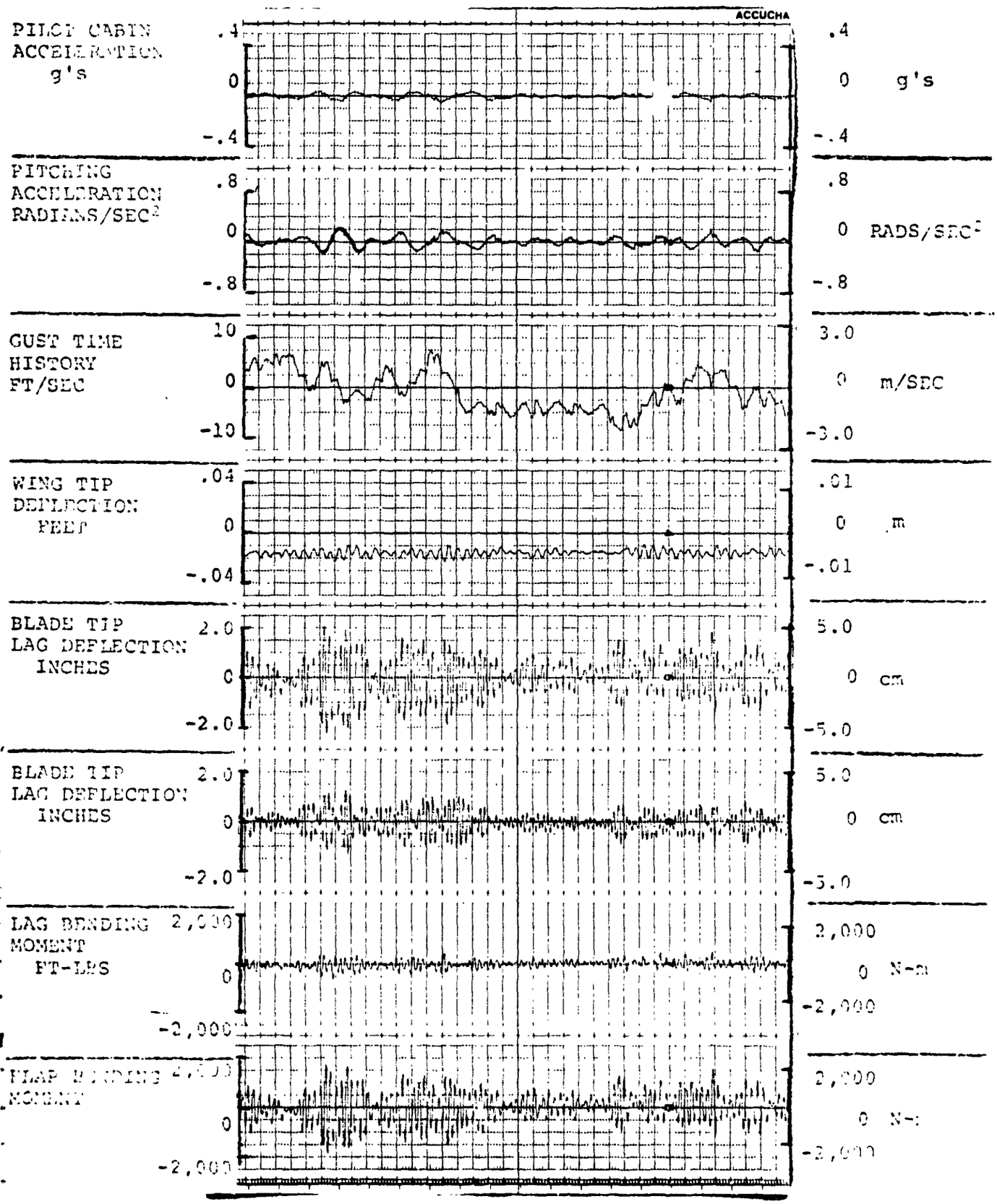

FIGURE 3.8.1.0.0.2. RESPONSES FOR GAIN F = 4.0, GAIN E = .6

ORIGINAL PAGE IS OF POOR QUALITY

FLIGHT CONDITION: 280 KNOTS, 10,000 FEET, (3,049m), FORWARD CG

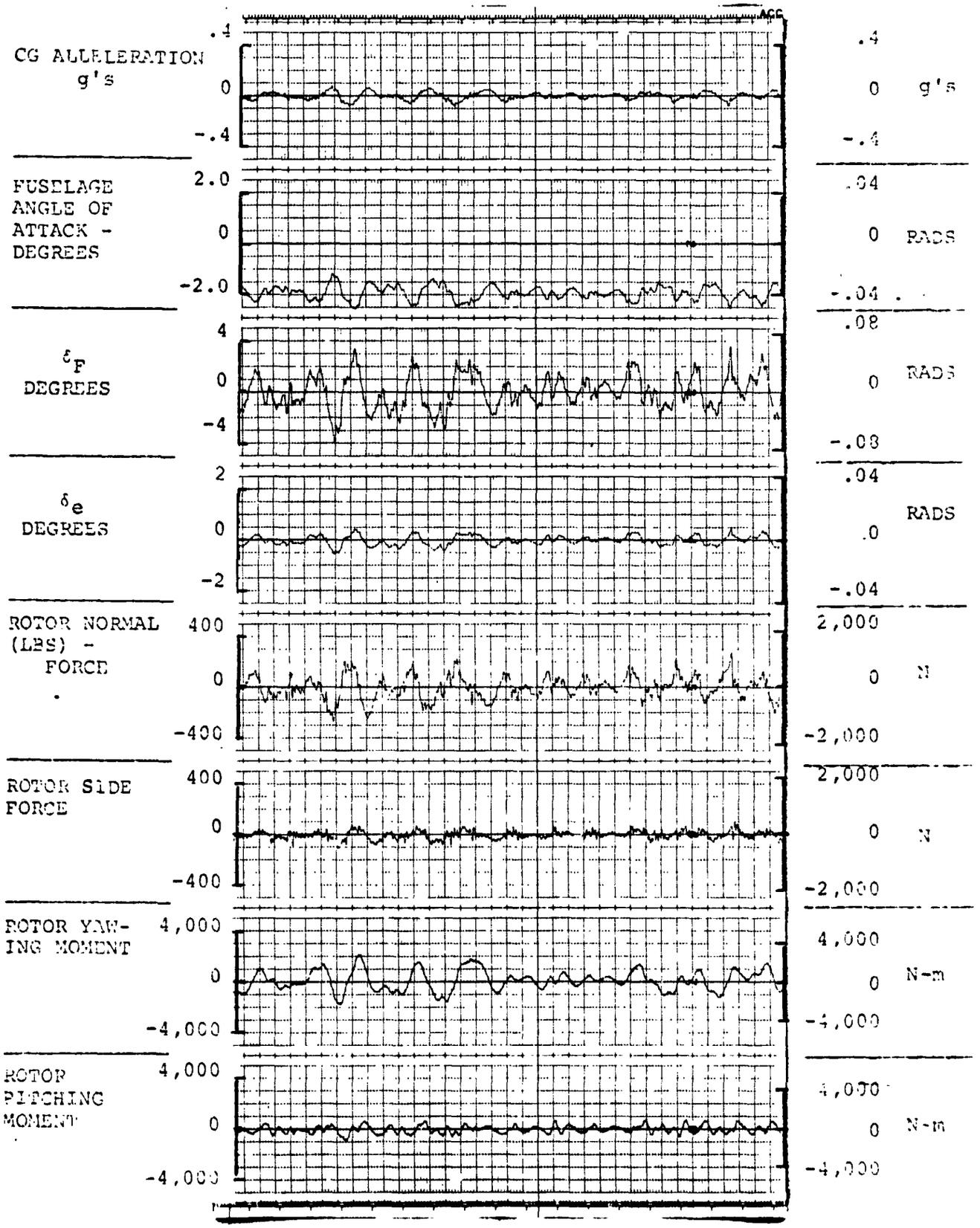

FIGURE 4.8.1.0.0.2. RESPONSES FOR GAIN F = 4.0, GAIN E = .6

FLIGHT CONDITION: 280 KNOTS, 10,000 FEET, (3,049m), FORWARD CG

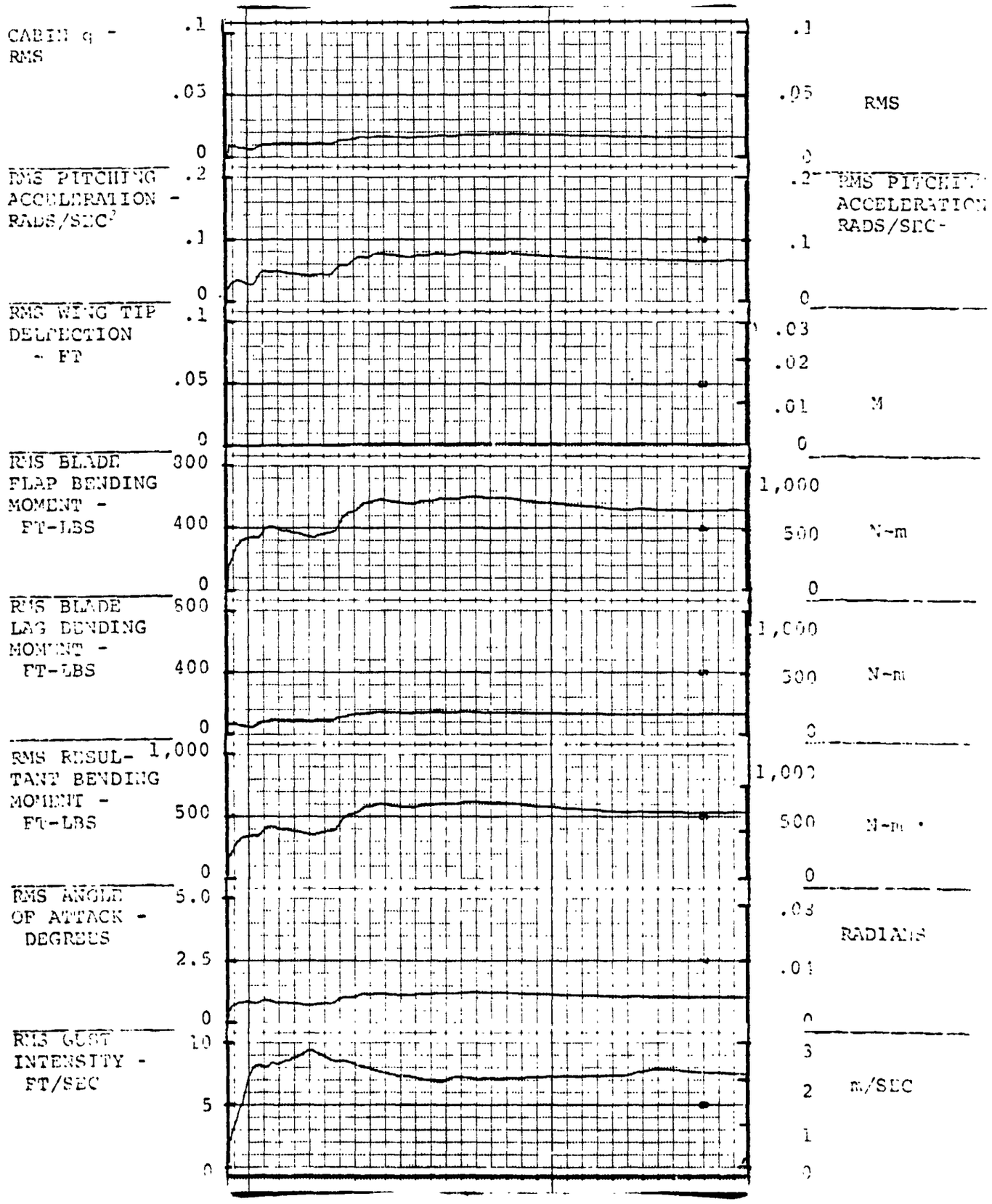

FIGURE 5.8.1.0.0.2. RESPONSES FOR GAIN F = 4.0, GAIN F = .6

ORIGINAL PAGE IS OF POOR QUALITY

FLIGHT CONDITION: 280 KNOTS, 10,000 FEET, (3,049m), FORWARD CG

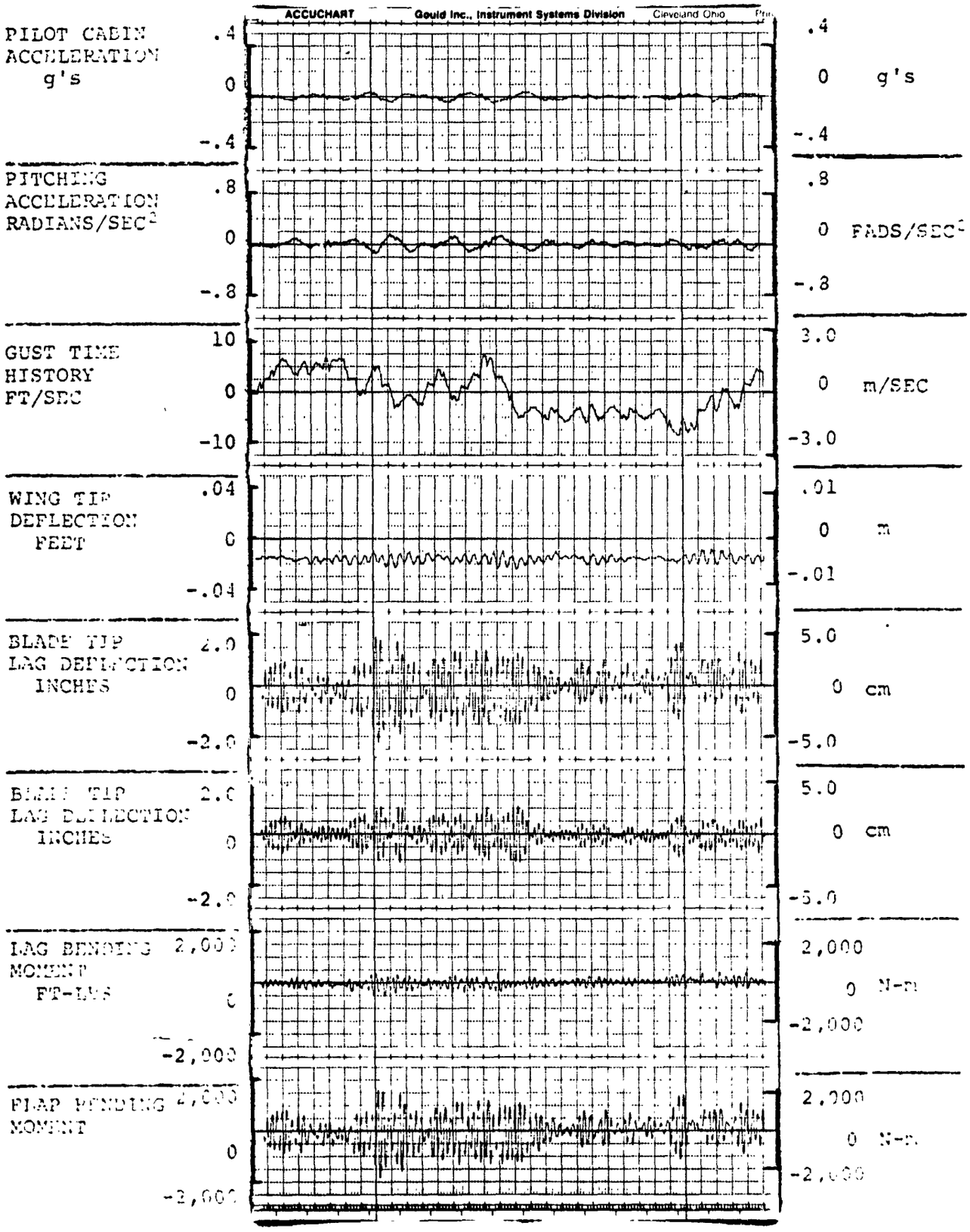

FIGURE 3.8.1.0.0.3. RESPONSES FOR GAIN F = 4.0, GAIN E = .7

FLIGHT CONDITION: 280 KNOTS, 10,000 FEET, (3,049m), FORWARD CG

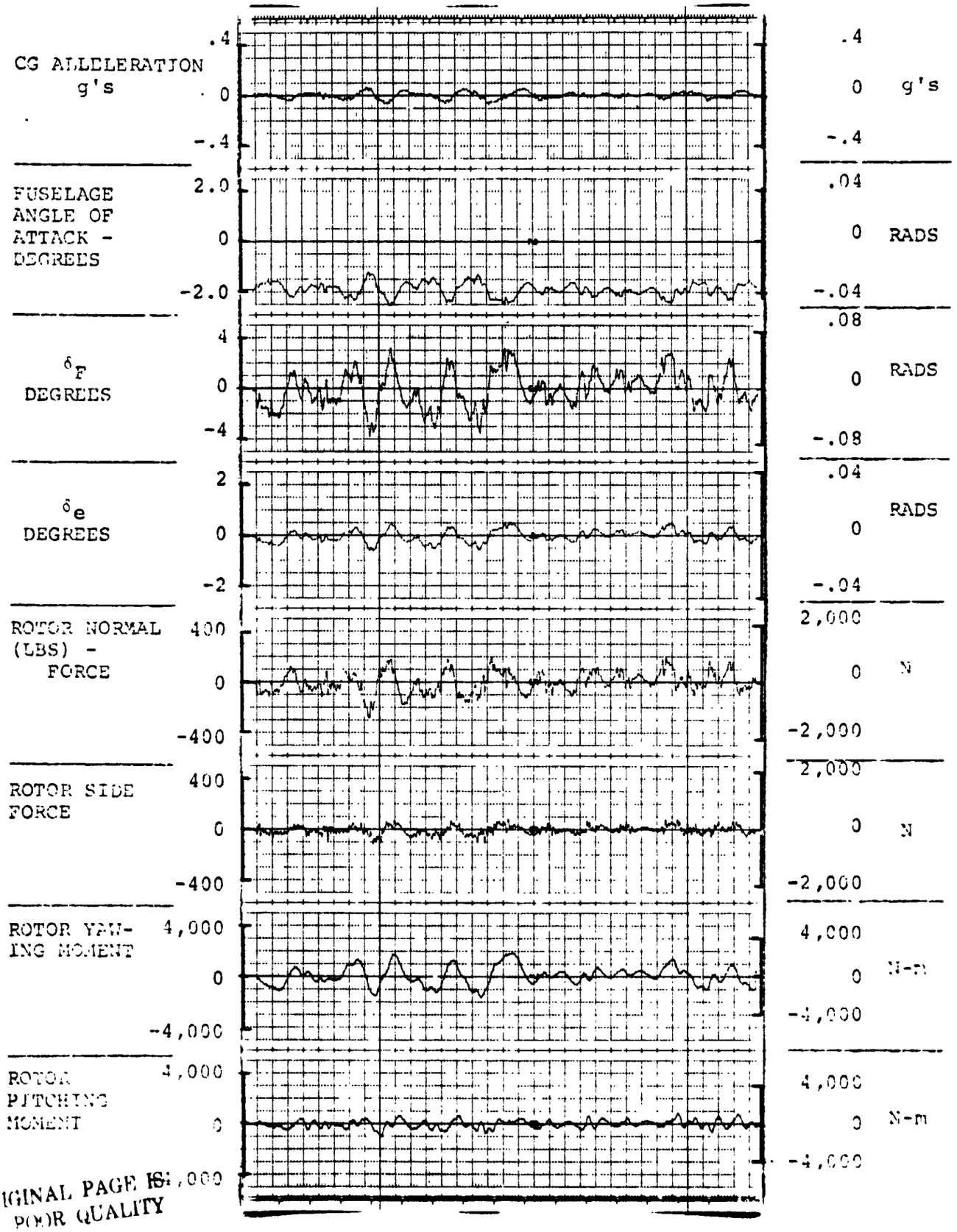

ORIGINAL PAGE IS
POOR QUALITY

FIGURE 4.8.1.0.0.3. RESPONSES FOR GAIN F = 4.0, GAIN E = .7

FLIGHT CONDITION: 280 KNOTS, 10,000 FEET, (3,049m), FORWARD CG

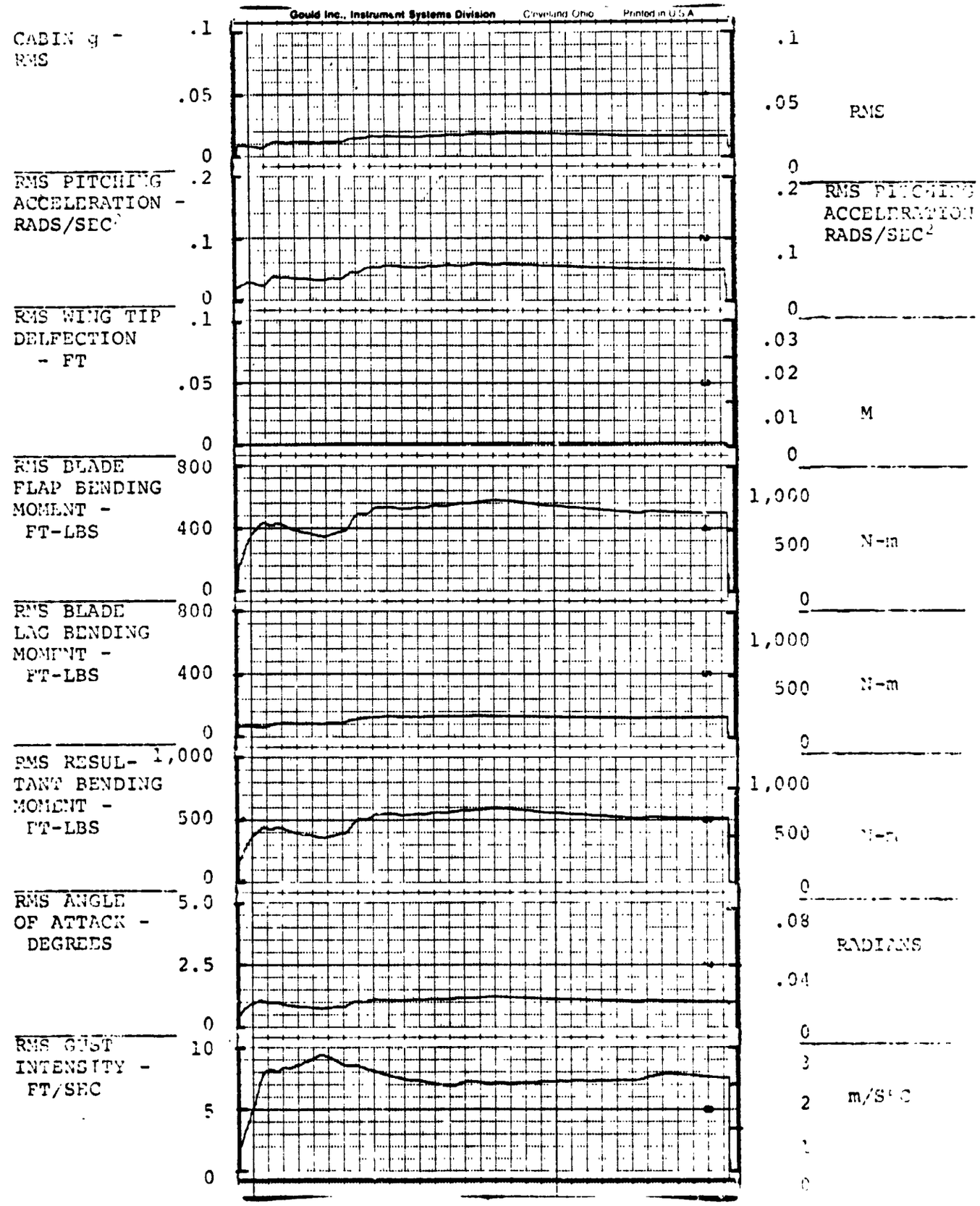

FIGURE 5.8.1.0.0.3. RESPONSES FOR GAIN F = 4.0, GAIN E = .7

FLIGHT CONDITION: 280 KNOTS, 10,000 FEET, (3,049m), AFT CG

D210-11231-2

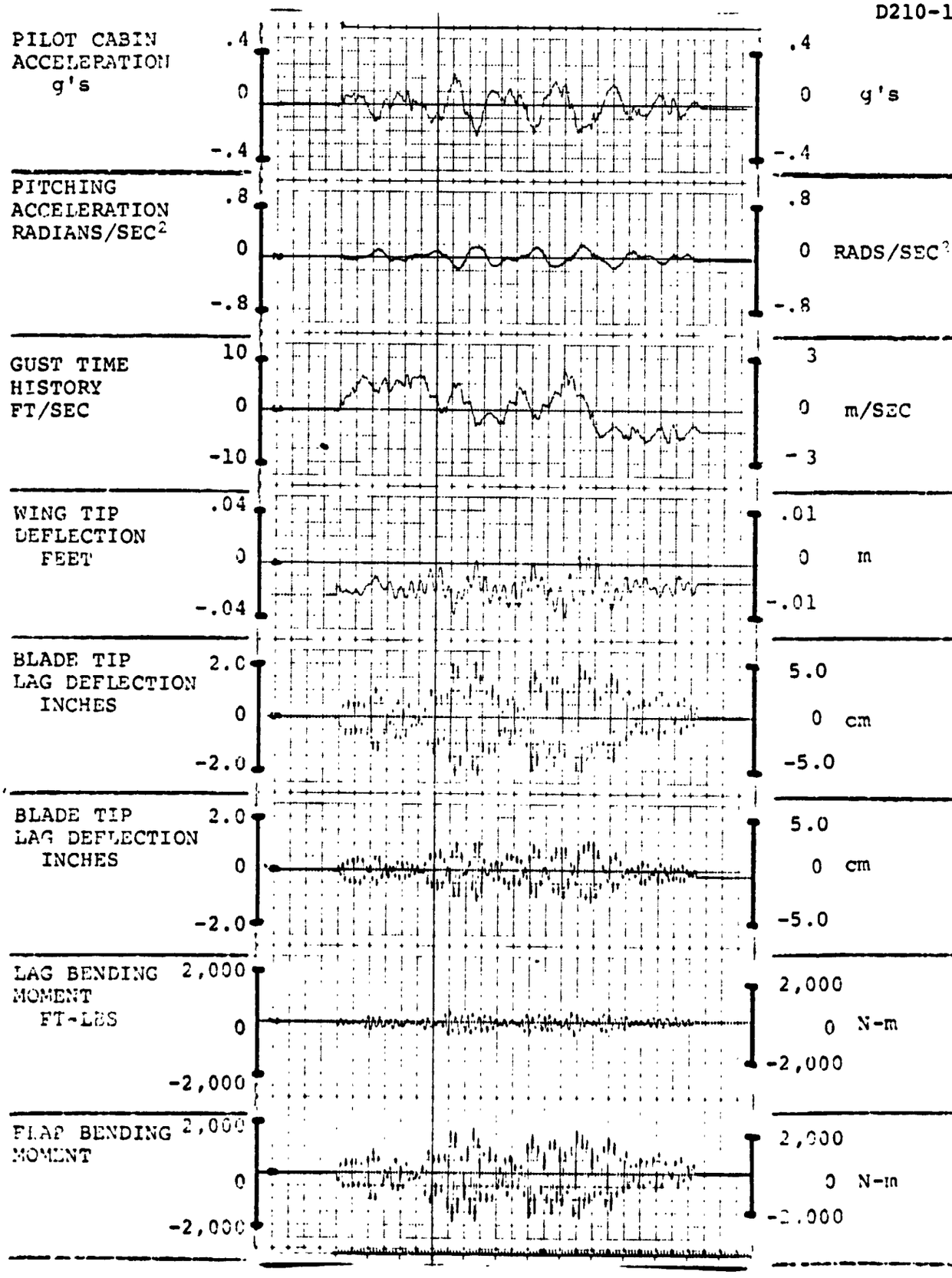

FIGURE 3.8.2.0.0.1. RESPONSES FOR GAIN F = 0, GAIN E = 0

ORIGINAL PAGE IS
OF POOR QUALITY

FLIGHT CONDITION: 280 KNOTS, 10,000 FEET, (3,049m), AFT CG

D210-11231-2

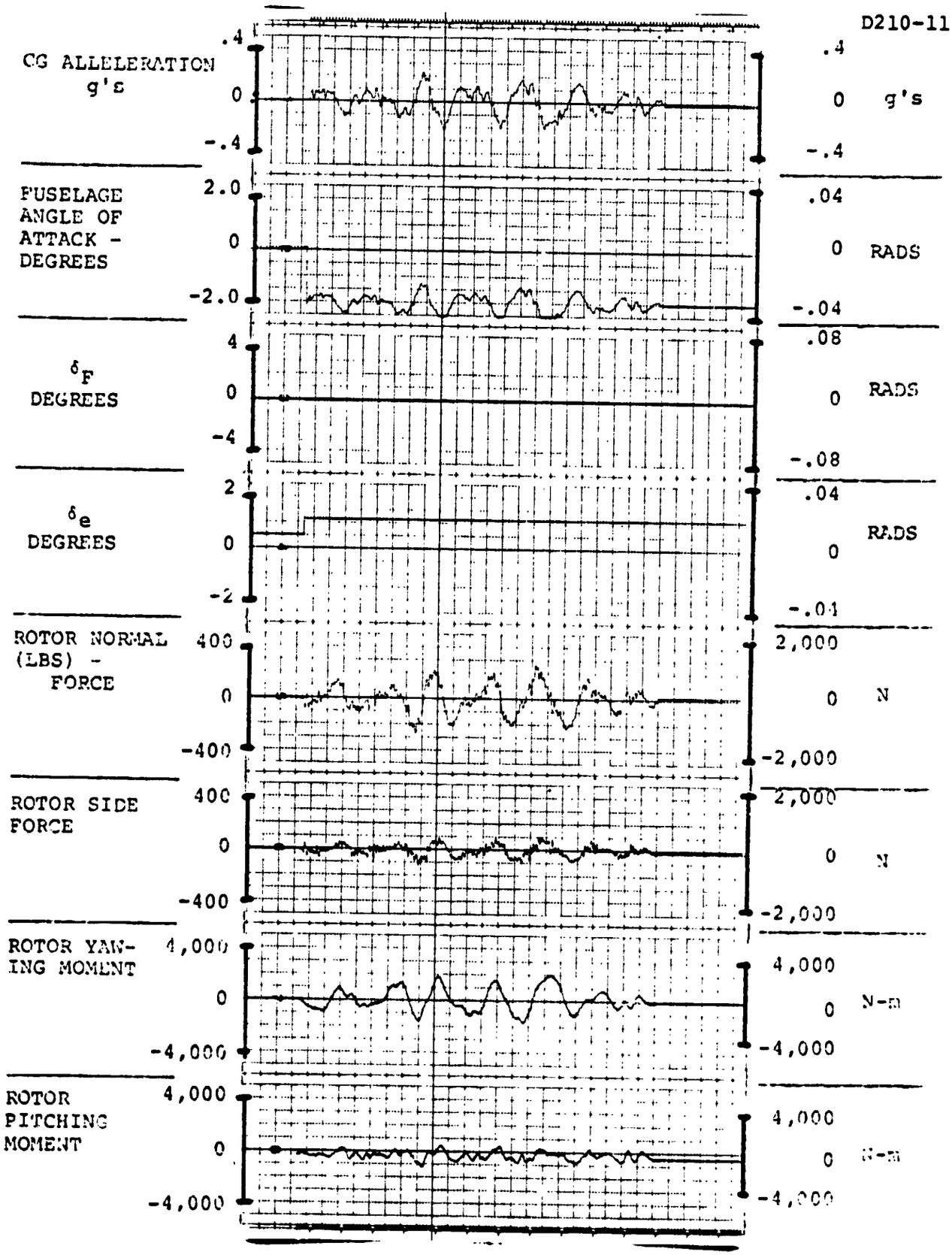

FIGURE 4.8.2.0.0.1. RESPONSES FOR GAIN F = 0, GAIN E = 0

FLIGHT CONDITION: 280 KNOTS, 10,000 FEET, (3,049m), AFT CG

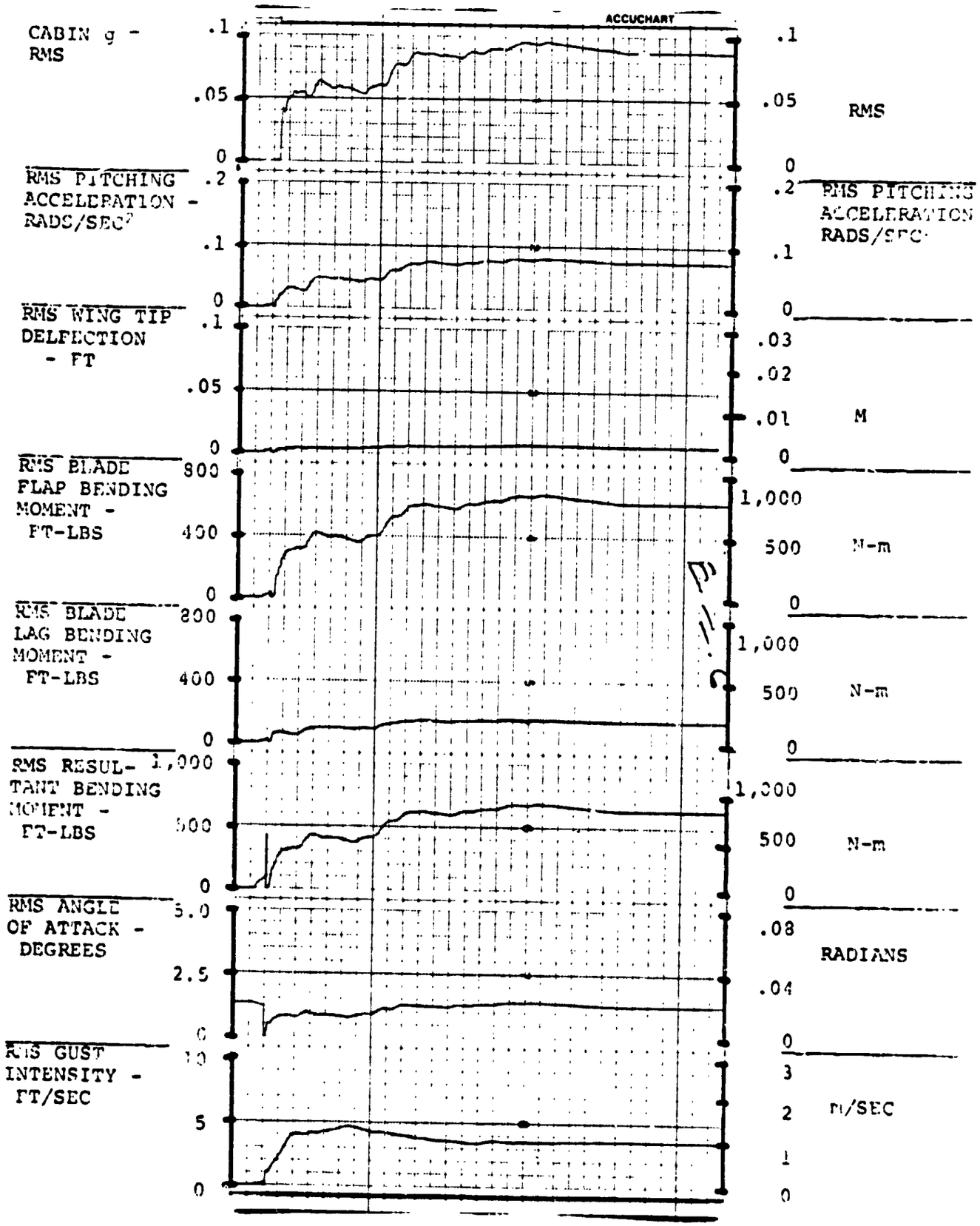

FIGURE 5.8.2.0.0.1. RESPONSES FOR GAIN F = 0, GAIN E = 0

AIV.231

ORIGINAL PAGE IS OF POOR QUALITY

ORIGINAL PAGE IS
OF POOR QUALITY

FLIGHT CONDITION: 280 KNOTS, 10,000 FEET, (3,049m), AFT CG

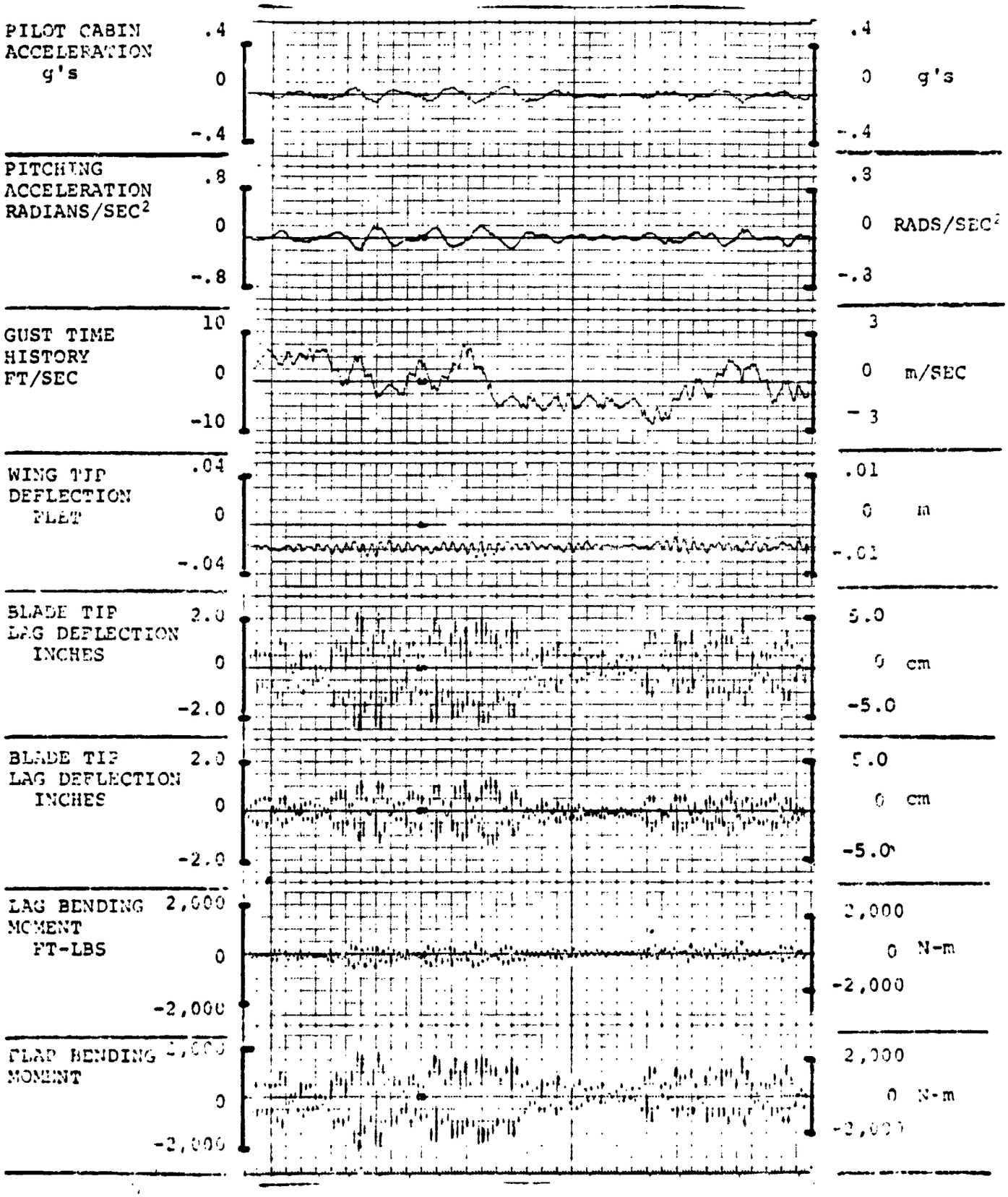

FIGURE 3.8.2.0.0.8. RESPONSES FOR GAIN F = 3.34, GAIN E = .51

FLIGHT CONDITION: 280 KNOTS, 10,000 FEET, (3,049m), AFT CG

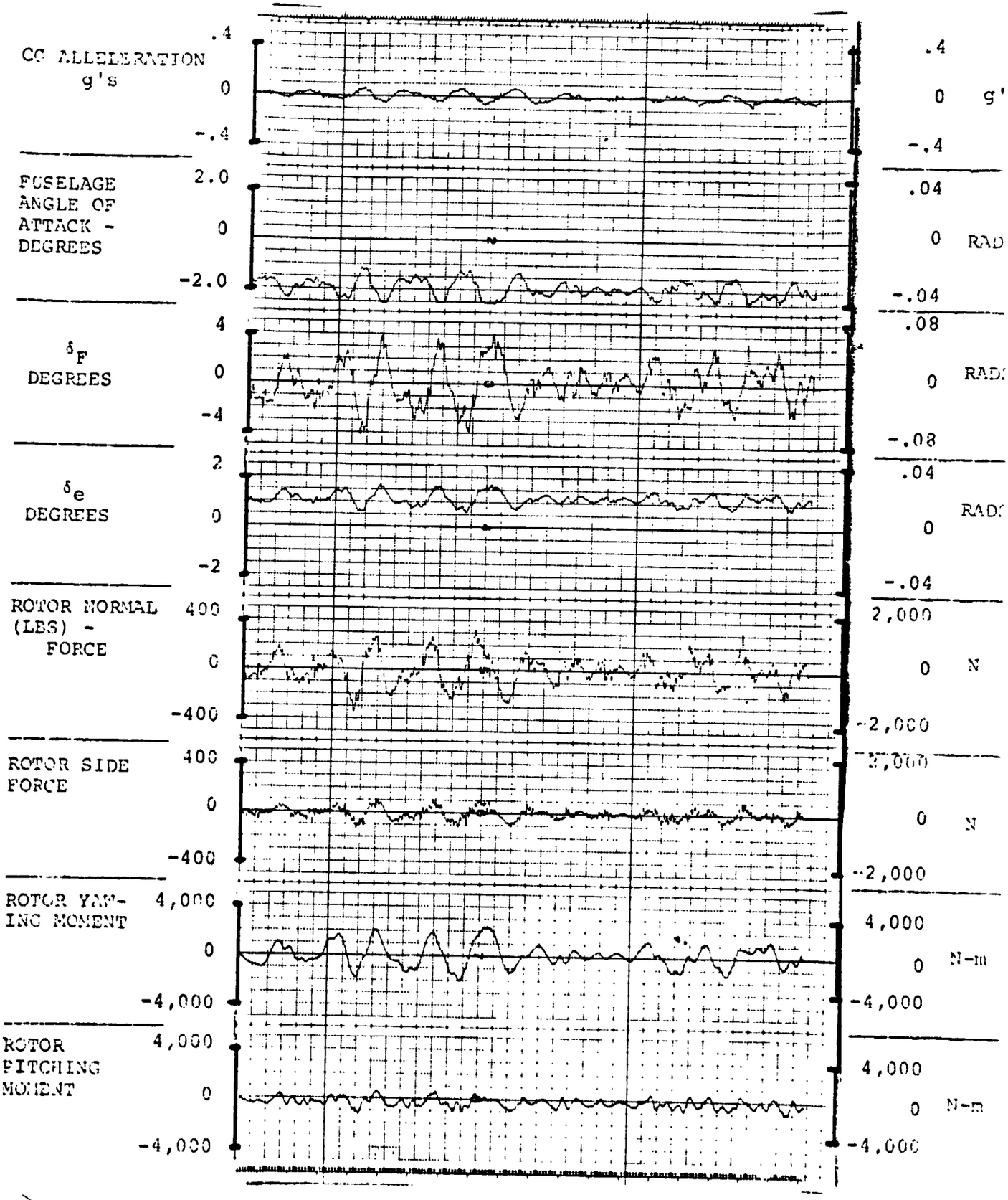

FIGURE 4.8.2.0.0.8. RESPONSES FOR GAIN F = 3.34, GAIN E = .51

FLIGHT CONDITION: 280 KNOTS, 10,000 FEET, (3,049m), AFT CG

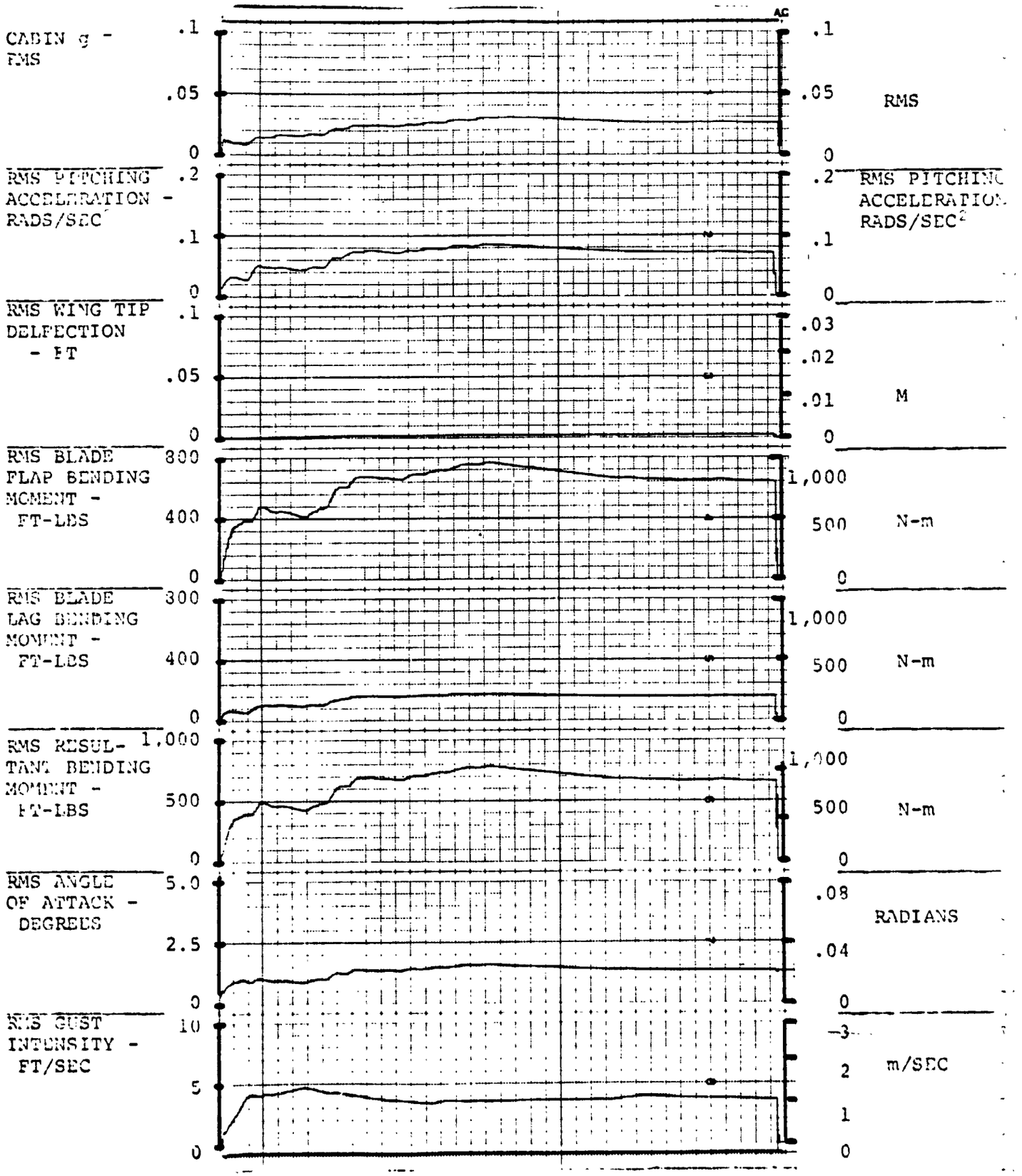

FIGURE 5.8.2.0.0.8. RESPONSES FOR GAIN F = 3.34, GAIN E = .51

ORIGINAL PAGE IS
OF POOR QUALITY

FLIGHT CONDITION: 280 KNOTS, 10,000 FEET, (3,049m), AFT CG

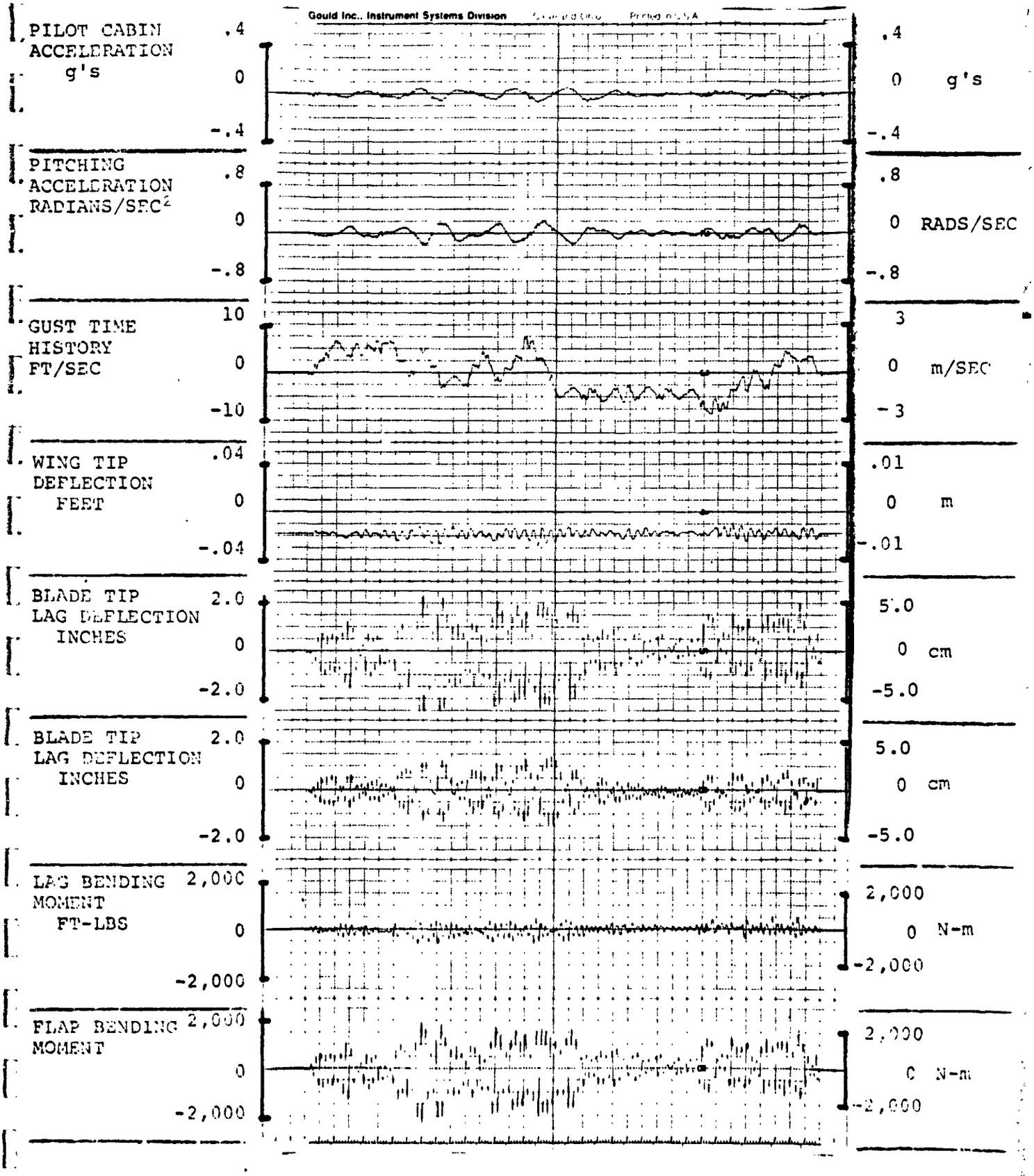

FIGURE 3.8.2.0.0.2. RESPONSES FOR GAIN F = 4.0, GAIN E = .6

FLIGHT CONDITION: 280 KNOTS, 10,000 FEET, (3,049m), AFT CG

D210-11231-2

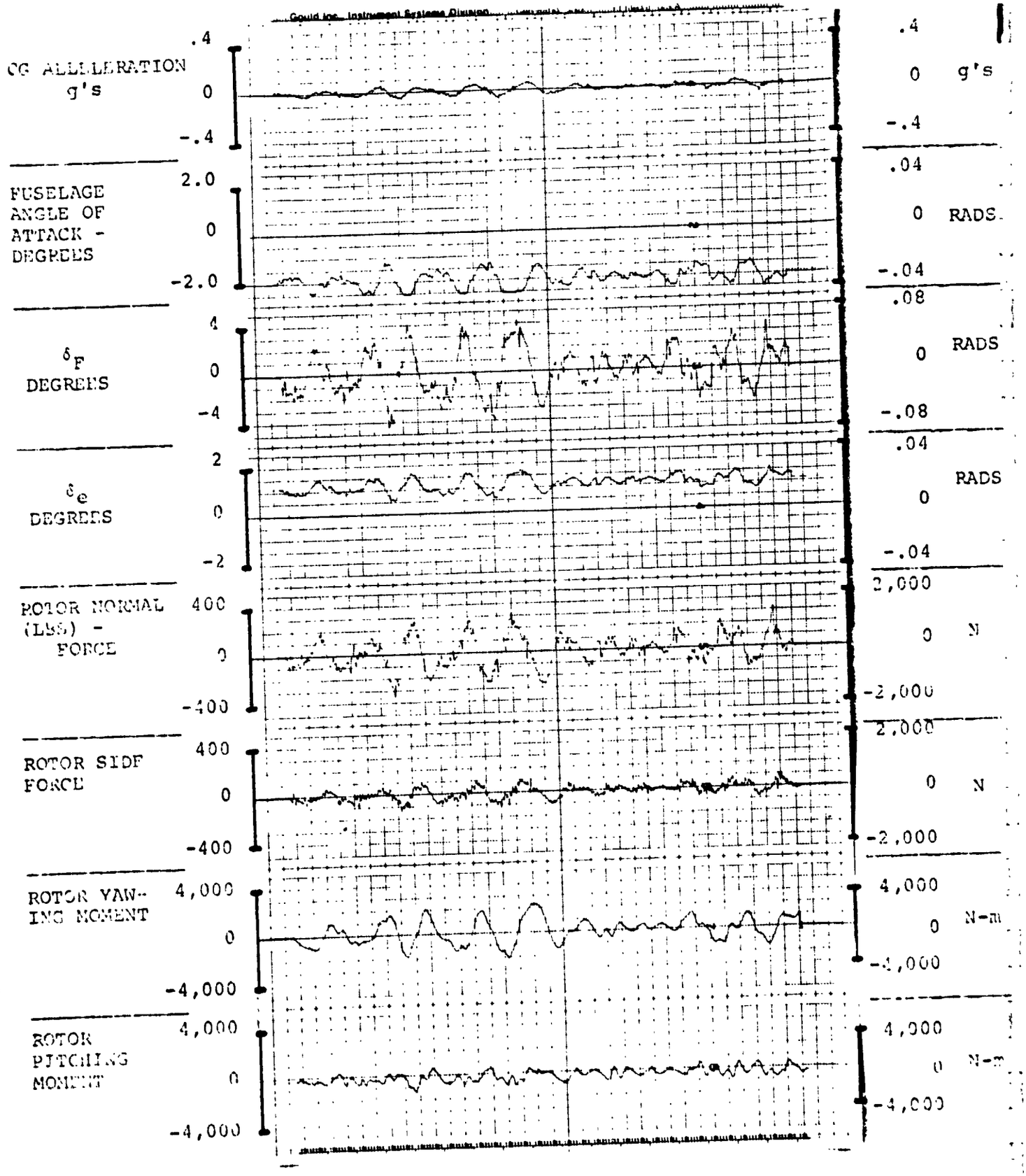

FIGURE 4.9.2.0.0.2. RESPONSES FOR GAIN F = 4.0, GAIN E = .6

FLIGHT CONDITION: 280 KNOTS, 10,000 FEET, (3,049m), AFT CG

D210-11231-2

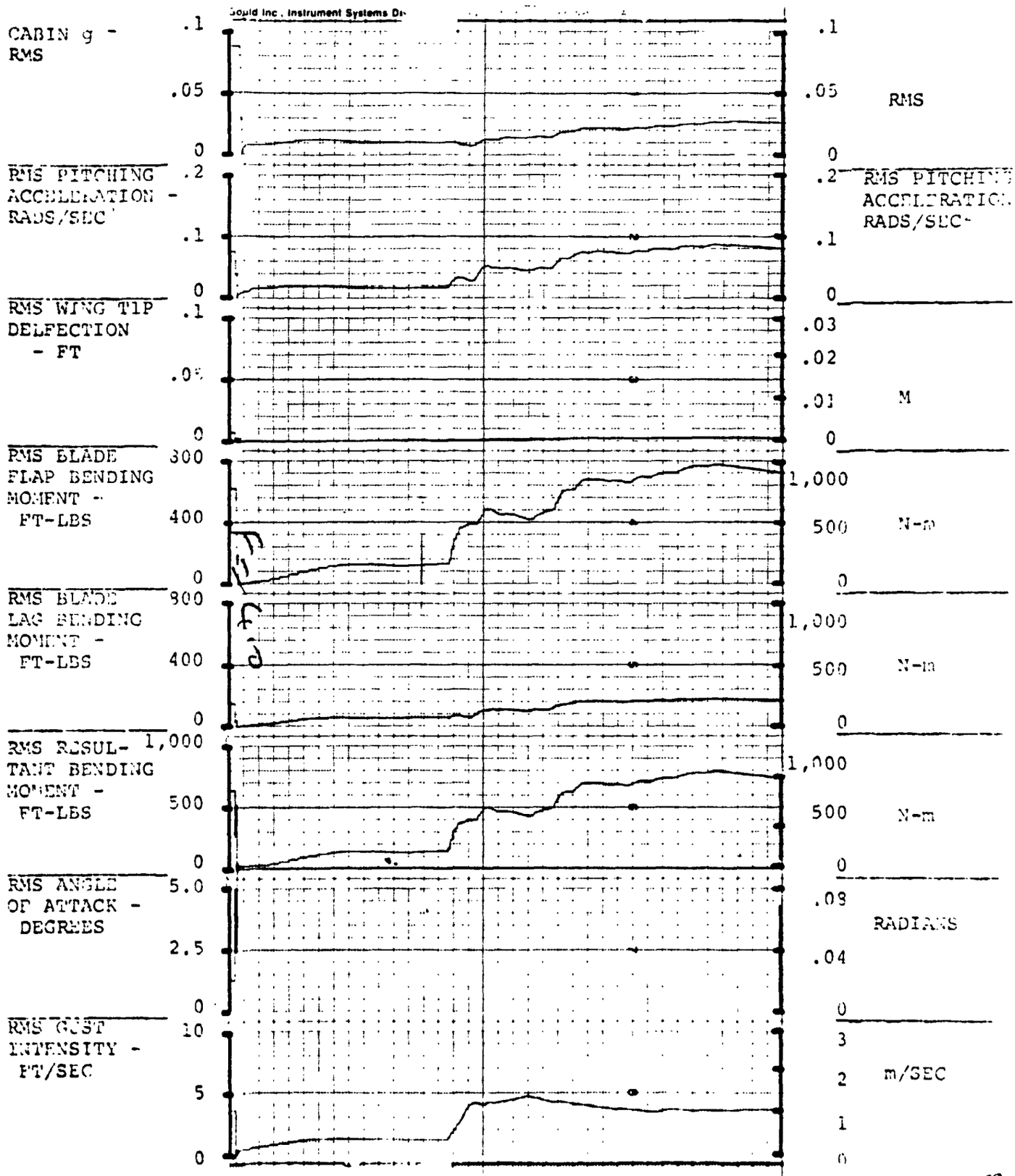

FIGURE 5.8.2.0.0.2 RESPONSES FOR GAIN F = 4.0, GAIN E = .6

ORIGINAL PAGE IS OF POOR QUALITY

FLIGHT CONDITION: 280 KNOTS, 10,000 FEET, (3,049m), AFT CG

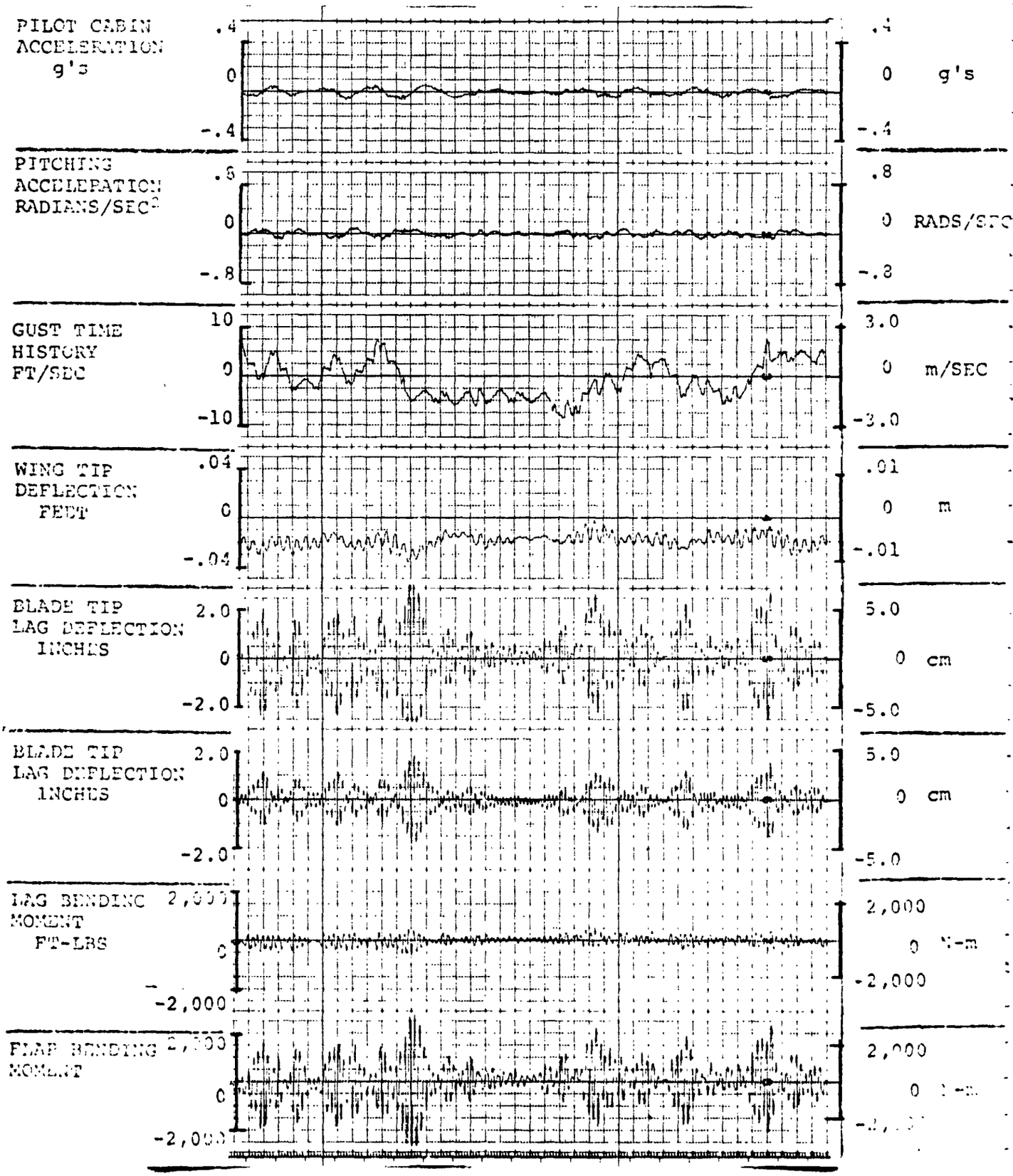

FIGURE 3.8.2.0.0.3. RESPONSES FOR GAIN F = 4.0, GAIN E = .7

ORIGINAL PAGE IS
OF POOR QUALITY

FLIGHT CONDITION: 280 KNOTS, 10,000 FEET, (3,049m), AFT CG

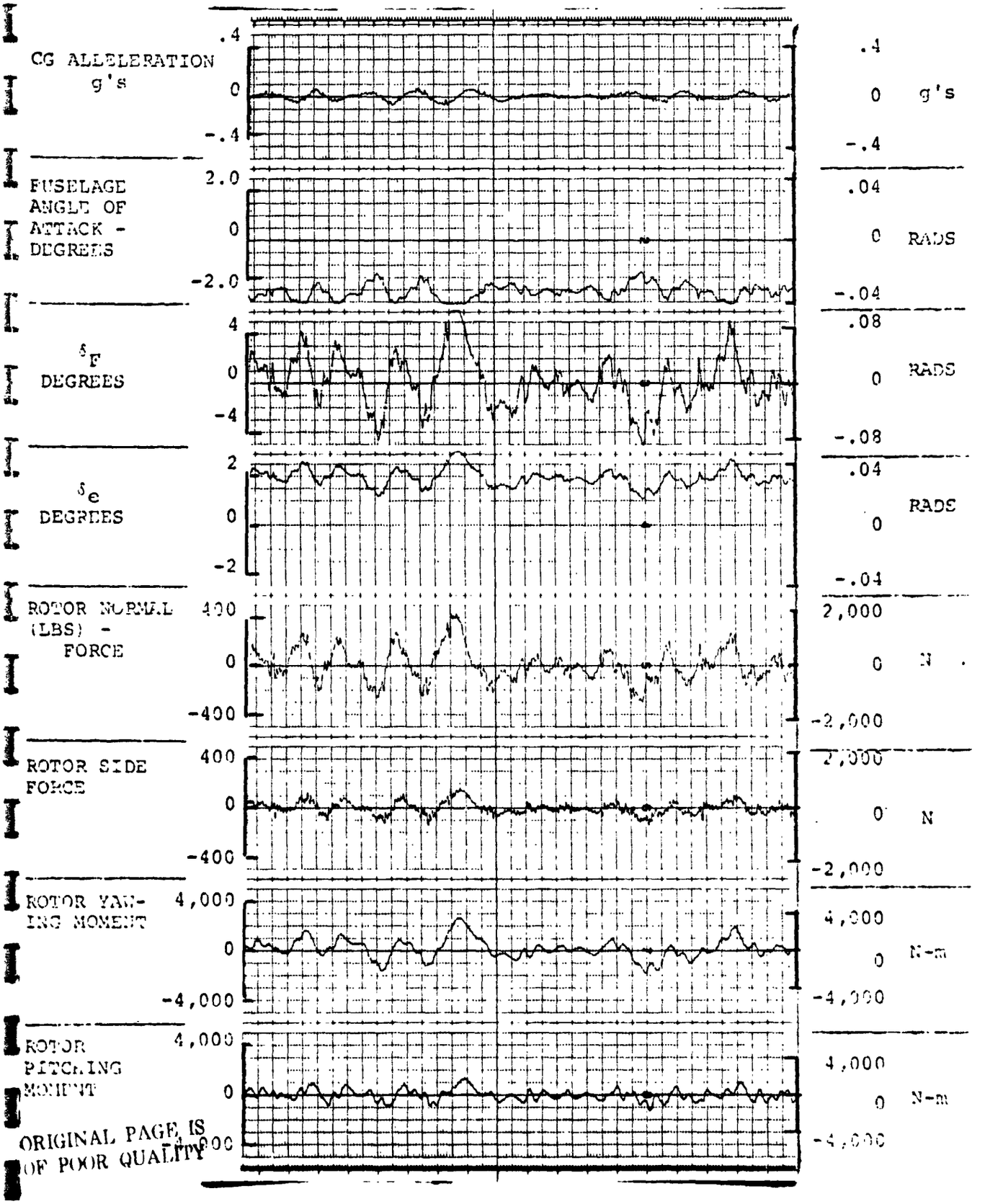

ORIGINAL PAGE IS OF POOR QUALITY

FIGURE 4.8.2.0.0.3. RESPONSES FOR GAIN F = 4.0, GAIN E = .7

FLIGHT CONDITION: 280 KNOTS, 10,000 FEET, (3,049m), AFT CG

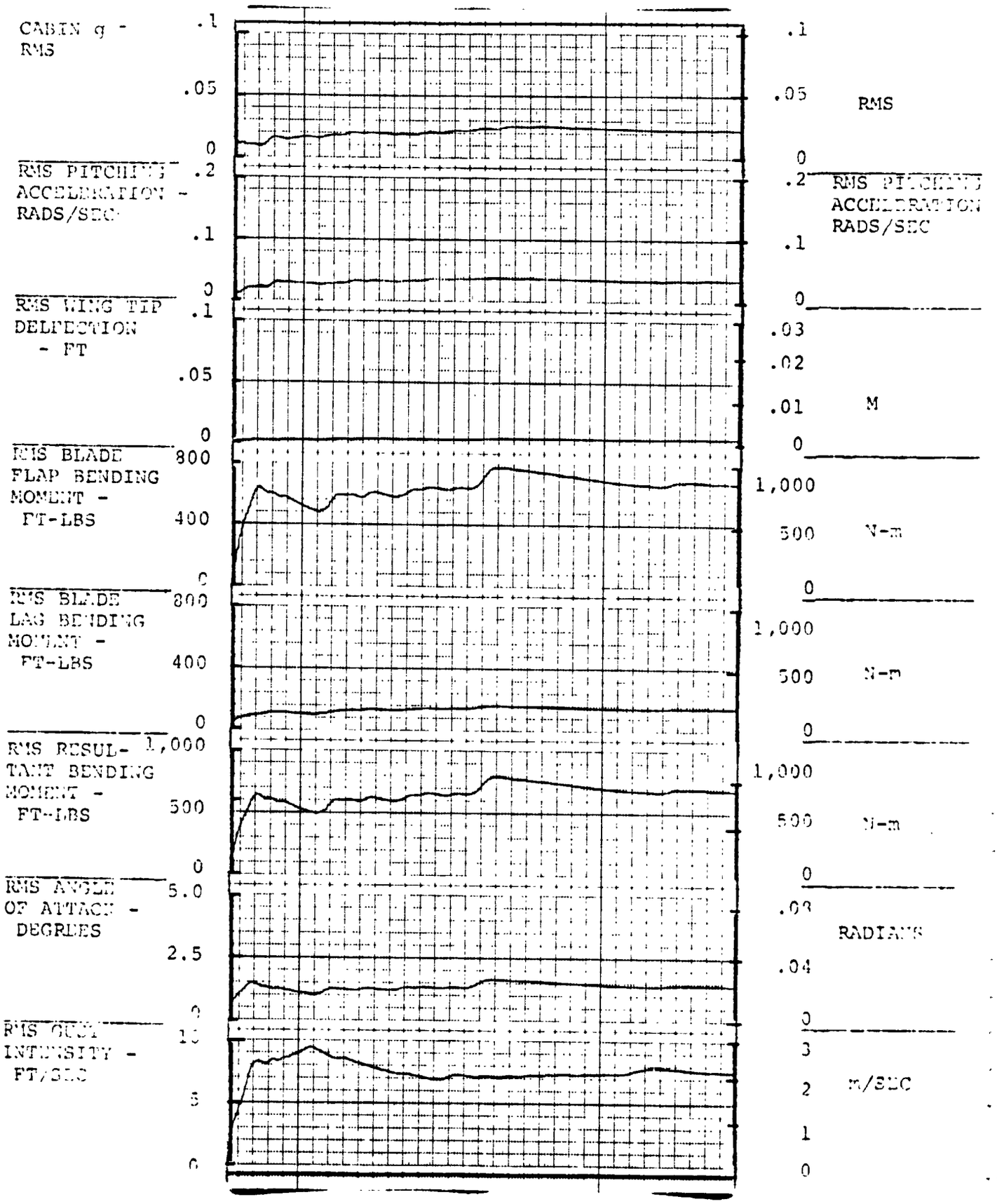

FIGURE 5.8.2.0.0.3. RESPONSES FOR GAIN F = 4.0, GAIN E = .7

FLIGHT CONDITION: 280 KNOTS, 10,000 FEET, (3,049m), AFT CG

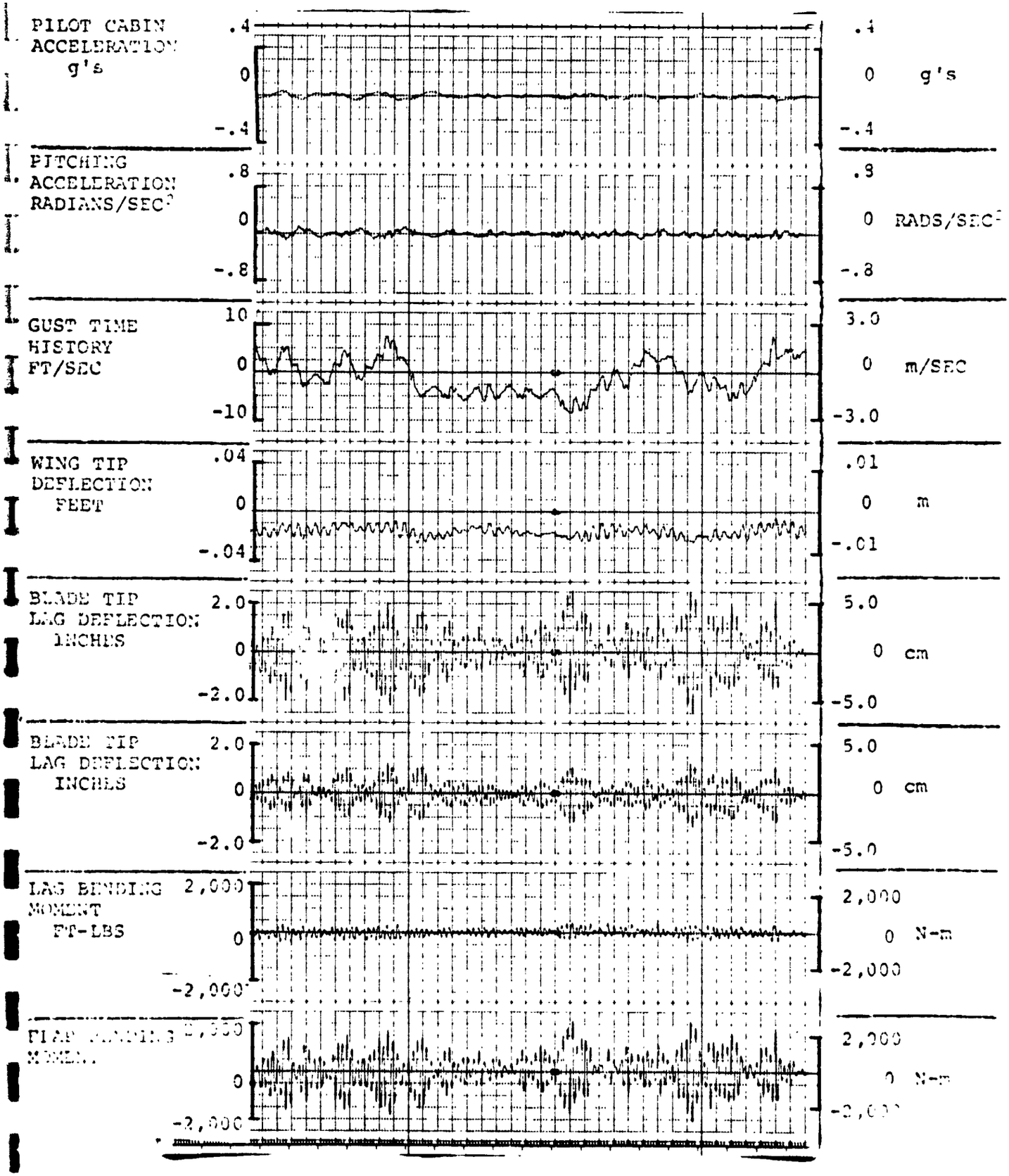

FIGURE 3.8.2.0.0.4. RESPONSES FOR GAIN F = 4.0, GAIN E = .8

ORIGINAL PAGE IS
OF POOR QUALITY

FLIGHT CONDITION: 280 KNOTS, 10,000 FEET, (3,049m), AFT CG

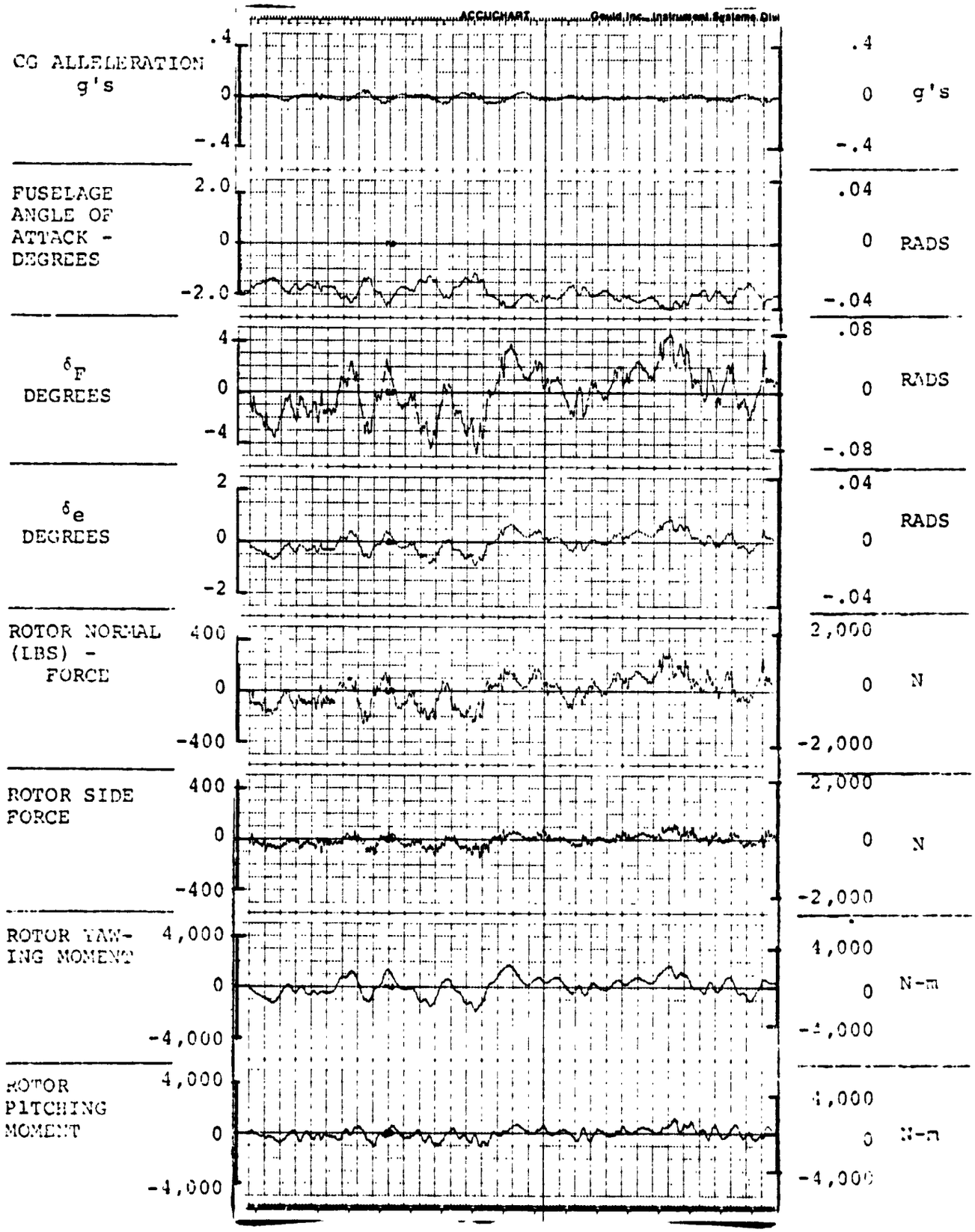

FIGURE 4.8.2.0.0.4. RESPONSES FOR GAIN F = 4.0, GAIN E = .8

FLIGHT CONDITION: 280 KNOTS, 10,000 FEET, (3,049m), AFT CG

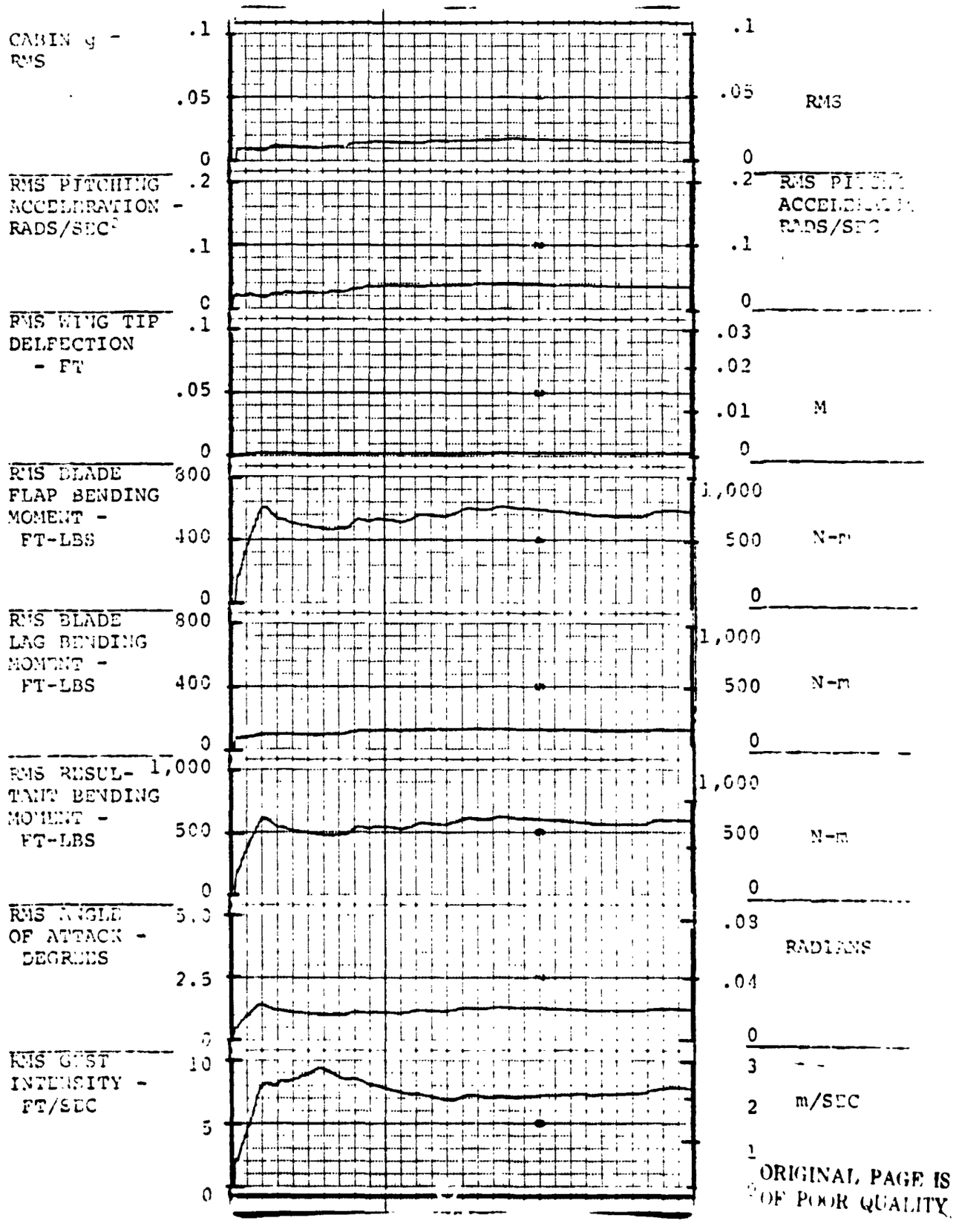

ORIGINAL PAGE IS OF POOR QUALITY

FIGURE 5.8.2.0.0.4. RESPONSES FOR GAIN F = 4.0, GAIN E = .8

K+E LOGARITHMIC 2 X 3 CYCLES
KEUFFEL & ESSER CO. MADE IN U.S.A.
46 7323

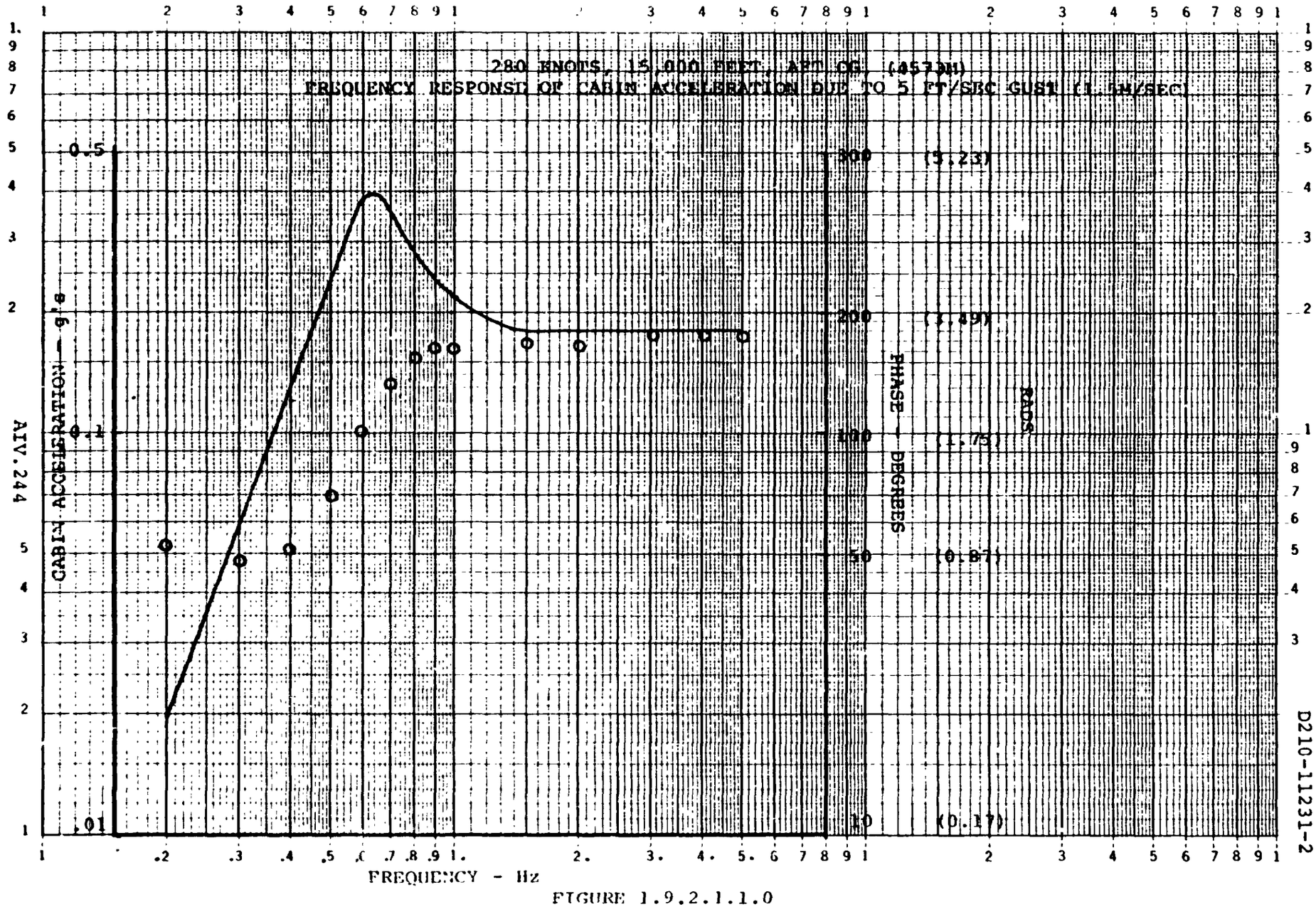

FIGURE 1.9.2.1.1.0

K+E LOGARITHMIC 2 X 3 CYCLES KEUFFEL & ESSER CO. MADE IN U.S.A.
46 7323

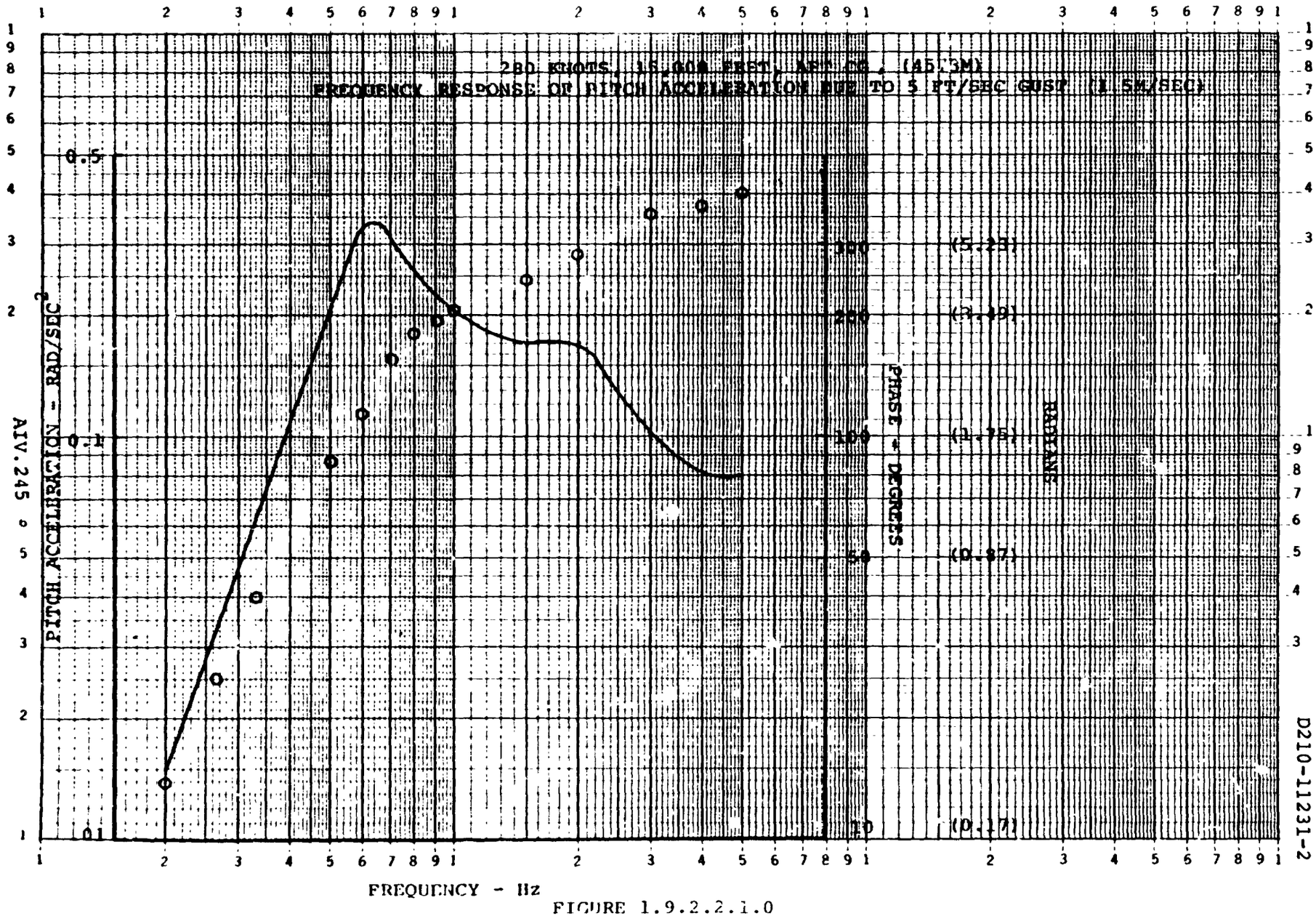

FIGURE 1.9.2.2.1.0

K+E LOGARITHMIC • 2 X 3 CYCLES
KEUFFEL & ESSER CO MADE IN U.S.A.

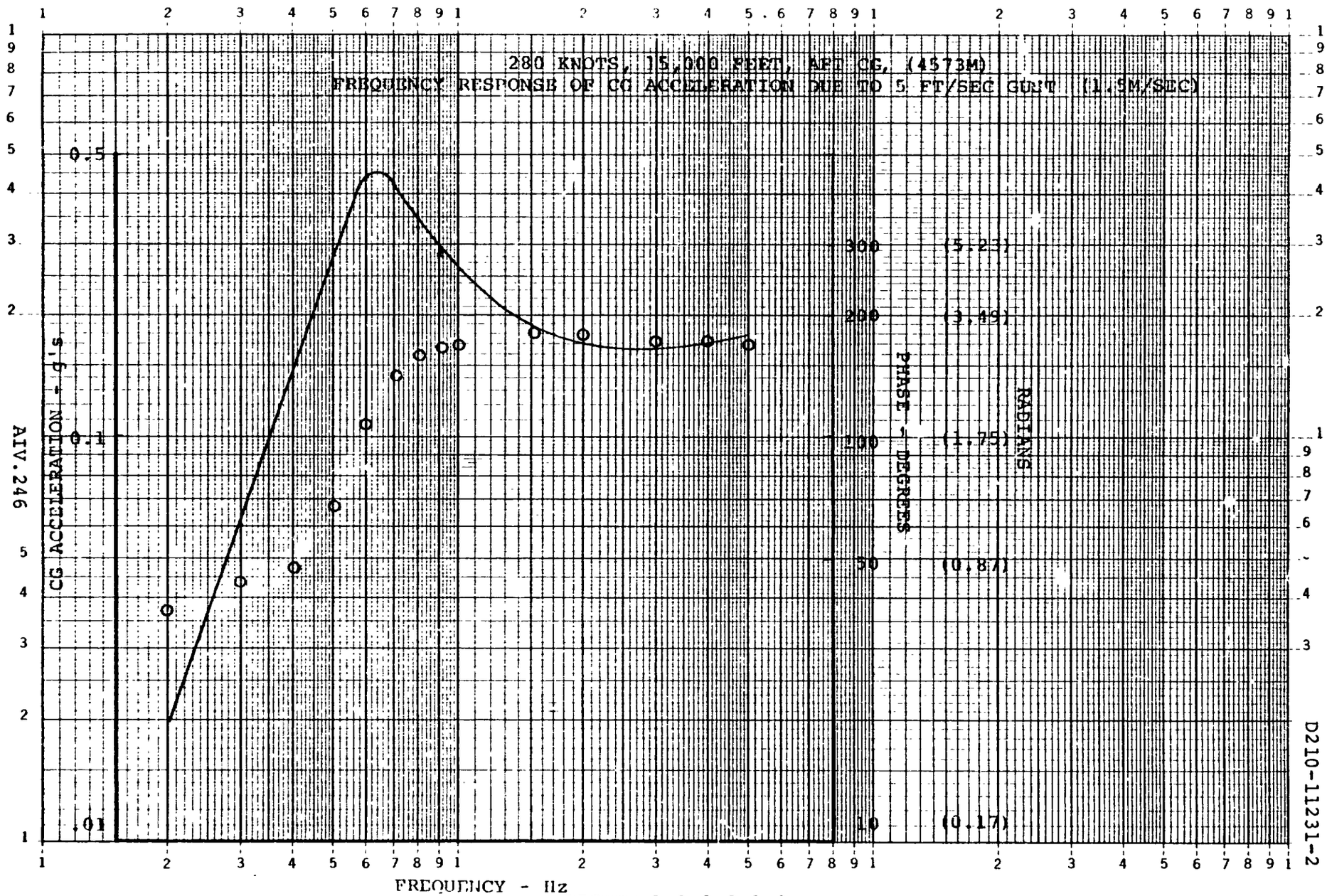

FIGURE 1.9.2.3.1.0

K•E LOGARITHMIC • 2 X 3 CYCLES
KEUFFEL & ESSER CO. MADE IN U.S.A.
46 7323

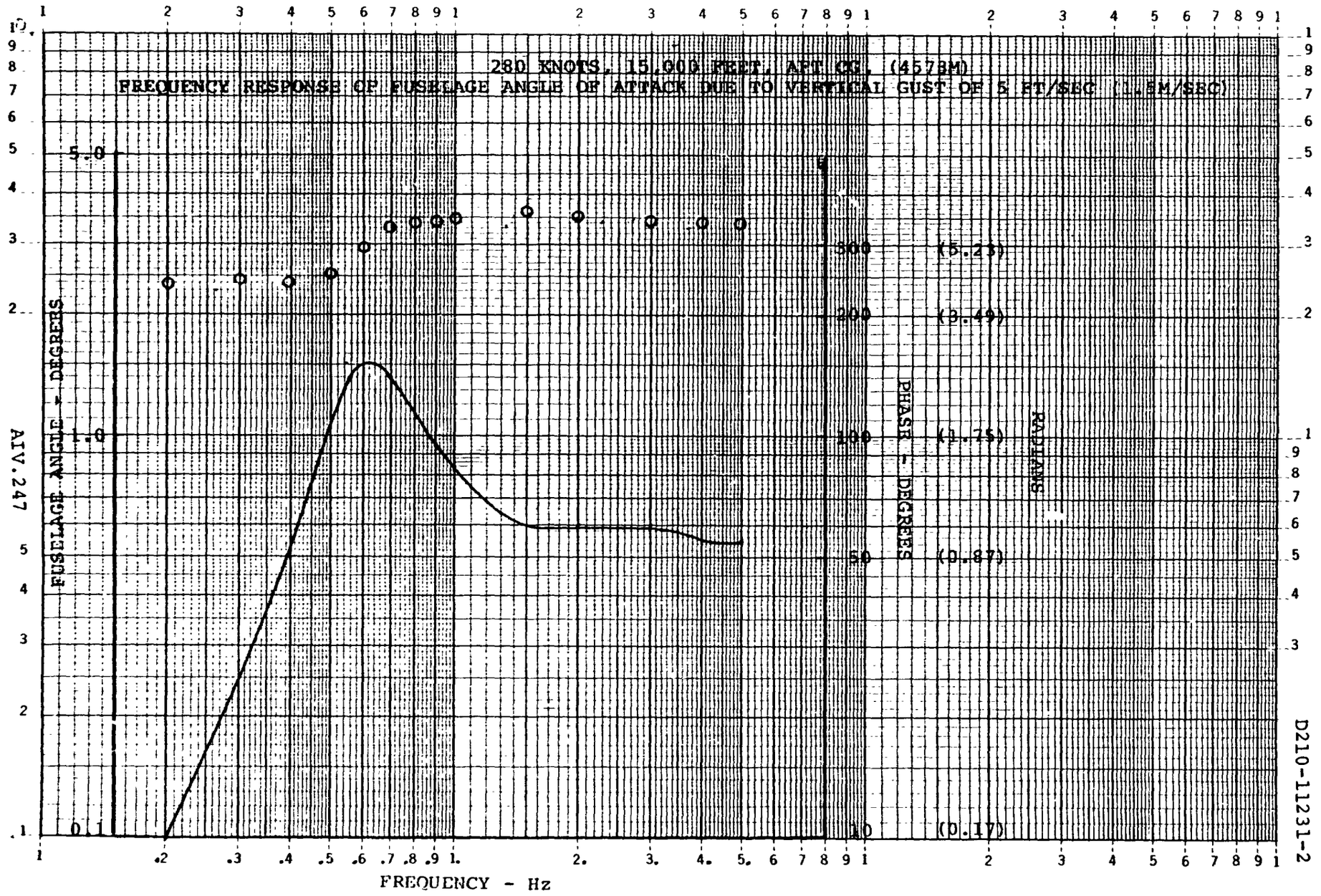

FIGURE 1.9.2.4.1.0

K·E LOGARITHMIC • 2 X 3 CYCLES KEUFFEL & ESSER CO. MADE IN U.S.A.

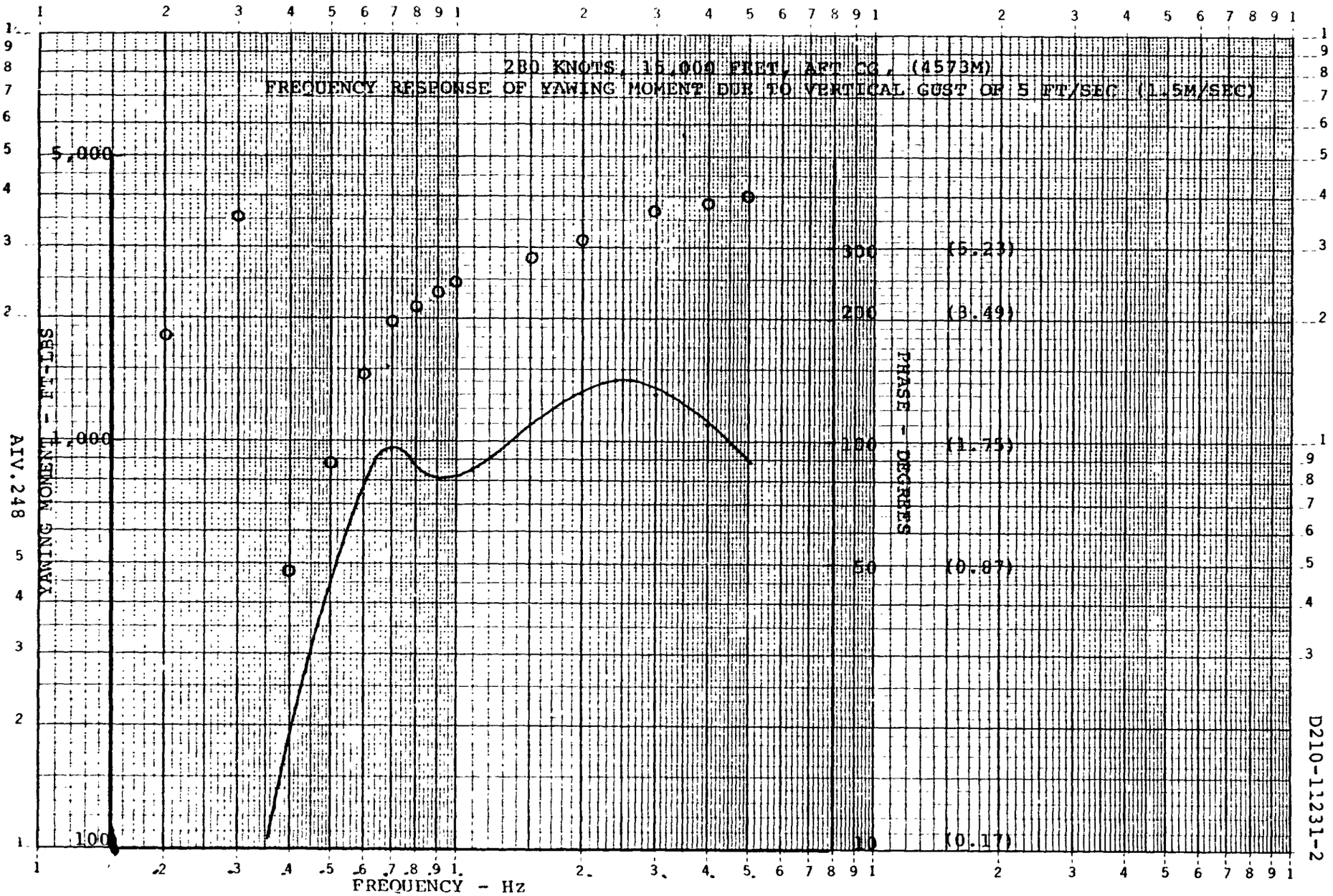

FIGURE 1.9.2.5.1.0

K·E LOGARITHMIC • 2 X 3 CYCLES
KEUFFEL & ESSER CO. MADE IN U.S.A.
46 7323

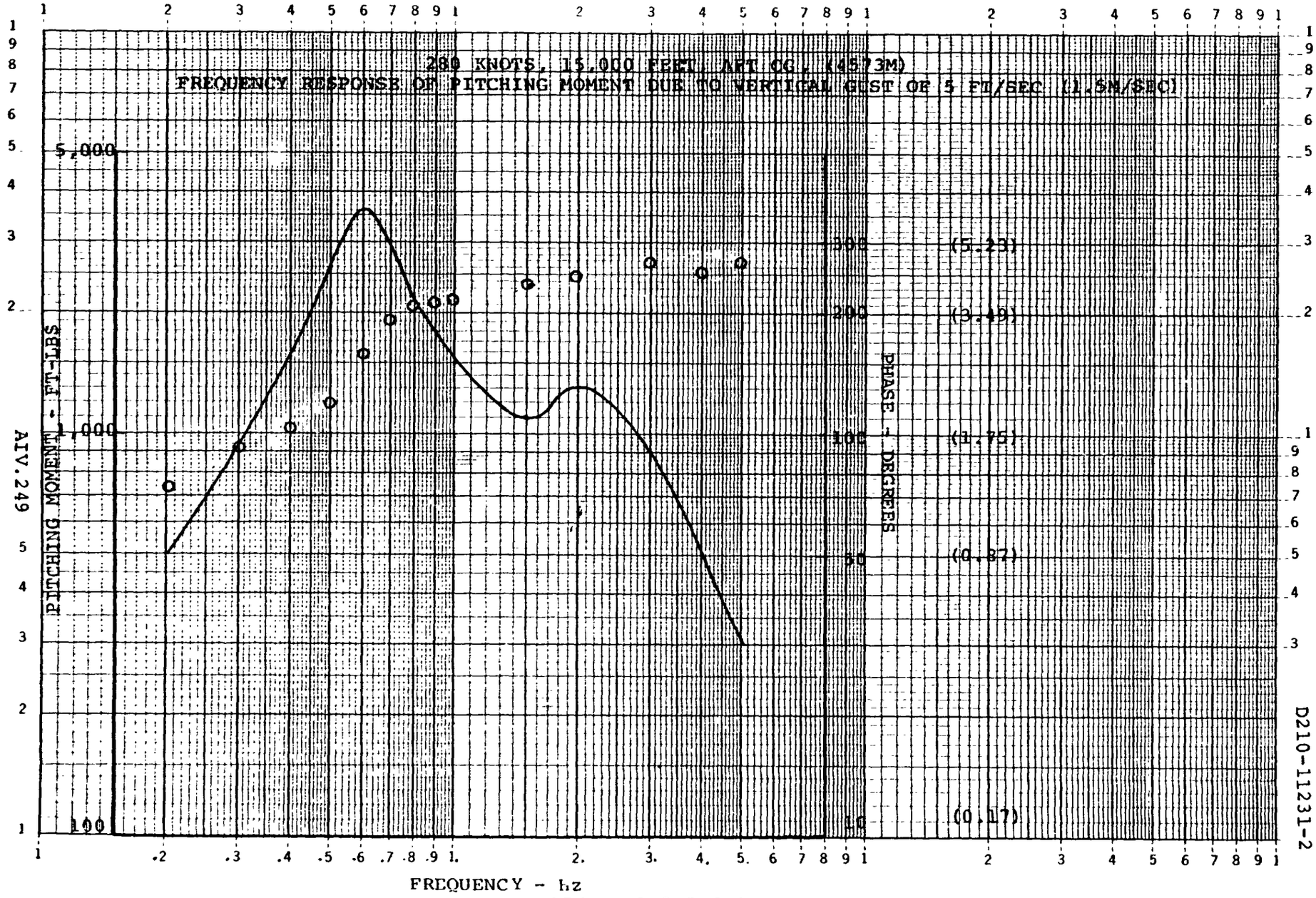

FIGURE 1.9.2.6.1.0

K·E LOGARITHMIC • 2 X 3 CYCLES
KEUFFEL & ESSER CO. MADE IN U.S.A.

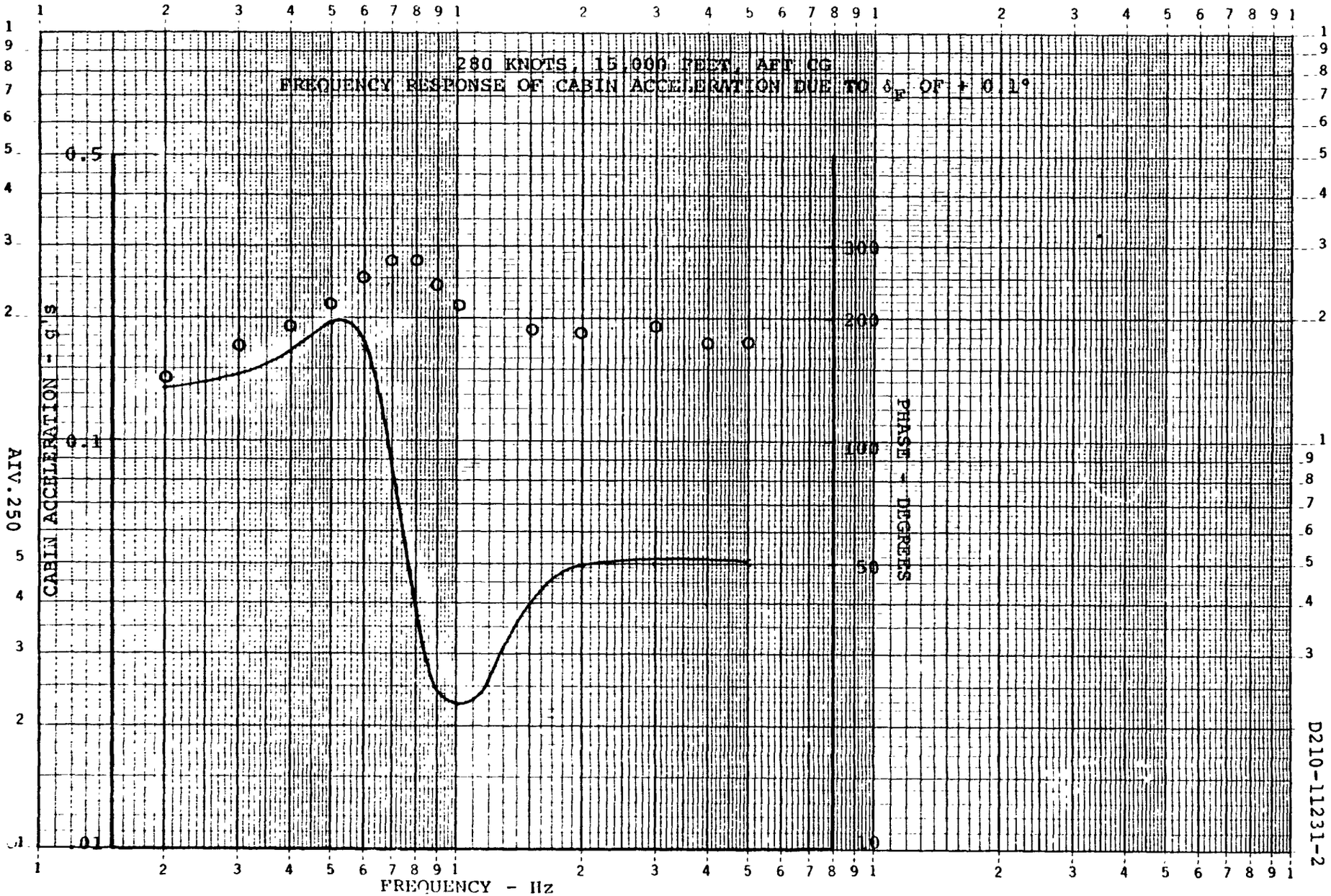

FIGURE 1.9.2.1.2.0

K•E LOGARITHMIC •2 X 3 CYCLES
KEUFFEL & ESSER CO MADE IN U.S.A.
46 7323

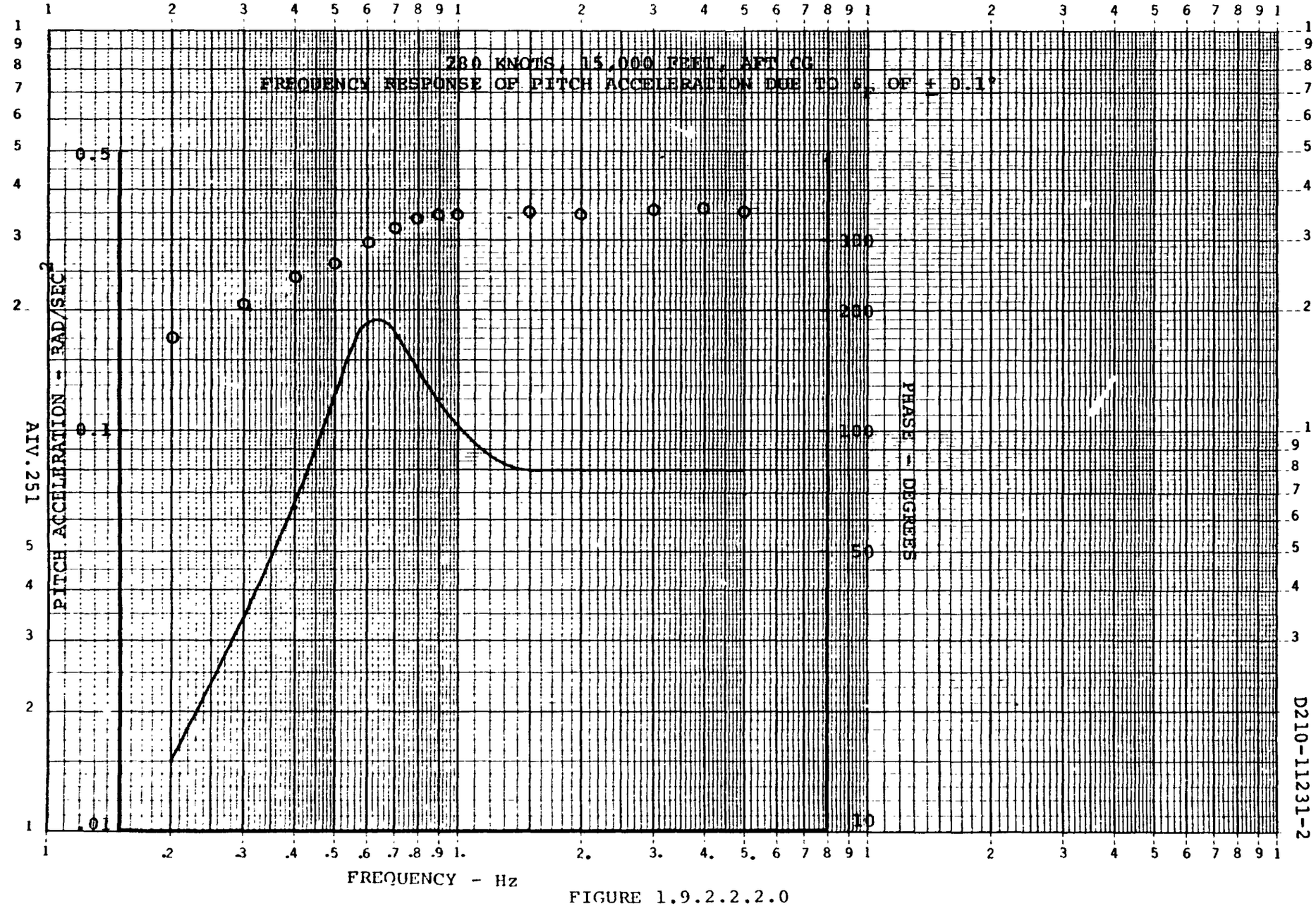

FIGURE 1.9.2.2.2.0

K+E LOGARITHMIC • 2 X 3 CYCLES
KEUFFEL & ESSER CO MADE IN U.S.A.

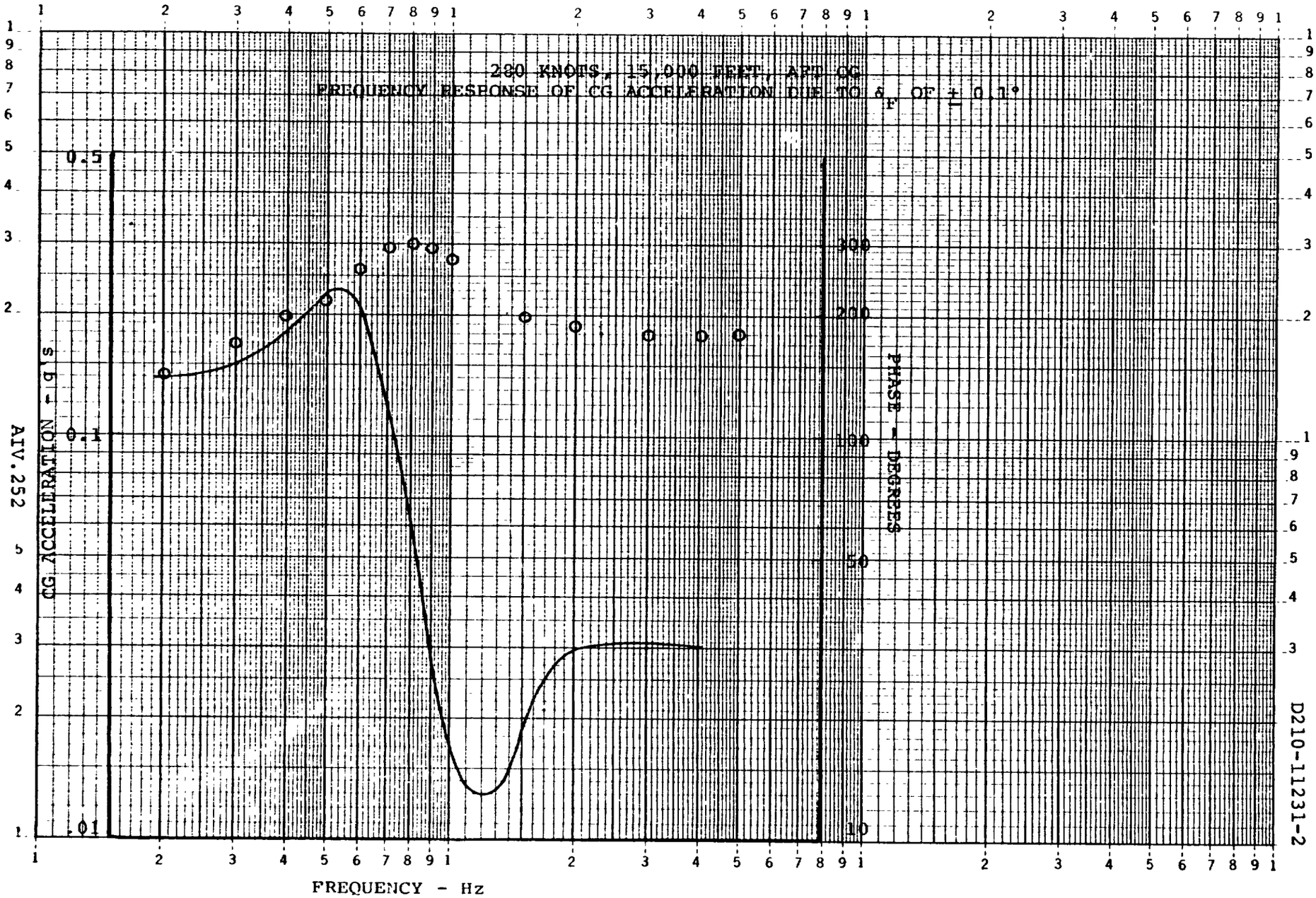

FIGURE 1.9.2.3.2.0

K•E LOGARITHMIC • 2 X 3 CYCLES
KEUFFEL & ESSER CO. MADE IN U.S.A.
46 7323

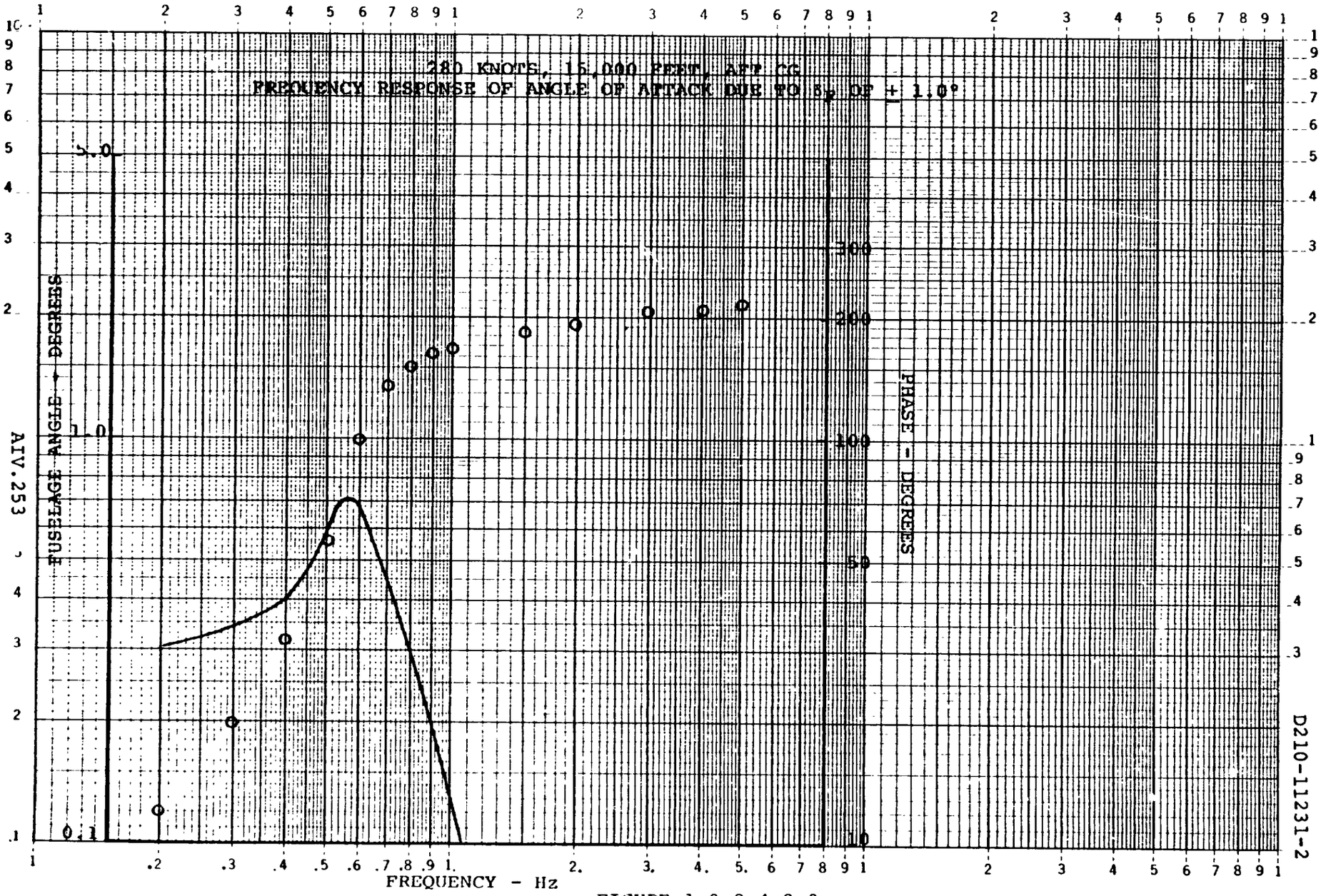

FIGURE 1.9.2.4.2.0

K+E LOGARITHMIC 2 X 3 CYCLES
KEUFFEL & ESSER CO. MADE IN U.S.A.

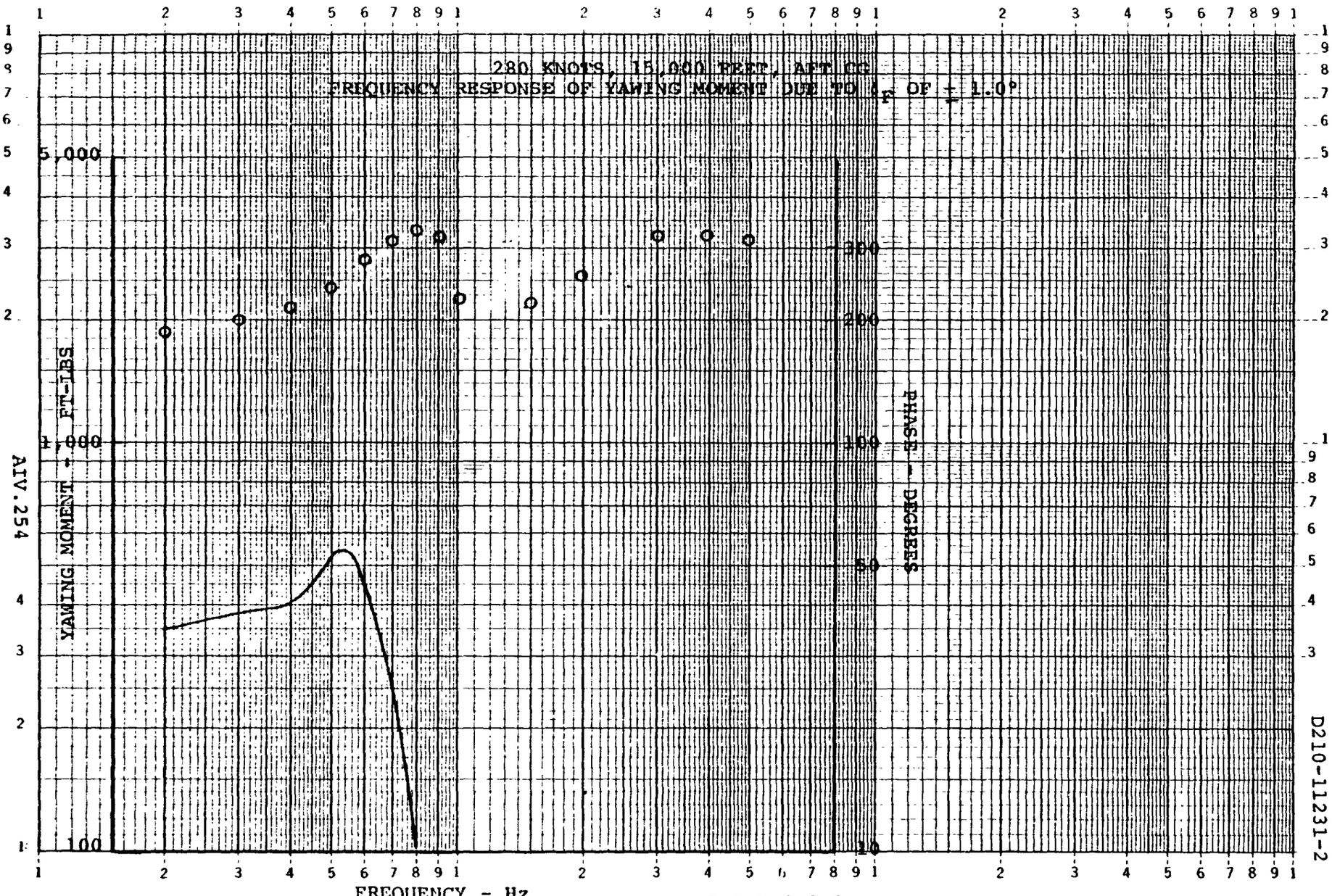

FIGURE 1.9.2.5.2.0

K·E LOGARITHMIC • 2 X 3 CYCLES
KEUFFEL & ESSER CO MADE IN U.S.A.
46 7323

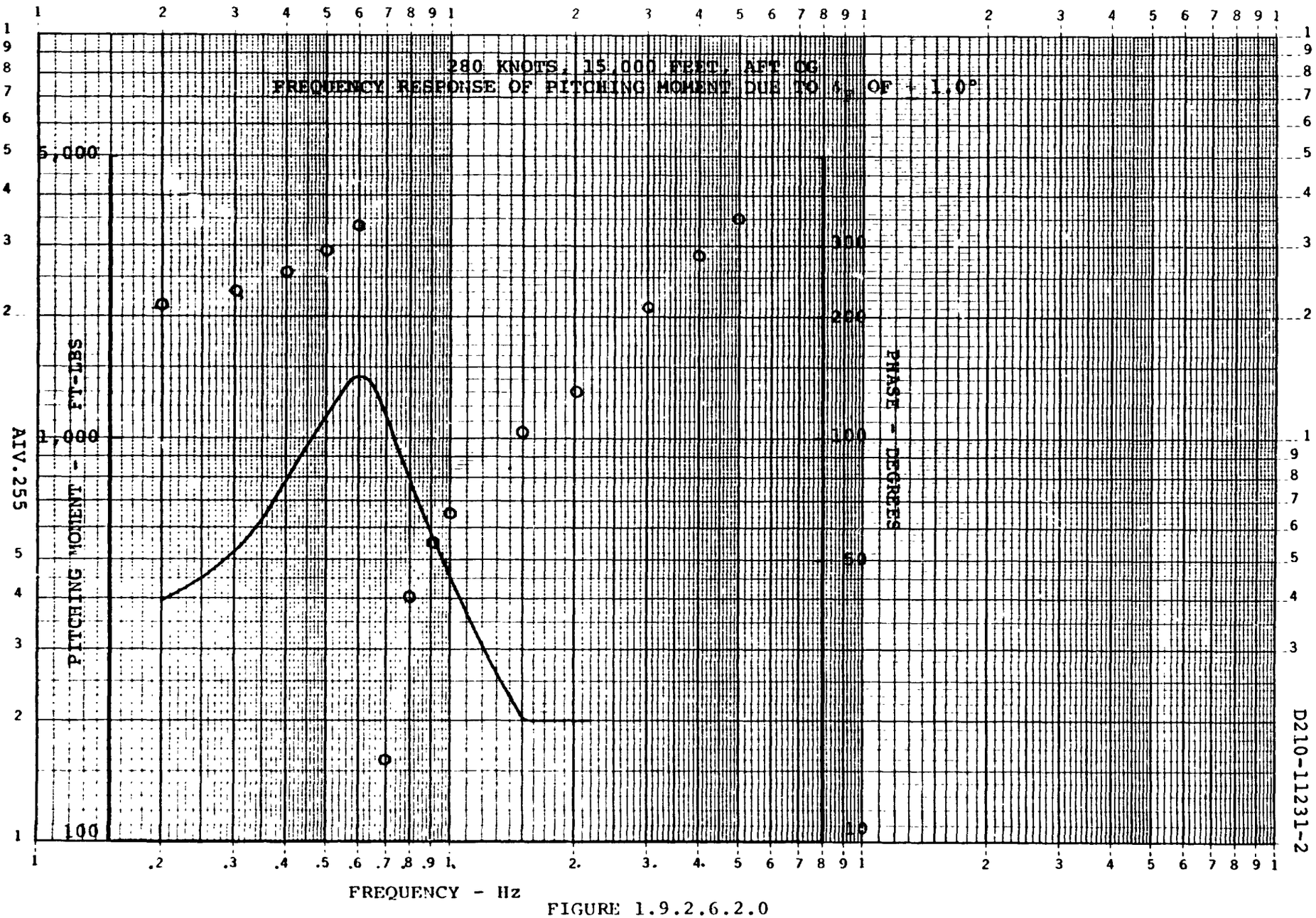

FIGURE 1.9.2.6.2.0

K+E LOGARITHMIC 2 X 3 CYCLES
KEUFFEL & ESSER CO. MADE IN U.S.A.

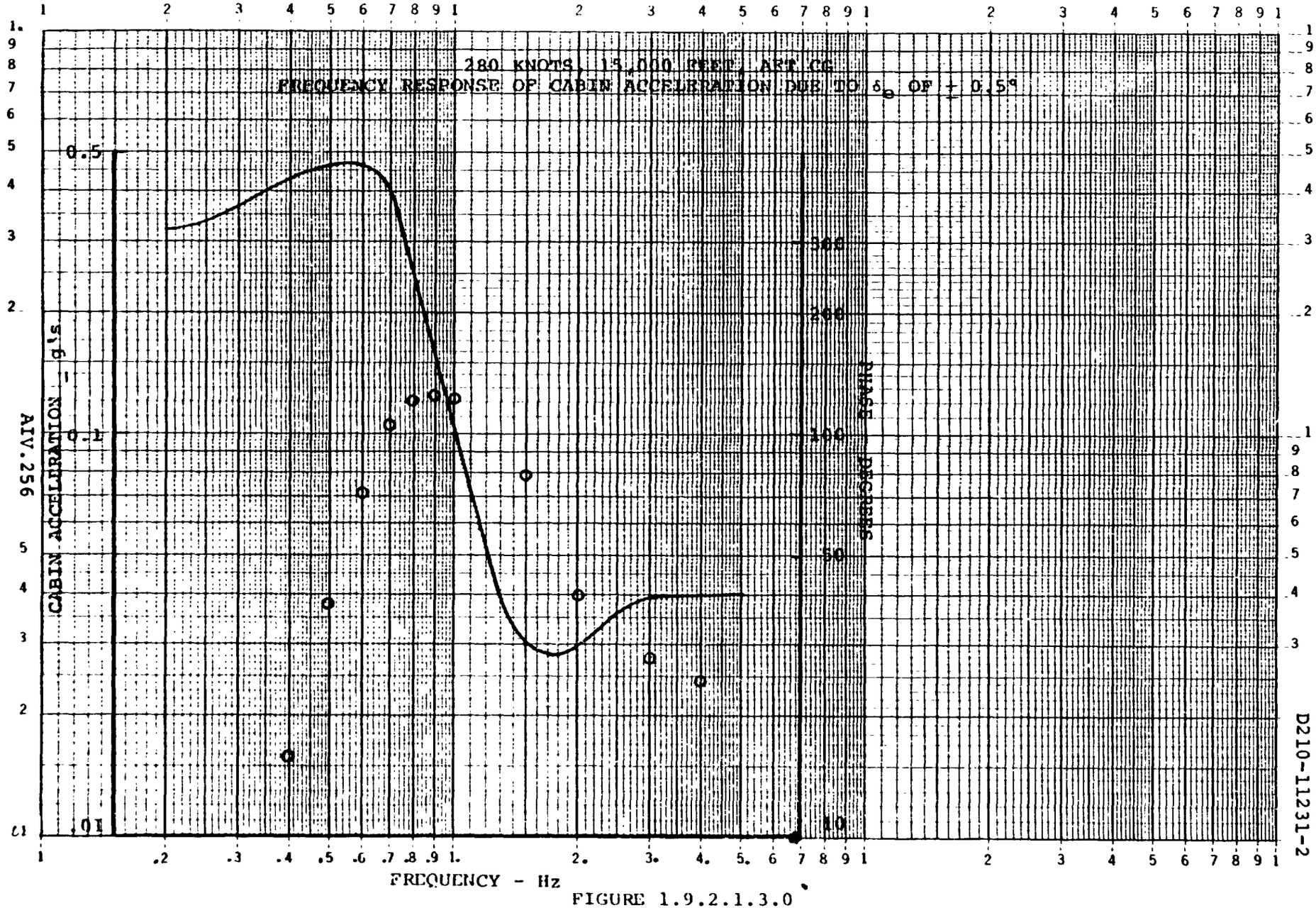

FIGURE 1.9.2.1.3.0

K•Σ LOGARITHMIC • 2 X 3 CYCLES KEUFFEL & ESSER CO. MADE IN U.S.A.

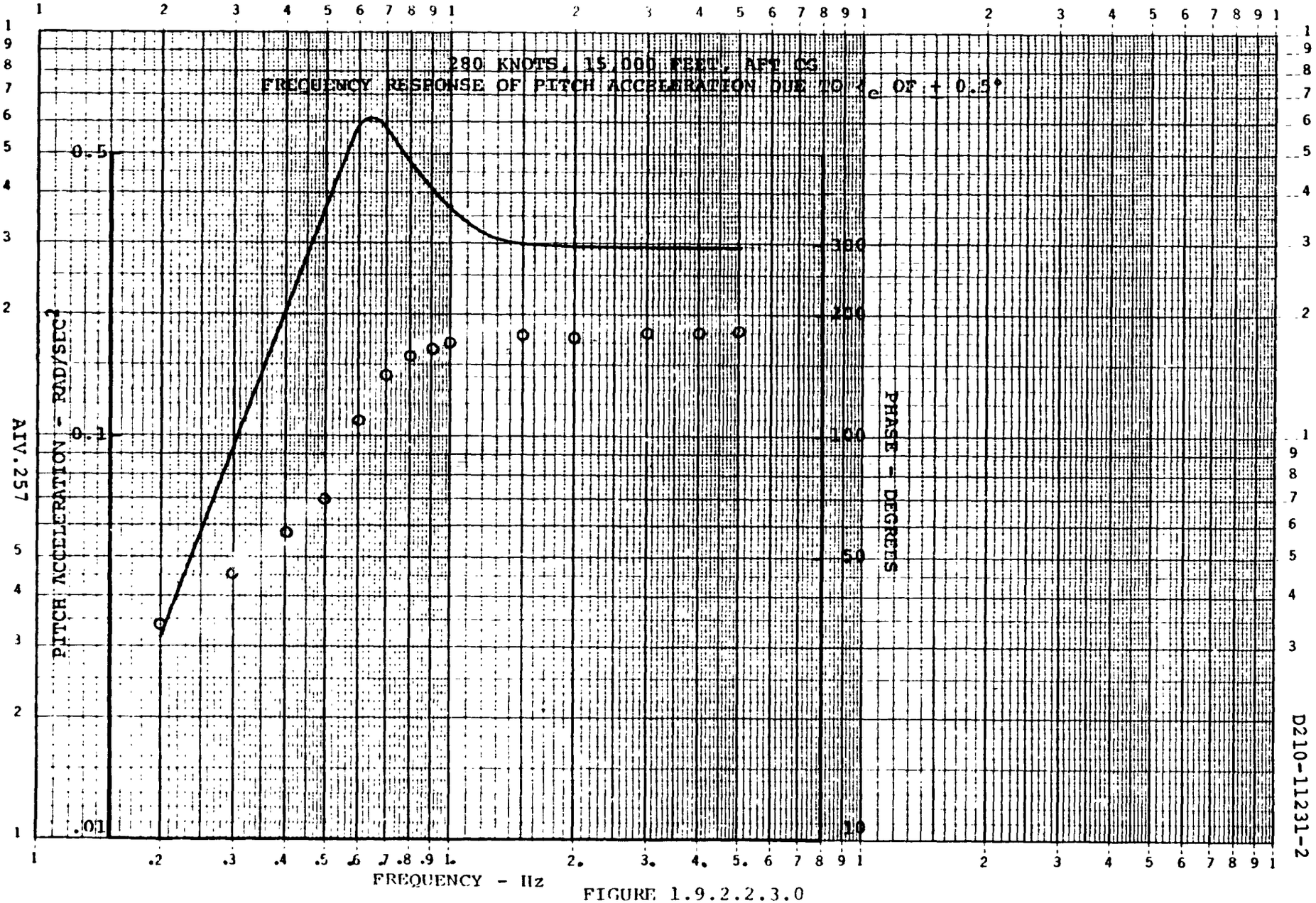

FIGURE 1.9.2.2.3.0

K·E LOGARITHMIC 2 X 3 CYCLES
KEUFFEL & ESSER CO. MADE IN U.S.A.

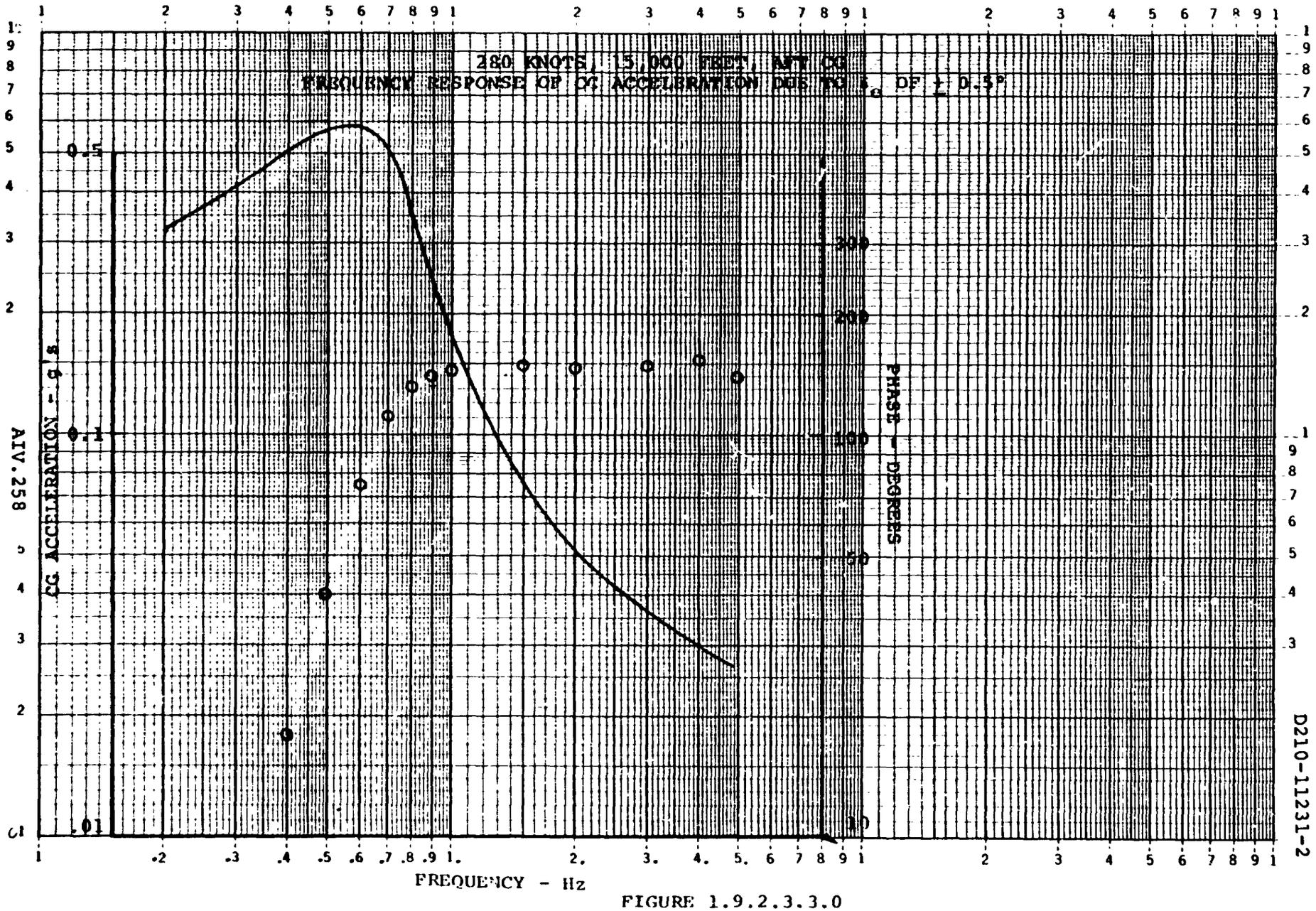

FIGURE 1.9.2.3.3.0

K·E LOGARITHMIC 2 X 3 CYCLES KEUFFEL & ESSER CO. MADE IN U.S.A.

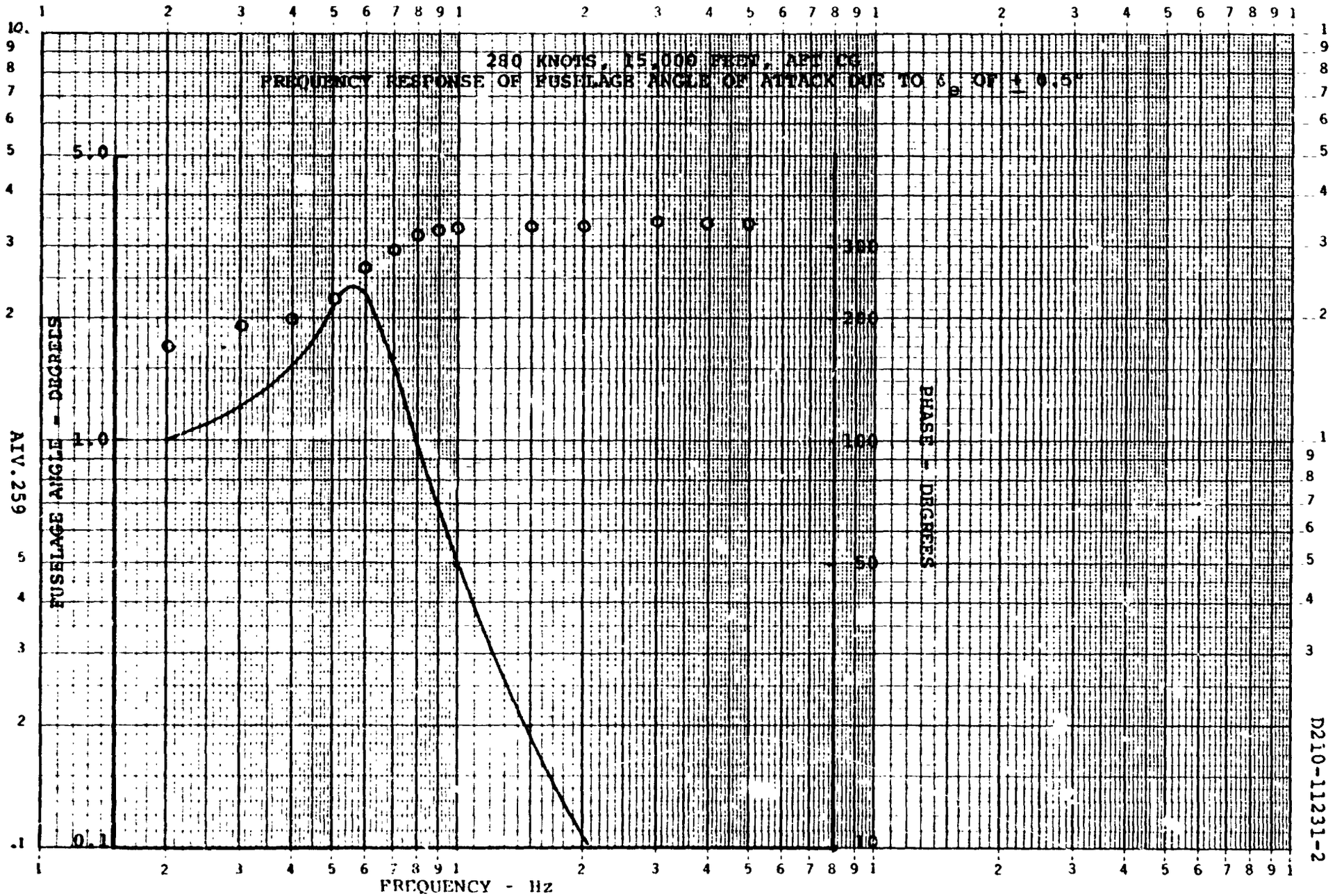

FIGURE 1.9.2.4.3.0

K•E LOGARITHMIC • 2 X 3 CYCLES
KEUFFEL & ESSER CO. MADE IN U.S.A.

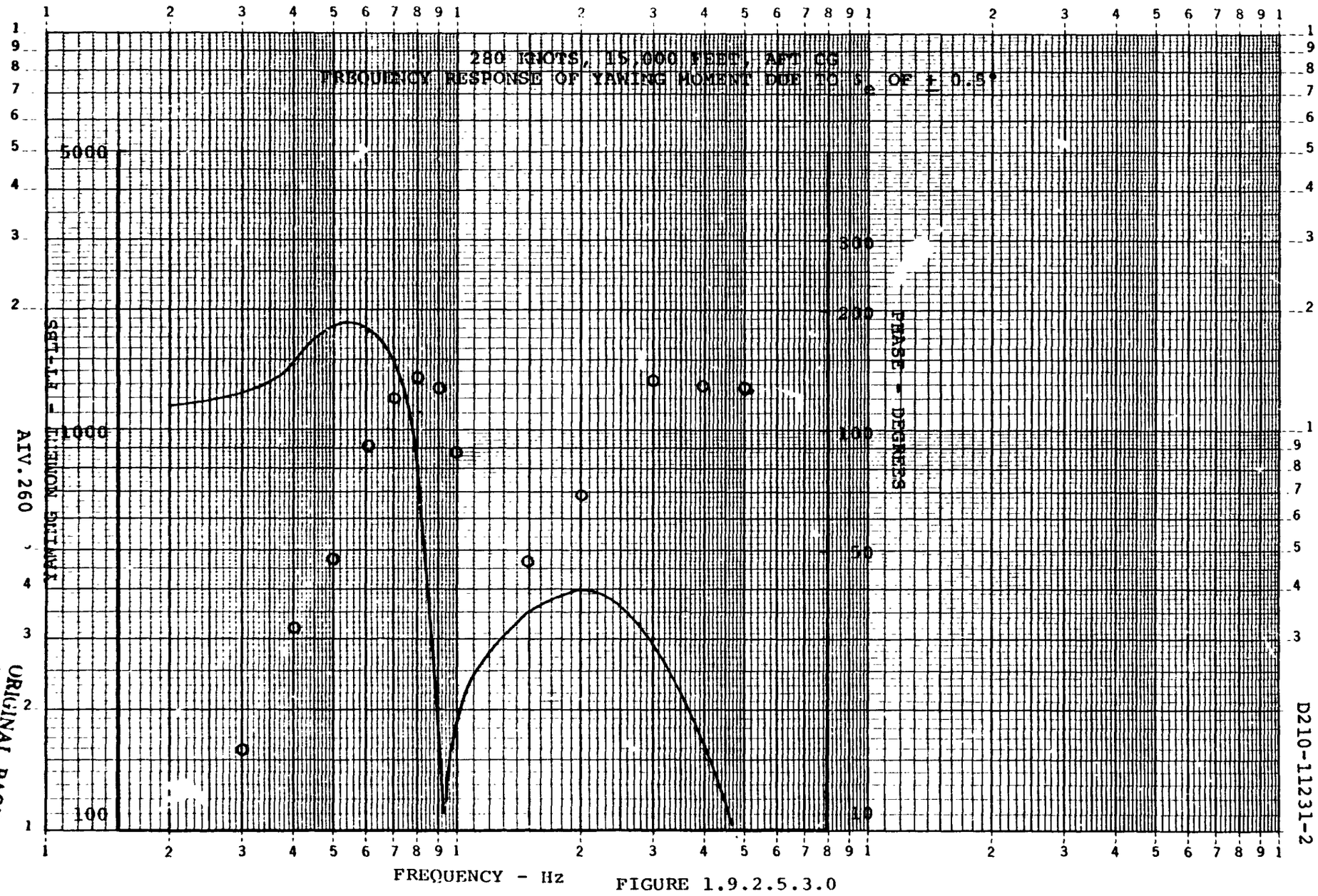

FIGURE 1.9.2.5.3.0

ORIGINAL PAGE IS
OF POOR QUALITY

K•E LOGARITHMIC • 2 X 3 CYCLES
KEUFFEL & ESSER CO. MADE IN U.S.A.

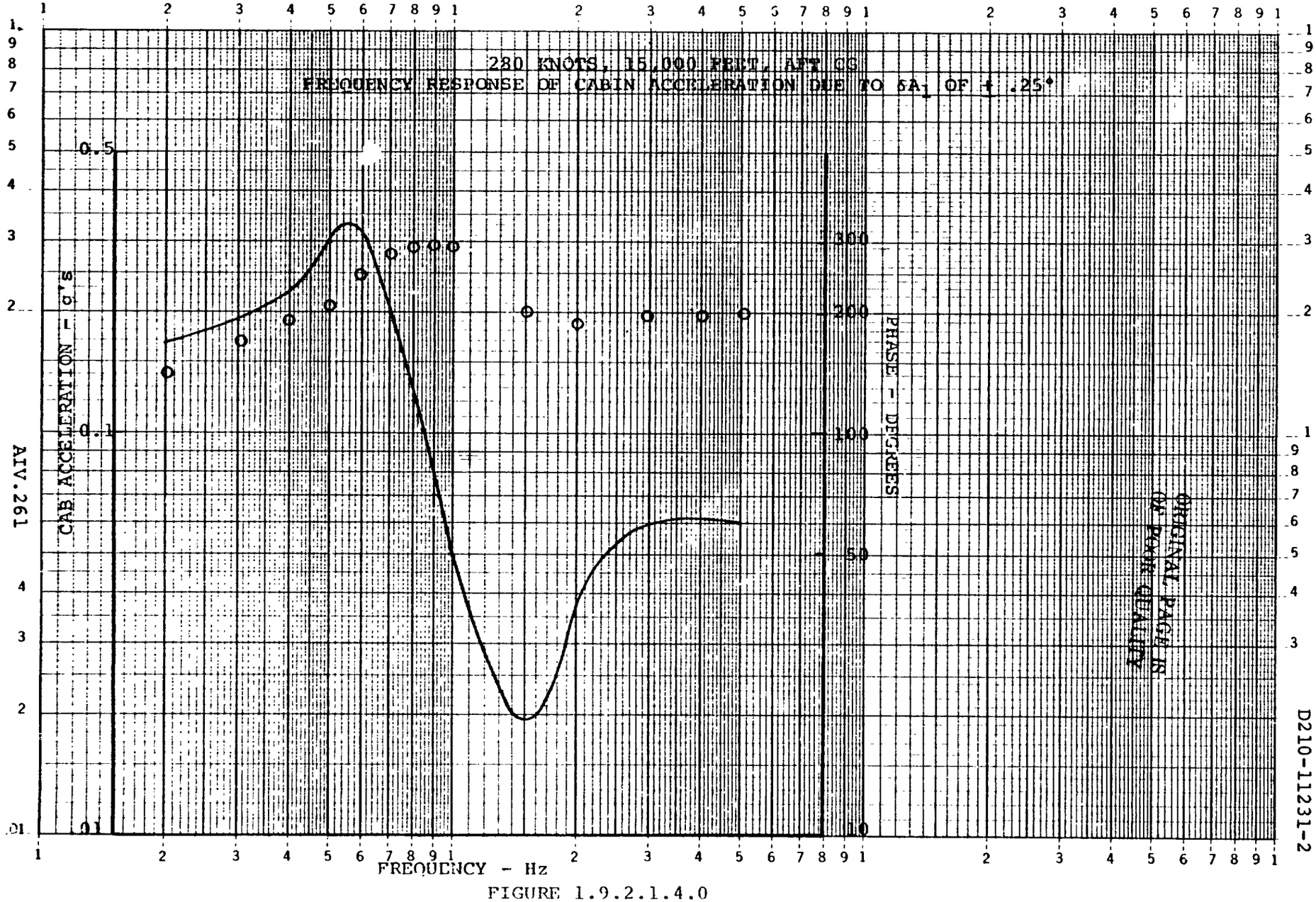

FIGURE 1.9.2.1.4.0

ORIGINAL PAGE IS
OF POOR QUALITY

K•E LOGARITHMIC • 2 X 3 CYCLES
KEUFFEL & ESSER CO. MADE IN U.S.A.

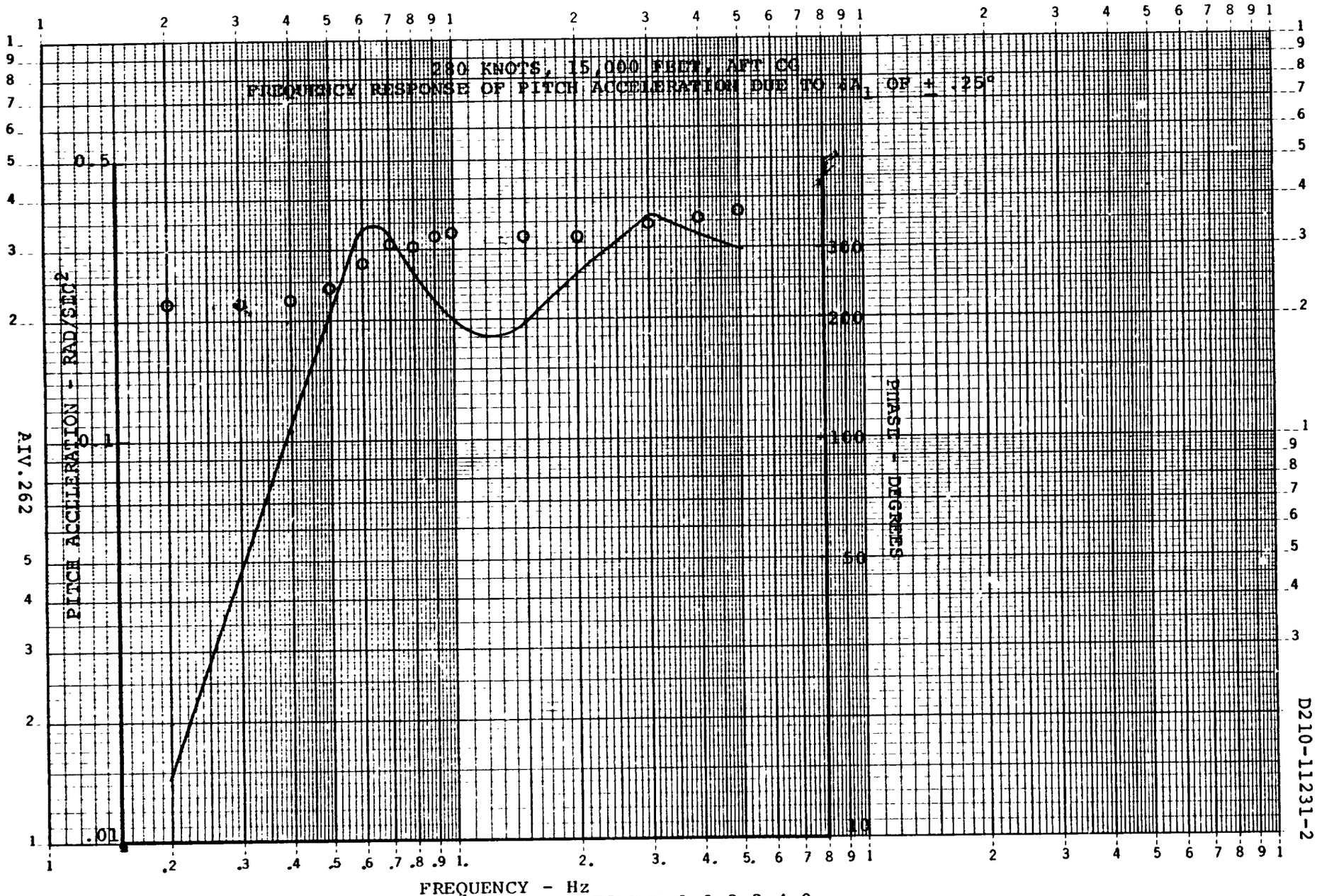

FIGURE 1.9.2.2.4.0

K+E LOGARITHMIC • 2 X 3 CYCLES
KEUFFEL & ESSER CO. MADE IN U.S.A.
46 7323

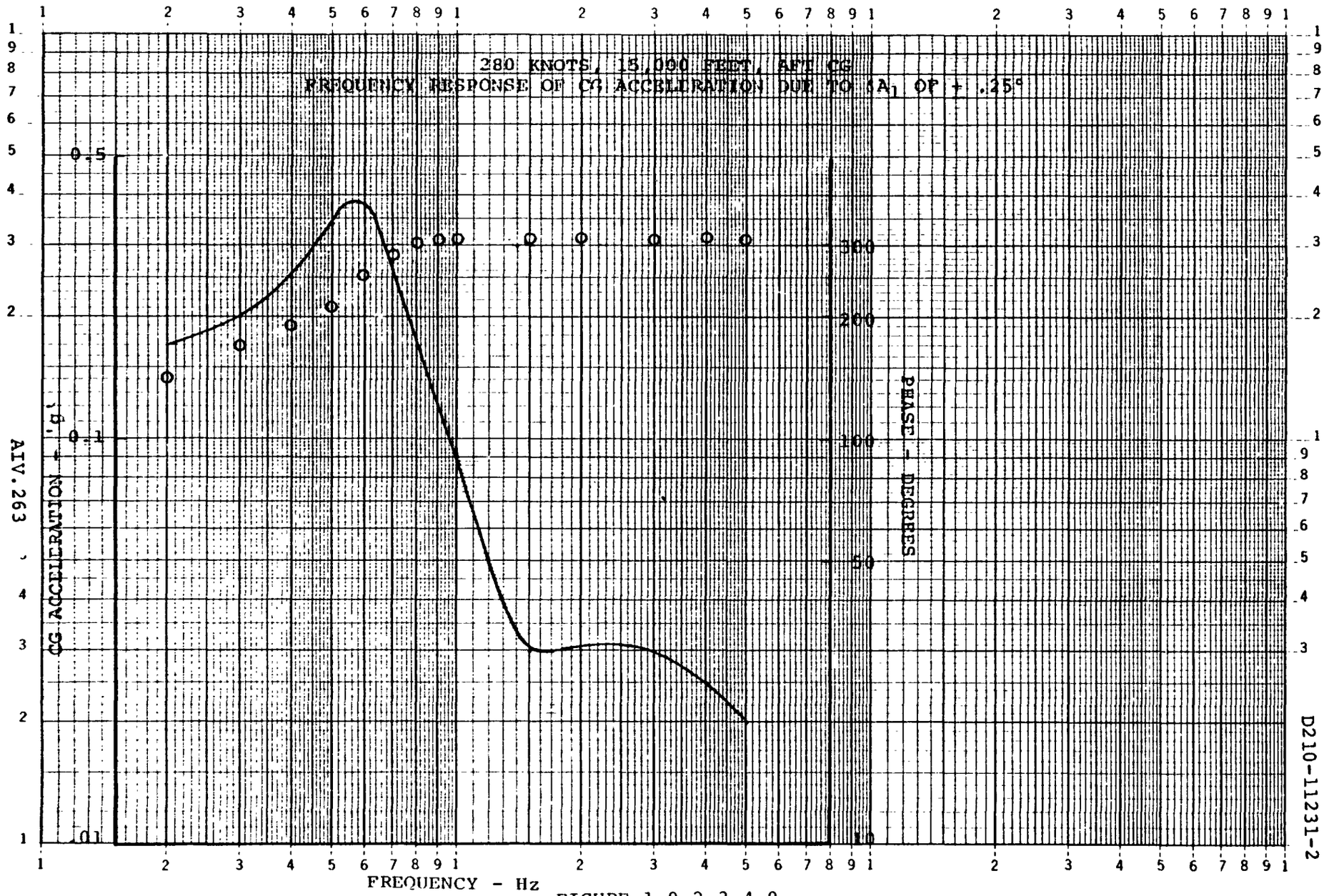

FIGURE 1.9.2.3.4.0

K+E LOGARITHMIC • 2 X 3 CYCLES
KEUFFEL & ESSER CO MADE IN U.S.A.

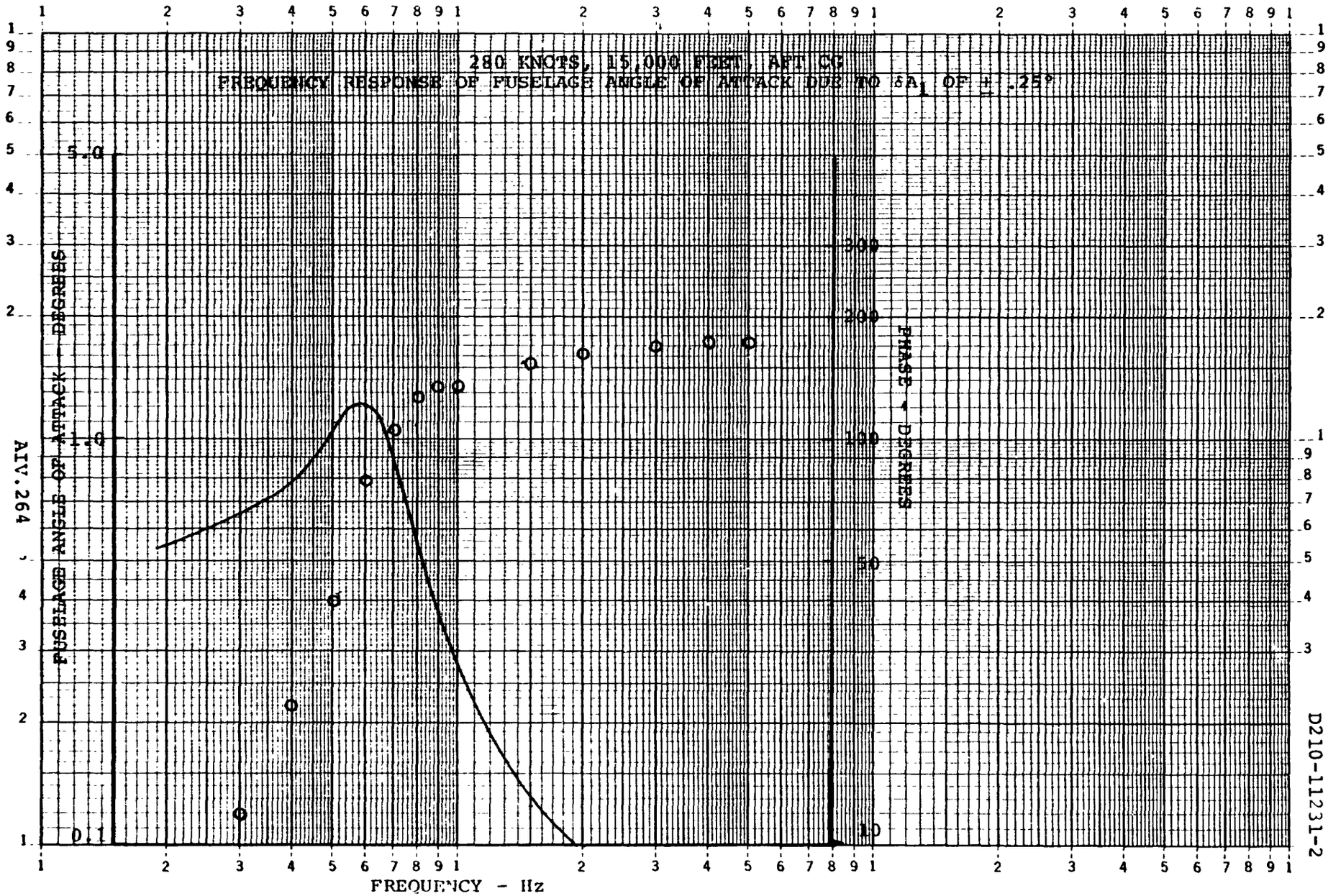

FIGURE 1.9.2.4.4.0

K+E LOGARITHMIC 2 X 3 CYCLES
KEUFFEL & ESSER CO. MADE IN U.S.A.
46 7323

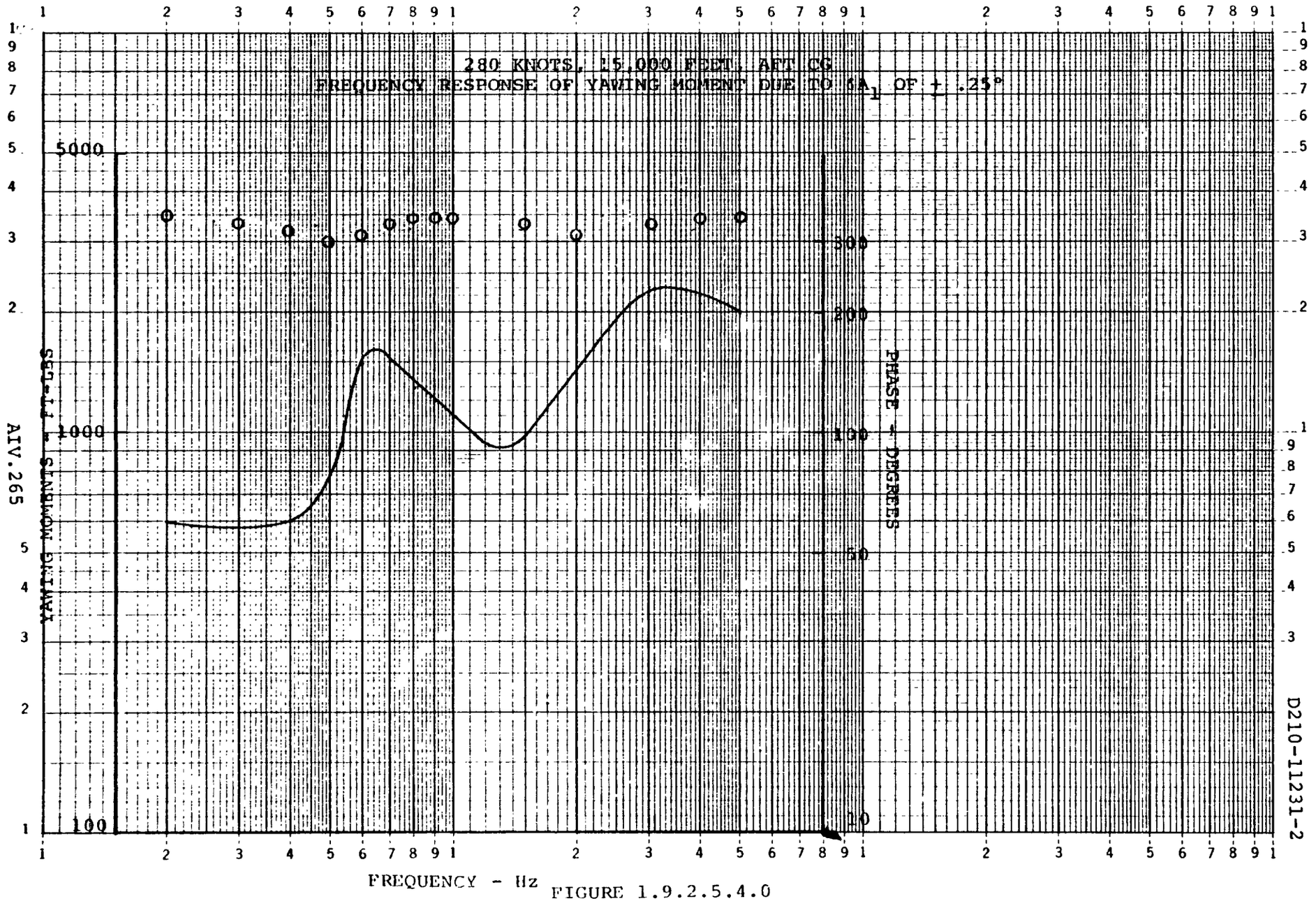

FIGURE 1.9.2.5.4.0

K+E LOGARITHMIC • 2 X 3 CYCLES
KEUFFEL & ESSER CO MADE IN U.S.A.

46 7323

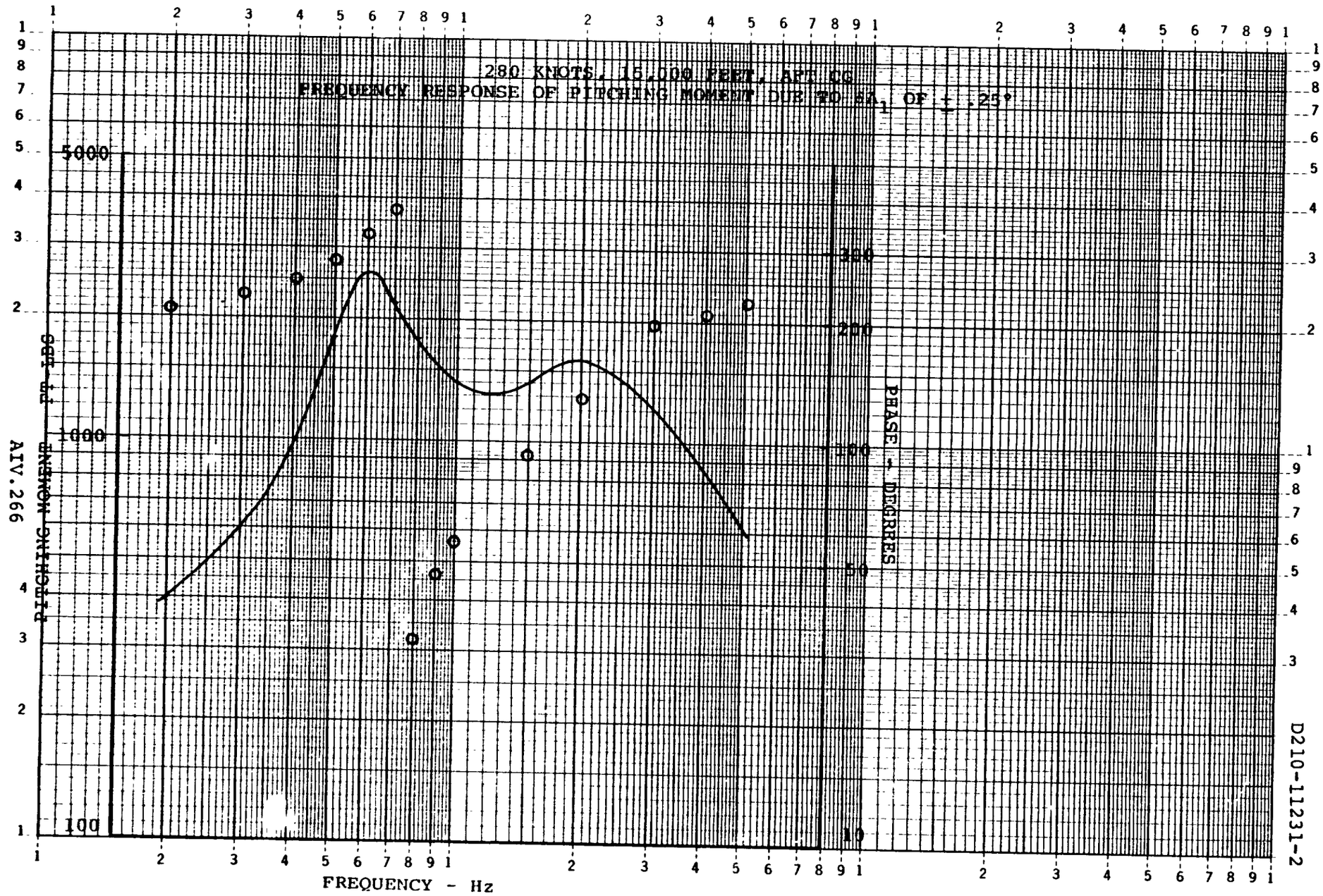

FIGURE 1.9.2.6.4.0

D210-11231-2

K•E LOGARITHMIC •2 X 3 CYCLES
KEUFFEL & ESSER CO MADE IN U.S.A.
46 7323

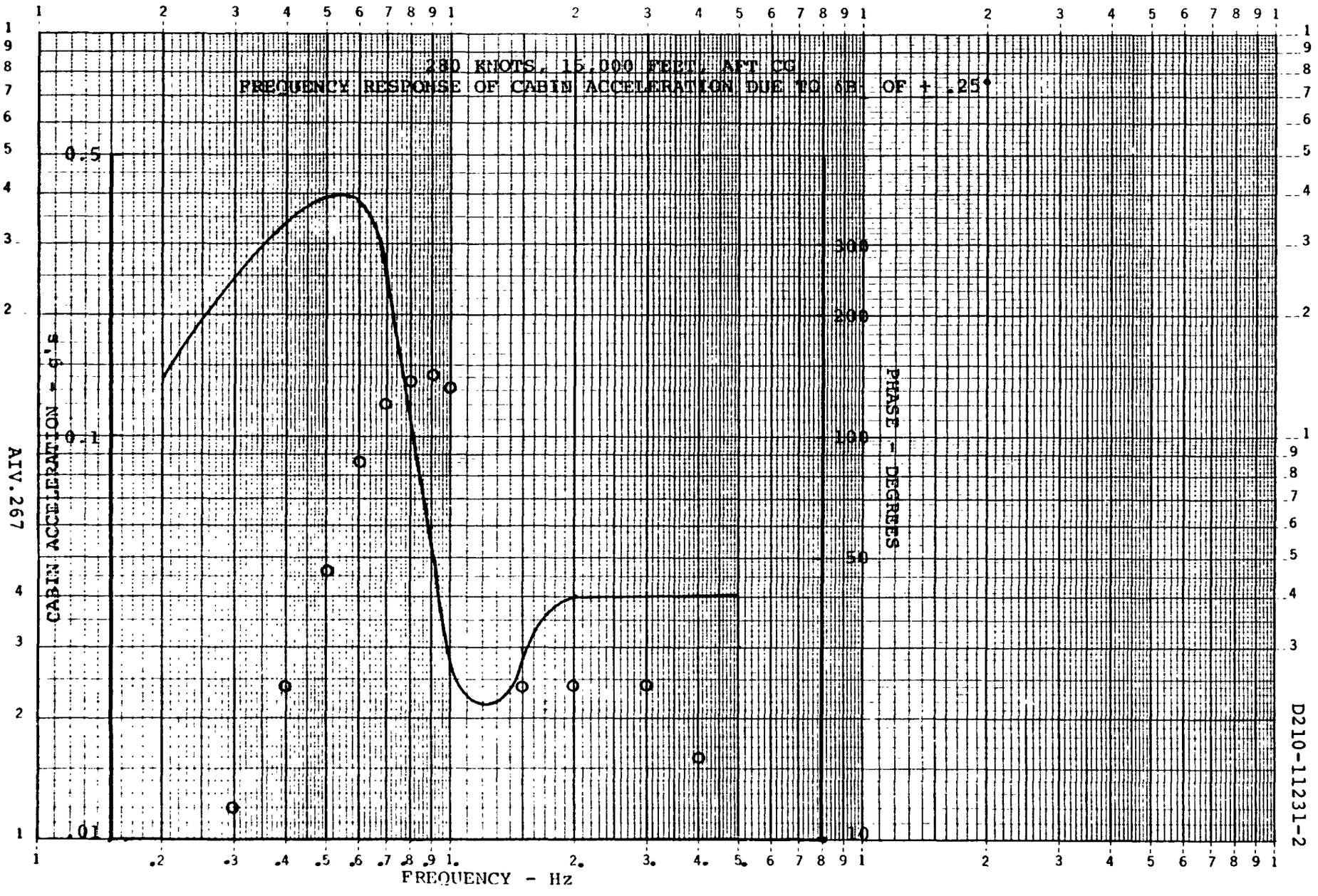

FIGURE 1.9.2.1.5.0

K•Σ LOGARITHMIC • 2 X 3 CYCLES
KEUFFEL & ESSER CO. MADE IN U.S.A.

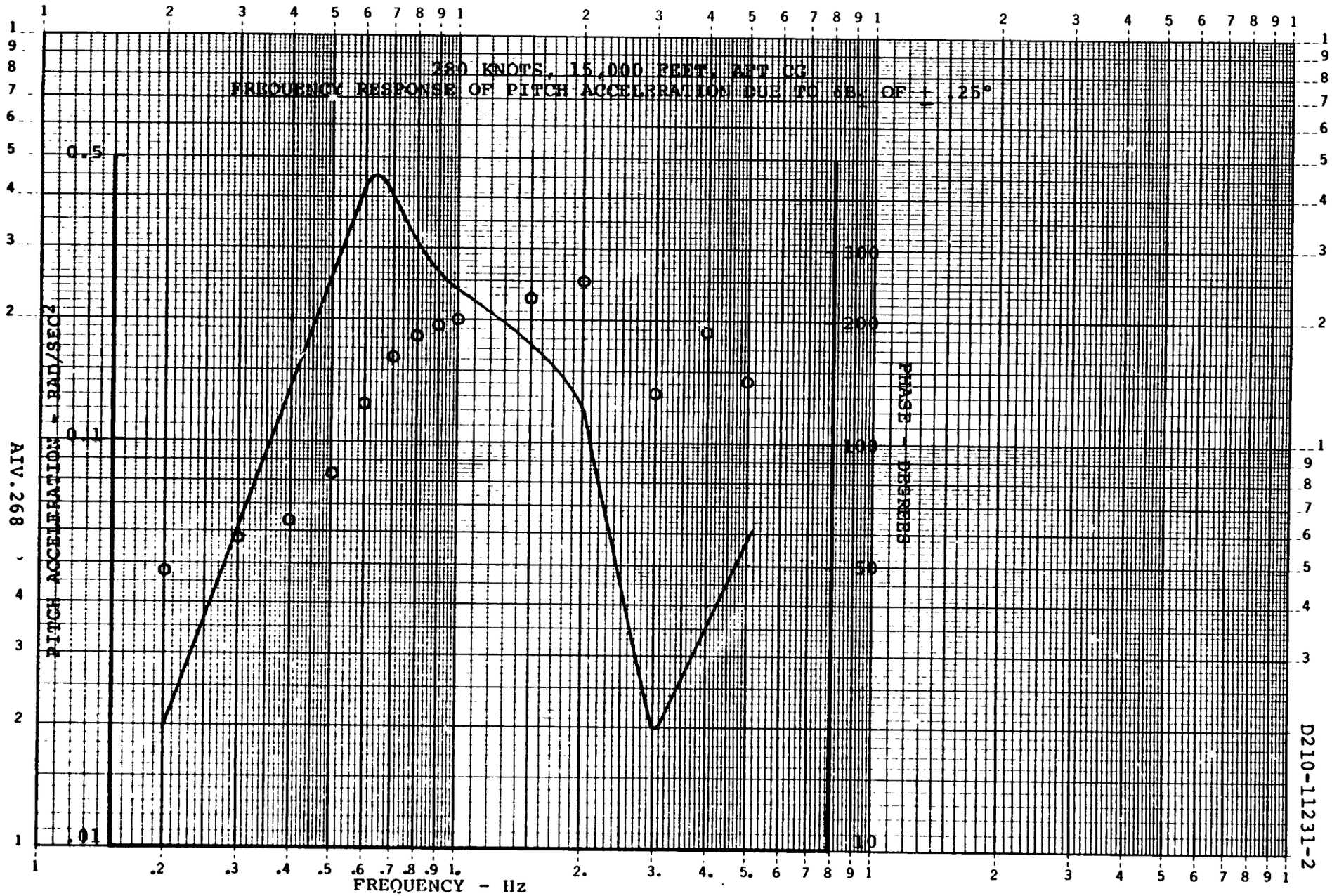

FIGURE 1.9.2.2.5.0

K·E LOGARITHMIC 2 X 3 CYCLES
KEUFFEL & ESSER CO. MADE IN U.S.A.
46 7323

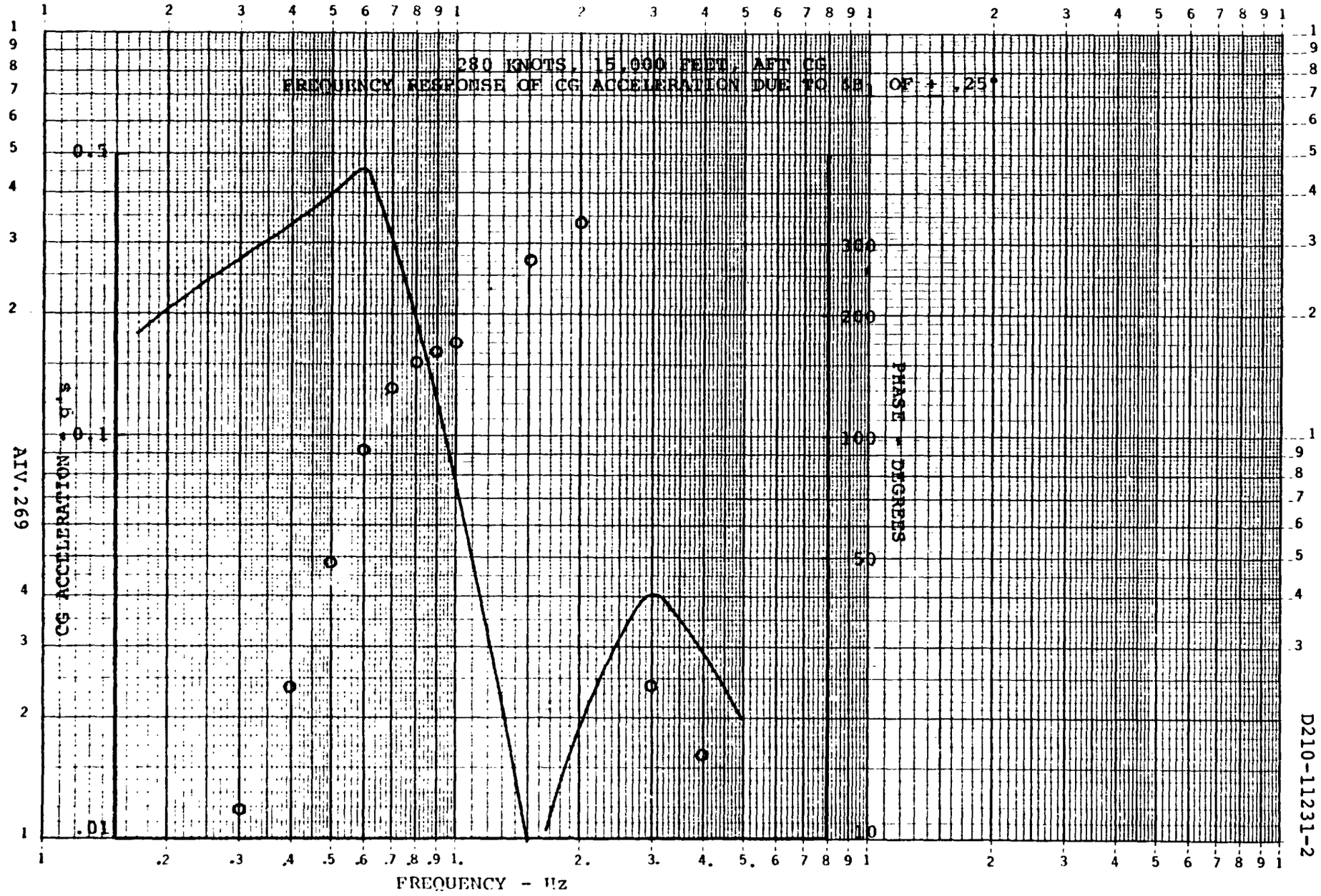

FIGURE 1.9.2.3.5.0

K•E LOGARITHMIC • 2 X 3 CYCLES
KEUFFEL & ESSER CO. MADE IN U.S.A.

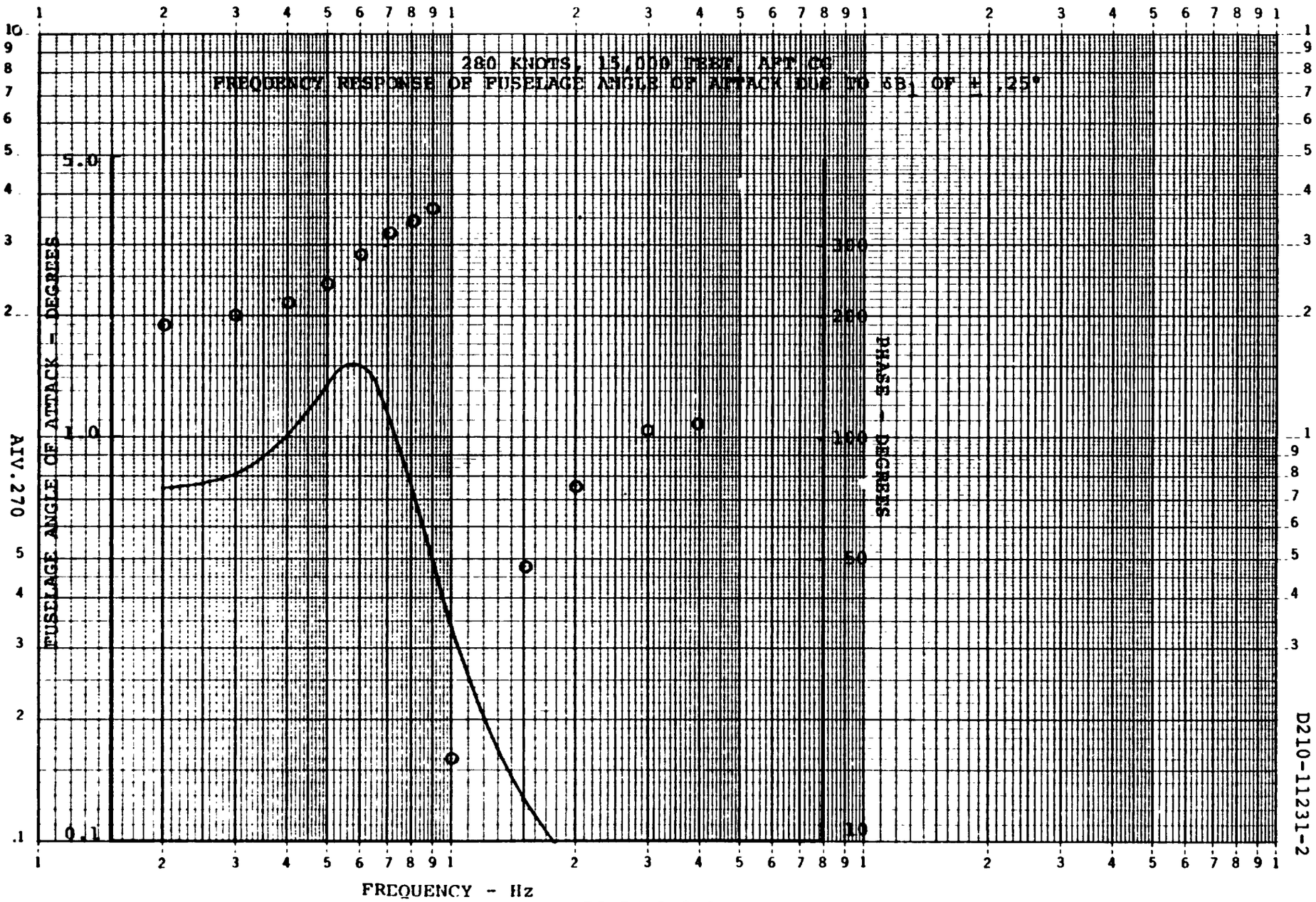

FIGURE 1.9.2.4.5.0

K•E LOGARITHMIC 2 X 3 CYCLES
KEUFFEL & ESSER CO. MADE IN U.S.A.
46 7323

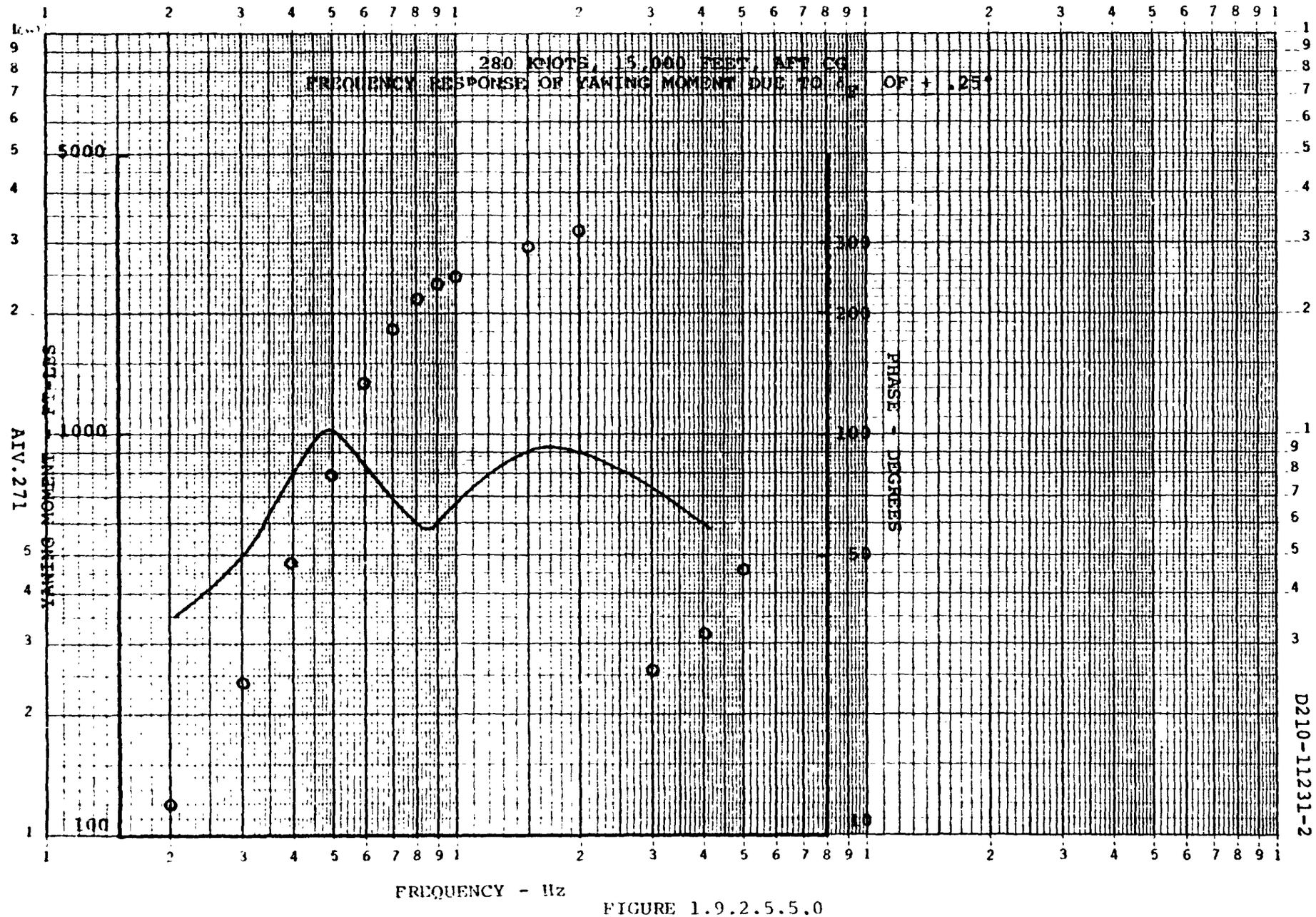

FIGURE 1.9.2.5.5.0

K·E LOGARITHMIC 2 X 3 CYCLES
KEUFFEL & ESSER CO. MADE IN U.S.A.

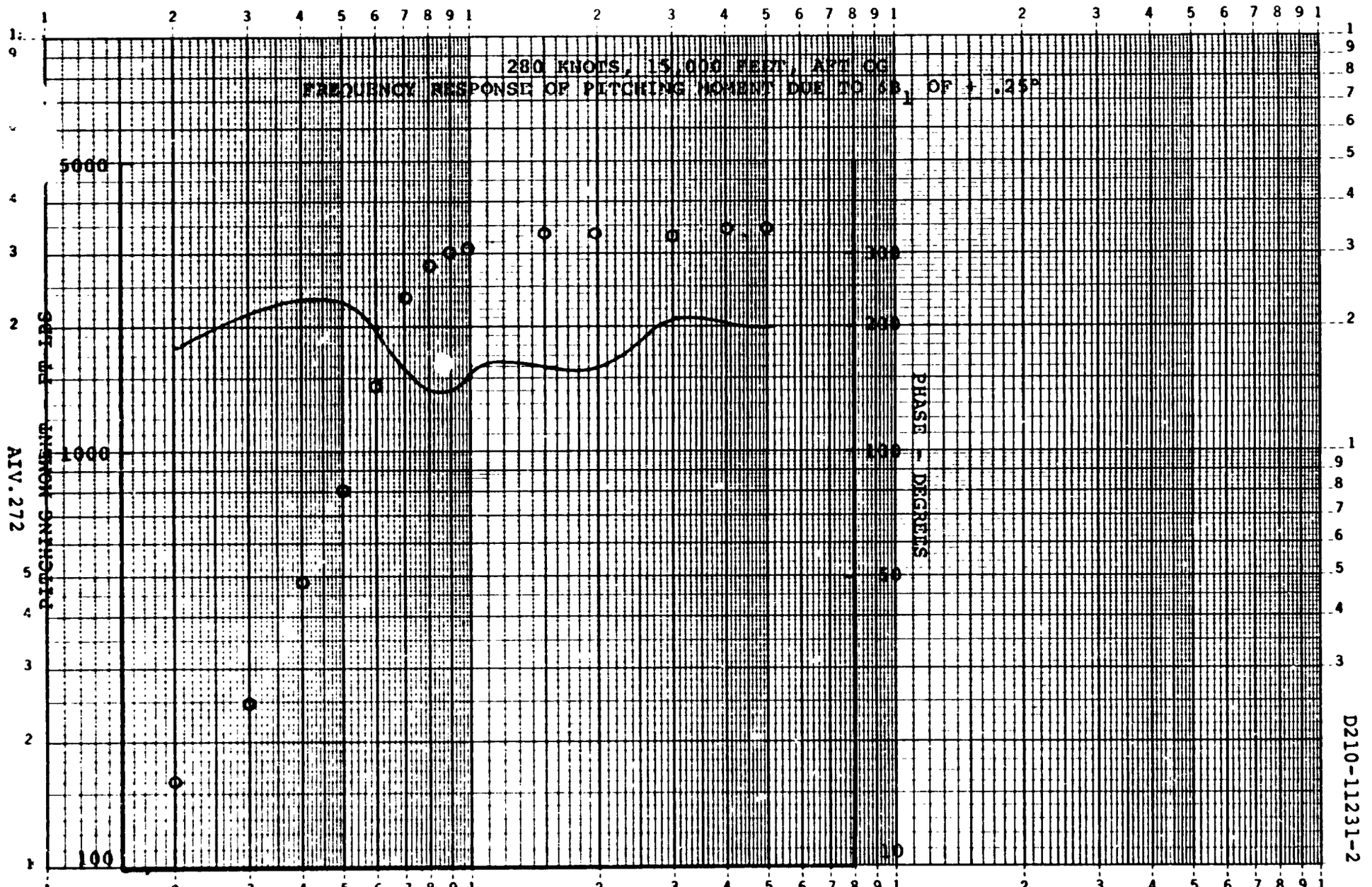

FIGURE 1.9.2.6.5.0

NO 340R-L410 DIETZGEN GRAPH PAPER
SEMI-LOGARITHMIC
4 CYCLES X 10 DIVISIONS PER INCH
EUGENE DIETZGEN CO.
MADE IN U. S. A.

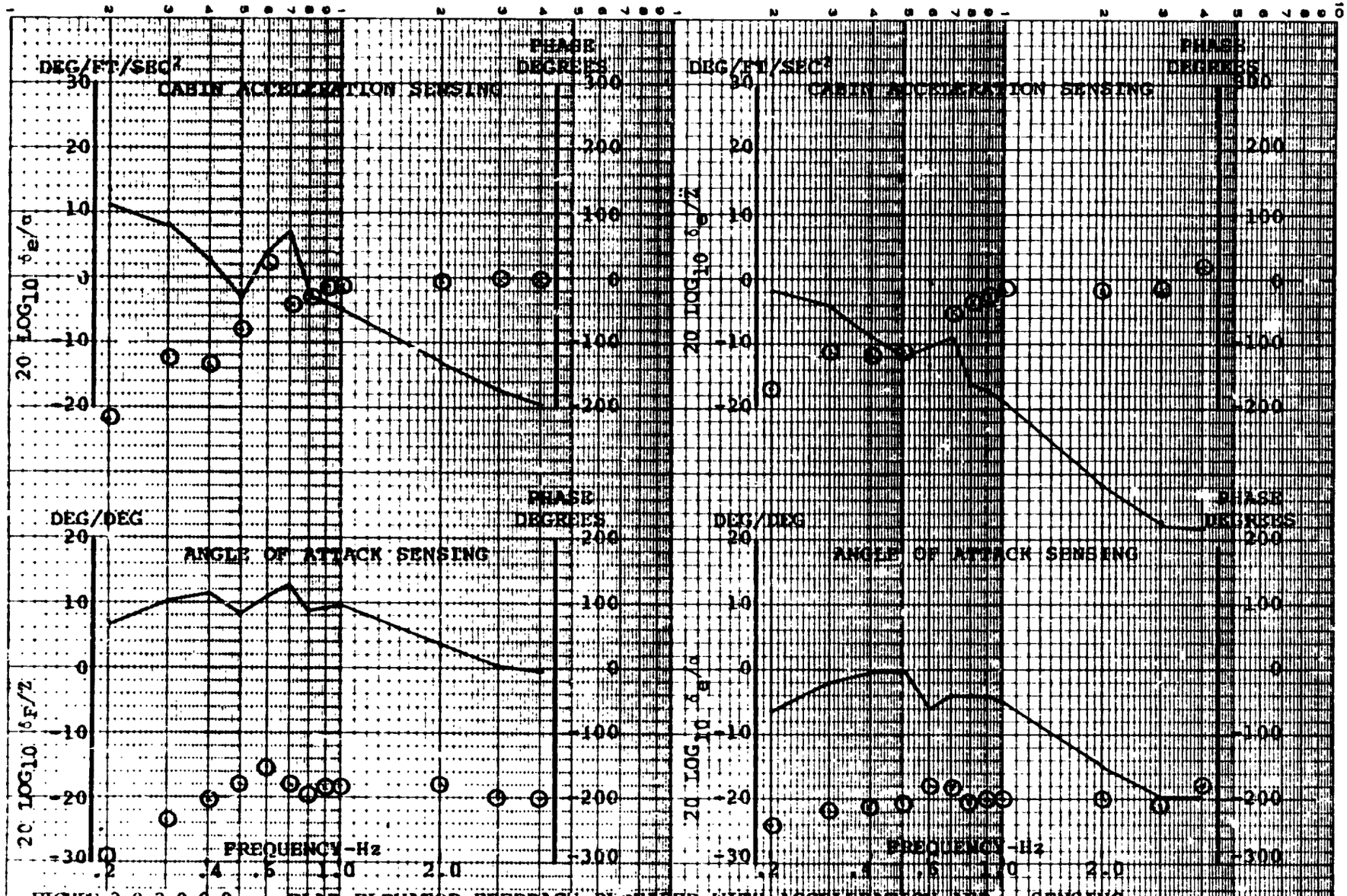

FIGURE 2.9.2.0.0.0. FLAP ELEVATOR FEEDBACK BLOCKED WITH ACCELERATION AND α SENSING, 280 KNOTS, 15,000 FEET, AFT CG, NO A_1 OR B_1 FEEDBACK

ORIGINAL PAGE IS
OF POOR QUALITY

OF POOR QUALITY

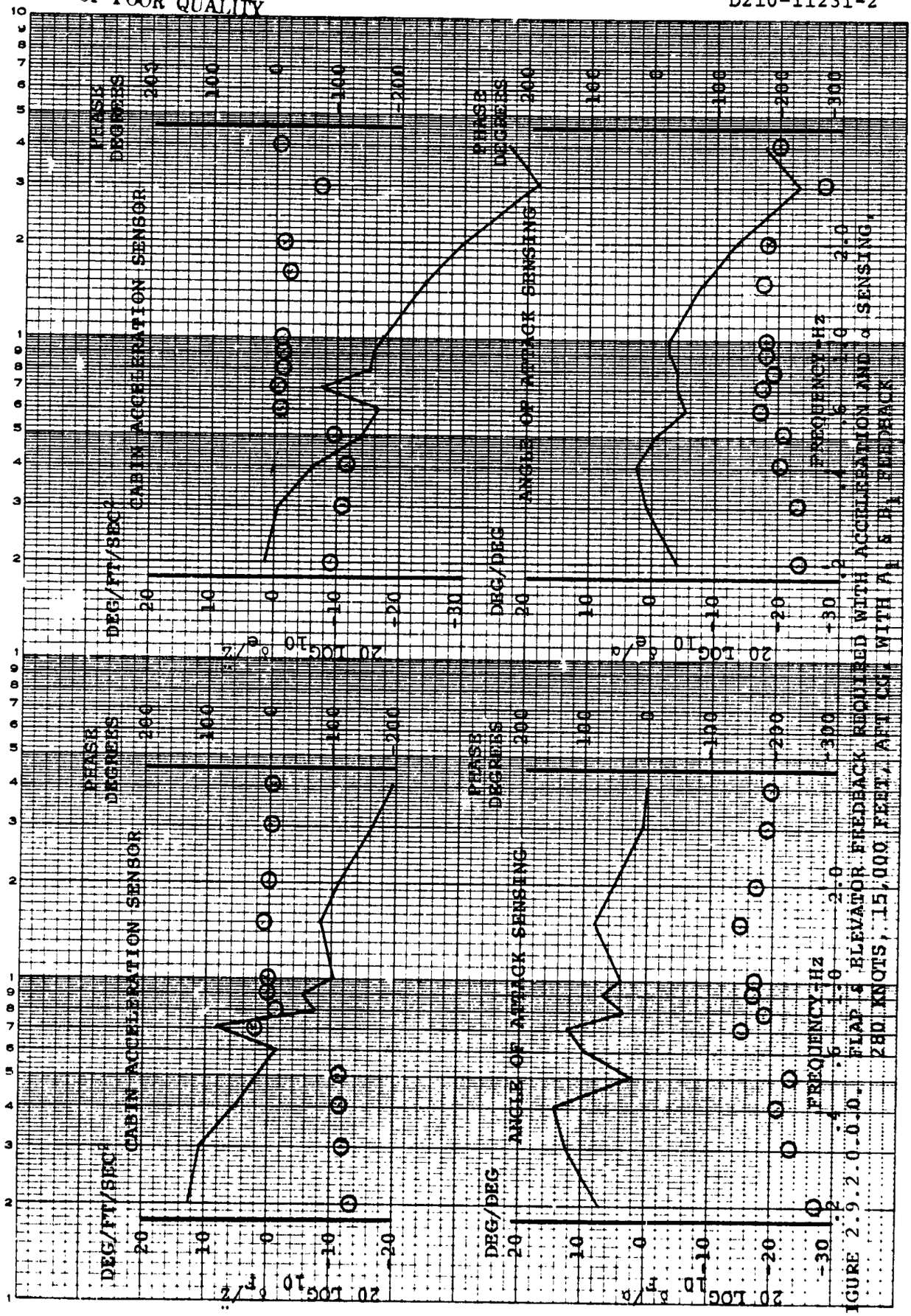

FIGURE 2.9.2.0.0.0. FLAP & ELEVATOR FEEDBACK REQUIRED WITH ACCELERATION AND α SENSING, 280 KNOTS, 15,000 FEET, AFT CG, WITH AL & HL FEEDBACK

EUGENE DIETZGEN CO.
MADE IN U.S.A.

NO. 340R-L410 DIETZGEN GRAPH PAPER
SEMI-LOGARITHMIC
4 CYCLES X 10 DIVISIONS PER INCH

NO. 340R-L410 DIETZGEN GRAPH PAPER
SEMI-LOGARITHMIC
4 CYCLES X 10 DIVISIONS PER INCH

EUGENE DIETZGEN CO.
MADE IN U.S.A.

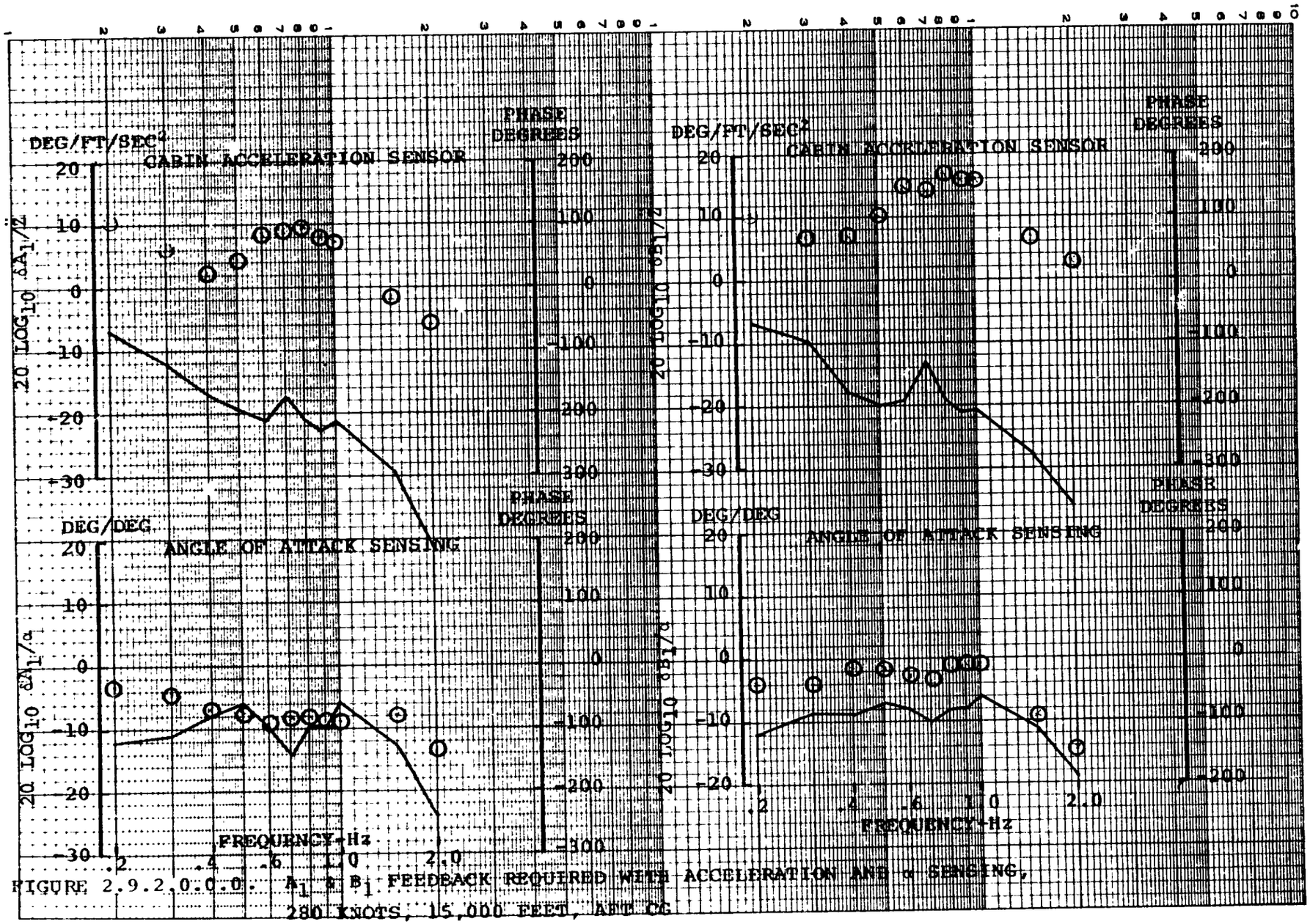

FIGURE 2.9.2.0.0.0. A_1 & B_1 FEEDBACK REQUIRED WITH ACCELERATION AND α SENSING, 280 KNOTS, 15,000 FEET, AFT CG

ORIGINAL PAGE IS
OF POOR QUALITY

FLIGHT CONDITION: 280 KNOTS, 15,000 FEET, (4,573m), FORWARD CG

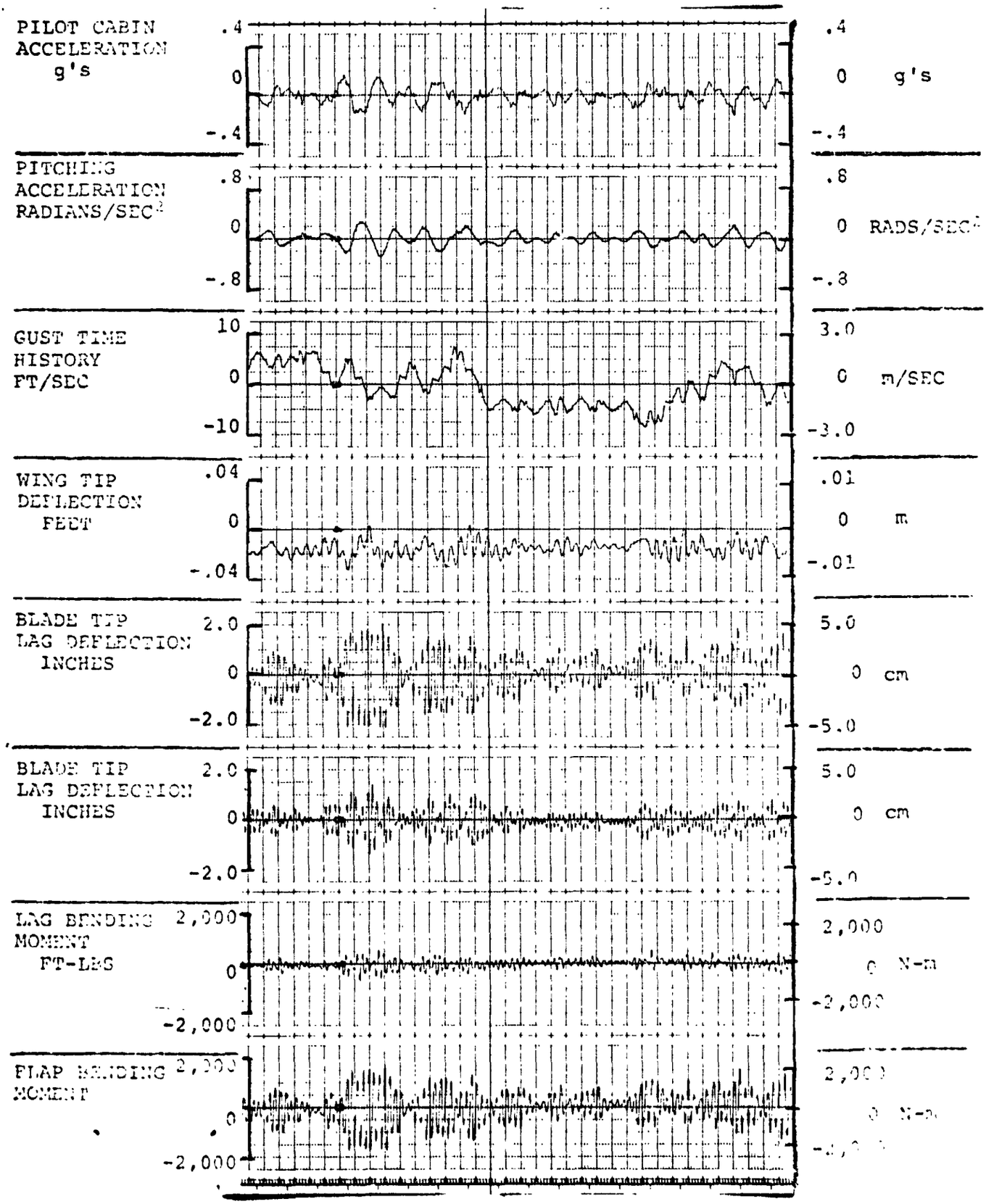

FIGURE 3.9.1.0.0.1. RESPONSES FOR GAIN F = 0, GAIN E = 0

FLIGHT CONDITION: 280 KNOTS, 15,000 FEET, (4,573m), FORWARD CG

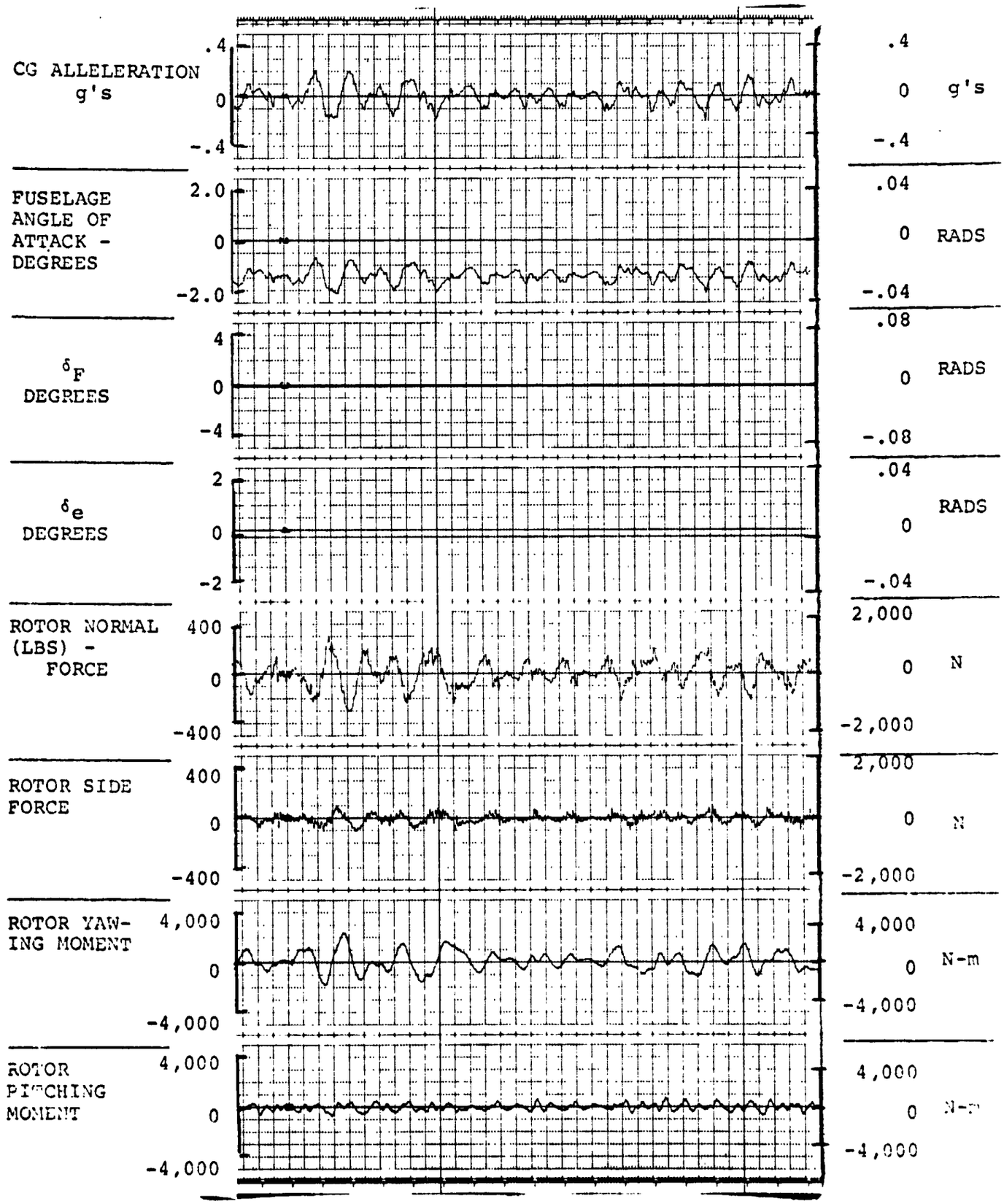

FIGURE 4.9.1.0.0.1. RESPONSES FOR GAIN F = 0, GAIN E = 0

ORIGINAL PAGE IS OF POOR QUALITY

FLIGHT CONDITION: 280 KNOTS, 15,000 FEET, (4,573m), FORWARD CG

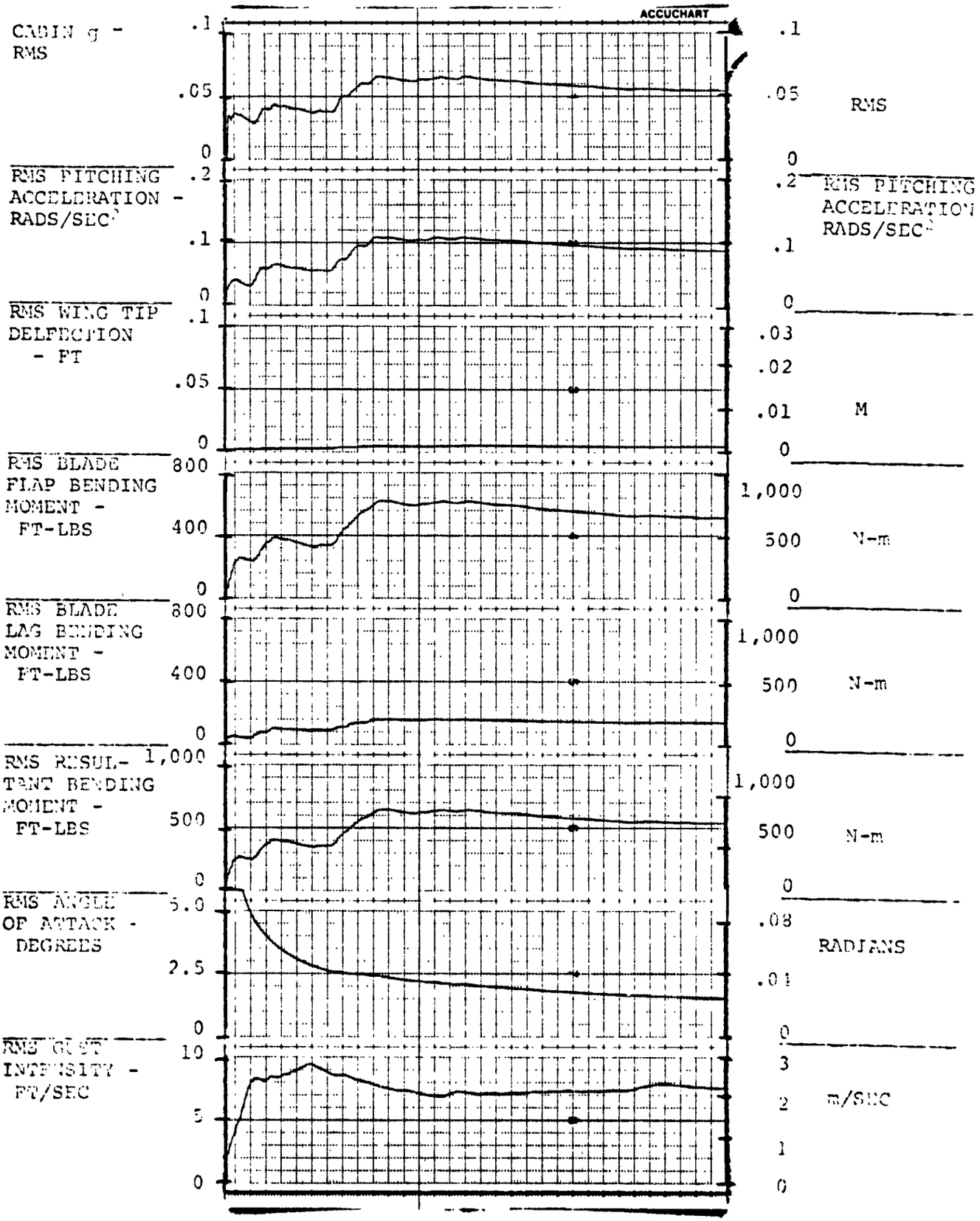

FIGURE 5.9.1.0.0.1. RESPONSES FOR GAIN F = 0, GAIN E = 0

FLIGHT CONDITION: 280 KNOTS, 15,000 FEET, (4,573m), FORWARD CG

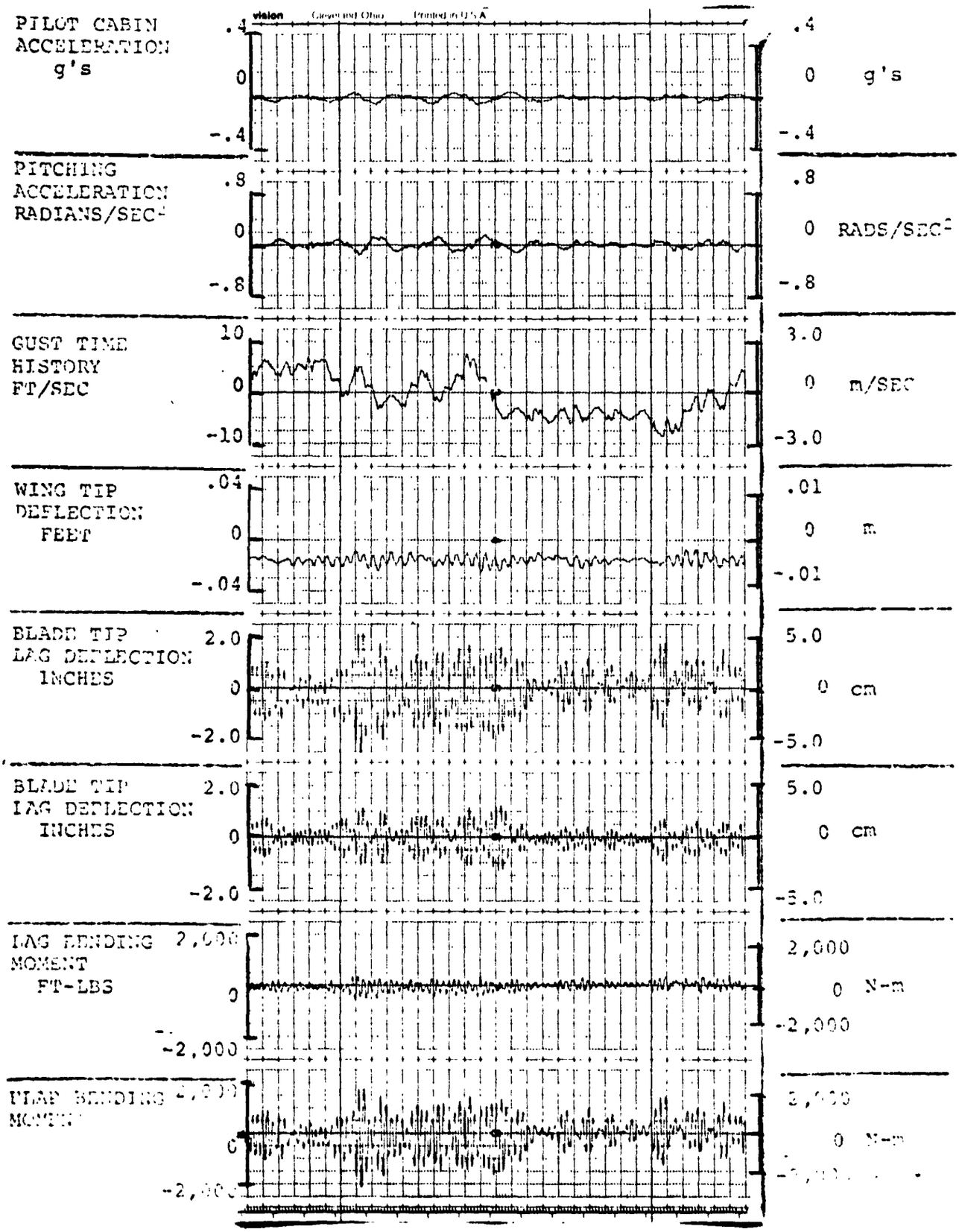

FIGURE 3.9.1.0.0.3. RESPONSES FOR GAIN F = 4.0, GAIN E = .7

ORIGINAL PAGE IS OF POOR QUALITY

FLIGHT CONDITION: 280 KNOTS, 15,000 FEET, (4,573m), FORWARD CG

D210-11231-2

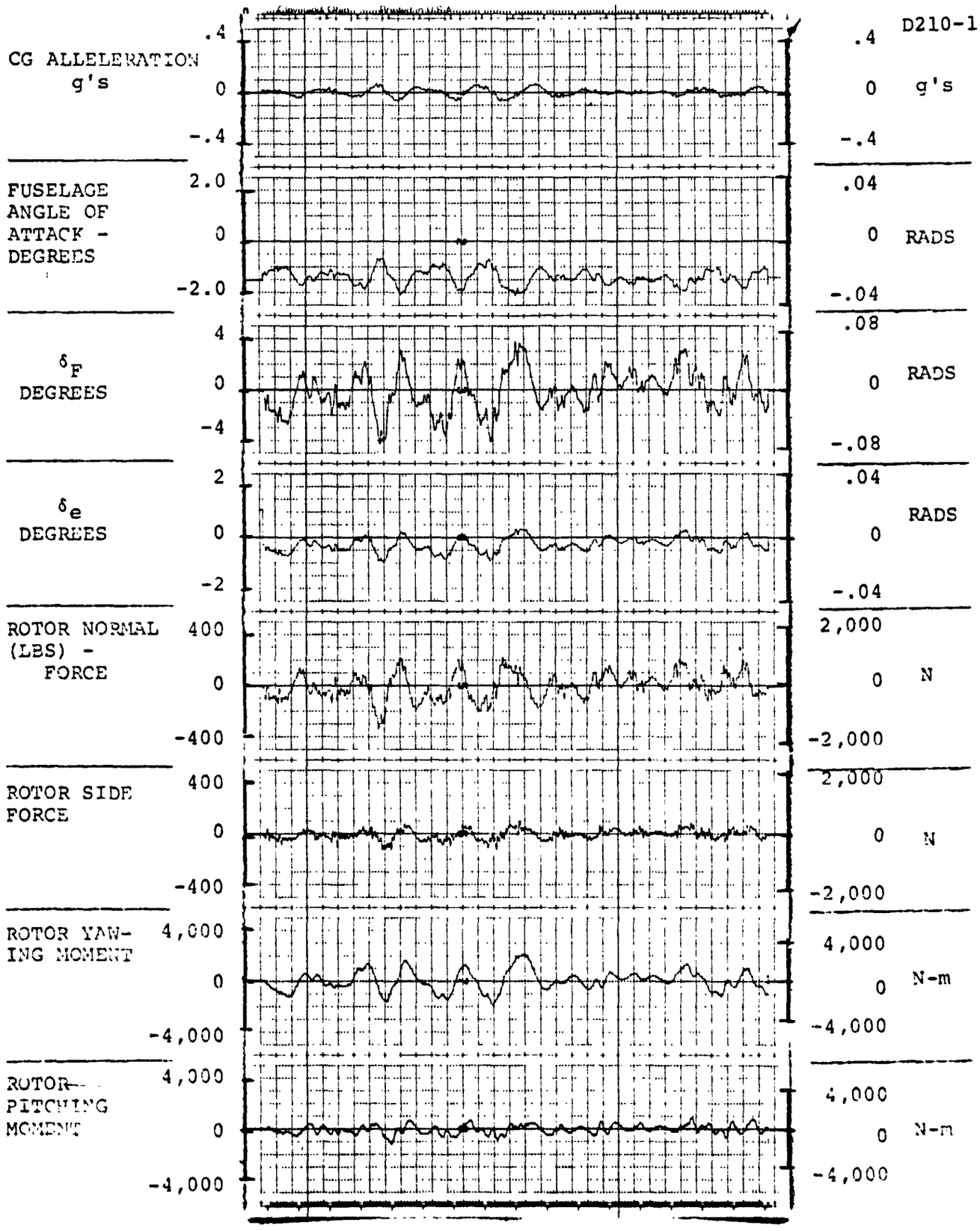

FIGURE 4.9.1.0.0.3. RESPONSES FOR GAIN F = 4.0, GAIN E = .7

FLIGHT CONDITION: 280 KNOTS, 15,000 FEET, (4,573m), FORWARD CG

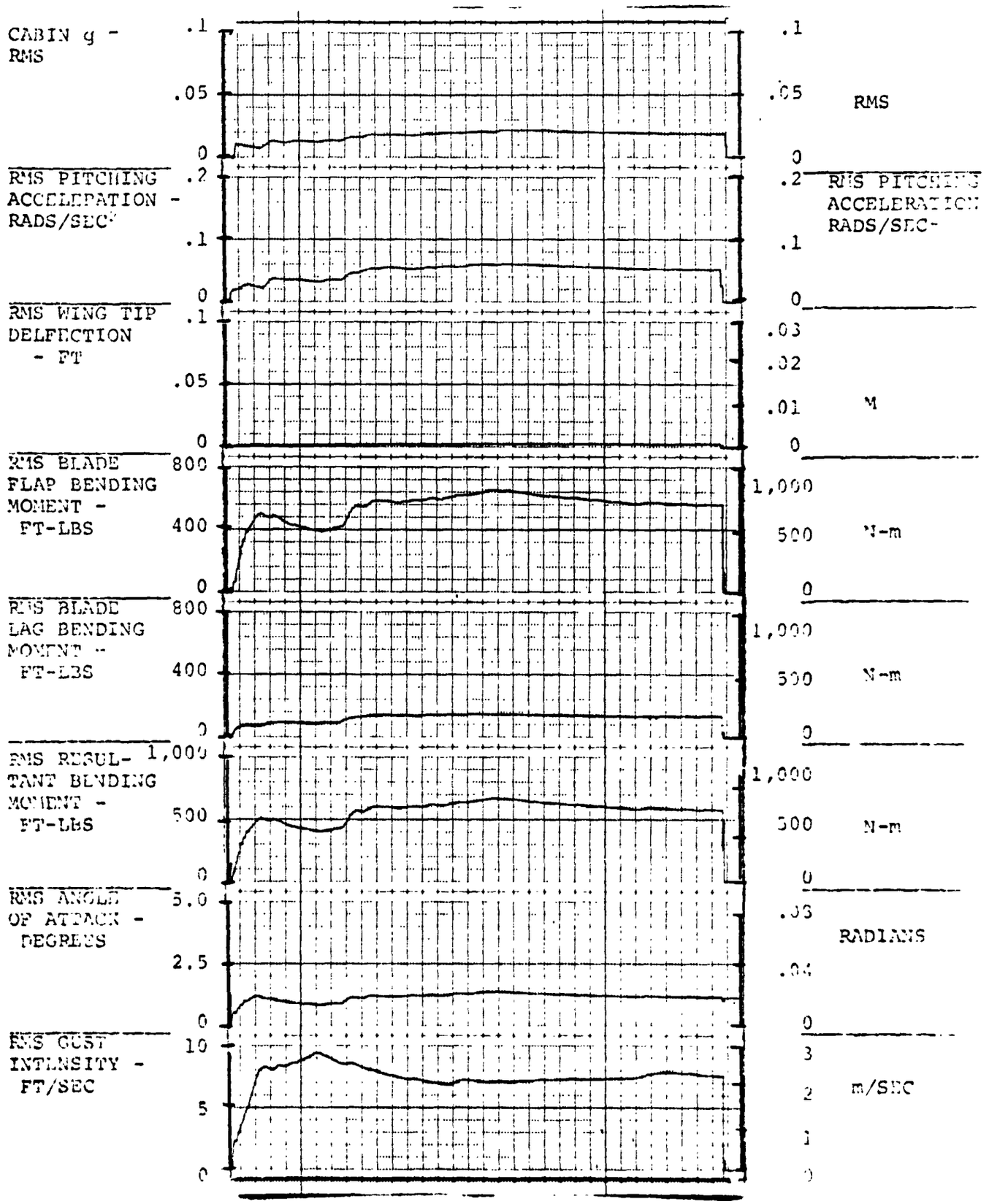

FIGURE 5.9.1.0.0.3. RESPONSES FOR GAIN F = 4.0, GAIN E = .7

ORIGINAL PAGE IS
OF POOR QUALITY

FLIGHT CONDITION: 280 KNOTS, 15,000 FEET, (4,573m), AFT CG

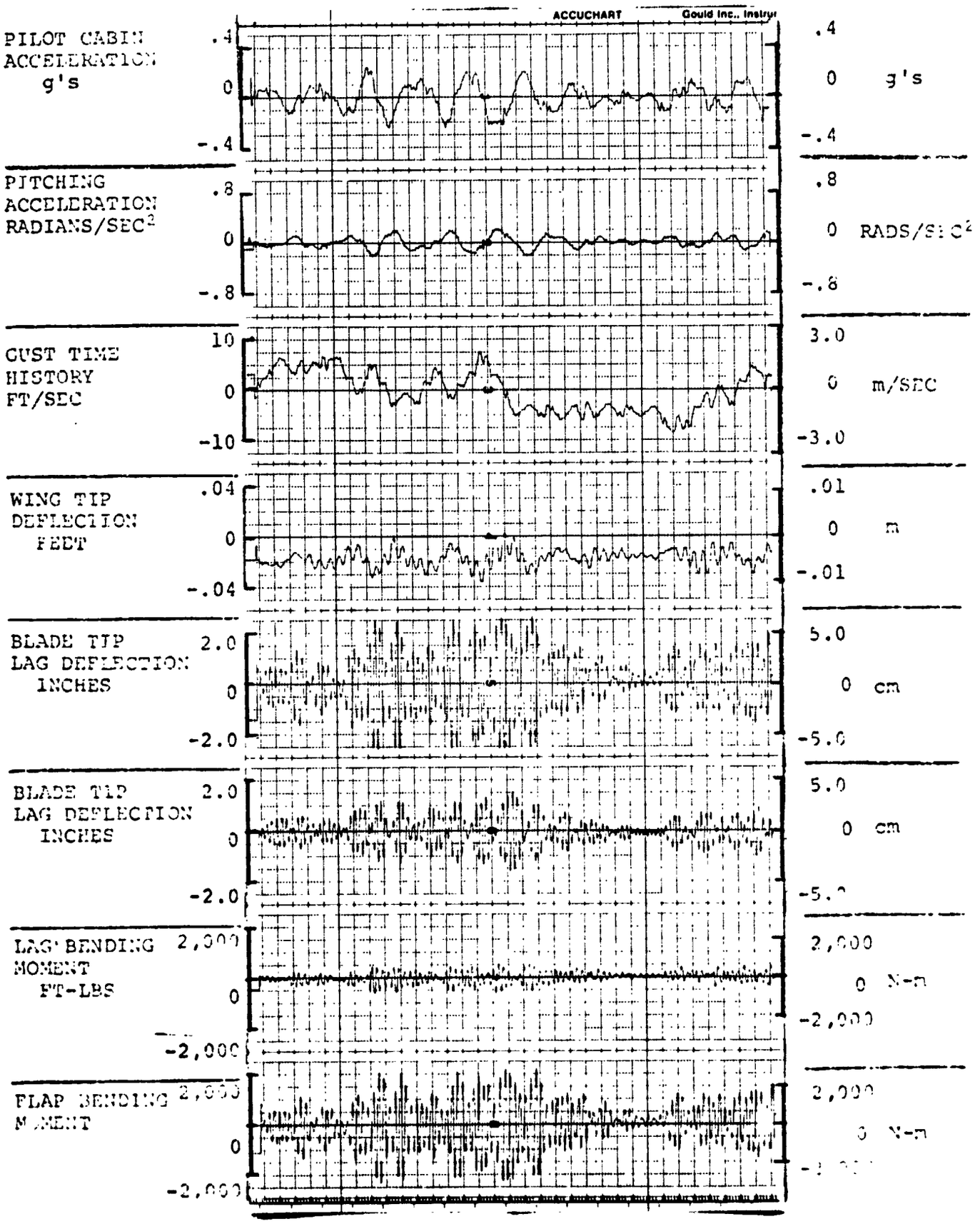

FIGURE 3.9.2.0.0.1. RESPONSES FOR GAIN F = 0, GAIN E = 0

FLIGHT CONDITION: 280 KNOTS, 15,000 FEET, (4,573m), AFT CG

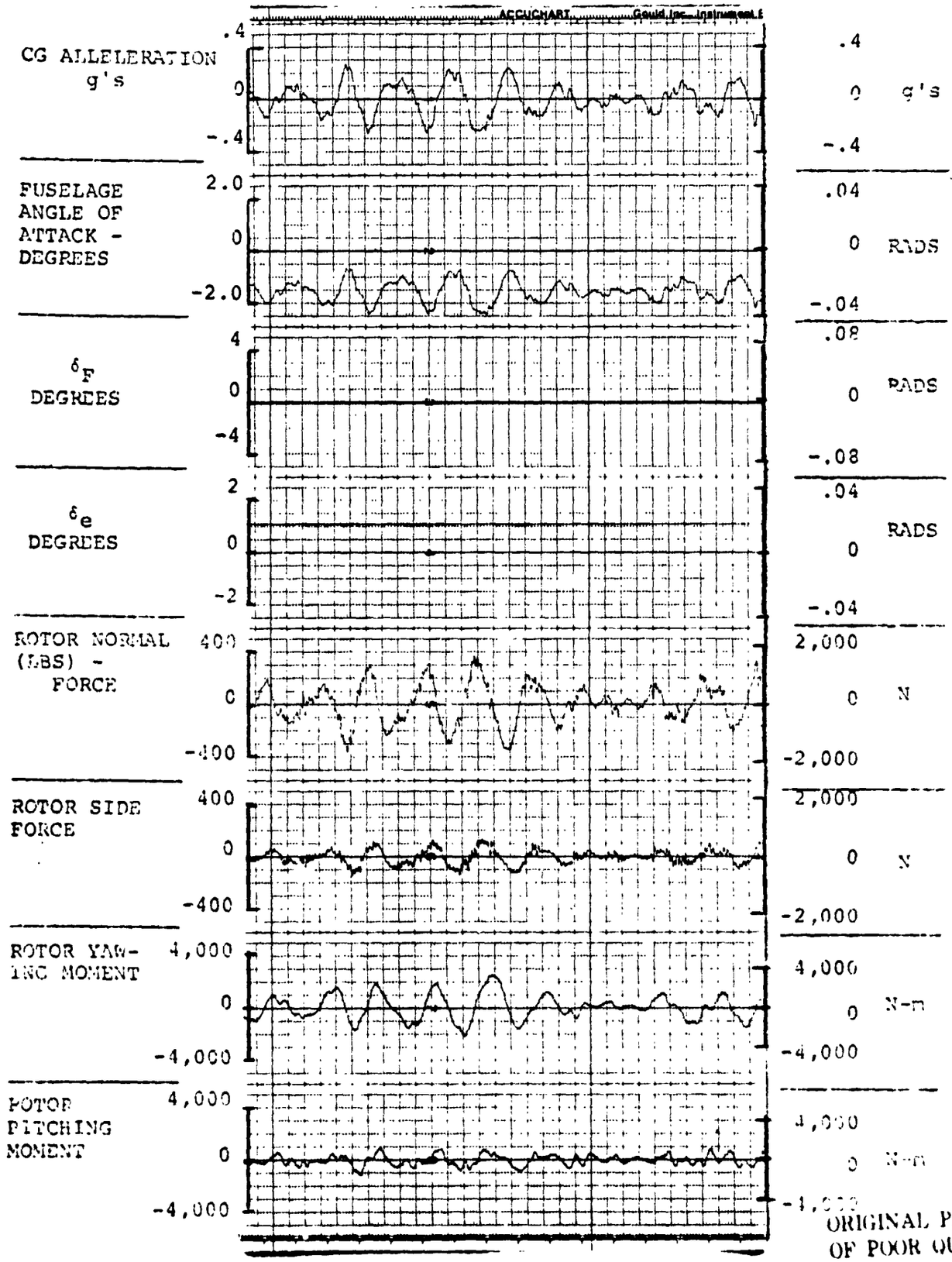

ORIGINAL PAGE IS
OF POOR QUALITY

FIGURE 4.9.2.0.0.1. RESPONSES FOR GAIN F = 0, GAIN E = 0

FLIGHT CONDITION: 280 KNOTS, 15,000 FEET, (4,573m), AFT CG

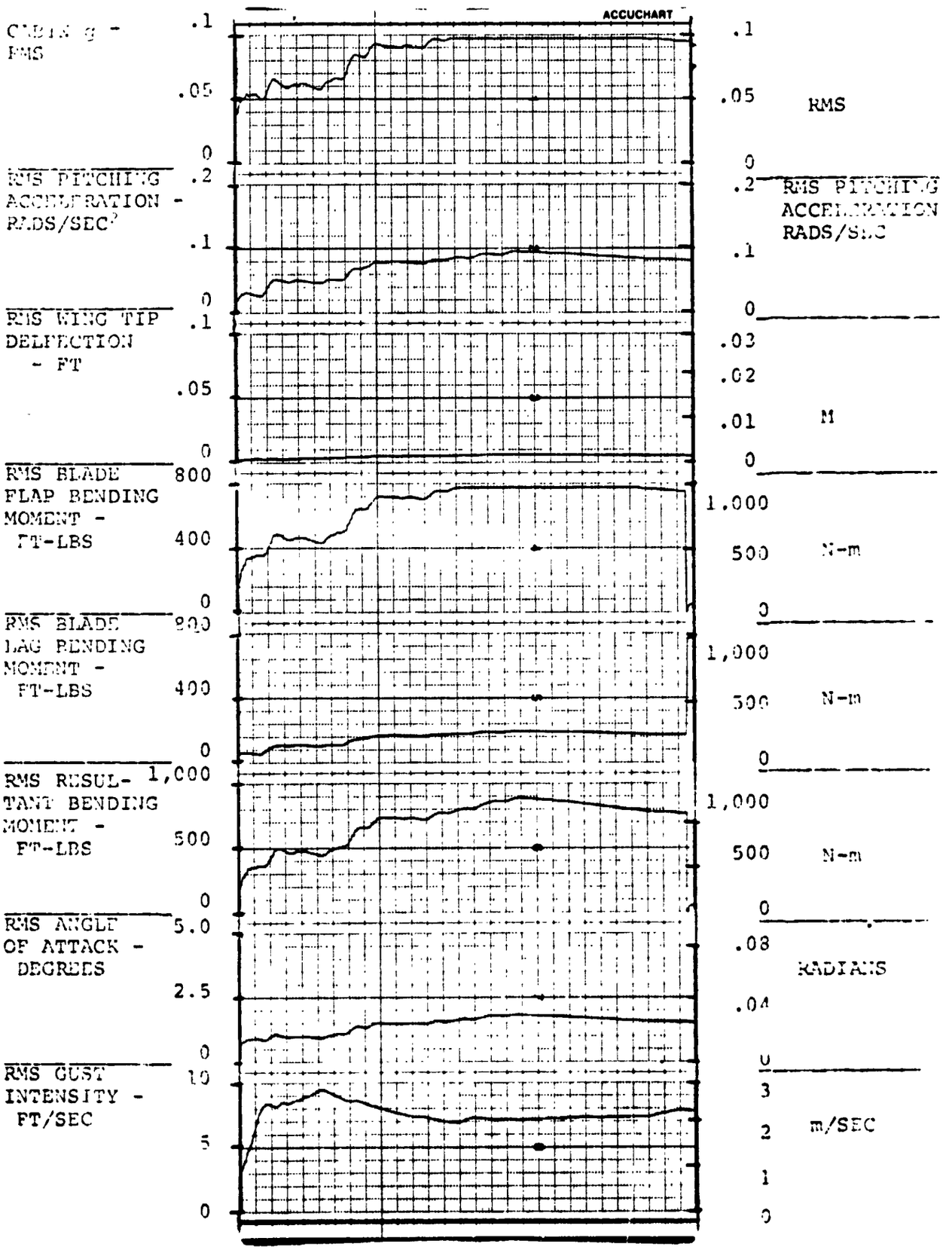

FIGURE 5.9.2.0.0.1. RESPONSES FOR GAIN F = 0, GAIN E = 0

FLIGHT CONDITION: 280 KNOTS, 15,000 FEET, (4,573m), AFT CG

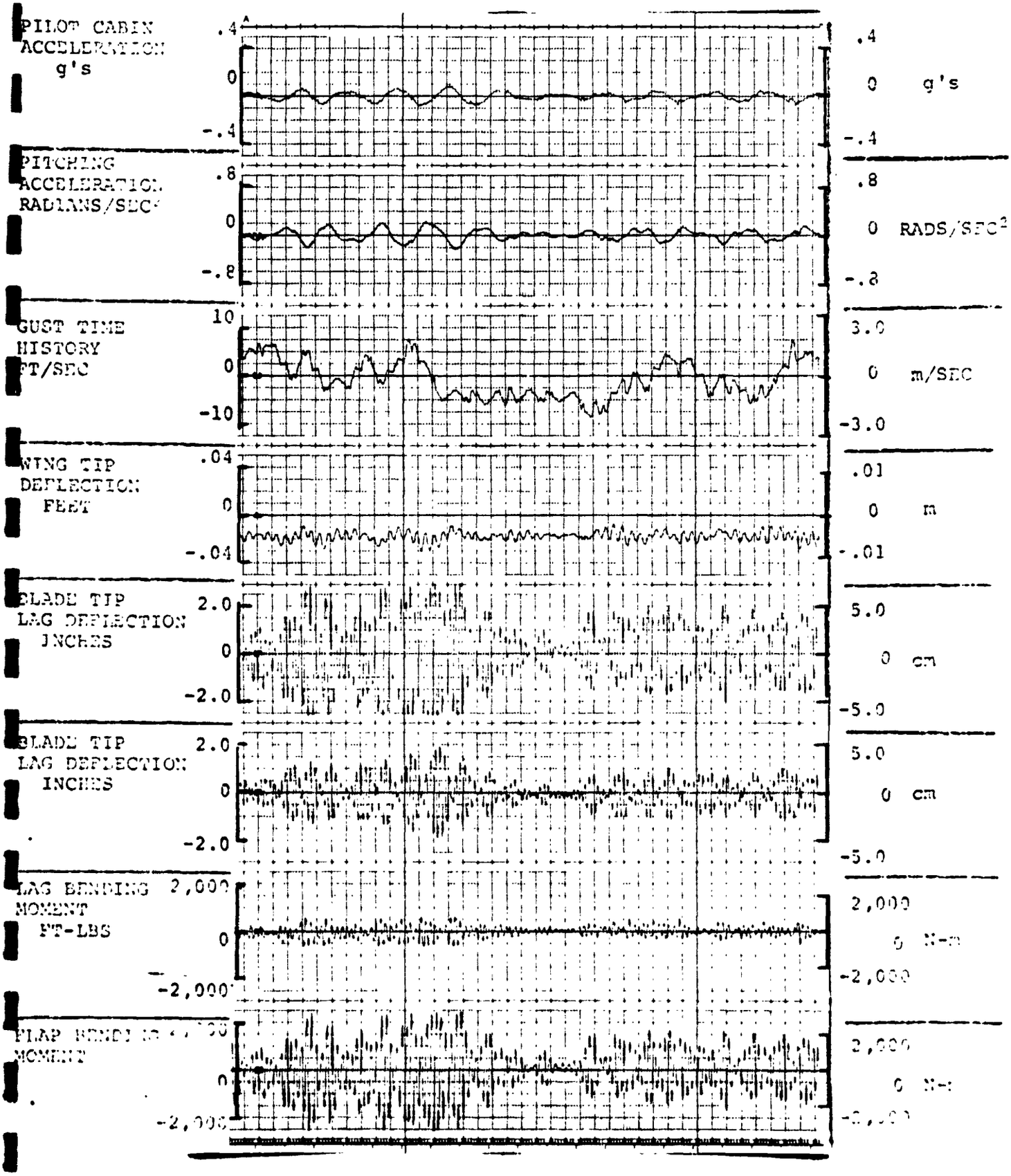

FIGURE 3.9.2.0.0.2. RESPONSES FOR GAIN F = 4.0, GAIN E = .6

FLIGHT CONDITION: 280 KNOTS, 15,000 FEET, (4,573m), AFT CG

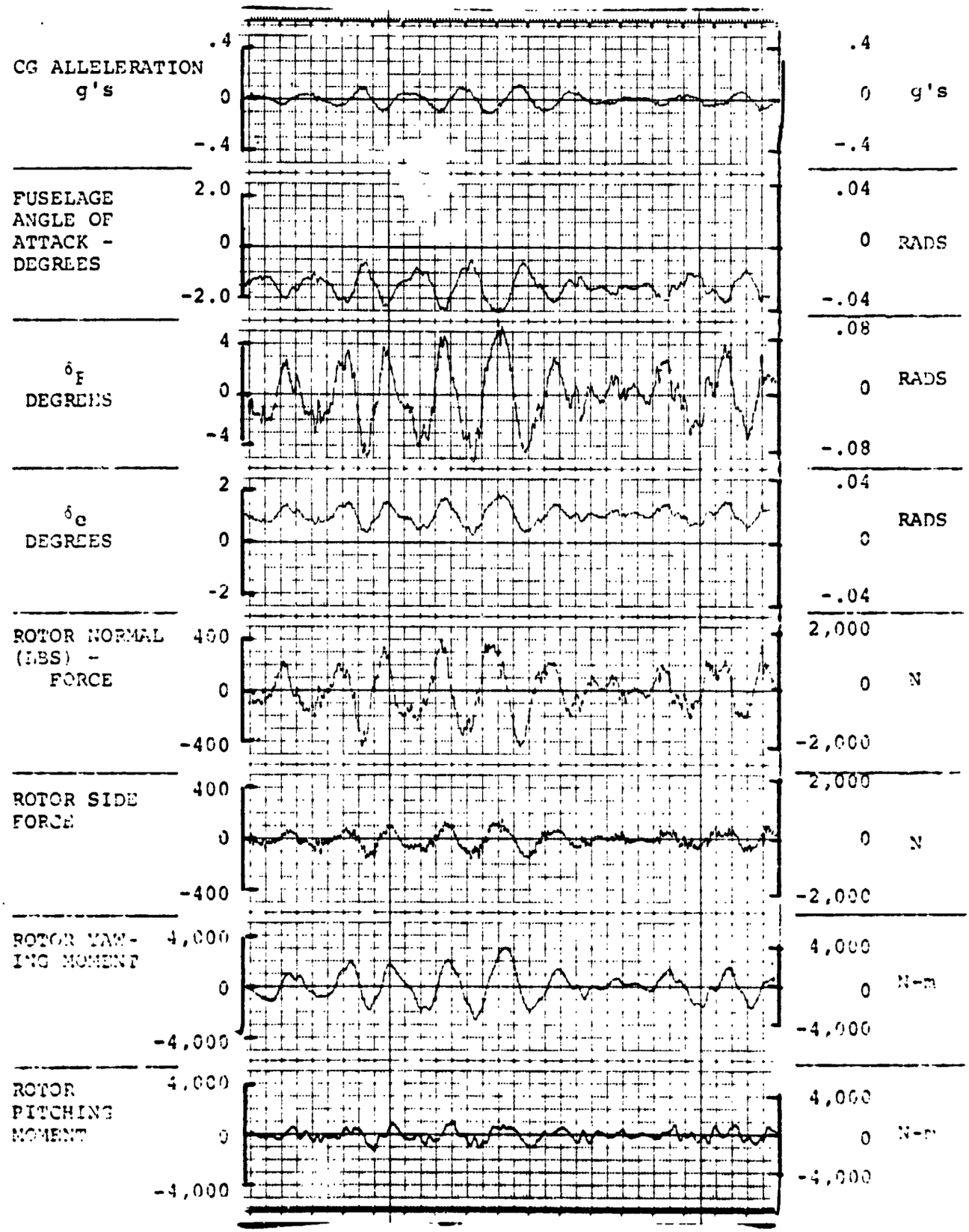

FIGURE 4.9.2.0.0.2. RESPONSES FOR GAIN F = 4.0, GAIN E = .6

FLIGHT CONDITION: 280 KNOTS, 15,000 FEET, (4,573m), AFT CG

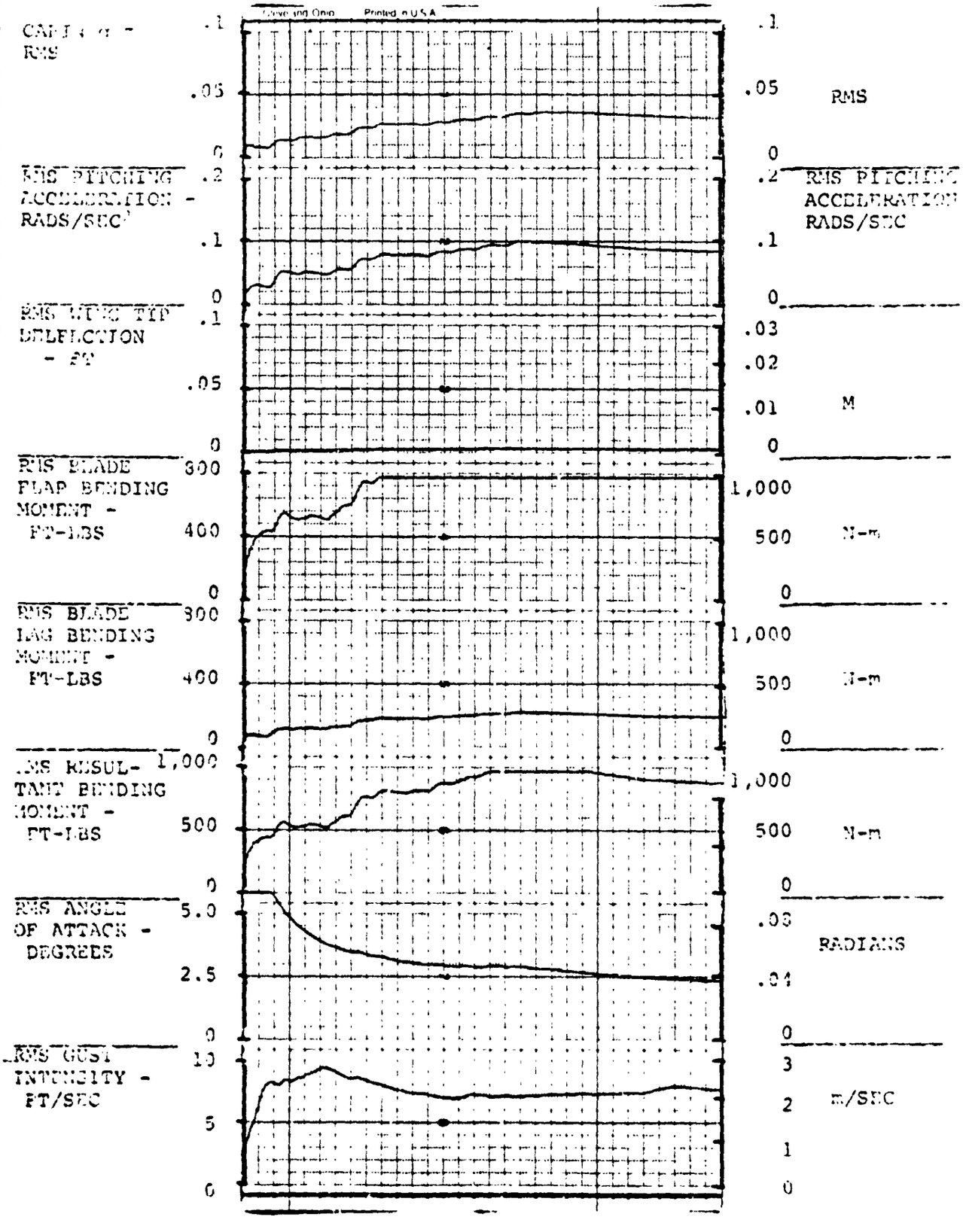

FIGURE 5.9.2.0.0.2. RESPONSES FOR GAIN F = 4.0, GAIN E = .6

FLIGHT CONDITION: 280 KNOTS, 15,000 FEET, (4,573m), AFT CG

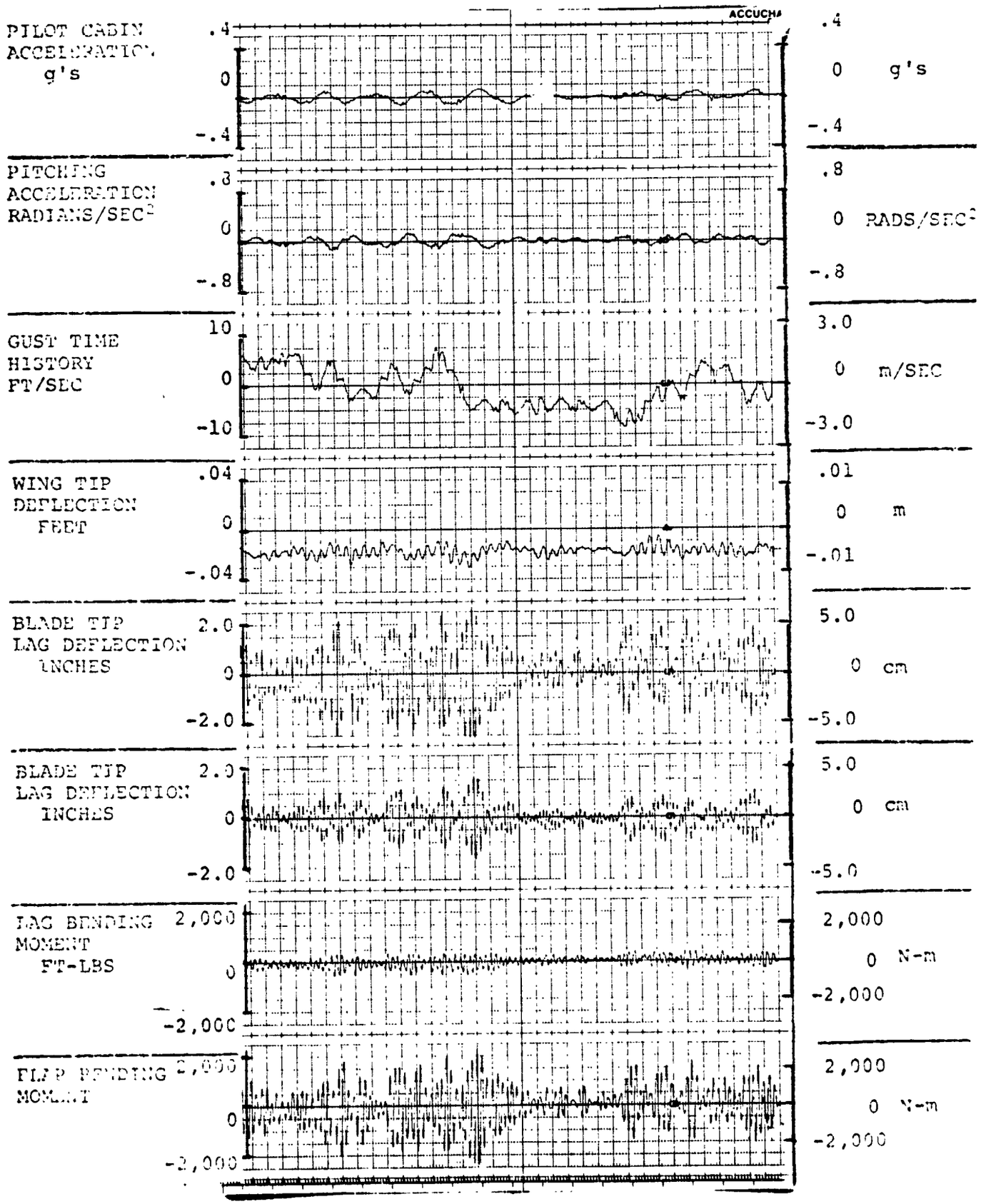

FIGURE 3.9.2.0.0.3. RESPONSES FOR GAIN F = 4.0, GAIN E = .7

ORIGINAL PAGE IS
OF POOR QUALITY

FLIGHT CONDITION: 280 KNOTS, 15,000 FEET, (4,573m), AFT CG

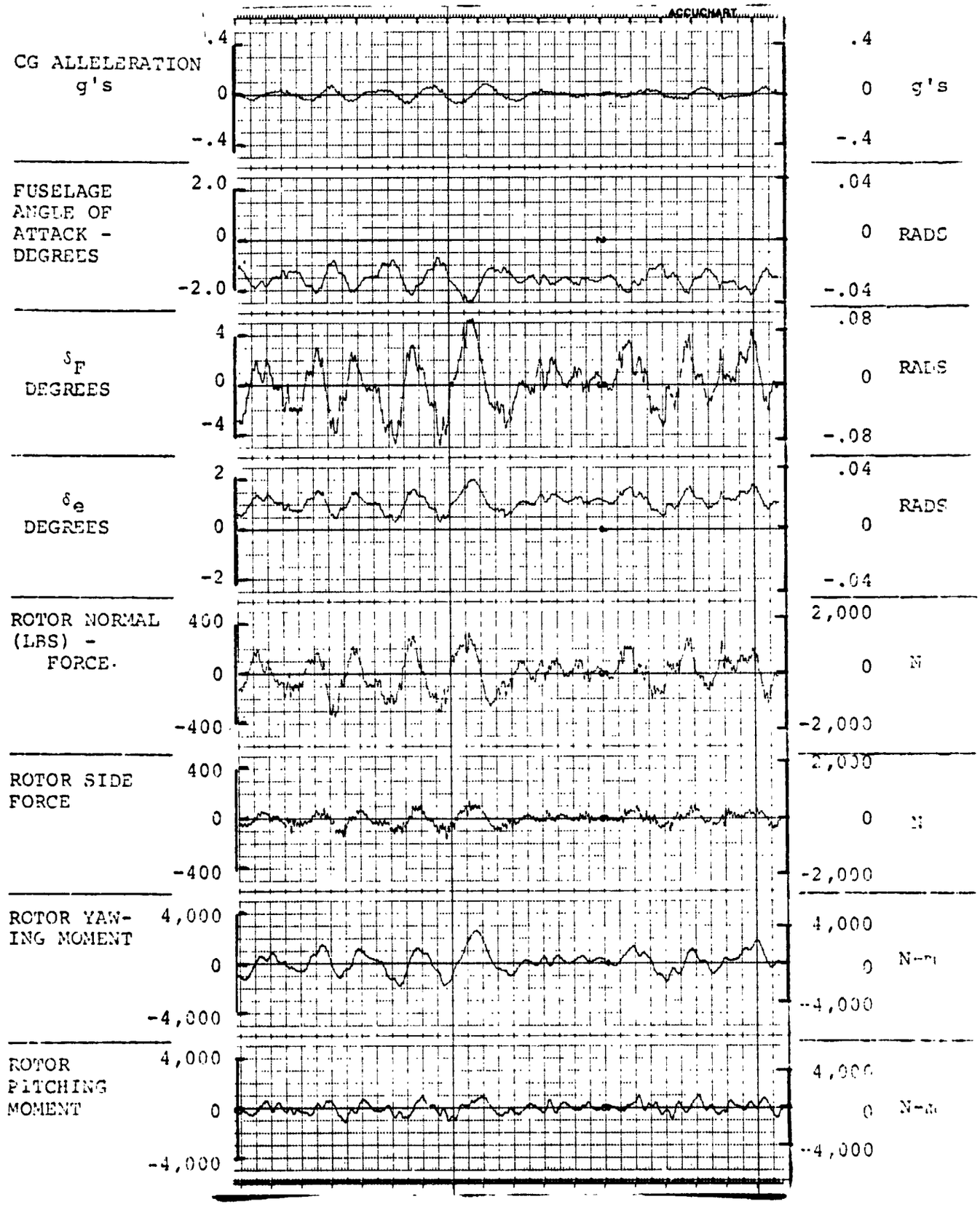

FIGURE 4.9.2.0.0.3. RESPONSES FOR GAIN F = 4.0, GAIN E = .7

ORIGINAL PAGE IS OF POOR QUALITY

FLIGHT CONDITION: 280 KNOTS, 15,000 FEET, (4,573m), AFT CG

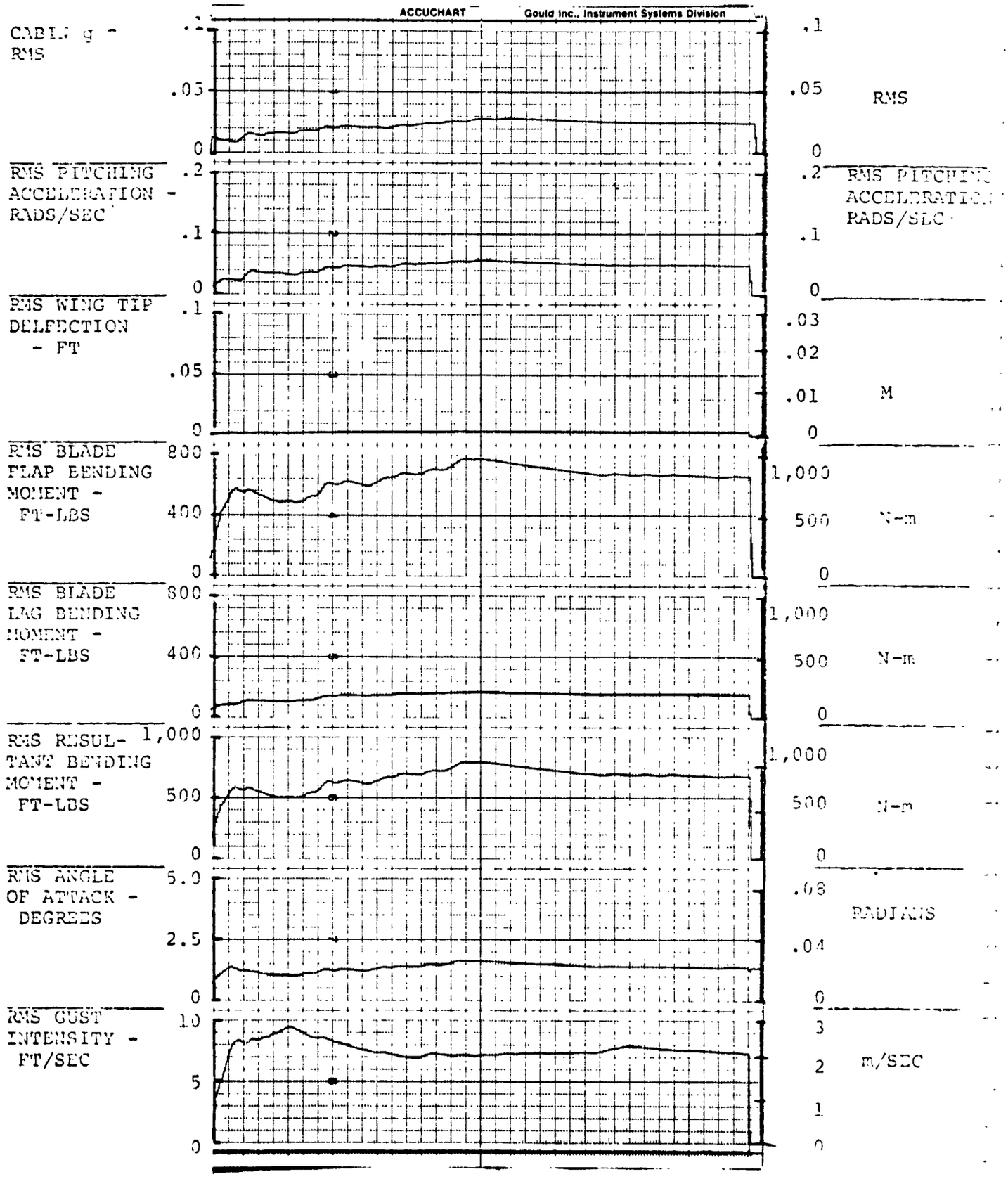

FIGURE 5.9.2.0.0.3. RESPONSES FOR GAIN F = 4.0, GAIN E = .7